

The 4th International Gem and Jewelry Conference

The Exquisite Gem Connectivity

GIT 2014

PROCEEDINGS



December 8-9, 2014

Holiday Inn Hotel, Chiang Mai, Thailand

December 10-12, 2014

Post-Conference Excursion; Lampang-Phrae-Sukhothai, Thailand



สถาบันวิจัยและพัฒนาอัญมณีและเครื่องประดับแห่งชาติ (องค์การมหาชน)
The Gem and Jewelry Institute of Thailand (Public Organization)

The 4th International Gem and Jewelry Conference (GIT 2014)

The Exquisite Gem Connectivity

December 8-9, 2014
Holiday Inn, Chiang Mai, Thailand



PROCEEDINGS

Copyright ©2014

Proceedings of the 4th International Gem & Jewelry Conference – GIT 2014

Owner: The Gem and Jewelry Institute of Thailand (Public Organization) – GIT

Bangkok, Thailand

<http://www.git.or.th/>

All rights reserved. No part of this proceedings may be reproduced by means of any mechanical photographic or electronic processes or in form of a phonographic recording, nor may it be sorted in a retrieval system, transmitted, or otherwise copied for commercial purposed, without a written permission of the GIT

Disclaimer:

This proceedings volume contains abstracts, extended abstracts and full papers submitted for the "GIT 2014" conference. The selection of the contributions has been made to assure pertinence to the conference topics; however, the contents and opinions expressed in the proceedings are of, and fully responsible by, the authors.

ISBN:

Printed in Thailand



The Gem and Jewelry Institute of Thailand (Public Organization)

Welcome Message from the Chairman of the Executive Board of the Gem and Jewelry Institute of Thailand

Thailand has been recognized as a competitive production base in gems and jewelry industry for decades. While undergoing rapid growth, the industry in Thailand still has plenty of room for development. In 2013, this industry was the fourth rank of Thailand's export earners and approximately contributed 9.3 percent to the total exports value of Thailand.

The Gem and Jewelry Institute of Thailand (GIT), the major supporter of Thai gem and jewelry Industry, has played a vital role in the success of the industry. We continue providing support and development to the industry through international technical conferences and other activities each year. Our technical conference underlines Thailand's leadership role in the gems and jewelry industry at the global level.

This year, it is our great pleasure to welcome you all to our renowned conference, the 4th International Gem and Jewelry Conference (GIT2014) under the theme of "The Exquisite Gem Connectivity". The technical conference will be held from December 8-9, 2014 at Holiday Inn, Chiang Mai, Thailand together with the post-conference excursion which will be held on December 10-12, 2014 in Lampang, Phare and Sukhothai.

The conference is a significant opportunity to connect all stakeholders across the industry as well as being a platform to share latest development in gemology, innovation, manufacture, jewelry design, trends, and marketing by the world's leading gemological experts and honorary speakers. I wish all participants a fruitful gathering, as well as a memorable, engaging and enjoyable experience at the 4th International Gem and Jewelry Conference in Chiang Mai, Thailand.



Mr. Siripol Yodmuangcharoen
Chairman of the Executive Board
The Gem and Jewelry Institute of Thailand (Public Organization)

Welcome Message from the GIT Director

I am honored to have the opportunity to welcome you all to GIT Conference once again. The Gem and Jewelry Institute of Thailand has hosted the Gem and Jewelry Conference ever since 2006, each time we have met with the warmest reception and overwhelming success. The past conferences have not only proved to serve as academic platform, but also as the networking forum amongst the peers, academia and industrial experts, to name but a few. From the series of GIT Conference, I am sure that many of you have acquainted with each other before, though, some are about to meet each other for the first time. So, this is a chance to see old friends and making a new, as well as, for all of us to continue to build a firm network for future cooperation.

This year, the 4th International Gem and Jewelry Conference (GIT 2014) will welcome you to the Northern hill scenic paradise of Thailand, with the theme "The Exquisite Gem Connectivity". This theme was chosen with the chief purposes of enhancing regional and international understanding and cooperation among scientists and major stakeholders as well as explore new avenues for better future in the areas of gemological field. On behalf of GIT 2014 Organizing Committee, I have the utmost pleasure and honor to cordially invite you to GIT 2014. The Conference begins with Pre-Conference Excursion to Mogok, Myanmar, during December 3-7, 2014 and to be followed with technical session, to be held during December 8-9, 2014 at Holiday Inn, Chiang Mai. Just make the Conference complete, the last part of the Conference will be the Post Conference Excursion, which will take place during December 10-12, 2014. Whereby you will have the opportunity to visit the Northern gem field in Phare-Sukhothai.

The Conference venue in the city of Chiang Mai, the Holiday Inn, is a charming locale, you will enjoy the dinner reception in relaxed atmosphere beside the Mae Ping River with harmonious northern Thai folk dance, music, arts and authentic taste of Northern Thai cuisine. This vibrant city has countless fascinated attractions. I am fully confident that the intensive conference session, the networking opportunities, the richness of the Thailand's Northern culture and lush greenery will definitely make your trip worthwhile.

I thank you all for your contributions and supports and hope to have them in our next effort to strengthen the GIT conference series for the benefit of us all. I also would like to express my deep appreciation to the GIT 2014 organizing committee, all staff and supporting agencies for the job well done.

See you all again in the GIT 2016


Pornsawat Wathanakul

Director
The Gem and Jewelry Institute of Thailand
(Public Organization)

Conference Committee

Advisory Committee

Somporn Chongkum
Surin Intayot
Panjawan Thanasuthipitak
Kanjana Chookruvong
Rak Hansawek
Henry Ho
Kageeporn Wongpreedee
Phannarat Sornprachoom
Pichet Limsuwan
Pongchan Chanthayot
Vincenzo Liverino
Wilson Yuen

International Technical Committee

Barada Kanta Mishra, India	Kenneth Scarratt, Thailand
Brendan Laurs, USA	Karl Schmetzer, Germany
Bhuwadol Wanthanachaisaeng, Thailand	Khin Zaw, Australia
Christoph A. Hauzenberger, Austria	Lu Taijin, China
Christopher P. Smith, USA	Lore Kiefert, Switzerland
Claudio Milisenda, Germany	Nguyen Ngoc Khoi, Vietnam
Dietmar Schwarz, Thailand	Puwanart Rattanaarungsikul, Thailand
Elena Gambini, Italy	Richard W. Hughes, Thailand
Ekasit Nisaratanaporn, Thailand	Supatra Srisook, Thailand
Gamini Zoysa, Sri Lanka	Taweesak Molsawat, Thailand
Henry A. Hanni, Switzerland	Tay Thye Sun, Singapore
James Shigley, USA	Theerapongs Thanasuthipitak, Thailand
Jayshree Panjekar, India	Tobias Haeger, Germany
Joerg Fischer-Buehner, Germany	Walter A. Balmer, Switzerland
Jongwan Park, Republic of Korea	Yoichi Horikawa, Japan
Yuri Shelementiev, Russia	

International Gem and Jewelry Association

Conference Committee

Organizing Committee

Advisors

Sakda Siripant
Pornsawat Wathanakul
Wilawan Atichat
Boontawee Sriprasert
Chakkaphan Sutthirat
Narong Praphairaksit
Chanutcha Siwamogsatham
Surapon Chaiumnuay

Committee Members

Visut Pisutha-Arnond
Jumpol Denmayca
Su-Arpa Waigayee
Jantima Chatchaisittigul
Thanong Leelawatanasuk
Thitintharee Leelawatanasuk
Jakraphan Suwanvijit
Komson Worakul
Kanyarat Boonsaem
Nalin Narudeesombat
Jirapit Jakkawanvibul
Thidarat Muangthai
Satit Phuangboonton

Secretariat

Wandee Mansrisuk
Malin Sawatekitithum

Contents

Table of Contents

	Page
Welcome Message from the Chairman of the Executive Board of the Gem and Jewelry Institute of Thailand	2
Welcome Message from the GIT Director	3
Conference Committee	4
Contents	6
Overview of Thai Gems and Jewelry Industry	11
The Gem and Jewelry Institute of Thailand (Public Organization)	15
Conference Program	17
Host City Chiang Mai	20
Holiday Inn Chiangmai Hotel	24
Keynote Speakers	26
List of Presenters	32
Keynote's Addresses	46
Extended Abstracts	63
Post Conference Excursion (Lampang-Phare-Sukhothai)	325
Sponsors	351
Author Index	364

Keynote's Address

No.	Keynote Title	Speaker	Page
1	The Role of AEC in Global Gem and Jewelry Market	Prida Tiasuwan	46
2	Past, Present and Future Prospects of World's Colored Stones	Jean Claude Michelou	47
3	Corporate Responsibility in the Gems and Jewelry Business: From Mine to Market	Burak Cakmak	51
4	Jewelry Designs: Creativity in Action	Franco Pianegonda	52
5	Developing at 10,000 Pieces of Jewelry per Hour	Thomas Nyborg	58
6	Raman Micro-spectroscopy of Diamond	Lutz Nasdala	59

Technical Contributions December 8 - 9, 2014

Oral and Poster Presentation

Gems and Precious Metals : deposits, exploration and mining

No.	Title	Presenter	Page
1	Diamond Exploration, Mining And Processing	John Chapman	63
2	Geomorphological Study At Ban Bo Kaeo Sapphire Deposit, Den Chai District, Phrae Province, Northern Thailand	Krit Won-In	65
3	Internal Features Of Ruby From Various Localities In Madagascar	Thanong Leelawatanasuk	69
4	Mineralogy And Petrology Of The An Phu Marble Hosted Spinel And Corundum Deposit, Luc Yen, N-Vietnam	Christoph Hauenberger	76
5	Update On Opal From Pedro Ii, Piauí State, Brazil	Claudio Milisenda	79

Treatment and Synthetics: update and disclosure

No.	Title	Presenter	Page
1	Applications Of Mid- And Near Infrared Spectroscopy To Indicate Conditions Of Heat Treatment In Synthetic Ruby Samples	Natthapong Monarumit	82
2	Carbon Isotope And Cl Analysis Of Natural Type Iia And Cvd Synthetic Gem Diamonds	Wuyi Wang	87
3	Electron-Beam Irradiation And Heat Treatment Of Corundums From New Deposits Of Krong Nang District, Dak Lak Province, Vietnam	Jongwan Park	91
4	From Hpht To Lpht Treatment Of Type Iia Diamonds	Katrien De Corte	95
5	Heat Treatment Of Aquamarine	Nantharat Bunnag	97
6	Influence Of Irradiation And Heating On The Ratanakiri Zircon Structure	Bhuwadol Wanthanachaisaeng	101
7	New Treated Blue Sapphire By Hpht Apparatus	Hyun-Min Choi	104
8	Rusgems Synthetic Opal	Panjawan Thanasuthipitak	106
9	Russian Demantoid Color Heat Treatment	Roman Serov	109
10	Separation Of Natural Argyle Pink And Blue Diamonds From New Generation Of Cvd-Grown Diamonds In Asia	Branko Deljanin	113
11	Spectroscopic Characterization Of Electron-Beam Irradiated Zircon	Sungwon Park	118
12	Thermal Enhancement Of Zircon Samples From Chanthaburi And Kanchanaburi Provinces, Thailand And Rattanakiri, Cambodia	Rattanawalee Chooyoung	122
13	Treated "Black Sapphire" Update	Boontawee Sriprasert	126
14	Treated Black Diamond Earring	Tay Thye Sun	131

Innovative identification and characterization - Manufacturing and cutting edge technology

No.	Title	Presenter	Page
1	A Study Of Color Changes In Natural Quartz By Heat Treatments.	Aram Ham	134
2	“Application Of Cathodoluminescent Technique On Fei Cui (Jadeite Jade) Research”	Miro Ng	137
3	Application Of Fourier Transform Infrared Spectroscopy For The Identification Of Treated Sapphires In Sri Lanka	Sandun Illangasinghe	142
4	Aquamarine From Karur, Tamil Nadu India	Jayshree Panjekar	145
5	Aquamarine From The Gilgit Baltistan Of Northern Areas, Pakistan	Sungjae Kim	149
6	Blue Sapphires From Ban Bo Keaw And Ban Na Poon Deposits In Phrae Province, Northern Thailand	Somruedee Satitkune	153
7	Causes Of Colour And Optical Phenomenon Of Cat’s Eye Opal From Tanzania	Boontarika Srithai	157
8	Characteristic And Physical Properties Of Freshwater Cultured Pearls From Kanchanaburi Province	Nutwatcharee Noirawe	161
9	Characteristics Of Cyanguu Sapphire From Rwanda	Tasnara Sripoonjan	165
10	Characteristics Of The Weyama Diamond From Weyama Gbapolu Country, Liberia	Kim Hyeonki	169
11	Chemical And Spectroscopic Study Of Zircon From Dak Lak, Central Highlands Of Vietnam	Huong Le	172
12	Classification Of Synthetic Diamonds By Using Fourier Transform Infrared Spectroscopy	Jurn Jinhee	177
13	Comparison On The Geochemical Methods For Fingerprinting Of Greenlandic Gem-Corundum (Rubies)	Majken Poulsen	180
14	Crystal Chemistry Of Coloration In Chrysoberyl	Janyaporn Witthayarat	184
15	“Discovering Effect Of Synchrotron Light Interaction On Color Of Freshwater Cultured Pearls: A New Identification Technique For Gamma Irradiated Pearls, A Disclosure Of Synchrotron Exotic Golden Pearls, And A High-Definition Golden Pattern Imprinting Process”	Nirawat Thammajak	187
16	Emeralds From Jharkhand, India	Gagan Choudhary	191
17	Gem Sapphires From A New Deposit In The Krong Nang District, Dak Lak Province, Vietnam: Spectroscopy In Color Investigation	Diep Thi Minh Phan	195
18	Gemological Characteristics Of Rhodolite Garnet From Madagascar	Kanyarat Kwansirikul	199
19	Geographic Origin Determination Of Ruby And Blue Sapphire: An Application Of La-Icp-MS	Kentaro Emori	203

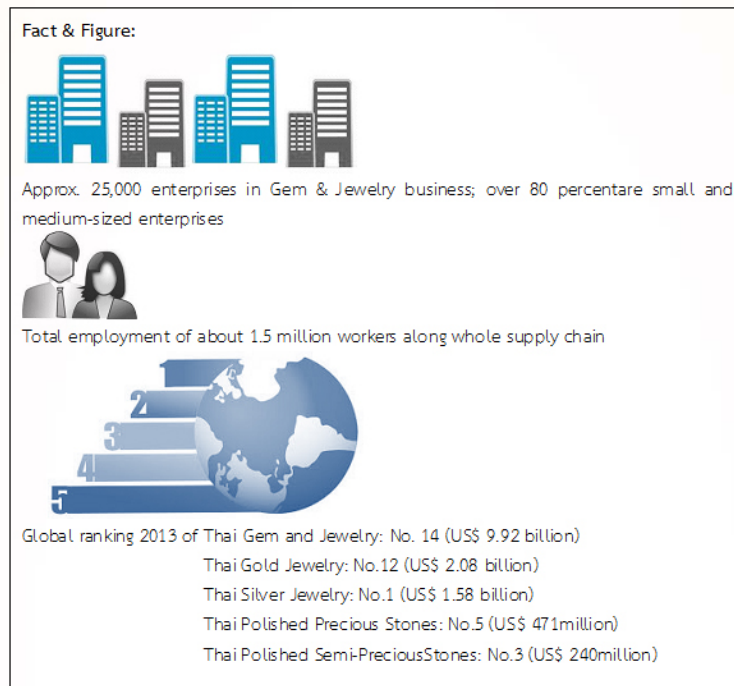
20	High Resolution Computed Microtomography: Insights into a Hollow Beaded Cultured Pearl	Laura M. Otter	207
21	If Diaspore Is Responsible For The 3309 cm ⁻¹ Peak in the FTIR Spectra of Heated Ruby Samples	Aumaparn Phlayrahan	211
22	Introduction of The New Gem-Corundum Sources from Krong Nang District, Dak Lak Province, Vietnam	Nguyen Khoi	217
23	“Mineralogical And Gemological Properties of Orange Johachidolite From Northwest of Mogok, Myanmar”	Yongkil Ahn	221
24	Mineralogy of Blue Pectolite Claimed to be from the Dominican Republic	Weerapan Srichan	224
25	More on Photoluminescence of Emeralds	Elena Gambini	228
26	Natural and Heated Blue Sapphire from Nigeria	Thanong Leelawataasuk	232
27	New Opal From Ethiopia	Lore Kiefert	237
28	Non-Destructive Differentiation of African And Asian Ivory by Ft-Raman Spectroscopy and Chemometric Methods	Ursula Wehrmeister	240
29	Peculiar Natural Type II Diamonds Showing Pseudo-Synthetic Characteristics	Hiroshi Kitawaki	244
30	Raman and Photoluminescence Spectroscopy in Gem Identification	Wolf Kuehn	248
31	Raman Spectroscopic Identification of Geographical Origins of Sapphires	Ssiwon Lee	253
32	Rubies, Sapphires and Quartzes with Double Stars	Karl Schmetzer	256
33	Smoky Quartz From Hod, Chiang Mai, Northern Thailand	Phisit Limtrakun	260
34	Spectroscopic Characterization of Zircon Inclusions of Gem Corundum from Mercaderes, Cauca, Colombia	Manuela Zeug	262
35	Surface Morphology of Natural and Irradiated Diamond Samples	Muzdareefah Thudsanapbunya	264
36	Three-Phase Inclusions in Emerald and Their Impact on Origin Determination	Sudarat Saeseaw	268
37	Update on the Characteristics of Amber from Indonesia	Nalin Narudeesombat	271
37	XRF Analysis in Thai’s Ivory Samples from Lampang Province, Northern Thailand	Chakkrich Boonmee	277

Others

No	Title	Presenter	Page
1	About Bead Nucleus used for Pearl Culturing	Shigeru Akamatsu	280
2	Ancient Glass Beads: a Gemstone of the Log Coffin Culture at Pang Mapha, Mae Hong Son, Thailand	Seriwat Saminpanya	284
3	Dynamic Korea, Dynamic Jewelry Design by Ye Myungji	Myungji Ye	287
4	Forests and Trees: 10 Lessons in Gemology	Richard W. Hughes	291
5	Gemological Research Status on Jades in China	Lu Taijin	292
6	Laminated Type Zirconia Ceramics	Minwoo Park	296
7	Micro-Raman Technology with Fas Imaging and Its Applications	Y.Y. Yang	298
8	Myanmar - The Past, Present and Future	Kennedy Ho	299
9	Preliminary Study on the Use of Lead Free Fire Assay for the Determination of Gold Fineness	Kageeporn Wongreedee	300
10	Should Laboratories Make Degree of Clarity Enhancement Calls? Controversy and Consequences.	Shane McClure	304
11	The Stars Fall from Heaven: Gems with Asterism. An Update.	Martin Steinbach	307
12	Top Ten Trends and Colors in Designer Jewelry for 2015	Cynthia Unninayar	311
13	Building Consumer Confidence in Dubai Gem and Jewelry Industry	Sutas Singbamroong	314
14	The Microstructures and Bending Test of Cu-Based Shape Memory Alloy for Jewelry Application	Chutimun Chanmuang	317
15	Phrae Sapphire Deposit Style	Pornsawat Wathanakul	321
16	The GIT Standard Color Master Sets for 'Pigeon Blood' Ruby, 'Royal Blue' and 'Cornflower Blue' Sapphires	Pongchan Chandayot	323

Overview of Thai Gems and Jewelry Industry

Thai Gem and Jewelry Industry at a Glance



Leading Center of Colored Stones

Thailand is internationally recognized as the world's leading center of colored stones manufacturing and trading with a wide range of gemstones available in various categories and sizes. Precious stones in the corundum family like ruby and sapphire enjoy popularity in the global market and are famous precious stones of Thailand.

Invaluable Local Wisdom

Heat treatment in corundum stones is the method of processing ruby and sapphire through both low and very high temperature under proper conditions. This technique was discovered by Thai craftsmen forty years ago and are kept secret by each craftsman to be shared only among his descendants. The local wisdom not only benefits domestic colored stones manufacturing, but also creates a groundbreaking phenomenon in the global market which has added to the incomparable expertise of Thai craftsmen.

Famous Gemstone Markets

Chanthaburi Gemstone Market (Sri Chan Road) is a major colored stone market in Thailand widely known among Thai and foreign gem traders. Trading activities here start on Thursdays and go on until weekends, with Saturdays as the busiest. Gemstones traded on Sri Chan Road are mainly polished colored stones of various types and sizes, while rough stones are slightly available, but their numbers are growing due to African traders bringing their rough stones to the market.

Mae Sot Gemstone Market is located in Mae Sot district, Tak province, bordering with Myanmar's Myawaddy district, having Moei River as their boundary line. A large variety of gemstones at different price levels can be found in the market. There have been precious stones,



semi-precious stones as well as some alternative gemstones for collectors of rare gems. Most rough stones come from Myanmar while some are from South Africa.

Bangkok is another colored stone trading center in Thailand and is also considered as one of the world's largest centers for high quality colored stones. Most business is concentrated on Silom and Mahaesak Road where gemstones in various grades and sizes can be purchased at reasonable prices.

Notable Jewelry Trading Areas

Yaowaraj gold quarter or "The Golden Road" is situated along Yaowaraj Road in Bangkok, crowded with gold jewelry retail stores along both sides of the road. With 96.5 percent gold purity or 23.16 karat gold according to the international standard of precious metal fineness, Yaowaraj gold



jewelry, which is sold mostly to Thai customers and occasionally to foreign tourists, has shiny golden color and high durability, a unique charm of distinguished quality.

Sukhothai is a province where antique gold ornaments called “Sukhothai gold jewelry” can be purchased. The product is renowned for its unique quality from its entirely handmade process and 99.99 percent gold. With manufacturing techniques restored from traditional gold weaving methods,



while integration of new creative inventions, these precious pieces of jewelry feature outstanding patterns and design elements. In particular, the process of enameling some colors which are red, green and blue, to add colorful patterns into the piece instead of decorating with diamonds or colored stones, has become one of the unique features in Sukhothai’s gold jewelry.



Charoenkrung Road and Khao San Road in Bangkok, where have been so crowded with silver jewelry manufacturers’ stores and wholesale shops, are widely known as Thailand’s silver jewelry trading centers among international buyers. High quality 925 sterling silver jewelry in different forms:

plain jewelry, enamel jewelry and gemset jewelry can be found on these roads. Numerous items with various styles including simple classic and modern elegant looks at competitive price levels are offered.



Chiang Mai's silver jewelry has long been known for its distinctive patterns and exquisite craftsmanship. The making of silverware and silver jewelry can be found in several areas such as Srisuphan village and Wualai community in Mueang district. The handmade silver jewelry and outstanding pieces with hammered patterns on their finish are mostly traded on Wua Lai Road which is the largest manufacturing center of silver products in Chiang Mai province.

The Gem and Jewelry Institute of Thailand (Public Organization)

The Gem and Jewelry Institute of Thailand (Public Organization) - “GIT PO”

The Gem and Jewelry Institute of Thailand (Public Organization) is the governmental agency established as a public organization in accordance with the Public Organization Act B.E. 2542 by Royal Decree on Establishment of the Gem and Jewelry Institute of Thailand (Public Organization) B.E. 2546. The establishment was announced in the Royal Gazette on December 31st, 2003. The institute is under the supervision of Minister of Commerce.

Background

On September 1st, 1998, Ministry of Commerce, Ministry of Industry, and Thai Gem and Jewelry Traders Association had held the meeting to discuss the establishment of the Gem and Jewelry Institute of Thailand and reached the conclusion that both ministries approved such establishment, with the cooperation from Faculty of Science, Chulalongkorn University, in terms of premise and personnel. The meeting has assigned Ministry of Commerce the leading role to propose the institute establishment project to the Cabinet which, on September 8th, 1998, approved the establishment of the Gem and Jewelry Institute of Thailand as an independent organization of which management is not bound to the rules and regulations of bureaucracies and state enterprises. Public Organization Act was stipulated when it was subsequently stipulated.

Once the Public Organization Act B.E. 2542 was announced in the Royal Gazette on February 24th, 1999, the Institute proceeded to draft the Royal Decree on Establishment of the Gem and Jewelry Institute of Thailand (Public Organization) in accordance with the guideline and process specified by Bureaucratic System Reform Commission, the Office of the Civil Service Commission (OCSC). On June 3rd, 2003, the Cabinet had the resolution to approve the principle of the Royal Decree and promulgated “the Royal Decree on Establishment of the Gem and Jewelry Institute of Thailand (Public Organization)” in the government gazette. Afterwards, the name of the institute was changed into “The Gem and Jewelry Institute of Thailand (Public Organization) or GIT, principally purported to promote and support the Thai gem and jewelry industry for its competitiveness in terms of domestic and international trade.

Vision

To be the world-class leading professional in gem and jewelry organization with excellences in standard and services.



Missions

To be the major institute promoting and supporting Thai gem and jewelry business so that it can compete in the world's markets, with the following duties:

1. To analyze, examine, classify, create standards and certify the quality of gem and jewelry as well as precious metals, in order to build up confidence in the quality of Thai gem and jewelry in such a way that it is accepted internationally.
2. To conduct research and develop gem and jewelry in full scale and to be in line with the needs of the gem and jewelry business.
3. Develop the quality of personnel in response the needs of the industry.
4. To prepare in-depth database of gem and jewelry marketing and publicize such among the gem and jewelry business circle.
5. Act as the center in coordinating a cooperation between the government and the private sectors domestically and abroad in order to upgrade the Thai gem and jewelry business to the international forefront level.

Institute's Values

"GIT PO" abbreviated from

G = Good Service

I = International Standard

T = Trustworthy

P = Professional

O = Outstanding

Conference Program

GIT 2014 Conference Program

December 8-9, 2014

Holiday Inn, Chiang Mai, Thailand

Day One- December 8, 2014		
08.00- 17.00	Registration at 2 nd Floor, the Holiday Inn Chiang Mai Hotel	
09.00- 09.30	Opening Ceremony	
09.30- 10.00	<p><u>Keynote Speaker 1 – Prida Tiasuwan</u> <i>“The Role of AEC in Global Gem and Jewelry Market”</i></p>	
10.00- 10.30	Coffee Break and Silent Auction of Original Paintings by the Elephants	
10.30- 11.00	<p><u>Keynote Speaker 2 – Jean Claude Michelou</u> <i>“Past, Present and Future Prospects of World’s Colored Stones”</i></p>	
11.00- 11.30	<p><u>Keynote Speaker 3 – Burak Cakmak</u> <i>“Corporate Responsibility in the Gems and Jewelry Business: From Mine to Market”</i></p>	
11.30- 13.00	Lunch and Poster Viewing	
	Grand Nanta Ballroom I & II (Main)	Tharathong Ballroom I (Break out)
	Session 1: Innovative Identification and Characterization- Manufacturing and Cutting Edge Technology Chairperson: <i>Tay Thye Sun</i>	Session 2: Miscellaneous Chairperson: Brendan Laurs
13.00- 13.20	Characteristics of Cyangugu Sapphire from Rwanda By <i>Chakkaphan Sutthirat</i>	The Stars Fall from Heaven: Gems with Asterism: An Update By <i>Martin Steinbach</i>
13.20- 13.40	Three-Phase Inclusions in Emerald and Their Impact on Origin Determination By <i>Sudarat Saeseaw</i>	About Bead Nucleus Used for Pearl Culturing By <i>Shigeru Akamatsu</i>
13.40- 14.00	Rubies, Sapphires and Quartzes with Double Stars By <i>Karl Schmetzer</i>	Gemological Research Status on Jades in China By <i>Lu Taijin</i>
14.00- 14.20	Geographic Origin Determination of Ruby and Blue Sapphire: an Application of LA-ICP-MS By <i>Kentaro Emori</i>	Application of Cathodoluminescent Technique on Fei Cui (Jadeite Jade) Research By <i>Miro Ng</i>

14:20- 14:40	Peculiar Natural Type II Diamonds Showing Pseudo-Synthetic Characteristics By <i>Hiroshi Kitawaki</i>	Ancient Glass Beads: a Gemstone of the Log Coffin Culture at Pang Mapha, Mae Hong Son, Thailand By <i>Seriwat Saminpanya</i>
14.40- 15.10	Coffee Break and Silent Auction of Original Paintings by the Elephants	
	Grand Nanta Ballroom I & II (Main)	Tharathong Ballroom I (Break out)
	Session 3: Innovative Identification and Characterization- Manufacturing and Cutting Edge Technology (cont.) Chairperson: <i>Claudio Milisenda</i>	Session 4: Miscellaneous (cont.) Chairperson: <i>Nguyen Ngoc Khoi</i>
15.10- 15.30	Aquamarine from Karur, Tamil Nadu India By <i>Jayshree Panjekar</i>	Top Ten Trends and Colors in Designer Jewelry for 2015 By <i>Cynthia Unninar</i>
15.30- 15.50	New Opal from Ethiopia By <i>Lore Kiefert</i>	Dynamic Korea, Dynamic Jewelry Design By <i>Myungji Ye</i>
15.50- 16.10	Causes of Colour and Optical Phenomenon of Cat's Eye Opal from Tanzania By <i>Boontarika Srithai</i>	Preliminary Study on the Use of Lead Free Fire Assay for the Determination of Gold Fineness By <i>Kageeporn Wongpreedee</i>
16.10- 16.30	Chemical and Spectroscopic Study of Zircon from Dak Lak, Central Highlands of Vietnam By <i>Huong Le</i>	Micro-Raman Technology with Fast Imaging and its Applications By <i>YY Yang</i>
16.30- 16.50	Blue Sapphires from Ban Bo Kaeo and Ban Na Poon deposits in Phrae Province, Northern Thailand By <i>Somruedee Satitkune</i>	Building Consumer Confidence in Dubai Gem and Jewelry Industry By <i>Sutas Singbamroongand</i>
18.30- 21.30	Welcome Reception and Silent Auction Winners Announcement at The River Pavilion	

Day Two - December 9, 2014	
08.00 - 12.00	Registration at 2nd Floor, the Holiday Inn Chiang Mai Hotel
09.00 - 09.30	Keynote Speaker 4 – Franco Pianegonda <i>"Jewelry Designs: Creativity in Action"</i>
09.30 - 10.00	Keynote Speaker 5 – Thomas Nyborg <i>"Developing at 10,000 Pieces of Jewelry per Hour"</i>
10.00 - 10.30	Coffee Break
10.30 - 11.00	Keynote Speaker 6 – Lutz Nasdala <i>"Raman Micro – Spectroscopy of Diamond"</i>
11.00 - 12.30	Poster Viewing & Meet the Authors
12.30 - 13.30	Lunch

	Grand Nanta Ballroom I & II (Main)	Tharathong Ballroom I (Break out)
	Session 5: Gem and Precious Metal Deposits, Exploration and Mining Chairperson: <i>Karl Schmetzer</i>	Session 6: Treatment and Synthetics: Update and Disclosure Chairperson: <i>Yoichi Horikawa</i>
13.30- 13.50	Diamond Exploration, Mining and Processing By <i>John Chapman</i>	Separation of Natural Argyle Pink and Blue Diamonds from New Generation of CVD-Grown Diamonds in Asia By <i>Branko Deljanin</i>
13.50- 14.10	Update on Opal from Pedro II, Piauí State, Brazil By <i>Claudio Milisenda</i>	From HPHT to LPHT Treatment of Type IIa Diamonds By <i>Katrien De Corte</i>
14.10- 14.30	Mineralogy and Petrology of the An Phu Marble Hosted Spinel and Corundum Deposit, Luc Yen, N-Vietnam By <i>Christoph Hauzenberger</i>	Russian Demantoid Color Heat Treatment By <i>Roman Serov</i>
14.30- 14.50	Geomorphological Study at Ban Bo Kaew Sapphire Deposit, Den Chai District, Phrae Province, Northern Thailand By <i>Krit Won-in</i>	Carbon Isotope and CL Analysis of Natural Type IIa and CVD Synthetic Gem Diamonds By <i>Wuyi Wang</i>
14.50- 15.10	Gem Sapphires from A New Deposit in the Krong Nang District, Dak Lak Province, Vietnam: Spectroscopy in Color Investigation By <i>Diep Thi Minh Phan</i>	Natural and Heated Blue Sapphire from Nigeria By <i>Thanong Leelawatanasuk</i>
15.10- 15.40	Coffee Break	
	Grand Nanta Ballroom I & II (Main)	
	Session 7: Closing Highlights Chairperson: <i>Jayshree Panjkar</i>	
15.40- 16.00	Treated "Black Sapphire" Update By <i>Boontawee Sriprasert</i>	
16.00- 16.20	Should Laboratories Make Degree of Clarity Enhancement Calls? Controversy and Consequences By <i>Shane McClure</i>	
16.20- 16.40	Myanmar- The Past, Present and Future By <i>Kennedy Ho</i>	
16.40- 17.00	Forests and Trees: 10 Lessons in Gemology By <i>Richard W. Hughes</i>	
17.00	End of Conference	

Host City of Chiang Mai

Destination Fast Fact



Get to know Chiang Mai

The rose of the North, Chiang Mai, is a wonderful small city with a history more than 700 years old. Chiang Mai impresses guests with its natural charm. Chiang Mai has its own very distinctive culture, arts, festivals, and traditions as well as an exciting mix of local, ethnic and expatriate communities from all over the world. It has been voted one of the top destinations to live in Asia and is a modern and cosmopolitan city, while not having lost its traditional old charm. Today, Chiang Mai is the economic, communications, cultural and tourism centre of Northern Thailand.

Travel from Bangkok to Chiang Mai

Chiang Mai is about 700 kms from Bangkok. There are variety of transportations from Bangkok to Chiang Mai such as airplane, train, bus and even car.

Attractions

Chiang Mai is blessed with natural, cultural and religious attractions as well as the historical places. Other attractions include Zoo, Chiang Mai Night Safari, Chiang Mai Night Bazaar, Saturday Market, Sunday Market and many more.

- **Wat Phra Singh** is contained within the city walls and moat. The main entrance is guarded by Singhs (lions).



- **Wat Chedi Luang** is a Buddhist temple in the historic centre of Chiang Mai. The current temple grounds were originally made up of three temples — Wat Chedi Luang, Wat Ho Tham and Wat Sukmin.



- **Chiang Mai Night Safari** is the world's third nocturnal zoo and is a government nature theme park. It is considered by many to be the most beautiful Night Safari in the world where you can discover the night life of wild animals from the safety of an open sided tram here! Please visit [www.Chiang Mainightsafari.com](http://www.ChiangMainightsafari.com) .



- Chiang Mai is a shopper's paradise, and nothing beats shopping for a bargain more than in the famous **Chiang Mai Night Bazaar**.



- **The Saturday Market** (or Wui Lai Market) is located to the south west of the old city opposite the Chiang Mai Gate. The Saturday Market is open every Saturday from 4pm till midnight. The road is closed to all vehicular traffic so you can browse the goods on display, bargain with vendors for a good price and wander freely around without traffic worries.



- **The Sunday Market** (or Walking Street) is a large market located right in the centre of the old walled city area of Chiang Mai. Starting at the Tha Phae Gate at one end the Sunday Market extends for roughly 1km down the full length of Ratchadamnoen Road. You can go to the Market every Sunday from 4pm till midnight.



Staying in Chiang Mai

Chiang Mai can claim to some of the finest accommodations in the world. In Chiang Mai, you have a superb selection of hotels in all categories; modern, luxurious, homely and ensure you that all are comfortable. Additionally, you can touch and feel the Thai Lanna style everywhere from staying in Chiang Mai.

Delicious Dining

Chiang Mai has hundreds options of dining and many are internationally famous for its delicious and piquant tastes. For examples:-

- **Khao Soi:** The grande dame of northern Thai cuisine is Khao Soi-- yellow noodles perched in a shallow pool of thick coconut milk curry, topped off with crispy fried noodles and served with wedges of lime, pickled cabbage and shallots.
- **Sai Ua:** Sai Ua, known to foreigners as “Northern-style” or “Chiang Mai” sausages, is salivated over for their gustatory complexity. Minced pork is stuffed with an orgy of herbs and spices including lemongrass, cilantro, shallot, black pepper and galangal, which is mixed with chili paste to burst forth with a cornucopia of flavors.
- **Nam Prik Noom:** Roasted green chilies are pounded with garlic, shallots and other ingredients to create a fibrous wet mess that gives a kick to sticky rice, vegetables or kaeb moo (pork rinds).

Getting around Chiang Mai

Chiang Mai is relatively easy to get around, since it is a very tourist oriented town. The major means of public transport in Chiang Mai town is mini-buses (or locally called Rod Daeng). Plying around town, they are in vivid colours and look like small pick-up with a roof. Tell the destination to the driver and negotiate the price before getting on. Normally the rides cost between 10 and 20 baht.



Holiday Inn Chiangmai Hotel

Holiday Inn Chiangmai is ideally located on the banks of Mae Ping River with easy access to the business and shopping districts. It is the only riverside international hotel brand on the Northern bank of Chiang Mai with 526 rooms and 25-storeys offering expansive riverside views from both guest and functional rooms. The hotel is only minutes away from the famous temples and the renowned night bazaar.

The Guest Rooms are the largest in Chiang Mai and have been designed with every comfort in mind. Every room has beautiful views over the idyllic Mae Ping River and towards Doi Suthep, the sacred mountain or Chiang Mai city views. At Holiday Inn Chiangmai, we guarantee your comfort with a double size for twin bed and pillow menu. Holiday Inn is the world's most recognized hotel brand offering genuine service and quality amenities, catering to the needs of both business and leisure travelers.

Holiday Inn Chiangmai Hotel

318/1 Chiang Mai-Lamphun Road, Tumbol Wat Kate, ChiangMai, 50000, Thailand

Tel: +66 (0) 5327 5300

Toll Free 001 800 656 888

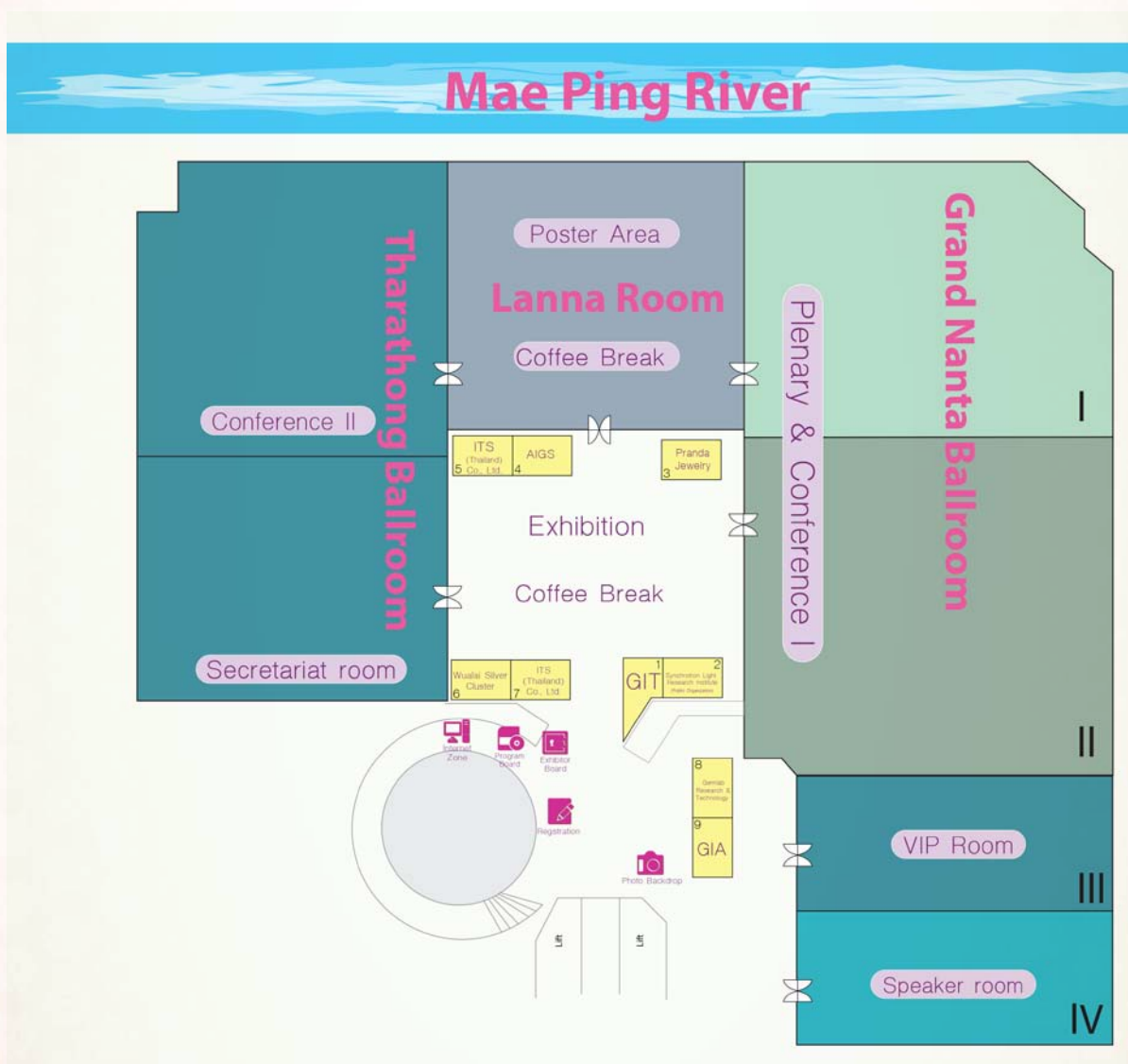
www.ihg.com/holidayinn/hotels/us/en/hd/thailand/chiangmai-hotels



Conference Room

The conference rooms are Grand Nanta Ballroom and Tharathong Ballroom where both are located at the 2nd floor of Holiday Inn Chiangmai. The rooms have specially been designed for catering meetings and conferences.

The poster area is in the Lanna room which is the connecting room of Grand Nanta Ballroom and Tharathong Ballroom. Additionally, we can see the attractive view of Mae Ping River from Lanna room.



Holiday Inn Chiangmai Hotel

Keynote Speaker



Prida Tiasuwan

Board Chairman of Pranda Jewelry Group

“The Role of AEC in Global Gem and Jewelry Market”

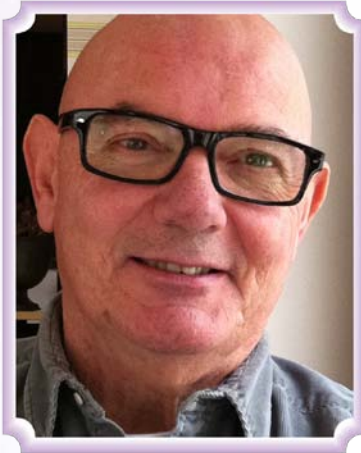
Prida Tiasuwan Is The Chairman Of Pranda Jewelry Public Company Limited, Manufacturer And Exporter Of Jewelry. Pranda Jewelry Is A Global Company, With A Manufacturing Capacity With Nearly 5,000 Highly Skilled Workers In 6 Factories Located Throughout S.E. Asia & Germany.

Mr. Tiasuwan Is Also Member (5Th Class) Of The Most Noble Order Of The Crown Of Thailand. He Received H.N.D. In Business Studies From Thames Valley University, England In 1971 And Distinguished Senior Executive Program In Government And Business At Harvard University, U.S.A. In 1991.

He Was A Founding Chairman Of Social Venture Network Asia (A Business For Society And Environmental Grouping), Vice President Of Thai Gem & Jewelry Traders Association, Vice President Of International Coloured Gemstone Association, Director Of Assembly Of Thailand Reform, And Presently Director On Sub Committee On Competitor Law Reform.

He Also Served On The Board At Duang Prateep Foundation, The Thai Chamber Of Commerce, Thai Listed Companies Association, And Thailand Us Business Council.

Keynote Speaker



Jean Claude Michelou

ICA Vice President

*“Past, Present and Future Prospects of
World’s Colored Stones”*

Jean Claude Michelou, ICA’S Vice President has been active in Colombian emerald trading, cutting and export since 1977 as well as rough colored gemstones sourcing strategist from different origins.

More recently he has been active as a consultant for USAID and the World Bank where he has worked on the development of infrastructures and policies from mine to market for the gemstone industry in different countries.

He has been working on the development of Fair and Ethical Trade and Mining Standards and certification and traceability models from counties of origins as well as Social responsibilities initiatives for Artisanal and Small Scale mining communities.

He is the chairman of the ICA fair trade and Ethical Mining committee. He is also ICA’Chairman of the Ambassadors and Communication committees as well as the Editor-in-Chief of ICA’s InColor magazine.

Keynote Speaker



Burak Cakmak

**Vice President of Corporate Responsibility, Corporate
Communication and Design Service, Swarovski**

*“Corporate Responsibility in the Gems and Jewelry
Business: From Mine to Market”*

Burak Cakmak is a sustainability expert with a focus on businesses and the environment. Currently he is the Vice President, Corporate Responsibility at Swarovski, the world’s leading producer of precision-cut crystal and gemstones. Mr. Cakmak is the first person to hold this role at the company and is establishing the global sustainability agenda through identifying and implementing the social, environmental and giving strategies for the brand. He is a frequent speaker with a focus on luxury brands and sustainability and has lectured throughout the world on this topic.

Prior to Swarovski, Mr. Cakmak worked as General Manager of MADE-BY Benelux, a European not-for-profit organization with a mission to make sustainable fashion common practice.

Mr. Cakmak has also held the role of Director of Corporate Sustainability in the Gucci Group (now Kering). At Gucci Group, he was responsible for the implementation of the sustainability framework to help the Group and its brands develop tailored initiatives to stay committed to business ethics, human rights and environmental stewardship in alignment with company’s Code of Business Practices and CSR principles. Previously, Mr. Cakmak was a part of Gap Inc.’s Social Responsibility department in San Francisco and London where he contributed to sustainable design, environmental and community initiatives.

Mr. Cakmak received a Bachelor of Science degree in International Relations from the Middle East Technical University and his MBA from San Francisco State University with a concentration on International Business as well as an MBA from CERAM Sophia Antipolis. He recently completed the postgraduate certificate degree in Sustainable Business at the University of Cambridge. Mr. Cakmak is also a visiting professor SKEMA Business School, lecturing at the Sophia Antipolis campus in Nice, France and Suzhou, China. Mr. Cakmak resides in London, United Kingdom.

Keynote Speaker



Franco Pianegonda

CEO of Franco Pianegonda

“Jewelry Designs: Creativity in Action”

1994: The brand “Pianegonda” was born in Vicenza from the entrepreneurial and creative capacities of Franco Pianegonda. The idea was to create new jewels in silver, combining design and fashion according to the highest tradition of the Italian jewellery. Artisan perfection and the most modern techniques were used for a brand that represented Made in Italy worldwide.

Constant research, far-sighted marketing and strong communication turned the brand into an expression of the latest jewelry and the fashion trends. Pianegonda was a dynamic entity that faced international competition boldly and competently.

The brand was distributed in Italy and worldwide in the best jewellery shops and department stores. Flagship stores were located in major cities: Milan, Venice, Rome, Florence, Paris, Athens, Dubai, Hong Kong and Beijing, among others

Keynote Speaker



Thomas Nyborg

Managing Director, Pandora Thailand

*“Developing at 10,000 Pieces of
Jewelry per Hour”*

Thomas Nyborg helms PANDORA’s manufacturing arm, PANDORA Production Thailand (PPT), which comprises seven production facilities in Gemopolis, Bangkok. It is here where PANDORA’s universe of contemporary, feminine and meticulously crafted jewellery, cherished by women the world over, is created by more than 8,000 Thai craftsmen and -women. Thomas is thus responsible for the largest manufacturing process of jewellery in Thailand, which uniquely combines modern production techniques with traditional craftsmanship and hand-finishing. Thomas brings a wealth of expertise to PANDORA spanning nearly 30 years in the sphere of jewellery: from gemstone trading to jewellery design, retailing and manufacturing. Thomas is also a Graduate Gemologist from the Gemological Institute of America (GIA).

Keynote Speaker



Lutz Nasdala

**Professor for Mineralogy and Spectroscopy,
Institute of Mineralogy and Crystallography,
University of Vienna, Austria**

“Raman Micro-Spectroscopy of Diamond”

Lutz Nasdala is a professor for mineralogy and spectroscopy at the University of Vienna, Austria. He is mineralogist by training and obtained his PhD at the Institute of Theoretical Physics, Freiberg Mining Academy (Germany). After several PostDocs at the University of Hawaii, the Curtin University of Technology, Perth, Western Australia, and the University of Vienna, Austria, he finished his habilitation in Mainz, Germany, where he then worked as mineralogy professor.

In 2006, Prof. Nasdala was awarded a three-year Marie Curie Chair of Excellence for Mineral Spectroscopy, funded by the European Commission. In 2009 he became full professor at the University of Vienna and served as head of the Institute of Mineralogy and Crystallography since.

Prof. Nasdala's main research interests include real structures and internal textures of minerals, optically active defect centers, and phenomena of radiation damage. He is an expert in the application of non-destructive micro-analysis techniques to the characterization of gem and their enhancement. Prof. Nasdala provides spectroscopy teaching and training on an international scale; in the last year he organized and conducted short-courses for instance in Bogota, Beijing and at several European institutions, and he delivered lectures in more than ten countries worldwide.

For the 2014–2015 academic year, Prof. Nasdala was awarded the honor to serve as Mineralogical Society of America Distinguished Lecturer.

List of Presenters



Name: Aram Ham
Address: Gemological engineering, Hanyang University, Seoul
Republic of Korea
Post Code: 133-791 Tel: +82-10-94635767 Fax: +82-2-2220-4011
Email: lilyham7@gmail.com
Title: A Study of Color Changes in Natural Quartz by Heat Treatments



Name: Aumaparn Phlayrahan
Address: Department of Earth Sciences, Faculty of Science, Kasetsart
University, Chanthaburi, Thailand
Post Code: 22170 Tel: +66 2940 6966 Fax: +66 2940 6966
Email: a.phlayrahan@gmail.com
Title: If Diaspore is Responsible for the 3309 cm^{-1} Peak in the FTIR Spectra
of Heated Ruby Samples



Name: Bhuwadol Wanthanachaisaeng
Address: Faculty of Gems, Burapha University, Chanthaburi, Thailand
Post Code: 22170 Tel: Fax:
Email: bhuwadol@yahoo.com
Title: Influence of Irradiation and Heating on the Ratanakiri Zircon
Structure



Name: Boontarika Srithai
Address: Department of Geological Sciences, Faculty of Science, Chiang
Mai University, Chiang Mai, Thailand
Post Code: 50200 Tel: +66 5394 3417 Fax:
Email: boontarika.s@cmu.ac.th
Title: Causes of Colour and Optical Phenomenon of Cat's Eye Opal from
Tanzania



Name: Boontawee Sriprasert
Address: The Gem and Jewelry Institute of Thailand (Public Organization),
Bangkok, Thailand; Department of Mineral Resources, Bangkok, Thailand
Post Code: 10400 Tel: +66 2621 9676 Fax: +66 26219554
Email: boontawee@gmail.com
Title: Treated "Black Sapphire" Update

List of Presenters



Name: Branko Deljanin
Address: CGL – GRS Swiss Canadian Gemlab, Vancouver, Canada
Post Code: BC V6C 1T2 Tel: Fax:
Email: info@cglworld.ca
Title: Separation of Natural Argyle Pink and Blue Diamonds from New Generation of CVD-grown Diamonds in Asia



Name: Chakkrich Boonmee
Address: Department of Earth Sciences, Faculty of Science, Kasetsart University, Bangkok, Thailand
Post Code: 10900 Tel: +66 2940 6966 Fax:
Email: Chakkrich_b@hotmail.com
Title: XRF Analysis in Thai's Ivory Samples from Lampang Province, Northern Thailand



Name: Christoph Hauzenberger
Address: Karl Franzens, University of Graz, Graz, Austria
Post Code: A-8010 Tel: Fax:
Email: christoph.hauzenberger@uni-graz.at
Title: Mineralogy and Petrology of the an Phu Marble Hosted Spinel and Corundum Deposit, Luc Yen, N-Vietnam



Name: Chutimun Chanmuang
Address: Faculty of Gems, Burapha University, Chanthaburi, Thailand
Post Code: 22170 Tel: +66 8 7537 2555 Fax:
Email: Chutimunta@hotmail.com
Title: The Microstructures and Bending Test of Cu-based Shape Memory Alloy for Jewelry Application



Name: Claudio Milisenda
Address: DSEF German Gem Lab, Idar-Oberstein, Germany
Post Code: D-55743 Tel: +496 7815 0814 Fax:
Email: info@gemcertificate.com
Title: Update on Opal from Pedro II, Piauí state, Brazil

List of Presenters



Name: Cynthia Unninayar
Address: Editor in Chief, CIJ Trends & Colours Magazine, Columbia, USA
Post Code: 21044 Tel: +1410 715 4680 Fax:
Email: cynthiau@gmail.com
Title: Top Ten Trends and Colors in Designer Jewelry for 2015



Name: DiapThi Minh Phan
Address: Institute of Geosciences, Johannes Gutenberg University, Mainz, Germany
Post Code: D55099 Tel: +491 7656 400 848 Fax:
Email: sjk310700@gmail.com
Title: Gem Sapphires from a New Deposit in the Krong Nang District, Dak Lak Province, Vietnam: Spectroscopy in Color Investigation



Name: DongwookShin
Address: Department of Advanced Gemology and Division of Materials Science and Engineering, Hanyang University, Seoul, Republic of Korea
Post Code: 133-791 Tel: +82-2-2220-0503 Fax: +82-2-2220-4011
Email: dwshin@hanyang.ac.kr
Title: Classification of Synthetic Diamonds by using Fourier Transform Infrared Spectroscopy, Classification of Synthetic Diamonds by Using Fourier Transform Infrared Spectroscopy



Name: Elena Gambini
Address: INNOVHUB SSI- CIGEM Laboratory, Milan, Italy
Post Code: 30 20149 Tel: +39 02 8515 5325 Fax: +39 02 8515 5258
Email: elena.gambini@mi.camcom.it
Title: More on Photoluminescence of Emeralds



Name: Gagan Choudhary
Address: Gem Testing Laboratory, Jaipur, India
Post Code: 302003 Tel: +911412568221 Fax:
Email: gagan@gjpcindia.com
Title: Emeralds from Jharkhand, India

List of Presenters



Name: Hiroshi Kitawaki
Address: Central Gem Laboratory, Tokyo, Japan
Post Code: 110-0005 Tel: +81-35817-4664 Fax: +81-35817-4665
Email: kitawaki@cgl.co.jp
Title: Peculiar Natural Type II Diamonds Showing Pseudo-Synthetic Characteristics



Name: Huong Le
Address: Faculty of Geology, VNU University of Science, Hanoi, Vietnam
Post Code: 10000 Tel: +008 4912 201 167 Fax:
Email: leth@vnu.edu.vn
Title: Chemical and Spectroscopic Study of Zircon from Dak Lak, Central Highlands of Vietnam



Name: Hyeonki Kim
Address: Hanyang Univ/Advanced Gemology, Advanced Materials & Chemical Engineering, Seoul, Republic of Korea
Post Code: 133-791 Tel: +82-2-776-2288 Fax: +82-2-752-9824
Email: k10547@nate.com
Title: Characteristics of the Weyama Diamond from Weyama Gbapolu Country, Liberia



Name: Janyaporn Witthayarat
Address: Chiang Mai University, Lampang, Thailand
Post Code: 52000 Tel: +6686-3752709 Fax:
Email: dana_mul@hotmail.com
Title: Crystal Chemistry of Coloration in Chrysoberyl



Name: Jayshree Panjekar
Address: PANGEMTECH- Panjekar Gem Research & Tech Institute, Pune, India
Post Code: 411001 Tel: +919822286288 Fax: +912026059359
Email: jayshreepanjekar@gmail.com
Title: Aquamarine from Karur, Tamil Nadu India

List of Presenters



Name: John Chapman
Address: Rio Tinto Diamonds, Perth, Western Australia, Australia
Post Code: 6000 Tel: +61 489 6133 Fax:
Email: John.chapman@riotinto.com
Title: Diamond Exploration, Mining and Processing



Name: Jongwan Park
Address: Division of Materials Science & Engineering, Hanyang University, Seoul, Republic of Korea
Post Code: 133-791 Tel: +82-2-2220-0386 Fax: +82-2-2298-2850
Email: jwpark@hanyang.ac.kr
Title: Electron-Beam Irradiation and Heat Treatment of Corundum from New Deposits of Krong Nang District, Dark Lak Province, Vietnam



Name: Kanyarat Kwansirikul
Address: Department of Geological Sciences, Faculty of Science, Chiang Mai University, Chiang Mai, Thailand
Post Code: 50200 Tel: 053 943417-9 EXT.331 Fax:
Email: kanyarat.k@cmu.ac.th
Title: Gemological Characteristics of Rhodolite Garnet from Madagascar



Name: Karl Schmetzer
Address: DPMA, Petershausen, Germany
Post Code: 85238 Tel: +4981377770 Fax:
Email: SchmetzerKarl@hotmail.com
Title: Rubies, Sapphires and Quartzes with Double Stars



Name: Kennedy Ho
Address: AIGS Laboratory, Bangkok, Thailand
Post Code: 10500 Tel: Fax:
Email: info@aigsthailand.com
Title: Myanmar- The Past, Present and Future

List of Presenters



Name: Kento Emori
Address: Central Gem Laboratory, Tokyo, Japan
Post Code: 110-0005 Tel: +81-35817-4664 Fax: +81-35817-4665
Email: emori@cgl.co.jp
Title: Gemological Characteristics of Rhodolite Garnet from Madagascar



Name: Krit Won-in
Address: Department of Earth Sciences, Faculty of Science, Kasetsart University, Bangkok, Thailand
Post Code: 10900 Tel: +662-562-5555 ext 1422 Fax:
Email: kritwonin@yahoo.com, fscikrit@ku.ac.th
Title: Geomorphological Study at Ban Bo Kaeo Sapphire Deposit, Den Chai District, Phrae Province, Northern Thailand



Name: Laura M. Otter
Address: Department of Geosciences and Earth System Science Research Centre, Johannes Gutenberg-University, Mainz, Germany
Post Code: D-55128 Tel: +016098552777 Fax:
Email: ottelaur@students.uni-mainz.de
Title: High Resolution Computed Microtomography: Insights into a Hollow Beaded Cultured Pearl



Name: Lore Kiefert
Address: Gubelin Gem Lab, Luzern, Switzerland
Post Code: 6006 Tel: +41 41 4291537 Fax: +41 41 429 1734
Email: lore.kiefert@gubelingemlab.com
Title: New Opal from Ethiopia



Name: Majken D. Poulsen
Address: Geological Survey of Denmark and Greenland (GEUS), Nuuk Office c/o the Greenland Institute for Natural Resources, Nuuk, Greenland
Post Code: 3900 Tel: +00299361221 Fax:
Email: madp@geus.dk
Title: Comparison on the Geochemical Methods for Fingerprinting of Greenlandic Gem-Corundum (Rubies)

List of Presenters



Name: Martin Steinbach
Address: AG; FGG, Idar-Orberstein, Germany
Post Code: D-55743 Tel: +0049-6781-509942 Fax: +0049-6781-569627
Email: gstargems@aol.com
Title: The Stars Fall from Heaven: Gems with Asterism: An update



Name: Miro F. Y. Ng
Address: The Hong Kong Institute of Gemmology, Central, Hong Kong
Post Code: Tel: (+852) 2815 1880 Fax: (+852) 2854 3970
Email: miro.ng@gmail.com
Title: Application of Cathodoluminescent Technique on Fei Cui (Jadeite Jade) Research



Name: Muzdareefah Thudsanapbunya
Address: Department of Earth Sciences, Faculty of Science, Kasetsart University, Bangkok, Thailand
Post Code: 10900 Tel: Fax:
Email: muzdareefah.t@gmail.com
Title: Surface Morphology of Untreated and Irradiated Diamond Samples



Name: Myungji Ye
Address: Division of Materials Science & Engineering, Hanyang University Seoul, Republic of Korea
Post Code: 133-791 Tel: +82-2-2220-0386 Fax: +82-2-2298-2850
Email: jwpark@hanyang.ac.kr, myungji.ye@hotmail.com
Title: Dynamic Korea, Dynamic Jewelry Design by Ye Myungji



Name: Nalin Narudeesombat
Address: The Gem and Jewelry Institute of Thailand (Public Organization), Bangkok, Thailand
Post Code: 10500 Tel: +662 634-4999 ext. 409 Fax: +662 634-4970
Email: nnalin@git.or.th
Title: Update on the Characteristics of Amber from Indonesia

List of Presenters



Name: Nantharat Bunnag
Address: Faculty of Gems, Burapha University, Chanthaburi, Thailand
Post Code: 22170 Tel: Fax:
Email: b_nantharat@yahoo.com
Title: Heat Treatment of Aquamarine



Name: Natthapong Monarumit
Address: Department of Earth Sciences, Faculty of Science, Kasetsart University, Bangkok, Thailand
Post Code: 10900 Tel: Fax:
Email: mu_earthsci.03@hotmail.com
Title: Applications of Mid- and Near Infrared Spectroscopy to Indicate Conditions of Heat Treatment in Synthetic Ruby Samples



Name: Nguyen Ngoc Khoi
Address: Hanoi University of Science, Hanoi, Vietnam
Post Code: 10000 Tel: +84 4 38585097 Fax: +84 4 38583061
Email: khoinn@vnu.edu.vn
Title: Introduction of the New Gem- Corundum Sources from Krong Nang District, Dak Lak Province, Vietnam



Name: Nirawat Thammajak
Address: Synchrotron Light Research Institute, NakhonRatchasima, Thailand
Post Code: 30000 Tel: +66 090-9235362 Fax: +66 044-217047
Email: n.thammajak@gmail.com
Title: Discovering Effect of Synchrotron Light Interaction on Color of Freshwater Cultured Pearls: A New Identification Technique for Gamma Irradiated Pearls, A Disclosure of Synchrotron Exotic Golden Pearls, and A High-Definition Golden Pattern Imprinting Process©



Name: Nutwatcharee Noirawee
Address: Department of Earth Sciences, Faculty of Science, Kasetsart University, Bangkok, Thailand
Post Code: 10900 Tel: Fax:
Email: fscisrd@sci.ku.ac.th
Title: Characteristic and Physical Properties of Freshwater Cultured Pearls from Kanchanaburi Province

List of Presenters



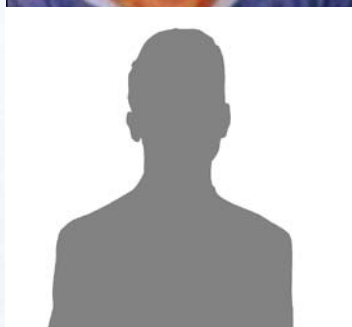
Name: Panjawan Thanasutthipitak
Address: Gemology program, Department of Geological Science, Chiang Mai University, Chiangmai, Thailand.
Post Code: 50200 Tel: 089-6352175 Fax:
Email: panjawan.t@cmu.ac.th
Title: Rusgems Synthetic Opal



Name: Park Minwoo
Address: Gemological Engineering, Hanyang University, Seoul, Republic of Korea
Post Code: 133-791 Tel: +82-10-31201315 Fax:
Email: yupgisun@naver.com
Title: Laminated Type Zirconia Ceramics



Name: Phisit Limtrakun
Address: Department of Geological Sciences, Faculty of Sciences, Chiang Mai University, Chiang Mai, Thailand
Post Code: 50200 Tel: +66-53-943417 Fax: +66-53-943444
Email: phisitlim@gmail.com
Title: Smoky Quartz from Hod, Chiang Mai, Northern Thailand



Name: Pongchan Chandayot
Address: Asian University, Banglamung, Chonburi, Thailand
Post Code: 20260 Tel: Fax:
Email:
Title: The GIT Standard Color Master Sets for 'Pigeon Blood' Ruby, 'Royal blue' and 'Cornflower blue' Sapphires



Name: Pornsawat Wathanakul
Address: The Gem and Jewelry Institute of Thailand (Public Organization), Bangkok, Thailand
Post Code: 10500 Tel: +66 2634 4999 Fax: +66 2634 4970
Email: pwathanakul2@gmail.com
Title: Phrae Sapphire Deposit Style

List of Presenters



Name: Rattanawalee Chooyoung
Address: Department of Earth Sciences, Faculty of Science, Kasetsart University, Bangkok, Thailand
Post Code: 10900 Tel: +66 2940 6966 Fax:
Email: rattanawalee.c@gmail.com
Title: Thermal Enhancement of Zircon Samples from Chanthaburi and Kanchanaburi Provinces, Thailand and Rattanakiri, Cambodia



Name: Richard W. Hughes
Address: Lotus Gemology Co. Ltd, Bangkok, Thailand
Post Code: 10500 Tel: +662 117 3616 Fax:
Email: richard@lotusgemology.com
Title: Forests and Trees: 10 Lessons in Gemology



Name: Roman Serov
Address: Gemological Center, Lomonosov Moscow State University, Moscow, Russia.
Post Code: 119992 Tel: +7-926-561-04-16 Fax:
Email: potom_skajy@mail.ru
Title: Russian Demantoid Color Heat Treatment



Name: Sandun Illangasinghe
Address: Gemmological Institute of Pelmadulla, Pelmadulla, Sri Lanka
Post Code: 70070 Tel: +00 71 8160 944 Fax:
Email: sillangasinghe@gmail.com
Title: Heat Treatment of Aquamarine



Name: Seriwat Saminpanya
Address: Department of General Science, Faculty of Science, Srinakharinwirot University, Bangkok, Thailand
Post Code: 10110 Tel: +66 2649 5000 ext 18668 Fax:
Email: seriwat@hotmail.com
Title: Ancient Glass Beads: A Gemstone of the Log Coffin Culture at Pang Mapha, Mae Hong Son, Thailand

List of Presenters



Name: Shane McClure
Address: GIA GTL, California, USA
Post Code: 92008 Tel: +911 412 568 221 Fax:
Email: smcclure@gia.edu
Title: Should Laboratories Make Clarity Enhancement Calls?
Controversy and Consequence



Name: Shigeru Akamatsu
Address: Central Gem Laboratory, Tokyo, Japan
Post Code: 110-0005 Tel: +813 3836 3219 Fax:
Email: s-akamatsu@mikimoto.net
Title: About Bead Nucleus Used for Pearl Culturing



Name: Siwon Lee
Address: Department of GEMOLOGICAL, Hanyang University, Seoul,
Republic of Korea
Post Code: 133-791 Tel: +82 10 8901 8944 Fax:
Email: ludia7788@gmail.com
Title: Raman Spectroscopic Identification of Geographical Origins of
Sapphires



Name: Somruedee Satitkune
Address: Department of Earth Sciences, Faculty of Science, Kasetsart
University, Bangkok, Thailand
Post Code: 10900 Tel: +66 84 674 4192 Fax: +662 579 3711
Email: somruedeesk@gmail.com, fscisrd@ku.ac.th
Title: Blue Sapphires from Ban Bo Keao and Ban Na Poon Deposits in
Phrae Province, Northern Thailand



Name: Sudarat Saeseaw
Address: GIA Research (Thailand), Bangkok, Thailand
Post Code: 10500 Tel: +66 2632 4090 Fax:
Email: ssaeseaw@gia.edu
Title: Three-phase Inclusions in Emerald and Their Impact on Origin
Determination

List of Presenters



Name: Sungjae Kim
Address: Department of Materials Science and Engineering, Hanyang University, Seoul, Republic of Korea
Post Code: 133-791 Tel: +82 10 3019 5297 Fax:
Email: sjk310700@gmail.com
Title: Aquamarine from the Gilgit Baltistan of Northern Areas, Pakistan



Name: Sungwon Park
Address: Division of Materials Science & Engineering, Hanyang University, Seoul, Republic of Korea
Post Code: 133-791 Tel: +82-2-2220-0386 Fax: +82-2-2298-2850
Email: sungwon96@naver.com
Title: Spectroscopic Characterization of Electron-Beam Irradiated Zircon



Name: Sunki Kim
Address: Hanmi Gemological Laboratory, Seoul, Republic of Korea
Post Code: 100-390 Tel: +82 2 3672 2800 Fax: +82 2 3672 2803
Email: skkimmy@hanmail.net
Title: New Treated Blue Sapphire by HPHT Apparatus



Name: Sutas Singbamroong
Address: Dubai Central Laboratory, Dubai Arab Emirates
Post Code: Tel: +971 4302 7300 Fax:
Email: sutas.singbamroong@gmail.com
Title: Building Consumer Confidence in Dubai Gem and Jewelry Industry



Name: Taijin Lu
Address: National Gems & Jewelry Technology Administrative Center (NGTC), Beijing, China
Post Code: 100013 Tel: +861058276120 Fax:
Email: lutj@ngtc.gov.cn
Title: Gemological Research Status on Jades in China



Name: Tasnara Sripoonjan
Address: The Gem and Jewelry Institute of Thailand (Public Organization), Bangkok, Thailand
Post Code: 10500 Tel: +66 2634 4999 Fax: +66 2634 4970
Email: stasnara@git.or.th
Title: Characteristics of Cyangugu Sapphire from Rwanda

List of Presenters



Name: Tay Thye Sun
Address: Far East Gemological Laboratory, Singapore
Post Code: 409958 Tel: Fax:
Email: tay@gem.com.sg
Title: Treated Black Diamond Earring



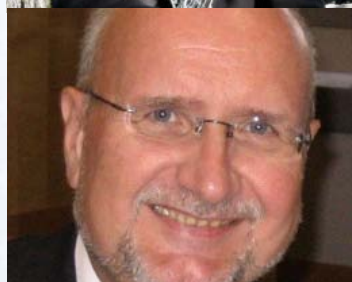
Name: Thanong Leelawatanasuk
Address: The Gem and Jewelry Institute of Thailand (Public Organization),
Bangkok, Thailand
Post Code: 10500 Tel: +66 2634 4999 Fax: +66 2634 4970
Email: lthanong@git.or.th
Title: Internal Features of Ruby from Various Localities in Madagascar



Name: Ursula Wehrmeister
Address: Department of Geosciences and Earth System Science Research
Centre, Johannes Gutenberg University, Mainz, Germany
Post Code: D-55128 Tel: +49 6131 3923170 Fax:
Email: wehrmeis@uni-mainz.de
Title: Non-Destructive Differentiation of African and Asian Ivory by
FT-Raman Spectroscopy and Chemometric Methods



Name: Weerapan Srichan
Address: Department of Geological Sciences, Faculty of Science, Chiang
Mai University, Chiangmai, Thailand
Post Code: 50200 Tel: +66-53-943417 Fax: +66-53-892261
Email: weerapan.s@cmu.ac.th
Title: Mineralogy of Blue Pectolite from the Dominican Republic



Name: Wolfgang Kuehn
Address: Gemlab Research & Technology, C/O Canadian Institute of
Gemmology, Vancouver, B.C., Canada
Post Code: V5k 5G6 Tel: +16 045 308 569 Fax:
Email: gemlab@cigem.ca
Title: Raman and Photoluminescence Spectroscopy in Gem Identification



Name: Wuyi Wang
Address: Gemological Institute of America, New York, Ny, Usa
Post Code: 10036 Tel: +1-917-286,3507 Fax:
Email: wwang@Gia.Edu
Title: Carbon Isotope and CI Analysis of Natural Type IIa and CVD
Synthetic Gem Diamonds

List of Presenters



Name: Yongkil Ahn
Address: Division Of Crafts Design, Kongju National University,
Chungnam, Republic Of Korea
Post Code: 314-701 Tel: +82-41-850-0382 Fax: +82-41-850-0389
Email: ykahna@gmail.com
Title: Mineralogical and Gemological Properties of Orange Johachidolite
from Northwest of Mogok, Myanmar



Name: Y Y Yang
Address: Its (Thailand) Co., Ltd., Bangkok, Thailand
Post Code: 10310 Tel: +66 (0) 2369 1793 Ext 22 Fax: +66 (0) 2369 1794
Email: info@its-thailand.com
Title: Micro-Raman Technology with Fast Imaging and Its Applications



Name: Kageeporn Wongpreedee
Address: Gems and Jewelry Program, Faculty of Science, Srinakharinwirot
University, Bangkok, Thailand
Post Code: 10110 Tel: +662-649-5630 Fax:
Email: kageeporn@gmail.com
Title: Preliminary Study on the Use of Lead Free Fire Assay for the
Determination of Gold Fineness



Name: JinheeJurn
Address: Department of Advanced Gemology, Hanyang University,
Seoul, Republic of Korea
Post Code: 133-791 Tel: +82-10-2045-2065 Fax:
Email: jinny006@naver.com
Title: Classification of Synthetic Diamonds by Using Fourier Transform
Infrared Spectroscopy



Name: Katrien De Corte
Address: HRD Antwep, Antwerp, Belgium
Post Code: 2018 Tel: +323-222-0705 Fax: +323-222-0704
Email: kdc@hrd.be
Title: From HPHT to LPHT Treatment of Type IIa Diamonds



Name: Sandun Illangasinghe
Institute/Company Name: Gemmological Institute of Pelmadulla
Address: ., Pelmadulla, Sri Lanka.
Post Code: 70070 Tel: +00 71 8160 944 Fax:
Email: sillangasinghe@gmail.com
Title: Heat Treatment of Aquamarine

Keynote's Address

The Role of AEC in Global Gem and Jewelry Market

Prida Tiasuwan

Chairman of Pranda Jewelry PCL.

The Association of Southeast Asian Nations (ASEAN) was established as a regional organization in 1967 to accelerate economic growth, promote regional peace and stability, and enhance cooperation on economic, social, cultural, technical, and educational matters among Southeast Asian countries. The five founding countries – Indonesia, Malaysia, Philippines, Singapore, and Thailand – were later joined by Brunei Darussalem (1984), Vietnam (1995), Laos (1997), Myanmar (1997) and Cambodia (1999). ASEAN has a goal of achieving full regional economic integration, known as AEC or ASEAN Economic Community, by 2015. The AEC, which creates ASEAN as a single market and production base, turns the diversity that characterizes the region into opportunities for business complementation and makes ASEAN a more dynamic and stronger segment of the global supply chain as well as an emerging market.

Among major economic powerhouses like United States and European countries, ASEAN is now recognized as a driver of global economic growth. In 2013, the combined population of ASEAN countries was about 616 million whereas the combined gross domestic product was US\$ 2.4 trillion.

By December 2015, the AEC will show a clearer picture of the situation on production and distribution within the region. As set in the AEC blueprint, AEC envisages the following key characteristics: (a) a single market and production base, (b) a highly competitive economic region, (c) a region of equitable economic development, and (d) a region fully integrated into the global economy. There will be free flow of goods, services, investment, skilled labor and freer capital flow. These will include tariff reductions and streamlining of certain administrative procedures so as to further facilitate the integration of ASEAN into a single market and production base as well as to enhance competitiveness.

At present, ASEAN countries have eliminated their import duties but still have some existing measures as trade barriers i.e. rule of origin that incurs additional cost and more procedures to businesses. Hopefully, non-tariff measures applied in ASEAN countries will be eased and removed within 10- 15 years after the launch of AEC in 2015, transforming ASEAN into a truly single market.

Moreover, ASEAN now takes further steps to establish the RCEP or Regional Comprehensive Economic Partnership. ASEAN has five free trade agreements with six dialogue partners, namely China, India, Japan, South Korea, Australia and New Zealand. Under RCEP scheme, ASEAN and the six dialogue partners will create a highly potential trading bloc, with a combined GDP of about US\$ 21.4 trillion and total population of 3,430 million. As a product in gem and jewelry category is covered in the Early Harvest Scheme under all five free trade agreements, gem and jewelry businesses can enjoy trade benefit from these agreements enhancing access to a huge potential market. We believe that both the AEC and the RCEP will certainly benefit to Thai gem and jewelry businesses.

Full name: PridaTiasuwan
Affiliation: Chairman, Pranda Jewelry Public Company Limited,
28 SoiBangna-Trad 28, Bangna-Trad Rd., Bangna, Bangkok, 10260, Thailand.
Email: prida@pranda.co.th

Keynote's Address

Past, Present and Future Prospects of World's Colored Stones

Jean Claude Michelou

Vice President ICA

The global gemstone and jewelry trade globally is showing intriguing characteristics when broken down into its constituent parts. While the European market is still somewhat slow, and China is striving to catch up with sales levels seen up to a couple of years ago, the United States is quite robust despite its economy still not managing to show a strong break out of a five-year slowdown.

Of most concern is, undoubtedly, the European market. Worries about the economy are rippling through Europe. Even Germany, the powerhouse economy of Europe, is seeing a fall in business confidence.

The Eurozone has shown zero growth for most of this year after a weak recovery from the economic crisis as a result of government debts and economic issues related to the Ukraine–Russia crisis.

After years of double-digit growth, China's economic growth is expected to be around 7.5 percent this year, falling to 7 percent in 2015. The government is moving to restructure the economy to stimulate local demand. Meanwhile, regulations against the giving of luxury items – considered as bribe-giving to win lucrative alliances, remain in force and have had an impact, in particular, on gemstone-set watches and other high-end jewelry items. Meanwhile, 2014 confirmed a rapid growth of middle class consumption of jewelry set with commercial gemstones.

U.S. jewelry sales in 2013, were revised downward to \$76.9 billion from \$79.2 billion. However, there have been average monthly rises for jewelry and watch retailers in the first half of 2014 of around 2 percent, based on preliminary US government figures.

Results from luxury and other retail jewelers show a solid performance. Tiffany & Co reported a 7 percent rise in revenue in its second fiscal quarter to almost \$1 billion. Sales across the Americas rose 9 percent year on year. And luxury group Richemont, whose units include Cartier and Van Cleef&Arpels, earlier this year, reported that sales rose 5 percent year on year. Sales in the Middle East and Africa rose 11 percent, and by 14 percent across the Americas while jumping 23 percent in Japan.

Although there are new gemstone sources in Africa, demand from the BRICs countries, as well as those in the ASEAN grouping, will surpass supply in the coming decade and beyond ensuring rising prices for gemstones.

We should be cautious in welcoming the moves, however, since the Mogok mines with their exquisite rubies, and closed for the past decade, are not being opened to foreign investors who could provide efficient and speedy development. Although there has been a headlong rush into the area, foreign miners and investors are not being given mining licenses since they are being limited to domestic firms.

The Myanmar regime would do well to look at what is happening in the world of rubies in order not to get left behind in a quickly developing world. The United States earlier this year extended its ban on the import of Burmese rubies for a further 12 months. Although China and India are increasing their purchases of rubies, the United States nonetheless remains the world's most important consumer market for rubies. Until human rights and business transparency are properly addressed, Myanmar can expect the ban to continue.

And in Africa, there is a new source of rubies, with Gemfields acquiring 75 percent of the Montepuez deposit in Mozambique, and saying that it expects the mine to eventually account for 20 percent of global supply. Early studies show that the quality of rubies is exceptional and comparable to the Burmese 'pigeon blood' rubies, says Gemfields. In contrast to the situation in Myanmar, Gemfields was awarded a 25-year mining license. What does that mean in practise? Critically for foreign investors, it brings stability and transparency, and for the Mozambique government, increased income, development of the area close to the mine and employment for locals.

Mozambique with its rubies and Zambia with its emerald assets, may be able to go some way to filling the void that has long existed since the supply of rubies and emeralds was largely limited to Myanmar and Colombia. They will help fill the gap by providing the stones to the global market.

Sourcing has become a key issue for all jewelry manufacturers and the upstream supply chain. Colored Stones, historically considered as secondary, and wrongly called Semi Precious stones, are in tremendous demand in China, the fastest growing jewelry market in the world. This is also the case for tourmaline of all kinds, with the strongest demand and unprecedented price increases being seen for pink and red tourmalines from their two major sources, Nigeria and Brazil.

The most important issue, sourcing, goes together with constant flow and reasonably steady production. Therefore mining has become crucial for the industry. Investing in colored gemstones mining has proven to be a sound business.

TanzaniteOne opened the way a decade ago; in recent years Gemfields has been proven right, with its successful move to emerald and ruby mining in Zambia and Mozambique. More recently junior listed Canadian company True North Gems has entered into ruby mining in Greenland.

Several Canadian venture capital mining companies have been reportedly looking for a breakthrough in emerald mining in Colombia, while a number of Chinese mining groups of investors have either entered the colored stones fields in Africa, or are also looking for mine buying opportunities both in Africa and South America.

Artisanal mining is still supplying the vast majority of colored stones to the market, while mechanized and industrial mining now accounts for 25% of total supply from just 10% previously and is expected to double in the next few years to eventually overtake artisanal mining within the next 10-15 years.

As geological exploration for gemstones and prospecting by mining companies increases, new deposits will be found in new areas, mostly in Africa and South America. And demand is likely to further outpace supply, thus pushing gemstone prices higher.



Keynote's Address



47 MAIN GEMSTONE SUPPLIER COUNTRIES



AFRICA	ASIA	AMERICAS	EUROPA	OCEANIA
<u>East Africa</u> Ethiopia Somalia Madagascar Kenya Uganda Tanzania Mozambique Zambia Zimbabwe Malawi Rwanda	<u>Central Asia</u> Congo Angola <u>West Africa</u> Nigeria Mali <u>South Africa</u> Namibia South Africa	<u>Central Asia</u> Afghanistan Tajikistan Kazakhstan Pakistan <u>Eastern Asia</u> China India Sri Lanka Burma Vietnam Thailand Cambodia	<u>Middle East</u> Iran Turkey <u>North America</u> USA Canada Greenland Mexico <u>Central America</u> Dominican Rep. Guatemala Honduras <u>South America</u> Colombia Brazil	<u>Czech Rep.</u> Russia Australia Uruguay Chile

Full name: Jean Claude Michelou
 Affiliation: Vice President, International Colored Gemstone Association (ICA).
 ICA Anchor, 62 West 47th Street, Suite 905, New York, NY 10036, USA.
 Email: claudiu@gemstone.org
 jcmichelou@gmail.com

Keynote's Address

Keynote's Address

Corporate Responsibility in the Gems and Jewelry Business: From Mine to Market

Burak Cakmak

Vice President, Corporate Responsibility, Swarovski

Swarovski designs, manufactures, and sells jewelry and high-quality crystal, genuine gemstones, created stones, and finished products such as accessories and lighting solutions. The company was founded in 1895 by Daniel Swarovski in the Austrian village of Wattens. His founding values included a deep sense of responsibility for his employees, nature and society at large. Over the years, Swarovski has strived to remain true to these values. However, in the 120 years since the company was founded, the world has become ever increasingly complex with unprecedented challenges faced in economic, social and environmental spheres. This is no less true for the gems and jewelry industry where growing consumer awareness adds to pressures from NGOs and regulators to ensure responsible business practices from mine to market. From traceability and transparency to respect for nature and society, there is progress to be made by the industry in order to safeguard our reputation in the eyes of all stakeholders.

As part of the gems and jewelry industry, Swarovski is very much aware of, and participating in, the industry's journey towards more responsible practices. We, like many large global companies, have formalized our approach to corporate responsibility in an effort to tackle these challenges head-on and live up to the expectations that we embrace as a company that is still 100% family owned. In my presentation, I briefly outline the company's history with special attention on our gems business as well as a particular focus on the founding values that inspire our corporate responsibility efforts today. I outline Swarovski's efforts to live up to these values through the development of a corporate responsibility strategy with six main focus areas. I put this in context by exploring the challenges – from mine to market – involved in coloured gems sourcing. At each stage of the process, I highlight current issues demanding the attention of the industry. These range from labour and human rights concerns during mining to trust and loyalty of our end consumers. I compare and contrast Swarovski's experience with the collective experience of the industry – drawing on examples of where we are actively engaged at the industry level as well as where, due to our unique circumstances, we have preferred to move at a different pace. Finally, I share my own thoughts on the way forward for corporate responsibility within the gems and jewelry industry.

The course we chart as an industry must be based on traceability and transparency as fundamental pillars supporting a framework that addresses: human rights, environment and illicit activity. The question of an international standard is one that requires breadth of consensus and depth of treatment for issues along the gems supply chain. But for this to happen, fundamental decisions need to be made. Main challenges will include determining who should be responsible and the best way to organise and implement an effective standard among all stakeholders involved in the coloured gems industry with the aim to address the real needs on the ground.

Full name: Burak Cakmak
Affiliation: Vice President, Corporate Responsibility, Swarovski
Email: burak.cakmak@swarovski.com

Keynote's Address

Jewelry Designs: Creativity in Action

Franco Pianegonda

CEO of Franco Pianegonda

It is a great honor and pleasure for me to meet all of you and to have this very rare opportunity to talk with you.

Creativity is the most profound motivation of our existence on Mother Earth. Many great thinkers have left messages for us on creativity over centuries. For me, the question is, "How can I be more creative in making contributions during my short time as a participant in the life of our world?"

My thoughts are modest because I am a self-made person from a family of farmers and am not an intellectual. I am an artisan who works with his hands. My hands express my heart. And my heart is always filled with respect for all persons and love for the gifts that Mother Nature gives every day to all her children, including all of us in this room.

I use my hands like a sculptor to take Nature's best materials and transform them into jewelry. I always hope that each of my jewels will become an intimate friend of the person who wears it. That is my goal in life.

I use my creativity for this purpose. I can only work to the best of my abilities. Therefore, I have one main obsession. That obsession is to learn all the time. I want to learn more and still more. I am convinced that I cannot give my best performance as a jewelry designer without trying to learn more all the time.

My guiding principle is a quotation from the great artist Leonardo da Vinci, who was born in Vinci near Florence, which is famous around the world for its art and sculpture. He said, "Simplicity is the ultimate sophistication."

I think this applies in particular to jewelry. This type of simplicity is what I always seek when I start my creative process to design jewelry or anything else.

I am an Italian from the Veneto region. The most famous city of our region is Venice. It has been a meeting place of all civilizations for centuries because it was a great port and center for trade with other countries. It is also full of art from all cultures and religions.

I work in a city called Vicenza, near Venice. For many centuries, my city has been the most famous center in Italy for the quality of its artisans. They are experts in making jewelry and other objects from gold, silver and precious stones.

We work in small laboratories. We use combinations of ancient and modern techniques of production. Therefore, we are not industrial. We do not make hundreds of thousands of pieces of anything. We make objects one by one, with love and dedication.

I felt very honored when I received the invitation from the organizers of this event to speak to all you about creativity. But I also felt worried. How can I explain to you in words such a profound and beautiful subject.

I am not very good at talking. I think with my heart and my instincts. Often, friends ask me why I made this design or that design. What was I feeling? What was I thinking?

I have to admit that I do not know the answers. I sometimes feel a little ashamed about this inability to explain. But my brain does not cooperate whenever I try to explain why I created something.

The best and only answer I can give all of you is that I think of the woman who will wear the jewelry. I admire a special type of woman. I make jewelry for her. Luckily, so far I have sold more than €150 million worth of jewelry over about 12 years.

That makes me happy because it proves that so many women enjoy my creations.

I am not capable of explaining to you why I create a specific piece of jewelry or why I create a specific design.

But I can explain **for whom** I create. Who inspires me to create, And, why each item of jewelry is like a piece of my heart given to the person who wears it.

I am inspired by a personality I call the "TOTAL WOMAN". She is a person who wants to be complete in every sense.

She wants it all. She wants to be an excellent mother and a great professional. She wants to be sensual and sexy but also very refined, very elegant and very chic.

She enjoys falling in love and she enjoys the gifts of life. But she is also a strong and responsible person who is capable of sacrifice and hard work.

I know that to many of you, my words may sound like the dreams of a teenage boy about his ideal woman.

You will have to forgive me. I cannot change my feelings. For me, a woman is more mysterious than a man. She is also profound and strong.

A woman-- any woman-- is like a like a ball of light emerging from the darkness of space. She has a universe **inside** her, which is full of surprises and mystery.

She can be kind but also violent. She can be beautiful but also have darker aspects in her character.

At the same time, each woman is surrounded by the universe **outside** her. She is a part of the universe.

This outer universe places many limitations on her because she is a woman. She is also unique because she can be a mother and that places responsibilities on her.

In addition, society, culture and religion place other limitations on her. Those limitations are often more difficult because of traditions in her community and family.

She lives with her inner universe and her outer universe. Both are very complex. Both can bring great happiness and also many difficulties.

In this complicated situation, I believe that jewelry can **make her shine**. It can be her friend, who never demands anything. Who never criticizes. Who never complains.

A jewel can make her happy, particularly if it suits her personality and allows her to feel good about herself.

I do not create jewels so that a woman can show off to other people or boast to her friends.

I create jewels so that she can enjoy **WHO** she is. Through the jewelry, I say to her, "Enjoy all you are"!

I feel proud and satisfied only if she feels happier because of my jewelry. I want her to feel more beautiful, *more* refined and more sensual.

I feel that I am creative only when she says, "These are my most loved jewels".

To tell you the truth, I do not know how that special type of creativity happens. I want her to love the jewels, just like she loves her family and friends.

But I do not know how I reach that point. I sit in front of a blank piece of paper. Then I fall into the world of my imagination. Suddenly, my heart moves and I draw a sketch.

Then I work on the sketch for days to transform it into a piece of jewelry. My friends help with computers and 3-D models. Eventually, over a period of months, the jewelry becomes real and the collections become real.

Then I try to find persons who will enjoy them and like to wear them.

After that, the sale happens because creating jewelry is also **a business** that employs many people.

Without sell out, and enough profit, the business cannot survive. It cannot continue. Many people lose their jobs.

Therefore, for me, creativity is also about finding new and innovative ways to reach the persons who enjoy my creations and are willing to pay for them so that I can continue the business.

In short, for me, creativity has **two main requirements**.

The first requirement for creativity is that we must know for **whom** we create. We must understand and appreciate that person.

We must be sincere. We should see the person in her totality.

We should not see her just as a neck, or finger, or wrist, or ears that we want to decorate with our jewelry.

We should see her together with the complexity of her life, in the place where she lives and the culture from which she comes.

Then we should use our best abilities to contribute to her happiness and good feelings about herself.

Of course, we can only contribute to her in our professional sector, and with the **skills** that we have.

We cannot give her an ocean of happiness and good feelings. But we can contribute pure and sincere drops for her ocean, according to our talents.

That is the best we can do. For me, that is **creativity**.

I believe that the only truly creative force on earth is Mother Nature. Each of us is her child.

In my capacity as Her child, I try every day to channel Her creativity through my heart and my hands.

My goal is to transfer some drops of Mother Nature's creativity to the women and men who enjoy my jewelry.

In that way, the cycle of my creativity becomes complete.

The second requirement for creativity is that we must take **great care of the business.** We must learn to innovate and accept new methods.

In this context, the biggest danger is refusing to change. It is good to be successful but it is also a great danger.

Sometimes, because of success we refuse to change. Instead, we think that we will succeed again by working much harder with the methods that brought success earlier.

That is wrong. We must change before change forces us to use different methods. By that time, the business becomes weak and making it successful becomes harder.

We must always be very vigilant and open-minded to learn new things. We must learn, learn and then learn again.

We are never good enough. We must always learn more because the market is always changing.

We must anticipate the changes and take action before the business becomes weak.

Another danger is to criticize persons who work in our business or complain that clients are not being loyal to us.

*In a business, we have to **earn** trust all the time. Continuously.*

If somebody inside the business is not giving the right performance, it is our job to coach and mentor that person.

However, even the best collaborators cannot make our business successful if the methods are out of date.

In other words, if the business model is out of date. It was effective in past but now it is not.

Now the market has changed. The world has changed. Therefore, the old business model is out of date. We must change our methods.

We should not remain stuck to our opinions.

Leonardo da Vinci also said, **"The greatest deception men suffer is from their own opinions."** His words are still true. Refusing to change opinions quickly enough is dangerous for a business, especially a small enterprise.

Our success depends on the success of our clients. They will not pay on time, if they are not able to sell out our jewelry quickly enough. That will make their business weak.

Then, they will no longer buy from us.

Therefore, innovation done **quickly** and **on time** is vital for a small or medium-sized enterprise. We are not rich enough to establish brand names by spending millions on publicity and marketing.

Our strength must come from *better **services** delivered more **quickly*** to clients. Those services must be relevant for the client. They should help his business and they should not take too much of his time.

In the current globalized economy, changes happen very fast because knowledge and information are travelling instantly, in real time, across all distances and across all cultures. There are no barriers anymore.

Languages are not a problem. No customer is isolated.

She can buy anything from anywhere in the world. She has more choices than ever before in history.

She can pay in minutes, and the products will be delivered to her home in a few days.

If we sell jewelry through retail stores and boutiques, we must remember that our **clients** have many more choices. They have many more suppliers.

Loyalty does not mean the same thing as in the past. We have to earn the trust of our clients again, and again.

Each client is operating a business of his own. His business cannot stand still because we are slow to change our methods. We must innovate fast enough to meet the new desires of the customers of our clients.

Therefore, we must have **detailed** knowledge about our client's business, particularly the profile of his customers.

We cannot help a client to succeed in his business if we do not know enough about his working methods and his customers.

Currently, there are many tools to obtain knowledge about our clients and to provide support very quickly for the sellout of our products through his business.

The main tool is digital networking and software improve relationships with clients.

We can even conduct digital marketing on behalf of a retail client who sells our products. We can build social media and web communication networks to tie the client into our own digital and web marketing systems.

Such services deliver real and concrete benefits to the client's own business. At the same time, they raise awareness about our products sold in the client's store.

They help to bring our business closer to the client and his customers. In this way, the client will remain with us in both good and bad times because our digital marketing efforts will include the needs of his business.

In summary, for me, creativity requires deep knowledge about the persons for whom you are creating.

It also requires the ability to adopt new methods of business without hanging on to past opinions and ideas.

That includes finding new ways to provide useful services for retail clients, to continue earning their trust and loyalty.

I hope some of you found these ideas to be interesting.

I thank all of you for your attention.

Full name: Franco Pianegonda
Affiliation: CEO of Franco Pianegonda
HEAD OFFICE; MorellatoS.p.A. Via Commerciale, 29 35010 Fratte di Santa
Giustina in Colle (PD), Italy.
Phone: +39 049 9323780
Email: sofia.marinelli@pianegonda.com
info@francopianegonda.com

Keynote's Address

Developing at 10,000 Pieces of Jewelry per Hour

Thomas Nyborg

Senior Vice President, Pandora Group Manufacturing

Affordable Luxury: What Pandora has learned about people, quality and agility from delivering more than 80 million pieces of jewellery per year from Thailand to the World.

From the start as a small traditional jewelry store in Denmark just over 30 years ago, to its current position as one of the world's largest jewelry brands, PANDORA has undergone a dramatic transformation.

In 2008, shortly after selling a majority stake in his company to private equity partner Axcel, the company's founder Danish goldsmith Per Enevoldsen selected Thomas Nyborg to lead the company's manufacturing operations in Thailand.

Though Thomas Nyborg had extensive experience from working in Thailand's gem and jewelry industry since the late 1980's, the challenges of ensuring that PANDORA's factory could support the explosive growth, the brand witnessed, required drawing on best practices not commonly used in the gem and jewelry industry.

In his presentation, Thomas will explain how the company has addressed the need for rapid, large-scale staff development, for systems and standardized processes, in addition to also meeting the corporate governance requirements expected of a NASDAQ-listed company, during a time where the manufacturing team has 6-doubled to its current level of 7,800 people at the company's manufacturing facilities in Gemopolis in Bangkok, Thailand.

Thomas will explain how PANDORA defines and manages quality, what the 4Cs means at PANDORA, as well as what terms like SQDC, PDCA, PPM, PMS, ILP, 4M and R&I stand for.

Earlier this year, the team's efforts and achievements were recognized by JNA Jewellery News Asia's "2014 Employer of the Year"-award, with PANDORA being elected winner among 91 international jewellery companies competing for this award.

ABOUT PANDORA

PANDORA designs, manufactures and markets hand-finished and modern jewellery made from genuine materials at affordable prices. PANDORA jewellery is sold in more than 80 countries on six continents through approximately 9,800 points of sale, including more than 1,300 Concept stores.

Founded in 1982 and headquartered in Copenhagen, Denmark, PANDORA employs over 11,000 people worldwide of whom approximately 7,800 are located in Gemopolis, Thailand, where the company manufactures its jewellery.

PANDORA is publicly listed on the NASDAQ OMX Copenhagen stock exchange in Denmark. In 2013, PANDORA's total revenue was DKK 9.0 billion (approximately EUR 1.2 billion). For more information, please visit www.pandoragroup.com.

Full name: Thomas Nyborg
Affiliation: Senior Vice President, Pandora Group Manufacturing,
Pandora Production Co., Ltd., Gemopolis, Bangkok, Thailand.
Email: thn@pandora.net

Keynote's Address

Raman Micro-Spectroscopy of Diamond

Lutz Nasdala

Institut für Mineralogie und Kristallographie, Universität Wien, Althanstr. 14, A-1090 Wien, Austria

The analysis of diamond requires the application of truly non-destructive techniques. Separating natural from synthetic stones, unravelling potential colour-enhancement procedures, or getting provenance information, are analytical objectives that need to be addressed without any damage or change of the valuable specimen. For this reason, light-spectroscopy methods are used extensively in studying diamond. First of all, infrared absorption spectroscopy is used to detect defects that determine the Type of diamond (Breeding and Shigley, 2009). Second of all, optical absorption and luminescence spectroscopy reveal optically active defects whose detection provides a wealth of information on the natural or synthetic origin stones and their treatment (Collins, 2001; Hainschwang *et al.*, 2014). Raman spectroscopy is in contrast used more rarely in the diamond community (except from the simple identification of diamond as such). In this plenary lecture, some modern applications of confocal Raman spectroscopy and hyperspectral mapping are summarized.

Due to this mineral's high lattice symmetry, the first-order Raman spectrum of diamond possesses only one main band near $\sim 1332 \text{ cm}^{-1}$ (Solin and Ramdas 1970). This band has a narrow FWHM (full width at band half-maximum) of $\sim 1.6 \text{ cm}^{-1}$. It is assigned to a triply degenerate optical phonon, consisting of longitudinal and transversal atomic movements (hence described as LO=TO phonon). The detection of this band in Raman spectra allows one to quickly identify diamond, or even minute amounts of diamond within geological samples. The latter are however not necessarily due to naturally formed microdiamond but may alternatively be caused by minute amounts of abrasives (Dobrzhinetskaya *et al.*, 2014).

Under conditions of elevated pressures or compressive stress, the diamond LO=TO phonon broadens appreciably, accompanied by notable band up-shift which has been well calibrated (Hanfland *et al.*, 1985). Confocal micro-analysis of diamond adjacent to inclusions hence provides an indirect but nevertheless precise in-situ measure of the stress acting on solid inclusions within the diamond (Nasdala *et al.*, 2003; 2005). Such compressive stress is also referred to as fossilised pressure, remnant pressure, or overpressure). It develops during uplift of the diamond from the mantle to the Earth's surface. Compressive stress is caused by heterogeneous volume expansion of the diamond-inclusion couples upon pressure release, provided the stress is not released through fracturing of the surrounding diamond. Near the ends of such fractures, notable dilative stress can be observed. Hyperspectral Raman mapping (Figure 1) allows one to evaluate quantitatively complex internal stress patterns within diamond crystals, i.e. to estimate both the strength and the lateral extension of stress haloes around inclusions. This is of interest in reconstructing the diamond genesis as well as for technical applications (such as the selection of stress-free diamonds for anvil cells).

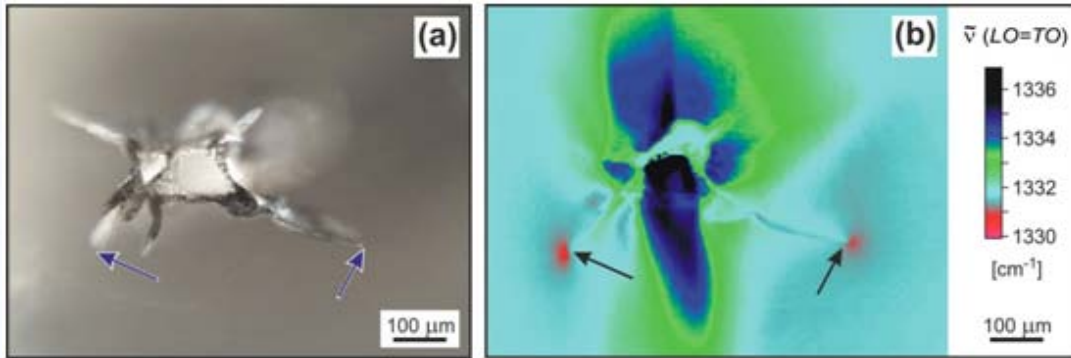


Figure 1: (a) Photomicrograph of a Ca-silicate inclusion in a diamond crystal from the Kankan district, Guinea). (b) Raman map, revealing compressive stress (up-shifted Raman band; blue-black color-coding) in non-fractures areas, and dilative stress (down-shifted Raman band; red color-coding) near the ends of two fractures (arrows). Images modified from Nasdala *et al.*, (2003).

Hyperspectral Raman mapping has also been applied successfully to unravel and visualize internal growth textures that are invisible under the optical microscope (Figure 2). Growth zones within diamond crystals are characterized by slight differences in the FWHM (full width at band half-maximum) of the **LO=TO** phonon (Nasdala *et al.*, 2005). These minor variations may be due to non-uniform concentrations of trace elements and structural defects. Hyperspectral Raman maps revealing the zoning are of particular importance as the visualization of textural relationship of inclusions and growth zones may for instance help to assign inclusions as either protogenetic (Figure 2), syngenetic, or epigenetic.

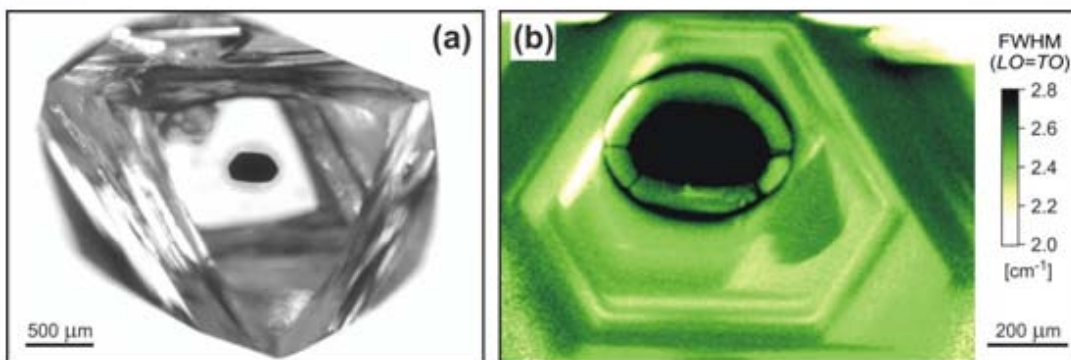


Figure 2: (a) Photomicrograph of a diamond crystal from the Panda kimberlite, Ekati mines, showing a large graphite inclusion surrounded by a small disc-like, ellipsoidal fracture in the diamond (light grayish color). View along the [111] axis. (b) Raman map revealing that the diamond's growth starts from the graphite inclusion. This implies that graphite must have been the primary phase and was overgrown by diamond. The growth zoning is overprinted by a pattern (black) of intense stress in the diamond host, close to the graphite crystal and right outside the ellipsoidal fracture. Images modified from Nasdala *et al.*, (2005).

Another example for the application to Raman combined with other light-spectroscopy techniques is the study of surficial, green or brown stains at the surface of rough stones. Green radiocoloration is caused by the impact of alpha radiation emanating from radioactive substances (i.e. minerals or fluids) located in direct contact with, or in close proximity to, the diamond surface.

The green color is controlled by a broad absorption band near ~ 620 nm wavelength, assigned to the GR1 centre (neutral vacancy). It turns orange-brown after heating to temperature of a few hundred degrees Celsius (Vance and Milledge, 1972). The color change is caused by the destruction of the GR1 absorption, due to trapping of vacancies at A defects (nitrogen pairs) to form the H3 center ($N-V-N$)⁰. Intensely colored centers of spots were found to represent elevated levels of structural irradiation damage, with FWHMs of the LO=TO band exceeding 20 cm^{-1} (Nasdala *et al.*, 2013). Also, Raman analyses showed that the temperature-induced green-to-brown color change is connected with only minor structural reconstitution. Comparative Raman analyses of natural radiohaloes and diamond irradiated with MeV helium ions helped to estimate defect densities in the former. It was concluded that the formation of intense radiocoloration stains may have required irradiation over long periods of time, presumably hundreds of millions of years in many cases (Nasdala *et al.*, 2013).

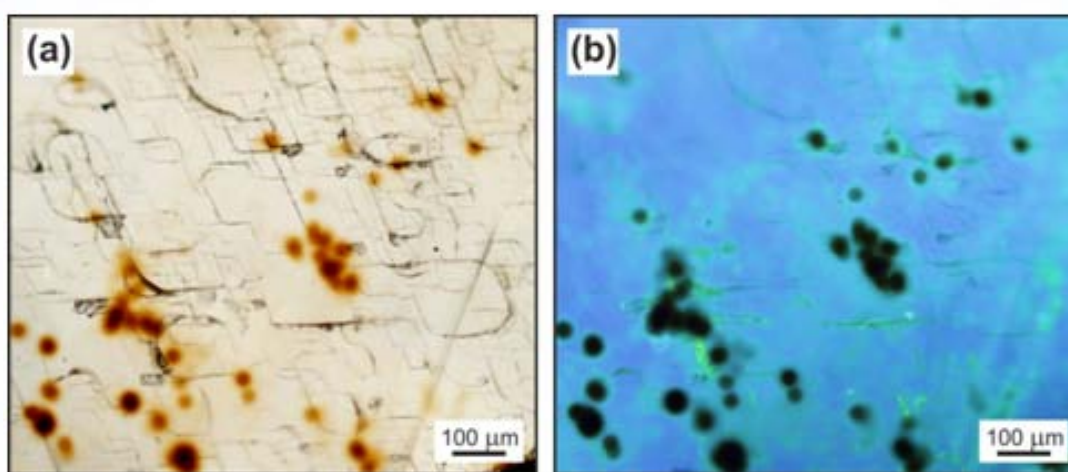


Figure 3: Pair of photomicrographs of the surface of a rough diamond from Namaqualand, R.S.A., with numerous orange-brown radiocoloration spots. Images were obtained in transmitted white-light **(a)** and under long-wave ultraviolet light **(b)**. Mildly radiation-damaged areas show enhanced luminescence, which is mainly due to the yellowish green emission of the H3 defect center. Strongly radiation-damaged areas show generally depleted photoluminescence.

Information on a diamond's origin and its post-growth history can be obtained by the in situ identification and characterization of micrometer-sized inclusions inside the stone (Nasdala *et al.*, 2003). For instance, the discovery of serpentinisation of olivine inclusions in diamond may indicate a "wet" alteration history. Another example was published just recently by Pearson *et al.*, (2014) who reported the first discovery of terrestrial ringwoodite included in a diamond from Juína, Brazil. The presence of ringwoodite (a high-pressure polymorph of olivine that is stable in the Earth's lower transition zone, between ca. 520 and 660 kilometers depth) characterizes that Juína sample as super-deep in origin. Last but not least, the identification of "man-made inclusions", that is, highly refracting organics used to fill drill holes and fractures (Kiefert *et al.*, 2000), bears important information for the trade.

References

- Breeding, C.M., and Shigley, J.E., 2009, The "Type" classification system of diamonds and its importance in gemology, *Gems & Gemology*, Vol.45, No.2, p.96-111.
- Collins, A.T., 2001, The colour of diamond and how it may be changed, *Journal of Gemmology*, Vol.27, No.6, p.341-359.
- Dobrzhinetskaya, L., Wirth, R., and Green, H., 2014, Diamonds in Earth's oldest zircons from Jack Hills conglomerate, Australia, are contamination, *Earth and Planetary Science Letters*, Vol.387, p.212-218.
- Hainschwang, T., Karampelas, S., Fritsch, E., and Notari, F., 2013, Luminescence spectroscopy and microscopy applied to study gem materials: a case study of C centre containing diamonds, *Mineralogy and Petrology*, Vol.107, No.3, p.393-413.
- Hanfland, M., Syassen, K., Fahy, S., Louie, S.G., and Cohen, M.L., 1985, Pressure dependence of the first-order Raman mode in diamond, *Physical Review B*, Vol.31, p.6896-6899.
- Kiefert, L., Haenni, H.A., and Chalain, J.-P., 2000, Identification of gemstone treatments with Raman spectroscopy, in *Proceedings of SPIE, The International Society for Optical Engineering*, Vol.4098, p.241-251.
- Nasdala, L., Brenker, F.E., Glinnemann, J., Hofmeister, W., Gasparik, T., Harris, J.W., Stachel, T., and Reese, I., 2003, Spectroscopic 2D-tomography: Residual pressure and strain around mineral inclusions in diamonds, *European Journal of Mineralogy*, Vol.15, No.6, p.931-935.
- Nasdala, L., Hofmeister, W., Harris, J.W., and Glinnemann, J., 2005, Growth zoning and strain patterns inside diamond crystals as revealed by Raman maps, *American Mineralogist*, Vol.90, No.4, p.745-748.
- Nasdala, L., Grambole, D., Wildner, M., Gigler, A.M., Hainschwang, T., Zaitsev, A.M., Harris, J.W., Milledge, J., Schulze, D.J., Hofmeister, W., and Balmer, W.A., 2013, Radio-colouration of diamond: a spectroscopic study, *Contributions to Mineralogy and Petrology*, Vol. 165, No.5, p.843-861.
- Pearson, D.G., Brenker, F.E., Nestola, F., McNeill, J., Nasdala, L., Hutchison, M.T., Matveev, S., Mather, K., Silversmit, G., Schmitz, S., Vekemans, B., and Vincze, L., 2014, Hydrous mantle transition zone indicated by ringwoodite included within diamond, *Nature*, Vol.507, No.7491, p.221-224.
- Solin, S.A., and Ramdas, A.K., 1970, Raman spectrum of diamond, *Physical Review B*, Vol.1, No.4, p.1687-1698.
- Vance, E.R., and Milledge, H.J., 1972, Natural and laboratory α -particle irradiation of diamond, *Mineralogical Magazine*, Vol.38, No.299, p.878-881.

Full name: Lutz Nasdala

Affiliation: Institut für Mineralogie und Kristallographie, Universität Wien, Althanstr.
14, A-1090 Wien, Austria.

Email: lutz.nasdala@univie.ac.at

Diamond Exploration, Mining and Processing

John Chapman

Rio Tinto Diamonds, Perth, Western Australia

Extended Abstract

Diamond is notorious for its hardness and to a lesser extent its high refractive index (2.42), but other physical characteristics feature in the journey of the cubic-structured crystal from the depths of Earth to a polishing wheel.

The diamond industry is worth near \$10 billion annually and comprises extractions from either a primary deposit of an ancient volcano or from a volcano's eroded state of gravels in a stream or seabed – producing alluvial diamonds. Alluvial diamonds were first recognised more than 3000 years ago, and the first primary deposit was not identified until 150 years ago in South Africa. The location of primary deposits is limited to those regions where the crust is thick enough to provide the temperature and pressure regimes necessary for diamond growth, some 3 billion years ago.

Locating diamonds deposits is achieved on the ground by stream sampling and from the air using magnetic or gravity surveys to detect anomalies. Kimberlite indicator minerals are formed in similar conditions to diamond, they are more abundant than diamonds so their presence during sampling is used as a key indicator for diamond deposits.

Mining takes the form of open pit extraction initially progressing to underground operations when the economics justify the expensive infrastructure. For example the recently completed Argyle underground operation comprising 40 km of tunnels and a development cost of over \$2b. A combination of trucks and conveyors deliver ore to a recovery plant in which the first operation is to crush the rocks to release diamonds within. One of the challenges to optimise the upper crushing size based on the expected frequency of occurrence and gem value.



Figure 1: The Diavik diamond mine in Canada was initially underwater. A dyke allowed open pit working and currently it is being mined underground.

The concentration of diamonds in commercial mines is typically less than 1 carat per tonne of ore and the objective of the recovery operation is to separate diamonds from ore. The mineral's specific gravity of $3.52 \text{ g}^{\text{cm}^{-3}}$ contrasts with most rocks sufficiently to employ density separation methods to produce a concentrate containing diamonds. These methods include pans, pressure jigs and most commonly for larger operations – cyclone separators. This concentrate is normally presented to either a surface of grease to which diamond sticks or presented to x-rays to which they fluoresce. However the fluorescence of some non-diamond minerals and the low-fluorescence of some diamond types have led to more recent methods using Raman luminescence and x-ray transmission. A more complex system using gamma rays is being researched to detect diamonds within rocks.

The recovery operation is completed after chemical cleaning using caustic and acidic chemicals to remove surface contaminants and residual non-diamond minerals followed by sieving into size classifications. Further sorting of each stone into categories based on their size, colour, shape and clarity prepares the diamonds for sale after which they start their journey to become a sparkling faceted gem.

Corresponding Author

Full name: John Chapman
Affiliation: Rio Tinto Diamonds, Perth, Western Australia.
Phone: +61 4896133
Email: John.chapman@riotinto.com

Geomorphological Study at Ban Bo Kaew Sapphire Deposit, Den Chai District, Phrae Province, Northern Thailand

Krit Won-in, Somruedee Satitkune, Padon Tangulrat, and Thitiporn Kaewlungka

Department of Earth Sciences, Faculty of Science, Kasetsart University, Bangkok, 10900, Thailand

Extended Abstract

Den Chai-Wangchin area is the most important blue sapphire deposit in Northern Thailand. The origin of Denchai sapphire is closely associated with the CO₂-rich alkaline basaltic magmatism (Limtrakun *et al.*, 2002). This research focuses on the geomorphology of the sapphire area to support the future exploration of this sapphire deposit. The investigated area is located in Ban Bo Kaew, Sai Yoi subdistrict, Den Chai district, Phrae province, northern Thailand, 480 kilometers away from Bangkok. This area is a small mountain basin with an area of 25 square Kilometer. The Huai Mae Sung river to the west acts as a boundary.

The geology of this area was studied by Department of Mineral Resource (DMR) in 1999 (Figure 1). The eastern and western parts of this study area are Triassic sedimentary rocks that consist of mudstone, shale, siltstone, sandstone and conglomerate. The Permo-Triassic volcanic rocks are found in the northeastern area. The Cenozoic basalt has flowed over and now covers the old topographic in the central area (Ban Bo Kaew investigation area). Barr and Macdonald (1981) classified the Phrae basaltic units into seven flows of magmas, and the age of the uppermost basaltic flow was dated by K/Ar technique to be 5.64±0.28 Ma.

Figure 1: Geological map of Ban Bo Kaew (modified from DMR, 1999).

The geomorphology in Ban Bo Kaeo can be divided into 3 landform units as High land unit, Eluvium unit and Alluvium unit (Figure 2). The High land unit is the mountainous area, 500-750 meters above the mean sea level. The Eluvium unit (Figure 3) covers the area resulting from the in situ weathering of the basaltic rocks that overly most of the study area. The Alluvium unit (Figure 4) is located along the stream/river and composed of the young sediments, such as gravel, sand, silt and clay. The gem sapphires are found as eluvial deposits in the Eluvial unit and as placer deposits in the Alluvial unit. The sapphires are of various shades from light to dark blue (Figure 5).

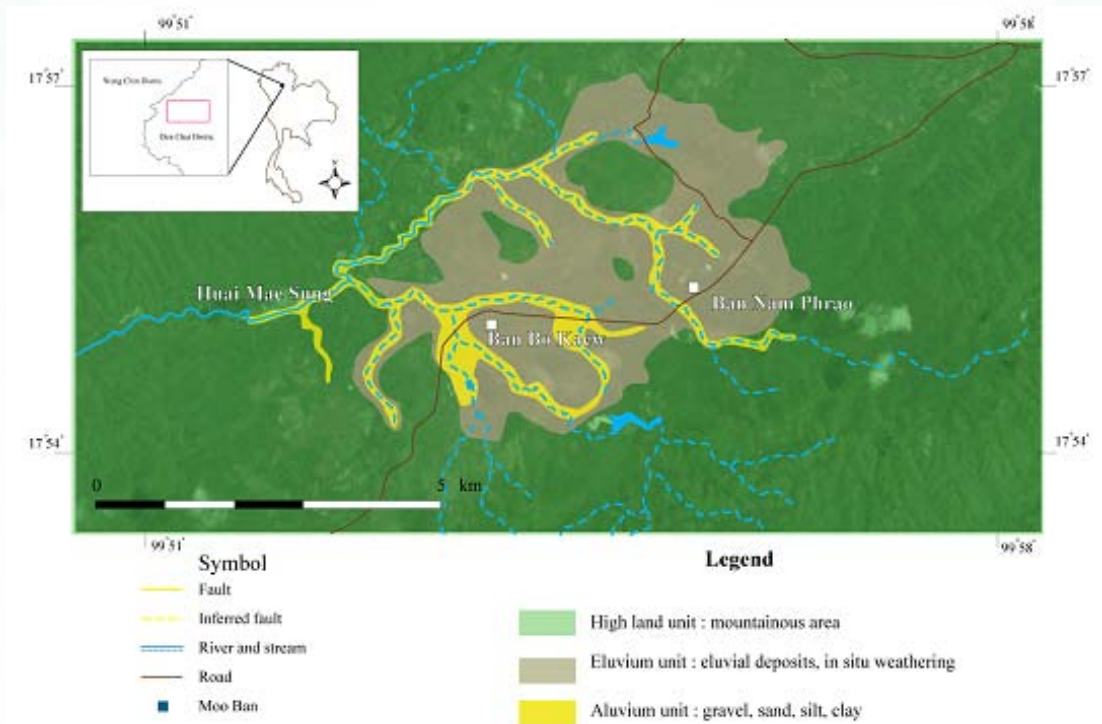


Figure 2: Geomorphological map of Ban Bo Kaeo study area.



Figure 3: Test pit in the Eluvium unit (17° 54' 29.36"N, 99° 53' 39.47"E).



Figure 4: The Quaternary section of fluvial deposit in the Alluvium unit.



Figure 5: Blue sapphire samples from Ban Bo Kaeo area

Acknowledgements

The authors are very grateful to Assist. Prof. Dr. Pornsawat Wathanakul, the director of The Gem and Jewelry Institute of Thailand (GIT), for the support and consultant and Dr. Panu Trivej for editing.

References

- Barr, S.M. and Macdonald, A.S., 1981, Geochemistry and geochronology of late Cenozoic basalts of Southeast Asia, Geological Survey of America Bulletin, Part II, Vol.92, p.1069-1142.
- Department of Mineral Resources, 1999, Geological map of Ban Bao Kaew Sheet 4944 I (1:50,000). Geological Survey Division, Department of Mineral Resources, Thailand.
- Limtrakun, P., Zaw, K., Ryan, C.G., and Mernagh, T.P., 2001, Formation of Denchai gem Formation of the Denchai gem sapphires, northern Thailand: evidence from mineral chemistry and fluid/melt inclusion characteristics, Mineralogical Magazine, Vol.65, No.6, p. 725-735.

Corresponding Author

Full name: Krit Won-in
Affiliation: Department of Earth Sciences, Faculty of Science, Kasetsart University, 50 Ngamwongwan Road, Chatuchak, Bangkok, 10900, Thailand.
Phone: +662-562-5555 ext 1422
Email: kritwonin@yahoo.com, fscikrit@ku.ac.th

Internal Features of Ruby from Various Localities in Madagascar

Thanong Leelawatanasuk¹, Tasnara Sripoonjan¹, Nataya Nilhud¹,
Wilawan Atichat¹ and Visut Pisutha-arnond^{1,2}

¹The Gem and Jewelry Institute of Thailand (Public Organization), Bangkok, 10500, Thailand

²Department of Geology, Faculty of Science, Chulalongkorn University, 10330, Thailand

Introduction

Madagascar is one of the world famous sources of various gemstones such as sapphire, ruby, emerald, alexandrite, tourmaline, garnet, etc. In the last decade, ruby has been reportedly found in many localities in Madagascar, for examples, Vatomaniry, Andilamena and Antsirabe. Vatomaniry deposit is located in Atsinanana Region, eastern Madagascar (Figure 1) (Modified Spaltenstein and Semenova, 2014: Online). Andilamena deposit is located in a part of Alaotra-Mangoro Region, northeast of Madagascar (Pardieu, 2012). Both Vatomaniry and Andilamena deposits are the famous sources that were first discovered in September and October 2000, respectively. Ruby from these two areas has been produced since 2002. The Antsirabe deposit was discovered in 2005 (Hughes *et al.*, 2014: Online). Ruby deposits from all three areas are mainly of secondary in origin.



Figure 1: Location map of the ruby deposits in Madagascar where the rough stones were used in this study.



Figure 2: Ruby samples from Vatomandry (**bottom right**), Andilamena (**top center**) and Antsirabe (**bottom left**) in Madagascar. Photo by T. Sripoonjan.

Materials and Methods

Three batches of naturally-occurring ruby roughs from Vatomandry, Andilamena and Antsirabe deposits in Madagascar (Figure 2) were used in this study. Most of the samples show smooth water-worn surface, indicating that the original crystals were probably eroded and transported from the primary sources. Some representative samples from each locality were slab-cut and polished for microscopic investigation, micro-photography and Raman spectroscopic analysis. The inclusions in those samples were firstly observed by using standard gemological microscope and later were identified by Laser Raman Spectroscope (Renishaw inVia Model). The system was equipped with Leica microscope DM2500M having objectives lens from 10 to 50 times magnification that could allow the confocal Raman spectral measurement to be better than 2.5 μm depth resolution. All Raman spectra were collected with green laser 532 nm.

Result

Ruby from Vatomandry

Ruby from this deposit contains mainly of rounded isolate (some cluster) of subhedral colorless crystal inclusions together with silk-like inclusions and some brown crystals. The Raman spectroscopic analysis proved that the majority of the colorless crystals are mostly zircon, minor apatite and monazite. The brown crystal was identified as rutile. Besides, several splendid elongate platy inclusions were also identified as mica. Typically, zircon inclusions appear as shiny, relatively high birefringence and round-shaped crystals (Figure 3). Its structure may partly or completely damage and turn into amorphous states (metamictization) due to self-radiation (α -decay) of U and Th that are commonly present as trace constituents. Rutile inclusions formed as black-to-dark-brown or bright-reddish-orange crystals, sometimes appear as cone shape (Figure 4). Other form of rutile also occurs as thinly short-to-long needles (known as rutile silks; Figure 5). Apatite was found as euhedral crystals with polygonal shape (Figure 6). Other inclusions occasionally present are unknown rounded crystals, negative crystals, mica, boehmite needles and monazite (Figures 7 and 8).

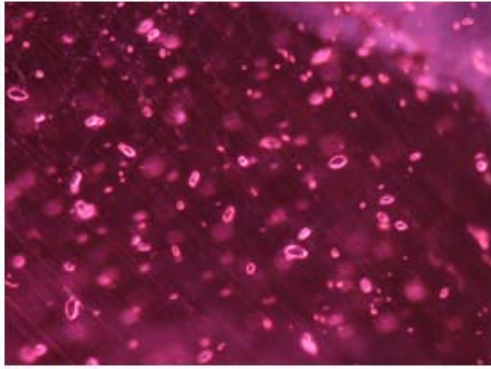


Figure 3: Abundant zircon inclusions occurring as transparent, high birefringence, shiny, round-shaped crystals in ruby from Vatomandry. Photomicrograph by T. Sripoonjan; magnified 40X



Figure 4: Dark-brown, cone-shaped crystals of rutile inclusions in Vatomandry ruby. Photomicrograph by T. Sripoonjan; magnified 30X



Figure 5: Brilliant colors of very finely short rutile silks in Vatomandry ruby. Photomicrograph by T. Sripoonjan; magnified 15X

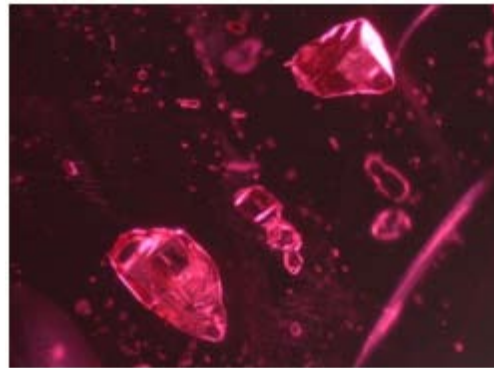


Figure 6: The polygonal crystals of apatite inclusions in Vatomandry ruby. Photomicrograph by T. Sripoonjan; magnified 30X

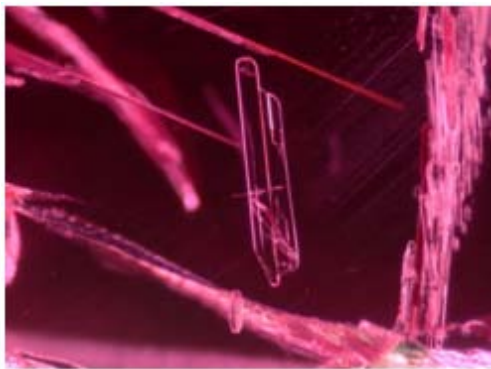


Figure 7: Transparent tabular crystals of mica inclusion in ruby from Vatomandry. Photomicrographs by T. Sripoonjan; magnified 25X

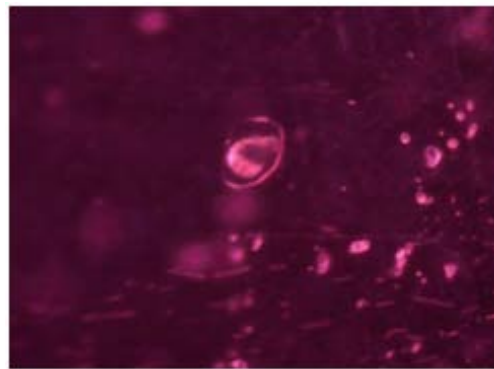


Figure 8: An isolated monazite inclusion associated with zircon clusters in Vatomandry ruby. Photomicrographs by T. Sripoonjan; magnified 40X

Ruby from Andilamena

Ruby from this deposit contains numerous inclusions inside. The most abundant one is hexagonal-shaped apatite present as isolated crystals and group of crystals (Figure 9). Apatite crystals commonly occur with zircon and rutile inclusions. Furthermore, short rutile needles are usually associated with cloud, fingerprint, mica and iron-stain (Figure 10).

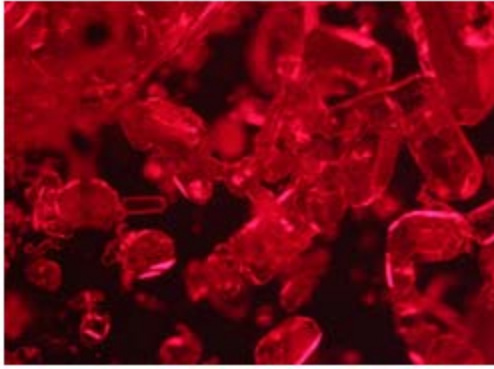


Figure 9: Well-shaped apatite inclusions occurred as individual crystal and group of crystals in ruby from Andilamena. Photomicrograph by N. Nilhud; magnified 30X

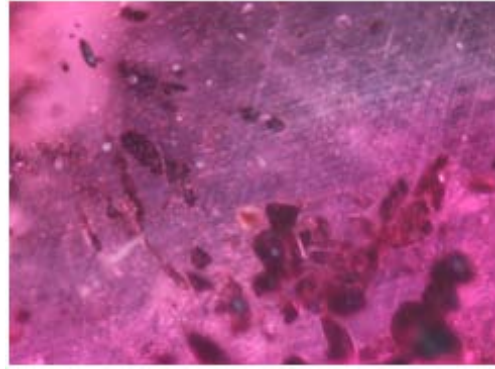


Figure 10: Subhedral crystals of brown-to-black rutile inclusion associated with short rutile needles and cloud in Andilamena ruby. Photomicrograph by N. Nilhud; magnified 30X

Ruby from Antsirabe

The Antsirabe ruby seems to show the internal features that are quite similar to those found in the Andilamena stones (Figure 11). However, zircon inclusions in Antsirabe samples are apparently differed from the other source in the way that they usually occur as smaller crystals or crystal aggregate, commonly known as “zircon cluster” similar to those found in pink sapphire from Ilakaka. Furthermore, this ruby also shows the distinctive characteristic of short and long boehmite needles intersecting in three-directions along rhombohedral planes (Figure 12). Other internal features that were occasionally found are rutile inclusions, iron-stain, milky cloud, fingerprint, fractures and, surprisingly, a rare quartz inclusion (Figures 13-14).

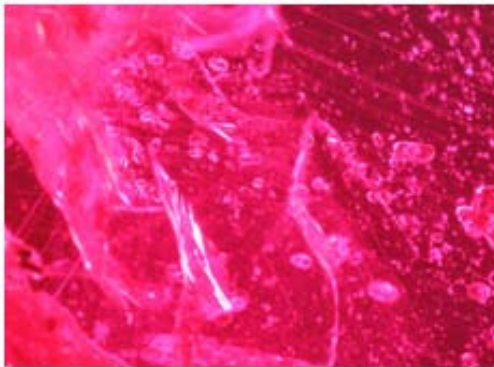


Figure 11: Small group of idiomorphous apatite crystals (middle right) associated with needles and zircon clusters (smaller inclusions in background) in ruby from Antsirabe. Photomicrograph by N. Nilhud; magnified 30X

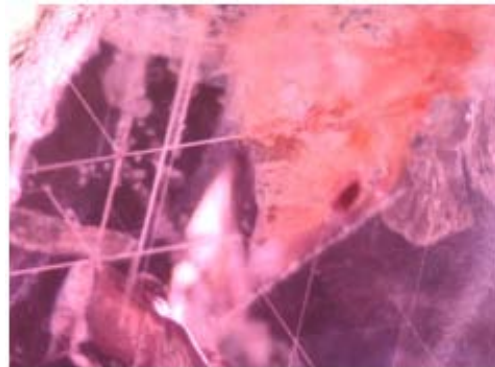


Figure 12: Boehmite needles oriented in three directions along rhombohedral planes in Antsirabe ruby. Photomicrograph by N. Nilhud; magnified 25X

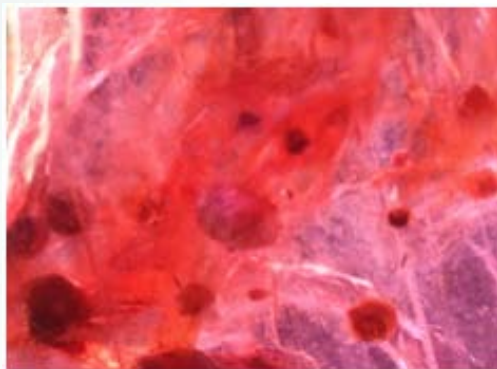


Figure 13: Rounded red-brown inclusions, dust-like particles along with iron-strain in Antsirabe ruby. Photomicrograph by N. Nilhud; magnified 25X



Figure 14: A quartz inclusion (confirmed by Raman Spectroscopy shown in Figure 15) rarely found in ruby from Antsirabe. Photomicrograph by N. Nilhud; magnified 40X

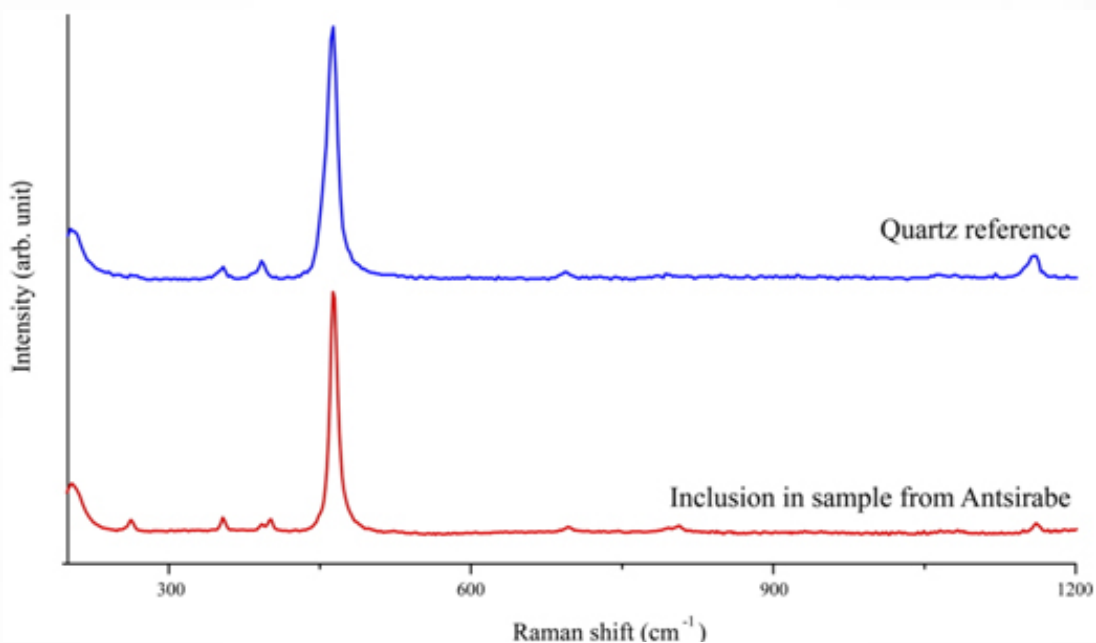


Figure 15 : Raman spectrum of a rarely found quartz inclusion

Discussion and Conclusion

While ruby can occur in differing rock types under various geological environments that could reflect by different inclusion assemblages hosted in ruby samples. However, the inclusion assemblages in ruby samples from these three localities in Madagascar appear to show many similarities. As such geological condition of ruby formation in these three localities could possibly be fairly similar. Nevertheless, subtle differences in the shape and abundance of those inclusions are noticeable from one locality to the others (Table 1). Vatomandry stones contain abundantly round-isolated zircon inclusions as its distinct characteristic with some rutile and monazite crystals. While the Andilamena samples usually contain well-formed apatite crystals with lesser amount of zircon and rutile. The ruby from Antsirabe contains mineral inclusion similar to those from Andilamena, but it also contains a rare quartz inclusion, including boehmite. Rutile silks seem to be common in all localities.

Table 1 : Mineral inclusions and their abundance in ruby samples from three localities

Inclusions Deposits	Zircon	Apatite	Rutile	Monazite	Mica	Quartz
<u>Vatomandry</u>	xxx	xx	xxx	x	xx	-
<u>Andilamena</u>	xx	xxx	xx	-	xx	-
<u>Antsirabe</u>	xx	xx	xx	-	-	x
xxx: commonly found xx: occasionally found x: rarely found -:not found						

Acknowledgements

We are thankful to CWS Gems for providing samples. This study was supported by the GIT. All the analyses were carried out at the GIT Gem Testing Laboratory.

References

- Andriamarofahatra, J., de la Boisse, H. and Nicollet, C., 1990, Datation U-Pb sur monazites et zircons du dernier Episode tectonométamorphique granulitique majeur dans le Sud-Est de Madagascar, Comptes Rendus de J Académicit des Science .Vol 310 p.1643-1648
- Besairie, H., 1964, Carte géologique de Madagascar: Antananarivo, Service Géologique de Madagascar, scale: 1:1,000,000, color (3 sheets).
- Hughes, R., Pardieu, V., and Schorr, D. 2014, Sorcerers & Sapphires: A Visit to Madagascar, Ruby-sapphire, Available from: http://www.ruby-sapphire.com/madagascar_ruby_sapphire.html [2014, October 28]
- Paquette, J.L., Nédelec, A., Moine, B. and Rakotondrazafy, M., 1993, U-Pb single zircon Pb evaporation and Sm-Nd dating of the SE Madagascar domain: a prevailing Pan-African event, Terra Abstract, Vol.5, p.393.
- Rakotondrazafy, A.F.M., Giuliani, G., Ohnenstetter, D., Fallick, A.E., Rakotosamizanany, S., Andriamamonjy, A., Razanatseheno, M., Offant, Y., Garnier, V., Maluski, H., Dunaigre, C., Schwarz, D., and Ratrimo, V., 2008, Gem corundum deposits of Madagascar: A review, Ore Geology Reviews, Vol.34, p.134-154.
- Pardieu, V., and Rakotosaona, N., 2012, Ruby and sapphire rush near Didy, Madagascar, GIA: On going research. Available from http://www.giathai.net/pdf/Didy_Madagascar_TH.pdf.
- Spaltenstein, W., and Semenova, J., 2014, Multicolor, Available from: <http://www.multicolour.com/columns/mguide/column122001L.html> Wang, W., Scarratt, K., Emmett, J.L., Breeding, C.M. and Douthit, T.R., 2006, The Effects of Heat Treatment on Zircon Inclusions in Madagascar Sapphires, Gems & Gemology. Vol.42, No.2, p.134-150.

Corresponding Author

Full name : Thanong Leelawatanasuk
Affiliation : The Gem and Jewelry Institute of Thailand (Public Organization)
140, 140/1-3, 140/5 ITF Tower building. 1st- 4th and 6th Floor,
Silom Road, Suriyawong, Bangrak, Bangkok. 10500, Thailand.
Phone: +66 2634 4999 Fax: +66 2634 4970
Email : lthanong@git.or.th

Mineralogy and Petrology of the An Phu Marble Hosted Spinel and Corundum Deposit, Luc Yen, N-Vietnam

Christoph A. Hauzenberger¹, Carina Bagola¹, Tobias Haeger², Christian Muellen², Nguyen Ngoc Khoi^{3,4}, and Le Thi-Thu Huong^{3,5}

¹Karl-Franzens-University of Graz, A – 8010, Graz, Austria

²Johannes Gutenberg-University of Mainz, D55099, Mainz, Germany

³Hanoi University of Science, 334 Nguyen Trai, Thanh Xuan, Hanoi, Vietnam

⁴DOJI Gold & Gems Group, 44 Le Ngoc Han, Hai Bat Trung, Hanoi, Vietnam

⁵Department of Education, Vietnam National University, Hanoi, Vietnam

Extended Abstract

Ruby and spinel are commonly found in the northern part of Vietnam, especially in the Yen Bai area. Both minerals are typically found in marbles, but in different mineral paragenesis: (1) Corundum (ruby), brown amphibol, and phlogopite bearing calcite marbles, and (2) spinel, green amphibole ± forsterite ± clinohumite ± chlorite calcite-dolomite marbles. Here, we will report mineral chemistry and petrology of these two types of gem deposits from An Phu and surrounding areas, close to the city of Luc Yen, Yen Bai province.

Geological Setting

The northern part of Vietnam consists of a series of metamorphic and magmatic rocks, as well as sedimentary successions which are crosscut by the Cenozoic Ailao Shan – Red River shear zone. Around Yen Bai and Luc Yen, high grade metamorphic rocks are exposed within the shear zone. The mainly granulite facies rocks can be divided into two main units (1) the Day Nui Con Voi complex and (2) the adjoining Lo Gam zone. (Figure 1).

Both units consist mainly of mylonitic gneisses and schists with variable amounts of intercalated marbles and amphibolites. The investigated area of An Phu belongs to the Lo Gam zone, where marbles, partly silicate and oxide (corundum, spinel) bearing dominate. K/Ar, Ar/Ar, and U/Pb ages indicate a young age of metamorphism and deformation (80- 29 Ma) (Leloup *et al.* 1995).

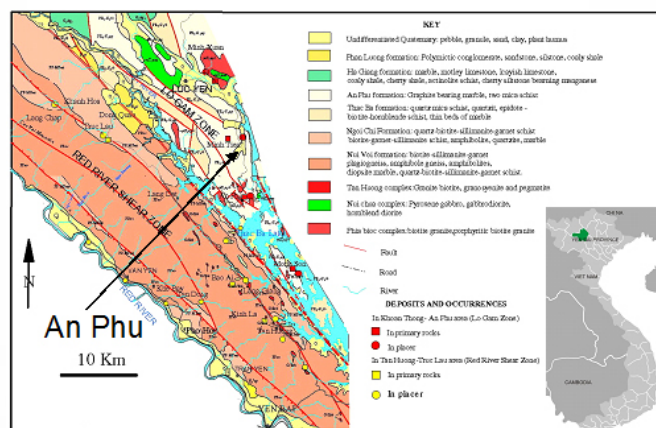


Figure 1: Schematic geological map of the Day Nui Con Voi and Lo Gam structural zones, which are part of the Ailao Shan- Red River shear zone.

Mineral Chemistry

The corundum bearing samples consist mainly of red corundum (ruby), amphibole, phlogopite, some sphene, and calcite (Figure 2). Sphene, phlogopite, and amphibole have significant amounts of fluorine in their crystal structure. Amphiboles have high Al_2O_3 (21.5- 22.3 wt.%), high alkalis (Na_2O 3 wt.%, K_2O around 1 wt.%) and high F (1.2- 1.5 wt.%) contents. They can be classified as aluminopargasites and aluminomagnesiosadanagaites. Nearly a quarter of phlogopite is replaced by its F- bearing variety (F content 1.85- 2.2 wt.%). Sphene has an Al_2O_3 content of 3.8 wt.% and F values of around 1.2 wt.%. Calcite contains about 1.3 wt.% MgO.

Spinel bearing samples comprise the mineral assemblage red to purple coloured spinel, forsterite, clinohumite, greenish amphibole, phlogopite, and chlorite (Figures 2, 3). Spinel contains only minor amounts of Cr_2O_3 (< 0.34 wt.%) and FeO (< 1.13 wt.%). Olivine is nearly pure endmember forsterite with FeO < 1 wt.% ($X_{\text{Mg}} > 0.99$). Clinohumite, amphibole, and chlorite have high F values. Clinohumite has TiO_2 values of 3.1- 3.6 wt.%, high F values of 2- 2.6 wt.% and $X_{\text{Mg}} > 0.99$. Amphiboles contain Al_2O_3 (11.9- 14.2 wt.%), high Na_2O (1.9- 2.4 wt.%) and high F (1.2- 1.5 wt.%) values. They are classified as pargasite, tschermakite, and magnesiohornblende.



Figure 2: (left) Corundum – pargasite/sadanagaite calcite marble. **(right)** Spinel- chromian pargasite calcite-dolomite marble.

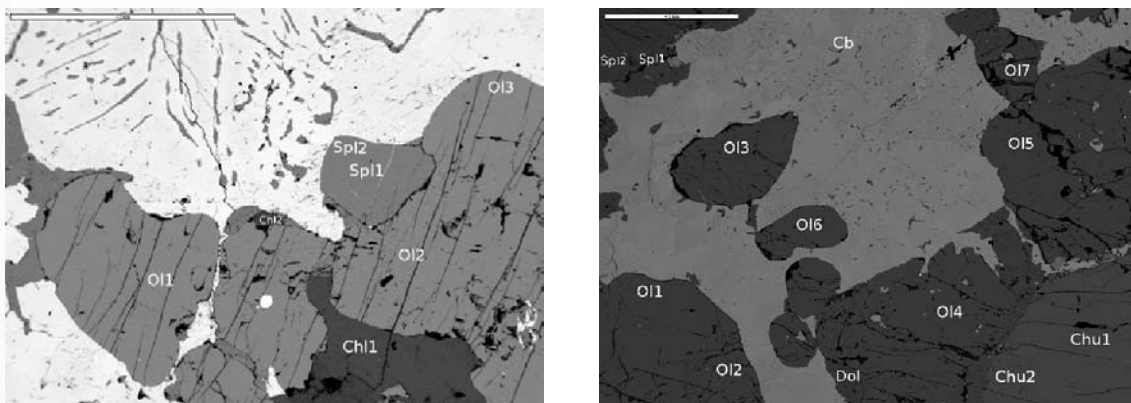


Figure 3: (left) BSE image of a forsterite (Ol) – spinel (Sp) – chlorite (Chl) marble. **(right)** BSE image of a forsterite (Ol) – clinohumite (Chu) – spinel (Spl) marble.

Petrology and P-T- X_{CO_2} Conditions of Metamorphism

The mineral rich spinel-clinohumite-pargasite-forsterite±chlorite-calcite-dolomite assemblages are well suited to estimate metamorphic T- X_{CO_2} conditions. The phase diagrams in

Figure 4 were calculated with the internally consistent thermodynamic database of Holland and Powell 1998 and updates. Activity corrections for solid solutions in minerals have been applied according to the activity models given by Holland and Powell 1998. The mineral assemblage clinohumite (Chum) - calcite (Cc) - forsterite (Fo) - dolomite (Dol) - spinel (Sp) represents peak metamorphic conditions. A minimum temperature of about 700°C is obtained from Figure 4. The composition of the involved fluid phase is constrained by the reaction $\text{Chum} + \text{Chl} = \text{Sp} + \text{Fo} + \text{H}_2\text{O}$ in sample AP1 (Figure 4, left) and $\text{Chum} + \text{Cc} + \text{CO}_2 = \text{Fo} + \text{Dol} + \text{H}_2\text{O}$ in sample V1 (Figure 4, right), which is found to be on the water rich fluid side of the diagrams ($X_{\text{CO}_2} < 0.3$ and 0.12, respectively). Corundum is not present in the dolomite bearing samples. During prograde metamorphism $\text{Cor} + \text{Dol}$ is replaced by $\text{Sp} + \text{Cc}$.

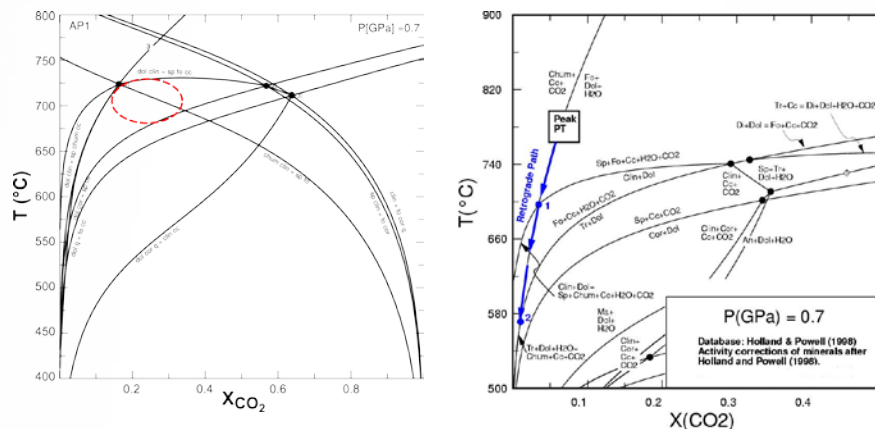


Figure 4: T- X_{CO_2} diagrams from two spinel-clinohumite-pargasite-chlinochlor-forsterite-calcite-dolomite marbles. Temperature can be estimated with 700-750 °C and mineral assemblages are only stable at water rich fluid composition. Pressure was estimated from a garnet-sillimanite metapelite which was collected nearby.

Acknowledgements

The support from ASEA-Uninet is gratefully acknowledged.

References

- Holland, T.J.B. and Powell, R., 1998, An internally consistent thermodynamic data set for phases of petrological interest, *Journal of Metamorphic Geology*, Vol.16, No.3, p.309-343. Leloup, P.H., Lacassin, R., Tapponier, P., Schärer, U., Zhong, D., Liu, X., Zhang, L., Ji, S., Phan Trong Trinh, 1995, The Ailao Shan-Red River shear zone (Yunnan, China), Tertiary transform boundary of Indochina, *Tectonophysics*, Vol.251, No.1-4, p.3-84.

Corresponding Author

Full name: Christoph A. Hauzenberger
Affiliation: Karl-Franzens-University of Graz, A – 8010, Graz, Austria.
Email: christoph.hauzenberger@uni-graz.at

Update on Opal from Pedro II, Piauí state, Brazil

Claudio C. Milisenda¹ and Jochen Knigge²

¹DSEF German Gem Lab, Prof.-Schlossmacher-Str. 1, D-55743 Idar-Oberstein, Germany

²Brasilopal, Andreasstr. 27, D-68623 Lampertheim, Germany

For many years, Brazil was the second largest producer of bright precious opal in the world. By far the most important deposits are located in the northeastern state of Piauí. More than 30 occurrences exist within a radius of 25 km surrounding the town Pedro II (“Pedro Segundo”), which is located approx. 220 km northeast of the state’s capital Teresina.

In this area the dominant rocks are sediments consisting of coarse- to fine-grained sandstones and claystones of the Mid-Devonian Cabeças Formation, which are cut by a series of quartz-dolerite dykes (Jobbins, 1980). Opal has been recovered both from secondary and primary deposits. At Boi Morto, by far the largest mine in the area, opal occurred in and around the contact between the dolerite and the sedimentary rocks.

Piauí has produced fine-quality bright precious opal similar to Australian material. The vast majority of the samples are translucent to semi-transparent and belong to the white or light opals (Figure 1). Some of the material has a very distinct, layered structure (Figure 2). Brazilian opals are known for their remarkable resistance against temperature changes and ultrasonic baths. This is most probably due to a relatively low water content (< 6 wt. %, e.g. de Brito Barreto and Bretas Bittar, 2010) compared to opals from other sources.

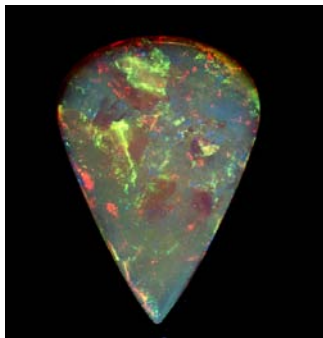


Figure 1: A 31 cts. precious opal from Pedro II, Piauí, Brazil. Photo by Konrad Götz, Starnberg, Germany.



Figure 2: A distinct, layered structure is obvious in this 4.7 grams rough opal from Pedro II, Piauí, Brazil. Photo by Boris Garaud, St. Etienne, France.

After a very productive period in the mid-1970s with an annual production of 10.000 to 30.000 kg, a second “rush” occurred at the Roça mine from around 1987 to 1992. Since then the opal production decreased and has been erratic. Nevertheless, between the mid-1990s and 2005, about 150 to 350 “garimpeiros” were working in Pedro II with hand tools and a couple of old diesel-engines (e.g. Knigge and Milisenda, 1997; de Brito Barreto and Bretas Bittar, 2010). Early in 2012 an interesting find was made in the Mamoeiro mine (Figure 3) about 5 km NW of Pedro II along the main road to Piripiri.



Figure 3: The Mamoeiro mine approx. 5 km NW of Pedro II.

That year the rainy season (which usually renders all mining activities impossible at the start of the year) came late. Hamilton, the owner of the mine borrowed some heavy machinery from the municipality that was not being used during the Carnival season. After the equipment was returned, they continued with hand digging and found the first opal. During three weeks of manual work, several pockets were discovered. Some of the stones reached spectacular sizes for precious opal, with the heaviest stone weighing 2,487 grams (Figure 4).



Figure 4: This high quality precious opal weighing 2,487 grams was discovered in 2012 in the Mamoeiro mine near Pedro II, Piauí, Brazil.

The total output of opal from that “Carneval-Bamburro” was estimated at around 50- 80 kilograms. Almost all of the material went into the local jewellery trade, because the price for bright precious opal on the international market declined after the huge opal finds in Ethiopia. Because of this, there is not a single organized mining operation taking place in Pedro II today. The handful of kilograms of precious opal still being produced per year are a product of sheer luck or leftovers from formerly successful mining sites. This is most deplorable, because Pedro II opal is supposedly the least “treatable” and most resistant i.e., stable of all known precious opals. After the achievements of altering the colour and appearance of Ethiopian opal, the determination of the provenance of opal have become more and more important.

References

- De Brito Barreto, S., and Bretas Bittar, S.M., 2010, The gemstone deposits of Brazil: occurrences, production and economic impact, *Boletín de la Sociedad Geológica Mexicana*, Vol.62, No.1, p.123-140.
- Jobbins, E.A., 1980, Opal in Piauí State, Brazil, *Zeitschrift der Deutschen Gemmologischen Gesellschaft*, Vol.29, No.1-2, p.40-54.
- Knigge, J., and Milisenda, C.C., 1997, Brazilian opals from Pedro II, *Zeitschrift der Deutschen Gemmologischen Gesellschaft*, Vol.46, No.2, p.99-105 (in German).

Corresponding Author

Full name: Claudio C. Milisenda
Affiliation: DSEF German Gem Lab, Prof.-Schlossmacher-Str. 1, D-55743 Idar-Oberstein, Germany.
Phone: +49-6781-50814
Email: info@gemcertificate.com

Applications of Mid- and Near Infrared Spectroscopy to Indicate Conditions of Heat Treatment in Synthetic Ruby Samples

***Natthapong Monarumit¹, Thanapong Lhuaamporn², Somruedee Satitkune¹,
Wiwat Wongkokua³, and Pornsawat Wathanakul²***

¹Gemmology and Mineral Sciences Special Research Unit, Department of Earth Sciences, Faculty of Science, Kasetsart University, Bangkok, 10900, Thailand

²The Gem and Jewelry Institute of Thailand (Public Organization), Bangkok, 10500, Thailand

³Department of Physics, Faculty of Science, Kasetsart University, Bangkok, 10900, Thailand

Extended Abstract

Introduction

Corundum undergone heating with beryllium (Be), Be atoms were believed to have caused structural defects in corundum structure (Wathanakul *et al.*, 2009). The beryllium atoms were not suggested to be located in the environment of Cr³⁺ ions proved by X-ray Absorption Spectroscopy (Monarumit *et al.*, 2012).

In the present time, synthetic ruby is widely used instead the natural one in gem product because of the natural ruby is very rare in gem market. There are the synthesize methods to produce synthetic ruby including Verneuil, Czochralski, floating zone, flux growth and hydrothermal processes. In this study, the synthetic ruby samples from Verneuil process were selected. The content of doped element impurities has been measured.

Mid Infrared (MIR) and Near Infrared (NIR) Spectroscopy were applied to study the identification of heat treatment conditions in synthetic ruby samples. In this work, the unheated, the conventional heating and heating with beryllium conditions were focused.

Samples and Methods

The synthetic ruby samples were used referring as Syn 30 and Syn 60 for containing approximately 3000 and 6000 ppm of Cr content, respectively, measured by LA-ICPMS. Both samples were cut into 3 pieces; one of them was kept as the reference as the unheated sample; the others were treated by traditional and Be heating methods shown in Figure 1.

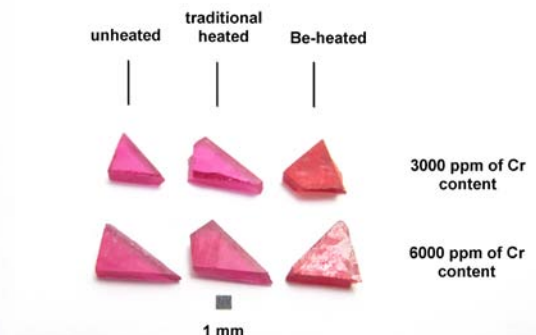


Figure 1: The synthetic ruby samples (**Syn 30 on the upper row, Syn 60 on the lower row**) were used in this study.

MIR and NIR measurements of the synthetic ruby samples were carried out in reflectance mode. MIR spectra were obtained at Department of Earth Sciences, Kasetsart University by using the Thermo Nicolet FT-IR spectrometer (Nexus 470). Unless, NIR spectra were measured at Department of Physics, Kasetsart University; using the Perkin Elmer FT-IR/FT-NIR spectrometer (Spectrum 400 model). This experiment was set to detect at 400-4000 cm^{-1} for MIR and 4100-10000 cm^{-1} for NIR region and it was taken five times per sample to obtain the precise spectrum.

Results and Discussions

The major trace elements content of synthetic ruby samples measured by LA-ICPMS is shown in Table 1.

Table 1: Chemical concentration (ppm) of synthetic ruby samples between unheated, traditional heated and Be-heated conditions.

Element	Sample					
	Syn 30 (unheated)	Syn 30 (traditional heated)	Syn 30 (Be-heated)	Syn 60 (unheated)	Syn 60 (traditional heated)	Syn 60 (Be-heated)
Be	0.92	1.19	15.65	0.96	0.98	15.71
Cr	3940.98	3539.22	3828.96	6646.02	6318.39	6396.53
Ti	11.44	9.14	11.47	28.28	23.59	23.42
Fe	15.59	19.05	57.73	12.24	16.54	18.74

The MIR spectra of unheated Verneuil synthetic ruby samples are different from the spectra of heated ones shown in Figure 2. The structural OH absorption peaks at 3309, 3237 and 3184 cm^{-1} were presented in unheated samples (also as in Volynets *et al.*, 1972), whereas they disappear when the samples were already undergone a conventional high temperature (at 1650 °C) heating; due to the metal-OH (-M-OH) bond were broken by heat (also as in Lhuaamporn, 2012), and the Be heating. The 3309 cm^{-1} peak would be related to-Ti-OH (Phlayrahan *et al.*, 2014), and Be would possibly catch up with most of Ti, deminishing the 3309 cm^{-1} peak accordingly.

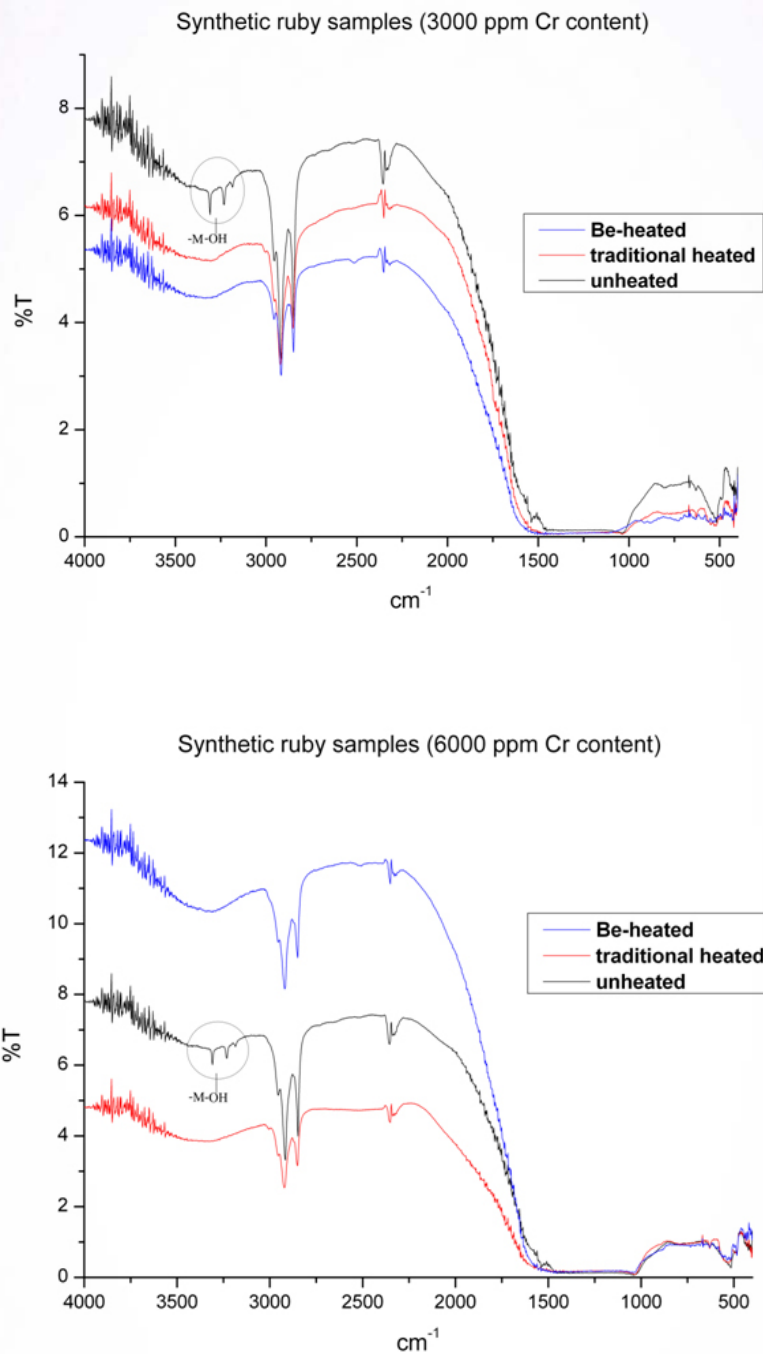


Figure 2: The MIR spectra of synthetic ruby samples at various condition (**above:** 3000 ppm of Cr content, **below:** 6000 ppm of Cr content).

The Figure 3 shows the NIR spectra of synthetic ruby samples at various conditions considered in both of the sample set (3000 ppm and 6000 ppm of Cr content). The NIR spectra of Be-heated synthetic ruby samples were different from unheated and traditional heated ones. The presence of 7700 cm⁻¹ on Be-heated samples were the distinctive absorption peak showing in NIR region, it could be suggested that this is the vibration mode of Be-O in corundum structure.

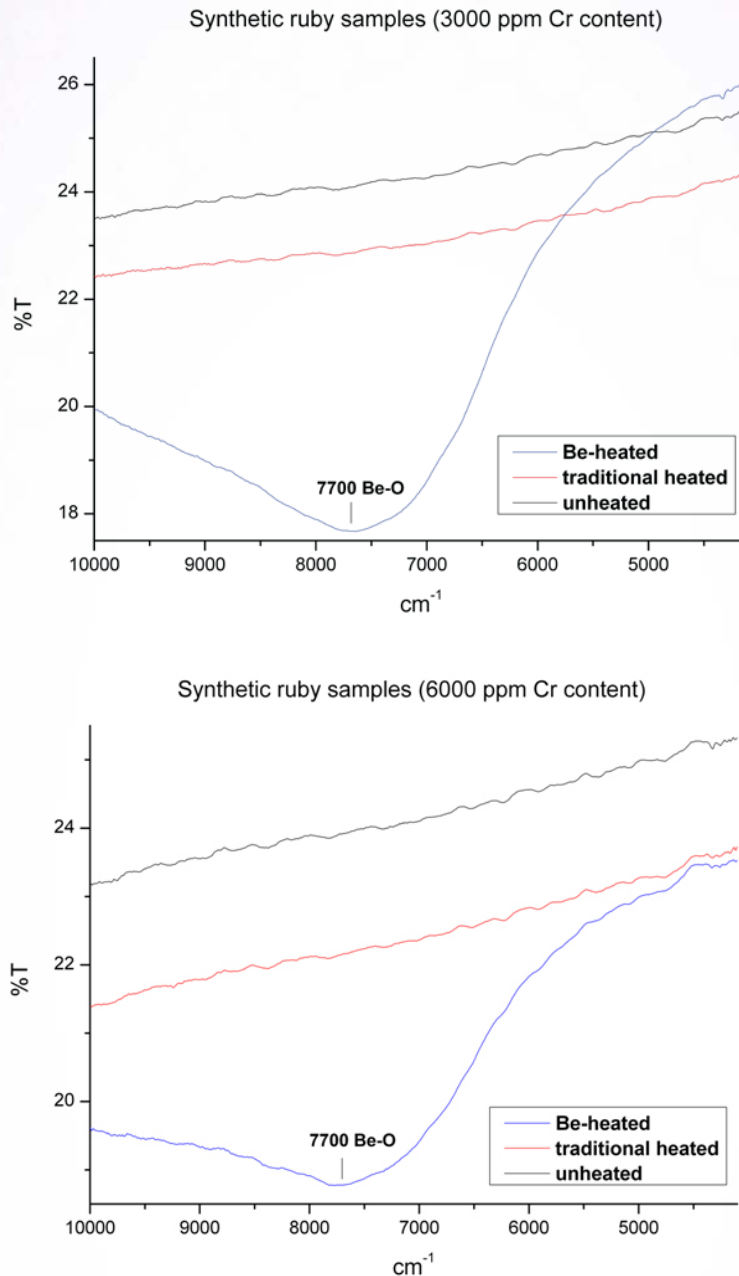


Figure 3: The NIR spectra of synthetic ruby samples at various condition (**above:** 3000 ppm of Cr content, **below:** 6000 ppm of Cr content).

Conclusions

The combination data from MIR and NIR spectroscopy can be used for identifying the synthetic ruby samples at various conditions; unheated, traditional heated and Be-heated. MIR spectra can widely give the information of heat treatment of samples and the unheated ones. Besides, NIR spectra (7700 cm⁻¹) can be used to indicate the samples undergone Be-heating. This technique is non-destructive and suitable for gemstone treatment identification. The experiments would lead to the applications in both natural ruby and sapphire samples.

Acknowledgements

The authors would like to appreciate the Department of Earth Sciences and Department of Physics, Faculty of Science, Kasetsart University for supporting the facility and the Gem and Jewelry Institute of Thailand (Public Organization) for research funding.

References

- Lhuaamporn, T., 2012, Atomic Force Microscopy of Synthetic Corundum before and after Annealing, M.S. Thesis, Kasetsart University.
- Monarumit, N., Wongkokua, W., and Wathanakul, P., 2012, Effect of Be on the Cr K-edge in Synthetic Ruby Samples, in Proceedings of the 3rd International Gem and Jewelry Conference (GIT 2012), p.175-178.
- Phlayrahan, A., Monarumit, N., Satitkune, S., and Wathanakul, P., 2014, If diaspore is responsible for the 3309 cm⁻¹ peak in the FTIR spectra of heated ruby sample, GIT 2014 submission.
- Volynets, F.K., Vorobev, V.G., and Sidorova, E.A., 1972, Infrared Absorption Bands in Corundum Crystals, Journal of Applied Spectroscopy, Vol.10, No.6, p.665-667.
- Wathanakul, P., Wongkokua, W., and Pongkrapan, S., 2009, XAS study on Cr³⁺ local environment in ruby samples, in abstracts of the 19th annual V. M. Goldschmidt conference, p.A1421.

Corresponding Author

Full name: Natthapong Monarumit
Affiliation: Gemmology and Mineral Sciences Special Research Unit, Department of Earth Sciences, Faculty of Science, Kasetsart University, Bangkok, 10900, Thailand.
Email: mu_earthsci.03@hotmail.com

Carbon Isotope and CL Analysis of Natural Type IIa and CVD Synthetic Gem Diamonds

Wuyi Wang

Gemological Institute of America, 50 West 47 Street, New York, NY 10036, USA

Extended Abstract

Introduction

Natural gem diamonds crystallized in the earth's mantle at high pressure and temperature. In contrast, chemical vapor deposition (CVD) technology can grow single-crystal diamond from low-pressure gases (e.g., mixture of CH₄ and H₂) activated by plasmas, hot filaments, or combustion flames. CVD diamond is a maturing material with a wide variety of technological impacts, including jewelry industry. During the past decade, the quality of single-crystal CVD synthetic diamond has improved significantly (Martineau *et al.*, 2004; Wang *et al.*, 2012). In recent years, many CVD synthetic diamonds have been introduced to the jewelry market, generating tremendous concern. Faceted gem diamonds, up to 3 carats in sizes, colorless or near-colorless and with good cuts, are available in the trade. Fancy colors, such as pink and blue with varying saturations, are also produced through post-growth treatments.

The ability to confidently separate these synthetic diamonds from natural ones is critical for consumer confidence. Current identification methods focus on optical properties, including types and concentrations of impurities or combinations of impurities and their distribution in the diamond lattice. The main technologies include deep UV fluorescence image, FTIR absorption spectroscopy, and laser photoluminescence spectroscopy, in addition to gemological observations. This approach has proven very successful for separating CVD synthetics from HPHT synthetics and natural diamonds. However, continuous improvement of CVD growth technology, control of impurity, in particular post-growth treatments introduces new identification challenges. In an effort to proactively confront these challenges, we present an evaluation of carbon isotope analysis and CL image analysis as tools for comparison of CVD synthetic diamonds with natural ones.

Samples and Analysis

Carbon isotope of twenty CVD synthetic diamonds from three manufacturers (Gemesis=8; SCIO=11; Element Six=1) and nine natural type IIa diamonds were analyzed by SIMS using the Cameca IMS1280 Ion Probe in the Canadian Center for Isotope Microanalysis at the University of Alberta. All samples (0.12 – 1.36 ct) were gem quality, carefully polished with a large flat surface. Linearly crossing the table face, 5 to 10 spots were analyzed for each crystal. Cathodoluminescent (CL) image of the same set samples were collected using Electron Scanning Microscope on the table faces. Geographic source of the natural type IIa diamonds is unknown. FTIR absorption spectroscopic analysis confirmed that all the samples in this study are type IIa diamonds, with no absorption detectable in one-phonon region at all.

Observations and Results

Comparing with fluorescence images obtained by deep-UV activation (DiamondView), CL images revealed significantly more detailed growth features and defect distribution (Figure 1). CVD diamonds showed mainly the “worm-like” and “layered-growth” patterns. In contrast, natural type IIa diamonds showed very sharp lines from plastic deformation and dislocation networks. Many of these samples were featureless under DiamondView.

All the CVD synthetic diamonds exhibited very homogeneous carbon isotope compositions. Standard deviation among multiple analyses on each sample was less than 0.6‰, which is close to the instrument analytical uncertainty. Carbon isotope compositions ($d^{13}C$) of CVD diamonds from SCIO were in the range -35 to -45‰, whereas samples from Gemesis were -55 to -75‰. The single sample from Element Six was -63.7‰, consistent with the Gemesis range (Figure 2). Unlike natural type I diamonds, which typically show heterogeneous carbon isotope distributions, the type IIa diamonds in this study were all very homogeneous in carbon isotope distribution, but covered a very large range ($d^{13}C$: -0.6 to -28.1‰).

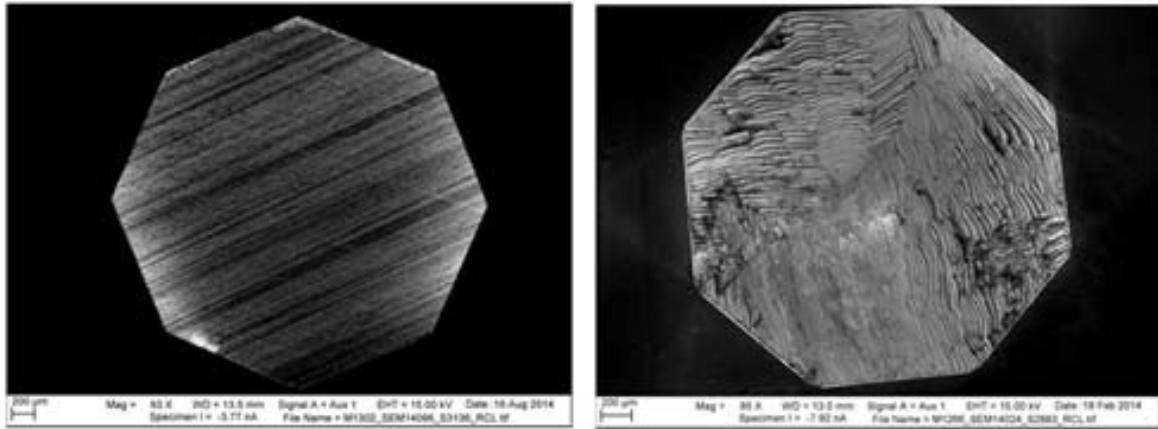


Figure 1: CL image revealed very different growth features and defect distribution between natural type IIa diamond (**left**) and CVD synthetic diamond (**right**).

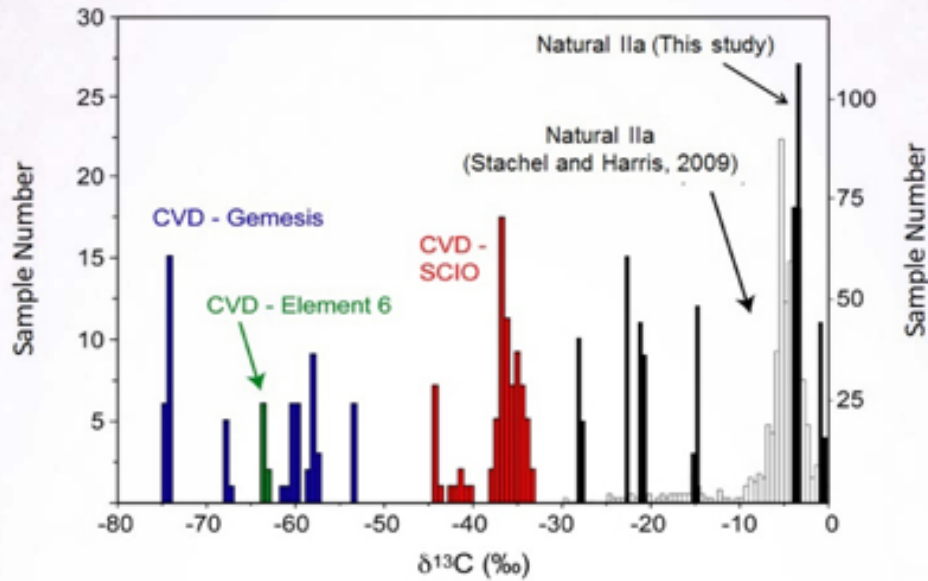


Figure 2: Carbon isotope compositions of CVD synthetic diamonds in comparison with that of natural type IIA diamonds. They are entirely different and no overlap was detected.

Discussions and Conclusions

Results obtained in this study revealed that CVD synthetic diamonds from various sources are much lighter in carbon isotope composition than natural diamonds (Stachel *et al.*, 2007), which occur in the range $\delta^{13}\text{C} = -10$ to 0‰ (peridotitic) or extend to values as low as -30‰ (eclogitic). They are much lower than those natural IIA diamonds in this study. Effectively, no overlap is observed in carbon isotope chemistry between natural and CVD diamonds. In combination with the homogenous distribution of carbon isotopes in CVD diamonds, this difference in $\delta^{13}\text{C}$ values could be a very useful feature for separating natural diamonds from CVD synthetics. In addition, very large differences were revealed between CVD diamonds from different manufacturers, as well as among CVD diamonds from the same manufacturer. Variations in CH_4 gas chemistry or growth conditions (pressure and temperature) may have contributed to this observed fractionation of carbon isotopes. In addition, it is confirmed that CL image is much more sensitive in detecting growth features and defect occurrence in a diamond than that of using DiamondView, and could be a very useful tool for identification.

Type IIA diamonds are rare in natural but gemologically important. Formation of type IIA diamond is poorly understood comparing with natural type Ia diamonds, for shortage of constrains such as mineral inclusions, nitrogen and hydrogen impurities. For the first time in this study, we confirmed that carbon isotope distribution in natural type IIA diamonds is very homogeneous. This result has significant implication in formation of natural type IIA diamonds. To form type IIA diamonds, in contrast to type Ia, sufficient amount of fluid/melt is required to avoid fractionation of C isotope during its crystallization. Nitrogen concentration in the melt/fluid must be extremely low, considering nitrogen is highly compatible. In addition, the environment for crystallization has to be very stable as many large natural diamonds are type IIA.

Acknowledgements

Ulrika F.S. D’Haenens-Johansson, Karen Smit, Christopher M. Breeding from GIA laboratory, and Richard Stern from University of Alberta are thanked for analysis and many helpful discussions.

References

Martineau, P.M., Lawson, S.C., Taylor, A.J., Quinn, S.J., Evans, D.J.F., and Crowder, M.J., 2004, Identification of synthetic diamond grown using chemical vapor deposition (CVD), *Gems & Gemology*, Vol.40, No.1, p.2-25.

Stachel, T., Harris, J.W., and Muehlenbachs, K., 2009, Sources of carbon in inclusion bearing diamonds, *Lithos*, Vol.112, Supplement 2, p.625-637.

Wang, W., D’Haenens-Johansson, U.F.S., Johnson, P., Moe, K.S., Emerson, E., Newton, M.E., and Moses, T.M., 2012, CVD synthetic diamonds from Gemesis Corp., *Gems & Gemology*, Vol.48, No.2, p.80-97.

Corresponding Author

Full name: Wuyi Wang
Affiliation: Gemological Institute of America, 50 West 47 Street, New York, NY 10036, USA.
Phone: +1-917-286,3507
Email: wwang@gia.edu

Electron-Beam Irradiation and Heat Treatment of Corundum from New Deposits of Krong Nang District, Dark Lak Province, Vietnam

Jongwan Park¹, Sora Shin¹, Nguyen Ngoc Khoi², Nguyen Thuy Duong², Duong Anh Tuan³, Hauzenberger Christoph Anton⁴ and Haeger Tobias⁵

¹Material Science and Engineering, Hanyang University, Korea

²Geochemistry, Hanoi University of Science, Hanoi Vietnam

³Gems and Jewelry manufacturing, DOJI Gold & Gems Group, Hanoi Vietnam

⁴Earth Sciences, Graz University, A-8010

⁵Gemstones, Mainz University, Desu95 Hanoi Germany

Extended Abstract

Sapphire belongs to the same “aluminium oxide” mineral family (corundum) as ruby, but sapphire is far more abundant due to the larger occurrence of its chromium, iron, and titanium coloring agents. Sapphire colors range from canary yellow to blue, brown, gray, green, orange, pink, purple, and colorless.

The color formation in sapphire is well known to occur as a result of inter-valence charge transfer (IVCT) in the sapphire crystals. Iron impurities are generally either in a Fe²⁺ or Fe³⁺ state in the sapphire crystal.

This study investigates the origin of sapphire from Krong Nang district, Dark Lak Province, Vietnam and the change of color and spectral characteristics after electron beam irradiation and heat treatment. Figure 1 shows the starting materials were classified as six groups including dark greenish blue, dark green, light green, yellowish green, yellowish orange and two tone color (dark blue and orange, dark blue and light green) according to the predominant color observed.

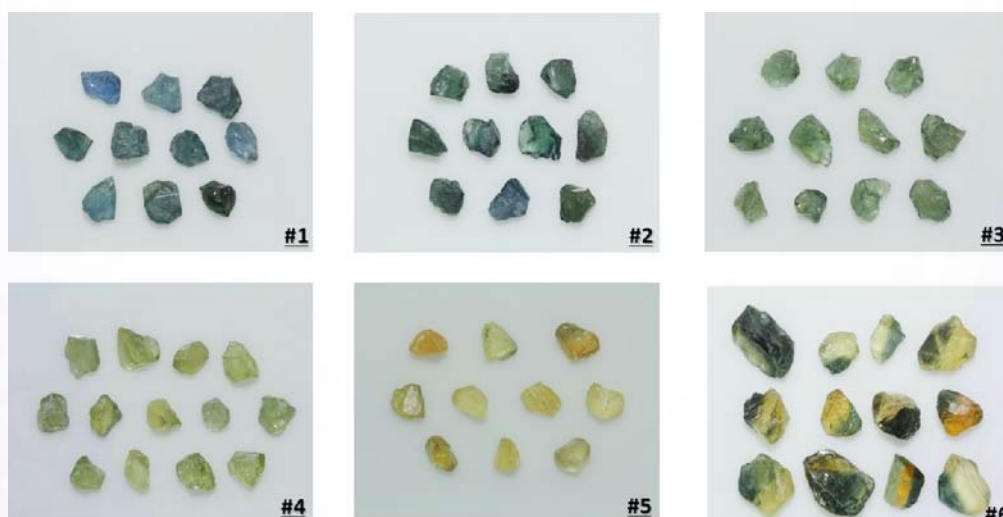


Figure 1: Sample collection under this study: **(1)** dark greenish blue, **(2)** dark green, **(3)** light green, **(4)** yellowish green, **(5)** yellowish orange, and **(6)** two-tone color (dark blue and orange, dark blue light green)

The irradiation was performed with electron dose densities of $1 \times 10^{17} / \text{cm}^2$ at 10 MeV for one hour, and the samples were analyzed before and after electron-beam irradiation by using WD-XRF, UV-Vis-NIR, FT-IR spectroscopy. Table 1 presents the results of chemical analyses of sapphire. Most of the sapphires from Vietnam are associated with basalts, and are notable for their high Fe content.

Table 1: Composition data of the typical six groups of sapphire samples by wavelength dispersive X-ray fluorescence (Unit: wt %).

Oxides (wt.%)	No.1 Dark greenish blue	No.2 Dark green	No.3 Light green	No.4 Yellowish green	No.5 Yellowish orange	No.6 Two-tone color
Al ₂ O ₃	99.207	99.132	99.201	99.219	99.148	98.83
Fe ₂ O ₃	0.759	0.81	0.699	0.694	0.751	0.855
ZnO	-	0.018	0.036	0.032	0.039	0.031
TiO ₂	0.023	0.009	0.033	0.021	0.03	0.053
Ga ₂ O ₃	0.01	0.02	0.015	0.011	0.02	0.012
Cr ₂ O ₃	-	0.01	0.016	0.024	0.021	0.013
K ₂ O	-	-	-	-	-	0.122
CaO	-	-	-	-	-	0.085

Figure 2 shows that the UV-Vis absorption spectra of No. 1, 4, 5 and 6 group sapphire were changed to yellow color after electron. For the sapphire samples of all groups, the 377 and 450 nm peaks which are related to Fe²⁺/Fe³⁺ increased and the 388 nm absorption peak related to Fe³⁺ increased, while in NO. 3 group sapphire, the increase in 565 and 699 nm peak absorption peak is related to inter-valence charge transfer (IVCT).

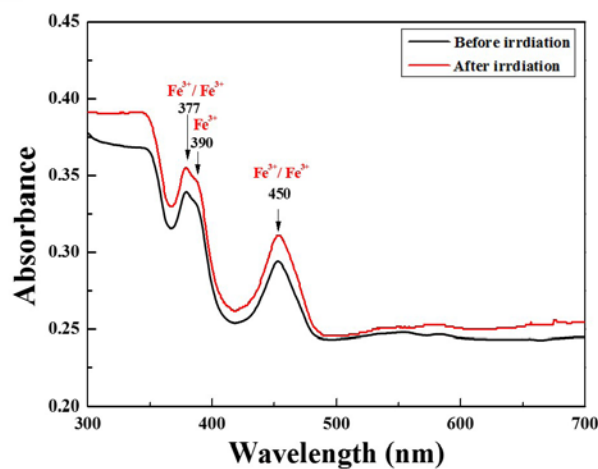


Figure 2: The 1, 4, 5, 6 group sapphire were changed to yellowish green color after electron beam irradiation.

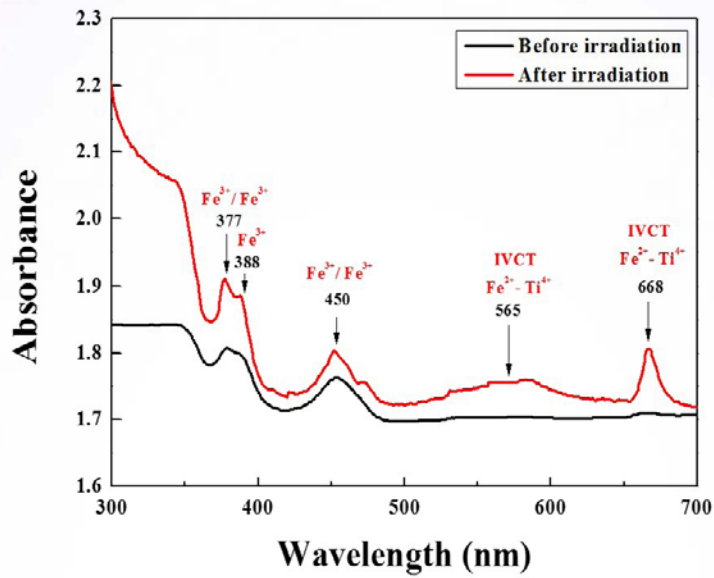


Figure 3: The 3 group sapphire were changed to light blue color after electron beam irradiation.

FT-IR analysis after electron beam irradiation in all samples shows that 1000-1600 cm^{-1} vibration absorption band of Al-O Stretching as a whole decreased.

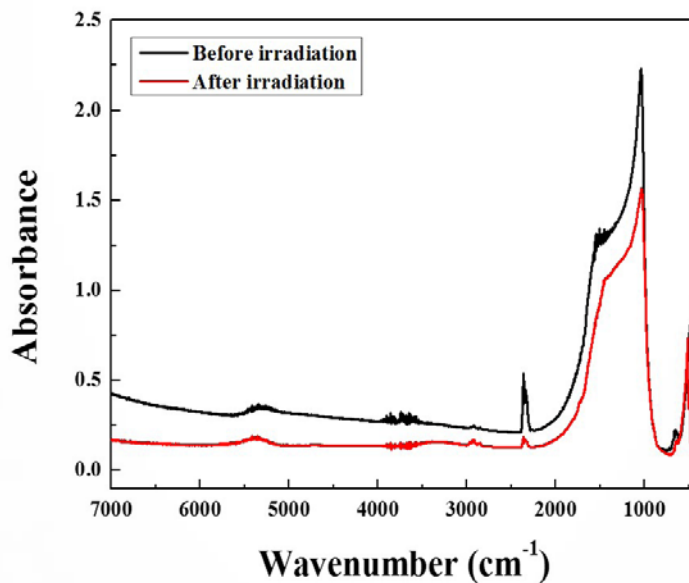


Figure 4: Comparison of the FT-IR spectra of the all color group sapphire before and after electron beam irradiation.

After heat treatment, the irradiated sapphires of various colors recovered their original colors. The electrons detached from the irradiated lattices can cause charge transfer transition. Then, it is expected that electrons are moved from unstable states to stable states by external energy, such as heat.

References

Nassau, K. 1978, The origins of color in minerals, American Mineralogist, Vol.63, No.1-4, p.219-229. Nguyen, N.K., Nguy, T.N., Nguyen, T.M.T., and Phan, V.Q., 2007, Characteristics of corundums from Phuoc

Hiep occurrence, Journal of science (Vietnam National University, Hanoi), No.23, p.152-158.

White, W.B, Matsumura, M., Linnehan, D.G., Furukawa, T. and Chandrasekhar, B.K., 1986,

Absorption and luminescence of Fe³⁺ in single-crystal orthoclase, American Mineralogist, Vol.71, No.11-12, p.1415-1419.

Corresponding Author

Full name: Jongwan Park

Affiliation: Division of Materials Science & Engineering, Hanyang University, Seoul
133-791, Korea.

Phone : +82-2-2220-0386 Fax : +82-2-2298-2850

Email: jwpark@hanyang.ac.kr

From HPHT to LPHT Treatment of Type IIa Diamonds

Katrien De Corte

HRD Antwerp, HOveniersstraat 22, 2018 Antwerp, Belgium

Extended Abstract

LPHT is a colour treatment procedure that stands for Low Pressure- High Temperature. Just like HPHT, the LPHT treatment aims to decrease the brown colour in type IIa diamonds. We expect that LPHT processors will focus on treating CVD lab-grown diamonds. As far as we know, there are so far no natural stones in the market that have been LPHT treated.

In 2008 an alternative to High Pressure High Temperature (HPHT) colour treatment of type IIa diamonds, was presented by a group of researchers at the Carnegie institution of Washington D.C. (Meng *et al.*, 2008). This new treatment was Low Pressure High Temperature (LPHT) annealing. A technique performed out of the range of stability of diamond. Just like HPHT, they used LPHT treatment to decrease brown colour in type II diamonds by annealing at temperatures up to 2200°C using a microwave plasma at pressures below atmospheric pressure. They point out that a significant advantage of LPHT is that it can improve both colour and clarity of a diamond. Furthermore, it can be applied to a larger quantity of diamonds at a single time making the process half the cost of the HPHT treatment.

Although the process is not yet commercially available, it is currently being studied in laboratories in Belgium, USA and Russia, where the focus is on refining the treatment and expanding the use of the treatment to all types of diamonds. At the same time detection protocols are being developed to identify diamonds that have undergone LPHT treatment. This because any new diamond treatment that enhances a stone's natural properties is a concern to an industry where full disclosure is the fundamental for consumer confidence.

Distinguishing colourless polished natural diamonds from polished synthetic diamonds using today's conventional gemological equipment is almost impossible which only adds to the market turmoil. Only measurements generated by sophisticated equipment can determine whether or not a diamond is synthetic. Such equipment is available in professional, well equipped laboratories such as the HRD Antwerp lab. All lab grown diamonds processed in the HRD Antwerp lab are laser inscribed and accompanied by a specific lab grown certificate.

For larger stones the cost of a certificate and thus the research of its origin (natural or synthetic) is negligible. This cost is however more significant for smaller stones, especially for melee (0.03-0.07 ct) and smaller goods. This is why the diamond sector needs advanced screening devices. The core function of such a screening device is to provide a 100% secure solution to separate natural stones from possibly synthetic stones or stones requiring further investigation. This type of screening essentially means that type II stones are separated from the other types as colourless CVD synthetic diamonds and colourless HPHT synthetic diamonds are (still) type II diamonds.

Type II diamond has a characteristic absorption of the electromagnetic spectrum and depending on the light source used during the screening, one speaks of infrared (IR) screening, ultraviolet (UV) screening or visible light (VL) screening. Two types of screening devices exist today: equipment that allows screening each stone individually and (manually and devices screening multiple stones automatically and often simultaneously. An overview of these available screening instruments will be discussed during the presentation.

HRD Antwerp advises everyone to submit all type II stones for investigation by a reputable diamond lab so both their growth origin — natural or lab-grown— as well as the origin of their colour — natural or treated colour — can be identified. This is all in the interest of full disclosure.

Reference

Meng Y.F., Yan C.S., Lai J., Krasnicki S., Shu H., Yu T., Ling Q., Mao H.K., and Hemley R.J., 2008, Enhanced optical properties of chemical vapor deposited single crystal diamond by low-pressure/high-temperature annealing, in Proceedings of the National Academy of Sciences, Vol.105, No.46, p.17620-17625.

Corresponding Author

Full name: Katrien De Corte
Affiliation: HRD Antwerp, HOveniersstraat 22, 2018 Antwerp, Belgium.
Email: kdc@hrd.be

Heat Treatment of Aquamarine

Nantharat Bunnag^{1,2} and Bhuwadol Wanthanachaisaeng^{1,3}

¹Faculty of Gems, Burapha University, Chanthaburi, 22170, Thailand

²Jewelry Material Research and Development, Faculty of Gems, Burapha University, Chanthaburi, 22170, Thailand

³Gems Enhancement Research Unit, Faculty of Gems, Burapha University, Chanthaburi, 22170, Thailand

Extended Abstract

Aquamarine is the trade name of greenish blue, yellowish blue and yellowish green beryl, which the top color is deep blue. The purpose of this study is to investigate the effect of heating environment between atmospheric and reducing condition at 400-500°C with 3 and 5 hours dwell time to the changing of colors in aquamarine.

Materials and Methods

A total of 80 rough samples, unconfident source which the merchant selling as Madagascar stone, were separated into 8 groups with 10 samples in each of them. The samples were polished at least a pair of parallel flat surface.

Standard gemological properties and spectroscopic data were measured at the Burapha Gemological Laboratory (BGL). Ultraviolet through visible and near-infrared (UV-Vis-NIR) spectra and color measurement were collected with a PerkinElmer Lambda 1050 spectrophotometer at 2 nm resolution, scan speed 300 nm/min. The color measurement in CIE L*a*b* were converted from the visible spectra by the PerkinElmer UV win LAB. Then the color difference (ΔE) was calculated.

The samples were heated by electric furnace in 8 conditions as shown in Table 1. The experiment uses 2 steps heating rate; step 1 is 100°C/hr from room temperature to 100°C; step 2 is 150°C/hr from 100°C to a maximum temperature until the end of soaking time. Samples remained in the furnace until the temperature decrease to room temperature. Argon was feeding in the furnace to create a reducing condition.

Table 1: Heating experiments in this study

	Max. Temp.(°c)	Dwell time (Hour)	Heating Condition
Group 1	400	3	atmosphere
Group 2	400	5	atmosphere
Group 3	500	3	atmosphere
Group 4	500	5	atmosphere

	Max. Temp.(°c)	Dwell time (Hour)	Heating Condition
Group 5	400	3	reducing
Group 6	400	5	reducing
Group 7	500	3	reducing
Group 8	500	5	reducing

Results and Discussions

After the heating experiments, gemological properties are not change. The fractures are extended; the yellow iron stains are changed into reddish brown color (Figure 1).

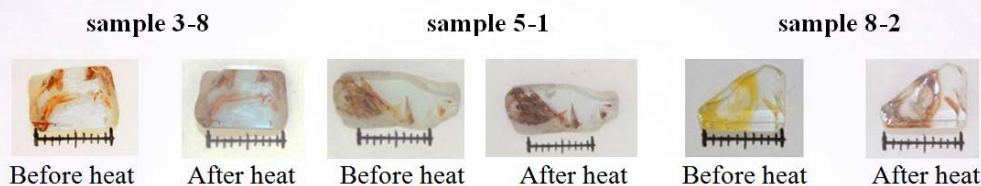


Figure 1: Changing of iron stains color after heat treatment.

The color measurement in CIE L* a* b* shows that heat treatment in reducing condition reduced green color (a* increasing) in the samples better than heating in atmosphere. After heating, saturation of the samples heated in reducing condition increased more than the samples heated in atmospheric condition.

Group 8-samples which heated at the maximum temperature of 500°C with 5 hours dwell time under reducing condition show the highest average value of the color difference (Table 2). However, the b* of four samples are decreased (Table 3). The b* decreasing is related to yellow color decreasing and blue color increasing (-b*). This means that the heat treatment cannot increase blue color in all samples but the sample color is changed by reduce green and yellow color.

Table 2: Color difference (ΔE) of the samples.

	Min. ΔE	Max. ΔE	ΔE average		Min. ΔE	Max. ΔE	ΔE average
Group 1	0.40	3.08	1.26	Group 5	0.12	7.65	2.40
Group 2	0.04	6.63	2.30	Group 6	0.38	10.46	2.80
Group 3	0.41	6.85	2.60	Group 7	0.33	6.56	1.85
Group 4	0.08	6.55	1.79	Group 8	0.24	13.07	3.14

Table 3: ΔE and L* a* b* of the samples group 8 comparison between before and after heat treatment.

Sample	L*			a*			b*			ΔE
	before heat	after heat	ΔL^*	before heat	after heat	Δa^*	before heat	after heat	Δb^*	
8-1	28.11	24.77	-3.34	-0.20	-0.15	0.05	0.50	0.60	0.10	3.34
8-2	31.08	26.78	-4.30	-0.51	0.78	1.29	3.00	3.46	0.46	4.51
8-3	28.32	27.56	-0.76	-0.78	-0.54	0.24	0.50	0.96	0.46	0.92
8-4	26.55	26.09	-0.46	-0.86	-0.70	0.16	0.38	-0.02	-0.40	0.63
8-5	27.67	27.50	-0.17	-0.76	-0.69	0.07	0.53	0.68	0.15	0.24
8-6	18.94	15.33	-3.61	-0.47	-0.04	0.43	1.12	1.70	0.58	3.68
8-7	30.67	30.22	-0.45	-0.42	-0.30	0.12	0.82	0.63	-0.19	0.50
8-8	26.87	25.21	-1.66	-0.73	-0.53	0.20	0.59	1.30	0.71	1.82
8-9	26.10	23.64	-2.46	-1.98	-1.40	0.58	-0.23	-1.16	-0.93	2.69
8-10	28.15	15.12	-13.03	-1.07	-1.16	-0.09	1.11	0.15	-0.96	13.07
ΔE average										3.14

The absorption spectra indicate that blue color in samples is related to the continuous absorption of Fe²⁺-Fe³⁺ charge process and Fe²⁺ in channel site at approximately 650-1000 nm, centered at 820 nm. The extending of the band into 600 nm ranges is effect to increase blue in sample as shown in sample 8-9 and 8-10 (Figures 2 and 3). After heat treatment, samples that are not increasing blue but decreasing green and yellow are related to the increasing of the Fe³⁺ absorption at 370 and/or 427 nm and unknown narrow absorption band at 470-510 nm as shown in sample 8-6 (Figure 4).

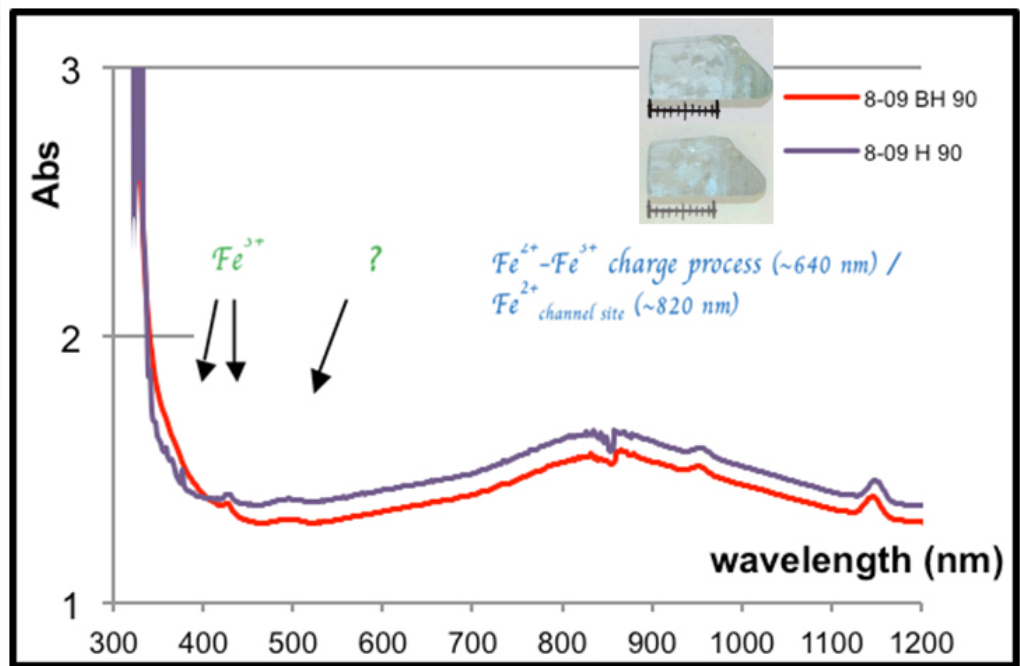


Figure 2: Absorption spectra of sample 8-9, comparison between before (**red line**) and after (**violet line**) heat treatment.

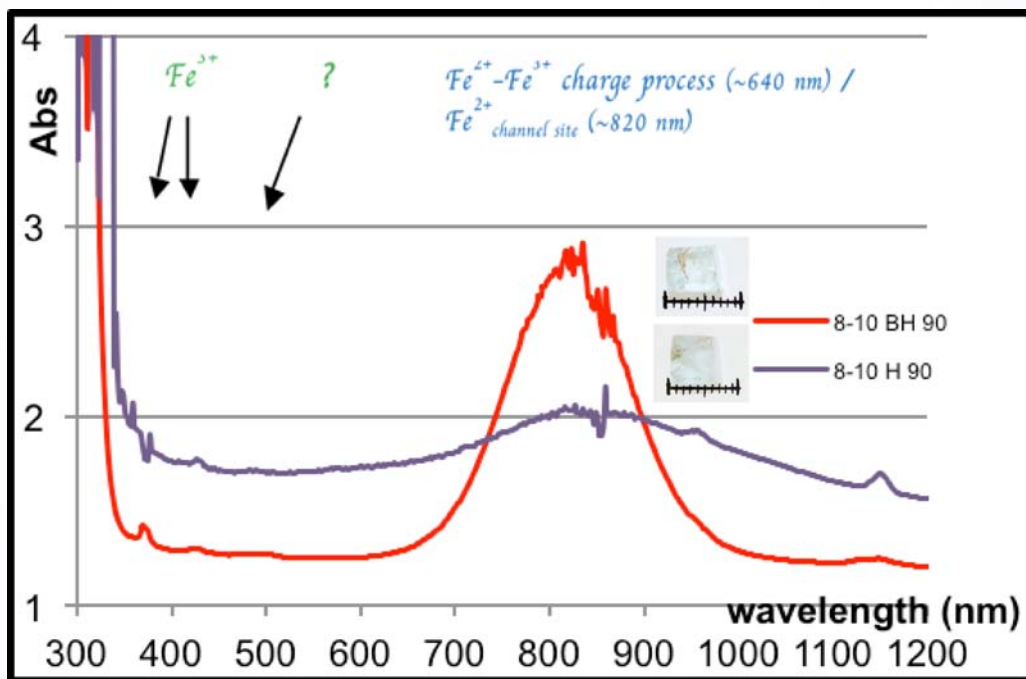


Figure 3: Absorption spectra of sample 8-10, comparison between before (**red line**) and after (**violet line**) heat treatment

Treatment and Synthetics: update and disclosure

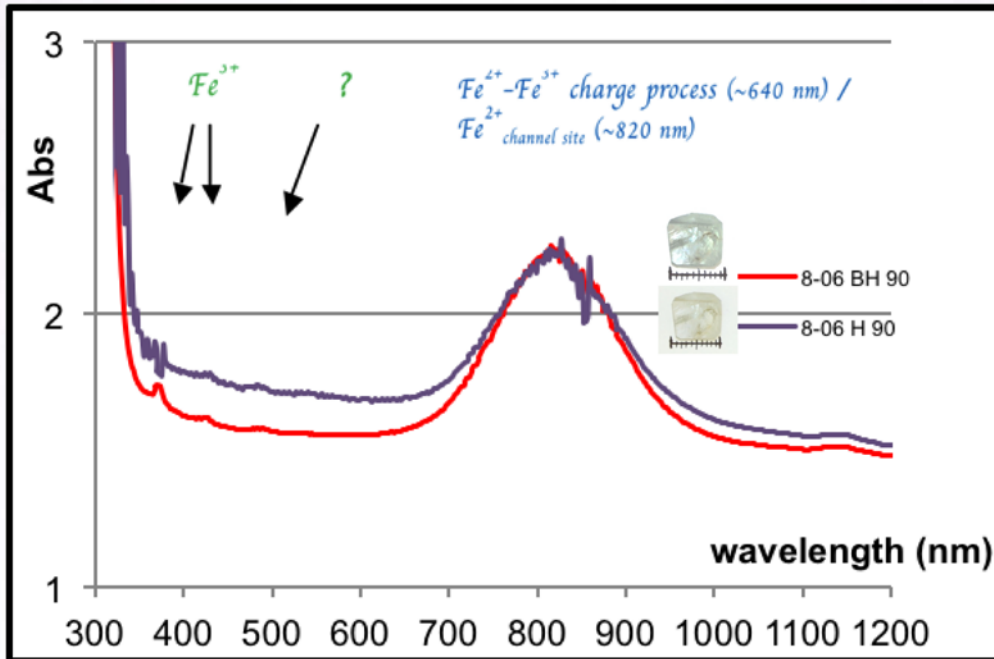


Figure 4. Absorption spectra of sample 8-6, comparison between before (**red line**) and after (**violet line**) heat treatment

Conclusions

Both atmospheric and reducing conditions can increase blue in aquamarine because both condition can cause $\text{Fe}^{2+}\text{-Fe}^{3+}$ charge process. However the reducing condition seem to give a better blue because this condition can also increase Fe^{2+} in channel site.

References

- Chankhantha, C., 2012, Heat treatment of aquamarine and morganite from Madagascar, Paper presented at the 38th Congress on Science and Technology of Thailand, Available from http://www.scisoc.or.th/stt38/proceedings38/pdf/m/STT38_M_M0005F.pdf. (Retrieved August 20, 2013).
- Nassau, K., 1994, Gemstone enhancement: History, Science and State of the Art, Manchester: Redwood Books, 252 p.
- Ruzeng, Y., Hongyi, X., and Minjie, L., 2007, The effect of heat treatment on color, quality and inclusions of aquamarine from China, The Journal of Gemmology, Vol.30, No.5-6, p.297-301.

Corresponding Author

Full name: Nantharat Bunnag
Affiliation: Faculty of Gems, Burapha University, Chanthaburi, 22170, Thailand.
Email: b_nantharat@yahoo.com

Influence of Irradiation and Heating on the Ratanakiri Zircon Structure

Bhuwadol Wanthanachaisaeng¹, Nantharat Bunnag², Somruedee Satitkune³, Papawarin Ounorn⁴, Chakkaphan Sutthirat^{4,5} and Visut Pisutha-Arnond^{4,5}

¹Gems Enhancement Research Unit, Faculty of Gems, Burapha University, Chanthaburi, 22170, Thailand

²Jewelry Material Research and Development, Faculty of Gems, Burapha University, Chanthaburi, 22170, Thailand

³Department of Earth Sciences, Faculty of Science, Kasetsart University, Bangkok, 10900, Thailand

⁴The Gems & Jewelry Institute of Thailand, (Public Organization), Bangkok, 10500, Thailand

⁵Department of Geology, Faculty of Science, Chulalongkorn University, Bangkok, 10330, Thailand

Extended Abstract

Zircon is a famous gemstone in the world markets. The attractive properties of this stone is derived from its sub-adamantine luster with moderate dispersion. The colors of natural zircon are commonly reddish brown which can be found in many deposits such as in Ratanakiri, Pailin and Preah Vihear in Cambodia, Chanthaburi and Kanchanaburi in Thailand, and also many localities in Sri Lanka. However, the most preferred color in the gem market is blue which is normally accomplished by heat treatment. The well-known zircon that can be heat-treated into beautiful blue since the early 20th century is the rough stones from Ratanakiri deposit in Cambodia (Balmer *et al.*, 2009). In this investigation, more than 50 samples from Ratanakiri deposit were heated and irradiated for investigation of the influences of heating and irradiation to zircon structure.

The unheated zircon from Ratanakiri is a high type based on its specific gravity values of 4.6-4.7. The visible spectra of the untreated brown samples (Figure 1) show a continuous increase of non-polarised absorption (i.e., showing similar patterns for both e- and o-rays) from around 650 nm towards the UV region with a shoulder or hump at ~500 nm. This selective absorption feature give brown to reddish brown color to those samples. Based on such absorption characteristic, the reddish brown color of this zircon has been interpreted to be due to the defect center causing by the self irradiation of uranium and thorium that are commonly present as trace elements in its structure (Wanthanachaisaeng *et al.*, 2008, Pisutha-Arnond *et al.*, 2011). To further confirm such interpretation and to investigate the impact of the irradiation on color, in this study, the samples were also irradiated by gamma ray at 900 kGy. As the result, the irradiated zircons turned even more intense reddish brown color. The absorption spectrum after irradiation showed a similar pattern to that of the unheated zircon but with much higher intensity (Figure. 1). This result proves that the cause of reddish brown color of Ratanakiri zircon is the color center caused by self irradiation.

In the traditional heat treatment of zircon, the rough stone is normally carried out in charcoal furnace for certain period of time and its color can turn from reddish brown to blue fairly easily. In our experiments, however, we preferred to heat them in an electric furnace that was able to control both temperature and heating condition more accurately. The zircon samples were firstly annealed at 400°C for one hour in a reducing atmosphere. The reddish brown color turned to almost colorless. Therefore, the low temperature heat treatment can remove the low level defect centers in zircon (Figure 1). The zircons were further heated at 1000°C under the reducing atmosphere. The color of all samples turned to blue.

It was found in our experiments that some samples of unheated zircon show the absorption sharp peak at around 650 nm which was assigned to U^{4+} (Richman *et al.*, 1967; Vance, 1974). After the heat treatment at 1000°C, the blue zircon shows a broad absorption band from 550 to 800 nm which coincides with the position of U^{4+} sharp peak (Figure 1). Even though Pisutha-Arnond *et al.*, (2011) have earlier pointed out the overlapping of the 650nm- U^{4+} sharp peak and the broad absorption band, but they have ruled out the relationship of such broad band intensity with the U content in zircon structure and possibly U^{4+} as well. However, because the n_3 Raman peak after heat treatment shifted red only in the blue zircon (Wanthanachaisaeng *et al.*, 2008). Hence the broad absorption band could still possibly be related to U^{4+} and its structure in other ways.

The Ratanakiri zircons were also heated at 1400°C and its color turned into translucent white color. The absorption spectrum shows several small sharp peaks that many of them were not appeared in the unheated samples. As reported by Wang *et al.* (2006) and Váczi *et al.* (2009), the zircon started to subsolidus decomposed into baddeleyite and SiO_2 -rich phase at 1400°C. Therefore, the high temperature heat treatment can destroy the zircon structure.

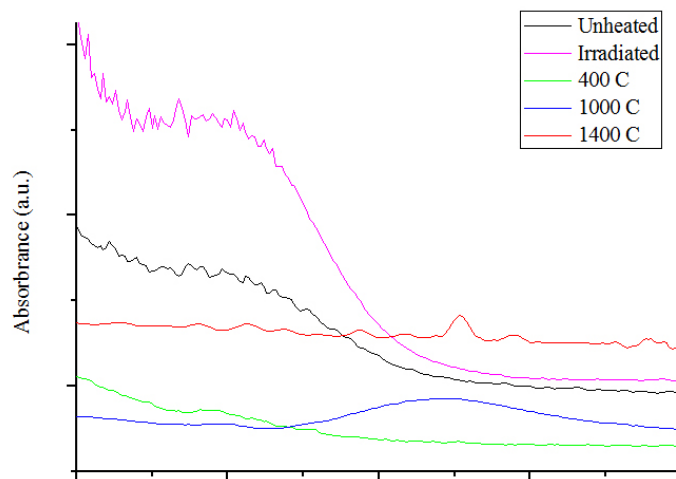


Figure 1: Absorption spectra of Ratanakiri zircons before treatment and after irradiation and heating at various temperatures.

Acknowledgments

Financial support has been provided by The Gems and Jewelry Institute of Thailand (Public Organization) (GIT).

References

- Balmer, W.A., Smith, M.H., Sriprasert, B., and Wanthanachaisaeng, B., 2009, Ratanakiri, the legendary zircon province of Cambodia, 3rd European Gemmological Symposium, Bern, Switzerland.
- Pisutha-Arnond, V., Hentoog, A., Atichat, W., and Leelawatanasuk, T., 2011, Blue coloration of heat-treated zircon, the 32nd International Geological Conference (IGC2011), Interlaken, Switzerland, p.89-94.

- Richman., I., Kisliuk, P., Wong, E.Y., 1967, Absorption spectrum of U⁴⁺ in zircon (ZrSiO₄), Physical Review, Vol.155, No.2, p.262-267.
- Vácz, T., Nasdala, L., Wirth, R., Mehofer, M., Libowitzky, E., and Häger, T., 2009, On the breakdown of zircon upon “dry” thermal annealing, Mineralogy and Petrology, Vol.97, No.1-2, p.129-138.
- Vance, E.R., 1974, The anomalous optical absorption spectrum of low zircon, Mineralogical Magazine, Vol.39, No.306, p.709-714.
- Wang, W., Scarratt, K, Emmett, J.L., Breeding, C.M. and Douthi, T.R., 2006, The effects of heat treatment on zircon inclusions in Madagascar sapphire, Gems & Gemology, Vol.42, No.2, p.134-150.
- Wanthanachaisaeng, B., Bunnag, N., Sutthirat, C., Papawarin, O., and Pistha-Arnond, V., 2008, Metamictization and color of zircon from Chanthaburi, Kanchanaburi, Cambodia, and Sri Lanka, The Gems and Jewelry Institute of Thailand (GIT).

Corresponding Author

Full name: Bhuwadol Wanthanachaisaeng
Affiliation: Faculty of Gems, Burapha University, Chanthaburi Campus, 57
M.1 Chonlaprathan Rd., Kamong, Thamai, Chanthaburi, 22170, Thailand.
Email: bhuwadol@yahoo.com

New Treated Blue Sapphire by HPHT Apparatus

Hyun-Min Choi, Sun-Ki Kim and Young-Chool Kim

Hanmi Gemological Institute Laboratory (Hanmi Lab, GIG), Seoul, 110-390, Korea

Extended Abstract

There are some treatments for valuable color of blue sapphire such as dyeing, heating, diffusion. Among of them, heat treatment with development of techniques and effort has been performed for deriving beautiful blue color of sapphire until nowadays. This tendency has been recognized that corundum is commonly undergone heat-treatment or enhancement.

Improvement of the blue color of sapphire by heating started from the 19th century, it was started in earnest in the 20th century (Themelis, 1992). It needed oxidizing-reducing conditions by gas diffusion. The process modifies color of too dark or pale blue sapphire or removes unnecessary inclusions for clarity enhancement (Nassau, 1994). According to geographic origins of corundum, it has different characteristics such as color, impurities, inclusions, etc. So, it needs to use a proper technique to change color. Therefore, it requires various conditions and skills with experience of heat treatment to change color of sapphire.

Some Koreans have a lot of interesting in treatment techniques of gemstone for creating added value. A Korean company has developed a technique to enhance color of blue sapphire by applying with HPHT (high pressure and high temperature) apparatus. Originally, the apparatus was designed to grow synthetic diamond. It took many attempts with thousands of conditions to finally get to valuable blue color from pale blue color, which is an unique process. The owner of the company explained that he had remade the HPHT apparatus and developed a mold for new treatment. It is noticeable news like Be-diffused corundum and HPHT treated diamond.

The characteristic of new treated sapphire is found in infrared region. Earlier undetected, a strong absorption band at 3040-3050 cm^{-1} was observed after new treatment process. Therefore, infrared spectroscopy is effective in identifying the new treated sapphire, although we still unable to ascertain the absorption band around 3040-3050 cm^{-1} . We need to study to get more information of the newly treated sapphire by HPHT apparatus.

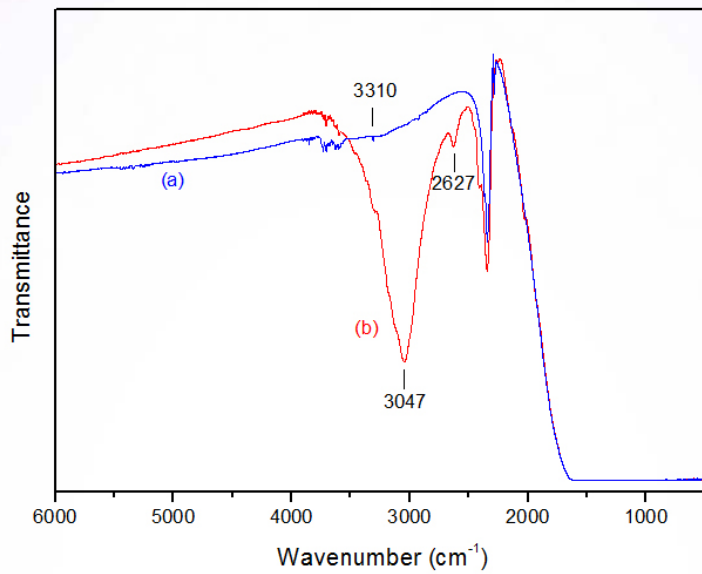


Figure 1: This infrared spectra show a blue sapphire before **(a-blue line)** and after **(b- red line)** new treated process by HPHT apparatus. After treatment, a strong band is observed at 3040-3050 cm⁻¹.



Figure 2: These two illustrations show the sample before **(left, light blue color)** and after **(right, blue color; 6.55 ct)** treated by HPHT apparatus.

References

- Nassau, K., 1994, Gemstone enhancement: History, Science and State of the Art – 2nd Rev.eds, Butterworth Heinemann, p.122-131.
Themelis, T., 1992, The heat treatment of ruby and sapphire, Gemlab Inc., USA, p.11-14.

Corresponding Author

Full name: Hyun-Min Choi

Affiliation: Hanmi Gemological Institute Laboratory (Hanmi Lab, GIG), Seoul 110-390, Korea.

Rusgems Synthetic Opal

Panjawan Thanasuthipitak¹ and Suchart Kiatwattanacharoen²

Department of Geological Science, Chiang Mai University, Chiang Mai 50200, Thailand

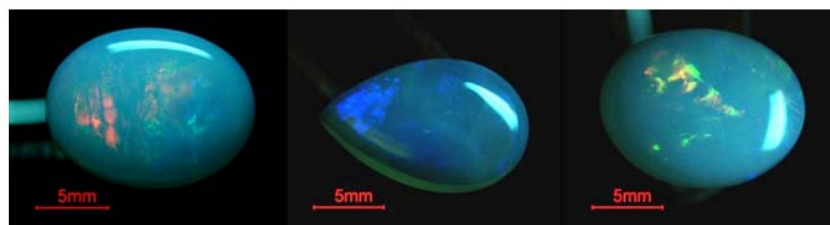
Extended Abstract

Introduction

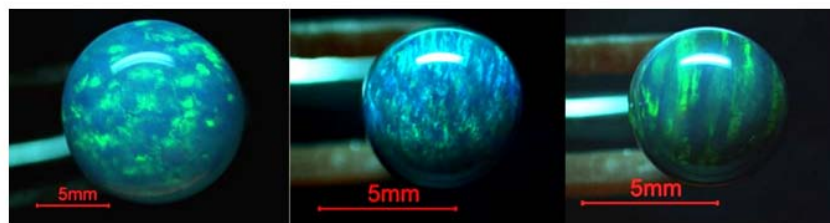
Synthetic opals were first manufactured and sold by P. Gilson since 1974. The products resembled the appearance of white and black opal having “play of colors” like those found in natural Australian opal. Since then several colors of synthetic opal including fire opal were available on the gemstone market from many companies. Recently, synthetic opals by the Rusgems Company from the Russian Federation, a leader in the manufacturer of man-made gem materials have been introduced in the trade. This work describes the gemological properties of these Rusgems synthetic opals.

Materials and Methods

15 black and white synthetic opals (0.77-1.24 ct.) and 12 natural white and crystal Australian opals (0.63-0.86 ct.) are studied for comparison. Gemological properties were collected on all samples, which appear semi-transparent to translucent, displaying blue and green play of color with various patterns (Figure 1). Two natural samples and two synthetics were analyzed for chemical compositions using EDXRF. Infrared spectra of all samples were recorded in the mid infrared (4000-400 cm^{-1}) range. Scanning electron microscopy (SEM) testing was performed on one synthetic sample.



Natural opals



Synthetic opals

Figure 1: Samples of some natural and synthetic opals

Result and Discussion

The Rusgems samples have S.G. value in the range of 2.2-2.24 slightly higher than the tested natural opals which show S.G. value of 2.03 to 2.13. Their refractive index cannot be measured. All natural opals fluorescence strong bluish white to long-wave UV and no reaction to short-wave UV. All Rusgems opals are inert to both long- and short-wave UV. Microscopic observation reveals white cristobalite (?) and brown hematite (?) presented in some natural samples (Figure 2). Chicken-wire or lizard skin pattern (Filin *et al.*, 2002; Schmetzer, 1984; and Smallwood, 2003) typical of synthetic opals cannot be observed in all synthetic samples (Figure 3).

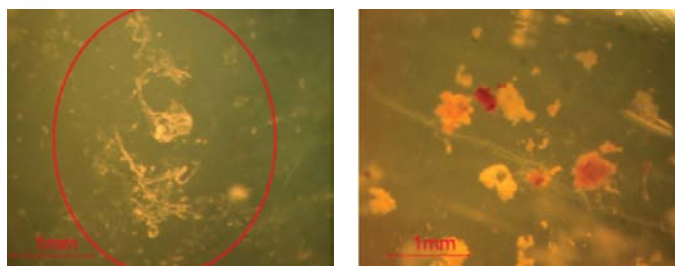


Figure 2: Inclusions of cristobalite? (**left**) and brown hematite? (**right**) in Australian natural opals

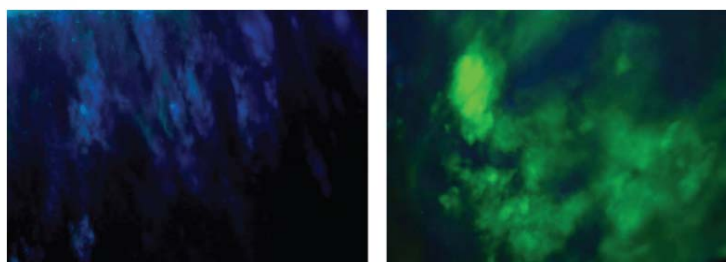


Figure 3: Lizard skin cannot be observed in synthetic opals

EDXRF analysis of natural opal detected Ca and Al as minor elements in addition to the main component Si. Small amount of Zr was found in the two synthetic opal samples while that in the natural ones was undetectable (Table 1).

Table 1 : Chemical composition of natural opal (Nat) and synthetic (Syn) in wt.%.

Specimen No.	SiO ₂	Al ₂ O ₃	CaO	ZrO ₂	Total
Nat_opl_05	98.68	0.54	0.78	-	100
Nat_opl_12	98.58	1.42	-	-	100
Syn_opl_05	98.66	-	-	1.34	100
Syn_opl_15	98.04	-	-	1.6	100

Scanning electron micrograph image of synthetic stone shows a loose staking of the sphere, unlike the structure of normal synthetic opal (Figure 4).

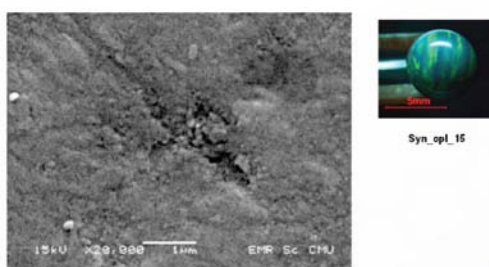


Figure 4 : SEM micrograph of synthetic opal structure (x 20000)

Mid-IR spectroscopic feature of synthetic samples are distinct from those of natural opal (Figure 5). The synthetic spectrum exhibits the distinct absorption peaks probably related to water and hydroxyl unit at ~ 3667 , 2850 , 2780 , and 2285 cm^{-1} . This result is consistent with synthetic opal from other company (Du Toit, 1996). No polymer peaks are detected.

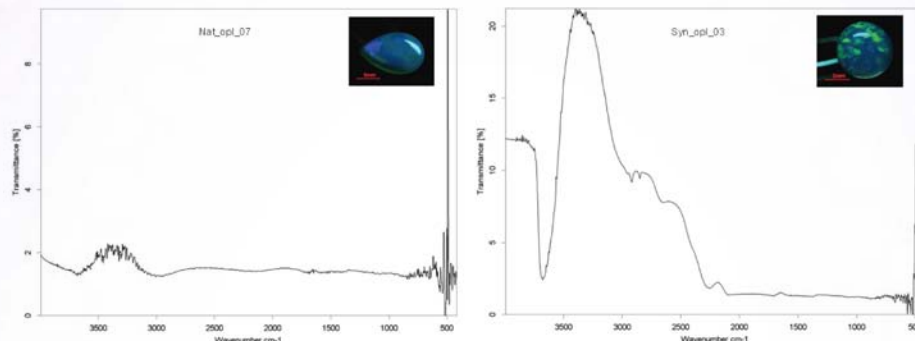


Figure 5: FTIR spectrum of natural (**left**) and synthetic opal (**right**)

Conclusion

An outstanding features of the Rusgems synthetic opals are the lack of the “lizard skin” feature which is the characteristic of synthetic opal, higher S.G. value than natural opal and the presence of Zr, which has been used for stabilizing opal, in their structure. Polymer is not presented in these Rusgems opals.

References

- Du Toit, G., 1996, Synthetic opal, Jewel Siam, Vol.13, No.7, p.78.
Filin, S.V., Puszynin, A.I., and Samoilov, V.N., 2002, Some aspect of precious opal synthesis, The Australian Gemologist, Vol.21, No.7, p.278-282. Schmetzer, K., 1984, An investigation of the synthetic products of Gilson showing a play of colors, The Journal of Gemology, Vol.19, No.1, p.27-41. Smallwood, A., 2003, 35 Year on new look at synthetic opal, The Australian Gemologist, Vol.21, No.11, p.438-447.

Corresponding Author

Full name: Panjawan Thanasutthipitak
Affiliation: Gemology program, Department of Geological Science, Chiang Mai University, Chiangmai, 50200 Thailand.
Phone: 089-6352175
Email: panjawan.t@cmu.ac.th

Russian Demantoid Color Heat Treatment

Roman Serov¹, Yuri Shelementiev¹, A. Serova¹, and Dmitry Filimonov²

¹*Gemological Center, Lomonosov Moscow State University, Moscow, Russia*

²*Chemistry Department, Lomonosov Moscow State University, Moscow, Russia*

Extended Abstract

Introduction

Demantoid is famous for its vivid green color and high dispersion. The heat treatment usually applies to improve the color and reduce brown tint of demantoids mined in Russia. Despite of numerous studies the causes of demantoid color alteration during the heat treatment process remain controversial.

Recent experiments with andradite garnets from Madagascar and Namibia (Chatagnier, 2012; Pezzotta, 2011) shown no color improvement during heat treatment. In our work, we focused on the heat treatment of demantoids from Russia and the reasons of its color alteration.

Samples and Methods

A set of untreated brown and green rough demantoid crystals from Karkodino, Urals, Russia was investigated. UV-VIS-NIR spectra were recorded on Ocean Optics QE65000 spectrometer in the range of 400-1100 nm, 30 scans. Mössbauer spectra were measured on MS 1104 Em Mössbauer spectrometer using a ⁵⁷Co radioactive source with activity of 50 microcurie. Samples were heated at temperature 650° C. The heating rate to the required temperature was carried out at 300°/hour. The cooling rate of the sample was at about 150°/hour. Air atmosphere was used for heat treatment in oxidizing conditions. Samples were sealed in crucible with charcoal powder for heat treatment in reducing conditions.

Results

All samples were heat treated at 4 successive stages (Figure 1) with different red-ox conditions and heat treatment duration.

First stage was performed in reducing atmosphere for 1 hour. All samples showed the reduction of brown tint. Initially brown samples became green.

Second stage was performed in oxidizing atmosphere for 2 hours. All samples became brown to orange-brown.

Stages three and four were performed in reducing atmosphere for 2 and 6 hours, respectively, and showed gradual decreasing of brown coloration in all samples.

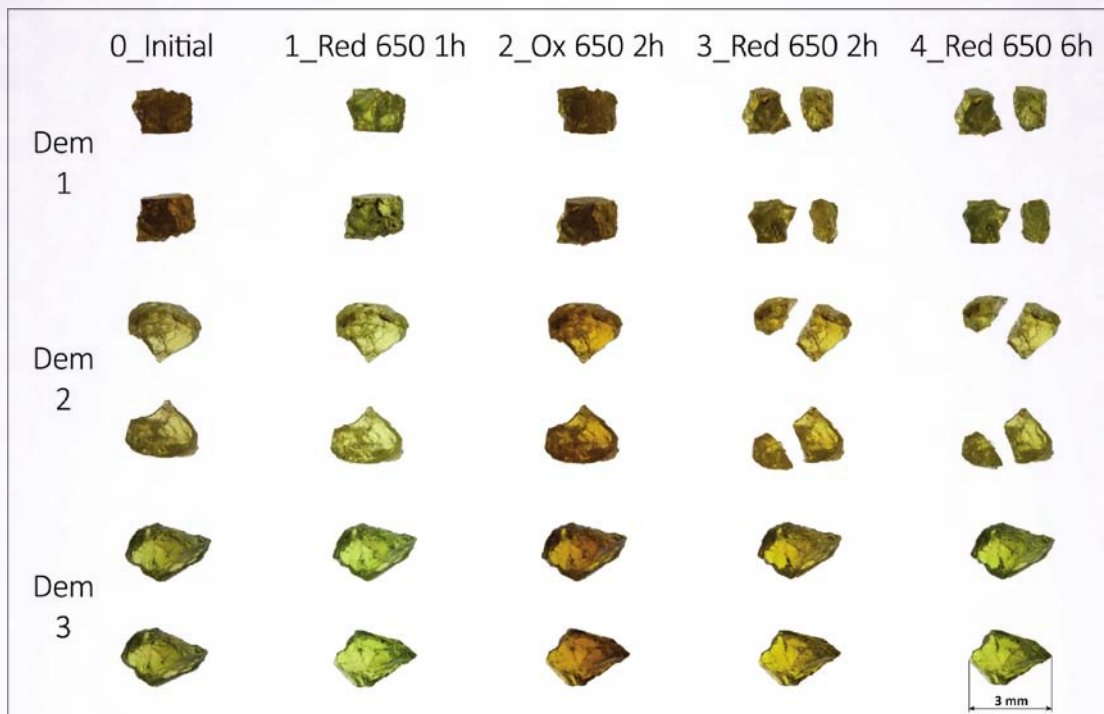


Figure 1: Demantoid crystals color alteration during heat treatment processes.

The VIS-NIR spectra of initial brown samples or samples with brown tint (Figure 2a) always show the edge of very broad absorption band with the center about 430 nm that determines the brown color of the sample. The character of that band resembles the absorption bands in melanite-schorlomite garnets (Locock, 1995) or pyralspite garnets (Platonov, 1991) where it was assigned to $\text{Fe}^{2+}\text{-Ti}^{4+}$ charge-transfer. Together with broad 430 nm band, the spectra show Fe^{3+} -related features at 855, 617 and 575 nm (Figure 2b). Some samples also exhibit Cr^{3+} -related absorption band at 621 nm (Figure 2c).

Heat treatment in oxidizing atmosphere results in the very effective formation of 430 nm band and changing the color of all samples to brown (Figure 1, the second and third column). There is no evidences that heat treatment in oxidizing atmosphere alters other Fe- and Cr-related absorption bands.

On the contrary, heat treatment in reducing conditions decreases the intensity of 430 nm band. In Figure 2d, the subtraction spectra between stage 1 and stages 2, 3, 4 are shown. It is clear that heat treatment in oxidizing atmosphere on stage 2 produces 430 nm band only, while the

absorption of Fe- and Cr-related bands remains exactly the same. The heat treatment at stages 3 and 4 in reducing conditions can progressively decrease the intensity of 430 nm band.

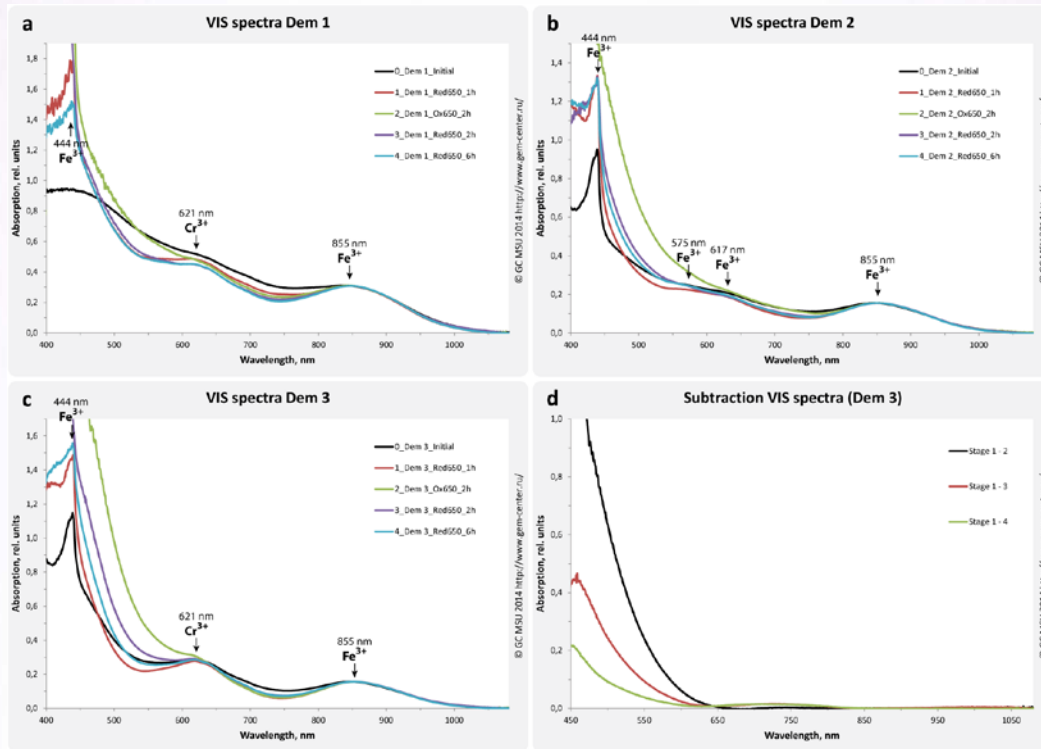


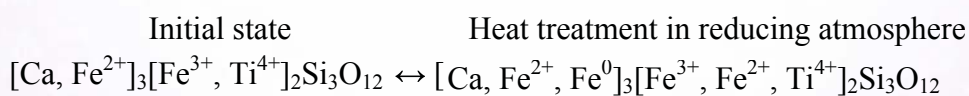
Figure 2: VIS-NIR spectra of demantoid samples during heat treatment processes.

Mössbauer spectra of unheated brown and green samples shows only Fe³⁺ in octahedral site (Figure 3). Spectra after the heat treatment in reduced conditions exhibit the remaining Fe³⁺ as well as Fe²⁺ in octahedral site and weak lines of metallic α-Fe.

Conclusion

Series of experiments in different conditions show that the color of demantoid could be altered from brown to green in reducing condition and back to brown again in oxidizing condition. The most probable cause of color changes is determined by the oxidation state of iron and/or titanium in garnet structure and thus remains reversible.

The most probable reason of brown coloration for studied samples from Karkodino is Fe²⁺-Ti⁴⁺ charge-transfer as it has been established in other garnets (Platonov, 1991). Fe²⁺-Fe³⁺ charge transfer seems to be unlikely the reason of brown color. As noted by Taran (2007) Fe²⁺-Fe³⁺ charge transfer required much higher concentrations of Fe²⁺ than those occur in demantoid garnets. The following scheme describing the heat treatment process can be suggested:



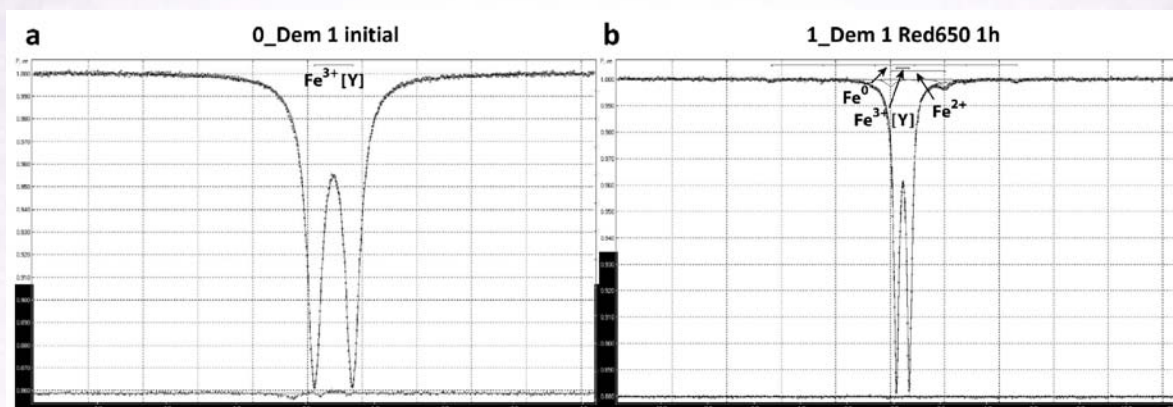


Figure 3: Mössbauer spectra of sample Dem 1 before heat treatment and after heat treatment in reducing atmosphere for 1 hour.

References

- Locock, A., Luth, R.W., Cavell, R.G., Smith, D.G.W., and Duke, M.J.M., 1995, Spectroscopy of the cation distribution in the schorlomite species of garnet, *American Mineralogist*, Vol.80, No.1-2, p.27-38.
- Pezzotta, F., Adamo, I., and Diella, V., 2011. Demantoid and topazolite from Antetazambato, northern Madagascar: review and new data, *Gems & Gemology*, Vol.47, No.1, p.2-14.
- Pierre-Yves, C., 2012, Le traitement thermique de l'andradite, *DIPLÔME D'UNIVERSITÉ DE GEMMOLOGIE*, 77 p.
- Platonov, A.N, Langer, K., Matsuk, S.S, Taran, M.N., and Hu, X., 1991, Fe²⁺-Ti⁴⁺ charge-transfer in garnets from mantle eclogites, *European Journal of Mineralogy*, Vol.3, No.1, p.19-26.
- Taran, M.N., Dyar, M.D., and Matsyuk, S.S., 2007, Optical absorption study of natural garnets of almandine-skiagite composition showing intervalence Fe²⁺ + Fe³⁺ → Fe³⁺ + Fe²⁺ charge-transfer transition, *American Mineralogist*, Vol.92, No.5-6, p.753-760.

Corresponding Author

Full name: Roman Serov
Affiliation: A-429, Leninskie gory, GSP-1, Gemological Center, Lomonosov Moscow State University, Moscow, Russia.
Phone: +7-926-561-04-16
Email: potom_skajy@mail.ru

Separation of Natural Argyle Pink and Blue Diamonds from New Generation of CVD-Grown Diamonds in Asia

Branko Deljanin¹ and Adolf Peretti²

¹CGL – GRS Swiss Canadian Gemlab, 510-409 Granville street, Vancouver, BC V6C 1T2, Canada

²GRS GemResearch Swisslab, Switzerland

Extended Abstract

The Argyle mine in Western Australia has been the major source of natural pink diamonds since the 1980s, and 90 per cent of the world's supply of pink diamonds come from this source. Argyle also produce rare gray-violet-blue type Ia diamonds that could be separated from type IIa boron rich diamonds from other world localities. There has been an increasing number of synthetic diamonds in the jewelry market over the past decade, and they can be irradiated and annealed to produce pink color. We are reporting on 'natural looking' CVD-grown treated pink and as-grown blue (Si doped) type IIa diamonds by Orion (PDC) company in Hong Kong. They could be separated from similar looking natural pink and blue diamonds from Argyle mine by using of combination of standard instruments (cross polarized filters, UV lamp) and advanced spectrometers (UV-VIS, FTIR and PL at LN temperatures).

Samples and Methods

50 natural and 10 CVD-grown pink and gray-blue loose diamonds from 0.05 to 1.20 carats were studied using standard and advanced (UV lamp at 254nm and 365nm, cross polarizers, gemological microscope, visible and infrared spectrometer) instruments at CGL-GRS in Vancouver and research instruments (infrared and custom-made visible and photoluminescence spectrometers at liquid nitrogen temperature) at GRS gem labs in Hong Kong and Lucerne.



Figure 1: Variety of natural colours of Argyle (**left**) and CVD-grown by Orion (**right**) pink and blue diamonds.

Results with Standard Instruments

Visually, CVD-grown pink and blue diamonds by Orion Diamond company look similar to natural Argyle diamonds because they are not as saturated as irradiated HPHT-grown or natural pink and blue diamonds. CVD-grown Orion diamonds are of high clarity (VS and higher) and it's difficult to separate them from natural by microscopy only, though pink ones are likely to have blackish and colourless inclusions.

A quick screening of loose and mounted diamonds is possible by using strong **UV illumination** in a dark room. Argyle pink diamonds fluoresce medium to strong blue under LWUV and a bit weaker under SWUV while Orion CVD-grown and treated pink fluoresce strong orange under both LW and SW light. Argyle blues usually fluoresce medium yellow under LW and weak yellow under SW (due to hydrogen) and Orion CVD-grown blue diamonds in most cases shows no reaction, both to LWUV and SWUV excitation.

The **birefringence patterns** of natural Argyle diamonds of type Ia are well recognized (intense interference colours, sample on the left). Whereas the birefringence of CVD-grown diamonds, have distinct differences that assist with identification of these diamonds. All new pink and blue colour CVD samples are type IIa diamonds. Observed between cross-polarized filters, they produce two general patterns: 1) a natural-looking pattern similar to 'tatami pattern' of type IIa natural diamonds, and 2) typical CVD pattern with strong parallel "columnar" pattern perpendicular to the table (sample on the right).

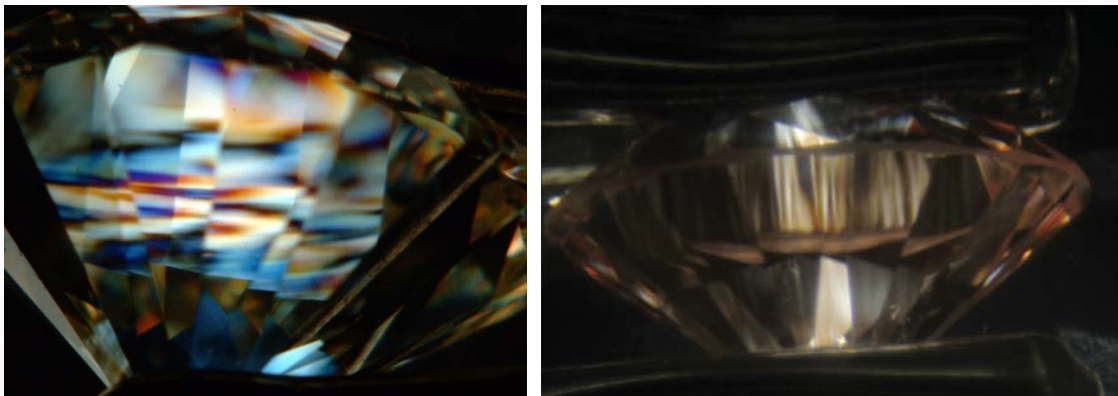


Figure 2: Images of Argyle (**left**) and pink (**right**) CVD-grown diamonds by Orion under Cross Polarized Filters.

Results with Advanced Instruments

FTIR spectroscopy

Natural Argyle pink diamonds are type IaAB having low concentrations of nitrogen with typically more in B form than A form. Orion CVD-grown diamonds are type IIa with negligible absorption of nitrogen at 1450 (H1a centre), 1340 and 1332 (N+ centre) and some display a peak at 3107 cm^{-1} related to hydrogen. Gray-violet-blue Argyle natural diamonds are typically IaAB with very high amounts of nitrogen and hydrogen. The CVD-grown blue diamonds by Orion reveal no presence of boron or nitrogen, thus they can be classified as type IIa, though sometimes with 1332 cm^{-1} peak (N+ centre).

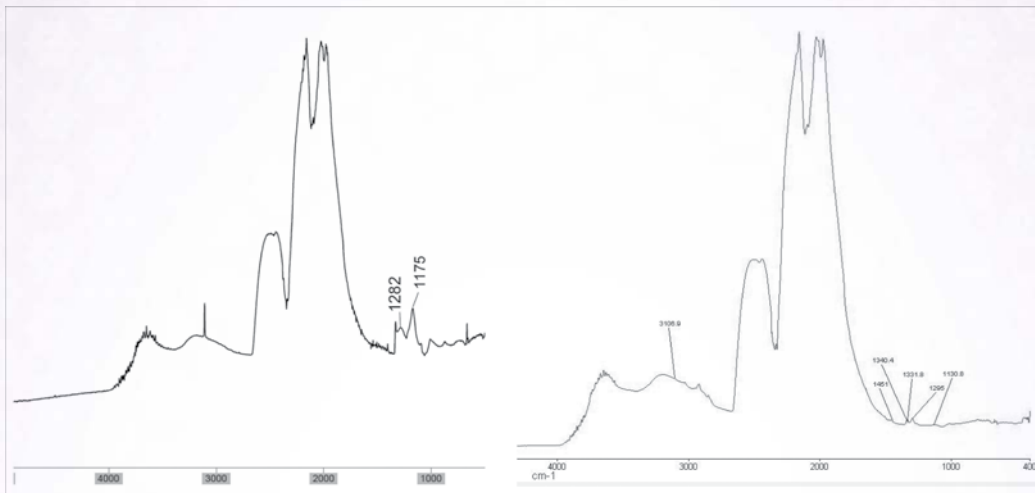


Figure 3: Typical infrared spectra of Argyle type Ia pink (**left**) with higher B (1175 cm^{-1}) nitrogen than A (1282 cm^{-1}) nitrogen aggregation next to infrared spectra of CVD-grown pink type IIa (**right**) diamond with N^+ traces (1131.8 cm^{-1})

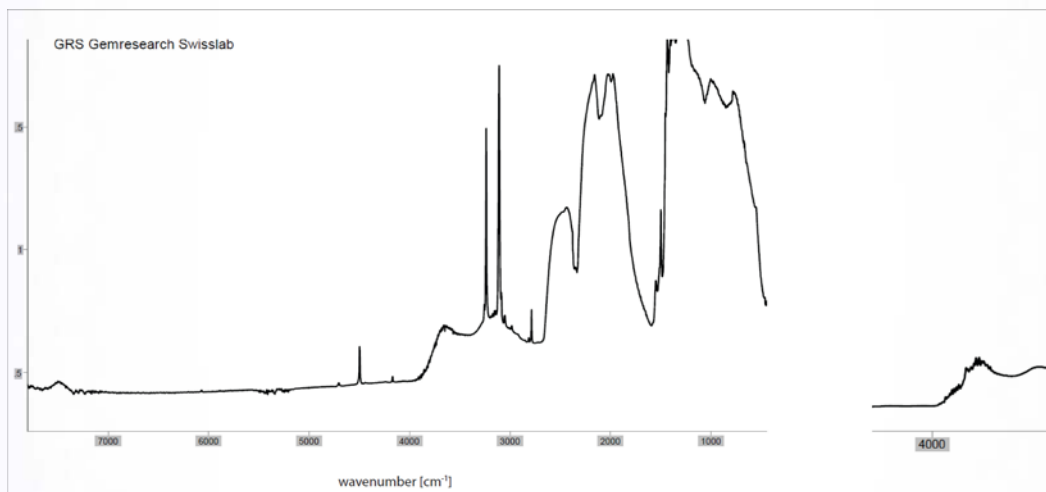


Figure 4: Infrared spectra of natural grayish blue Argyle type Ia diamond with very high hydrogen (3107 and 3237 cm^{-1}) type IIa spectra of CVD-grown gray-blue diamond by Orion with traces of N^+ center (1131 cm^{-1}).

UV-VIS-NIR and PL spectroscopy

The main absorption feature in the visible spectrum distinguishing the studied natural Argyle pink diamonds from their CVD-grown and treated counterparts is a pronounced N_3 center, which together with the 550 nm band (“Natural” Pink Band) and the 380 nm band are the dominating color centers. A very intense SiV^- centre with zero-phonon line at 737 nm (the most characteristic optical centre of CVD-grown diamonds) was found as the dominating feature in both absorption and PL spectra of CVD pink and blue diamonds. Although the absorption spectrum of SiV^- centre has a very complex multi-line structure in CVD-grown Orion blue diamonds, on average, its development over the visible spectral range is similar to that produced by boron. The UV-Vis-NIR spectra of Argyle gray-violet-blue diamonds are characterized by a strong bands around 545 and 730 nm.

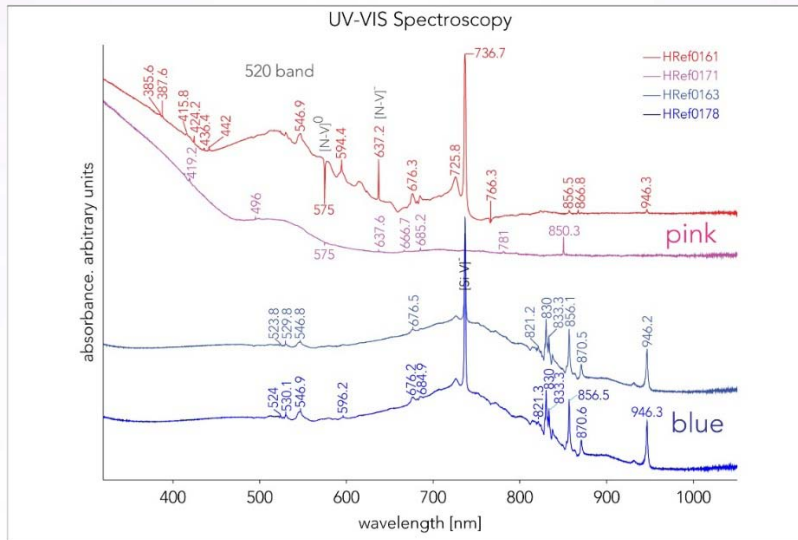


Figure 5: Common feature for both pink and blue CVD-grown diamond in UV-VIS spectra is strong Si-V center at 737 nm.

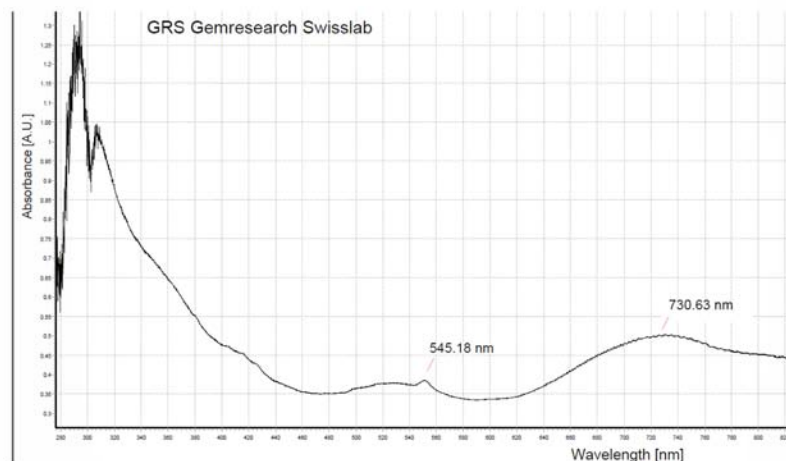


Figure 6: UV-VIS spectra measured at LN temperature of Argyle blue diamond.

Discussion

As fancy natural diamonds increase in price to world-record levels, the technology to make imitations of natural colored diamonds using synthetic diamonds is ready now. Pink colour in CVD-grown diamonds by Orion is caused by a 520 nm band from the nitrogen related N-V center (induced by irradiation and annealing). Blue color of CVD-grown diamonds can be induced by boron, and most recently, with silicon as discussed here. We are reporting that the new generation of lab-grown colored CVD-grown diamonds have appeared on Asian market, but they could be separated from natural blue and pink diamonds of similar color (like Argyle) in well-equipped gem laboratories. Other “natural-looking” colors are also possible to produce with CVD technology with different dopants or treatment techniques (like HPHT), which are current research project of GRS and CGL-GRS labs.

Today, there is increasing number of facilities that grow diamonds, especially in Asia due to lower production costs. It appears that the CVD technology is increasingly employed to grow both near-colorless and colored diamonds (brown, yellow, pink and blue). In comparison to pink CVD-grown diamonds, blue CVD-grown diamonds are still relatively rare on the diamond market.

Acknowledgements

Authors is grateful to M. Alessandri and W. Biéri of GRS GemResearch Swisslab in Hong Kong and Switzerland for joint research on natural and synthetic pink and blue diamonds and J. Chapman of Rio Tinto Diamonds for supplying natural Argyle pink diamonds for testing.

References

- Peretti, A., Herzog, F., Bieri, W., Alessandri, M., Günther, D., Frick, D., Cleveland, E., Zaitsev, A.M., and Deljanin, B., 2014, New Generation of Synthetic Diamonds Reaches the Market: Lab-grown Blue, Pink and Yellow CVD Diamonds (Part A, B, C 3 articles), Contribution to Gemology, March 2014, No.14.
- Simic, D., and Deljanin, B, 2010, Identifying Diamond Types and Synthetic Diamonds with CPF (Cross Polarized Filters)', GHI Booklet.

Corresponding Author

Full name: Branko Deljanin
Affiliation: CGL – GRS Swiss Canadian Gemlab, 510-409 Granville street, Vancouver, BCV6C 1T2, Canada.
Phone: 1(604) 687-0039
Fax: 1(604) 687-0091
Email: info@cglworld.ca

Spectroscopic Characterization of Electron-Beam Irradiated Zircon

Sungwon Park¹, Sora Shin² and Jongwan park²

¹Material Science and Engineering, Hanyang University / Gemological engineering, Seoul Korea

²Material Science and Engineering, Hanyang University, Seoul Korea

Extended Abstract

Most natural gem quality zircons shows pale brown or yellowish to reddish brown colors. But heat treatment can be carried out to change brown color to blue or colorless which are more preferable color in the gem.

The crystal structure of the zircon ($ZrSiO_4$) consists of linked tetrahedral SiO_4 and polyhedral ZrO_8 . There are four $ZrSiO_4$ molecules per unit cell. The ZrO_8 polyhedral are related to each other by rotations of 90° about the c-axis, implying that the four substitutional Zr^{4+} sites should be magnetically indistinguishable (Nassau, 1978).

In this study, we performed spectroscopic analysis of natural zircon before and after electron-beam irradiation in order to investigate the changes in color of brown zircon and the cause of color formation by electron beam irradiation. The starting materials were classified into three groups including colorless, light blue and reddish brown according to the predominant color observed as showed in Figure 1.



Figure 1: Sample collection in this study: **(A)** colorless, **(B)** light blue and **(C)** reddish brown.

We performed irradiation with electron dose densities of $1 \times 10^{17} / \text{cm}^2$ at 10 MeV for one hour and the sample spectra were recorded for comparative analysis before and after electron-beam radiation using UV-Vis, FT-IR spectroscopies.

The composition in weight % of the elemental components of the zircon samples were determined by WD-XRF spectroscopy. Zircon samples contain high Zr and Si, low Sn and Hf, and very traces amounts of other elements as shown Table 1.

Table 1: Chemical composition of representative zircon samples by wavelength dispersive X-ray fluorescence (wt %).

Element (wt.%)	No.1 Colorless	No.2 Light blue	No.3 Reddish brown
Zr	47.991	46.95	51.069
O	35.457	33.643	30.005
Si	16.133	15.746	16.290
Sn	0.183	0.491	1.03
Hf	-	0.704	0.939
Nb	0.082	0.078	0.109
Fe	-	0.034	0.419
Ti	0.012	-	0.081
Cu	-	0.043	0.026
Zn	-	-	0.019

Figures 2 and 3 show the UV-Vis absorption spectra of the zircon before and after electron beam irradiation respectively. The zircon samples of colorless, light blue, reddish brown color were all changed to dark brown color by electron beam irradiation. The absorption bands were observed at 500~550 nm. These absorption bands were attributed to the hole center (Lang and Zhang, 2008).

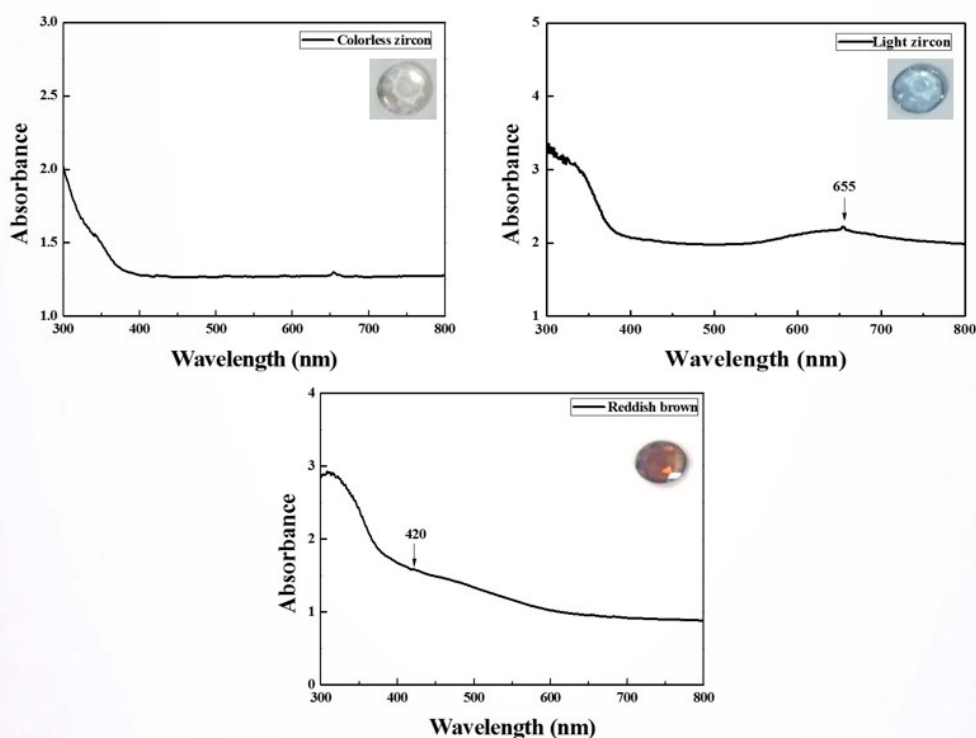


Figure 2: The UV-Vis absorption spectra of the natural zircon. (Top left) colorless, (Top right) light blue, and (Bottom) reddish brown.

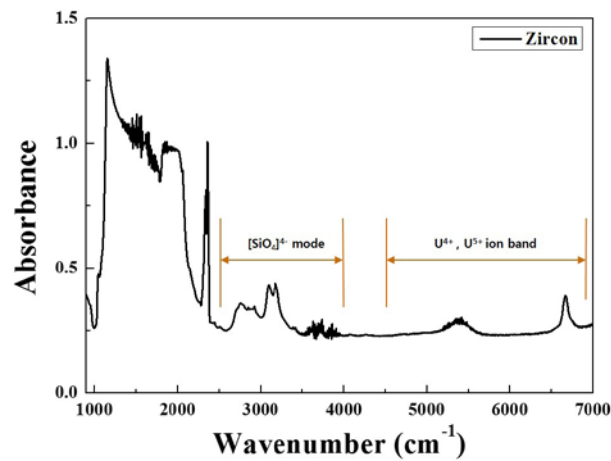


Figure 3: The UV-Vis spectra zircon samples after electron beam irradiation.

FT-IR spectroscopy analysis of zircon samples showed that 3-phonon combination mode of $[\text{SiO}_4]^{4-}$ internal vibration in the region of $3100\text{--}3400\text{ cm}^{-1}$ are broad and some of them disappear. Also, U^{4+} peak which can detect the uranium content in zircon appears at near 4800 cm^{-1} as shown Figure 4. (Laruhin *et al.*, 2002)

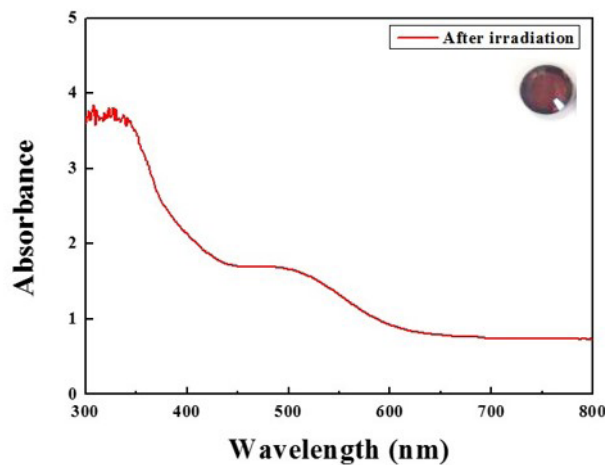


Figure 4: The FT-IR absorption spectra of the natural zircon.

References

- Lang, M., and Zhang, F., 2008, Irradiation-induced stabilization of zircon (ZrSiO_4) at high pressure, *Earth and Planetary Science Letters*, Vol.269, No.1-2, p.291-295.
- Laruhin, M.A., van Es, H.J., Bulka, G.R., Turkin, A.A., Vainstein, D.I., and den Hartog, H.W., 2002, EPR study of radiation-induced defects in the thermoluminescence dating medium Zircon (ZrSiO_4), *Journal of Physics: Condensed Matter*, Vol.14, No.14, p.3813-3831.
- Nassau, K., 1978, The origins of color in minerals, *American Mineralogist*, Vol.63, No.3-4, p.219-229.

Corresponding Author

Full name: Jong-Wan Park

Affiliation: Division of Materials Science & Engineering, Hanyang University, Seoul
133-791, Korea.

Phone : +82-2-2220-0386

Fax : +82-2-2298-2850

Email: jwpark@hanyang.ac.kr

Thermal Enhancement of Zircon Samples from Chanthaburi and Kanchanaburi Provinces, Thailand and Rattanakiri, Cambodia

***Rattanawalee Chooyoung, Natthapong Monarumit, Chakkrich Boonmee,
Aumaparn Phlayrahan, and Somruedee Satitkune***

*The Gem and Mineral Sciences Special Research Unit, Department of Earth Sciences, Faculty of Science, Kasetsart University,
Bangkok, 10900, Thailand*

Extended Abstract

Introduction

Natural zircon mainly shows brown to reddish brown color. Brown zircon is poorly demanded whereas blue zircon is beautiful, popular and expensive in gems market. Thus, the enhancement of valueless zircon samples is the most important method to improve their quality, value and color. Heat treatment of zircon is popular method for a decade. Satitkune *et al.* (2013) and Therdteppitak *et al.* (2007) reported that the brown coloration of zircon could be changed to blue, causing of color center, by heat treatment. The Thailand Institute of Nuclear Technology (n.d.) and Trongsilat (2008) also reported that the gamma irradiation can turn the color of zircon from colorless to brown or red. Therefore, this study is focused on the color improvement of zircon samples from Kanchanaburi and Chanthaburi Provinces, Thailand and Ratanakiri, Cambodia by thermal enhancement.

Materials and Methods

The zircon samples were selected from Kanchanaburi and Chanthaburi Provinces, Thailand and Ratanakiri, Cambodia (Figure 1). The conditions of this study are summarized as Flowchart in Figure 2. The absorption spectra of samples in UV-Vis-NIR range (~350-2000 nm) were acquired by Perkin-Elmer UV-Vis-NIR spectrophotometer, Lambda 900 model.



Figure 1: Zircon samples used in this study.

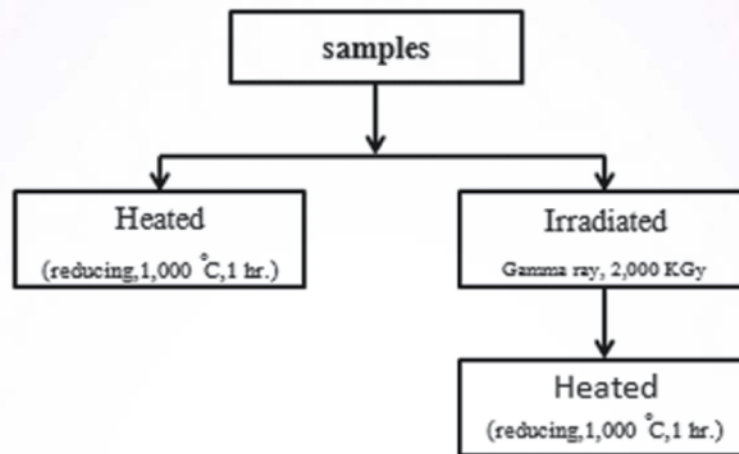


Figure 2: Flowchart of the conditions of the experiment.

Results and Discussions

The zircon samples from Kanchanaburi and Chanthaburi Provinces, Thailand and Ratanakiri, Cambodia show the distinct change of their colors after subjected to various types of treatment condition Table 1.

Table 1: Colors of zircon samples before and after treatments

Source	Natural color	Heating	After Irradiation	After Irradiation followed by Heating
<u>Kanchanaburi</u>	Brown-reddish brown	Colorless	Dark reddish brown	Colorless
<u>Chanthaburi</u>	Brown-reddish brown	Blue	Dark reddish brown	Blue
<u>Ratanakiri</u>	Brown-reddish brown	Dark blue	Dark reddish brown	Blue

The UV-Vis-NIR absorption spectra of those zircon samples were measured before enhancement showing the absorption band around 600 nm to the UV range causing by color center (Satitkune *et al.*, 2013; Therdteppitak *et al.*, 2007). The intensity of absorption peaks at 1100 and 1500 nm are due to U⁵⁺ content related with the brown color degree (Satitkune *et al.*, 2013; Therdteppitak *et al.*, 2007) shown in Figure 3a.

After heat treatment, zircon samples from Chanthaburi and Ratanakiri show the absorption band around 650 nm assigned to U⁴⁺. However, there are no such absorption band in colorless zircon samples from Kanchanaburi (Figure 3b).

The irradiated zircon samples show absorption band around 600 nm to UV region. The intensity of band increases after irradiation relating to the appearance of the darker brown color. As irradiation normally creates defects in crystalline structure; hence, this treatment confirms that the naturally brown coloration of zircon is due color center. On the other hand, the absorption peaks of U^{5+} at 1100 and 1500 nm decrease (Figure 3c). Moreover, the spectra of irradiated samples followed heating show the absorption band around 650 nm (U^{4+}) and strong absorption peaks at 1100 and 1500 nm (Figure 3d). From those of UV spectrum, these data should be meticulously study more in the future.

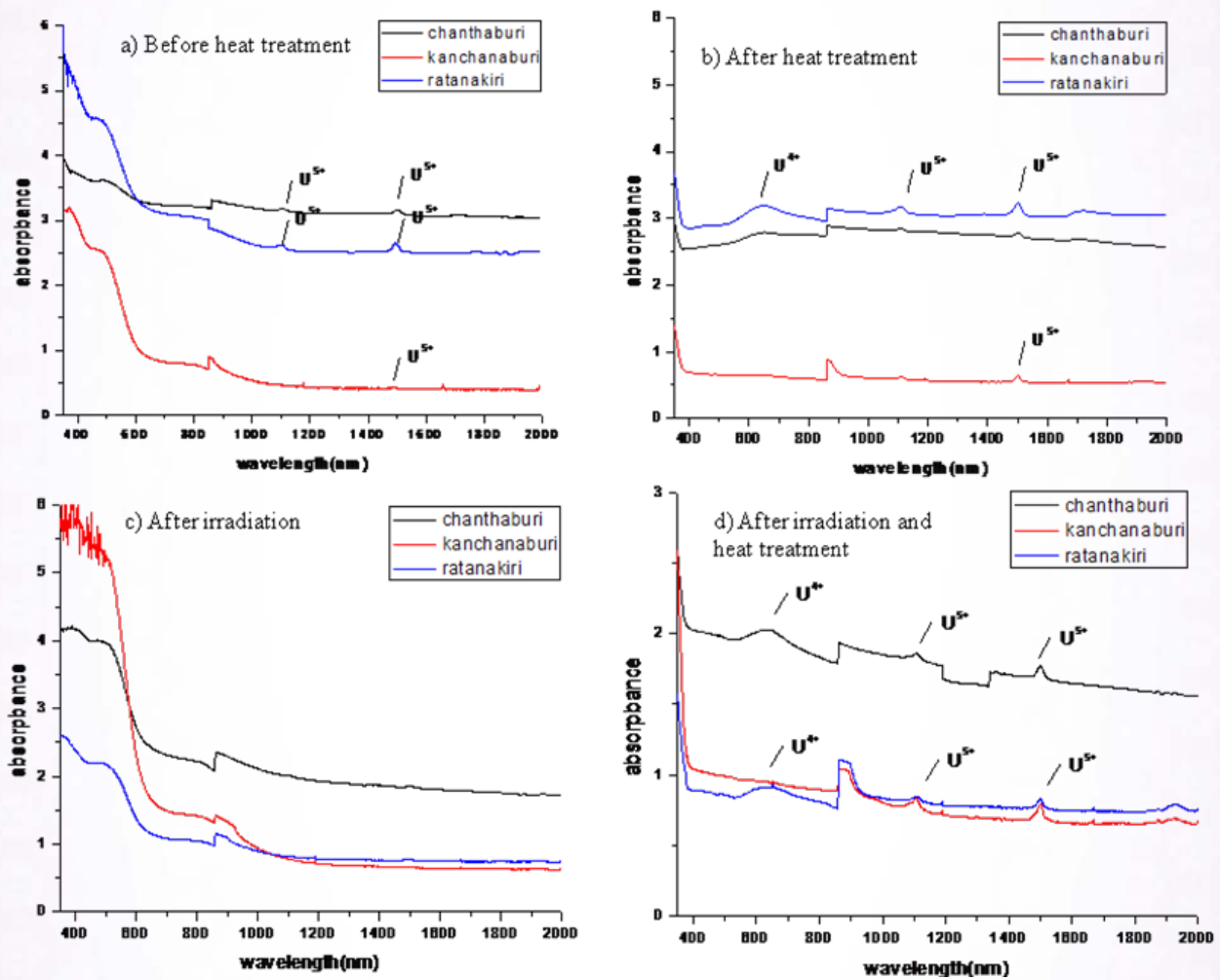


Figure 3: UV-Vis-NIR absorption spectra of zircon samples at different condition.

Conclusions

After thermal enhancement, zircon samples from Chanthaburi and Ratanakiri change from brown to blue colors, however, the samples from Kanchanaburi change from brown to colorless. The irradiation followed by heating can turn the color of zircon samples from Chanthaburi and Ratanakiri from brown to blue, while those from Kanchanaburi from brown to colorless.

Reference

- Satitkune, S., Wanthanachaisaeng, B., Won-in, K., Wongkokau, W., Chantararat, P., Leelawattasuk, T., and Wathanakul, P., 2013, Heat treatment of zircon samples from Kanchanaburi, Thailand and Ratanakiri, Cambodia, 33rd International Gemmological Conference (IGC 2013), 182, p.158-160.
- Thailand Institute of Nuclear Technology, (n.d.), Gems Enhancement by Nuclear Technology, Available from <http://www.tint.or.th/gems/gems5102.html>, accessed 28 August 2014.
- Therdteppitak, A., Thongnopkun, P. and Chindudsadegul, P., 2007, Color development of zircon by heat treatment, Gems College, Burapha University, Chanthaburi IT Campus, Chanthaburi, 52 p.
- Trongsilat, W., 2008, Color alteration of failed heat treated zircon by Gamma Irradiation, Abstract in M.S. Thesis, Department of Nuclear Technology, Chulalongkorn University, 1 p.

Acknowledgement

The authors gratefully acknowledge the supporting from The Gem and Mineral Sciences Special Research Unit, Department of Earth Sciences, Faculty of Science Kasetsart University.

Corresponding Author

Full name: Rattanawalee Chooyoung
Affiliation: Department of Earth Sciences, Faculty of Science, Kasetsart University, 50 Ngamwongwan Road, Ladyao, Chatuchak, Bangkok, 10900, Thailand.
Phone: 0-2940-6966
Email: rattanawalee.c@gmail.com

Treated “Black Sapphire” Update

**Thanong Leelawatanasuk¹, Namrawee Susawee¹, Saengthip Saengbuangamlam¹,
Supparat Promwongnan¹, Nicharee Atsawatanapirom¹, Wilawan Atichat¹,
Visut Pisutha-Arnon^{1,2} and Boontawe Sripasert^{1,3}**

¹The Gem and Jewelry Institute of Thailand (Public Organization), Bangkok, 10500, Thailand

²Department of Geology, Faculty of Science, Chulalongkorn University, Bangkok, 10330, Thailand

³Department of Mineral Resources, Bangkok, 10400, Thailand

Extended Abstract

Introduction

Diffusion treated corundum was introduced to the gem market in the late 1970s (Kane *et al.*, 1990). The process involved high-temperature heating of colorless or near-colorless corundum mixed with chemicals in crucible for a long time. Such treatment could allow color-causing elements (such as titanium for blue coloration, or chromium for red one) to penetrate into the gem surfaces and produced the desired gem products.

In January 2014, a parcel of gem, sold as “black sapphire” in the market, was submitted for identification at Gem Testing Lab of the Gem and Jewelry Institute of Thailand (GIT-GTL) by a gem treater. After testing (see GIT LAB INFO by Leelawatanasuk and Maneekrajangsaeng, January 2014), it was found that this gem material was not black sapphire but actually was a very dark blue treated stone. The starting raw material for this treated gem was low-quality, near-colorless-to-pale-colored sapphire with abundant open fissures from metamorphic origin (Leelawatanasuk and Maneekrajangsaeng, 2014). Hence, Ti-diffusion technique could create dark blue color zones extending outward from the fissures inside the stone and make it look very similar to a black sapphire.

Seven months later, in August 2014, GIT-GTL received another two unusual black stones for identification from a gem trader who informed that these stones were also sold as “black sapphire” in the market. This new set of black sapphire is different from the previous one in some aspects. This article will describe the characteristics of this new material.

Material and Methods

The two “black sapphire” samples are faceted stones that come in mixed cut, oval shapes, weighing 1.54 and 1.80 cts., respectively (Figure 1).

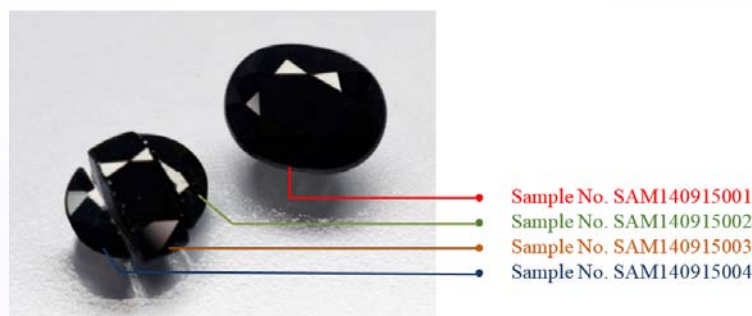


Figure 1: The stone on the left was sliced into three pieces and weighs totally 1.54 ct., and the one on the right weighs 1.80 ct. Photo by S. Saengbuangamlam.

As a routine testing, both stones were examined for standard gemological properties, such as refractive index (RI), specific gravity (SG), pleochroism, fluorescence and internal features under different lighting conditions and immersion method. For advanced testing, we used Fourier Transform Infrared Spectrometer (FTIR, model Nicolet 6700), UV-VIS-NIR spectrometer (Model Lambda 950), Soft X-Ray radiograph and Energy Dispersive X-ray Fluorescence Spectrometer (EDXRF, model Eagle III) and Raman Spectroscopy (Renishaw, InVia) to collect their specific spectroscopic data.

Results

General properties

On first observation, these two stones appeared extremely dark blue color to almost black with low transparency under daylight-equivalent light (Figure 1). The standard gemological properties of these stones are generally consistent with natural sapphire. These two stones are of double refractive substance with the RI values of 1.760- 1.770 and SG values of 3.950- 4.010. These stones showed none to moderate dichroism from blue to greenish blue through a dichroscope and no fluorescence under both LWUV and SWUV.

Microscopic features

Microscopic examination is a very important technique for the identification of this treated gem material. Under magnification with normal illumination, the stones clearly revealed many healed fissures which made it difficult to find natural inclusions (Figure 2). However, fiber-optic lighting technique would be very helpful method to find blue color concentration along the healed fissures throughout the whole stones (Figure 3).

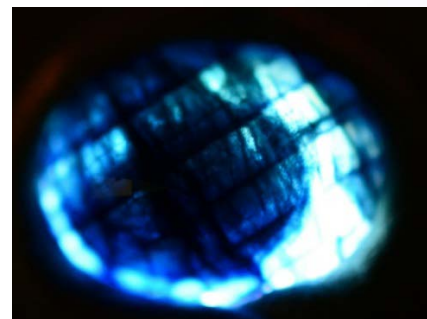


Figure 2: Many healed fissures with color concentration throughout the whole stone, noted also the white spots of residue material left-over along healed fissures after treatment (Sample No. SAM-14091500; left picture, 20x magnification; right picture, enlargement of the square area on the left picture, 40x magnification). Photos by S. Saengbuanglam.

Figure 3: Color concentration along healed fissures. Photo by S. Saengbuanglam

Due to the lack of transparency of these two stones, we decided to cut one stone (1.54 ct) into 3 pieces in order to see more inclusions and provide more accurate results of advanced testing. The polished slabs (~1 mm) revealed many features indicating the natural origin of raw material, such as cloud of silk pattern (Figure 4) and repeated twinning (Figure 5).

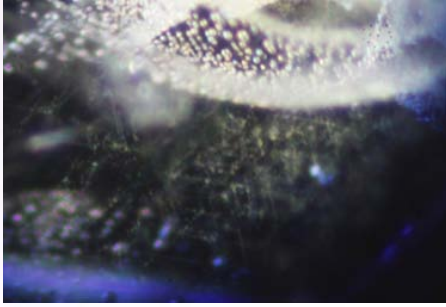


Figure 4: Cloud of silk pattern under darkfield illumination (50x magnification). Photo by N. Atsawatanapirom.

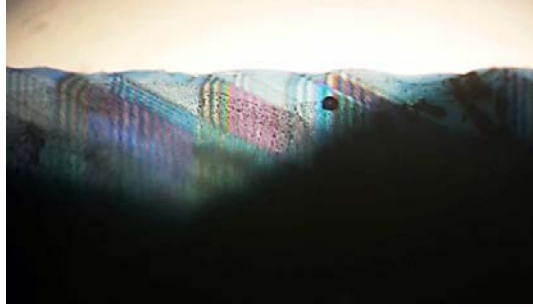


Figure 5: Repeated twinning seen under immersion in di-iodomethane solution. Photo by S. Saengbuangamlam.

Immersion in di-iodomethane (methylene iodide) revealed the unusual color concentration along healed fissures due to diffusion of color-causing element(s) outward from the fissures into the host sapphire. Blue color rim is also observed along the stone surface outline indicating color penetration inward from outside of the stone (Figure 6).

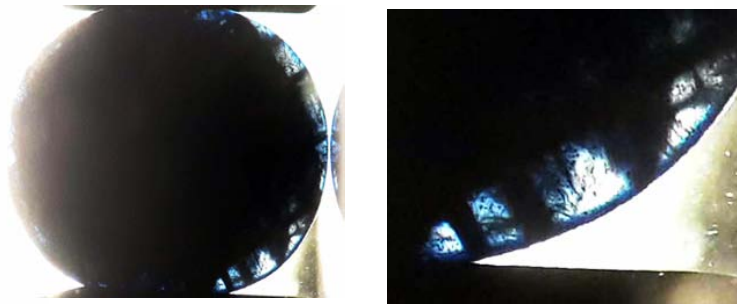


Figure 6: Color concentration along healed fissures and blue color rim along the stone surface outline seen under immersion in di-iodomethane solution. Photos by S. Saengbuangamlam.

Advanced instrumental analyses

We further collected the data on a polished slab and a faceted sample with DiamondView™, FTIR spectrometer, UV-Vis-NIR spectrometer, and EDXRF to help making more conclusive identification. Even though, the samples were inert in normal LWUV and SWUV lights, with high-intensity ultra-shortwave UV radiation of the DiamondView™ (~225nm), however, all samples showed strong chalky blue fluorescence along the healed fissures (Figure 7).

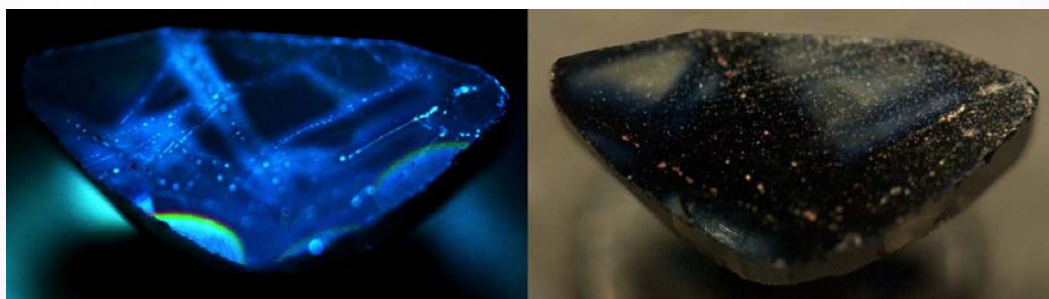


Figure 7: DiamondView™ images showing strong chalky blue fluorescence zones and bright dots in the slab sample no. SAM140915003 (**left**, SWUV light) that correspond to the dark blue diffusion bands and dots of residue material along the healed fissures (**right**, normal light). Photos by S. Promwongnan.

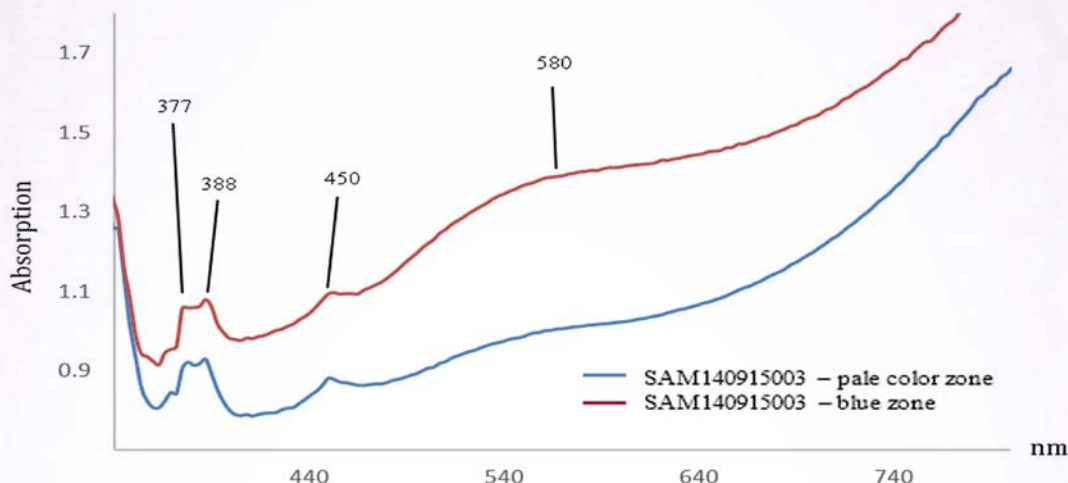


Figure 8: These non-polarized UV-Vis absorption spectra illustrating the differences in the blue and paler color zones of the slab sample no. SAM140915003, the spectra merely displayed up to 800 nm due to signal error at higher nm region.

As shown in Figure 8, the UV-Vis-NIR spectra of the sample clearly reveal iron-related absorption peaks at 377, 388, 450 nm, and $\text{Fe}^{2+}/\text{Ti}^{4+}$ Intervalent charge transfer (IVCT) at ~ 580 nm as well as $\text{Fe}^{2+}/\text{Fe}^{3+}$ IVCT absorption bands at ~ 900 nm that are perfectly matched the GIT reference spectra for “basaltic blue sapphire”. Notably the absorption spectrum of the blue zone shows higher intensity of $\text{Fe}^{2+}/\text{Ti}^{4+}$ IVCT absorption band near 580 nm than that found in the paler color zone of the same slab sample.

In order to determine the elements which cause the dark blue color, EDXRF analysis was also carried out. For the whole stone, we detected the major amounts of Al with minor to trace amounts of Fe, Ti, V, Cr and Ga without Pb, Bi or Ba. For the polished slab (no. SAM140915003), we analyzed the blue and paler color areas for comparison. It was found that both areas contained similar contents of Fe, V, Cr, and Ga, but the amount of Ti content of the blue area was higher than that in the paler color area.

Discussion and Conclusions

According to the ‘black sapphire’ article by Leelawatanasuk and Maneekrajangsaen in January 2014, those diffusion-treated stones were blue to dark blue in color and they were treated from starting raw material of metamorphic origin. Whereas the samples under this investigation apparently look much darker blue to almost black and their starting raw materials are basaltic sapphires. Although the internal characteristics of these samples are quite similar to the previously treated black sapphires, some different results are obtained due to the difference of the raw materials. Based on above testing, it seems to suggest that these stones were subjected to a common type of Ti-diffusion treatment using starting raw materials which were not white sapphire but were of light-blue-to-blue, low-quality and heavily fractured ones. Hence, these new products are recommended to be called “diffusion-treated black sapphire”, rather than ‘black sapphire’ in the market.

Acknowledgements

The authors sincerely appreciate the GIT director and her staff for supporting this research project.

References

- Kane, R. E., Kammerling, R. C., Koivula, J. I., Shigley, J. E., and Fritsch, E., 1990, The identification of blue diffusion-treated sapphires, *Gems & Gemology*, Vol. 26, No. 2, p.115-133.
- Leelawatanasuk, T., and Maneeakrajangsaeng, M., 2014., A treated stone sold as 'Black Sapphire', GIT LAB INFO, January 2014, 8 p. Available from http://www.git.or.th/2014/eng/testing_center_en/lab_notes_en/glab_en/2014/treated_black_diffused_sapphire.pdf

Corresponding Author

Full name: Boontawe Sripasert
Affiliation: The Gem and Jewelry Institute of Thailand (Public Organization), Bangkok, 10500, Thailand; Department of Mineral Resources, Bangkok, 10400, Thailand
Phone : 662 6219676
Fax : 662 6219554
Email: boontawe@gmail.com

Treated Black Diamond Earring

Tay Thye Sun¹, Wilawan Atichat², Thanong Leelawatanasuk² and Loke Hui Ying¹

¹Far East Gemological Laboratory, 12 Arumugam Road #04-02, Lion Building B, Singapore

²The Gems & Jewelry Institute of Thailand, Public Organisation, Bangkok, 10500, Thailand

Extended Abstract

A pair of black diamond earring was submitted to our lab for testing and customer would like to know whether the diamond earring is natural or not. The diamond earring weighs 13.21 grams and the measurement is approximately 2 x 1.6 x 0.4cm. The surface of the diamond is stud with many small rounded gold pin drilled into the diamonds.



Figure 1: A pair of black diamond earring weighs 13.21 grams with gold pin studs (Photo by Tay).

Our first test using the Presidium Diamond Test pen, and the result indicate diamond but it gave a beep sound. As it is rather unusual for test pen to give the beep sound on touching a diamond sample unless the probe touch gold or alloy metal. Tests were conducted on the front and back of the diamonds, all gave beep sound except in the cavities. Initially, we suspect the diamond could be a composite as mentioned before (Fritsch, 2000).

As the diamonds are opaque and only way to observe the diamond is through microscope using reflected lighting. Our observation shows that the surface of the diamonds have many irregular cavities (Figure 2). Also the jewellery manufacturer has drilled holes into the diamond and stud them with small round gold pins giving a rather attractive appearance. Actually the gold pins distraction the observation on the many cavities. The quality of polish is good, the facets are in shallow angles, and some of the polish overlap onto the gold pins (Figure 2). Natural black diamond is made up of naats and polishing it is very difficult. In this case, this pair of earring does not show polishing marks.

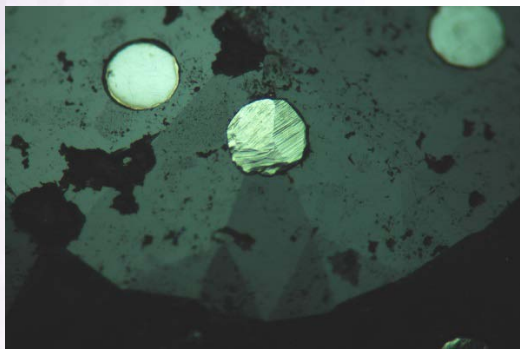


Figure 2: Many cavities and good quality of polishing with some polishing of diamond overlap onto the gold pin (15x).

Under higher magnification at 20x, the fissures of the diamonds are filled with black carbon like staining probably graphite.



Figure 3: Fissures show black carbon like staining probably graphite (20x under reflected lighting).

At the back of the earring, there are parallel groove marks run across the surface and the grooves seems to appear to fuse together along the centre creating a small ridge like appearance (Figure.4). No explanation could be given as this is our first time to observe such an unusual markings. Even the side of the earring are drilled holes at interval (Figure.5).

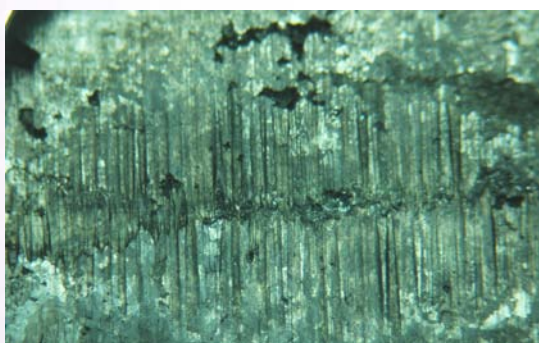


Figure 4: Parallel groove through the centre of the diamond, and looks like two materials fused together at the centre (10x).

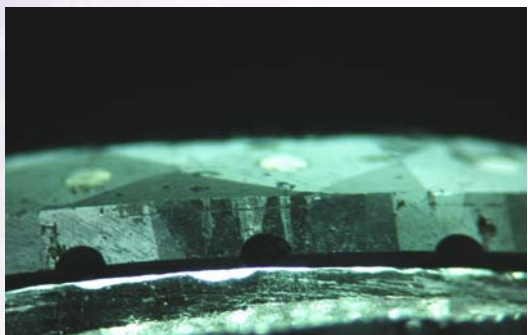


Figure 5: Drilled from the sides of the diamond earring (10x).

The diamond earring was brought to one of the Singapore government material science laboratory for further testing. EDAX was performed on one of the sample, the result was pure carbon 97.37 wt %, O 2.41 wt %, and Si 0.22 wt%. Further test using Raman spectroscopy was performed at the Gems & Jewelry Institute of Thailand (GIT) and found that there are graphite in the cavities.

Discussion

Through discussion with various senior gemologists around the world, it was concluded that this pair of black diamond has been heat treated from poor quality rough diamond material or boart. Heating under vacuum or under low pressure turns the diamond black along the fissures and cavities. As a result, the graphitisation of this treated black diamond sometimes gives metallic beep on diamond tester. This form of treatment became popular since 2008 and carried out in Surat (per comm. Dr Panjekar, 2014).

References

- A German and French Diamond magazine "Production et vente a Surat". Fritsch, E., 2000, Black diamond imitation, Gem News, Gems & Gemology, Vol.36, No.2, p.171-173. Hall, M., and Moses, T.M., 2001, Heat-Treated Black diamond: before and after, Gem Trade Lab Notes, Gems & Gemology, Vol.37, No.3, p.214-215.
- Roskin, G., 2008, Treatments and Lab-Grown Diamonds, JCK, November 1, 2008.

Acknowledgement:

Many discussion through email and kindly sharing of references, my sincere thanks to Dr. Jayshree Panjekar, Prof. Henry Hanni, staff at GIT, Prof. Emmanuel Fritsch, Dr. Hiroshi Kitawaki, Jean-Pierre Chalain of SSEF, Brendan Laurs and Masaki Furuya.

Corresponding Author

Full name: Tay Thye Sun
Affiliation: Far East Gemological Laboratory, 12 Arumugam Road #04-02, Lion Building B, Singapore.
Email: tay@gem.com.sg

A Study of Color Changes In Natural Quartz By Heat Treatments

Aram Ham and Dong Wook Shin

Material Science and Engineering, Hanyang University / Gemological engineering, Seoul Korea

Extended Abstract

Quartz is one of the most important minerals on earth and makes up one of the most popular gemstone groups in the world of colored stones. It is the second most abundant mineral found in Earth's continental crust, second only to the feldspars.

Figure 1 show the common structure of Quartz, or α -quartz, is the mineral form of SiO_2 stable at low temperatures and pressures. It occurs in igneous, sedimentary, metamorphic, and hydrothermal mineral environments, particularly in continental regions. As the structure is acentric, it occurs in both left and right-handed varieties and is both piezoelectric and pyroelectric. It is usually nearly pure and accepts only very limited amounts of other elements in substitution.

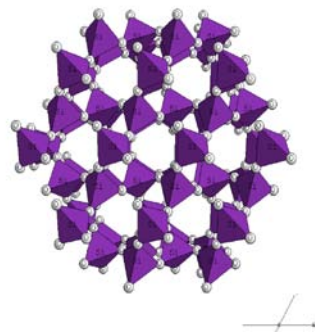


Figure 1: Crystal structure of quartz

In this study, we performed spectroscopic analysis of natural quartz before and after heat treatment in order to investigate the changes in color of brown or purple and the cause of color formation of each sample by heat treatment.

The starting materials were classified as three groups including purple (amethyst), yellowish brown (citrine) and grey (smoky-quartz) according to the predominant color observed as showed in Figure 2.



Figure 2: Sample collection in this study: **(A)** amethyst, **(B)** citrine and **(C)** smoky-quartz

The physical properties of quartz samples are summarized in Table 1. They showed refractive indices spanning 1.540 to 1.550 with a birefringence ranging between 0.009 and 0.010. Amethyst and smoky quartz showed an inert to long- and short-wave UV radiation. Citrine appeared with a weak and strong red fluorescence to short-wave UV radiation but was inert to long-wave UV.

Table 1: Physical properties of the investigated quartz gems.

NO.	Sample	Refractive indices	Birefringence	UV fluorescence	
				Long-wave	Short-wave
C1	citrine	1.540-1.550	0.010	Inert	Red: Strong red
C2	citrine	1.540-1.550	0.010	Inert	Red: Strong red
C3	citrine	1.540-1.550	0.010	Inert	Red: Weak red
C4	citrine	1.540-1.550	0.010	Inert	Inert
C5	citrine	1.540-1.550	0.010	Inert	Red: Strong red
A1	Amethyst	1.540-1.550	0.010	Inert	Inert
A2	Amethyst	1.530-1.540	0.010	Inert	Inert
A3	Amethyst	1.540-1.550	0.010	Inert	Inert
A4	Amethyst	1.540-1.550	0.010	Inert	Inert
A5	Amethyst	1.540-1.550	0.010	Inert	Inert
S1	Smoky quartz	1.540-1.550	0.010	Inert	Inert
S2	Smoky quartz	1.540-1.550	0.010	Inert	Inert
S3	Smoky quartz	1.540-1.550	0.010	Inert	Inert
S4	Smoky quartz	1.540-1.550	0.010	Inert	Inert
S5	Smoky quartz	1.540-1.550	0.010	Inert	Inert

We performed heat-treated in the temperature range of 500~600° C for one hour. Heat treatment, these were analyzed by using UV-Vis, FT-IR, WD-XRF and Raman spectroscopy. The amethyst after heating at 500° C green color changed to dark brown in at 500° C. There was no significant change in the color of citrine is then heat-treated. Finally, a light violet color turned 500° C and 600° C of smoky quartz are showed in Figure 3. The heat treatment may be associated with the mechanism of color centers.



Figure 3: The quartzes samples change of color before and after heat treatment.

Amethyst, Citrine and Smoky quartz for FT-IR study, had indicated 2,500~4,000 cm⁻¹ at mid infrared. In particular, it is at 3,000~3,800 cm⁻¹ that provide important clues to determine whether the range of natural and treatment of quartzes. Figure 3 shows that the FT-IR analysis after heating in all samples shows that 3450, 3595, 3613, 3750 cm⁻¹ vibration absorption band of OH⁻ Stretching as a whole decreased

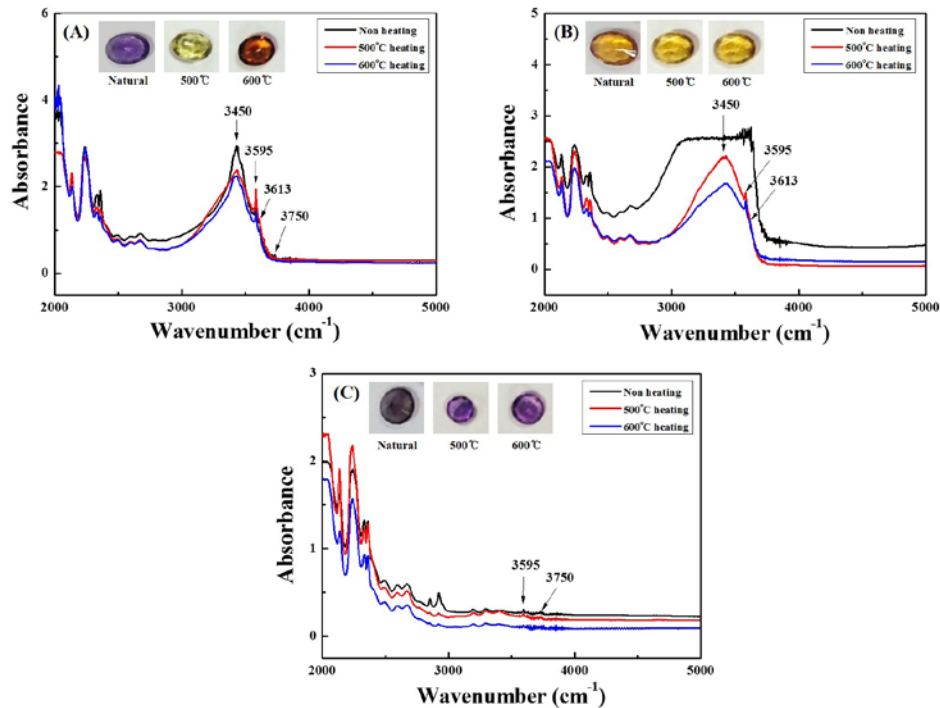


Figure 4: Comparison of the FT-IR spectra of the amethyst, citrine, smoky quartz before and after heat treatment; **black line:** non heating(natural), **red line:** 500 °C heating and **blue line:** 600 °C heating

References

- Balitsky, V.S., Baltisky, D.V., Bondarenko, G.V., and Balitskaya, O.V., 2004, The 3,543 cm⁻¹ Infrared Absorption band in natural and synthetic amethyst and its value in identification, *Gems & Gemology*, Vol.40, No.2, p.146-161.
- Nassau, K., 1981, Artificially induced color in amethyst citrine quartz, *Gems & Gemology*, Vol.17, No.1, p.37-39.
- Lehmann, G., and Bambauer, H.U., 1973, Quartz crystal and their colors, *Angewandte Chemie International Edition in English*, Vol.12, No.4, p.283-291.

Corresponding Author

Full name: Dong Wook Shin
 Affiliation: Division of Materials Science & Engineering, Hanyang University, Seoul 133-791, Korea.
 Phone : +82-2-2220-0503
 Fax : +82-2-2220-4011
 Email: dwshin@hanyang.ac.kr

Application of Cathodoluminescent Technique on Fei Cui (Jadeite Jade) Research

Mimi C. M. Ouyang, and Miro F. Y. Ng

The Hong Kong Institute of Gemmology, 4/F Tung Hip Commercial Building, 248 Des Voeux Road Central, Hong Kong

Extended Abstract

Introduction

Luminescence has long been used in gemmology. The emission of visible light upon the absorption of high energy light source by gemstones has proven to be a useful probe of the trace “impurities” or defects in the crystal lattice of gemstones. The sources of light are typically X-ray, ultraviolet light, visible light (photoluminescence, PL) or cathode ray (cathodoluminescence, CL).

In this study we have used CL microscopic techniques on Fei Cui (previously known as jadeite jade) to reveal the zonal growth structure as well as the texture and colours of the grains. During the work we have studied Fei Cui of i) different colours and varieties ii) different locality and iii) quality in terms of grain sizes and cracks and iv) treatment and imitations.

Experimental

CL analyses were performed on GI-CLB manufactured by Bao Guang Instruments. Typical operating voltage and current were 8 kV and 0.2 mA respectively. Digital images were recorded using a Canon EOS 700D camera connected to the microscope with open aperture, ISO 800 and various exposure time (Figure 1).



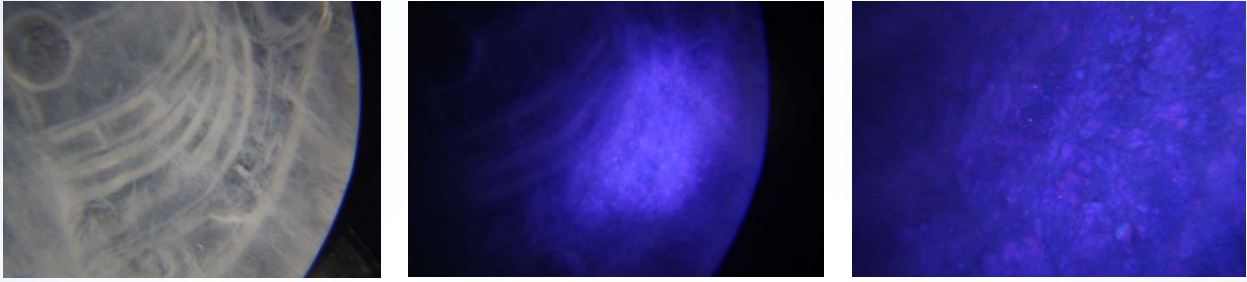
Figure1: Cathodoluminescence microscope used in this work.

Results

i. Analyses on different colours and varieties of Fei Cui

Generally different body colours give rise to different CL colours. For the colourless variety the chemical composition is nearly pure $\text{NaAlSi}_2\text{O}_6$, the CL colours are mainly blue and purplish blue. For the purple series of which Mn ions are present in the crystal lattice, the CL colours are mainly a mixture of purple and reddish purple. For the green Fei Cui of which Fe and / or Cr in the crystal l

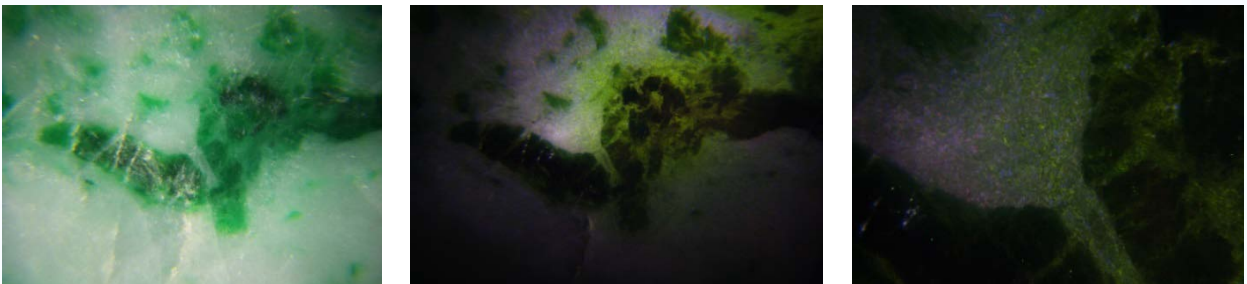
Attice give rise to the body colour, the CL colours are usually dull green to dull yellowish green (Figure 2).



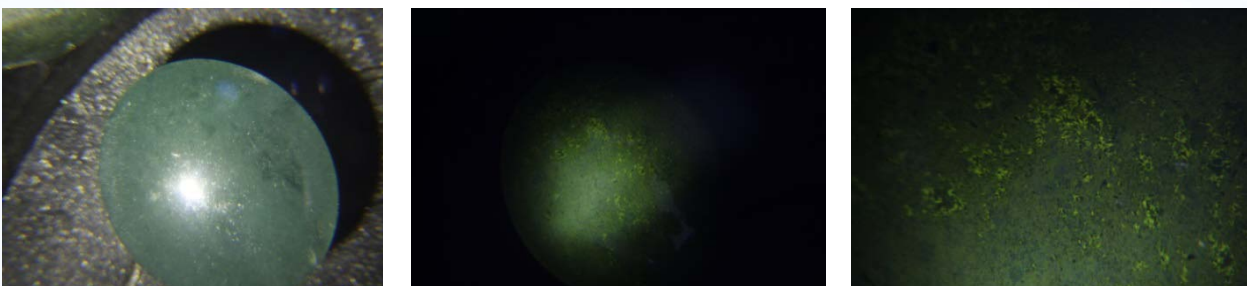
A colourless “Icy Variety” Fei Cui (**left**) with cathode ray on, 6.5X (**middle**) and 20X (**right**).



CL images of 3 different purple Fei Cui, 45X. Note that different grain sizes and zonal structures are evident.



“Green on Snow Variety” Fei Cui (mainly jadeite) (**left**), its corresponding CL images. 6.5X (**middle**) and 20X (**right**).



“Oily Green Variety” Fei Cui (mainly omphacite) (**left**), its corresponding CL images. 6.5X (**middle**) and 20X (**right**).

Figure 2: CL analyses on different colours and varieties of Fei Cui.

During our work we have also performed CL analyses on the red / yellow Fei Cui. It is well known that such coloration is a result of the presence of (hydrus) ferric oxides. In general the presence of iron inside a gemstone will inhibit luminescence. While red / yellow Fei Cui gives little response under UV light, it shows a bright orange to yellow glow with a purple core (more pure jadeite crystals) under cathode ray (Figure 3).

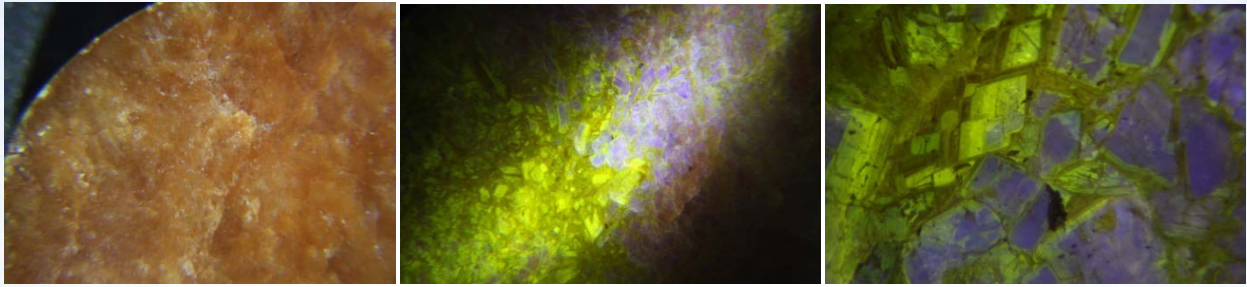
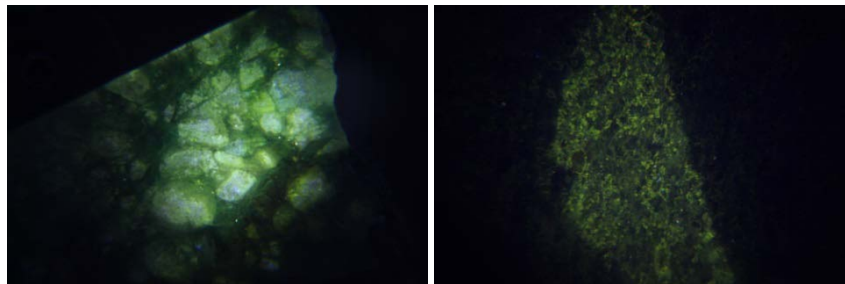


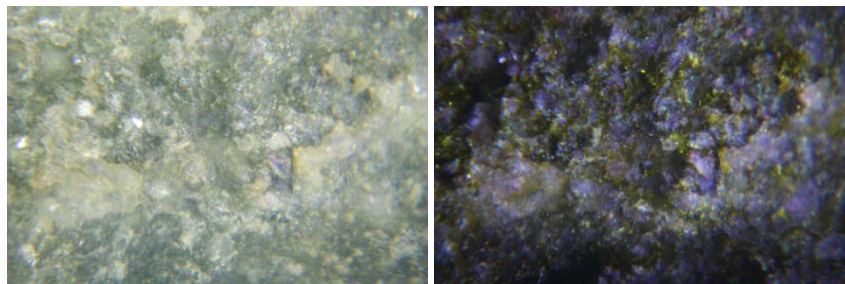
Figure 3: CL analyses on a “Red Variety” Fei Cui (**left**) with cathode ray on, 6.5X (**middle**) and 45X (**right**). Zonal structure are obvious.

ii. Analyses on Fei Cui from different locality

We have extended our work to cover Russian and Guatemala Fei Cui. Preliminary work reveals that there is no significant difference between the crystal grain shapes or CL colours of Burmese, Russian and Guatemalan Fei Cui. Further investigations are required for the possible locality determination.



CL images of 2 Russian Fei Cui, 6.5X (**left**) and 10X (**right**).



CL images of Guatemalan Fei Cui. 6.5X (**left**) and 20X (**right**).

Figure 4: CL analyses on Russian and Guatemalan Fei Cui.

iii. Quality assessment

One of the judging factors for quality assessment of Fei Cui is the texture analysis. In other words it is the assessment of the size, shape and spatial arrangement of the composing grains. Except optical microscopy so far there is no simple way to objectively give such information. However CL can be used to clearly reveal the grains so as to convincingly classify the quality in terms of grain size (Figure 5).

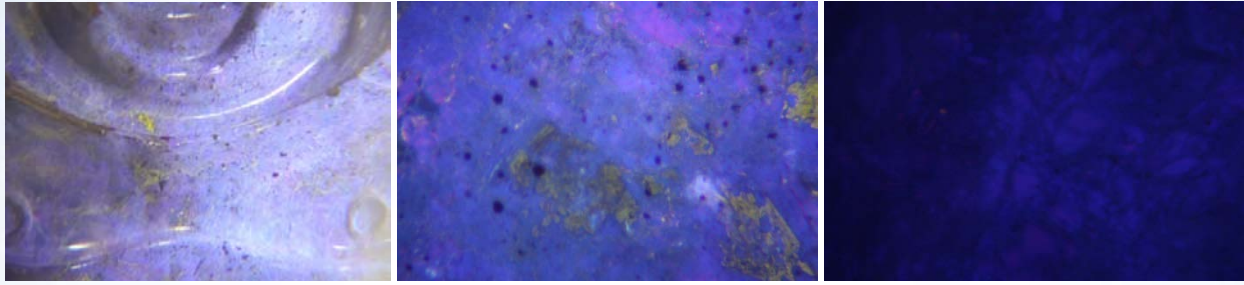


Figure 5: CL images of “Glassy Variety”, very fine grains **(left)**, “Icy Variety” **(middle)** and “Nor Variety”, coarser grains **(right)**.

Another important parameter of quality assessment is the presence of cracks. In the trade there is a saying “one crack in a Fei Cui bangle halves the price”. Yet one can hardly tell whether a “line” in a finished product is truly a crack or just the grain boundary line. Under CL imaging if the “line” appears dark and it breaks nearby crystals, it is a crack (Figure 6).

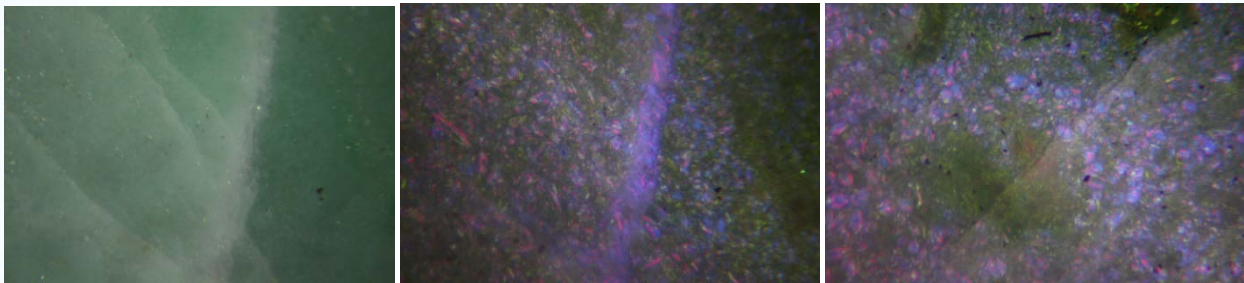


Figure 6: A Fei Cui slab with a line **(left)**. CL reveals it is only a grain boundary line **(middle)**. On another part of the same piece, CL shows a dark line and breaks crystal grains alongside **(red circles, right)**.

iv. Identification of treatments and imitations

Under CL imaging B-jade (acid washed and polymer impregnated) will show rounded grains and even green coloration between grains. Absence of zonal structure may be a clue that the sample under test is indeed an imitation (Figure 7).

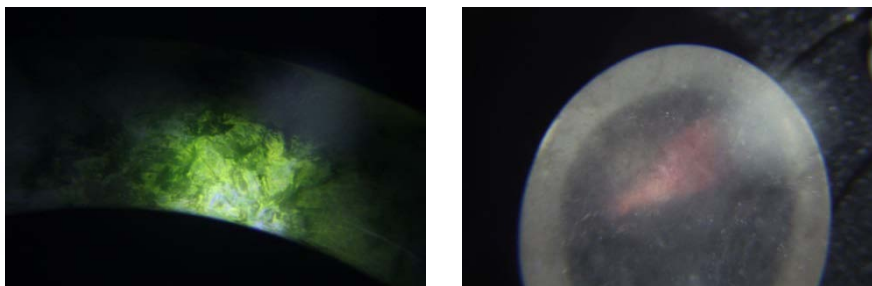


Figure 7: CL images of a hydrogrossular garnet bangle **(left)** and a quartzite cabochon **(right)**. Both do not possess zonal structure as Fei Cui.

Acknowledgements

The authors would like to acknowledge the National Center of Supervision and Inspection on Quality of Gold and Silver Product (NGSTC) for their instrumental support on this project.

References

- Hong-wei, Z., Guo Ying, G., and King-king, L., 2011, Cathodoluminescence Study of Jadeite, *Acta Petrologica et Mineralogica*, Vol.30, p.219-224.
- Nai, Z., Jin-fa, H., and Hongli, G., 2000, Identification of jadeite jade with cathodoluminescence Microscope, *Journal of Gems & Gemmology*, Vol.2, No.3, p.13-16.
- Ponahlo, J., 1999, Cathodoluminescence du jade, *Revue de Gemmologie A.F.G.*, No.137, p.10-16.
- Schertl, Götte, H.P. T., Neuser, R. D., and Richter, D. K., 2009, Cathodoluminescence (cl) Studies of Uhp-metamorphic Rocks From Dora Maira/Western Alps: Petrological Applications And High Resolution Spectroscopy, Micro-Raman Spectroscopy and Luminescence Studies, p.3026
- Xin-qiang, Y., Li-jian, Q., and Sen, Z., 2005, Characteristics of Cathodoluminescence Spectra of Jadeite Jades from Burma, *Journal of Gems & Gemmology*, Vol.7, No.2, p.9-13.
- Ying, Z., 2002, Cathodoluminescence Texture of Jadeite and its gemological significance, *Journal of Gems & Gemmology*, Vol. 4, No.3, p.31-35.

Corresponding Author

Full name: Miro F. Y. Ng
Affiliation: The Hong Kong Institute of Gemmology, 4/F Tung Hip Commercial Building, 248 Des Voeux Road Central, Hong Kong.
Phone: Tel : (852) 2815 1880
Fax : (852) 2854 3970
Email: cmouyang@hkgemslab.com.hk

Application of Fourier Transform Infrared Spectroscopy for the Identification of Treated Sapphires in Sri Lanka

Sandun Illangasinghe¹, Hasintha Wijesekara², Meththika Vithanage² and Chandana P. Udawatte³

¹*Gemmological Institute of Pelmadulla, Ratnapura Rd., Pelmadulla, 70070, Sri Lanka*

²*Institute of Fundamental Studies, Hantana Road, Kandy, Sri Lanka*

³*Sabaragamuwa University of Sri Lanka, PO Box 02, Belihuloya, Sri Lanka*

Extended Abstract

Introduction

Gem treaters pay more attention to these low quality sapphires in order to improve their quality by developing new treatment methods. Heat treatment is the common practice of converting the low quality sapphire to fine quality ruby and sapphire. Transparency and color of the Sri Lankan low quality sapphires can easily be improved by heat treatment at elevated temperature and changing atmospheric condition. However, due to advance in technology and increased demand for low priced gems, newly treated ruby and sapphires appear in the gem market (McClure *et al.*, 2000).

Most of the cases, the appearance of the treated and synthetic ruby and sapphires are similar with the corresponding high value natural gem stones. However, some gemological features exist to disclose the treatment methods but it is difficult to identify without sophisticated equipments (Shigley, 2000). Other hands, insuring of integrity on natural ruby and sapphires to international gem market is essential. Thus, world leading gemological laboratories and researches struggle to disclose the treated gems. Recently, sophisticated equipments have being successfully applied to identify the treated stones. Among these methods, infrared absorption spectra using Fourier Transform –Infra Red (FTIR) spectroscopy was a popular method for disclose treatment state of ruby and sapphire. Treated ruby and sapphires enter the Sri Lankan gem market. Moreover, Sri Lankan sapphires are sold in the international gem market at high price. Thus, Sri Lankan gemological laboratories and responsible institutes try to help insuring the integrity of the Sri Lankan sapphires to the international market. However, sophisticated instruments used for the gemological field yet to be. In addition to that, detail investigation of infrared absorption spectrum on ruby and sapphires in the country is rear. Thus in this research, we investigated the possibility of distinguishing treated ruby and sapphires found in the Sri Lankan gem market by FT-IR spectroscopy.

Materials and Methodology

In order to study on infrared absorption spectrum of ruby and sapphires in the gem market, 60 samples of different colors of natural, synthetic, glass filled and heat treated ruby and sapphires were obtained from private collectors in the Ratnapura area. Samples were carefully cleaned and maintained in the dry condition. 50 samples were rough and rest were cut and polished. The weight is ranging from 1 to 6 ct.

In this study, heat treated ruby, blue and yellow sapphires were used to FT-IR analysis. Three yellow sapphires and ten blue sapphires were performed infrared absorption spectrum study prior and after the heat treatment. Most of the heat treatment was performed by using gas furnace under supervision of the authors. Blue sapphires were obtained by heat treatment at 1800°C at reducing condition. While ruby and yellow sapphires were obtained by heat treatment in oxidizing atmospheric condition and temperature at 1200 and 1850°C respectively. Moreover, in this study we analyzed on infrared absorption spectrum of Cobalt doped glass filled blue sapphires. Previous studies (Leelawatanasuk *et al.*, 2013) have described on Cobalt doped glass filled blue sapphires.

Samples of ruby and sapphires were examined in the mid infrared spectral region by using the Nicolet 7600 FTIR spectrophotometer. Unpolarized infrared spectra were recorded from 4000 to 2100 cm^{-1} on Nicolet 7600 FTIR spectrometer operating 4 cm^{-1} resolution. Background and sample spectra were respectively obtain from 64 scans in air and through sample crystal. Subsequently, resulted infrared spectra of natural, synthetic, heat treated and glass filled sapphires were compared in mid infrared region.

Results and Discussion

Resulted infrared absorption spectrum of the samples showed distinguish absorption peaks at different energy levels and saturated by bonds of Al-O below the 1500 cm^{-1} . It evidenced that all the samples belong to the corundum gem family. Beran and Rossman (2006) have identified two peaks at 2920 and 2851 cm^{-1} due to goethite mineral phase in ruby and sapphires from different localities. Resulted infrared absorption spectra of Sri Lankan natural blue sapphires clearly revealed that the most of analyzed sapphires have goethite (FeOOH) impurity inclusion phases at 2920 and 2851 cm^{-1} (Figure 1a). During the heat treatment process, goethite inclusion phase may be dissolve and iron would be forced to reduced to Fe^{2+} ions in order to formed blue colour through Intervalance Charge Transfer (IVCT) process. Therefore, the resulted infrared absorption spectrum of heat treated sapphires did not show goethite inclusion phase (Figure 1b).

However, the heat treated blue sapphires demonstrated a new peak appeared at 3309 cm^{-1} corresponding to hydroxyl stretching bonds (Figure 1b). Thus this phenomenon can be used for distinguished heated blue sapphires from natural Sri Lankan blue sapphires.

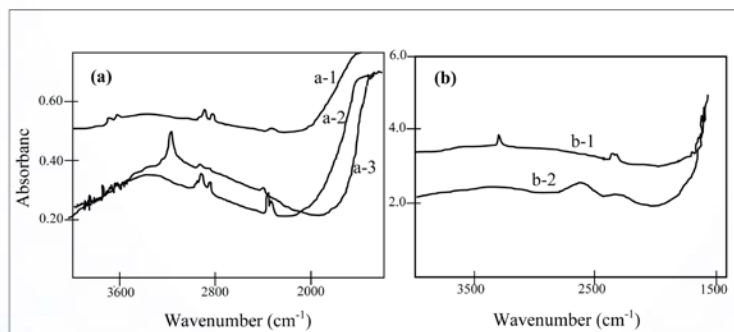


Figure 1: Infrared absorption spectrum of **(a)** non-heated sapphires of a-1) low quality Sri Lankan sapphire (Geuda), a-2). Natural blue sapphire, a-3). Natural yellow sapphire. **(b)** b-1, Heat treated sapphire, b-2, glass filled sapphires.

Graph of b-2 in Figure 1b showing IR absorption spectrum of cobalt colored glass filled blue sapphires and demonstrated characteristic broad peaks at 2597 and 2256 cm^{-1} (Figure 1b) which are common in glass filled ruby due to Si-OH bond vibration (Efimov *et al.*, 2003). These peaks do not appear in natural, heat treated or synthetic sapphires. Moreover, synthetic sapphires are given the hydroxyl bond absorption band at 3309 cm^{-1} , additional weak absorption bands from 3100 to 3300 cm^{-1} with absorption bands of goethite inclusion phase.

Yellow and pink natural sapphires were analyzed and some samples demonstrated hydroxyl stretching bond absorption peak at 3160 cm^{-1} (Figure 1a). However, heat treated yellow sapphires did not show this peak. Subsequently, results of this study clearly revealed that the infrared absorption spectrum of sapphires using FT-IR spectroscopy is a powerful tool to distinguish treat and natural sapphires available in the Sri Lankan gem market.

Conclusions

Most common problem in gem trade is to distinguishing synthetic and treated sapphires from natural sapphires because the value of a sapphire mainly depends on treatment state of the stone. Therefore, identification of the treatment state of sapphire is important and infrared absorption pattern in mid-infrared region can be used as an accurate method to distinguish treated and natural sapphires available in the Sri Lankan gem trade.

References

- Efimov A.M., Pogareva V.G., and Shashkin, A.V., 2003, Water-related bands in the IR absorption spectra of silicate glasses, *Journal of Non-Crystalline Solids*, Vol.332, No.1-3, p.93-114.
- Leelawatanasuk T., Atitchat W., Pisutha-Arnond V., Wattanakul P., Ounorn P., Manorotkul, W., and Hughes, R.W., 2013, Cobalt-doped glass-filled sapphires: An update, *The Australian Gemmologist*, Vol.25, No.1, p.14-20.
- McClure S. F., Kane R. E., and Sturman, N., 2000, Gemstone Enhancement and its Detection in the 2000s, *Gems & Gemology*, Vol.46, No.3, p.218-240.
- Shigley J. E., 2000, Treated and synthetic gem materials, *Current Science*, Vol.79, No.11, p.1566-1571.

Corresponding Author

Full name: Sandun Illangasinghe
Affiliation: Gemmological Institute of Pelmadulla, Ratnapura Rd., Pelmadulla, 70070, Sri Lanka.
Email: sillangasinghe@gmail.com

Aquamarine from Karur, Tamil Nadu India

Jayshree Panjekar and Aatish Panjekar

PANGEMTECH - Panjekar Gem Research & Tech Institute, 10 Sangeeta Building, Tadiwala Road, Pune 411001, India

Extended Abstract

Gemmological and spectroscopic features of aquamarine from Karur, Tamil Nadu have been investigated. Karur Kangyam gemstone belt in Tamil Nadu has been known for gem minerals like beryl, corundum, garnet, sillimanite and feldspars. Large crystals of aquamarine are very commonly found in this area. In fact in the 2009 Mineralientage Exhibition in Munich had displayed a 9.8 kg aquamarine crystal from Karur, Tamil Nadu. Aquamarine occurs in the pegmatite which traverses the hard consolidated crystalline rocks of Archaean age represented by the weathered, fissured and fractured formations of gneisses, granites and charnockites.

In the present study aquamarines from Pallapatti village (Lat: 10.77deg Long: 77.90deg) in Karur district of Tamil Nadu have been investigated. Ten faceted samples ranging from 1.02 carats to 12.01 carats with visible inclusions were selected. Laser Raman, FTIR, UV-Vis spectroscopy and EDXRF were used. The characteristic microscopic inclusions were a variety of fluid inclusions, two phase, three phase, liquid films, liquid filled capillaries, feathers, healed feathers, large cavities filled with original magmatic fluids. These fluid inclusions were observed to be of different generations with specific orientation with respect to the c-axis. Nature of inclusions, spectroscopic analyses have helped to throw light on the crystallization of the aquamarine in the pegmatite.



Figure 1: Ten specimen of aquamarine from Pallapatti village, Karur region used in this study

Materials and Methods

Ten faceted aquamarine and two rough crystals were examined using standard gemmological methods to determine their optical properties, hydrostatic specific gravity, UV

fluorescence and microscopic features. Non-polarized UV-Vis spectra for all samples were collected using JASCO F660 spectrophotometer over the 350 nm – 800 nm range. Mid Infrared spectra of 5 samples were collected in transmission mode by a JASCO FT/IR-6600 with a resolution of 4cm⁻¹. Qualitative analyses were carried out using EDXRF. Raman spectra were used to determine the nature of the inclusions.

Results

The colour of the faceted aquamarine ranged from medium blue to blue to greenish blue. Refractive indices determined showed values as RI $n_o = 1.580-1.590$ and $n_e = 1.572-1.579$ with birefringence = 0.008-0.009 having optic character uniaxial negative. Specific gravity was determined using hydrostatic method, and was SG = 2.69-2.72. All samples were totally inert under long wave and short wave ultraviolet radiations.

Microscopic Inclusions

Under microscope mostly fluid inclusions were observed. These fluid inclusions could be categorized: 1. Multiphase inclusions, three phase inclusions with solid + liquid + gas, liquid films (Figure 2), 2. Two phase inclusions in cavities (Figure 3) and in thin flat planes (Figure.4), 3. Different generations of liquid feathers (Figure 5), 4. Cavities with two bubbles (Figure 6), 5. Cavities with long bubbles (Figure 7), 6. Healed feathers, 7. Large cavities filled with mother liquor of different generations with specific orientation with respect to the c-axis. Solid crystalline inclusions observed were biotite mica and quartz.

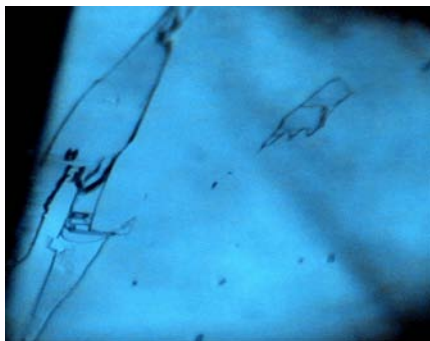


Figure 2: Multiphase inclusion.



Figure 3: Cavity with 2-phase.

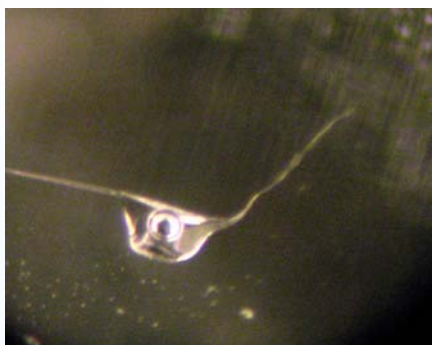


Figure 4: Two phase inclusion flat cavity.



Figure 5: Feathers of 2 generations.

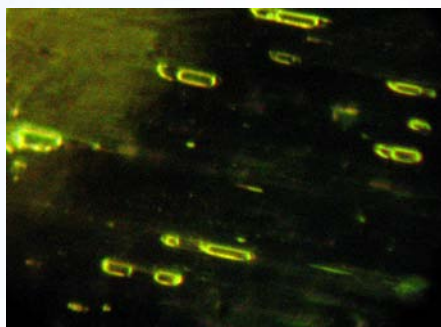


Figure 6: Cavities with two bubbles.

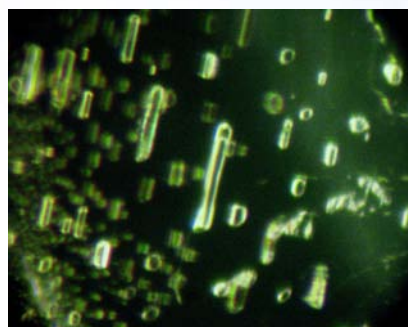


Figure 7: Cavities with large bubbles.

UV-Vis Spectra

The UV-Vis spectra were typical for aquamarine (Figure 8) with two peaks at 370 nm and 426 nm related to Fe³⁺ and a strong absorption after 760 nm assigned to Fe²⁺. Absorption peaks at 538 nm and 590 nm are attributed to a Fe²⁺-Fe³⁺ and inter valence charge-transfer process although some have assigned it to Fe²⁺.

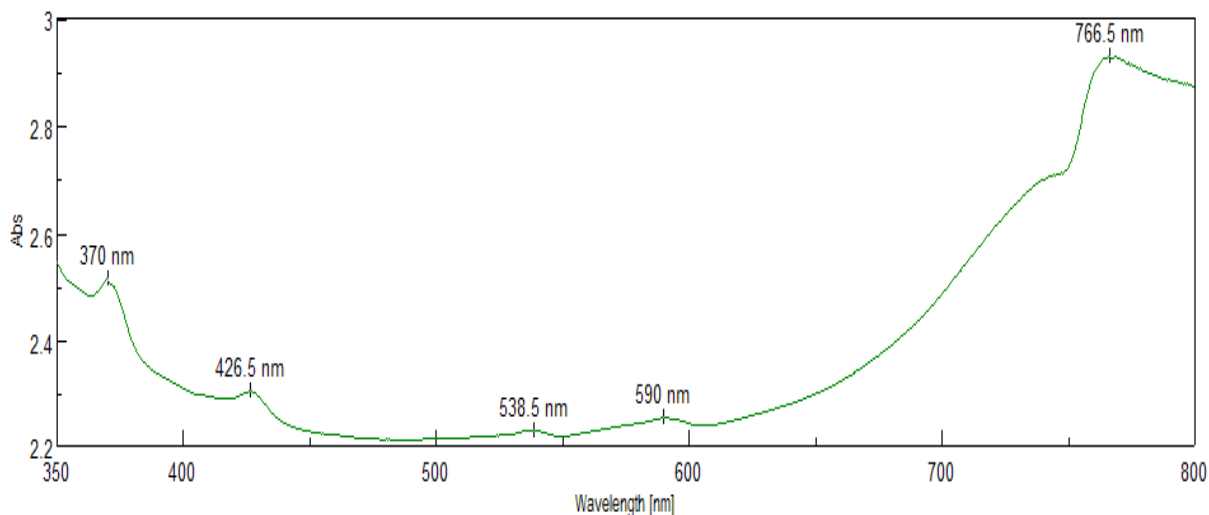


Figure 8: The UV-Vis spectrum of aquamarine from Karur.

FTIR Spectra

The infrared spectra contained the absorption bands below 1200 cm⁻¹ intrinsic to the beryl structure as well as the features originating from both type I 3699 cm⁻¹ and type II (3660 and 3597 cm⁻¹) water molecules trapped in the structural channels (Woods and Nassau, 1968). In agreement with chemical composition, the IR spectrum is typical of medium alkali bearing beryl.

Raman Spectroscopy helped to identify and confirm the biotite inclusion.

Chemical Composition

The aquamarine samples analysed gave rather high iron content (1.52-2.05%wtFeO) and medium contents of alkali (0.961- 0.526%wt Na₂O, 0.015- 0.046%wt K₂O).

Discussion

The Karur beryls display solid inclusions in the form of biotite and quartz and a large variety of fluid inclusions which are characteristic for pegmatites with significant hydrothermal activity (Sinkankas, 1981). This would mean that the Karur beryl have crystallized from a hot aqueous solution. The evidence for which can be further had from the fluid inclusions which show “Boiling and Necking” effect. Some of the multi-phase inclusions contain two crystals one of them being halite and other could not be identified, liquid phase, and sort of stretched effect. Besides, these fluid inclusions are distinctly categorised into first and second generation inclusions. The first generation fluid inclusions are larger and oriented with respect to the “c” axis whereas the other inclusions do not show any particular orientation. In this region large crystals must have developed in the pegmatites this is evident from the fact that 9.8 kg aquamarine crystal was discovered here.

Acknowledgements

Special thanks to Ms. Nirmala of WISMORE EXIM Coimbatore for helping to collect samples from the site. Authors are grateful to the technical staff of National Chemical Laboratory, Pune for EDXRF and Raman spectroscopy.

References

- Boehm, E., 2000, Aquamarine from southeast India, Gem News, Gems & Gemology, Vol.36, No.3, p.263-264.
- Koivula, J., 2006, Cuneiform aquamarine inclusions, Gem News, Gems & Gemology, Vol.42, No.1, p.70.
- Roedder, E., 1984, Fluid Inclusions, Reviews in Mineralogy, Vol.12, Mineralogical Society of America, 644 p.
- Sinkankas, J., 1981, Emerald and Other Beryls, Chilton Book Company, Radnor, 665 p.
- Wood, D.L., and Nassau, K., 1968, The characterization of beryl and emerald by visible and infrared spectroscopy, American Mineralogist, Vol.53, No.5-6, p.777-800.

Corresponding Author

Full name: Jayshree Panjekar
Affiliation: PANGEMTECH- Panjekar Gem Research & Tech Institute, Address: 10 Sangeeta Building, Tadiwala Road, Pune, 411001, India.
Phone: +919822286288
Fax: +912026059359
Email: jayshreepanjekar@gmail.com

Aquamarine from the Gilgit Baltistan of Northern Areas, Pakistan

Sungjae Kim and Dong wook Shin

Department of Materials Science and Engineering, Hanyang University, 222 Wangsimni-ro, Seong dong-gu, Seoul, 133-791, Korea

Extended Abstract

Introduction

Aquamarine are blue variety of beryl mineral group with chemical formula of $\text{Be}_3\text{Al}_2\text{Si}_6\text{O}_{18}$, as is emerald which is the green variety, better known, and most expensive beryl. The structure composes of 6-fold rings of linked SiO_4 tetrahedron, alternated with Be^{2+} in tetrahedral site, and bonded with Al^{3+} in octahedral site (Figure 1) (Wood and Nassau, 1967). The SiO_4 rings stack one above the other along the c-axis forming hollow channel site of quite large dimension for holding large molecules such as H_2O , CO_2 and alkali ions. The light blue coloration in aquamarine results from Fe^{2+} being in channel site. Aquamarine from the Gilgit Baltistan of Northern Areas, Pakistan occurs in big veins of Be-rich coarse pegmatite, consisting of quartz, orthoclase with some albite, tourmaline, muscovite, garnet and beryl. The best and most transparent aquamarines are found in cavities (Agheemet al., 2011). The color of the best specimens is not very deep, but of the true aquamarine shade.

In this study, aquamarine samples from the Gilgit Baltistan were investigated for their gemological characteristics.

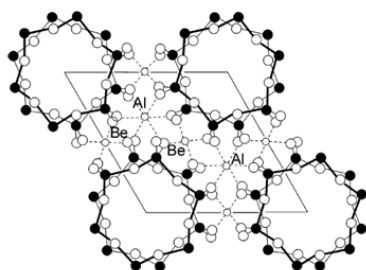


Figure 1: Projection of part of the structure of beryl on a plane perpendicular to the c axis. Modified after Bragg and Claringbull (1965).



Figure 2: Photograph of the aquamarine samples from the Gilgit Baltistan of Northern Areas, Pakistan.

Methodology

A total of 12 aquamarine faceted samples (2.74 to 15.89 ct) used in this study were purchased from a Pakistani gem dealer (Figure 2). Parallel plates were cut and polished from all samples for spectroscopy. The physical and optical properties (refractive indices, birefringence, specific gravity, ultraviolet fluorescence, and microscopic features) were examined using gemological instruments. UV-Vis-NIR spectroscopy (300-2400 nm) was used to investigate causes of coloration. Fourier Transform Infrared (FT-IR) spectroscopy ($7600\text{--}400\text{cm}^{-1}$) in absorption mode was used to characterize the types of water molecule in their channel. Microscopic Observation was used to

observe the inclusions and they were identified using a Raman spectroscopy (150~1800 cm⁻¹). Quantitative chemical analyses were performed using an X-ray Fluorescence Spectrometer (XRF) in energy dispersive. All of these analyses were carried out at the Department of Materials Science and Engineering, Hanyang University.

Results

Gemological property

The gemological testing of all samples used in this study indicates that they are consistent with natural aquamarine. Their properties are summarized in Table 1.

Table 1: Physical properties of aquamarines from the Gilgit-Baltistan of Northern Areas, Pakistan.

Color	Very light to medium blue, typically a saturated bluish green with a light to medium tone
Clarity	Very slightly included
Refractive indices	n _o = 1.583; n _e = 1.577
Birefringence	0.006
Specific gravity	2.69–2.70
Fluorescence	inert
Internal features	<ul style="list-style-type: none"> • Often homogeneous color distribution • Partially healed fissures with two-phase (Figure 3a) • Negative crystals, forming CO₂-rich two-phase inclusions • Parallel growth tubes • Extremely fine fiber-like inclusion (tantanlite) (Figure 4) • Mineral inclusions: crystal pyrite and silk-like sodic plagioclase (Figure 3b, 3c)

Microscopic characteristics

The most commonly encountered inclusions were partially healed fissures with two-phase fluid. Solid inclusions were uncommon. Inclusions of tantanlite (Figure 4) were identified by Raman analysis.



Figure 3: Photograph of the characteristic inclusions. **a)** healed fissures with two-phase, **b)** crystal pyrite, **c)** silk-like sodic plagioclase (albite, oligoclase).

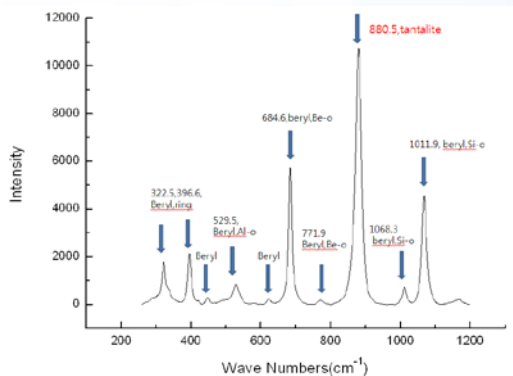


Figure4: Photograph and Raman spectra of fine fiber-like inclusion tantalite-Mn. The black arrows are indicative of tantalite. The dominant beryl peaks are also present in the spectra of the inclusion.

UV-Vis-NIR

The UV-Vis-NIR absorption spectra (Figure 5) of all samples were investigated in order to explain their colors. The absorption peak at 370 nm with a small peak at 427 nm are attributed to Fe³⁺ substitutes for Al³⁺ causing yellow coloration. A strong broad band centered at 820 nm, only apparent in aquamarine samples as causes of blue coloration, are assigned to Fe²⁺ replacing Al³⁺. In the near infrared region, all spectra show sharp bands due to type II H₂O at 1145, 1400, and 1890 nm whereas the weak bands of type I H₂O at 1830 and 1950 nm present in samples. This is typical of alkali bearing beryl.

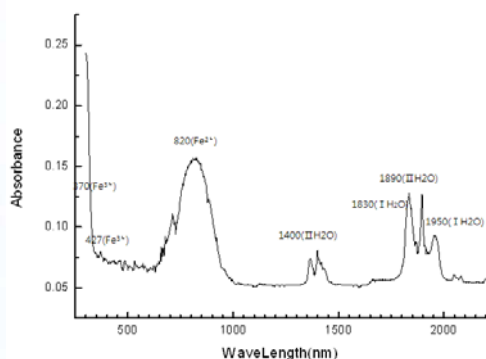


Figure5: UV-VIS-NIR absorption spectra in the region of 300 ~ 2400 nm.

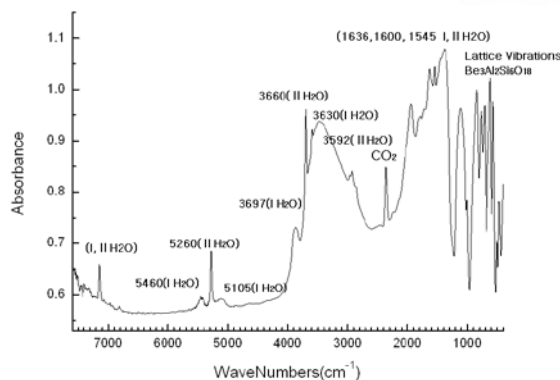


Figure6: FT-IR absorption spectra in the region of 7600 ~ 400 cm⁻¹.

FT-IR

FT-IR absorption spectra (Figure 6) reveal typical absorption in the range 400-1400 cm⁻¹ due to vibration of intrinsic structures (Be-O, Si-O, and Al-O stretching). The sharp band at around 2350 cm⁻¹ is assigned to CO₂ molecules. In the range from 3800 to 3500 cm⁻¹ always show important bands of both type I and II H₂O in channel site. The two weak bands at around 5460 and 5105 cm⁻¹ can be attributed to overtones of type I H₂O and the distinctive sharp band due to type II H₂O at around 5260 cm⁻¹ respectively.

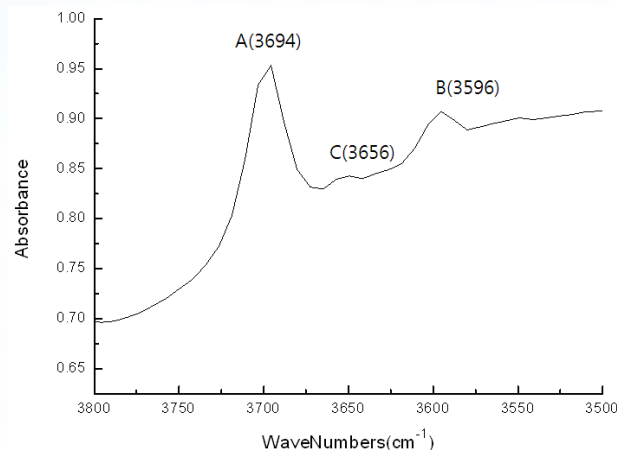


Figure 7: FT-IR absorption spectrum from KBr pellet in the range of the stretching modes of H₂O. **(A)** 3694 cm⁻¹, H₂O type I. **(B)** 3596cm⁻¹, H₂O type II. **(C)** 3656 cm⁻¹, H₂O type II.

According to classification of Schmetzer and Kiefert (1990) beryls from the Gilgit Baltistan belong to low alkali-bearing, for which the intensity of diagnostic three IR bands: at 3694 cm⁻¹ (A band), at 3592 cm⁻¹ (B band) and at 3655 cm⁻¹ (C band) is in the order A>B>>C (Figure 7). This is consistent with content 0.3 wt% of K₂O and Na₂O.

Conclusion

Aquamarine mineralization from the Gilgit Baltistan occurs in association with a big veins of Be-rich coarse pegmatite. The results of chemical analyses and infrared absorption spectra indicate that the aquamarine from Gilgit Baltistan is low alkali-bearing beryl with considerable CO₂.

References

- Agheem, M. H., Shah, M. T., Khan, T., Laghari, A., and Dars, H., 2011, Field features and petrography used as indicators for the classification of Shigar valley pegmatites, Gilgit-Baltistan region of Pakistan, *Journal of Himalayan Earth Sciences*, Vol. 44, No. 2, p. 1-7.
- Bragg, W.L., and Claringbull, G.F., 1965, *Crystal Structures of Minerals*, Bell and Sons Ltd, London, p. 213.
- Wood, D.L., and Nassau, K., 1967, Infrared spectra of foreign molecules in beryl, *Journal of Chemical Physics*, Vol. 47, No. 7, p. 2220-2228.
- Schmetzer, K., and Kiefer, L., 1990, Water in beryl—a contribution to the separability of natural and synthetic emeralds by infrared spectroscopy, *Journal of Gemmology*, Vol. 22, No. 4, p. 215-223.

Corresponding Author

Full name: Sungjae Kim
Affiliation: Department of Materials Science and Engineering, Hanyang University,
222 Wangsimni-ro, Seong dong-gu, Seoul, 133-791, Korea.
Phone: +82-10-30195297
Email: sjk310700@gmail.com

Blue Sapphires from Ban Bo Keao and Ban Na Poon Deposits in Phrae Province, Northern Thailand

***Somruedee Satitkune¹, Krit Won-in¹, Natthapong Monarumit¹, Sermrak Ingkawani¹,
Prayath Nanthasin¹, and Pornsawat Wathanakul²***

¹Department of Earth Sciences, Faculty of Science, Kasetsart University, Bangkok, 10900, Thailand

²The Gem and Jewelry Institute of Thailand (Public Organization), Bangkok, 10500, Thailand

Extended Abstract

Introduction

Sapphire and other associated minerals (i.e., black spinel, zircon and garnet) deposits have been found in Ban Bo Keao and Ban Na Poon in Denchai-Wangchin area, Phrae province, the well-known gem field in northern Thailand (Figure 1). Phrae basaltic units were classified into seven flows and the age of the uppermost basaltic flow was 5.64 ± 0.28 Ma (K/Ar) (Barr and Macdonald, 1981). The sapphire samples are recovered from both alluvial and eluvial deposits (Wathanakul *et al.*, 2013; Won-in *et al.*, 2014). In the past, the local people were digging and searching for sapphire samples along the stream.

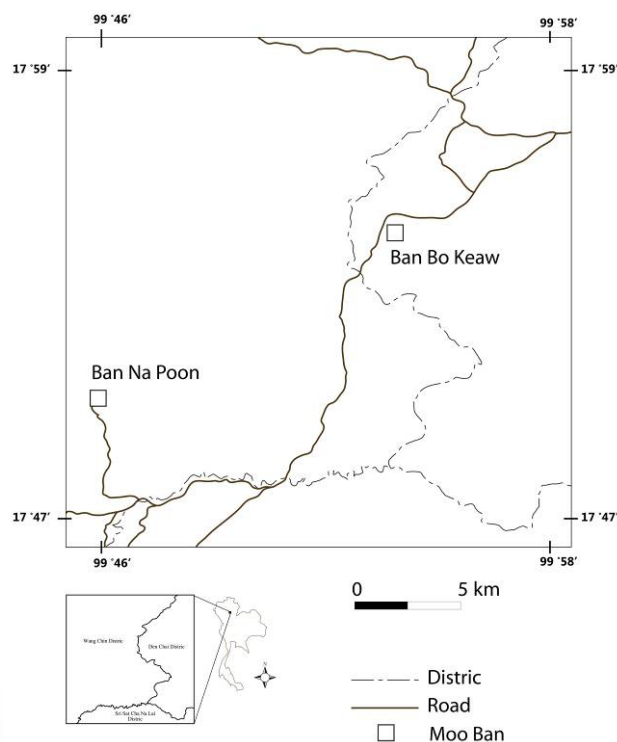


Figure 1: Map of Ban Bo Keao and Ban Na Poon sapphire deposits, Phrae.

Materials and Methods

Most of sapphire samples collected from Ban Bo Keao deposits are dark indigo blue colour as the Thai denim named “Mo Hom”, whereas sapphires from Na Poon deposits are bluish gray (Figure 2). Black spinel, garnet and zircon are found as by-products. Some ruby samples were also found in both areas (Wathanakul *et al.*, 2012). Most of the sapphire samples are broken but still show euhedral to subhedral hexagonal tabular crystals, and, barrel-shaped crystals.

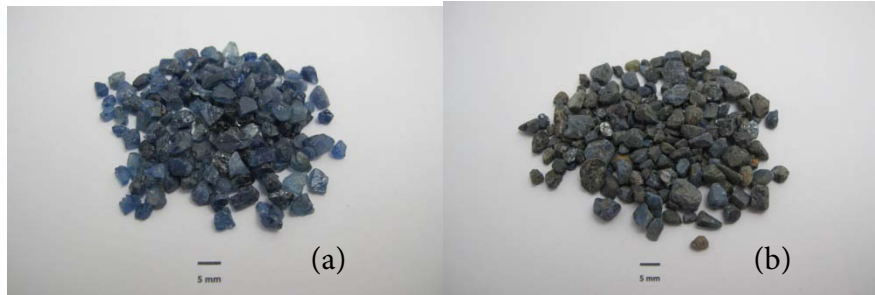


Figure 2: Sapphire samples from (a) Ban Bo Keao and (b) Ban Na Poon.

The internal features and growth structures (crystal inclusions, healing fracture of fluid inclusions and colour zoning) were observed using the gemological microscope (Figure 3).



Figure 3: (a) Crystal inclusion, minute particles and colour zoning and (b) crystal and fluid inclusions in sapphire samples from Phrae.

The FTIR spectra of blue sapphire samples from Ban Bo Keao and Na Poon deposits show the C-O, C-H and Ti-OH absorption peaks at 2350, 2846, 2915 and 3309 cm^{-1} (Phlayrahan *et al.*, 2014) respectively (Figure 4). The UV-Vis-NIR spectra of blue sapphire samples show Fe^{3+} absorption bands at 377, 388 and 450 nm, $\text{Ti}^{2+}/\text{Fe}^{4+}$ charge transfer at 570 nm and $\text{Fe}^{2+}/\text{Fe}^{3+}$ pair absorption at 870 nm, which cause blue colouration of the basaltic type origin (Sripoonjan, 2013) (Figure 5).

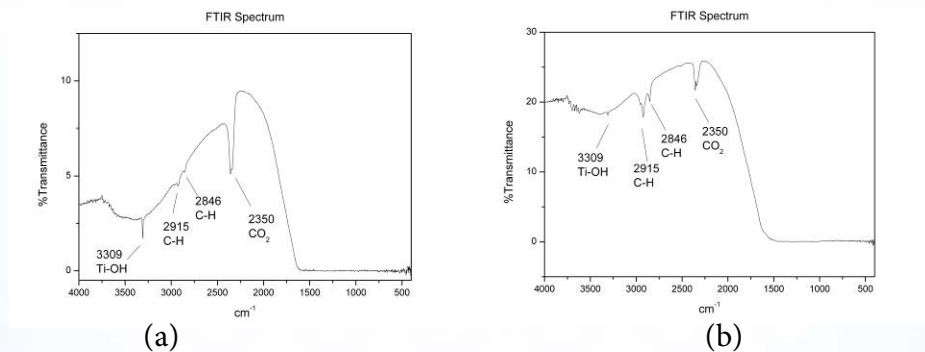


Figure 4: FTIR spectra of blue sapphire from (a) Baan Bo Kaeo and (b) Na Poon deposits.

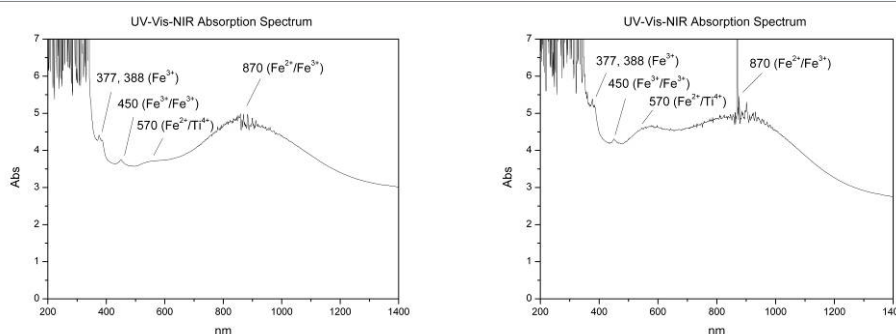


Figure 5: UV-Vis-NIR spectra of blue sapphire from **(a)** Baan Bo Kaeo and **(b)** Baan Na Poon deposits.

Chemical composition can also confirmed the basaltic origin of these sapphires. The EDXRF analyses show rather high Fe contents as well as traces of Ti, V, Cr and Ga (Table 1).

Table 1: EDXRF analyses of sapphires from Ban Bo Keao and Ban Na Poon deposits.

Deposit	Concentration (wt%)				
	TiO ₂	V ₂ O ₃	Cr ₂ O ₃	Fe ₂ O ₃	Ga ₂ O ₃
Ban Bo Keaw	0.02-0.21	0.005-0.048	0.002-0.012	0.21-1.17	0.016-0.055
Ban Na Poon	0.03-0.07	0.002-0.014	0.006-0.017	0.46-1.55	0.018-0.069

Discussions and Conclusions

The blue sapphire samples from Ban Bo Keaw and Ban Na Poon deposits show the hexagonal tabular and barrel-shaped habits with the broken ends. The internal features comprise crystal inclusions, fluid inclusions, minute particles and colour zoning. The UV-Vis-NIR absorption spectra show the typical pattern of the sapphire from basaltic origin.

Acknowledgements

Kasetsart University Research and Development Institute (KURDI) is thankful for research funding. Department of Earth Sciences, Faculty of Science, Kasetsart University and the Gem and Jewelry Institute of Thailand (Public Organization) are gratefully acknowledged.

References

- Barr, S.M., and Macdonald, A.S., 1981, Geochemistry and geochronology of late Cenozoic basalts of Southeast Asia, Geological Survey of America Bulletin, Part II, Vol.92, p.1069-1142.
- Phlayrahan, A., Monarumit, N., Satitkune, S., and Wathanakul, P., 2014, If diaspore is responsible for the 3309 cm⁻¹ peak in the FTIR spectra of heated ruby sample, in Proceedings of the 4rd International Gem and Jewelry Conference (GIT 2014).
- Sripoonjan, T., 2013, Influence of heat to silky-mineral inclusion in sapphire from Changwat Chathaburi, M.S. Thesis 2013, Department of Geology, Faculty of Science, Chulalongkorn University.

Wathanakul, P., Atichat, W., Ingavanija, S., Satitkune, S., Lhuaaporn, T., Monarumit, N., and Nanthasin, P., 2012, Blue sapphire from Phrae, Northern Thailand, in Proceedings of the 3rd International Gem and Jewelry Conference, GIT 2012, p.74-76.

Wathanakul, P., Satitkune, S., and Nanthasin, P., 2013, The management of gemstone deposits in Thailand (in Thai), KU report 2013.

Won-in, K., Satitkune, S., Tangulrat, P., and Kaewlunka, T., 2014, Geomorphological study at Ban Bo Kaew sapphire deposit, Den Chai District, Phrae Province, Northern Thailand, in Proceedings of the 4th International Gem and Jewelry Conference (GIT 2014).

Corresponding Author

Full name: Somruedee Satitkune

Affiliation: Department of Earth Sciences, Faculty of Science, Kasetsart University, 50 Ngamwongwan Road, Chatuchak, Bangkok, 10900, Thailand.

Phone: +66 2 562 5555 # 1406, +66 84 674 4192

Email: somruedeesk@gmail.com, fscisrd@ku.ac.th

Causes Of Colour and Optical Phenomenon of Cat's Eye Opal From Tanzania

Boontarika Srithai¹, Parichart Puangcharoen² and Weerapan Srichan¹

¹Department of Geological Sciences, Faculty of Science, Chiang Mai University, Chiang Mai, 50200, Thailand

²GRS Thailand, Silom 19 building, 5th floor, room 501, 45/1 Silom Road, Bangrak, Bangkok, 10500, Thailand

Extended Abstract

An amorphous substance 'opal' is one of the most important gem species that exhibits varieties of spectacular optical phenomena. It is generally classified according to its appearance as common opal, fire opal and precious opal. Structurally, they are divided into opal-A, opal-CT and opal-C, which correspond to the present or absent of tridymite and cristobalite (Elzea and Rice, 1996; Gaillou *et al.*, 2008; Herdianita *et al.*, 2000). Cat's eye opal is a variety that displays cat's eye effect resulting from group of tiny fibrous-like inclusions like goethite that was replaced by opal (Wentzell and Reinitz, 1998). 16 samples of cat's eye opal from Tanzania were studied for the causes of colour and the cat's eye effect by using varieties of techniques including standard gemological examination, mineral and chemical composition (XRD and SEM-EDS), and optical-vibrational spectroscopic analyses.

The studied samples are white, yellow, orangy brown, and blackish brown in colour. Their specific gravity is in the range of 2.03 to 2.15 and refractive indices are of 1.430 to 1.460. They appear inert under UV luminescent. Hematite, cristobalite, minute needle-like inclusions and iron-oxide stained fractures were observed as inclusions in these samples (Figure 1).

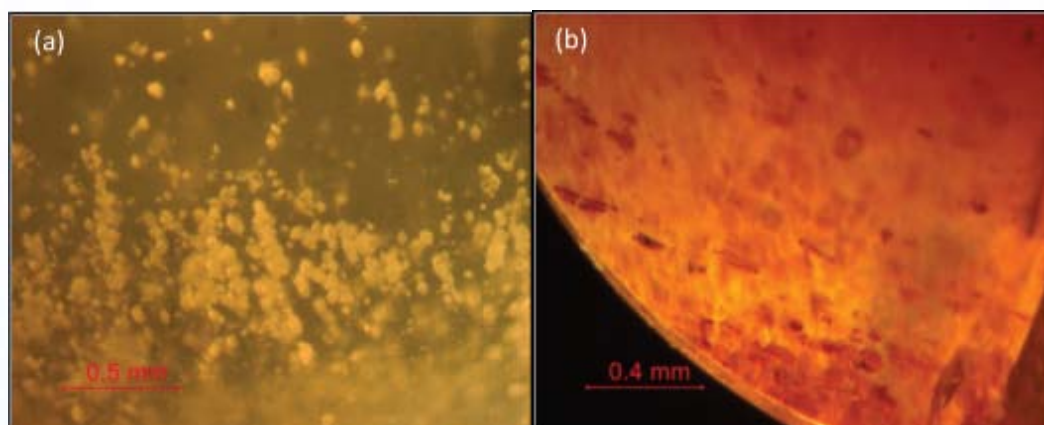


Figure 1: (a) Cluster of cristobalite inclusions (b) Trails of reddish brown hematite crystals.

X-Ray diffraction analyses indicated that the stones were amorphous and structurally opal-CT (Figure 2) with the presence of mineral phases including cristobalite, tridymite, quartz and goethite (clearly seen in the blackish brown samples).

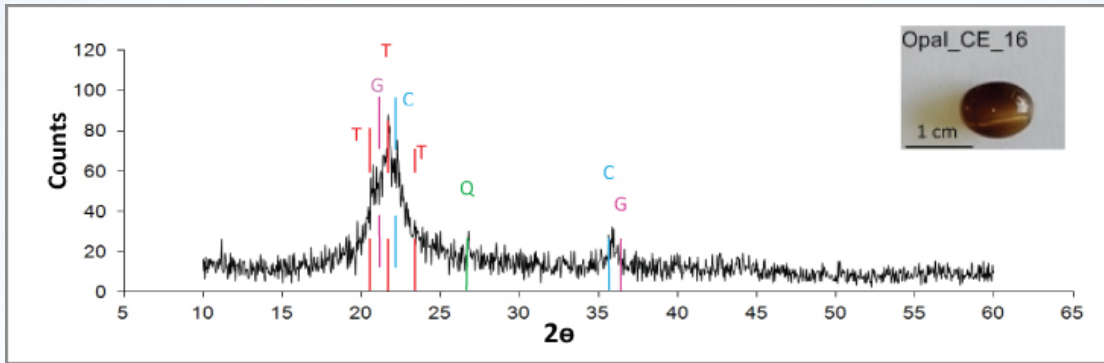


Figure 2: Diffraction pattern of cat's eye opal (**sample Opal_CE_16**), blackish brown colour, suggests the presence of tridymite (**T**), goethite (**G**), cristobalite, and quartz (**Q**) in opal structure.

Optical-vibrational spectroscopic study of these stones were carried out from 300 to 2500 nm (Figure 3 and 4) and the patterns exhibited general absorption bands at 300-600 nm suggesting the presence of ferric oxide (Fe^{3+}). In addition, the absorption band around 860-930 nm were seen in some samples which were related to goethite in the stones. Hydroxyl group and water molecules were found in the absorption bands at 1370 to 1600 nm and 1880 to 2050 nm, respectively. The absorption bands at 2150 to 2500 nm might be related to iron-hydroxyl bonding (Fe-OH).

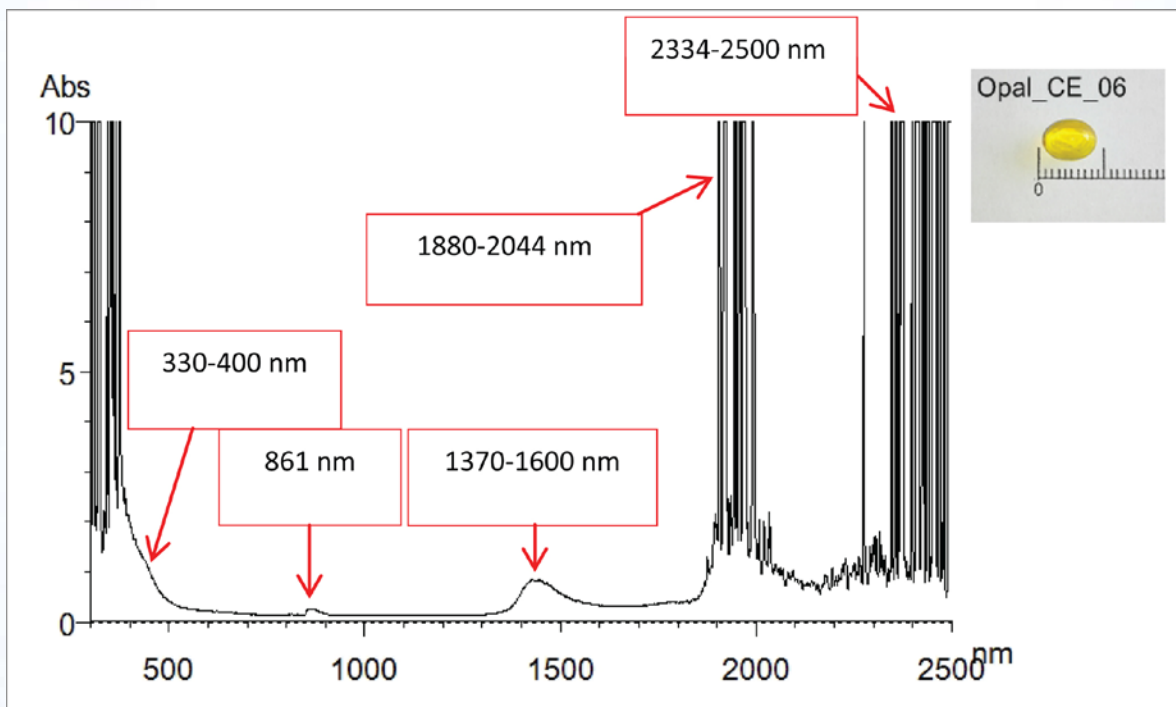


Figure 3: Optical-vibrational spectroscopy of yellow cat's eye opal.

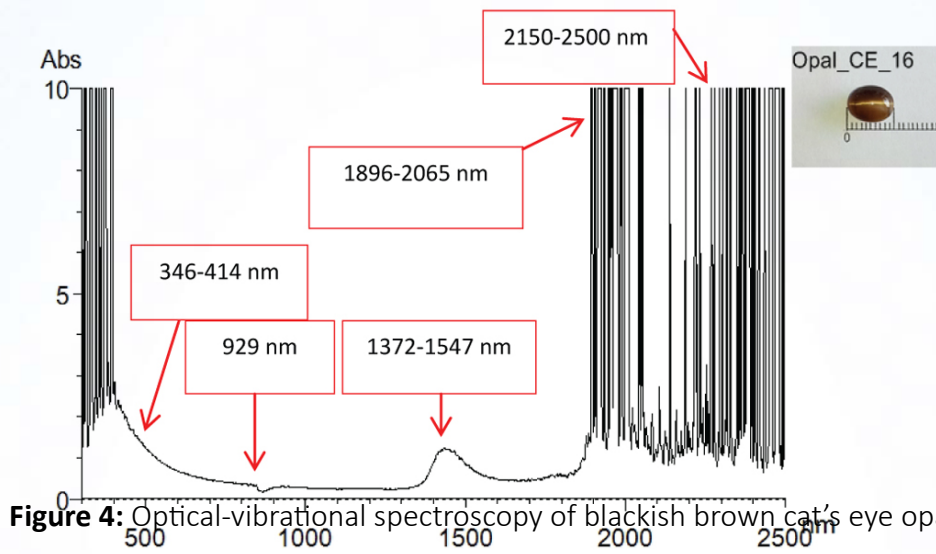


Figure 4: Optical-vibrational spectroscopy of blackish brown cat's eye opal.

The SEM images showed that the stones were composed of sphere beads having the sizes range from 0.01 to 0.05 μ m apparently without regular packing (Figure 5). The EDS analyses for chemical composition showed appreciable amount of Ti, Al, Fe, Mg, Ca and Mn additionally to the large amount of Si. Brown and blackish brown cat's eye opals contain significant amount of Ti and Fe suggesting the presence of Fe-Ti minerals also as inclusion in these opals.

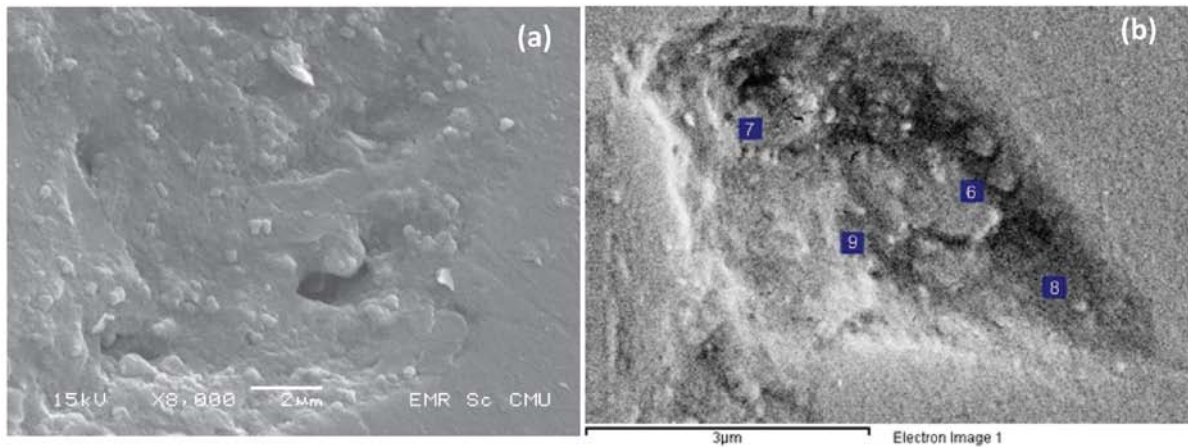


Figure 5: (a) SEM image of sphere beads in cat's eye opal structure (b) EDS analysis points of a blackish brown cat's eye opal and the chemical compositions were shown in Table 1.

Table 1: Chemical compositions of a blackish brown cat's eye opal at each analysis points from Figure 5(b).

	6	7	8	9
SiO ₂	46.38	57.28	86.48	65.62
TiO ₂	24.21	7.52	6.47	28.23
Al ₂ O ₃	8.35	2.23	0.00	1.75
Fe ₂ O ₃	5.95	1.28	0.77	1.91
MnO ₂	0.28	0.00	0.30	0.64
MgO	0.23	3.25	1.35	0.99
CaO	13.11	26.09	2.92	0.43
Na ₂ O	0.38	0.00	0.00	0.43
K ₂ O	0.74	2.34	0.18	0.00
ZnO	0.36	0.00	1.52	0.00
Total	99.99	99.99	99.99	100.00

The data obtained from these analyses provided the clue for the cause of colour of cat's eye opals that the presence of iron oxide/hydroxide minerals in the form of tiny goethite and hematite governed the colour mechanism of these stones. The cat's eye effect in these opals results from the needle-like inclusions, which was interpreted as goethite from its form and the confirmation from XRD analyses, however, the commonly presence of hematite may be possible candidate for the cause of this phenomenon.

References

- Elzea, J.M., and Rice, S., 1996, TEM and X- ray diffraction evidence for cristobalite and tridymite stacking sequences in opal, *Clays and Clay Minerals*, Vol.44, No.4, p.492-500.
- Gaillou, E., Delaunay, A., Rondeau, B., Bouhnik, I. M., Fritsch, E., Comenand, G., and Monnier, C., 2008, The geochemistry of gem opal as evidence of their origin, *Ore Geology Reviews*, Vol.34, No.1-2, p.113-126.
- Herdianita, N.R., Browne, P.R.L., Rodgers, K.A., and Campbell, K.A., 2000, Mineralogical and textural changes accompanying ageing of silica sinter, *Mineralium Deposita*, Vol.35, No.1, p.48-62.
- Wentzell, C.Y., and Reinitz, I., 1998, Cat's- Eye Opal, *Lab Notes, Gems & Gemology*, Vol.34, No.1, p.46.

Corresponding Author

Fullname: Boontarika Srithai
Affiliation: Department of Geological Sciences, Faculty of Science, Chiang Mai University, Chiang Mai, 50200, Thailand.

Characteristic and Physical Properties of Freshwater Cultured Pearls from Kanchanaburi Province

***Nutwatcharee Noirawee, Chakkrich Boonmee, Natthapong Monarumit,
Aumaparn Phlayrahan, and Somruedee Satitkune***

The Gem and Mineral Sciences Special Research Unit, Department of Earth Sciences, Faculty of Science, Kasetsart University, Bangkok 10900, Thailand

Extended Abstract

Introduction

Pearl, one of organic gems, is greatly demanded in the jewelry market due to the lack of natural one. Nowadays, the cultured pearl is the most popular organic gemstone in the world for serving the consumer desire. The inland fisheries research and development bureau Kanchanaburi is the only one institute in Thailand for developing and researching the freshwater cultured pearls, especially *Chamberlainia hainesiana* species. There are many kinds of pearl products which are different by colors, shapes and lusters. The pearl is formed by biomineralisation of calcium carbonate. The main composition of pearl is caused by CaCO_3 substance in aragonite and vaterite forms. Pearl is good example of polymorphs gem. The pearl can be studied using a Raman spectroscopy, such as aragonite, vaterite, calcite and amorphous CaCO_3 (Kiefert and Karampelas, 2011). Scanning Electron Microscope (SEM) is used to examine the micro-structure showing laminated character on the pearl surfaces. SEM images present the hexagonal shape of aragonite form (Xie *et al.*, 2009).

Material and Methods

The pearl samples (Figure 1) were collected from the inland fisheries research and development bureau Kanchanaburi. The good and poor luster samples were detected and prepared for studying micro-structure by using SEM.



Figure 1: The pearl samples (*Chamberlainia hainesiana* species) from Kanchanaburi.

Raman is the efficient technique to identify the chemical compounds, functional groups and the conformation of complex biomolecules. The Raman spectroscopic technique is caused by a photon interacts with a molecule and scatters into surrounding direction. The detector measures lost photon or receiving energy for spectrum analysis (Prance *et al.*, 2011).

Scanning Electron Microscope (Figure 2) is applied to study the micro-structure level on surface of materials. SEM image is caused by generated electron from the sample to the detector producing a highly resolution image.

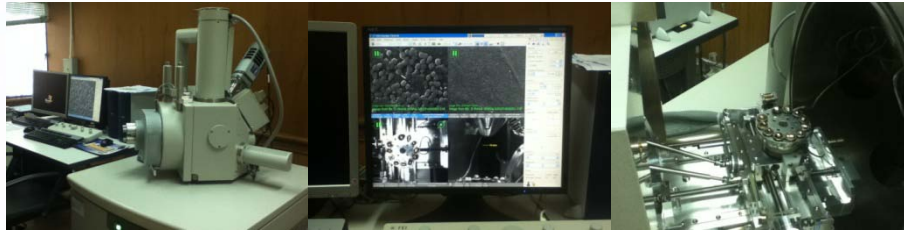


Figure2: The Scanning Electron Microscope (SEM) at Scientific Equipment Center, Faculty of Science, Kasetsart University (Quanta 450 FEI model).

Results

In this study, the characteristics of 25 pearl samples from Kanchanaburi are summarized in Table 1.

Table 1: Characteristics of pearl samples.

	Characteristics
shape	nearly round, slightly round, oval, semi oval, drop, baroque, semi baroque
color	white, nearly white, pale yellow, cream and purple
luster	good, medium, low, very low

Moreover, selected both samples of good luster and poor luster are identified the chemical compounds and surface feature of pearls by using Raman spectroscopy and SEM images, respectively. The Raman spectra of good luster pearl sample show peaks at 142, 152, 180, 191, 205, 213, 471, 705 and 1085 cm^{-1} (Figure 3a). Another, the poor luster pearl sample show peaks at 112, 152, 178, 191, 205, 210, 471, 705 and 1085 cm^{-1} (Figure 3b). Besides, the peaks mainly consist of aragonite, however, there are different two peaks of vaterite (210 cm^{-1}) and calcite (1085 cm^{-1}) (Gauldie *et al.*, 1997, Sodati *et al.*, 2007, Wehrmeister *et al.*, 2009).

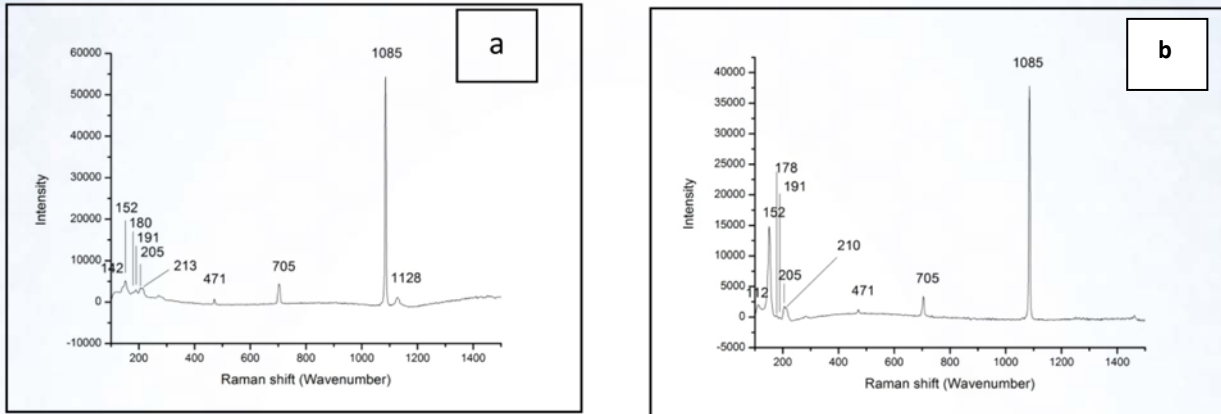


Figure 3: The Raman spectra of pearl sample **a)** good luster and **b)** poor luster

The SEM images show the hexagonal form (Figure 4) especially in good luster pearl and incomplete form (Figure 5) in poor luster pearl. *Chamberlainia hainesiana* pearls presented hexagonal form of aragonite in good luster pearl surface and round-like form or irregular form of vaterite in poor luster pearl surface (Bourrat *et al.*, 2011; Dechphrom, 2014; Murr and Ramirez, 2012).

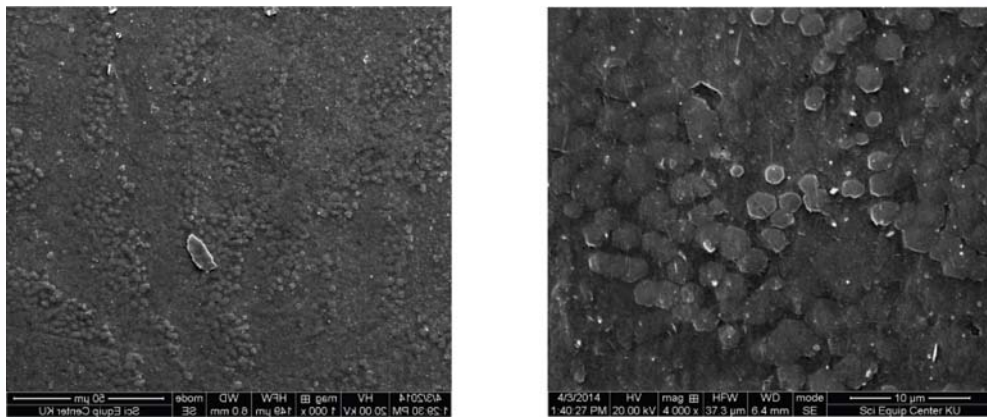


Figure 4: The hexagonal form on good luster pearl surface

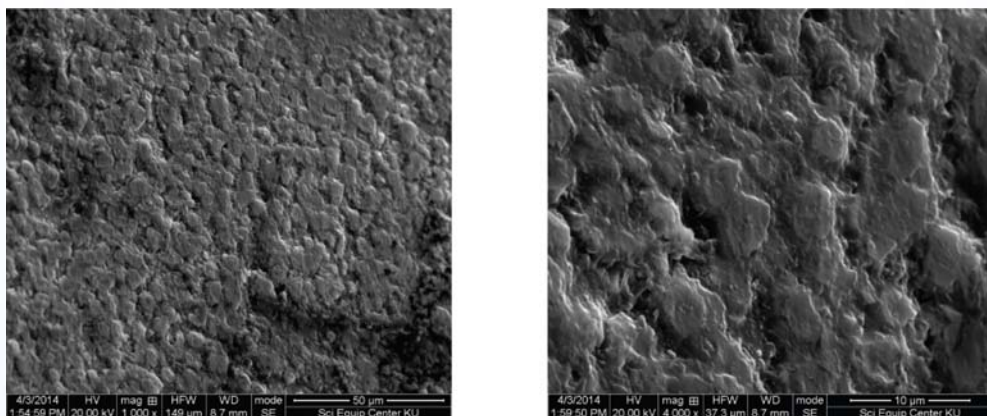


Figure 5: The incomplete hexagonal form on poor luster pearl surface

Conclusions

The pearl samples present various shapes, colors and lusters. The good luster pearl sample shows Raman spectra of aragonite phase and calcite phase whereas the poor luster pearl sample shows Raman spectra (weak peak) of vaterite phase at 210 cm⁻¹ and the other peaks of aragonite and calcite phase. The SEM images of good luster pearl could be indicated the hexagonal form. On the other hand, the other images show irregular form of poor luster pearl.

Acknowledgement

The authors are grateful for support from the Gem and Mineral Sciences Special Research Unit, Department of Earth Sciences, Faculty of Science, Kasetsart University and the Graduate School Kasetsart University, the inland fisheries research and development bureau Kanchanaburi for the pearl samples, the Gem and Jewelry institute of Thailand for supporting Raman spectrometer.

References

- Bourrat, X., Qiao, L., Feng, Q., Angellier, M., Dissaux, A., Beny, J.M., Barbin, V., Stempfle, P., Rousseau, M., and Lopez, E., 2012, Origin of growth defects in pearl, *Materials Characterization*, Vol.72, p.94-103.
- Dechphrom, P., 2014, Physical Characteristic and Spectroscopic Property of fresh water cultured pearl *Chamberlainia hainesiana*, B.T. Thesis, Kasetsart University.
- Gauldie, R.W., Sharma, S.K., and Volk, E., 1997, Micro-Raman Spectral Study of Vaterite and Aragonite Otoliths of the coho salmon, *oncorhynchus kisutch*, *Comparative Biochemistry and Physiology A-Physiology*, Vol.118, No.3, p.753-757.
- Kiefert, L., and Karampelas, S., 2011, Use of the Raman spectrometer in gemmological laboratories: Review, *Spectrochimica Acta Part A: Molecular and Biomolecular Spectroscopy*, Vol.80, No.1, p.119-124.
- Murr, L.E., and Ramirez, D.A., 2012, The Microstructure of the Cultured Freshwater Pearl, *JOM*. Vol.64, No.4, p.469-474.
- Prance, A., Peachey, J., Harvey, R., Hepel, M., Stobiecka, M., and Ewy, R., 2011, Chemical and Biological Applications of Raman Spectroscopy, University of New York, Learning and Research Fair, April 13, 2011, SUNY Potsdam, NY.
- Sodati, A.L., Jacob, D.E., Wehrmeister, U., Hager, T., and Hofmeister, W., 2007, Micro-Raman spectroscopy of pigments contained in different calcium carbonate polymorphs from freshwater cultured pearls, *Journal of Raman Spectroscopy*, Vol.39, No.4, p.525-536.
- Wehrmeister, U., Sodati, A.L., Jacob, D.E., Häger, T., and Hofmeister, W., 2009, Raman spectroscopy of synthetic, geological and biological vaterite: a Raman spectroscopic study, *Journal of Raman Spectroscopy*, Vol.41, No.2, p.193-201.
- Xie, L., Wang, X., and Li, J., 2009, The SEM and TEM study on the laminated structure of individual aragonitic nacre tablet in freshwater bivalve *H.cumingii* Lea shell, *Journal of Structural Biology*, Vol.169, No.1, p.89-94.

Corresponding Author

Full name: Nutwatcharee Noirawee
Affiliation: The Gem and Mineral Sciences Special Research Unit, Department of Earth Sciences, Faculty of Science, Kasetsart University, Bangkok, 10900, Thailand.
Email: fscisrd@sci.ku.ac.th

Characteristics of Cyangugu Sapphire from Rwanda

***Tasnara Sripoonjan¹, Thanapong Lhuaamporn¹, Nataya Nilhud¹,
Nisa Sukkee² and Chakkaphan Sutthirat^{1,2}***

¹The Gem and Jewelry Institute of Thailand (Public Organization), Bangkok, 10500, Thailand

²Department of Geology, Faculty of Science, Chulalongkorn University, Bangkok, 10330, Thailand

Extended Abstract

Introduction

East and Central Africa is one of the world's important sources of gem-quality corundum. Many sapphire deposits have been discovered continuously in the last three decades, such as at Uмба River in Tanzania, at Garbatula and Turkana in Kenya (Hughes, 1997; 2014). Since late 2013, an increasing number of sapphire materials from new mines have been reportedly supplied into the gem markets. One of those new sources of blue sapphire was recently found in Cyangugu Province, Southwestern Rwanda. These sapphires are associated with alkali basalt extruded during the Tertiary extensional regime along the east Africa rift (Krzemnicki *et al.*, 1996). Stones from this deposit showed specific surface features which were influenced by the primary magmatic corrosion of the basaltic melt during transportation process from deep-seated source to the earth's surface (Krzemnicki *et al.*, 1996; also as previously suggested for basaltic gem corundum from other sources; Levinson and Cook, 1994; Guo *et al.*, 1996; Pisutha-Arnond *et al.*, 2005).

In this investigation, 17 representative samples (Figure 1) were selected and used for collecting the gemological properties by basic equipment and various spectroscopic data by advanced instruments such as UV-Vis-NIR, FTIR and EDXRF.



Figure 1: Representative sapphire samples from Cyangugu, Rwanda.

Gemological Properties

Most samples from this locality show pleochroic colors ranging from greenish blue to blue with weak to moderate saturation. Other gemological properties include RI ($n_o=1.763$ - 1.766 , $n_e=1.769$ - 1.775), birefringence (0.007 - 0.009), and SG (3.96 - 4.02). All samples are inert under both short and long UV-radiation. Microscopic observation reveals that the most common internal features are silks oriented along crystallographic direction. Some samples show distribution of milky/cloudy inclusions throughout the whole stone (geuda-like) (Figure 2a). It occasionally exhibits clearly polysynthetic twinning (Figure 2b). Other solid inclusions randomly occurred are ferro-columbite (Figure 2c), feldspar with tension cracks (Figure 2d) and zircon clusters (Figure 2e) that were confirmed by Raman microscope. Apart from above, some distinct features i.e., unusual irregular color zones with polygon color patches and comet-like inclusions (red circle) are observed in one sample (Figure 2f).

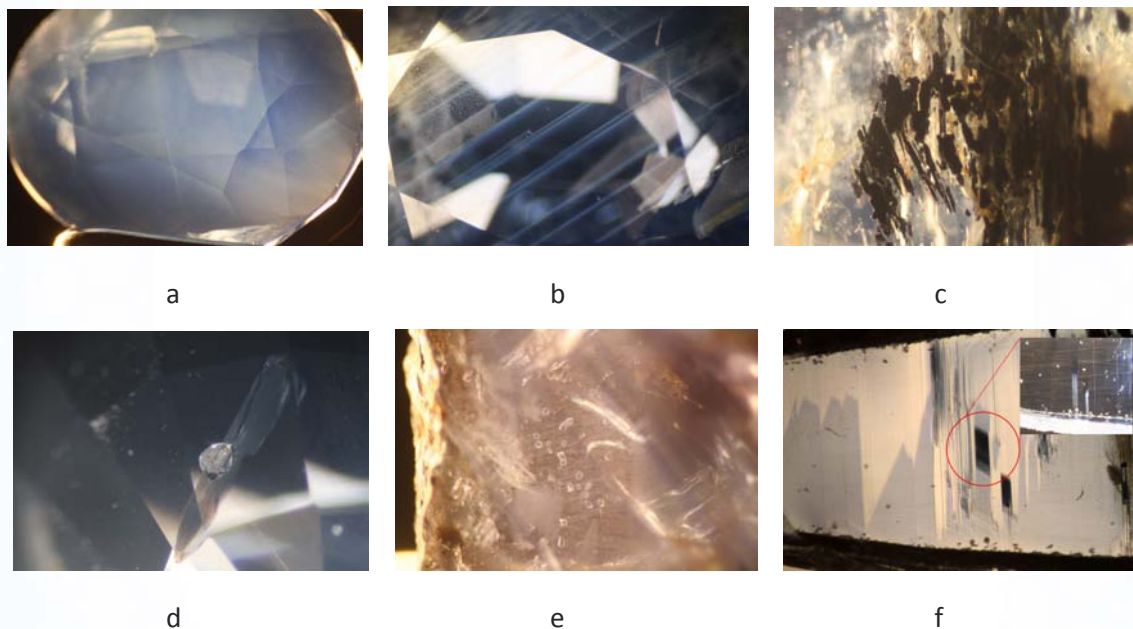


Figure 2: Microscopic images of inclusions in blue sapphires from Cyangugu, Rwanda.

Advanced Spectroscopy

EDXRF analysis gave Fe contents range between 0.13 and 0.54 wt% with an average of 0.37 wt%, Ga contents between 0.01 and 0.05 wt% with an average of 0.03 wt%, Ti contents between 0.01 and 0.03 wt% with an average of 0.02 wt%, V and Cr values below the detection limit (< 0.01 wt%). UV-Vis-NIR spectra (Figure 3) show broad absorption bands around 900 nm due to Fe^{2+}/Fe^{3+} IVCT and 585 nm due to Fe^{2+}/Ti^{4+} IVCT, as well as absorption peaks due to d-d transition of Fe^{3+} at 450 nm and 378/388 nm (as suggested by Ferguson and Fielding, 1971; Nassau and Valente, 1987; Burn, 1993; Fritsch, 1993; Häger, 2001). The spectra in Mid-IR region are related to structural OH-group absorption consisting of series of sharp peaks, placed around 3100 to 3600 cm^{-1} as suggested by Volynets *et al.*, (1972) and Smith (1995) (Figure 4).

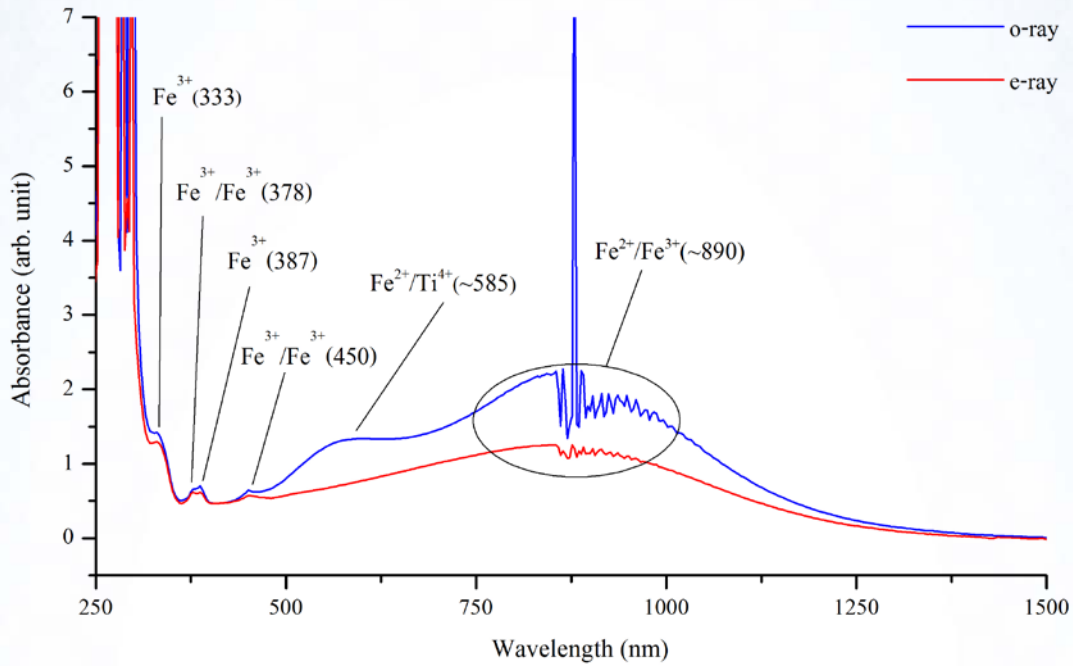


Figure 3: Representative UV-Vis-NIR spectrum of blue sapphire from Cyangugu, Rwanda.

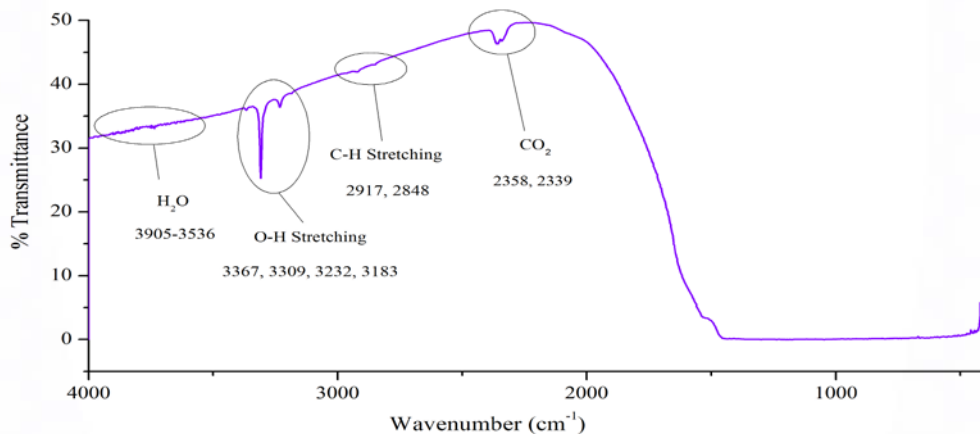


Figure 4: Representative Mid-IR spectrum of blue sapphire from Cyangugu, Rwanda.

Discussion and Conclusion

The analytical data obtained from this study indicate that the Rwanda sapphires are associated with magmatic-type origin similar to those found in Australia, Kenya, Madagascar, Nigeria, Cameroon and Southeast Asia. In addition, Rwanda sapphires commonly show “silky” inclusions. The sapphires with silk inclusions could be suitable for quality enhancement by heat treatment as the silk inclusions can be removed and the stone turns more transparent. Besides, the inclusion features appeared as unusual irregular color zones with polygon color patches and comet-like inclusions seem to be a distinct characteristic of sapphire from this source.

Acknowledgements

We are thankful to Mr. Chumphon Pijarnson for providing samples. This study was supported by the GIT. The authors would like to sincerely thank to the academic advisors and staff of GIT Gem Testing Laboratory (GIT-GTL) for analytical and technical assistances during the course of this study and the manuscript preparation. All the analyses were carried out at the GIT-GTL.

References

- Burns, R.G., 1993, Mineralogical applications of crystal field theory, 2nd ed., Cambridge, Great Britain: Cambridge University Press, 576 p.
- Ferguson, J., and Fielding, P.E., 1971, The origins of the colours of yellow, green, and blue sapphires, *Chemical Physics Letters*, Vol.10, No.3, p.262-265.
- Fritsch, E., and Mercer, M., 1993, Blue Color in Sapphire Caused by Fe²⁺/Fe³⁺ Intervalence Charge Transfer, *Letters, Gems & Gemology*, Vol.29, No.3, p.151 and 226.
- Guo, J, O'Reilly, S.Y., and Griffin, W.L., 1996, Corundum from basaltic terrains: a mineral inclusion approach to enigma, *Contributions to Mineralogy and Petrology*, Vol.122, No.4, p. 368-386.
- Häger, T., 2001, High temperature treatment of natural corundum, in Hofmeiser, W., Dao, N.Q., Quang, V.X. (eds.), in *Proceedings of the international workshop on material characterization by solid state spectroscopy: The Minerals of Vietnam*, Hanoi, Vietnam, p.24-37.
- Hughes, R.W., 1997, *Ruby & Sapphire*, Colorado, USA, RWH Publishing, 512 p.
- Hughes, R.W., 2014, *Ruby & Sapphire: a Collector's Guide*, with photos by Wimon Manorotkul & e. Billie Hughes, Gem and Jewelry Institute of Thailand, 384 p.
- Krzemnicki, M.S., Hänni, H.A., Guggenheim, R. and Mathys, D., 1996, Investigations on sapphires from an alkali basalt, South West Rwanda, *Journal of Gemmology*, Vol.25, No.2, p.90-106.
- Levinson, A.A., and Cook, F.A., 1994, Gem Corundum in Alkali basalt: Origin and Occurrence, *Gems & Gemology*, Vol.30, No.3, p.253-262.
- Nassau, K., and Valent, G.K., 1987, The seven types of yellow sapphire and their stability to light. *Gems & Gemology*, Vol.23, No.4, p.221-231.
- Pisutha-Arnond, V., Intasopa, S., Wathanakul, P., Griffin, W.L., Atichat, W., and Sutthirat, C., 2005, Sapphire xenocrysts in basalt from the Bo Phloi Gem Field, Western Thailand; in *Proceedings of the International Conference on GEOINDO 2005*, Khon Kaen, November 28- 30, p.338-344.
- Smith, C.P., 1995, A contribution to understanding the infrared spectra of rubies from Mong Hsu, Myanmar, *Journal of Gemmology*, Vol.24, No.5, p.321-335.
- Volynets, F.K., Sidorova, E.A., and Stsepuro, N.A., 1972, Oh groups in corundum crystals which were grown with the verneille technique, *Journal of Applied Spectroscopy*, Vol.17, No.6, p. 1626-1628.

Corresponding Author

Full name : Tasnara Sripoonjan
Affiliation : The Gem and Jewelry Institute of Thailand (Public Organization), Bangkok, 10500, Thailand.
Phone: +66 2634 4999 Fax: +66 2634 4970
Email : stasnara@git.or.th

Characteristics of the Weyama Diamond from Weyama Gbapolu Country, Liberia

Hyeonki Kim

Advanced Gemology, Hanyang University, Seoul, 133-791, Korea

Extended Abstract

Diamonds is the most valuable gem mineral in the world and has been generally traded with stable rates. It has been demanded by all countries. Properties of diamonds are quite interesting for scientific researches. It becomes more and more significant to study on gemological properties of diamonds for characterization of new diamond mines.

Recently, a new diamond mine has been discovered in the Weyama area of Liberia, West Africa. These diamonds found have high qualities for jewelry industry. Seven pieces of rough diamonds from the mine, were investigated under microscope weighting, and fluorescence testing. They were analyzed by FTIR, Raman, UV-VIS spectrometers, and XRF. There were not particular results in other experiments, but Micro-Raman test showed a unique peak near $2,600\text{ cm}^{-1}$.

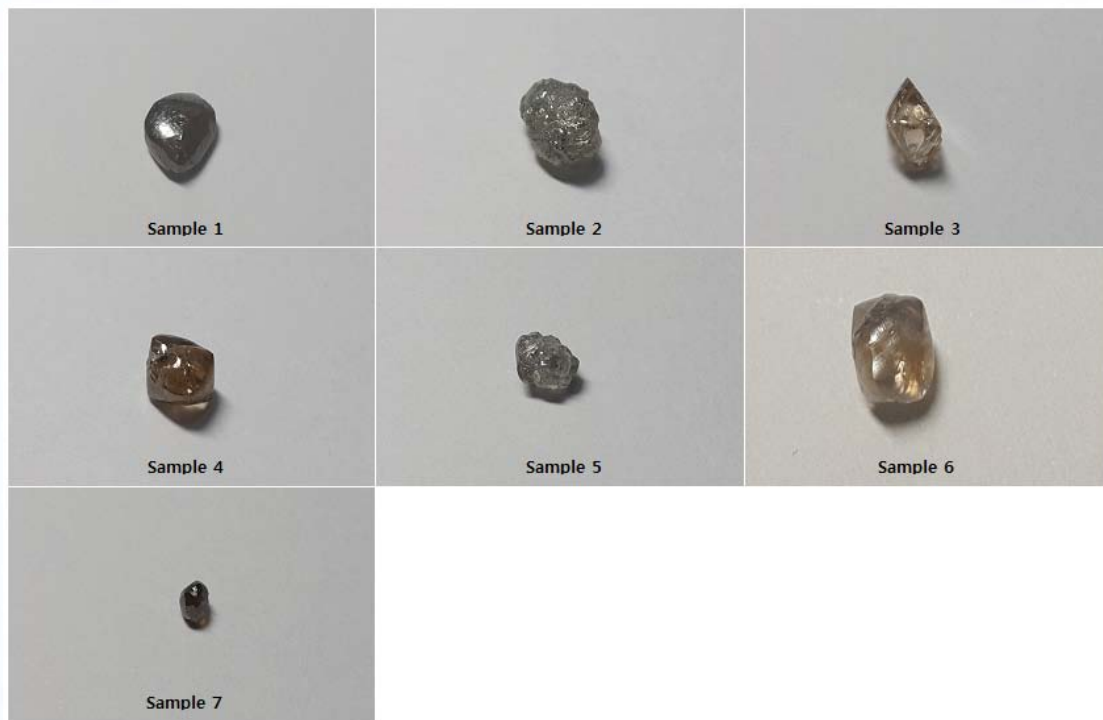


Figure 1: Natural Diamond from Weyama Gbapolu Country, Liberia

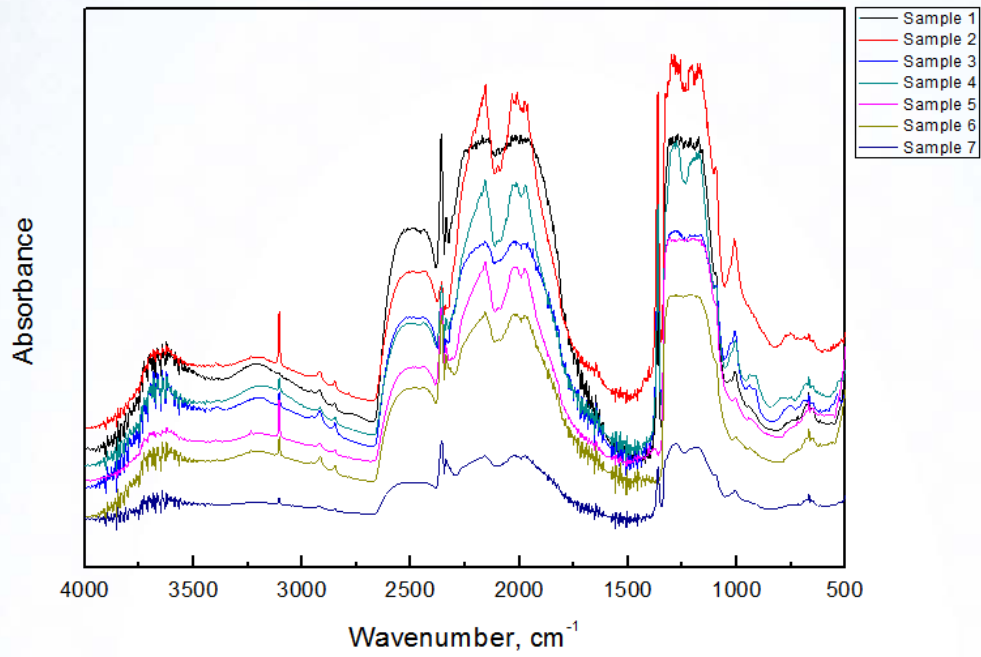


Figure 2: FTIR spectrum of Diamonds from Weyama Gbapolu Country, Liberia

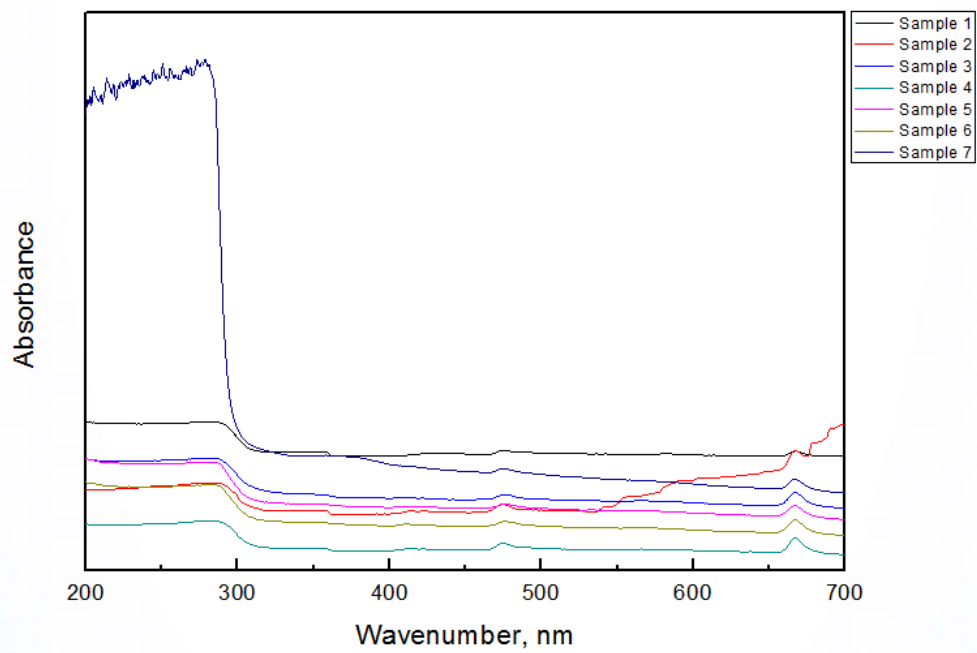


Figure 3: UV-Vis spectrum of Diamonds from Weyama Gbapolu Country, Liberia.

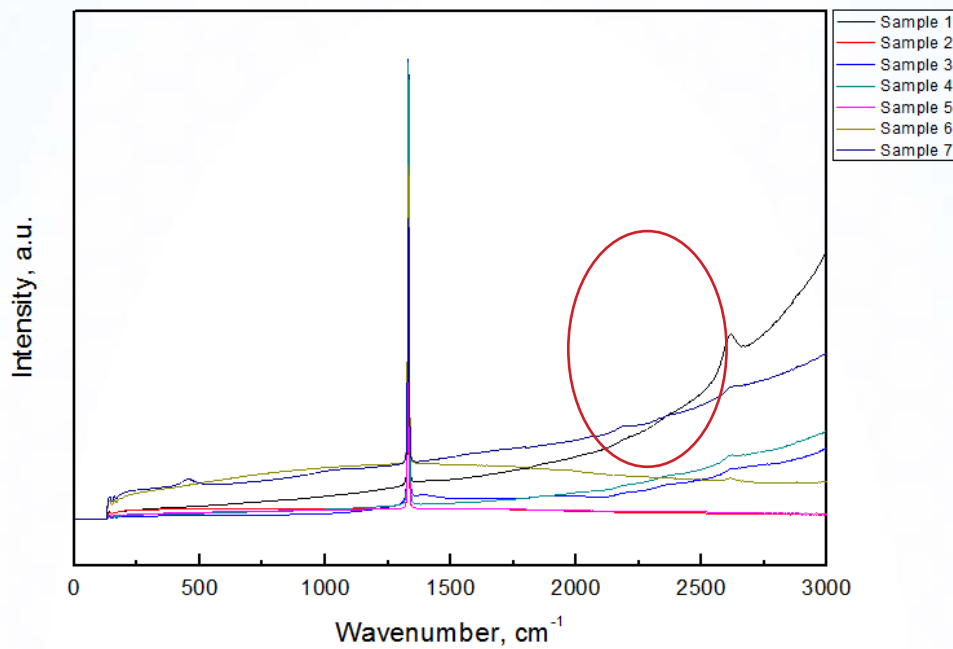


Figure 3: Raman spectrum of Diamonds from Weyama Gbapolu Country, Liberia. Samples showed unique peak near 2600 cm⁻¹

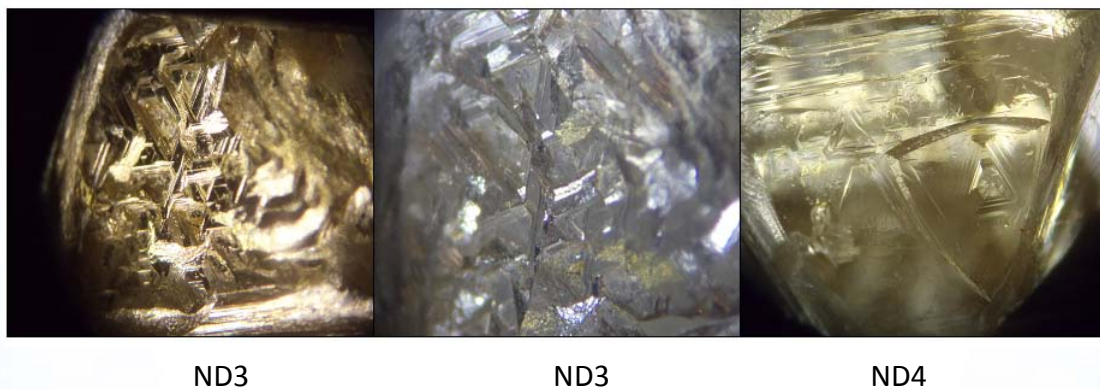


Figure 4: Microscope Images (Inclusion) of Diamonds from Weyama Gbapolu Country, Liberia. Some growth mark (trygon) was well observed from several samples.

Corresponding Author

Full name: Hyeonki Kim
 Affiliation: Advanced Gemology, Hanyang University, Seoul, 133-791, Korea.
 Email: k10547@nate.com

Chemical and Spectroscopic Study of Zircon from Dak Lak, Central Highlands of Vietnam

*Le Thi-Thu Huong¹, Bui Sinh Vuong¹, Somruedee Satitkune², and Bhuwadol
Wanthanachaiseng³*

¹Faculty of Geology, VNU University of Science, 334 Nguyen Trai, Hanoi, Vietnam

²Faculty of Science, Kasetsart University, Bangkok, 10900, Thailand

³Faculty of Gems, Burapha University, Chanthaburi, 22170, Thailand

Extended Abstract

Together with basaltic sapphires, zircon is recovered from placers in the provinces of Central Highlands including Kon Tum, Dak Lak, Dak Nong, and Gia Lai. In this study we reported some chemical and spectroscopic features of samples collected from currently exploited mine in Dak Lak province. The zircon colour of the mine ranges from colourless to orange, brownish orange and reddish brown (Figure 1). The crystals, typically combinations of the bipyramid and the tetragonal prism, are usually etched and waterworn, sized from 0.5 cm to 4 cm. The reddish brown zircon from the mine is typically heated to turn it blue, orange, or colourless.



Figure 1: Small scale exploiting zircon mine in Dak Lak province and the samples showing natural orange, brownish orange and reddish brown colour.

Materials and Methods

Eight samples (3 faceted and 5 rough some of which shown in Figure 2) were collected to study with EDXRF, UV-Vis-NIR, FTIR and Raman spectroscopy (Figure 2).

Chemical component of the samples are identified with EDXRF. Microprobe analyses were performed with an EDAX Eagle III microprobe. Measurements were made at 40 kV and 250 μ A with an EAGLE III spectrometer equipped with a rhodium tube and the environment will be in a vacuum.



Figure 2: Six samples which are representatives for the zircon mined from the area showing typical colours.

The UV-Vis-NIR spectra were obtained from a Perkin Elmer Lambda 900 spectrophotometer. The absorption spectra were recorded over the range of 200 to 1600 nm in absorbance mode at a scan speed of 300 nm/minutes and a slit width of 2.5 millimeters. The data were compiled by Perkin Elmer Spectrum V.5.0.1 program. The study before checking sample will calibrate using the automated system that comes with the machine.

The FTIR spectrum were obtained from a Thermo Scientific, Nicolet Model 6700 brands which uses a He-Ne Laser by the study of wave numbers between 400-7000 cm^{-1} in transmittance mode and scan 128 seconds. The standard resolution of the Nicolet 6700 spectrometer is 0.09 cm^{-1} . The data were compiled by OMNIC software program.

Raman spectra in this study were collected with a Laser Raman Spectroscope model 1000, Renishaw IR Laser 785 (Infrared) coupled with an Olympus BX41 optical microscope and a Si-based CCD (charge-coupled device) detector.

Results

Chemical features

EDXRF analysis showed that the zircon samples were commonly enriched in Y_2O_3 , heavy rare-earth elements (HREE), light and middle rare earths (LREE and MREE). The zircon structure

is adopted by numerous minerals and synthetic compounds with the general formula ABO_4 , in which: $A=Zr^{4+}$, Hf^{4+} , Ca^{2+} , Mn^{2+} , Mg^{2+} , Fe^{3+} and some REEs; $B=Si^{4+}$, P^{5+} , Al^{3+} , Fe^{3+} . The presence of REE which substitute for Zr^{4+} site contributes the colours of zircon. The concentration of Ti_2O_3 , La_2O_3 , CaO , MgO , Fe_2O_3 were more enriched in dark brown color area than the light brown and light yellow ones while the concentrations of Nd_2O_3 , Gd_2O_3 , Tb_2O_3 , Lu_2O_3 , Y_2O_3 , ThO_2 were reversible.

UV-Vis-NIR

All of the spectra showed a similar pattern with a similarly continuous increase in the absorption toward the UV region, in particular in the range of 400-600 nm with the shoulder at around 500 nm giving the absorption window toward the red end; hence as the result, the samples appear with the red-orange-yellow color components. This absorption pattern is likely to be due to the defect in crystal structure caused by the radiation damage from radioactive elements such as U and Th. Some spectra also revealed prominent absorption peaks at 1114 nm and 1505 nm which are probably due to U^{5+} (Figure 3).

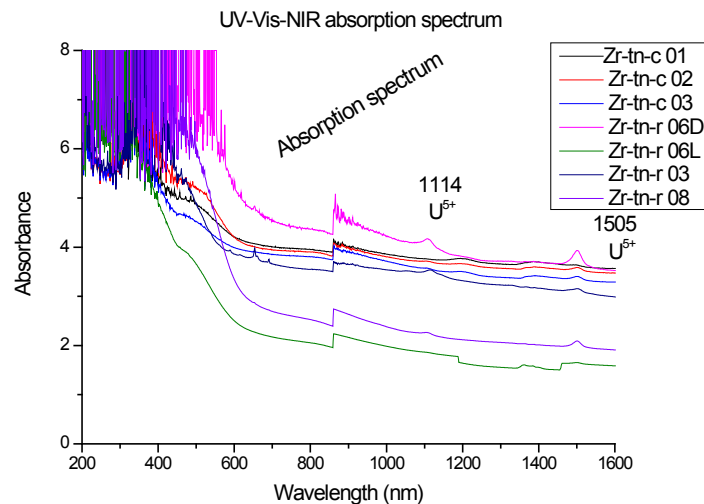


Figure 3: UV-Vis-NIR absorption spectra of Dak Lak zircon.

FTIR spectroscopy

The spectra showed strong absorptions at 2341, 2504, 2764, 2856, 2918, 3090, 3197 cm^{-1} (Figure 4). The particular attention was paid to the peak at 3197 cm^{-1} which is the evidence of OH stretching characteristic. Besides, the presence of peak at 6663 cm^{-1} indicates that a small number of U ions are in the pentavalent state (U^{5+} amorphous) in metamict natural $ZrSiO_4$ (Nasdala *et al.*, 1995). An absorption band in the 1,400-2,000 cm^{-1} interval is related to Si-O stretching which indicate a well crystalline zircon (Woodhead *et al.*, 1991). The appearance of peaks at 3420 cm^{-1} ($E \parallel c$) and 3385 cm^{-1} ($E \perp c$) are associated with Si occupied tetrahedrons and a peak at around 1730 cm^{-1} instead of the H-O-H bending mode near 1630 cm^{-1} and the lack of the combination (bending + stretching) mode at around 5200 cm^{-1} indicate a crystalline zircon with little radiation damage by radioactive elements (Woodhead *et al.*, 1991). Moreover, some spectra indicate two very weak bands located near 4069 and 4256 cm^{-1} which may be attributed to the combination of OH stretching and the vibrations of the framework.

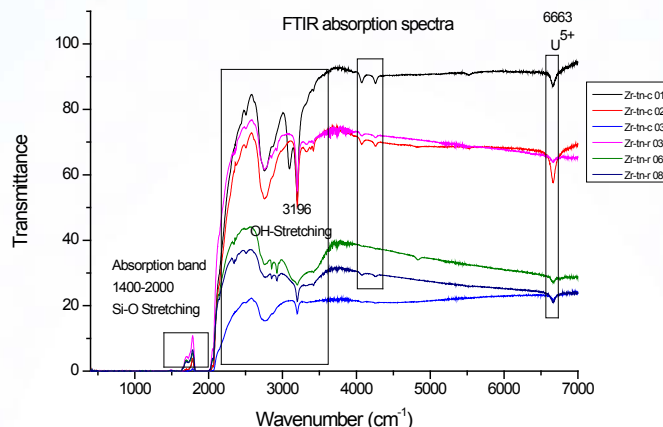


Figure 4: FTIR absorption spectra of Dak Lak zircon.

Raman spectroscopy

Raman spectra showed dominant peaks at 356, 440, 972, 1008 cm^{-1} (Figure 5). In general, the peaks appeared at 356 cm^{-1} are assigned to ν_4 antisymmetric SiO_4 bending, or lattice mode, at 440 cm^{-1} to ν_2 symmetric SiO_4 bending, at 972 cm^{-1} to ν_1 symmetric SiO_4 stretching, and at 1008 cm^{-1} to ν_3 antisymmetric SiO_4 stretching (Dawson *et al.*, 1971). Correspondingly, a low-intensity band at 649 cm^{-1} is assigned to internal ν_4 (SiO_4) vibrations whereas the strong 356 cm^{-1} band was described as external mode (Kolesov *et al.*, 2001). Moreover, the spectra also showed some bands at a 225, 321, 1256, 1539 cm^{-1} which are generally agreed to be lattice modes (i.e. vibrations involving movements of SiO_4 tetrahedrons and Zr ions). In addition, the most intense peak appearing at 1384 cm^{-1} in all samples is related to the vibration of CO_2 molecules (Zeming *et al.*, 2006)

Nasdala *et al.*, (1995) suggested that degree of metamictization can be best estimated from the Raman peak of ν_3 (SiO_4). The well crystalline zircon usually has ν_3 (SiO_4) peak at about 1008 cm^{-1} and its Full Width at Half Maximum (FWHM) value is about 3 cm^{-1} . In contrast, the amorphous (metamict) zircon can possess the ν_3 (SiO_4) peak below 900 cm^{-1} and its FWHM value is larger than 100 cm^{-1} . All Đăk Lăk zircon samples show the ν_3 (SiO_4) peak at 1008 cm^{-1} and their FWHM values varying from 3.09 to 3.57. These data therefore suggest that the Đăk Lăk zircons is very mildly radiation damage.

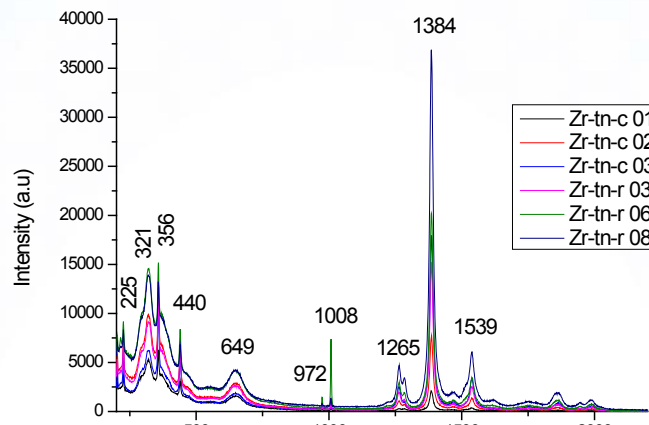


Figure 5: Raman spectra of Dak Lak zircon.

Acknowledgments

EDXRF analyses were carried out at The Gem and Jewelry Institute of Thailand; UV-Vis-NIR based at the Earth Science Faculty, Kasetsart University; FTIR and Raman measurements based at Center for Material Sciences, VNU University of Sciences. The authors are grateful for the supports.

References

- Dawson, P., Hargreave, M.M., and Wilkison, G.R., 1971, The vibrational spectrum of zircon ($ZrSiO_4$), *Journal of Physics C: Solid State Physics*, Vol.4, No.2, p.240-256.
- Kolesov, B.A., Geiger, C.A., and Armbruster, T., 2001, The dynamic properties of zircon studied by single- crystal X-ray diffraction and Raman spectroscopy, *European Journal of Mineralogy*, Vol.13, No.5, p.939-948.
- Nagasawa, H., 1970, Rare earth concentrations in zircons and apatites and their host dacites and granites, *Earth and Planetary Science Letters*, Vol.9, No.4, p.359-364.
- Nasdala, L., Irmer, G., and Wolf, D., 1995, The degree of metamictization in zircon: a Raman spectroscopic study, *European Journal Mineralogy*, Vol.7, No.3, p.471-478.
- Woodhead, J.A, Rossman, G.R, and Silver, L.T., 1991, The metamictization of Zircon: radiation dose-dependent structural characteristics, *American Mineralogists*, Vol.76, No.1-2, p.74-82.
- Zeming, Z., Kun, S., Yilin, X., Jochen, H., and Liou, J.G., 2006, Mineral and fluid inclusions in zircon of UHP metamorphic rocks from the CCSD-main drill hole: A record of metamorphism and fluid activity, *Lithos*, Vol.92, No.3-4, p.378-398.

Corresponding Author

Full name: Bui Sinh Vuong
Affiliation: Faculty of Geology, VNU University of Science, 334 Nguyen Trai, Hanoi, Vietnam.

Classification of Synthetic Diamonds by Using Fourier Transform Infrared Spectroscopy

Jinhee Jeon¹, Hunhyeong Lee², and Dongwook Shin^{1,2}

¹Department of Advanced Gemology, Hanyang University, Seoul, Korea

²Division of Materials Science and Engineering, Hanyang University, Seoul, Korea

Extended Abstract

In the past, synthetic diamonds and natural diamonds were easily distinguished due to the inclusions, impurities, and defects included in the process of making synthetic diamonds. However, recent technologies upgraded the qualities of synthetic diamonds which made it show less difference with natural diamonds. Because there is not much difference, synthetic diamonds are being sold as natural diamonds by salesman in markets. Therefore, delicate analysis equipment is vital to find synthetic diamonds among natural diamonds. However, not a lot of this equipment is made and these various amounts of equipment hold a very high price. Also, it is difficult, for jewelers, to own this high price equipment. There is no way to identify synthetic diamonds and natural diamonds just by using simple and cheap equipment at present. Therefore, the new technology for comparing natural and synthetic diamonds is needed.

In this work, experimental results show a simple method to tell the difference between synthetic diamonds and natural diamonds. For the experiment, natural diamonds type IaA, IaB, and IIa, and the CVD synthetic diamonds were prepared (Breeding and Shigley, 2009). Hundreds of natural diamonds were analyzed by FT-IR. After that, the several IIa diamonds were found and the others were IaA and IaB diamonds. Also, the ten samples of CVD diamonds were used for this experiment. The way of discrimination is defined on Table 1. Natural diamonds, type 1, significantly holds different characteristics compared to synthetic diamonds, while natural diamonds, type 2, holds very similar characteristics with CVD synthetic diamonds. The Fourier Transform Infrared Spectroscopy (FTIR) was used for the experiment. For high accuracy analysis, the integrating sphere accessory included in the FTIR was used. In general, when the diamonds are analyzed by the FTIR, the carbon structural peaks are observed in $1500 \sim 2700 \text{ cm}^{-1}$ and the nitrogen related peaks are observed in $1000 \sim 1500 \text{ cm}^{-1}$ (Howell *et al.*, 2012).

Figure 2 shows the typical absorbance spectrum of each type of diamonds by the FTIR. Because type I diamonds have nitrogen related peak, it is easy to classify between natural and synthetic diamonds. Comparing graph IIa and CVD, the FTIR results have critical two different points. First, it is shown that 2160 cm^{-1} peak of natural diamonds has higher intensity than 2030 cm^{-1} peak on the left, while CVD diamonds have lower peak of 2160 cm^{-1} than the 2030 cm^{-1} peak. Second, another big difference shown from these four graphs are at the 700 cm^{-1} peak. Not like the CVD, natural diamonds have an absorption peak on the 700 cm^{-1} peak. By understanding these two facts, it is shown that the natural diamonds and synthetic diamonds can be classified simply using by the FTIR analysis with integrating sphere.

Table 1: Classification of type of diamonds

	Group	N impurities (ppm)
Type I	Type Ia	10 ~ 5,500 (aggregated N impurities)
	Type Ib	25 ~ 50 (isolated single N impurities)
Type II	Type IIa	< 10 (no N or boron impurities)
	Type IIb	~ 0 (boron impurities)



Figure 1: The samples of (a) natural diamonds and (b) CVD synthetic diamonds.

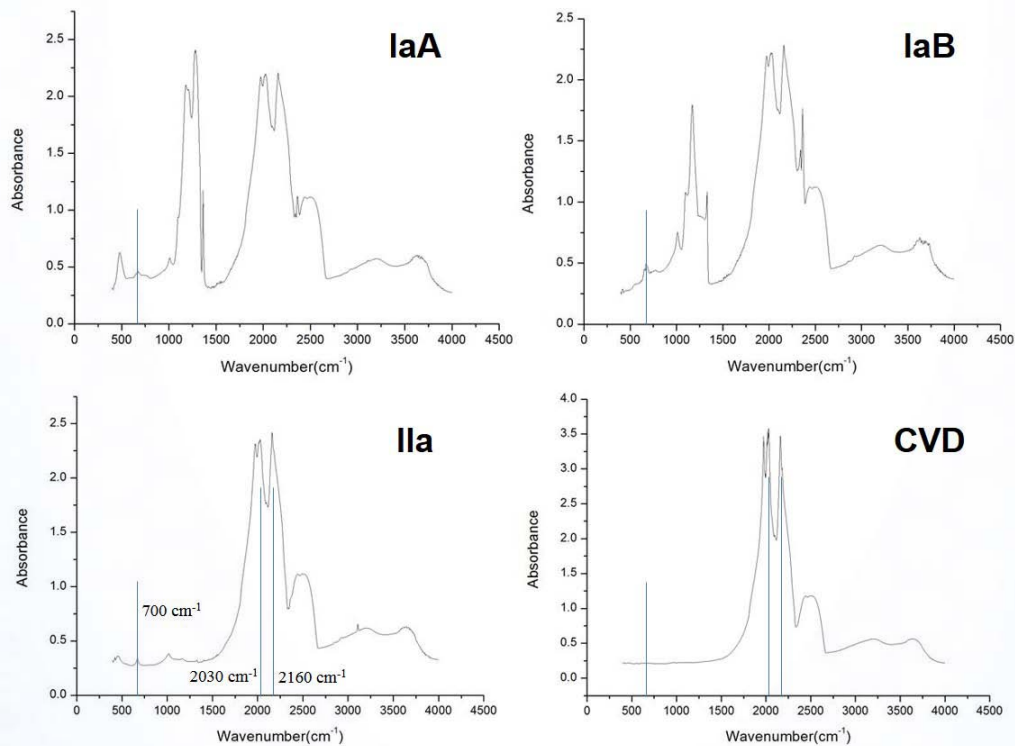


Figure 2: The spectrum of FTIR spectroscopy about diamonds.

References

- Breeding, C.M., and Shigley, J.E., 2009, The type classification system of diamonds and its importance in gemology, *Gems & Gemology*, Vol.45, No.2, p.96-111.
- Howell, D., O'Neill, C.J., Grant, K.J., Griffin, W.L., Pearson, N.J., and O'Reilly, S.Y., 2012, μ -FTIR mapping: distribution of impurities in different types of diamond growth, *Diamonds and Related Materials*, Vol.29, p.29-36.

Corresponding Author

Full name: Dongwook Shin
Affiliation: Department of Advanced Gemology and Division of Materials Science and Engineering, Hanyang University, Seoul, Korea.
Phone: +82-2-2220-0503
Fax: +82-2-2220-4011
Email: dwshin@hanyang.ac.kr

Comparison on the Geochemical Methods for Fingerprinting of Greenlandic Gem-Corundum (Rubies)

Majken D. Poulsen¹ and Nynke Keulen²

¹Geological Survey of Denmark and Greenland (GEUS), Nuuk Office c/o the Greenland Institute for Natural Resources, Kivioq 2, 3900 Nuuk, Greenland

²Geological Survey of Denmark and Greenland, Department for Petrology and Economic Geology, ØsterVoldgade 10, 1350 Copenhagen K, Denmark

Extended Abstract

Since the 1990's there has been considerable interest in investigating and exploiting the Greenlandic gemstone deposits with corundum (sapphire and ruby) at Fiskensættet in southern West Greenland and the Greenlandic Ministry for Industry and Mineral Resources (MIM) have issued a number of exploration and small scale licenses for the occurrences. The corundum is sitting in an extensive area measuring 30 by 70 km in the Fiskensættanorthosite complex (Windley *et al.*, 1973; Myers, 1985), which is part of the Archean basement in Greenland. The area contains more than 40 ruby localities and a few of those are well-developed and host gem-quality corundum.

Other Greenlandic ruby localities are found in West Greenland in the area around Maniitsoq and Nuuk. Rubies are also found in South-East Greenland in the Tasilaq area. The ruby localities in Greenland known so far are concentrated in the North Atlantic Craton, mainly near anorthosites, amphibolites and ultramafic bodies and are often related to intruding felsic sheets.

The company True North Gems Greenland (TNGG) has sought an exploitation license in Fiskensættet complex at one of the ruby localities called Aappaluttoq (Greenlandic for 'the red'). The research is collaboration between MIM and GEUS, and involves geochemical study of the Greenlandic corundum, with the purpose of finding good characteristics for recognizing the rubies from Aappaluttoq with a precise and non-destructive analytical method.

Here, we will describe results for LA-ICP-MS analyses and μ -XRF analyses. Major elements in rubies are Al and O, but 22 trace elements were investigated with LA-ICP-MS, where only Mg, Si, Ti, V, Cr, Fe, and Ga yielded significant results. These seven trace elements gave important characteristics for the Fiskensættet rubies that can be differentiated from the other Greenlandic occurrences (Kalvigand Keulen, 2013).

The samples from Fiskensættet are lower in Ti, Fe and V and higher in Cr compared to the other samples from Greenland. The Aappaluttoq samples have a very high Cr content (up to 16000 ppm) and are low in Mg, Ti and Fe. The rubies from other Fiskensættet localities show a strong resemblance to rubies from Aappaluttoq, when compared to other Greenlandic ruby occurrences

The Aappaluttoq rubies have been compared to international occurrences and are distinguishable from other ruby localities especially in ternary diagrams such as a Fe-Ti-Cr or Fe-Ga-V diagram (Figure 1). The samples from Aappaluttoq show only minor overlap with literature data on samples from other international localities, like Pailin, Bo Rai, Longido, Winza, and a number of occurrences in Madagascar. Rubies from these occurrences are all set in, or derived from, mafic or ultra-mafic rocks (Keulen and Poulsen, 2014). It is therefore important to analyze more samples from mafic-ultramafic ruby occurrences for comparison and thereby defining a good geochemical fingerprinting of the Aappaluttoq rubies.

In order to find a more non-destructive method for the analysis of rubies we compared micro-X-ray fluorescence (μ -XRF) to LA-ICP-MS analyses. μ -XRF is an elemental analysis method, which can examine very small sample areas. It uses direct X-ray excitation to induce characteristic X-ray fluorescence radiation from the sample for elemental analysis. Unlike conventional XRF, μ -XRF uses X-ray optics to restrict the excitation beam size or to focus the excitation beam to a small spot on the sample surface so that small features on the sample can be analyzed. A spatial resolution of down to about 10 micrometers can be reached. The μ XRF instrument applied in this study is a Bruker M4 Tornado based at the Roskilde University.

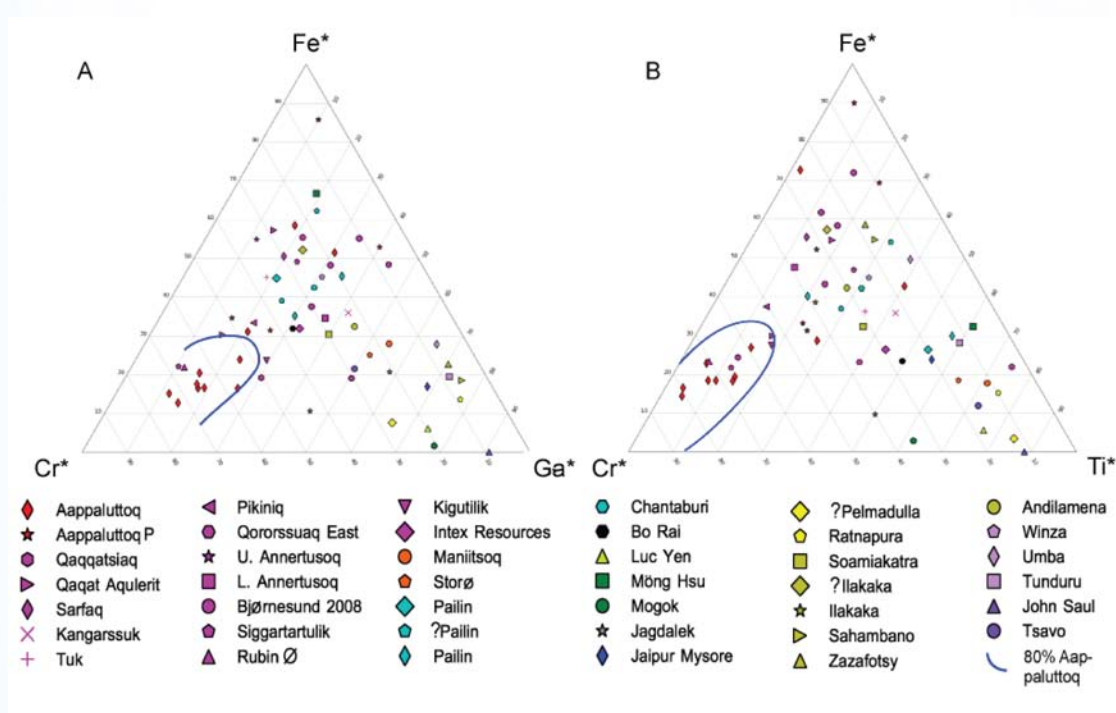


Figure 1: Normalized trace element distribution for Fe-Ga-Cr (A) and Fe-Ti-Cr (B). The Aappaluttoq samples are marked with a blue line. The Aappaluttoq samples are compared to international ruby localities (Calligaro, 1999; Calvo del Castillo, 2009; Rakotondrazafy *et al.*, 2008; Schwarz *et al.*, 2008).

The Greenlandic corundum samples from Aappaluttoq were analyzed for the purpose of fingerprinting of the Aappaluttoq corundum and to compare the results to the analyses on corundum from other localities in the Fiskenæsset complex: Bjørnesund, Rubin Ø, Kigutilik, Upper Annertusoq and Lower Annertusoq. Investigations concentrated on the elements O, Mg, Al, Si, Ti, V, Cr, and Fe. Results were compared to those obtained with LA-ICP-MS on the same grains in the same samples (Figure 2). μ XRF analyses are standard-less analyses.

When comparing some of the analytical methods, it becomes evident that there are quite big differences in the accuracy of trace element content. As LA-ICP-MS analyses were performed with standards and tested on known unknowns, these results are considered more reliable. The difference in values obtained with LA-ICP-MS and μ -XRF is too large and the spreading in the μ -XRF measurements is too random to consider μ -XRF as a suitable tool for geochemical fingerprinting. The LA-ICP-MS is not entirely non-destructive, whereas the μ -XRF is non-destructive, but the obtained results for the two methods makes the LA-ICP-MS the preferred analytical method (KeulenandPoulsen, 2014). Of all investigated analytical methods for characterizing the Aappaluttoq rubies so far, LA-ICP-MS has been the method, which gives the best possibilities for fingerprinting.

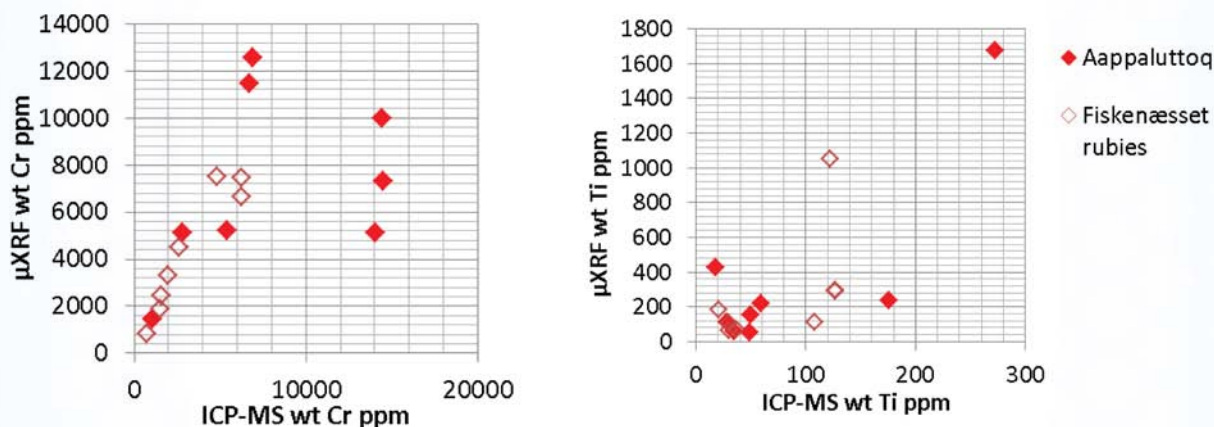


Figure 2: Comparison of the results from μ XRF and LA-ICP-MS. **Left:** The average of Cr in ppm for the two different methods. The differences between the measured element concentrations are not too divergent. **Right:** The average of Ti in ppm for the two different methods. The concentration of Ti measured with μ XRF is about 4 times larger than with the LA-ICP-MS.

References

- Calligaro, T., Poirot, J.-P., and Querré, G., 1999, Trace element fingerprinting of jewellery rubies by external beam PIXE, Nuclear Instruments and Methods in Physics Research Section B, Vol. 150, No.1-4, p.628-634.
- Calvo del Castillo, H., Deprez, N., Dupuis, T., Mathis, F., Deneckere, A., Vandenabeele, P., Calderón, T., and Strivay, D., 2009, Towards the differentiation of non-treated and treated corundum minerals by ion-beam-induced luminescence and other complementary techniques, Analytical and Bioanalytical Chemistry, Vol.394, No.4, p.1043-1058.

- Kalvig, P., and Keulen, N., 2011, Aktiviteter I Rubinprojektet, 2011- Samarbejdsprojekt med Råstofdirektoratet, Danmarks og Grønlands Geologiske Undersøgelse Rapport 2011/138, 41p.
- Kalvig, P., and Keulen, N., 2013, Fingerprinting of corundum (ruby) from Fiskensættet, West Greenland, Geological Survey of Denmark and Greenland Bulletin 28, p.53-56.
- Keulen, N., and Kalvig, P., 2013, Report on the activities in the ruby project 2012, A joint project with the Bureau of Minerals and Petroleum, DanmarksogGrønlandsGeologiskeUndersøgelse Rapport2013/9, 24p.
- Keulen, N., and Poulsen, M. D., 2014, Report on the activities in the ruby project 2011-2013, DanmarksogGrønlandsGeologiskeUndersøgelse Rapport 2014/36, 44p.
- Myers, J.S., 1985, Stratigraphy and structure of the Fiskensættet Complex, southern West Greenland. GrønlandsGeologiskeUndersøgelse Bulletin 150, 72 p.
- Rakotondrazafy, A.F.M., Giuliani, G., Ohnenstetter, D., Fallick, A.E., Rakotosamizanany, S., Andriamamojy, A., Ralantoarison, T., Razanatseheno, M., Offant, Y., Garnier, V., Maluski, H., Dunaigre, C., Schwarz, D., and Ratrimo, V., 2008, Gem corundum deposits of Madagascar: A review, The genesis of gem deposits, Ore Geology Reviews, Vol.34, No.1-2, p.134–154.
- Schwarz, D., Pardieu, V., Saul, J.M., Schmetzer, K., Laurs, B.M., Giuliani, G., Klemm, L., Malsy, A.-K., Erel, E., Hauzenberger, C., Du Toit, G., Fallick, A.E., and Ohnenstetter, D., 2008, Rubies and sapphires from Winza, Central Tanzania, Gems & Gemology, Vol.44, No.4, p.322–347.
- Windley, B.F., Herd, R.K., and Bowden, A.A., 1973, The Fiskensættet Complex, West Greenland, Part 1: A preliminary study of the stratigraphy, petrology, and whole rock chemistry from Qeqertarsuatsiaq, GrønlandsGeologiskeUndersøgelse Bulletin 106, 80 p.

Corresponding Author

Full name: Majken D. Poulsen
Affiliation: Geological Survey of Denmark and Greenland (GEUS), Nuuk Office c/o the Greenland Institute for Natural Resources, Kivioq 2, 3900 Nuuk, Greenland.
Phone: +00299361221
Email: madp@geus.dk

Crystal Chemistry of Coloration in Chrysoberyl

Janyaporn Witthayarat and Panjawan Thanasuthipitak

Gemology program, Department of Geological Science, Chiang Mai University, Chiang Mai, 50200, Thailand

Extended Abstract

Introduction

Gem chrysoberyl is a transparent variety with various shades of green, yellow, brownish to greenish black, or colorless. Since chrysoberyl has various shades of yellow and green, many publications mentioned only Fe³⁺ as cause of these colors without any details on the different shades. There is no clear relation between Fe content and the causes of color, and chemical analyses also show traces of Cr³⁺ and V³⁺ in chrysoberyl of some deposits. Recently, Hänni (2010) mentioned that V³⁺ is the cause of blue-green color in vanadium chrysoberyl. It is thus speculated that chromium and/or vanadium may be involved in coloration of chrysoberyl. Also, Schmetzer *et al.*, (2002) and Schmetzer *et al.*, (2013) indicated that the green chrysoberyl is caused by vanadium and chromium and the yellowness are due to the present of iron in chrysoberyl.

Materials and Methods

Twenty-six rough, yellow to green chrysoberyl samples from Ilakaka, Madagascar and Ratnapura, Sri Lanka were studied. They were divided into three color groups: 11 greenish yellow, 11 yellow-green, and 4 yellowish green. Basic instruments were used to determine gemological properties of the chrysoberyl samples. Chemical composition, including trace element contents, of the chrysoberyl samples were analyzed using electron probe microanalysis with wavelength dispersive spectrometry (EPMA-WDS). The cause of color in yellow to green chrysoberyl, which are related to the presence of transition elements, can be verified by UV-Vis-NIR spectrometer. X-ray absorption spectroscopy was used to investigate the local environment of iron in the chrysoberyl.

Result and Discussion

The chrysoberyl samples span a wide range of tone and saturation in color, displaying mixed color between yellow and green. Specific gravity of the chrysoberyl samples ranges from 3.68 to 3.75. Their refractive indices range from 1.745 to 1.747 for n_{α} , 1.748 to 1.750 for n_{β} , and 1.755 to 1.758 for n_{γ} with a birefringence of 0.008 to 0.010. All the samples were inert under long- and short-wave UV radiation. Microscopic examination revealed many fractures filled with dirt and small healed fractures, which is common for chrysoberyls.

Chemical analysis was done on all 26 samples using EPMA-WDS. The 11 greenish yellow samples show iron oxide content (FeO as total Fe) ranging from 0.823 to 4.605 wt%. Low contents of chromium oxide show values from below detection limit (BDL) to 0.032 wt%. Vanadium oxide contents are also low, BDL to 0.030 wt%. The 11 yellow-green samples show higher concentration of FeO ranging from 0.719 to 2.521 wt%. Chromium and vanadium oxides are BDL in some samples

while the highest values are 0.058 and 0.048 wt%, respectively. The 4 yellowish green chrysoberyl samples show iron oxide contents ranging from 0.734 to 1.554 wt%. Chromium oxide contents vary from 0.013 to 0.029, while vanadium oxide varies from 0.002 to 0.019 wt%.

Color-causing transition elements (Fe, Cr, and V) of yellow to green chrysoberyl are plotted against each other in Figure 1. The highest iron contents are in the greenish yellow group. Iron contents are lower in the yellow-green, and lower still in the yellowish green groups. In contrast, chromium contents increase with more intense greenish tint (Figure 1a). The chemical plots of V_2O_3 versus Cr_2O_3 (Figure 1b) shows that the more greenish samples have higher chromium contents, while vanadium shows no such relationship. This result agrees with Schmetzer *et al.*, (2002)'s finding that Cr has higher contents than V in causing yellowish green or green tints in chrysoberyl.

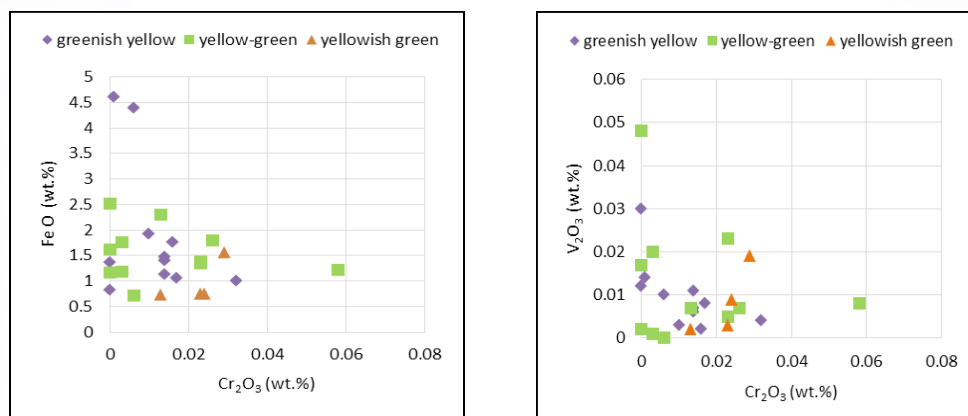


Figure 1: Chemical plots of greenish yellow, yellow-green and yellowish green chrysoberyls, **a)** FeO versus Cr_2O_3 and **b)** V_2O_3 versus Cr_2O_3 .

UV-Vis-NIR absorption spectra were recorded for the 26 samples. The main absorption spectra of the yellow to green chrysoberyls show only Fe^{3+} absorption peaks in the ultraviolet region at 364 nm and 372 nm, as well as in the visible region at 444 nm (Figure 2). All these absorption bands are due to spin-forbidden transitions of Fe^{3+} from 6A_1 ground state to the $^4A_1(G)$, $^4E(G)$, $^4T_2(D)$, and $^4E(D)$ states (Farrell and Newnham, 1965). While yellow-green sample that has highest Cr_2O_3 content, there is on significant absorption in chromium region. Although the greenish yellow sample has the highest V_2O_3 content, no sign of vanadium absorption.

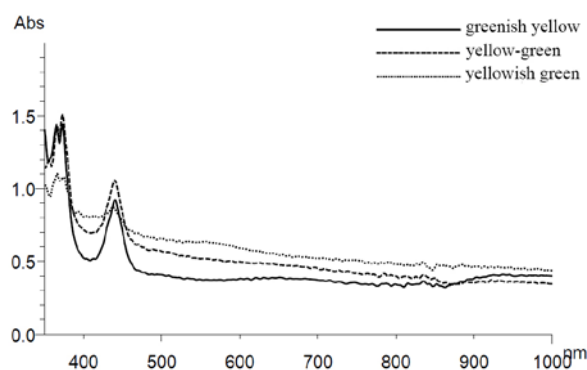


Figure 2: UV-Vis-NIR absorption spectra of greenish yellow (**solid line**), yellow-green (**dash line**), and yellowish green (**dot line**) chrysoberyl samples.

Room-temperature Fe K-edge XANES measurements were performed on two samples, greenish yellow and yellowish green, to investigate the local environment of iron in the chrysoberyl. The greenish yellow, and yellowish green showed pre-edge peak of Fe at 7112 - 7116 eV. Compared to Fe²⁺ and Fe³⁺ compound standard (FeO and Fe₂O₃ standards). It can be implied that Fe occurs in only the trivalent state and most of the literatures agree with this observation. The normalized spectrum of the greenish yellow sample is displayed in Figure 3.

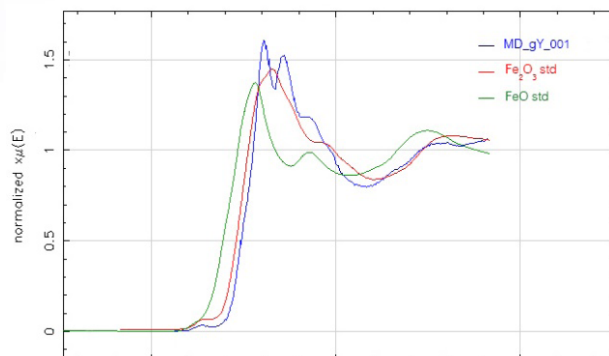


Figure 3: XANES spectra of greenish yellow sample compared with Fe²⁺ and Fe³⁺ compound. In the set the pre-edge peak of chrysoberyl is showed (**blue line**) with Fe₂O₃ (**red line**) and FeO (**green line**).

Conclusion

EPMA-WDS result shows that the causes of yellow to green colors in chrysoberyls is not only Fe but also Cr and V. Although there are no distinctive color boundaries between the yellow and green chrysoberyls, the transition element chemical plots are useful for certain differentiation. The result of this study agrees with Schmetzer *et al.* (2013)'s finding that the green color in chrysoberyl is caused by vanadium and chromium and the more yellowness are due to more iron in the chrysoberyl. Absorption spectra and Fe K-edge XANES spectra also confirm that the iron is present only in trivalent state.

References

- Farrell, E.F., and Newnham, R.E., 1965, Crystal-field spectra of chrysoberyl alexandrite, peridot, and sinhalite, *The American Mineralogist*, Vol.50, No.12-12, p.1972-1981.
- Hänni, H.A., 2010, Chrysoberyl: a gemstone with many faces, *The Australian Gemologist*, Vol.24, No.3, p.68-70.
- Schmetzer, K., Hainschwang, T., and Bernhardt, H.J., 2002, Yellowish green and green chrysoberyl from Ilakaka, Madagascar, *Gem News, Gems & Gemology*, Vol.38, No.3, p.261.
- Schmetzer, K., Krzemnicki, M.S., Hainschwang, T., and Bernhardt, H.J., 2013, Natural and synthetic vanadium-bearing chrysoberyl, *The Journal of Gemmology*, Vol.38, No.7-8, p.223-238.

Corresponding Author

Full name: Janyaporn Witthayarat
 Affiliation: Gemology program, Department of Geological Science, Chiang Mai University, Chiang Mai, 50200, Thailand.
 Email: dana_mul@hotmail.com

Discovering Effect of Synchrotron Light Interaction on Color of Freshwater Cultured Pearls: A New Identification Technique for Gamma Irradiated Pearls, A Disclosure of Synchrotron Exotic Golden Pearls, and A High-Definition Golden Pattern Imprinting Process©.

Nirawat Thammajak¹, Wantana Klysubun¹ and Sorapong Pongkrapan²

¹Synchrotron Light Research Institute, 111 University Avenue, Suranaree, Muang District, NakhonRatchasima, 30000, Thailand.

²Department of Earth Sciences, Faculty of Science, Kasetsart University, Bangkok, 10900, Thailand.

Extended Abstract

Freshwater Cultured Pearls (FWCPs) exhibit a wide variety of body colors, including whites, creams, oranges, yellows, purples, and greens. The major cause of body color variation has been ascribed to pigments (Elen, 2002). Commercial FWCPs, however, are often white and do not exhibit strong metallic luster. Some chemicals have been used to artificially color the white pearls, but the coloring often damages the natural luster. Since 1963, gamma radiation of radioactive cobalt-60 have been used to change the color of FWCPs to a more iridescent and fixed color of “metallic-gray” tone, similar to black Tahitian pearls (Chow, 1963). Nevertheless, there is no satisfactory accounting for an origin of the changed color and a mechanism of the radiation interaction.

X-ray Absorption Spectroscopy (XAS) is a powerful technique for studying local structure in materials using an energy-tuneable source of x-rays from a synchrotron. The absorption of x-rays by an atom can provide a meaningful spectrum which qualitatively and quantitatively related to its chemical compositions, forms, and bonding structure. The fine structure in the energy-dependence of the absorption arises when an emitted photoelectron is scattered back towards the source atom by other atoms in its close environment. XAS is therefore sensitive to the oxidation state, coordination geometry, and the distances, coordination number and species of the atoms immediately surrounding the selected element. Hence, the technique is capable to provide an effective analysis of trace elements and dilute compositions, which commonly affect the color of gemstones. BL8-XAS beamline is located at Synchrotron Light Research Institute (SLRI), NakhonRatchasima, Thailand. The beam line and its experimental setup diagram are shown in Figure 1.

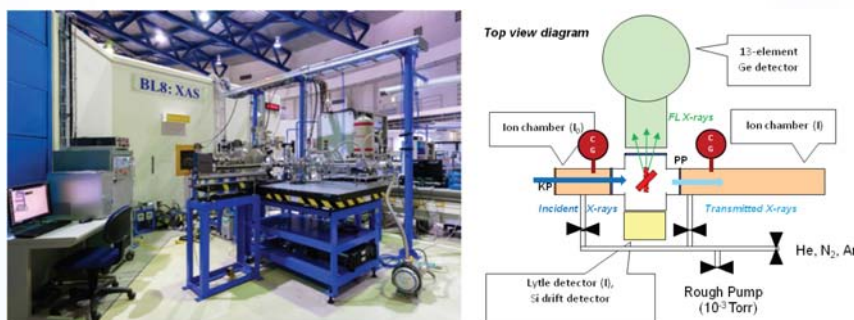


Figure 1: BL8: X-ray Absorption Spectroscopy (XAS) beamline and experimental diagram.

A study of gamma irradiated FWCPs by the XAS technique led to a fundamental knowledge of coloring mechanism caused by a trace color-forming composition combined with the calcareous base material of the pearl (Pongkrapan *et al.*, 2014). Different irradiation doses resulted in a shift of XAS spectra, including a development of a peak-shape feature near the absorption edge. This gamma dose dependence can provide a substantial evidence for irradiated pearl's identification. Besides, the revealed coloring mechanism can potentially be applied for FWCPs quality improvement.

In a feasibility study, an intense x-ray white beam generated by a synchrotron was employed to alter the color of freshwater pearls cultured in Thailand and China. It was observed that the original white pearls from both sources were enhanced to a metallic-golden pearls, as shown in Figure 2; contrary to the metallic-grey pearls obtained from gamma irradiation. This unexpected gold color is very unique; and surprisingly, the natural iridescence of the irradiated pearl has also been slightly improved. Since the more exotic colors have the greater commercial value, this synchrotron method can therefore be an effective option to produce a new, exotic color, and more valuable pearl (Thammajak *et al.*, 2014).



Figure 2 : Original white freshwater cultured pearl (**left**) and synchrotron metallic-golden pearl (**right**).

It should be noted that the intense x-ray beam from a synchrotron stimulates the color change, but does not activate the pearls through nuclear reactions, as in the case of cobalt-60 gamma irradiation. Not only the radiation safety; it also has an extra advantage of the synchrotron's specific beam direction that can be beneficially applied with a photolithography technique. This technique has consequently established a new and inventive process for imprinting an irradiated pattern on pearls by means of the intense x-rays irradiation through a designed mask that partially obscured the beam. The partly through x-ray beam resulted in a high-definition golden pattern with highly detailed line as fine as micrometer level, as shown in Figure 3 (Thammajak and Klysabun 2014). The imprinted pearl products by this technique can be used as a special jewelry that is very unique and valuable.

In conclusion, the synchrotron technique can be applied for gems and gemology as a new technique for irradiated pearl's identification, a method of creating a new exotic golden pearls, and a process of printing high-definition and high-resolution golden pattern on FWCPs. It is therefore a very useful tool to raise the value of FWCPs that possess less unique color and inferior luster, compared to seawater cultured pearls (SWCPs). In an occasion of a 60th year birthday anniversary celebration of HRH Princess Maha Chakri Sirindhorn in 2015, some selected prototypes of synchrotron golden pearls and golden pattern imprinted pearls with HRH Princess Maha Chakri Sirindhorn 'semblem will be presented. This project has patented two articles with Department of Intellectual Property (DIP). All copy rights reserved©.



Figure 3 : Selected FWCPs with imprinted golden-pattern.

References

- Chow, K.T., 1963, Process for irradiating pearls and product resulting therefrom, U.S. Patent, United States Patent Office, 3075906, 1963.
- Elen, S., 2002, Identification of yellow cultured pearls from the black-lipped oyster *Pinctada-Margaritifera*, *Gems & Gemology*, Vol.38, No.1, p.66-72.
- Pongkrapan, S., Thammajak, N., and Klysubun, W., 2014 XAS study of γ -irradiated freshwater pearls cultured in Thailand from bivalve species *Chamberlainahainesiana*, *Journal of Synchrotron Radiation*, 2014, In preparation of a research manuscript.
- Thammajak, N., and Klysubun, W., 2014, Process for golden pattern imprinting on pearls using synchrotron photolithography, Thailand Patent, Department of Intellectual Property, 2014, submitted.

Thammajak, N., Klysubun, W., and Pongkrapan, S., 2014, Synchrotron process for changing pearl's colour to iridescent gold, Thailand Patent, Department of Intellectual Property, 1401004449, 2014.

Corresponding Author

Full name: NirawatThammajak
Affiliation: Synchrotron Light Research Institute, 111 University Avenue, Suranaree,
Muang District, NakhonRatchasima, 30000, Thailand.
Phone: (+66) 090-9235362
Fax: (+66) 044-217047
Email: n.thammajak@gmail.com

Emeralds from Jharkhand, India

Gagan Choudhary

Gem Testing Laboratory, Rajasthan Chamber Bhawan, Mirza Ismail Road, Jaipur, 302003, India

Extended Abstract

Background

It was December 2013, when the news about emerald deposits in the state of Jharkhand broke out in the market and within few months time, some large quantities of these emeralds were already being mined. The deposit initially attracted attention because of the reports in local media about arrests for illegal mining and smuggling. In no time, these emeralds became quite popular in the local market and many traders have shown interest in these stones. As per a report published in the Journal of Gem & Jewellery Industry, Vol. 51, No. 5, "over 5,000 skilled and unskilled miners are digging nearly 15 kg of precious stones (emerald) per day". Although, we have seen some large lots of Jharkhand emeralds, most of which are relatively small in sizes, less than 5 ct in rough.

Emerald deposits in Jharkhand are located in Ghorabandha hills in Ghatshila sub-division of East Singhbhum district, bordering the state of Odisha (Orissa), which is already known for a variety of high quality gemstones. Mining in Jharkhand is carried out by local villagers, including children in at least 50 places and hence is illegal at this stage. However, the government of Jharkhand is working towards legalizing mining by seeking necessary approvals from the centre for reserving the mining areas for Jharkhand State Mineral Development Corporation. Meanwhile, these emeralds are gaining popularity amongst the traders and jewellers in Jaipur and hence, we also procured and studied few samples of these emeralds.

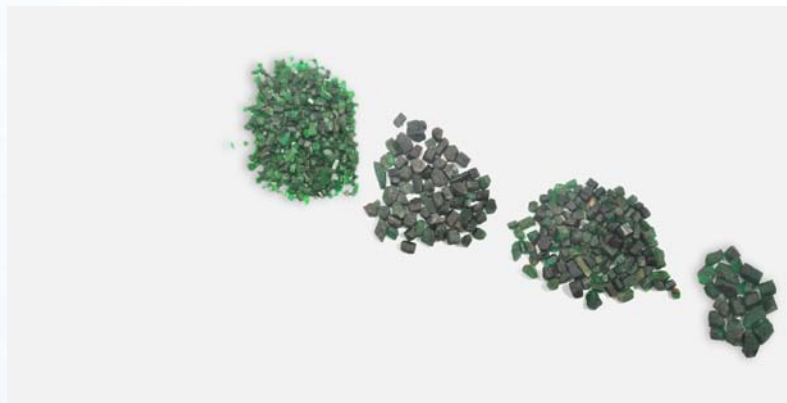


Figure 1: Emerald rough from Jharkhand in a range of colour, transparency and size. Photomicrograph by G. Choudhary

Visual Characteristics

The studied emeralds from Jharkhand displayed a range of colours from bluish green to yellowish green of medium to strong saturation (Figure 1 and 2). However, most of these emeralds are characterized by haziness while many rough crystals appear blackish due to presence of some mineralic substance, making the stones appear opaque. Although, these can be removed during cutting and polishing, some still make their way into the cut stones, making them appear too dark or blackish.

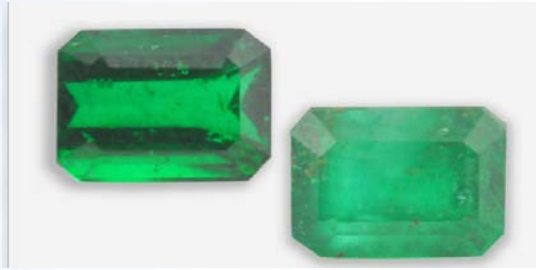


Figure 2: Representative samples of cut and polished emeralds from Jharkhand. Note the difference of colour shade in two specimens. Photomicrograph by G. Choudhary

Basic Properties

Gemmological properties namely, refractive index and specific gravity were measured at 1.580-1.588 and 2.70-2.71, respectively; displayed strong Cr-absorption in desk model spectroscope, and appeared inert under ultra-violet lamp and Chelsea filter.

Microscopic Features

As mentioned above, most of these emeralds are characterized by haziness, caused by minute inclusions, which could not be resolved under standard gemmological microscope, however, appeared to be some colourless mineral. In addition, the most common inclusions were black grains of spinel (chromite, magnetite or picotite), which were present scattered throughout the stone, as well as in zones and planes. Further, few specimens also contained numerous colourless to white rounded crystals of phenakite, elongated blades of actinolite, mica plates and most strikingly rounded colourless grains of zircon with stress cracks (zircon halos). We have never seen a zircon halo inclusion in an emerald from any other source before not we could find a reference of a previous report.



Figure 3: Most of the Jharkhand emerald appeared hazy due to presence of minute mineral inclusions. Photomicrograph by G. Choudhary, magnified 32x

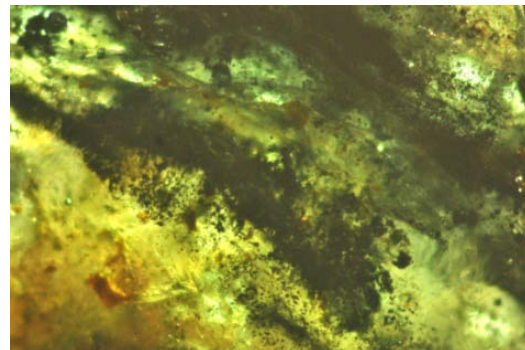
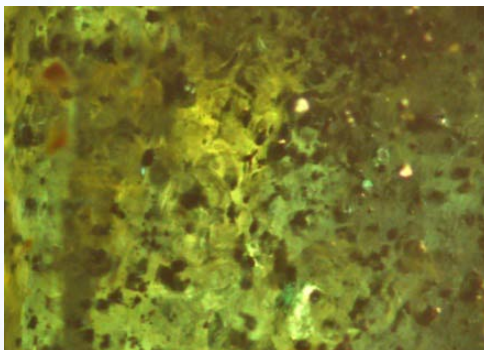


Figure 4: Majority of Jharkhand emeralds contained black grains (spinel group), which were present scattered throughout the stone or in planes or zones. Photomicrographs by G. Choudhary, magnified 48x (left), 32x (right)

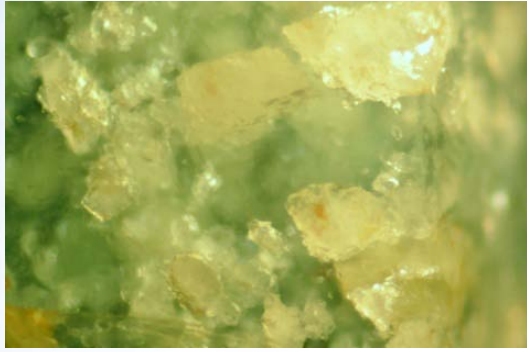


Figure 5: These whitish to colourless crystals in Jharkhand emerald have been identified as phenakite.
Photomicrograph by G. Choudhary, magnified 80x

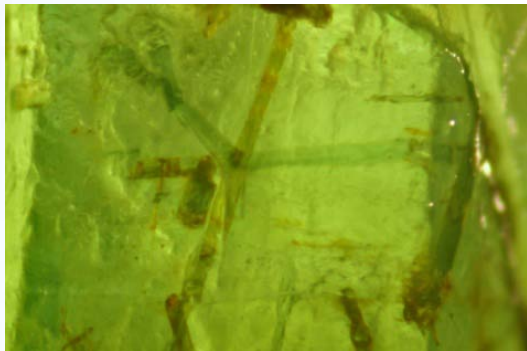


Figure 6: Actinolite blades were also seen in few specimens, which have been encountered in emeralds from other deposits too.
Photomicrograph by G. Choudhary, magnified 64x

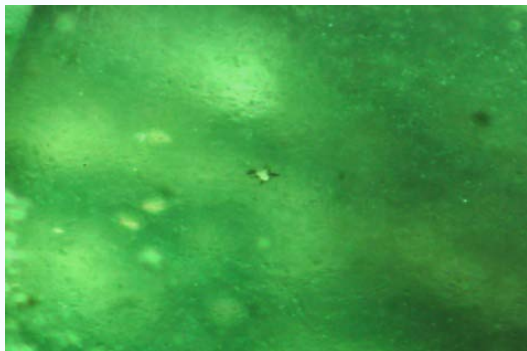


Figure 7: Zircon-Halo was the most striking inclusion seen in these emeralds, which were never seen before in emeralds.
Photomicrograph by G. Choudhary, magnified 80x

Conclusion

This relatively new find of emeralds from the East Singhbhum district of the state of Jharkhand has produced a lot of interest in the local market and at very good prices. However, currently the deposits are being excavated through illegal mining, but the state government has already sent the proposal to acquire mining rights and clearances, which will help to regulate the supply of these emeralds. As per preliminary observations, these emeralds appear to be of decent colour and transparency, although in relatively smaller sizes, less than 5 ct. Right now, it is too early to say, whether this deposit will contribute significantly to the emerald trade or is just another instance of 'sporadic encounter.

References

- Anonymous, 2012, Man arrested with emeralds, The Telegraph, Friday, November 9
Anonymous, 2012, Patrol plea for emerald hills, The Telegraph, Friday, December 21
Anonymous, 2013, Jharkhand emeralds cry for attention, Journal of Gem & Jewellery Industry, Vol. 51, No. 5, p.10-14.
Jenamani, K., 2012, Emerald hills eye state geology seal, The Telegraph, Friday, December 21

Corresponding Author

Full name: Gagan Choudhary
Affiliation: Gem Testing Laboratory, Rajasthan Chamber Bhawan, Mirza Ismail Road, Jaipur, 302003, India.
Phone: +911412568221
Email: gagan@gjepcindia.com

Gem Sapphires from a New Deposit in the Krong Nang District, Dak Lak Province, Vietnam: Spectroscopy in Color Investigation

***Phan Thi Minh Diep¹, Nguyen Ngoc Khoi^{2,4} Tobias Häeger, Christoph Hauzenberger³,
Duong Anh Tuan^{4,5} and Wolfgang Hofmeister¹***

¹Johannes Gutenberg-University Mainz, D55099, Mainz, Germany

²Hanoi University of Science, 334 Nguyen Trai str., Thanh Xuan dist., Hanoi, Vietnam

³Karl-Franzens-University of Graz, A – 8010, Graz, Austria

⁴DOJI Gold & Gems Group, 44 Le Ngoc Han str., Hai Ba Trung dist., Hanoi, Vietnam

⁵Institute of Material Science (Vietnam Academy of Science & Technology), 18 Hoang Quoc Viet str., Cau Giay dist., Hanoi Vietnam

Extended Abstract

The new sapphire deposit from Krong Nang was discovered by local gem diggers at the end of 2012. The color of these samples ranges from blue, greenish blue, bluish green, greenish yellow to yellow. This present study describes the UV-Vis-NIR and FTIR characteristics of those sapphires.

Sample Preparation And Analytical Methods

The sapphire samples in this study were purchased by two authors (Nguyen Ngoc Khoi and Duong Anh Tuan) at a gem mine in Dle Yea commune, Krong Nang district, Dak Lak province. Rough and cut Krong Nang sapphires are shown in Figure 1. Most of them occur as angular to partly round eroded fragments. The colors are commonly from light blue, bluish green, greenish yellow to yellow sapphires. We separated them into three color groups: (light) blue, (bluish) green and (greenish) yellow.

The samples were cut and polished in plane-parallel slices for UV-Vis-NIR and FTIR transmission measurements. Some samples were prepared in such a way, that the polished faces are parallel to the c-axis.

Chemical analyses of Krong Nang sapphires were performed by EPMA and LA-ICP-MS at Institute of Earth Sciences, Karl-Franzens-University of Graz, Austria. Spectral experiments were carried out in the Institute of Earth Sciences, Johannes Gutenberg-University Mainz, Germany.

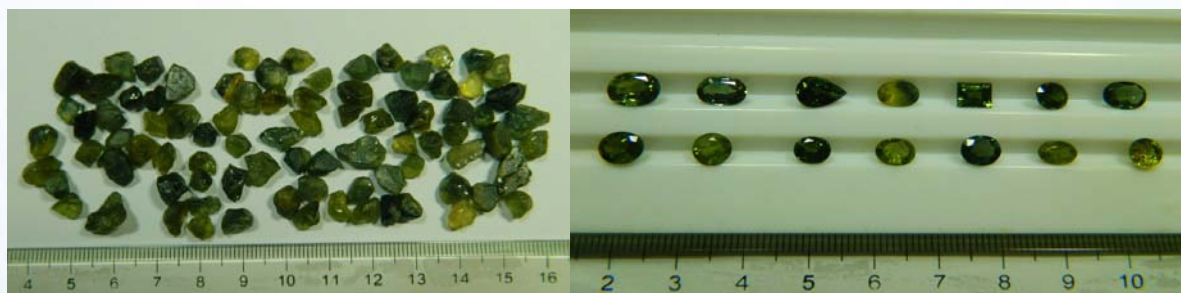


Figure 1: Rough and cut Krong Nang sapphires.

Results and Discussion

Chemical compositions

The chemical compositions of Krong Nang sapphire by EPMA and LA-ICP-MS are summarized in Table 1. The values of Al₂O₃ and Fe₂O₃ (total) were taken from EMPA and Mg, Ti, Cr, Ga and V from LA-ICP-MS analysis.

Table 1: Chemical analyses of three color groups of Krong Nang sapphires in wt% oxides and ppm with minimum, maximum and mean values.

Color	No. of samples	Al ₂ O ₃ (wt.%)	Fe ₂ O ₃ tot. (wt.%)	Mg (ppm)	Ti (ppm)	Cr (ppm)	Ga (ppm)	V (ppm)
Green	12	98.12-99.41 (98.71)*	1.61-2.72 (2.12)	13-39 (29)	22-175 (77)	bdl-27 (9)	166-246 (197)	2-6 (4)
Yellow	17	97.83-100.11 (98.70)	0.19-2.03 (1.79)	15-45 (19)	19-82 (33)	bdl-18 (8)	163-315 (210)	2-5 (3)
Blue	10	97.73-101.50 (99.14)	0.53-2.52 (1.46)	1-54 (25)	27-551 (115)	bdl-16 (11)	159-398 (231)	1-34 (11)

(98.71)* = mean value, bdl = below detection limit

Iron is the most significant minor element detected in all three color groups, where green sapphire samples have the highest average value and blue sapphires have the lowest. Gallium is recorded in all three groups with a similar value. Titanium was detected in all samples and the highest average value (115 ppm) is found in blue sapphire samples. Other trace elements (Mg, Cr, and V) are very small to negligible amounts or below the detection limit.

UV-Vis-NIR spectra and color of Krong Nang sapphires

The absorption spectra of Krong Nang sapphires are similar to those described for BGY magmatic sapphires (Schmetzer 1987; Smith *et al.*, 1995; Kiefert *et al.*, 1996; Schwarz *et al.*, 2000). Figure 2 shows polarized UV-Vis-NIR spectra of the three sapphire groups. All of these samples had intense absorption bands in the UV-region at 377, 387, in the visible range at 450 nm and two shoulders at 460 and 471 nm.

Blue sapphires show intense absorption bands due to Fe²⁺/Ti⁴⁺ IVCT with absorption maximum between 560 and 600 nm with a polarization E[^]c and 690 to 770 nm with a polarization E//c, as well as an Fe²⁺/Fe³⁺ IVCT toward the near infrared with absorption maximum between 850 and 900 nm. Green sapphires are indicated by intense Fe²⁺/Fe³⁺ IVCT with absorption maximum approximately 850 to 900 nm. Yellow sapphires show mainly absorption peaks related to pairs of Fe³⁺ at 377 and 387 nm, and single Fe³⁺ at 450, 460 and 471 nm. The polarization dependency in yellow sapphires is weak. In Figure 2, two peaks at 486 and 656 nm are due to artifact from the background.

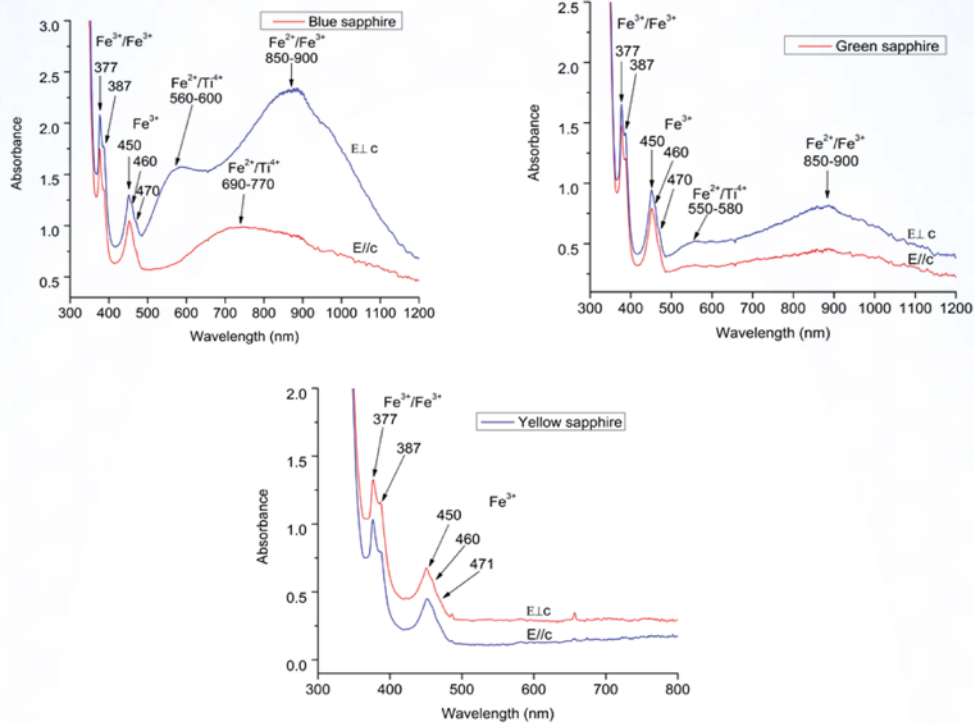


Figure 2: Polarized UV-Vis-NIR spectra of blue, green and yellow Krong Nang sapphires.

FTIR spectra – OH-groups in sapphire

We examined 14 Krong Nang sapphires with FTIR spectroscopy to determine OH-groups. All green and yellow samples do not show any OH-groups. Only one light blue sample contains very weak OH groups (Figure 3). The peak positions and intensity ratios of the OH groups are similar to those reported for basaltic sapphires (Moon and Philips, 1994) or sapphires from southern Vietnam (Smith *et al.*, 1995).

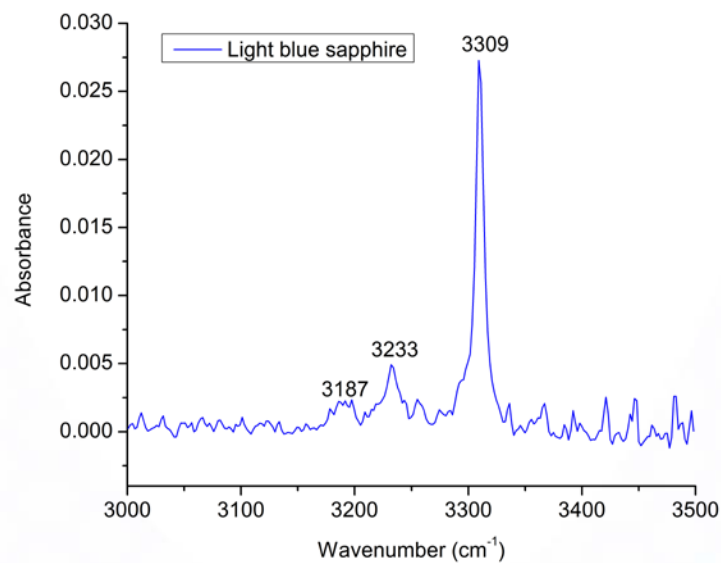


Figure 3: OH-groups in a light blue Krong Nang sapphire.

Conclusions

Krong Nang sapphires display the color range from blue to green to yellow. Blue sapphires show absorption bands due to $\text{Fe}^{2+}/\text{Ti}^{4+}$ and $\text{Fe}^{2+}/\text{Fe}^{3+}$ IVCT. Yellow sapphires are colored by absorption peaks of single and pairs of Fe^{3+} . Green sapphires are a combination out of blue and yellow causes of color. Very weak absorption of OH groups is only observed in a light blue sapphire.

Acknowledgements

The authors are thankful for experimental supports from Institute of Earth Sciences, Karl-Franzens-University of Graz, Austria and Institute of Geosciences, Johannes Gutenberg-University Mainz, Germany.

References

- Kiefert, L., Schmetzer, K., Krzemnicki, M.S., Bernhardt, H.-J., and Hänni, H.A., 1996, Sapphires from the Andranondambo area, Madagascar, *Journal of Gemmology*, Vol.25, No.3, p.185-209.
- Moon, A.R., and Philips, M.R., 1994, Defect Clustering and Color in $\text{Fe,Ti: } \alpha\text{-Al}_2\text{O}_3$, *Journal of The American Ceramic Society*, Vol.77, No.2, p.356-367.
- Schmetzer, K., 1987, Zur Deutung der Farbursache blauer Sapphire-eine Diskussion, *Neues Jahrbuch für Mineralogie Monatshefte*, Vol.1987, No.8, p.337-343.
- Schwarz, D., Kanis, J., and Schmetzer, K., 2000, Sapphires from Antsiranana Province, Northern Madagascar, *Gems & Gemology*, Vol.36, No.3, p.216-233.
- Smith, C.P., Kammerling, R.C., Keller, A.S., Peretti A., Scarratt, K.V., Khoa, N.D., and Repetto, S., 1995, Sapphires from southern Vietnam, *Gems & Gemology*, Vol.31, No.3, p.168-186.

Corresponding Author

Full name: Phan Thi Minh Diep
Affiliation: Johannes Gutenberg-University Mainz, D55099, Mainz, Germany.
Phone: +4917656400848
Email: thphan@students.uni-mainz.de

Gemological Characteristics of Rhodolite Garnet from Madagascar

Kanyarat Kwansirikul and Sasithorn Ya-in

Department of Geological Sciences, Faculty of Science, Chiang Mai University, Chiang Mai, 50200, Thailand

Extended Abstract

Garnets are silicate minerals that conform to the general formula $A_3B_2(SiO_4)_3$, where A site is occupied by calcium, magnesium, ferrous iron, or divalent manganese whereas B site is allocated for trivalent aluminum, iron, and more rarely chromium, titanium, zirconium and vanadium. Those garnets in which B corresponds to aluminum are referred to as the pyrope series (pyrope, almandine, spessatine species) while those in which A corresponds to calcium are referred to as the ugrandite series (uvarovite, grossularite, andradite species). Garnet with those pure species are really found in natural deposit. Most garnets commonly show solid solution between them.

Rhodolite is the name given to a light to dark purplish red through reddish purple garnet. It is a member of the pyrope-almandine solid solution series with approximate garnet composition of $Py_{70}Al_{30}$. Thus, the properties of rhodolite are intermediate between pyrope and almandine. Rhodolite was first described from North Carolina. However, commercial sources are currently from Tanzania, Zimbabwe, Mozambique, Kenya, Madagascar, Sri Lanka and India (Hurlbut and Kammerling, 1991).

Materials and Methods

Twenty rough rhodolite garnet samples ranging from 1.65-3.43 carats from Madagascar were examined gemological properties using fundamental gemological tools and advance equipments. Five samples were selected for chemical analysis using scanning electron microscope equipped with energy dispersive X-ray fluorescent spectrometer (SEM-EDS).

Results

The studied rhodolite samples are divided into two groups according to their color appearances including purplish red and orangey red groups (Figure 1). Their specific gravities vary from 3.79-3.84 and the refractive indices vary from 1.751-1.763. All rhodolite samples are inert in both shortwave and longwave ultraviolet radiations. The samples contain mineral inclusions of apatite (Figure 2), rutile needle (Figures 2 and 3) and healed fractures.

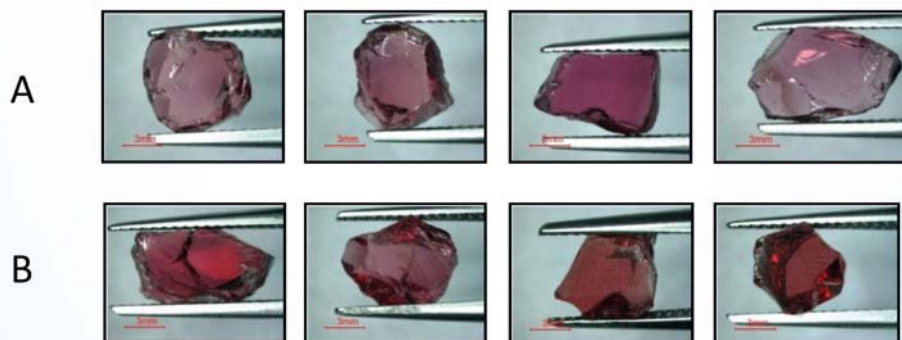


Figure 1: Some rhodolite samples in purplish red group (A) and orangey red group (B).

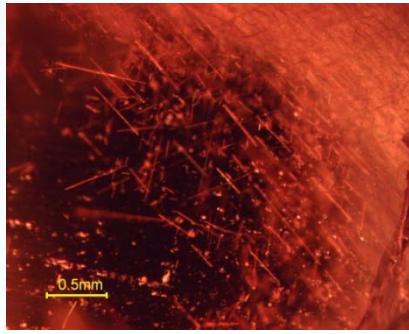


Figure 2: Apatite and rutile needles inclusions

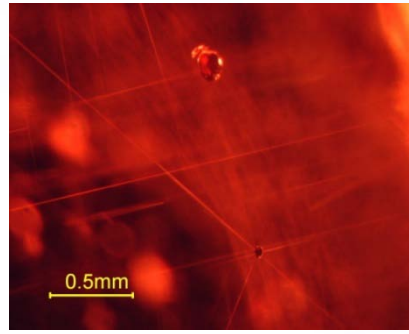


Figure 3: Rutile needles inclusion

The UV-Vis spectra of the rhodolite samples in both color groups show absorption bands at about 409, 504, 523, 572 and 574 nm, and a very weak broad band centered at about 694 nm (Figures 4 and 5).

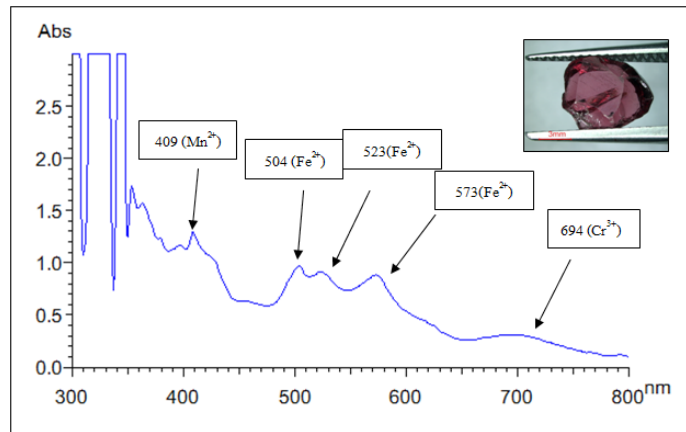


Figure 4: A representative UV-Vis absorption spectrum of the purplish red rhodolite samples.

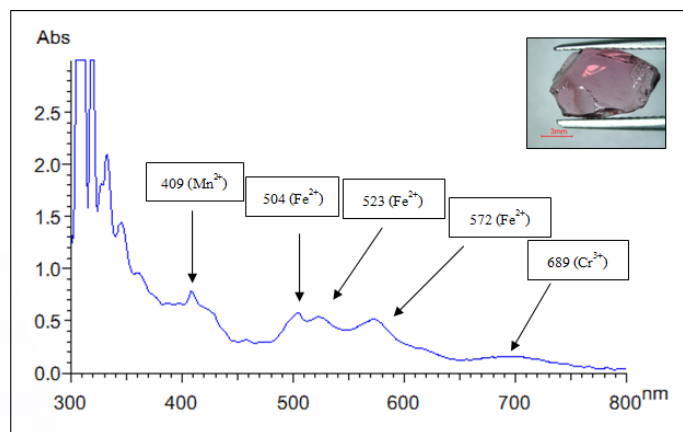


Figure 5: A representative UV-Vis absorption spectrum of the orangey red rhodolite samples.

The chemical analyses reveal that the studied samples fall within pyrope-almandine solid solution series that are quite rich in pyrope (Mg^{2+}) component (Figure 6). The atomic end-member components of the purplish red samples comprise about 56-64% pyrope, 28-44% almandine and 0.2-7.8% spessartine while the atomic end-member components of the orangey red samples comprise about 38-64% pyrope, 29-54% almandine and 6.4-10.2% spessartine.

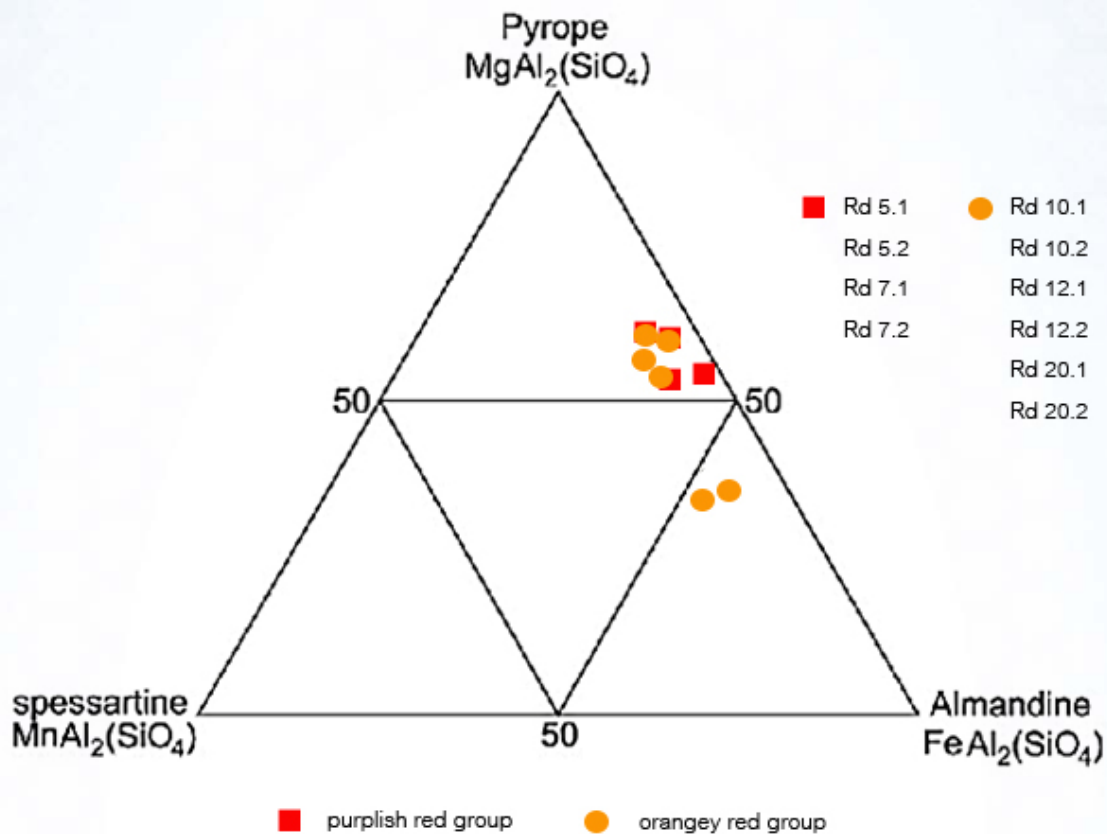


Figure 6: Ternary plots of pyrope (**Mg**), almandine (**Fe**) and spessartine (**Mn**) end-member components of the rhodolite garnets.

Discussion and Conclusion

The absorption bands obtained in this study are similar to those observed in almandine and rhodolite garnets from other localities (Adamo *et al.*, 2007). According to the chemical data obtained in this study, those spectral patterns, which are responsible for the purplish red and orangey color of those samples, are likely to be related to the crystal field transitions within divalent iron (Fe^{2+}) and manganese (Mn^{2+}) present in the garnet structures (Burns, 1983). Manganese content in the orangey red group is higher than that content in the purplish red group consistent with the cause of orange color in spessartine.

Acknowledgements

All the data were obtained by using the basic and advanced analytical equipments at Faculty of Science, Chiang Mai University for which the authors are appreciated.

References

- Adamo, I., Ajò, D., Diella, V., Pavese, A., and Prospero, L., 2007, Gem-quality garnet: correlations between gemological properties, chemical composition and infrared spectroscopy, *The Journal of Gemmology*, Vol.30, No.5, p.307-319.
- Burns, R.G., 1993, Colours of gems, *Chemistry in Britain*, p.1004-1007.
- Hurlbut, C.S. and Kammerling, R.C., 1991, *Gemology*, 2nd, John Wiley & Sons, Inc., New York, 336p.

Corresponding Author

Full name: Kanyarat Kwansirikul
Affiliation: Department of Geological Sciences, Faculty of Science, Chiang Mai University, Chiang Mai, 50200, Thailand.
Email: kanyarat.k@cmu.ac.th

Geographic Origin Determination of Ruby and Blue Sapphire: an Application of LA-ICP-MS

Kentaro Emori and Hiroshi Kitawaki

Central gem laboratory, Tokyo, Japan

Extended Abstract

Introduction

Gem minerals have information about their geological environment of the host rock and occurrence. Analyzing the component of gem minerals leads to identify geological environment of the host rock and occurrence and is important in determination of their geographic origin.

X-ray fluorescence analysis is commonly used for chemical analysis in gemological testing laboratories, but its sensitivity is not always satisfactory and it has disadvantage that it cannot detect light element such as Li, Be and B in particular.

LA-ICP-MS (laser ablation inductively coupled plasma mass spectrometer) is a tool to detect impurities of ppb to ppm level with simultaneous multi-element analysis including light elements in high-sensitivity performance. It has been applied in the gemological field as a new analytical technique that is essential for the identification of Be-diffused corundum, although the laser ablation gives a little damage, i.e. formation of tiny crater of 10 micro meters from several points on surface of samples (Abduriyim, 2006).

As one of the applications in gem identification using LA-ICP-MS analysis, we studied the possibility of geographic origin determination of ruby and blue sapphire.

Material and Method

We analyzed ruby from 9 pieces of Cambodia (Pailin), 4 pieces of Madagascar, 52 pieces of Myanmar (9 of Mo-gok, 38 of Mong-Hsu, 5 of Nam-Ya), 26 pieces of Tanzania (6 of Morogoro, 15 of Tanga, 5 of Winza), 17 pieces of Vietnam (Luc-Yen) and blue sapphires from 5 pieces of Cambodia, 5 pieces of China, 4 pieces of Laos, 24 pieces of Madagascar, 10 pieces of Myanmar, 9 pieces of Nigeria, 9 pieces of Sri Lanka, 5 pieces of Tanzania, 10 pieces of Thailand (5 of Kanchanaburi, 5 of Chanthaburi).

In this study, we used a LA-ICP-MS system, consisting of NEW WAVE UP-213 for laser ablation and Agilent 7500a ICP-MS. Analysis conditions were as follows: Laser ablation setting: laser wavelength 213 nm, crater size 30 μm and 80 μm , laser power 0.025mJ, laser frequency 20 Hz, ICP-setting: ICP 27.15 MHz, RF Power 1200 W, Plasma gas(Ar) 14.93 l/min, Auxiliary gas (Ar) 0.89l/min, Carrier gas(Ar) 1.44 l/min.

Result

Ruby: Rubies from Myanmar show higher content (above 120 ppm) of vanadium (V) than those from other locations. Magnesium (Mg) content of rubies from Cambodia tends to be higher than others and is at least 180 ppm.

Numerical range of analyzed elements is very close in rubies from Madagascar, Tanzania, and Vietnam but 3D-plot graph in Mg-V-Fe shows their difference. (Figure 1)

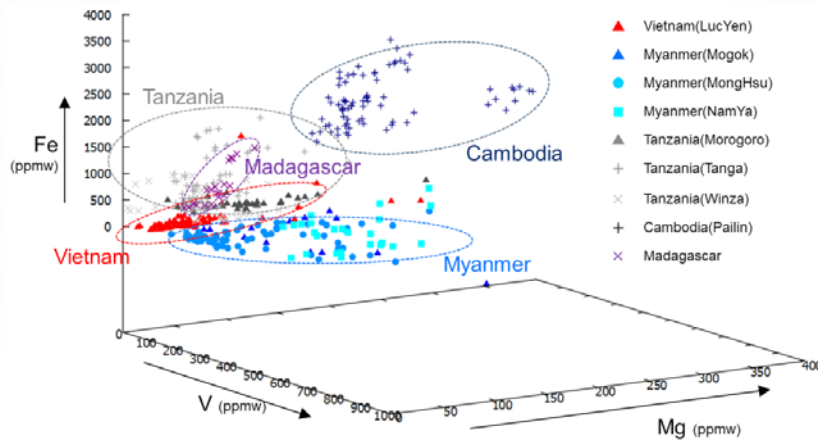


Figure 1: The 3D plot graph in Mg-V-Fe of rubies in this study.

Blue sapphire: It has been found that the graph plotted with Mg and Ga can separate blue sapphire of basaltic origin (Cambodia, China, Laos, Nigeria and Thailand) from metamorphic and metasomatic origin (Madagascar, Myanmar, Sri-Lanka and Tanzania). (Figure 2)

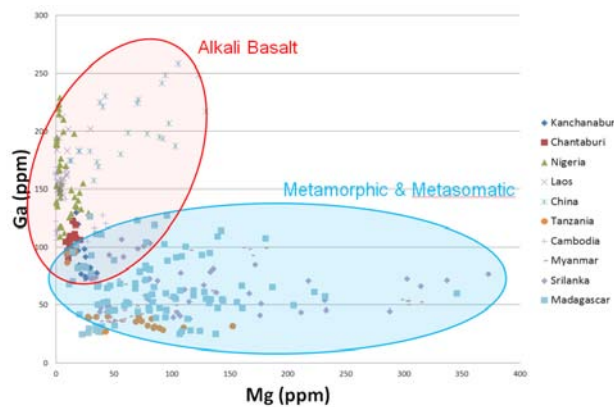


Figure 2: The graph plotted with Mg and Ga of blue sapphires in this study.

It has been found that ratio of Mg to Ti of the blue sapphires is good indicator of locality; Madagascar, Myanmar or Sri Lanka. They are not basaltic origin and have difficulty in origin determination from observation of inclusions and optical spectrometry. It is also found that the presence of trace element (Li, Be, B, Sc, Zn, Zr, Nb, Zr, In, Sn, Sb, La, Ce, Hf, Ta, W, Pb, Bi, Th) varies between locations. (Figure 3)

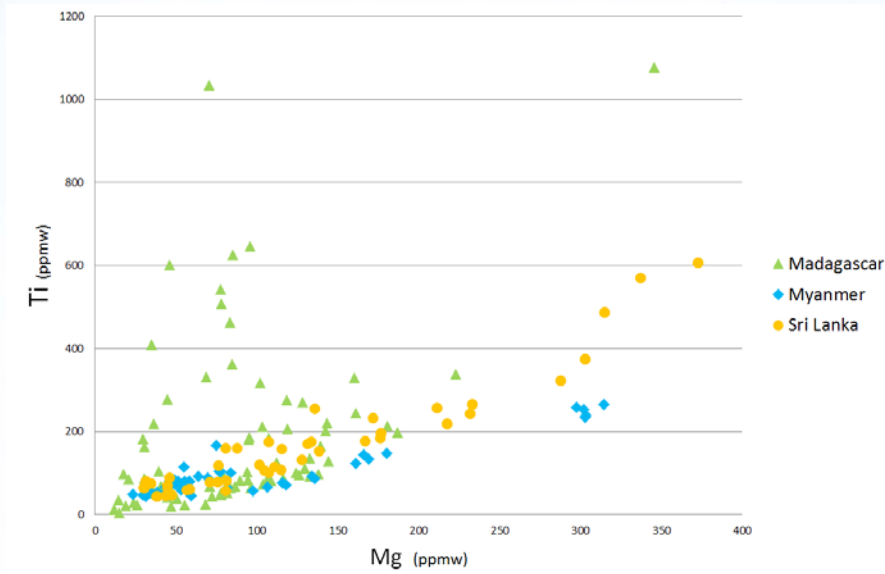


Figure 3: This graph shows Mg and Ti content of Blue sapphire from 3 localities: Madagascar, Myanmar and Sri Lanka in this study.

Conclusion

Trace element analysis of LA-ICP-MS shows information about geological environment of the host crystal and occurrence and leads to geographic origin determination of Ruby and Blue Sapphire. But origin determination in trace element analysis by LA-ICP-MS does not always bring reliable information because data obtained from different locations are sometimes the same. It must be used complementary with an observation of inclusions and gemological characteristics. For increase accuracy, it is necessary to collect samples with secure origin information and their chemical database.

Acknowledgements

I thank Yoichi Horikawa (Central Gem Laboratory, Japan) for supplying the corundum samples obtained the origin determination and discussing the data for this article. Dr. Hisao Kanda (Tsukuba Expo Center, Japan) kindly provided a critical reading of this manuscript.

Reference

Abduriyim, A., and Kitawaki H., 2006, Applications of Laser Ablation-Inductively Coupled Plasma-Mass Spectrometry (LA-ICP-MS) to Gemology, Gems & Gemology, Vol.42, No.2, p.98-118.

Corresponding Author

Full name: Kentaro Emori
Affiliation: Central gem laboratory, Tokyo, Japan
Phone: +81-35817-4664
Fax: +81-35817-4665
Email: emori@cgl.co.jp

High Resolution Computed Microtomography: Insights into a Hollow Beaded Cultured Pearl

Laura M. Otter¹, Ursula Wehrmeister¹, Frieder Enzmann¹, and Dorrit E. Jacob²

¹Department of Geosciences and Earth System Science Research Centre, Johannes Gutenberg-University, D-55128, Mainz, Germany

²Department of Earth and Planetary Sciences, Macquarie University, North Ryde, NSW 2109, Sydney, Australia

Extended Abstract

An exceptionally large (34.6 mm x 40.3 mm) baroque-shaped beaded South Sea cultured pearl was studied using high-resolution X-ray computed microtomography (X-ray μ -CT). The silver specimen was undrilled and shows a pink to blue overtone together with a good quality luster. It was cultured in an Indonesian *Pinctada maxima*.

The CT data revealed a large, internal cavity, filled with liquid, gas, and organic material. These substances are trapped within the pearl, due to the intact layer of nacre, measuring 2.3 mm in average. The bead was localized in the lower part of the cavity and is unconnected to the surrounding nacre. It measures 9.08 mm in diameter, being well within the range for beads used for grafting the oyster *Pinctada maxima*.

It is proposed here that the cavity was at first occupied by aqueous, spongy organic material produced by the young pearlsac, before nacre deposition was initiated at a distance from the small bead. A subsequent disintegration of the organic material started clearing the cavity and caused the liberation of gases, evolving to the present version of the pearl, as seen in the CT dataset. Therefore we refer to this development as an “inflated pearlsac”, giving that not the bead itself, but rather the organic material around it supported the deposition of nacre.

Materials and Methods

The Pearl

The studied specimen is a beaded South sea cultured pearl, from the island of Lombok. The silver, baroque shaped pearl shows a good quality luster and a pink to blue overtone. It measures 34.6 mm x 40.3 mm, thus making it the currently largest known beaded cultured pearl from the South Sea. It was produced in a *Pinctada maxima* oyster, which can reach shell sizes >30 cm in diameter (Strack, 2006). The presence of liquid inside the pearl could be heard when the pearl was gently shaken close to the ear.

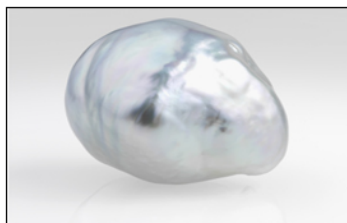


Figure 1: This baroque-shaped pearl is with 40.3 x 34.6 mm, the currently largest known beaded cultured pearl from the South Sea. It shows a silver bodycolor with a pink to blue overtone and a high quality luster (Foto by Gellner GmbH & Co).

X-Ray Computed microtomography

The X-ray μ -CT measurements were carried out with a Procon X-Ray CT-Alpha instrument (ProCon X-Ray GmbH, Sarstedt, Germany) at the Institute for Geosciences, Johannes Gutenberg-University of Mainz (Germany). The acceleration voltage was set to 100 kV, operating at a (diamond-) target current of 120 μ A. The x-ray beam was prefiltered by a 1 mm thick aluminium foil. The optimal distance between pearl and x-ray tube was 250 mm. Spatial resolution depends strongly on the sample size; for this pearl a nominal isotropic resolution of 22.4 μ m per voxel (volume pixel) was achieved. The pearl was mounted on the rotation stage without further pre-treatment, performing a single 360° turn, whilst 800 projections (with 10 images per projection) were recorded with an acquisition time of 1.5 seconds per image.

Reconstruction of the CT dataset was performed with “Octopus 8.5” software (inCT, Aalst, Belgium), while analysis and visualization were done using Avizo Fire 7.0 (Visualization Science Group (VSG), Burlington, USA).

Results and Discussion of the X-Ray μ -CT Dataset

As a major advantage, X-ray μ -CT measurements are non-destructive and the specimens require only minimal pre-treatment e.g. dismounting of samples (Karampelas *et al.*, 2010; Wehrmeister *et al.*, 2008). Analysis results in a dataset, with various options for 3D visualization, providing more extensive information than the traditional X-ray radiograms (Krzemnicki *et al.*, 2010; Wehrmeister *et al.*, 2008). It is capable to give information about nacre thickness, the presence or absence of a bead or drill hole, growth structures, cavities and the presence of vaterite- a CaCO_3 polymorph (Krzemnicki *et al.*, 2010; Otter *et al.*, 2014; Strack, 2006; Wehrmeister *et al.*, 2008). Altogether these aspects provide insights into a pearl’s formation and development. The 2D or 3D images, extracted from a CT dataset are comprised of different greyscale values. Each value depends on material thickness and its specific X-ray density, to the extent that bright values represent areas of high X-ray density and vice versa.

Processing the CT dataset revealed a large internal cavity within the pearl, following the periphery of the nacre layer. A manufactured bead was localized in the bottom of the cavity. Using a software measurement tool, the average nacre thickness was determined by 18 measurements across the pearl to be 2.3 ± 0.7 mm, with a min. value of 0.9 mm and a max. value of 3.3 mm. The bead measures 9.08 mm in diameter and is without contact to the surrounding nacre. Whereas nacre and bead exhibit light greyscale values (high X-ray densities) and appear white to light grey, three distinct, darker phases stand out within the cavity and are already distinguishable in the raw data image (Figure 2):

Phase 1 has the darkest greyscale value (lowest X-ray density) and is situated at the top of the cavity. Due to the low grayscale value and its similarity towards the surrounding air in the sample chamber this phase is interpreted to be a gas.

Phase 2 has an intermediate greyscale value (medium X-ray density) and occupies the middle and bottom region within the cavity. The transition between phases 1 and 2 is characterized by a clearly visible meniscus. Capillary rise is visible along the inside of the cavity, between single

layers of nacre (Figure, 2 and 4, blue arrow). The presence of the meniscus and the capillary rise along the sides, as well as the sound of the pearl upon shaking identify this phase as a liquid.

Lastly, phase 3 appears net-like at the bottom of the cavity, sharing its space here with phase 2 and also covering the bead. Its filigree appearance around the bead and the intermediate greyscale value between liquid and nacre, led us to consider this phase as the remains of an early organic layer. While processing the dataset with the Avizo software, all three phases were segmented individually, allowing the quantification of each volume and separate illustrations (Figures, 3 and 4).

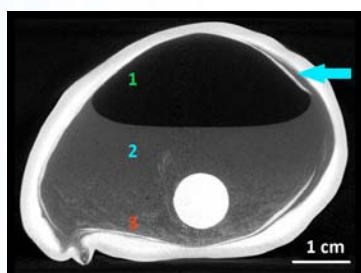


Figure 2: Shows a virtual transversal cut through the pearl (raw data image). Nacre and bead show a white to light grey greyscale value, whereas the different substances in the cavity (1-3) have darker values. Each phase is represented by an own, distinct grayscale value. We believe the substances to be gas (1), liquid (2) and organics (3). Note the capillary action (blue arrow) between spacing layers of nacre.

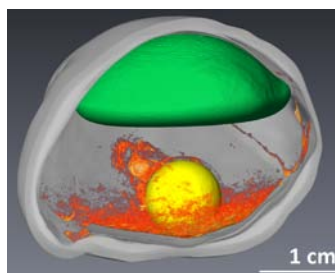


Figure 3: Segmentation of Phase 1, gas, (green) and 3, organics (red), while the bead is yellow. The bottom of the gas has an inward bent surface, which is a result of the meniscus between it and the liquid. The blank part of the void is occupied by the liquid (phase 2), but was faded out, to reveal the organic phase.

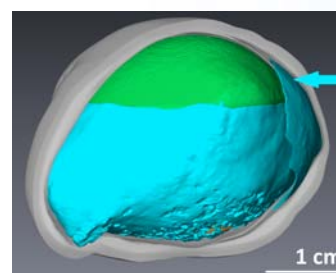


Figure 4: Segmentation of Phase 1, gas (green) and 2, liquid (blue). The flaky look of the liquids bottom is due to negative imprints of the organic substance. The blue arrow highlights capillary rise between single layers of nacre.

Table 1: The relative abundances of the pearl's phases calculated with the Avizo software.

	Volume [cm ³]	Vol. %
Nacre	7.72	44
Phase 1 Gas	3.40	19
Phase 2 Liquid	6.06	34
Phase 3 Organics	0.19	1
Total cavity (Phase 1+2+3)	9.65	54
Bead	0.39	2
Total pearl	17.76	100

Conclusions Drawn from Ct Datasets

X-ray μ -CT analysis is an excellent tool for studying the internal properties of valuable pearls. In the present case a series of conclusions is drawn from the CT dataset, depicting the pearl's development:

Its remarkable size is linked to the development of the large cavity, making up 54 Vol.-% of the pearl and therefore results neither from exceptional nacre growth nor an oversized bead.

We believe that a voluminous layer of organic material was deposited onto the small bead, before switching to the production of nacre and refer to this process as "inflation of the pearlsac" (Otter *et al.*, 2014).

The early production of this significant amount of organic material (ca. 9.65 cm³) may be due to contamination or inflammation of the pearlsac upon surgery or shortly after.

Later on, disintegration-processes consumed most of the organic material and cleared the cavity, liberating gases and liquids still present in the cavity today.

References

- Karampelas, S., Michel, J., Zheng-Cui, M.L., Schwarz, J.O., Enzmann, F., Fritsch, E., Leu, L., and Krzemnicki, M.S., 2010, X-ray computed microtomography applied to pearls: Methodology, advantages, and limitations, *Gems & Gemology*, Vol.46, No.2, p.122-127.
- Krzemnicki, M.S., Friess, S.D., Chalus, P., Hänni, H.A., and Karampelas, S., 2010, X-ray computed microtomography: Distinguishing natural pearls from beaded and non-beaded cultured pearls, *Gems & Gemology*, Vol.46, No.2, p.128-134.
- Otter, L.M., Wehrmeister, U., Enzmann, F., Wolf, M., and Jacob, D.E., 2014, A Look Inside A Remarkably Large Beaded South Sea Cultured Pearl, *Gems & Gemology*, Vol.50, No.1, p.58-62.
- Strack, E., 2006, *Pearls*. Rühle-Diebener Verlag, Stuttgart. ISBN: 978-3981084801.
- Wehrmeister, U., Götz, H., Jacob, D.E., Soldati, A. L., Xu, W., Duschner, H., and Hofmeister, W., 2008, Visualization of the internal structures of cultured pearls by computerized X-ray microtomography, *The Journal of Gemmology*, Vol.31, No.1-2, p.15-21.

Corresponding Author

Full name: Laura M. Otter
Affiliation: Department of Geosciences and Earth System Science Research Centre,
Johannes Gutenberg-University, D-55128, Mainz, Germany.
Phone: +016098552777
Email: ottelaur@students.uni-mainz.de

If Diaspore is Responsible for the 3309 cm⁻¹ Peak in the FTIR Spectra of Heated Ruby Samples

Aumaparn Phlayrahan¹, Natthapong Monarumit¹, Somruedee Satitkune¹, and Pornsawat Wathanakul²

¹The Gem and Mineral Sciences Special Research Unit, Department of Earth Sciences, Faculty of Science, Kasetsart University, Bangkok, 10900, Thailand

²The Gem and Jewelry Institute of Thailand (Public Organization), Bangkok, 10500, Thailand

Extended Abstract

Introduction

The 3309 cm⁻¹ peak in FTIR spectra is a significant indication of heat treatment in ruby samples. In the case of ruby samples from Mong Hsu, Myanmar specifically the sample with dark core, the 3309 cm⁻¹ peak is obviously shown with high intensity after heating at 1200°C (Wathanakul *et al.*, 2012). Smith (1995) reported that the result is related to the inclusions of diaspore and boehmite in the ruby structure. Nevertheless, some research such as Beran and Rossman (2006) reported that the 3309 cm⁻¹ peak is also observed in the ruby samples without the inclusion of diaspore. Hence, this study aims to find how exactly diaspore is related to the occurring of 3309 cm⁻¹ peak in FTIR spectra of ruby samples from Mong Hsu, Myanmar.

Materials and Methods

The diaspore samples from Turkey as shown in Figure 1B were selected for referencing. The samples were crushed into fine powder and mixed in analysis grade of KBr (AR grade). The concentration of the samples in KBr is 0.1%. Besides, the selected ruby samples from Mong Hsu, Myanmar were cut in perpendicular to c-axis (Figure 1A). The FTIR spectra of unheated ruby samples were recorded. All samples were heated in oxidizing atmosphere at 600, 800, 1000 and 1200 °C. The FTIR spectra of the samples were acquired by a NEXUS 470 FTIR spectrometer in transmission mode. The spectra were taken in the 400-4000 cm⁻¹ region with a resolution of 4 cm⁻¹ and 256 numbers of scan at room temperature.

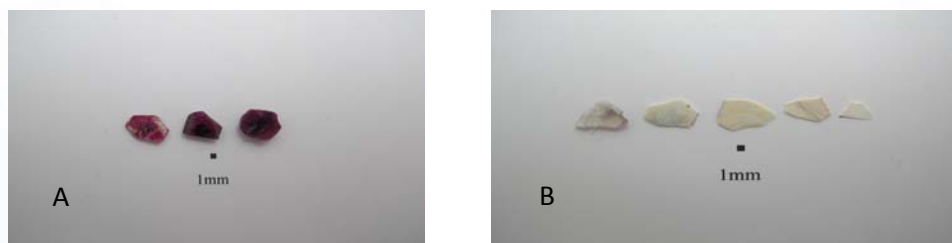


Figure: 1 ruby samples **(A)** and diaspore samples **(B)**.

Results and Discussion

The peaks position in FTIR spectra of ruby samples from Mong Hsu, Myanmar and diaspore samples are summarized in the Table 1 and Table 2, respectively.

Table 1: FTIR peaks position of the ruby samples.

Wavenumber (cm ⁻¹)					Assignment
unheated	heated at 600 °C	heated at 800 °C	heated at 1000 °C	heated at 1200 °C	
--	--	--	3309 3231 3188	3309 3234 3184	M-OH stretching [Beran and Rossman, 2006; Smith, 1995]
--	--	2920	--	--	M ²⁺ -OH stretching [Wu <i>et al.</i> , 2000]/ C-H stretching
2352	2354 2338	2352 2338	2352	2352	C-O stretching
2122 1986	2148 2037	2150 2036	--	2334	O-H stretching [Smith,1995]
536, 490	530, 485	536, 485	529, 486	526, 483	Al-O stretching [Smith,1995]

Table 2: FTIR band position of diaspore samples.

Wavenumber (cm ⁻¹)					Assignment
unheated	heated at 600 °C	heated at 800 °C	heated at 1000 °C	heated at 1200 °C	
--	2921 2852	--	--	--	M ²⁺ -OH stretching [Wu <i>et al.</i> , 2000]/ C-H stretching
--	2359 2334	2362 2330	2363 2341	2366	C-O stretching
2134 1989	--	--	--	2341	O-H stretching [Ruan <i>et al.</i> , 2001]
	1488	1482	1457	1456	C-H stretching [Saikai and Parthasarathy, 2010]
1078	--	1113	--	--	Si-O quartz [Saikai and Parthasarathy, 2010]
961	--	--	895	877	OH deformation [Saikai and Parthasarathy, 2010]
--	630	631	632	628	Si-O-Si bending [Saikai and Parthasarathy, 2010]
582, 557	563, 552	560	557	556	Fe-O, Fe ₂ O ₃ , Si-O-Al stretching [Saikai and Parthasarathy, 2010]
--	--	459	--	468	Si-O-Si bending [Saikai and Parthasarathy, 2010]

The FTIR spectra of ruby samples in different heating temperature are shown in Figure 2. The 3309 cm⁻¹ and the two side peaks at 3234 and 3185 cm⁻¹ are only observed in the sample at high temperature heating (1000 and 1200°C). On the other hand, the absorption peaks of hydrous minerals such as diaspore are only indicated in the unheated and heated sample at low temperature. The samples were heated at moderate to high temperature (1000- 1200°C), these peaks seem to be missing (Figure 3, Table 2). It means that if the 3309 cm⁻¹ peak occurs, the hydrous mineral peaks disappear. In addition, there are no significant changes in the peaks indicated around 2350- 2330 cm⁻¹ and the low wavenumbers at 536- 485 cm⁻¹ of C-O stretching and Al-O stretching respectively in all heating temperatures.

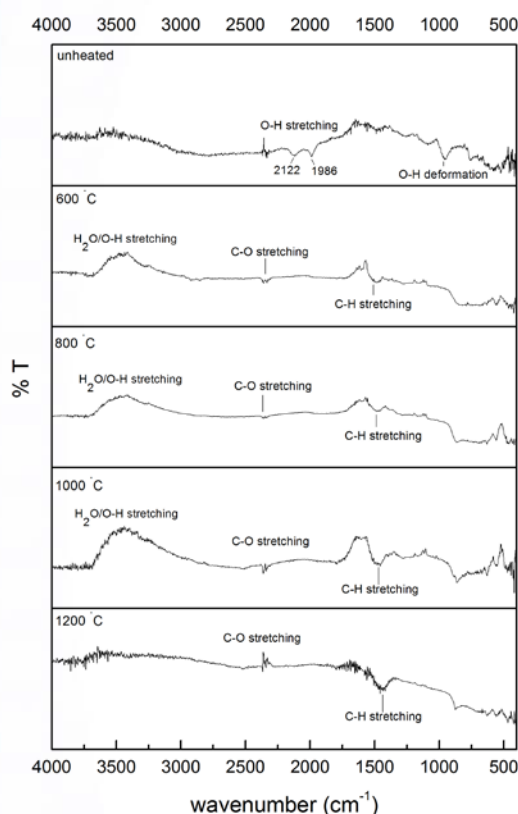


Figure 2: FTIR spectra of ruby samples from Mong Hsu, Myanmar at different heating temperatures.

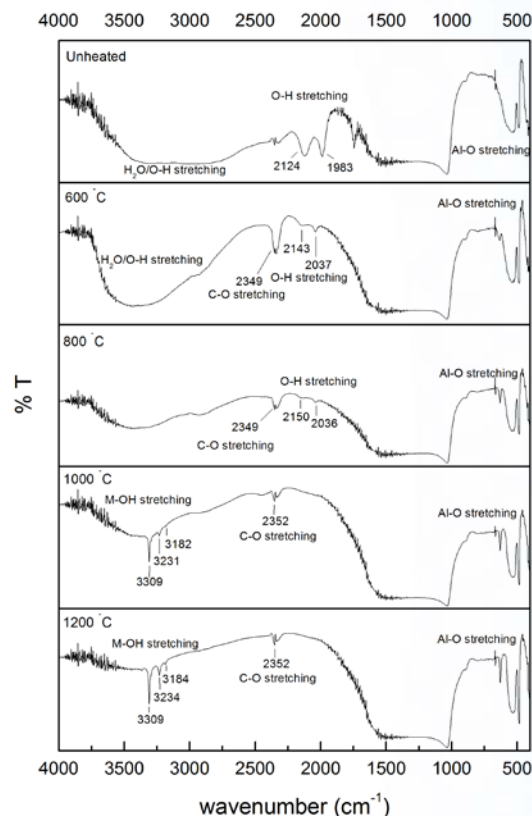


Figure 3: FTIR spectra of diaspore samples at different heating temperatures.

The diaspore samples are heated at different temperatures. After heating, the sample has been changed the physical appearance such as, turbidity, colour and weight. The FTIR spectra of a selected diaspore sample as shown in Figure 3 indicate the absorption peaks at 2122 and 1986 cm⁻¹ of O-H stretching. These peaks are only observed in unheated samples and disappeared in the heated ones. In addition, the other peaks in FTIR spectra of diaspore samples do not significantly indicate the changes of heated samples at different temperature. Importantly, there are no the set of peaks (3309, 3234 and 3185 cm⁻¹) in the diaspore samples. The temperatures of heating at 1000 and 1200 °C, the FTIR spectra of ruby samples obviously show the 3309 cm⁻¹. At the

same time, the O-H stretching peak of hydrous mineral slightly decreased. Nevertheless, there are no the 3309 cm⁻¹ peak appearing in FTIR spectra of diaspore samples. This result reveals that the 3309 cm⁻¹ peak does not directly occur from the inclusion of diaspore in ruby structure but is rather related to the M-OH, in which the OH might have been generated by some hydrous minerals, i.e. diaspore.

Corresponding to our research results (Wathanakul *et al.*, 2012; Monarumit *et al.*, 2014) of the ruby samples from the other sources and different features are summarized in table 3. It is obvious that the samples without inclusions of diaspore also indicated the peaks at 3309 cm⁻¹. Another interesting point is the ruby samples with blue patch/core usually show the 3309 cm⁻¹ peak, whether there is the inclusion of diaspore or not. Considering to the samples with the 3309 cm⁻¹ peak, most of them show the high content of Ti in their structure. This evidence could be assumed that the diaspore does not affect to the 3309 cm⁻¹ peak, but rather the trace element in the structure especially Ti plays an important role; and this could help solve problem in indication of heating in sapphire samples as well.

Table 3: The summary of 3309 cm⁻¹ peak in ruby samples from different sources and features observed.

Type of ruby samples	The 3309 cm ⁻¹ peak	Diaspore inclusions	Ti content
Ruby samples from Mong Hsu Myanmar	--- (unheated), xxx (after heated at 1200 °c)	xxx (unheated), --- (heated)	High
Ruby samples from Luc yen, Vietnam	--- (unheated), xxx (after heated at 1200 °c)	xxx (unheated), --- (heated)	High
Ruby samples from Mozambique (with blue patch/core)	xxx	---	High
Ruby samples from Mozambique (without blue patch/core)	---	---	Very Low
Ruby samples from Sri Lanka	---	---	Very Low
Ruby samples from Guinea	x	---	Low
Verneuil synthetic ruby samples	xx	---	Medium

Note: --- (absent), x = weak intensity, xx = moderate, xxx = strong intensity

Ti content; High = ~300-400 ppm, Medium = ~>100 ppm, Low = ~> 50 ppm, Very Low = ~>10 ppm

Therefore, the experiment on how diasporite is related to the occurring of the 3309 cm⁻¹ peak in FTIR spectra of ruby samples from Mong Hsu, Myanmar reveals the dehydration process in both of the ruby samples and diasporite. When diasporite was heated the chemical reaction on losing water in the structure also occurs. This process produces 2H⁺ and O²⁻ ions in the host structure. These ions formed the OH⁻ and bonding with the cation molecule [Beran and Rossman, 2006], which could be Ti⁴⁺. Corresponding to the physical appearance of diasporite, the sample has been changed the colour and turbidity undergone heating. It is due to losing of water in diasporite. Before heating, the chemical composition of diasporite is still an α -AlO(OH). After heating the composition remains only Al₂O₃ (B-alumina). In addition, the dehydration occurs in ruby structure by its own is also responsible for generating of OH. This process removes the broad absorption of O-H stretching in FTIR spectra. So, the 3309 cm⁻¹ clearly observed in the ruby sample which are undergone heating at high temperature (= and > 1000 °C).

Conclusion

The occurring of 3309 cm⁻¹ peak does not directly depend on the presence of diasporite but relate to the trace element in particular Ti along with the presence of O²⁻ and 2H⁺, produced by the dehydration while heating.

References

- Beran, A., and Rossman, R.G., 2006, OH in naturally occurring corundum, *European Journal of Mineralogy*, Vol.18, No.4, p.441-447.
- Monarumit, N., Lhuamporn, T., Satitkune, S., Wongkokua, W., and Wathanakul, P., 2014, Applications of Mid- and Near Infrared Spectroscopy to indicate conditions of heat treatment in synthetic ruby samples, GIT 2014 submission.
- Ruan, H.D., Frost R.L., and Kloprogge, J.T., 2001, Comparison of Raman spectra in characterizing gibbsite, bayarite, diasporite and boehmite, *Journal of Raman Spectroscopy* Vol.32, No.9, p.745-750.
- Saikai, B.J., and Parthasarathy, G., 2010, Fourier transforms infrared spectroscopic characterization of kaolinite from Assam and Meghalaya, northeastern India, *Journal .Modern Physics*, Vol.1, No.4, p.206-210.
- Smith, C.P., 1995, A contribution of understanding the infrared spectra of rubies from Mong Hsu, Myanmar, *Journal of Gemmology*, Vol.24, No.5, p.321-335.
- Wathanakul, P., Atichat, W., Pisutha-Arnond, V., Sriprasert, B., Leelawatanasuk, T., Satitkune, S., Monarumit, N., Lhuamporn, T., Sanguanphun, C., Phlayrahan, A., Chantrakul, T., Chaipaksa M. and Ingavanija, S., 2012, The study of AFM and FTIR spectroscopy of low temperature heated ruby samples, GIT report 2012
- Wu, Z., Jiang, Y., Xie, G., Cheng, X., Li, D., and Wang, T., 2000, The effect of irradiation on IR peaks in corundum at about 2850, 2920 and 2995 cm⁻¹, *Sensors and Actuators B: Chemical*, Vol.66, No.1-3, p.293-295.

Acknowledgements

The authors gratefully acknowledge support from The Gem and Mineral Sciences Special Research Unit, Department of Earth Sciences, Faculty of Science, Kasetsart University and the Graduate School Kasetsart University for the research fund.

Corresponding Author

Full name: Aumaparn Phlayrahan

Affiliation: The Gem and Mineral Sciences Special Research Unit, Department of Earth Sciences, Faculty of Science, Kasetsart University, Bangkok, 10900, Thailand.

Email: a.phlayrahan@gmail.com

Introduction of the New Gem - Corundum Sources from Krong Nang District, Dak Lak Province, Vietnam

***Nguyen Ngoc Khoi^{1,3}, Christoph Hauzenberger², Duong Anh Tuan^{3,6}, Jongwan Park⁴,
Tobias Häeger⁵, Phan Thi Minh Diep⁵ and Sora Shin⁴***

¹Hanoi University of Science, 334 Nguyen Trai, Thanh Xuan, Hanoi, Vietnam

²Karl-Franzens-University of Graz, A – 8010, Graz, Austria

³DOJ Gold & Gems Group, 44 Le Ngoc Han, Hai Bat Trung, Hanoi, Vietnam

⁴Hanyang University, 222 Wangshimni-ro, Seongdong-gu, Seoul 133-791, Korea

⁵Johannes Gutenberg-University of Mainz, D55099, Mainz, Germany

⁶Institute of Material Science (Vietnam Academy of Science and Technology), 18 Hoang Quoc Viet, Cau Giay, Hanoi, Vietnam

Extended Abstract

Vietnam is one of the major producers of gem corundum. Due to the high demand of ruby and sapphire, most of local mining sites are exhausted rapidly and the discovery of new sources is the great necessity for the country. The Krong Nang corundum deposit was discovered by the end of 2012; recently, monthly production is operated ranging from 200 to 300 kg. This report covers some gemological, mineralogical and geochemical characteristics of the gem-quality sapphires from this new deposit.

Location and Geology

The Krong Nang region is located approximately 180 km northeast of Ban Me Thuot city, Dak Lak province, in Tay Nguyen Highlands. Fancy sapphires occur in secondary (deluvial and alluvial) deposits that cover a surface area of approximately 30 km². The deposits are located in small valleys surrounded by hills, in coffee fields and along the streams crossing the area. The placer deposits are found in Quaternary sediments lying in a terrain of depressions and valley terraces. The gem-bearing sedimentary beds with an average of 2-3 m thick may be traced to tens of meters. The overburden ranges from less than a meter in some areas to 1.5-2 m.

Samples and Methods

For this study, two lots (about 1 kg) of representative gem-quality rough sapphire were purchased directly from the mining site in Krong Nang district. They were divided into small lots, based on color shades (Figure 1). Some representative pieces were then cut prepared for analytical methods. We used standard gemological equipments to record basic gemological properties of this material. Moreover, forty four sapphire pieces were mounted and embedded in resin, polished and then analyzed by EPMA and LA-ICPMS.



Figure 1: Some samples of cut sapphire used for this study

Results

Crystal Morphology, Visual Morphology and Basic Gemological Properties

Most of the gem-quality materials from these deposits range in size from 2 to 6 mm, but stones of tens to hundreds carats are also encountered. Stones with typical crystal shape are rare. Most common samples are angular to partly rounded fragments. They are mostly green, bluish green to yellow, greenish yellow sapphires, sometimes show BGY and blue colors. Diaphaneity is semitransparent to translucent or opaque. Basic gemological properties of Krong Nang sapphires fall within the common ranges of corundum (Table 1).

Table 1: Basic gemological properties of Krong Nang sapphire

Property	Number of sample	Result
Refractive index	14	$n_e = 1.761 - 1.764$; $n_o = 1.770 - 1.773$
UV Luminescence	15	SW: inert; LW: inert
Specific gravity	18	3.98 – 4.04

Internal Features

The typical feature of these sapphires is distinct light to medium and dark blue or yellow to green color zones. Straight and angular parallel growth features are also encountered. In some stones, well-developed laminated twinning planes were also observed.

The most common inclusions are irregular to angular in outline minute whitish to grayish particles concentrated along the color zones (Figure 2). Of these particles, short needle-like inclusions were identified by EPMA as iron oxide, most likely hematite and Fe-Ti oxide (ilmenite). Less common inclusions are very long, relatively coarse “needles” along the junctions of laminated twinning planes. Other solid inclusions are zircon (Figure 3) and feldspar which have been identified by Raman spectroscopy comparable to those reported by Guo *et al.*, (1996). Partially healed fractures, planes of gas/liquid and negative inclusions, and fractures were also commonly seen in this Vietnamese material.

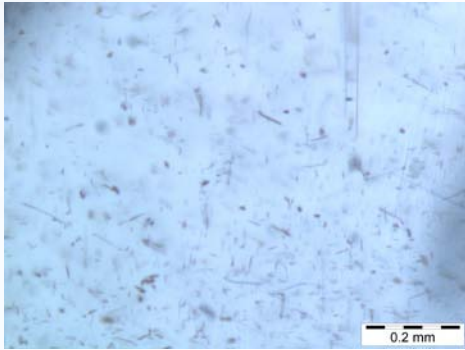


Figure 2: Minute particles appear to be hematite or ilmenite (90x)

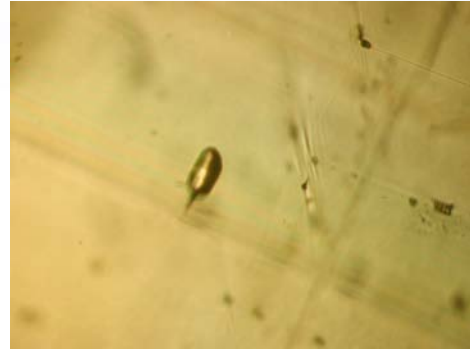


Figure 3: Zircon inclusions encountered as single crystals (50x)

Chemistry and Spectroscopy

The results of EPMA and LA-ICP-MS are summarized in Table 2, where values of Al₂O₃ and FeO were analyzed by electron microprobe and for other trace element analyses were carried out using ICP-MS.

Table 2: Compositional range of 3 main color groups of Krong Nang sapphire

Color	No of samples	Al ₂ O ₃ (w.%)	FeO _{tot.} (w.%)	Mg (ppm)	Ti (ppm)	Cr (ppm)	Ga (ppm)	V (ppm)
Green	12	98.12-99.41 (98.71)*	1.45-2.45 (1.91)	13-39 (29)	22-175 (77)	bdl-27 (9)	166-246 (197)	2-6 (4)
Yellow	17	97.83-100.11 (98.70)	0.17-1.83 (1.61)	15-45 (19)	19-82 (33)	bdl-18 (8)	163-315 (210)	2-5 (3)
Blue	10	97.73-101.50 (99.14)	0.48-2.27 (1.31)	1-54 (25)	27-551 (115)	bdl-16 (11)	159-398 (231)	1-34 (11)

(98.71)* = mean value, bdl = below detection limit

Iron is the most significant minor element in all color groups; however, green sapphire displays the highest average content whereas blue sapphire contains the lowest average concentration. Gallium concentration is similar in all color groups and varies from 159 to 398 ppm with an average of around 210 ppm. Titanium which is needed for the blue color-causing (Fe²⁺/Ti⁴⁺ IVCT charge transfer) is present mostly in blue sapphire (115 ppm). Other trace elements are present in very low and negligible amounts, including Mg, V and Cr (Table 2).

The color of sapphire samples of three main types (green, yellow and blue) is indicated using UV-VIS-NIR spectra (Figure 4). Most samples examined, not depending on their body color, show the entire iron 450 nm complex in their absorption spectra. The spectra of blue with part of green sapphires show absorption bands due to Fe²⁺/Ti⁴⁺ and Fe²⁺/Fe³⁺ IVCT with the maximum approximately at 571 and 877 nm, respectively, and absorption peaks due to Fe³⁺ at 377, 387, 450 nm as sharp peaks, and 459 and 471 nm as shoulder peaks. The absorption band in the near infrared (NIR) with a maximum at around 876 nm is typically found in basaltic sapphires elsewhere. The spectra of yellow sapphires show mostly absorption peaks related to Fe³⁺ at 377, 387, 450, 459 and 471 nm (Fritsch *et al.*, 1987; 1988).

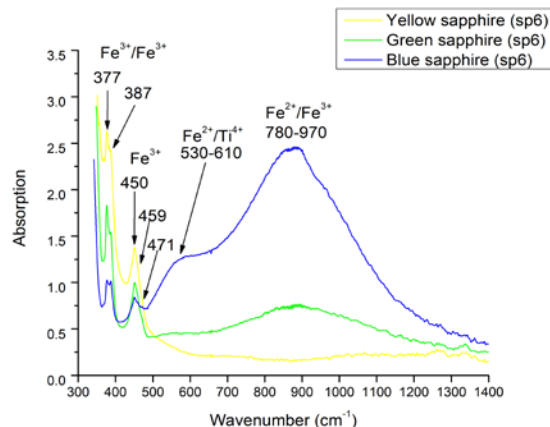


Figure 4: UV-VIS-NIR spectra of Krong Nang sapphires

Discussion and Conclusions

Krong Nang deposits yield mostly green and yellow sapphires, sometimes BGY ones. Color of this material is caused mostly by Fe. Stones with typical crystal shape are generally much rarer comparing to other deposits of basalt-related type in South Vietnam. Mineral inclusions, trace element composition and absorption spectra characteristics can be used to differentiate this material from other sources of basaltic origin in Vietnam (Garnier *et al.*, 2005; Smith *et al.*, 1995).

Acknowledgements

This research is funded by Vietnam National Foundation for Science and Technology Development (NAFOSTED) under grant number 105.02-2012.08.

References

- Fritsch, E., and Rossman, G.R., 1987, An Update on Color in Gems; Part 1: Introduction and Colors Caused by Dispersed Metal Ions, *Gem & Gemology*, Vol.23, No.3, p.126-139.
- Fritsch, E., and Rossman, G.R., 1988, An Update on Color in Gems; Part 2: Colors Involving Multiple Atoms and Color Centers, *Gem & Gemology*, Vol.24, No.1, p.3-15.
- Garnier, V., Ohnenstetter, D., Giuliani, G., T. Phan Trong, V. Hoang Quang, L. Pham Van, and Schwarz, D., 2005, Basalt petrology, zircon ages and sapphire genesis from Dak Nong, southern Vietnam, *Mineralogical Magazine*, Vol.69, No.1, p.21-38.
- Guo, J., O'Reilly, S.Y., and Griffin W.L., 1996, Corundum from basaltic terrains: a mineral inclusion approach to the enigma, *Contributions To Mineralogy and Petrology*, Vol.122, No.4, p.368–386.
- Smith, C.P., Kammerling, R. C., Keller, A.S., Peretti, A., Scarratt, K.V., Khoa, N. D., and Repetto, S., 1995, Sapphire from Southern Vietnam, *Gems & Gemology*, Vol.31, No.3, p.168-185.

Corresponding Author

Full name: Nguyen Ngoc Khoi
 Affiliation: Hanoi University of Science, 334 Nguyen Trai, Thanh Xuan, Hanoi, Vietnam
 Phone: +84 4 38585097
 Fax: +84 4 38583061
 Email: khoinn@vnu.edu.vn

Mineralogical and Gemological Properties of Orange Johachidolite from Northwest of Mogok, Myanmar

Yongkil Ahn¹, Kyungjin Kim¹ and U Tin Hlaing²

¹Division of Crafts Design, Kongju National University, 56 Gongjudaehak-Ro, Gongju-Si, Chungnam-Province, 314-701, Korea

²Bldg. No.C Room No. 205, Yoma Apartment, Myoma Quarter, Taunggyi, Myanmar

Extended Abstract

Orange Johachidolites were collected from Northwest of Mogok, Myanmar in recent months. They were analyzed by WD-XRF, UV-Vis spectroscopy. The crystal structure of Johachidolite is CaAlB_3O_7 , [Cmma, $a = 9.767(2)$, $b = 11.723(3)$, $c = 4.3712(5)$] as a borate mineral.

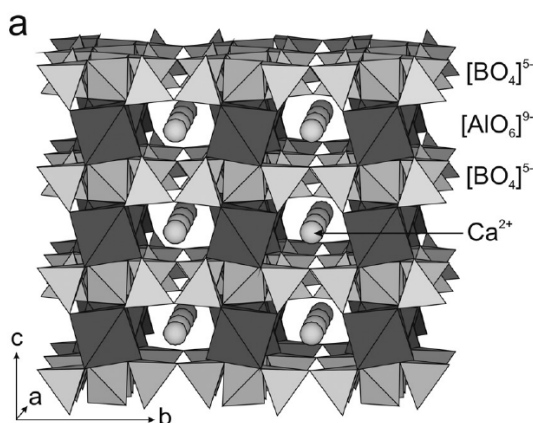


Figure 1: Polyhedral structure of Johachidolite (Kadiyski *et al.*, 2008).

Johachidolite is arranged compact walls parallel to (010). The unusual units of these walls are dense columns of $[\text{AlB}_4\text{O}_{12}]^{9-}$ composition parallel to the c axis. AlO_6 octahedra sharing edges with BO_4 are caused by strong bonds perpendicular to the borate sheet. Between the (010) walls, six-membered-ring channels are occupied by ten-coordinated Ca (Figure 1).

Johachidolite was originally named by Iwase & Saito in 1942. According to Tsuda (1969), the name of the region is Sangpal-dong, Chngbaeng-myon, Kilchu-gun, Northern Hmgryong Province, North Korea.

In this study, we investigated Johachidolites from Pain Mynit mining province which is located about 5 km Northeast of Mogok (Figure 2). The Pain Pyit mine is famous for occurrences of

gem quality spinels, sapphire and other gemstones. Rubies are also found in other areas of Mogok as shown in the Figure 2 (Peretti *et al.*, 2007). The occurrence of Johachidolite at the locality of Pyant Gyi is indicated on the map. Figure 2 shows the major gemstones mined in the vicinity of the Johachidolite occurrence.

Johachidolite mine from Pain Pyit belongs to Mogok Metamorphic Belt (MMB). This belt extends for 1500 km along the western margin of the Shan-Thai block and from the Andaman Sea north to the eastern Himalayan syntaxus (Searle *et al.*, 2007). In the northern MMB around Mogok the youngest phase of magmatism discovers to be a suite of nepheline syenites that contain gem quality sapphires intruded into marble, gneiss and cross cut metamorphic fabrics (Figure 2).

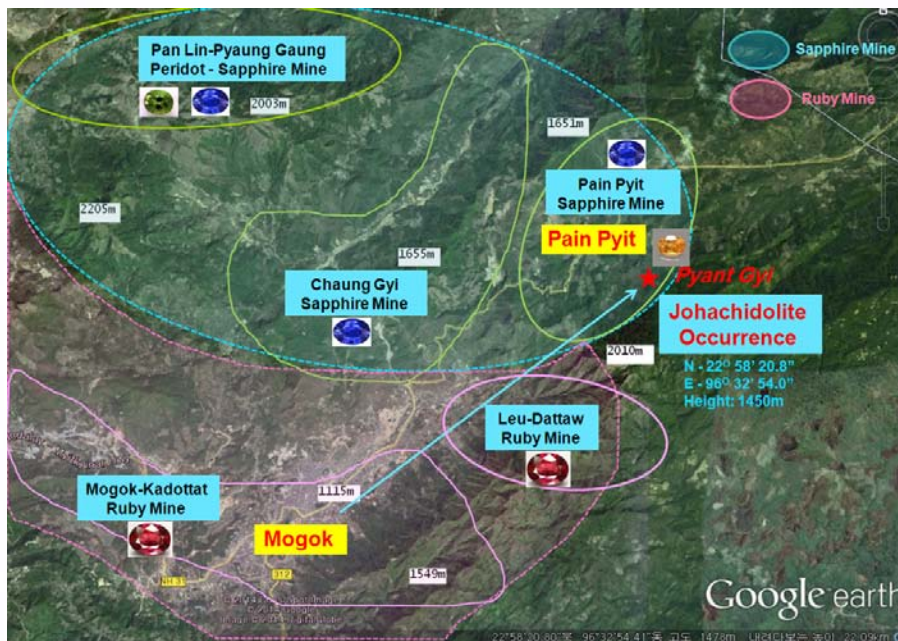


Figure 2: Satellite image of Pain Pyit region captured from Google earth showing some crucial deposits including Pain Pyit mine.

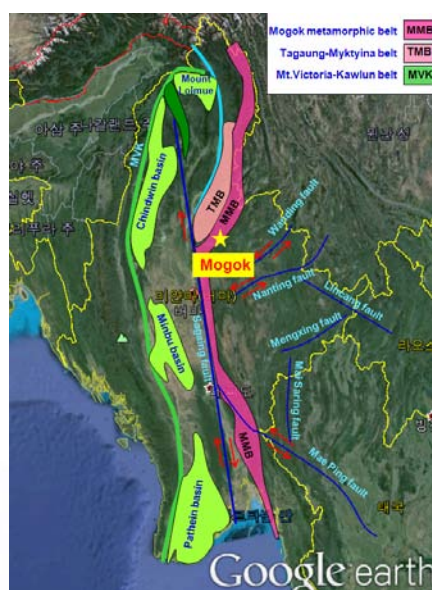


Figure 3: Satellite image (captured and modified from Google Earth) with some crucial geological features of Myanmar.



Figure 4: Orange johachidolite from Pain Pyit, Myanmar.

Intergrowth mineral assemblages are characterized by pegmatite as shown in Figure 4a. This orange johachidolite is combined with violet hackmanite. Figures 4b and c are rough stones and polished stones, respectively.

The physical properties were consistent in RI (1.717-1.725) and SG (3.32-3.54). The fluorescence to long- and short-wave UV radiation showed inert in all samples. These were similar to results of Chadwick and Breeding (2008).

WDXRF analysis identified the presence of the following elements: B, Al, and Ca (in major amounts), F (minor), Si, Sn, Na, Fe, and P (trace). Especially, U and Th of the small quantity as radioactive elements were detected in some samples.

References

- Kadiyski, M., Armbruster T., Günther, D., Reusser, E., and Peretti, A., 2008, Johachidolite, $\text{CaAl}[\text{B}_3\text{O}_7]$, a mineralogical and structural peculiarity, *European Journal of Mineralogy*, Vol.20, No.5, p.965-973.
- Peretti, A., Peretti, F., Tun, N.L., Günther, D., Hametner, K., Bieri, W., Reusser, E., Kadiyski, M., Armbruster, T., 2007, Gem quality Johachidolite: occurrence, chemical composition and crystal structure, *GRS Publications; Contributions to Gemology*, No.5, 53 p.
- Searle, M.P., Noble, S.R., Cottle, J.M., Waters, D.J., Mitchell, A.H.G., Tin Hlaing, and Horstwood, M.S.A., 2007, Tectonic evolution of the Mogok metamorphic belt, Burma (Myanmar) constrained by U-Th-Pb dating of metamorphic and magmatic rocks, *Tectonics*, Vol. 26, No.3, 24 p.
- Chadwick, K.M., and Breeding, C.M., 2008, Color variations and properties of johachidolite from Myanmar, *Gems & Gemology*, Vol.44, No.3, p.246-251.

Corresponding Author

Full name: Yongkil Ahn
 Affiliation: Division of Crafts Design, Kongju National University, 56 Gongjudaehak-Ro, Gongju-Si, Chungnam-Province, 314-701, Republic of Korea.
 Phone: +82-41-850-0382
 Fax: +82-41-850-0389
 Email: ykahna@gmail.com

Mineralogy of Blue Pectolite from the Dominican Republic

Weerapan Srichan and Nalida Jaiboon

Department of Geological Sciences, Faculty of Science, Chiang Mai University, Chiang Mai, 50200, Thailand

Extended Abstract

Nineteen samples of blue pectolite from the Dominican Republic were studied in gemological characteristic, petrography, surface feature, mineral composition and chemical composition. Samples are ranged from white, light blue, greenish blue to moderate dark blue. Specific gravity varied from 2.80 to 2.87. Most of samples fluoresces pinkish orange to short-wave U.V. but no react to long-wave U.V. Petrographically, five representative samples show fibrous and some amygdaloidal texture under polarizing microscope. Finely fibrous crystal of blue pectolites was also examined by Scanning Electron Microscope. Chemically, three representative samples of blue pectolites shown peaks of Si, Ca, Na and Cu on their SEM-EDX spectra. Two samples were confirmed their mineral identity as pectolite in associated with minor calcite by X-ray powder diffractometer. The small amounts of copper content have been interpreted as cause of color of blue pectolite, substitute for calcium in the crystal structure.

Introduction

Blue pectolite from the Dominican Republic known by the trade name Larimar (Woodruff and Fritsch, 1987). Larimar is a rock composed largely of pectolite, an acid silicate hydrate of calcium and sodium. Its coloration varies from white, light-blue, green-blue to deep blue. This blue color, distinct from that of other pectolites, is the result of copper substitution for calcium. The first mention of blue pectolite in the gemological literature was by Arem (1977). Previously, gem pectolite occurred only in an unattractive white to gray color and was considered rare because of its scarcity in pieces suitable for cutting (Webster, 1983; Liddicoat, 1976). The new and more plentiful supply of blue, and less commonly green, pectolite has helped it achieve recognition as an excellent lapidary material; carving are now on display in the Smithsonian Institution and the Lizzadro Museum (Lizzadro, 1987). Nineteen samples of blue pectolite from the Dominican Republic were found in the 53rd Bangkok Gems and Jewelry Fair, 2013. The samples were examined in gemological properties and mineralogy (Jaiboon, 2014) at Gemological Research Unit, Department of Geological Sciences, Chiang Mai University.

Gemological Properties

Nineteen samples of pectolite were polished for visualized observing. They are ranged from white, light blue, greenish blue to moderate dark blue. Some samples display fibrous radial aggregation. Specific gravity of all samples obtained by the hydrostatic methods varied from 2.80 to 2.87 and averaged at 2.83. All samples of blue pectolite were examined for their reaction to short- and long-wave radiation. The samples fluoresces pinkish orange to short-wave U.V. but no react to long-wave U.V.

Petrography

Five representative samples of blue pectolite were cut to be polished-section for petrographic study. Fibrous and radial textures are commonly found in all samples (Figure 1). Some samples are exhibited vesicular and amygdaloidal textures. Radiating pattern of fibrous crystals in vesicles indicated secondary deposit.



Figure 1: Microphotographs showing fibrous and radial textures for a representative sample of blue pectolite (**left;** plane polarized light and **right;** cross polar).

Three representative samples were examined by Scanning Electron Microscope (SEM: JEOL JSM-591LV) at Science Central Laboratory, Chiang Mai University. Finely fibrous crystals of blue pectolite are observed on their surfaces (Figure 2).

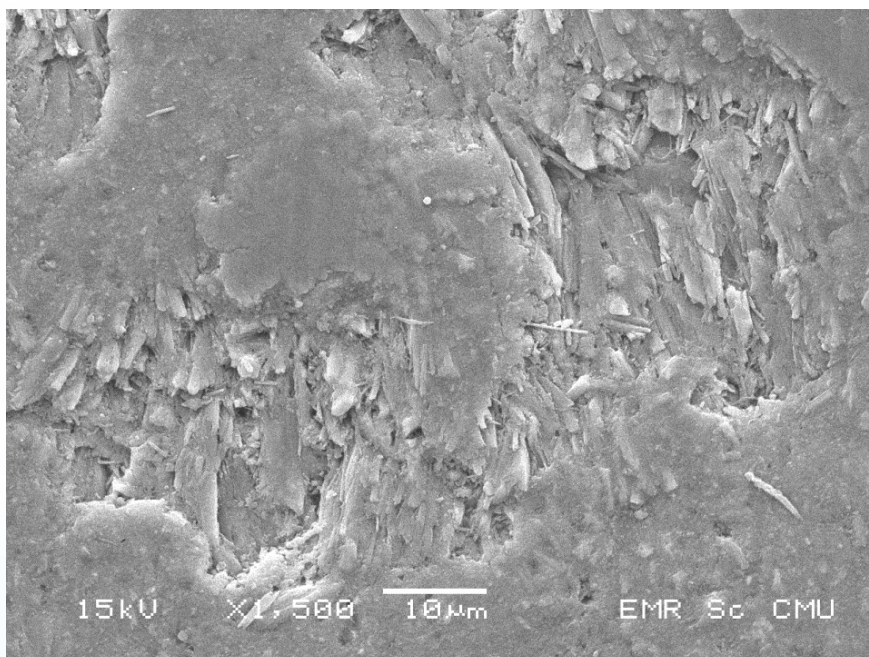


Figure 2: SEM-image showing fibrous crystals of a representative sample of blue pectolite.

Chemical and Mineral Composition

Three representative samples of blue pectolites were determined with Scanning Electron Microscope with Energy Dispersive X-ray analyzer (SEM EDX). The pectolite spectra have been shown peaks of Si, Ca, Na and Cu. The presence of small amounts of Cu^{2+} have been interpreted as cause of color of blue pectolite, substitute for calcium in the crystal structure.

Two representative samples of blue pectolites were tested by X-ray powder diffractometer for mineral composition. X-ray diffractograms show peaks of pectolite and calcite (Figure 3).

Conclusion

Most of mineralogical properties of nineteen samples of blue pectolites in this study are consistent with those previously reported for blue pectolite from the Dominican Republic. Radial, vesicular and amygdaloidal textures in petrographic observation is possibly indicated the secondary deposit in altered basalt.

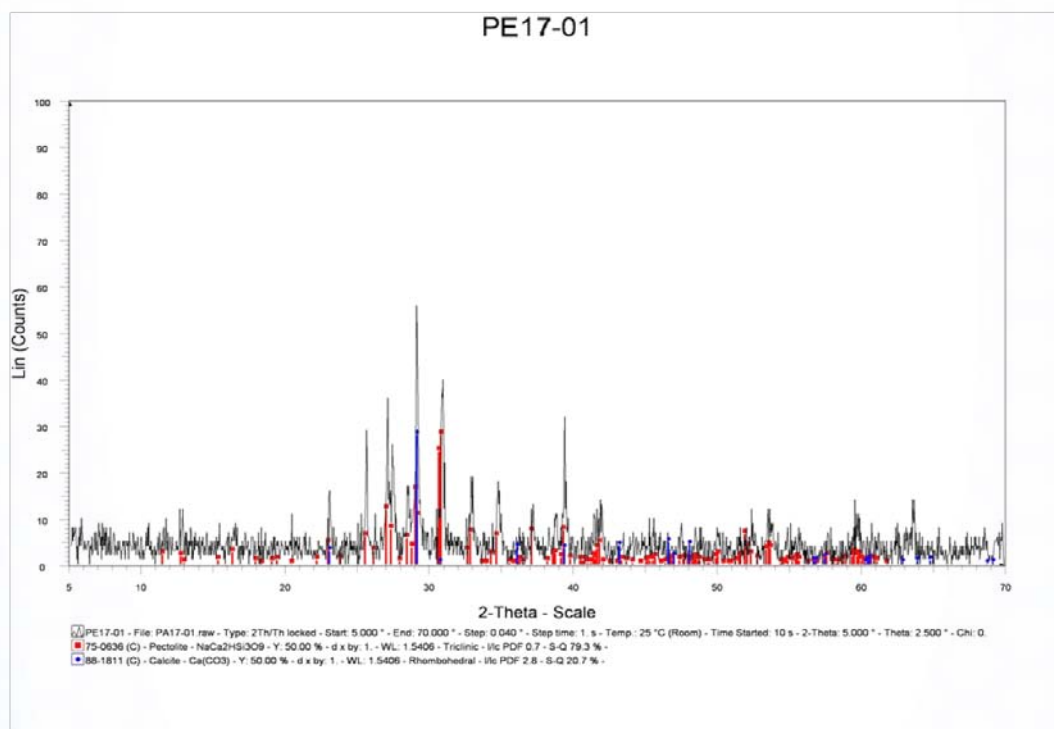


Figure 3: X-ray diffractogram of a representative sample of blue pectolite showing pectolite and calcite for mineral compositions.

References

- Arem, J.E., 1977, Color Encyclopedia of Gemstones, 1st ed., Van Nostrand Reinhold, New York, 139 p.
- Liddicoat, R.T. Jr., 1987, Handbook of Gem Identification, 12th ed., Gemological Institute of America, Santa Monica, CA, 364 p.
- Lizzadro, J., 1987, The interesting story of a new blue gem material called Larimar, Lizzadro Museum, Summer-Fall, p.13-14.
- Jaiboon, N., 2014, Mineralogy and Gemological Characteristic of Blue Pectolite Claimed to be from the Dominican Republic, Gemology Project, Department of Geological Sciences, Faculty of Science, Chiang Mai University, 27 p.
- Webster, R., 1983, Gems, Their sources, descriptions and identification, 4th ed., revised by B. W. Anderson, Butterworths, London, 1006 p.
- Woodruff, R. E., and Fritsch, E., 1989, Blue Pectolite from the Dominican Republic, Gems & Gemology, Vol.25, No.4, p.216-225.

Corresponding Author

Full name: Weerapan Srichan
Affiliation: Department of Geological Sciences, Faculty of Science, Chiang Mai University, Chiang Mai, 50200, Thailand.
Phone: +66-53-943417
Fax: +66-53-892261
Email: weerapan.s@cmu.ac.th

More on Photoluminescence of Emeralds

Elena Gambini, Emanuela Castaman, Antonello Donini, Andrea Marzola, and Giuliano Radice

INNOVHUB SSI - CISGEM Laboratory, Special Agency of the Chamber of Commerce of Milan, Italy

Extended Abstract

Introduction

For a gem testing laboratory, reliable instrumental data are of primary importance, as the identification of gemstones is based on careful observations and crossed comparison of the results obtained with different methods.

Among the tests carried out during the standard analyses, the CISGEM Laboratory has detected the photoluminescence of beryls from different geographical origins and genesis in order to collect more information about the importance of photoluminescence in coloured stones testing.

The additional data provided by photoluminescence to gemmological analyses represent a further step towards the determination of the geological environment/geographical origin of gemstones.

Samples and Methods

More than 70 samples of emeralds from Afghanistan, Brazil, Colombia, Nigeria, Madagascar, Pakistan, Russia and Zambia have been analysed by standard gem testing procedures as well as by photoluminescence. In addition, emerald samples from the Vigizzo Valley in Italy were tested. The Italian samples have no commercial interest, but are useful examples of geological environment origin.

Methods and instruments include, among others, visual comparison of samples with Munsell Color Charts under Standard Light Sources, Color Name Charts, EDXRF Quant'X, UV-Vis-NIR Zeiss McS 505, Raman System Renishaw 1000 (laser 633 nm). The photoluminescence spectra were collected on oriented samples.



Figure 1: A selection of the samples from Afghanistan.



Figure 2: Some of the emeralds and other beryls from Colombia.



Figure 3: Zambian emeralds and other beryls.

For each origin, different hues and saturations were chosen, in order to get the major number of possible variations

Results

The hue of the stones ranges from yellowish green to bluish green and the saturation from pale to deep (see Table 1).

EDXRF analyses on the samples allowed to put into evidence the variations of the colouring agents of the emeralds, even within the same geographical provenance.

In the same way the photoluminescence puts into evidence differences related to the relative abundance of the colouring agents (see maximum values of the band between 713-745 nm).

Table 1: Summary of the results obtained from the samples

Samples	Geographical origin	Geological environment	Hue and Saturation range based on Munsell Units	EDXRF	Photoluminescence band
G3373 to G3389	Afghanistan - Panjshir Valley	Contact zone schists/pegmatite dykes	green pale to strong	Cr ox: low to medium V ox: low to v. high Fe ox: v. low to low	727 to 742 nm
G3515 to G3516	Brazil - Minas Gerais - Itabira	Schists	bluish green very light to moderate	Cr ox: low to medium V ox: v. low to low Fe ox: v. low to low	726 to 730 nm
G3509 to G3510	Brazil - Bahia - Carnaiba/Socoto area	Contact zone granite pegmatites/serpentinites	green light	Cr ox: v. low V ox: v. low Fe ox: low	727 to 730 nm
G3521 to G3523	Brazil - Campo Verdes / Santa Terezinha de Goias	Schists	green moderate to strong	Cr ox: medium V ox: low Fe ox: high to v. high	738 to 739 nm
G1608 to G3404 to G3422	Colombia - Cordillera Oriental	Hydrothermal evaporitic veins in black shales	green to bluish green light to strong	Cr ox: v. low to med V ox: v. low to high Fe ox: v. low to low	725 to 735 nm
G3425 to G3432	Madagascar - Mananjary	Schists-amphibolites related to granitic pegmatite	green light to strong	Cr ox: low to medium V ox: low to high Fe ox: low to medium	731 to 742 nm
G3576 to G3587	Nigeria - Kaduna	Related to pegmatites/albitites	bluish green pale to light	Cr ox: low to medium V ox: low to medium Fe ox: v. low to medium	713 nm
G3448-9 to G3613-4	Pakistan - Swat Valley	Schists	green to bluish green strong	Cr ox: high V ox: medium Fe ox: medium to high	739 to 745 nm
G3601	Russia - Ural Mountains	Contact zone granite pegmatite/schists	green light	Cr ox: v. low to low V ox: medium Fe ox: medium to high	726 to 732 nm
G3390 to G3403	Zambia - Ndola District - Miku - Kafubu	Contact zone pegmatite/schists	green to bluish green light to strong	Cr ox: v. low to low V ox: v. low to low Fe ox: medium to high	723 to 745 nm
G0930 Vig01 to Vig03	Italy - Vigizzo Valley	Contact zone pegmatites (albitites)/ultramafic basement	green light	Cr ox: low V ox: v. low to low Fe ox: medium to high	732 to 734 nm

Note to Table 1 - EDXRF analyses: the indication very low to very high refers to the values obtained from semiquantitative analyses

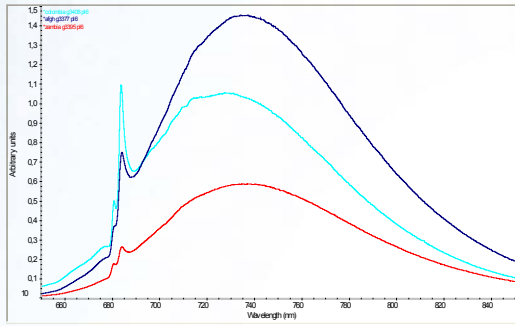


Figure 4: Photoluminescence spectra of three emeralds from different geographical origins. Dark blue: Afghanistan; light blue: Colombia; red: Zambia

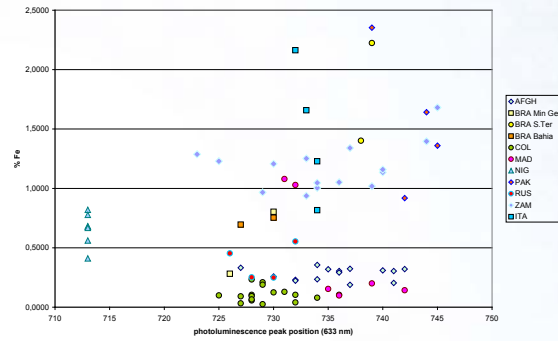


Figure 5: Correlation between the position of the broad photoluminescence band with the iron content (EDXRF).

Conclusions

As a follow up of already published studies (Bersani *et al.*, 2014; Huong, *et al.*, 2013 and Moroz *et al.*, 2000), the aim of this poster is to add more observations on the photoluminescence of emeralds, in order to give additional contribution to the distinction of their geographical origin.

Our investigation was focused on the band between 713 and 745 nm, in addition to the doublet at 680-684 nm, already studied by other Authors.

According to our first results, it seems that there is a relation between the band position and the geographical origin, in spite of the variability among the spectra obtained from samples of the same origin, but having different hues and saturations. We intend to carry out further tests in order to confirm if this criterion is applicable on a larger scale.

Acknowledgements

The Authors wish to express their gratitude to Margherita Superchi for her scientific advices, her careful inspection throughout this work and for providing the emerald samples from the Vigizzo Valley.

References

- Åström, M., and Scarani, A., 2013, Characterizing emerald types by chromium photoluminescence, Available from <http://www.gemmoraman.com/Articles/Emerald.aspx>.
- Bersani, D., Azzi, G., Lambruschi, E., Barone, G., Mazzoleni, P., Raneri, S., Longobardo, U., and Lottici, P.P., 2014, Characterization of emeralds by micro-Raman spectroscopy, *Journal of Raman Spectroscopy*, on line edition, John Wiley & Sons Ltd.
- Huong, L.T.-T., Haeger, T., Hofmeister, W., Karampelas, S., and Trung-Kien, N.D., in 2013, New features to identify natural and synthetic emerald by vibrational spectroscopy, *Proceedings of 33rd International Gemmological Conference*, Hanoi, Vietnam, 12-16 October 2013, p.82-83.

Kuehn, J.W., 2014, Raman and photoluminescence in mineral identification, 11th International GeoRaman Conference, St. Louis, Missouri, USA, June 15-19, 2014.

Mairani, M., 1985, Smeraldi in Val Vigizzo, Airone, aprile 1985, Giorgio Mondadori, p.96-103.

Moroz, I., Roth, M., Boudeulle, M., and Panczer, G., 2000, Raman microspectroscopy and fluorescence of emeralds from various deposits, Journal of Raman Spectroscopy, Vol.31, No.6, p.485–490.

Corresponding Author

Full name: Elena Gambini

Affiliation: INNOVHUB SSI- CISGEM Laboratory

Special Agency of the Chamber of Commerce of Milan, Italy

CISGEM Laboratory Viale Achille Papa, 30 20149 Milano – Italy.

Phone: +39 02 8515 5325 Fax: +39 02 8515 5258

Email: elena.gambini@mi.camcom.it

Natural and Heated Blue Sapphire from Nigeria

**Thanong Leelawatanasuk¹, Jirapit Jakkawanvibul¹, Marisa Maneekrajangsaeng¹,
ThanapongLhuaamporn¹, Wilawan Atichat¹, and Boontawee Sriprasert^{1,2}**

¹The Gem and Jewelry Institute of Thailand (Public Organization), Bangkok, 10500, Thailand

²Department of Mineral Resources, Bangkok, 10400, Thailand

Extended Abstract

Introduction

Blue sapphires from Nigeria was reported commercially since 1980. But in the last decade the production was very low, and sapphire from this deposit become less important in the market. However, since earlier this year, a large number of blue sapphire claimed to be from a new source in Nigeria has been flooded into Thailand gemstone market. This new deposit is located in Mambilla Plateau nearby the border of Cameroon, in the eastern Nigeria (Pardieu *et al.*, 2014).

Material and Methods

Two sets of rough blue sapphire (14 unheated stones ranging in weight from 0.33 ct. to 1.98 ct. and 21 heated stones ranging in weight from 0.13 ct. to 3.78 ct.) claimed to be from new mines in Mambilla area, Nigeria were used in this study. The unheated stones vary in their colors from light greenish blue to light blue. On the other hand, stones undergone traditional heat treatment show color ranging from medium blue and deep blue. All stones show corroded surface and some pieces still retain their original hexagonal crystal shape. (Figure 1).



Figure 1: Parcel of rough stones from Nigeria, including 14 unheated blue sapphires (**left**) and 21 sapphires undergone traditional heat treatment (**right**). (Photo by T. Sripoonjan)

Gemological properties were determined using standard gemological equipment such as the refractometer, polariscope, longwave (LW) and shortwave (SW) UV lamps and hydrostatic balance, at the GIT-Gem Testing Laboratory. Advanced instrumental analyses were carried out using the Raman spectroscope (Renishaw InVia), UV-Visible-NIR Spectrometer (Perkin 950), FTIR spectrophotometer (Thermo-Nicolet 6700) and EDXRF (EDAX Eagle III).

Basic Gemological Properties

The basic gemological testing of all unheated and heated stones gave refractive indices (RI) of 1.76-1.77 and specific gravity (SG) values between 3.97-3.99. Based on the basic physical properties, the stones can be identified as corundum (var. blue sapphire).

Unheated stones are inert under both LWUV and SWUV lights (only one sample is weakly red fluorescent under LWUV). However, heated stones are inert to weakly red fluorescent under LWUV, and inert to weakly or moderately chalky blue fluorescent under SWUV.

Microscopic Features

Under a microscope, the unheated sapphires showed brownish growth bands of minute particles (Figure 2a), dark brown opaque crystal (Figure 2b) and tube-like inclusions oriented in three directions (Figure 2c).

Some heated samples showed angular growth zones of minute particles (Figure 2d), melted crystals with discoid (Figure 2e) and ferrocolumbite crystals with induced fingerprints with (Figure 2f) indicating the stones had undergone heat treatment.

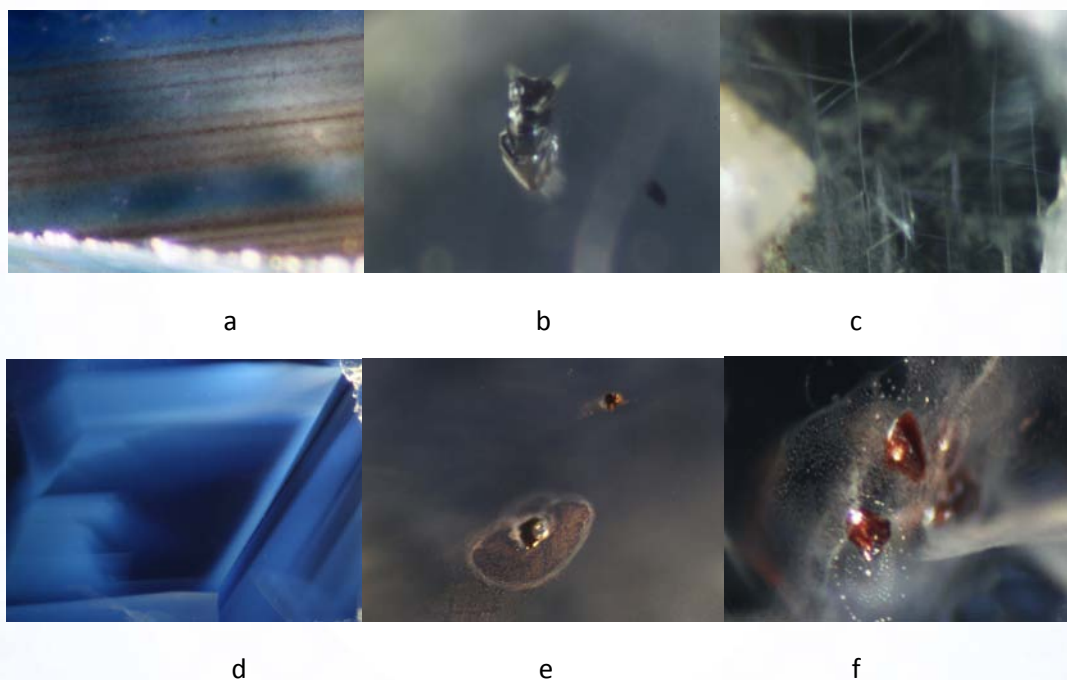


Figure 2: Microscopic images of inclusions in blue sapphires from Nigeria. (Photos by Jakkawanvibul and Maneekrajangsaeng).

Advanced Instrumental Analysis

The Raman Spectroscopy analysis has confirmed that the brown crystals in Figure 2f are ferrocolumbite (Figure 3).

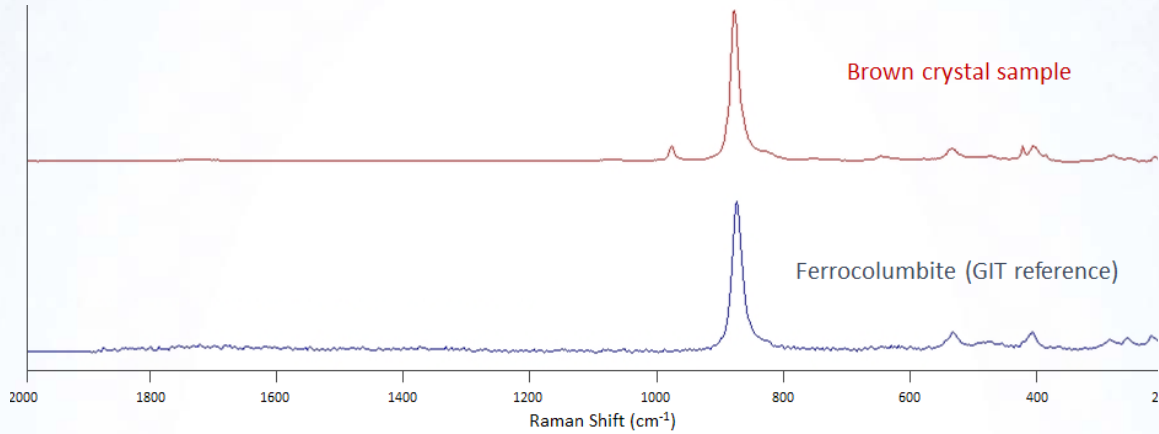


Figure 3: Raman spectrum of a brown crystal inclusion shown in Figure 2f perfectly matched with the spectrum of ferrocolumbite from the GIT reference database.

Semi-quantitative EDXRF analyses revealed that both groups of blue sapphire (35 samples) contained trace constituents that seem to vary in narrow ranges (0.2-0.6% Fe₂O₃, 0.001-0.2% TiO₂, 0.02-0.05% Ga₂O₃, 0.001-0.02% V₂O₅ and low 0.001-0.07% Cr₂O₃).

The UV-Vis-NIR spectra of unheated stones showed absorption peaks related to Fe³⁺ at 336/378/388 and 450 nm as well as a broad absorption band at around 900 nm due to Fe²⁺/Fe³⁺ intervalent charge transfer (IVCT) mechanism (Pisutha-Arnond *et al.*, 2010) (see Figure 4). In contrast, the spectra of heated deep blue sapphires not only showed absorption peaks and bands resembled those found in the unheated stones, but also displayed the distinct 585 nm absorption band (due to Fe²⁺/Ti⁴⁺ IVCT) and the stronger 900 nm band that are responsible for the deeper blue coloration (Sakkaravej, 2004).

Mid-IR spectra of unheated samples revealed series of sharp hydroxyl related peaks from 3100-3500 cm⁻¹ (Volynets, 1969) whereas heated samples usually showed peaks at 3309 and 3232 cm⁻¹ (Figure 5).

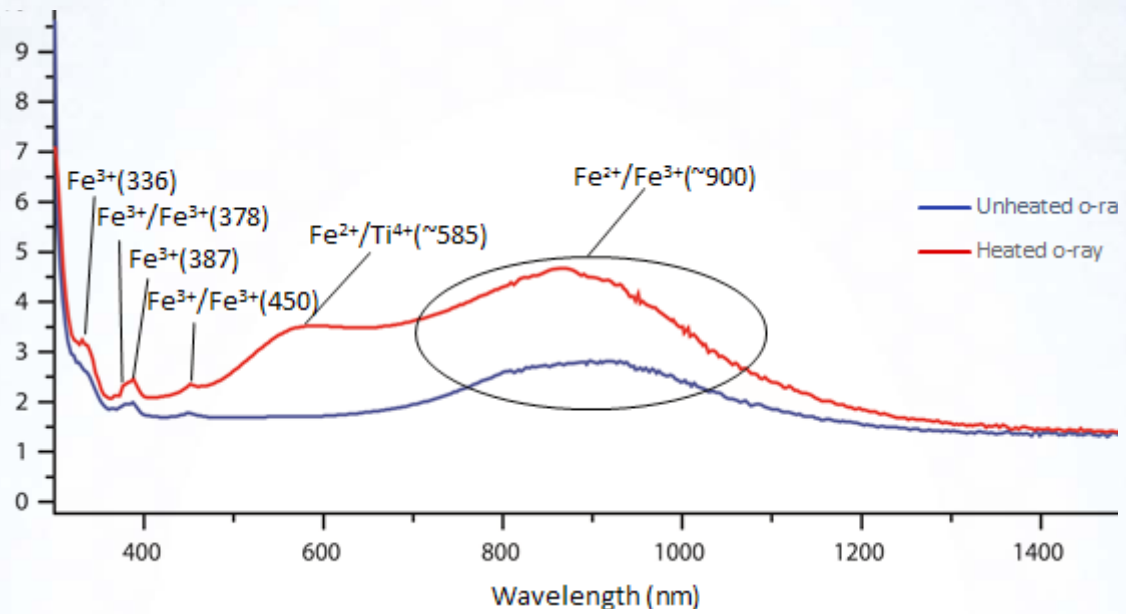


Figure 4: The representative UV-Vis-NIR spectra of unheated blue sapphire and heated blue sapphire from Nigeria.

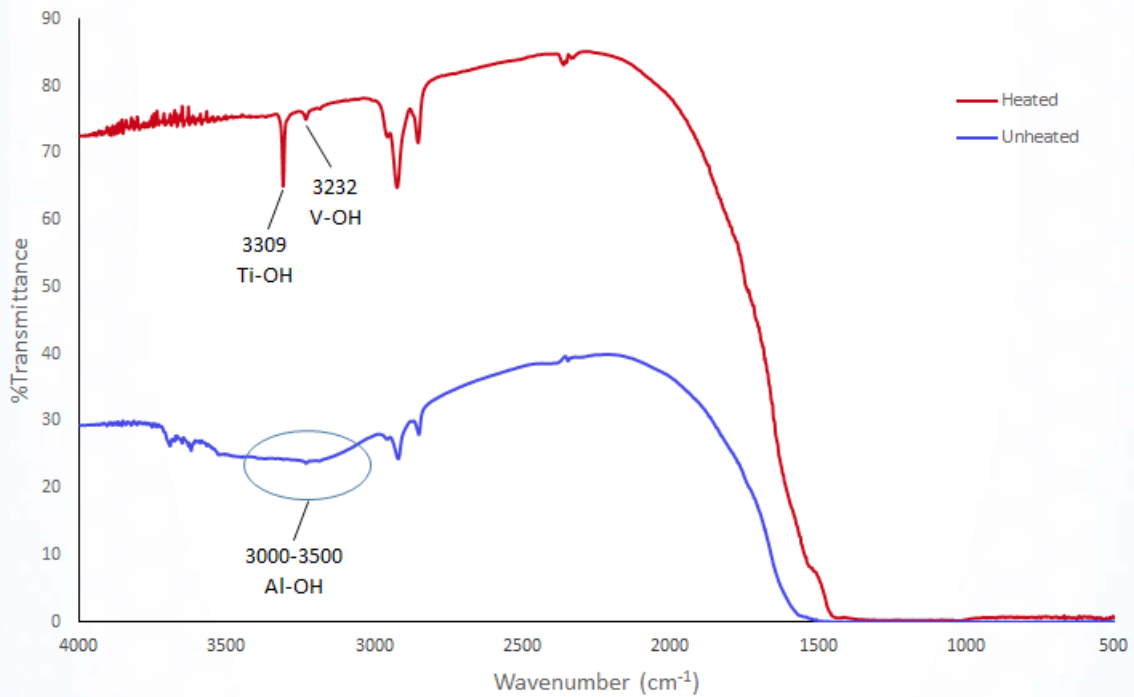


Figure 5: The represent Mid-IR spectra of unheated and heated blue sapphire from Nigeria.

Discussion and Conclusion

Our study of sapphires from Mambila, Nigeria revealed many typical characteristics of magmatic-related type origin similar to those found in other localities such as Australia, Thailand, Cambodia, South Vietnam and Cameroon. However, their iron contents are relatively lower than those found in other basaltic type deposits (GIT database, 2010). Dark brown opaque crystal inclusions are also present.

Because Nigeria and Cameroon are situated in the same geological setting (Wright, 1970; Wright *et al.*, 1985), the Nigerian blue sapphire and the Cameroon blue sapphire from previous study (Leelawatansuk *et al.*, 2012), do share many similar characteristics such as the type of inclusions as well as spectroscopic features.

Acknowledgements

The authors deeply appreciate many sapphire dealers, namely World Sapphire, Elegant Gems and Amorn Gems, for samples donated for this study. Special thank is also given to Mr. Tasnara Sripoonjan, a gemologist of GIT-GTL, for photography and data collection.

References

- Leelawatansuk, T., Atichat, W., Sriprasert, B., Pisutha-Arnond, V., Wathanakul, P., Sutthirat, C. and Sripoonjan, T., 2012, Some Characteristics of Blue Sapphire from Cameroon, The 3th International Gem and Jewelry Conference (GIT2012), p.127-130.
- Pardieu, V., Sangsawong, S., Muyal, J., and Sturman, N., 2014, Blue sapphires from the Mambilla Plateau, Taraba State, Nigeria, GIA News from Research, August 16, 47 p. Available from http://www.giathai.net/pdf/Nigeria_Mambilla_Sapphire_20140816_TH.pdf
- Pisutha-Arnond, V., Wathanakul, P., Sutthirat, C., Boonchai, A., and Somboon, C., 2010, Role of Trace Elements in Causing Color in Corundum, The Gem and Jewelry Institute of Thailand, p.122-128.
- Sakkaravej, S., 2004, Thermal enhancement of some blue sapphires from Madagascar. Master's thesis, Chulalongkorn University, Bangkok, Thailand.
- Volynets, F.K., Vorobev, V.G., and Sidorova, E.A., 1969, Infrared Absorption Bands in Corundum Crystals, Journal of Applied Spectroscopy, Vol. 10, No.6, p.665-667.
- Wright, J.B., 1970, High pressure phases in Nigerian Cenozoic lavas distribution and geotectonic setting, Bulletin of Volcanology, Vol.34, No.4, p.833-847.
- Wright, J.B., Hasting, D.A., Jones, W.B. and William, H.R., 1985, Geology and Mineral Resources of West Africa, George Allen & Unwin Publisher, UK, 197 p.

Corresponding Author

Full name : Jirapit Jakkawanvibul
Affiliation : The Gem and Jewelry Institute of Thailand (Public Organization), Bangkok, 10500, Thailand.
Phone: +66 2634 4999 Fax: +66 2634 4970

New Opal from Ethiopia

Lore Kiefert¹, Pierre Hardy¹ and Tewodros Siantayehu²

¹Gubelin Gem Lab, Maihofstrasse 102, 6006 Luzern, Switzerland

²Ethiopia

Extended Abstract

Opal has first been found in Ethiopia in the early 1990's. These opals from Mezezo in the Amhara-Province consist of nodules of brown sandstone on the outside with orange, reddish-brown or "chocolate-brown" precious opal inside of these nodules. The next big discovery was then in 2008, when white precious opal was found in the Welo province, about 550 km north of Addis Ababa (Mazzero *et al.*, 2009). To date, this deposit produces large amounts of white precious opal.

It was only in 2013 when yet another opal deposit in the Welo province was found (Figure 1), producing not only white but also black opal (Figure 2). The deposit is set in distinct opal-bearing layers in a mountainous area approximately 700 km northeast of Addis Ababa and 100 km away from Lalileba by road. Caves are dug into the mountain slope by the local villagers to reach the opal. Pieces up to approximately 10 cm were retrieved from this deposit (Figure 3).

The opals are usually very dark in colour (Figure 2), reminiscent of dyed or smoke treated opal. However, the surface does not show any staining in surface pits or fissures (Figure 4), as observed in smoked treated opal shown by Williams (2011) or Milisenda and Henn (2012). The stones also displayed an even dark colour all the way through the samples, unlike the sugar-acid treated opal as described by Fritsch *et al.*, (2011), where the darker colour is confined to a more or less thick surface layer.

FTIR spectrometry did not give conclusive results, due to the relative opaque character of our samples. Raman spectra gave very strong carbon peaks. These carbon peaks alone do not allow a safe distinction between natural-colour or treated black opal from Wollo. However, careful microscopic observation should reveal the natural character of this new deposit.

Acknowledgements

The authors thank Mr. Bill Marcue from D.W. Enterprises for financing this trip, as well as the Ministry of Mines of Ethiopia and the people from Welo for their help and hospitality.

References

- Fritsch, E., Mazzero, F., and Gauthier, J.-P., 2011, Sugar-acid treatment of opal from Wollo, Ethiopia, Gem News, Gems & Gemology, Vol. 47, No.4, p.333-334.
- Mazzero, F., Gauthier, J.-P., Rondeau, B., Fritsch, E., and Bekele, E., 2009, Nouveau gisement d'opales d'éthiopie dans la Province du Welo: Premières informations, Revue de Gemmologie a.f.g., Vol.167, p.4-5.

Milisenda, C., and Henn, U., 2012, Einige Besonderheiten der Opale aus Äthiopien, Some peculiarities of opals from Ethiopia, *Gemmologie: Zeitschrift der Deutschen Gemmologischen Gesellschaft*, Vol.61, No.1-2, p.43-54.

Williams, B., and Williams, C., 2011, Smoke treatment in Wollo opal, Available from www.stonegrouplabs.com/Smole-TreatmentWolloOpal.pdf



Figure 1: Local miners working the new opal deposit in the Welo Province, Ethiopia.
Photo: Tewodros Siantayehu.



Figure 2: Rough and faceted black opal from the Welo Province, Ethiopia. The large polished piece in the foreground weighs 90 ct. Photo: Lore Kiefert.



Figure 3: A rough piece of Ethiopian black opal, measuring approximately 10 cm.
Photo: Tewodros Siantayehu.

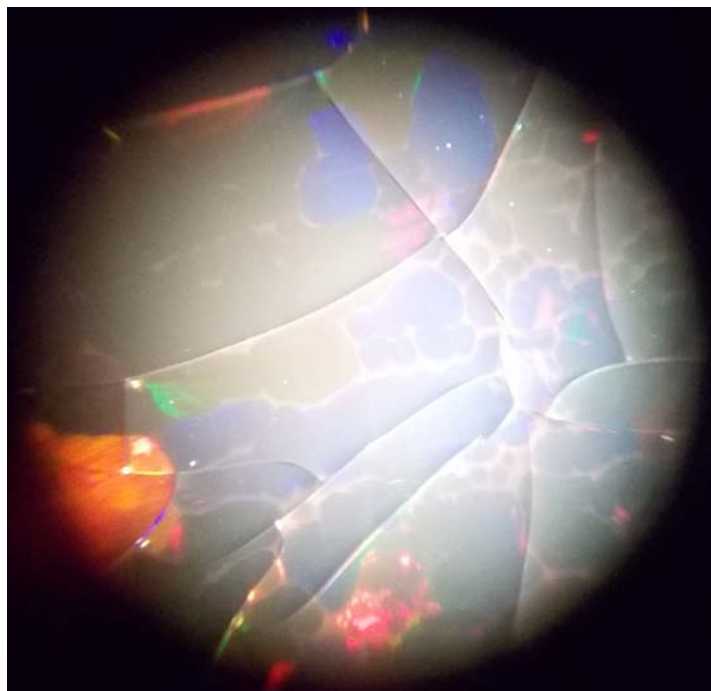


Figure 4: Microscopic image of an Ethiopian black opal. The stone shows some crazing, which is typical for some of this material, but no black staining is observed. 30x. Photo: Lore Kiefert.

Corresponding Author

Full name: Lore Kiefert
Affiliation: Gubelin Gem Lab, Maihofstrasse 102, 6006 Luzern, Switzerland.
Email: lore.kiefert@gubelingemlab.com

Non-Destructive Differentiation of African and Asian Ivory by FT- Raman Spectroscopy and Chemometric methods

Ursula Wehrmeister¹, Tatjana M. Gluhak¹, Hermann Götz², Laura M. Otter¹, and Dorrit E. Jacob³

¹Department of Geosciences and Earth System Science Research Centre, Johannes Gutenberg-Universität, D-55128, Mainz, Germany

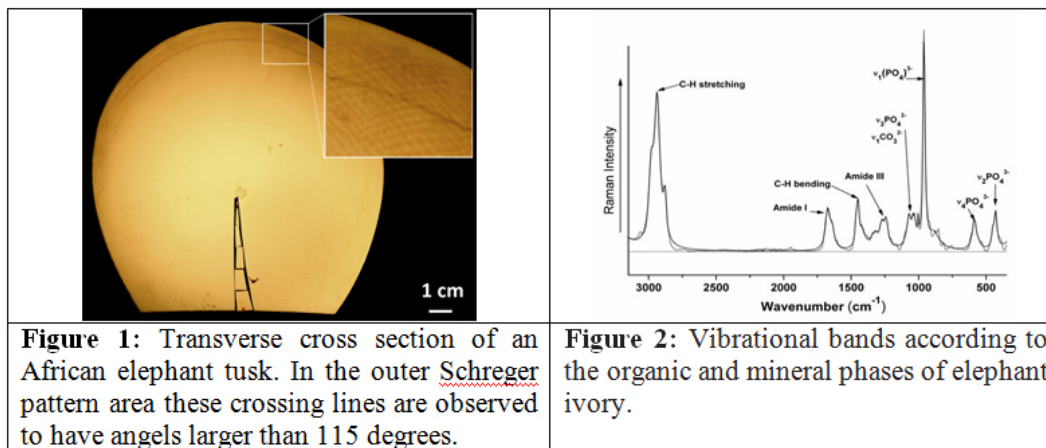
²Institute of Applied Structure and Microanalysis, Department of Medicine, Johannes Gutenberg-Universität, D-55128, Mainz, Germany

³Department of Earth and Planetary Sciences, Macquarie University, North Ryde, NSW 2109, Sydney, Australia

Extended Abstract

Ivory trade is a politically highly sensitive matter and a considerable proportion of the trade is illegal resulting in ivory to be found in different markets around Asia and Africa, but also in the US and Europe. Because of illegal ivory trade elephant populations declined in massive numbers in the 1970s and 1980s before the international trade was banned by CITES in 1989, when also the African elephant was uplisted from Appendix II (“managed commercial trade”) to Appendix I (“no commercial trade”) joining the Asian elephant already listed there. In 1997 Botswana, Namibia, Zimbabwe and later South Africa (in 2000) received limited trade rights for controlled sales of ivory stockpiles and their elephant populations were “downlisted”. Many scientists oppose these stockpiles sales, because they suspect further increase of poaching (Wasser *et al.*, 2010), which seems to be supported by the latest news in the media.

From the viewpoint of forensic science a non-destructive determination of the various ivories is very important in order to detect illegally imported ivory samples. The term ivory comprises teeth and tusks of different animals, which are of any commercial interest and large enough to be processed (Espinoza and Mann, 1991). Elephant dentine is relatively soft and strongly favoured by artists for its carvability. The desire for elephant ivory has been one of the major factors in the reduction of the world’s elephant population. The family of elephants (*Elephantidae*) within the order Proboscidea contains two genera: *Loxodonta* – the African and *Elephas* – the Asian elephant, including three different species.



Visually, ivories can be differentiated by observing the Schreger lines (Espinoza and Mann, 1991; Figure 1), which are natural growth features characteristic for elephant ivory. However, most samples are carved, and for these samples this method is often not applicable. Various Raman spectroscopic investigations provide rapid and non-destructive methods that do not require sample preparation. However, the organic materials intrinsic to ivory often cause fluorescence, which dominates the characteristic Raman signals. Reducing fluorescence is therefore of great importance for successful Raman analysis of ivory. The aim of the present study is to improve and develop further non-destructive analysis of ivories by use of FT-Raman spectroscopy and chemometric methods.

Materials and Experimental Methods

Analyses were carried out on 16 samples of *Elephas maximus* from different provenances in Asia as well as 22 ivory samples of *Loxodonta africana* from different African localities and one sample of *Loxodonta cyclotis* from DR Congo. FT-Raman spectra were collected with a NXR FT-Raman Module for FT-IR spectrometers (Nicolet 5700, Thermo Scientific) at the Medical Faculty, Johannes Gutenberg-University, Mainz. A near-infrared Nd:YAG laser operating at 1064 nm, a liquid nitrogen-cooled germanium detector (NXR Genie, Thermo Scientific) with a near-constant noise level over a very wide frequency range and a CaF₂ beam splitter were used. Spectra were recorded with a laser power of 0.5- 1.0 W in order to avoid damage to the material. In order to improve S/N ratio 256 spectra were collected at a resolution of 4 cm⁻¹ with Happ-Genzel apodization from (250-3700) cm⁻¹. For each sample 3 to 5 FT-Raman spectra were acquired at different locations. A MicroStage FT-Raman Microscope focuses the Laser Beam to a spot size of 50µm. To obtain the best comparability, all spectra were normalized to the highest Raman peak at 960 cm⁻¹. For each sample group, master spectra were calculated from all data points of Raman spectra. In order to collate the results we followed the essential studies of Edwards *et al.*, (2006) and Brody *et al.* (2001) with only minor changes in dividing the spectra into different wavenumber areas (labelled with letters – see also Table 1).

Vibrational Assignment of The Ft Raman Spectra of Elephant Ivory

Master spectra of five different sample groups are discussed according to both the different wavenumber regions and the mineral and organic components. A general view of an ivory FT-Raman spectrum is given in Figure 2 and shows the main vibrational bands according to the organic and mineral phases. Main diagnostic differences between African and Asian ivory are reported at 1721 cm⁻¹ and 1504 cm⁻¹ (areas B, C) for African, as well as at 720 cm⁻¹ and 453 cm⁻¹ (areas J, K) for Asian ivory (Edwards *et al.*, 1997; Carter and Edwards, 2001). However, we show here, based on our much larger data base, that differences of Raman band positions of inorganic and organic modes are neither diagnostic nor statistically significant for both Asian and African ivory. The areas under the bands within the different wavenumber areas (A-K) (Table 1), as well as the maximum height of peaks in every one of these are calculated and collated. Box- and Whisker-plots of the peak area and their intensity-values are shown in Figures 3 and 4. In general, the intensity values show less overlap than the corresponding peak area-values. Differences are

mainly found in bands assigned to organic components of dentine, showing higher protein content of African than of Asian ivory- previously established by other authors (e.g. Edwards *et al.*, 1998). Otherwise African ivory has lower intensities of the band at 1071 cm⁻¹ (area E- assigned to carbonate and phosphate) than Asian ivory- this contradicts earlier findings of Edwards *et al.*, (1998).

Table 1: The mean wavenumbers (cm⁻¹) and standard deviations (cm⁻¹) at the position of maximum peak heights in the spectral areas (A-K) for African and Asian ivory. The peak position is averaged from 78 and 110 spectra of Asian and African ivory, respectively.

Wavenumber-region	Vibrational assignment	African ivory		Asian ivory	
		wavenumber (cm ⁻¹)	SD	wavenumber (cm ⁻¹)	SD
A	v(CH ₂), v(CH ₃)	2939.0	0.9	2938.6	1.2
B	v(C=O), δ(NH) amide I	1668.8	1.5	1669.3	2.5
C	δ(NH), δ(CH ₂)	1450.2	0.4	1450.1	0.6
D	δ(NH) amide III	1244.2	1.0	1244.2	1.8
E	v ₃ (PO ₄ ³⁻), v ₁ (CO ₃ ²⁻), proline	1069.5	6.5	1071.0	0.8
F	v(CC), aromatic ring, phenylalaline	1002.8	0.2	1002.7	0.3
G	v ₁ (PO ₄ ³⁻)	960.9	0.2	960.8	0.3
H	v(CC), proline, hydroxyproline	853.9	0.8	853.7	0.9
I	v(COC), v(CC)	814.3	0.7	814.0	1.2
J	v ₄ (CO ₃ ²⁻)	588.7	3.4	589.7	1.2
K	v ₄ (PO ₄ ³⁻)	429.7	0.4	430.0	0.4

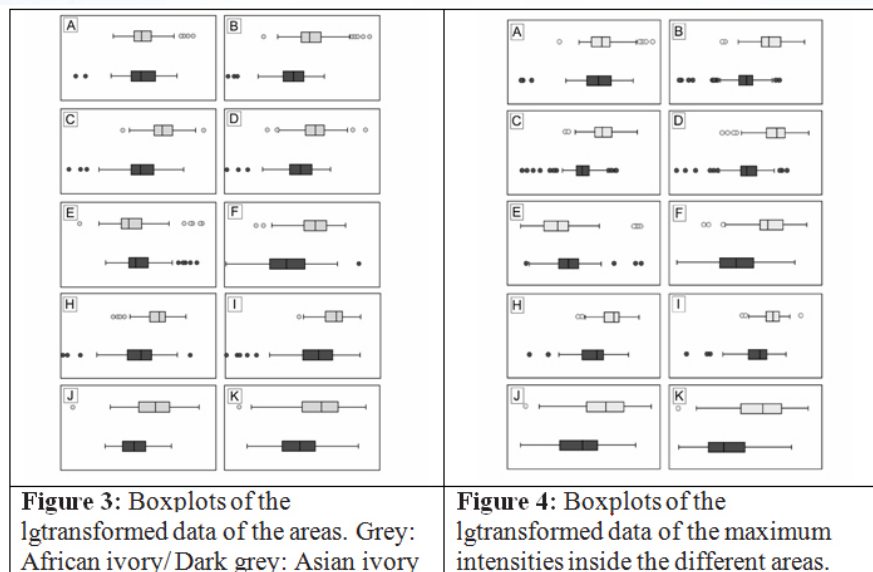
Statistical Data Evaluation

Hierarchical cluster (CA)-, principal component (PCA)-, and discriminant analyses (DA) are applied to the peak area-data as well as to the intensity-data to test if and, if yes, which one of the approaches achieves an adequate separation into African and Asian ivory. Furthermore, four samples of identical origin were treated as being of “unknown provenance” to test the statistical models. Outliers and extreme values are deleted from the statistical evaluation. Normal distribution was checked by the Kolmogorov-Smirnov-test.

The CA (average linkage, city block distance) shows that clustering based on the intensity-values affiliates 86.2% of all samples correctly to their respective group; the application of the area-values resulted in 81.9% correct grouping. However, both approaches came to concordant results for the test-group of unassigned origin: The CA of the intensity-as well as the area-values resulted in an affiliation to the Asian ivory group.

Neither the PCA of the area-, nor of the intensity-values results in a clear separation of African from Asian samples. Furthermore, including our test samples of “unknown provenance” into the PCAs shows that, although they plot in a field dominated by the Asian ivory samples, it is not possible to affiliate them unequivocally to either Africa or Asia.

The Discriminant Analysis (stepwise method) showed that, when based on the intensity-values, higher percentages of correct classifications were achieved in cross validation than based on the area-values (88.2% in comparison to 84.6%). Anyway, DA based on the intensity-values failed to affiliate the “unknown provenance” test samples correctly, whereas DA based on the area-values assigned them correctly to the Asian ivory-group, which is in accordance with the results from the CA. As results of DA have to be interpreted with caution, we recommend calculating a CA and PCA as first steps, then to study the general data structure, in order to be able to judge the classification by DA with the results of CA and PCA in the background.



The statistical evaluation shows that preference can be given neither to area- nor to intensity-values in deciding on the provenance of elephant ivory. We recommend always including both values into the statistical evaluation.

References

- Brody, R.H., Edwards, H.G.M., and Pollard, A.M., 2001, Chemometrics Methods Applied to the Differentiation of FT-Raman Spectra of Ivories, *Analytica Chimica Acta*, Vol.427, No.2, p.223-232.
- Edwards, H.G.M., Hassan, N. F. Nik, and Arya, N., 2006, Evaluation of Raman spectroscopy and application of chemometric methods for the differentiation of contemporary ivory specimens I: elephant and mammalian species, *Journal of Raman Spectroscopy*, Vol.37, No.1-3, p.353-360.
- Edwards, H.G.M., Howell, G.M., Farwell, D.W., Dennis, W., Holder, J.M., and Jacci, M., 1998, Fourier transform-Raman spectroscopy of ivory: a non-destructive diagnostic technique, *Studies in conservation*, Vol.43, No.1, p.9-16.
- Espinoza, E.O., and Mann, M.J., 1992, *Identification Guide for Ivory and Ivory Substitutes*, WWF Publications, Baltimore, USA, 2nd eds.
- Wasser, S. , Poole, J., Lee, P., Lindsay, K., Dobson, A., Hart, J., Douglas-Hamilton, I., Wittemyer, G., Granli, P., Morgan, B., Gunn, J., Alberts, S., Beyers, R., Chiyo, P., Croze, H., Estes, R., Go bush, K., Joram, P., Kikoti, A., Kingdon, J., King, L., Macdonald, D., Moss, C., Mu tayoba, B., Njumbi, S., Omondi, P., and Nowak, K., 2010, *Elephants, Ivory, and Trade*, *Science*, Vol.327, No.5971, p.1331-1332.

Corresponding Author

Full name: Ursula Wehrmeister
 Affiliation: Department of Geosciences and Earth System Science Research Centre, Johannes Gutenberg-Universität, D-55128, Mainz, Germany.
 Phone: +49 6131 3923170
 Email: wehrmeis@uni-mainz.de

Peculiar Natural Type II Diamonds Showing Pseudo-Synthetic Characteristics

Hiroshi Kitawaki, Mio Hisanaga, Masahiro Yamamoto, and Kentaro Emori

Central gem laboratory, Tokyo, Japan

Extended Abstract

Identification of CVD-grown or HPHT-grown synthetic diamonds requires advanced laboratory techniques using such as photoluminescence spectroscopy or DiamondView in addition to the standard gemological tests. In this report we introduce examples of natural type II diamonds that show pseudo-synthetic features superficially resembling synthetic stones in such advanced analyses.

1. All the colorless to nearly colorless CVD-grown synthetic diamonds of fifty-four samples in total that had been submitted to our laboratory since 2012 showed a Si-V peak at 737 nm (736.4/736.8 nm) in photoluminescence spectra. On the other hand, nine samples of natural type II diamond that had been analyzed around the same time showed the Si-V luminescence peak. This was accompanied by many other peaks including the one at 714 nm, and together with the existence of included minerals this indicates natural origin of the stones.
2. Distinct sector zoning that shows greenish blue color luminesce and phosphorescence has been observed by DiamondView™ in two type II diamonds, which were submitted by different clients independently. This is generally a characteristic feature seen in HPHT synthetic diamonds, but cloud inclusions observed under magnification revealed that these samples were natural diamonds containing CO₂ that gives rise to characteristic peaks in FTIR analysis

Background

An international diamond grading laboratory in Antwerp reported a large lot of CVD synthetic diamonds were found in gem market in 2012 and this caused a sensation in the diamond industry (Even-Zohar, 2012). Since then, the CVD synthetic diamonds were continuously reported from laboratories in India and China (Song *et al.*, 2012), and we also made a report on the CVD synthetic diamond over 1 carat which was submitted without disclosure to our laboratory (Kitawaki *et al.*, 2013). For HPHT synthetic diamonds, new suppliers of colorless diamonds such as Advanced Optical Technology Co. have been appearing (D'Haenens-Johansson *et al.*, 2014). In the jewelry industry, precise disclosure of information on synthetic diamonds as well as the establishment of definite identification techniques is strongly desired.

Samples and Analyses

The samples reported in this paper are made up of nine natural diamonds displaying the Si-V peak at 737 nm in the photoluminescence analysis (Min: 0.123 ct ~ Max: 5.018 ct, Ave. 0.743 ct) and two natural diamonds (0.376 ct and 1.117 ct) showing the features that are resemble to HPHT synthetic stones under the observation with DiamondView. Fifty-four colorless to near colorless CVD synthetic diamonds and about three hundred colorless to pale blue HPHT synthetic diamonds that had been tested around the same time were used for comparison.

JASCO FT/IR 4200 was used for infrared spectral analysis with 7000-400 cm^{-1} range, 4.0 cm^{-1} resolution and 20 accumulated scans. Renishaw Raman system- model 1000 equipped with Renishaw inVia Raman Microscope was used for photoluminescence (PL) analysis with the stones being immersed in liquid nitrogen, with the laser exciting sources at each wavelength of 633 nm, 514 nm, 488 nm and 325 nm. For observation of UV luminescence images, DTC DiamondView was used. Also gold coating was applied to the samples for SEM-CL observation by Topcon scanning electron microscope SM-350.

Results and Discussions

1. Natural type II diamonds showing Si-V luminescence peak in photoluminescence analysis

The luminescence peak at 737 nm (736.4/736.8 nm doublet) observed in photoluminescence analysis is supposed to originate in the CVD synthesizing apparatus such as a silica window and it seems difficult to avoid the contamination in the current commercial manufacturing process (Eaton-Magaña, and D'Haenens-Johansson, 2012). All the fifty-four CVD synthetic diamonds in total that had been analyzed at CGL showed the 737 nm peak and currently this becomes the positive indication of CVD synthetic origin.

On the other hand, the 737 nm peak is also reported in some natural diamonds (Breeding and Wang, 2008) and we have also confirmed the peak in nine pieces of natural type II diamond in these two years. As Breeding and Wang, 2008 report, the natural diamonds that show 737 nm peak are often accompanied by a series of peaks such as 714.7, 651.1, 649.4, 593.3, 573.5, 557.9, 554.3, 550.4 and 524.4nm that are not seen in CVD synthetic diamonds. These peaks are presumably related to Si but the details have not been understood so far. All the nine samples we confirmed also showed these additional peaks and they provide a good indication of natural origin.

The 737 nm peaks in photoluminescence analysis show almost constant intensity throughout the CVD synthetic diamonds regardless the measurement spot. This is supposedly because they accept little environmental change during the growth in the commercial synthesis of the stones. Contrary to this, natural diamonds show variations in the peak intensity according to the measurement spot. Among the nine natural diamonds that showed the 737 nm peak, five were SI or lower clarity and four were VS clarity or over. The lower clarity stones contained crystal inclusions, which were confirmed to be olivine by Raman spectra. However, there was no correlation between the olivine crystal inclusion and the intensity of the 737 nm peak, and the detail of the growth environment that forms Si-V effect has yet been unknown.

2. Natural type II diamond showing sector zoning in the observation by Diamond-View™

The analysis of UV luminescence images using the DiamondView is extremely important to determine natural/synthetic origin of diamonds. Natural diamonds typically show octahedral crystal habit consists of {111}, while HPHT synthetic diamonds, which require metal solvents for the synthesis, often show assemblage of {111} and {100}, sometimes accompanied by {110} or {113}. In natural type II diamonds, mosaic pattern of dislocation network caused by plastic deformation is observed. Figure 1 shows UV luminescence images of two diamonds, 0.376 ct and 1.117 ct, by

DiamondView. Blue luminescence color with slight greenish tint and phosphorescence of similar color were observed in the both stones. These two stones also showed distinct sector zoning, which made them similar to HPHT synthetic diamonds. In addition, both of them contained clouds composed of minute white inclusions. In the SEM-CL images, the area with darker contrast showed linear growth stripes, which presumably corresponds to the growth area on the smooth interface {111}. Another area with less dark contrast shows zigzag structure, which supposedly corresponds to the growth area of rough interface {100}.

In infrared spectra, absorptions related to CO₂ were recognized at 3754, 3625, 2376 and 653 cm⁻¹. The CO₂ peak in an infrared spectrum of natural diamond was reported in 1993 and at that time it was assumedly derived from the solid inclusion of CO₂ that had been generated under high pressure (Schrauder and Navon, 1993) but recently some suppose that CO₂ has been bonded in crystal lattice (Hainschwang *et al.*, 2008). Several absorptions are also observed in the nitrogen region between 1000~1500 cm⁻¹ but none of them corresponds to the A or B center of nitrogen impurities. Therefore, these diamonds are type II, and those absorptions between 1000~1500 cm⁻¹ are presumably originate in minute carbonate inclusions. The two diamonds that display the DiamondView images appearing almost like sector zoning of HPHT synthetic diamond are considered to be Mixed-habit growth stones, in which {111} and {100}, that have been generated due to the crystal growth under high supersaturation of such as CO₂, coexist.

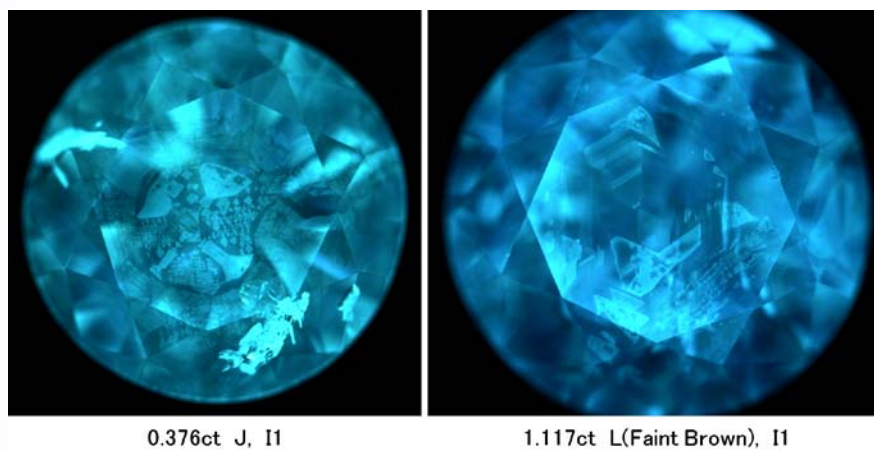


Figure 1: Natural type II diamonds displaying UV luminescence images similar to HPHT synthetic diamond.

Acknowledgements

We extend our thanks to Dr. Hisao Kanda of Tsukuba Expo Center who helped us observe SEM-CL images.

References

- Breeding, C.M., and Wang, W., 2008, Occurrence of the Si-V defect in natural colorless gem diamonds, *Diamond and Related Materials*, Vol.17, No.7-10, p.1335-1344.
- D'Haenens-Johansson, U.F.S., Moe, K.S., Johnson, P., Wong, S.Y., Lu, R., and Wang, W., 2014, Near colorless HPHT synthetic diamonds from AOTC group, *Gems & Gemology*, Vol.50, No.1, p.30-45.
- Eaton-Magaña, S., and D'Haenens-Johansson, U.F.S., 2012, Recent Advances in CVD synthetic diamond quality, *Gems & Gemology*, Vol.48, No.2, p.124-127.
- Even-Zohar, C., 2012, Synthetic specifically "made to defraud", *Diamond Intelligence Briefs*, Vol.27, No.709, p.7281-7290.
- Hainschwang, T., Notari, F., Fritsch, E., Massi, L., Rondeau, B., Breeding, C.M, and Vollstaedt H., 2008, HPHT treatment of CO₂-related brown diamonds, *Diamond and Related Materials*, Vol.17, No.3, p.340-351.
- Kitawaki, H., Yamamoto, M., Hisanaga, M., Okano, M., and Emori, K., 2013, Undisclosed sample of large CVD synthetic diamond., *Gems & Gemology*, Vol.49, No.1, p.60-61.
- Schrauder, M., and Navon, O., 1993, Solid carbon dioxide in a natural diamond, *Nature*, Vol.365, No.6441, p.42-44.
- Song, Z., Lu, T., Lan, Y., Shen, M., Ke, J., Liu, J, and Zhang, Y., 2012, The identification features of undisclosed loose and mounted CVD synthetic diamonds which have appeared recently in the NGTC laboratory, *Journal of Gemmology*, Vol.33, No.1-4, p.45-48.

Corresponding Author

Full name: Hiroshi Kitawaki
Affiliation: Central gem laboratory, Tokyo, Japan
Phone: +81-35817-4664
Fax: +81-35817-4665
Email: kitawaki@cgl.co.jp

Raman and Photoluminescence Spectroscopy in Gem Identification

J. Wolfgang Kuehn

Gemlab Research & Technology, c/o Canadian Institute of Gemmology, P.O. Box 57010, Vancouver, B.C., V5K 5G6, Canada

Extended Abstract

Raman spectroscopy is particularly useful for rapid identification of gemstones. Searchable data-bases such as in the RRUFF project (www.rruff.info) contain a large number of reference spectra and are in public domain; the data-bases can be modified and expanded to the user's requirements.

Raman Applications

Figure 1 demonstrates the quick identification of Zektzerite which is an extremely rare mineral; there are few gem quality specimen known and they could easily be mistaken for other gem materials.

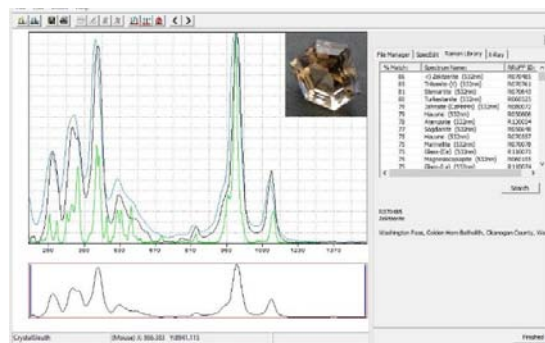


Figure 1: Zektzerite confirmed with RRUFF database

Gemmologists often have difficulty to identify gemstones set in finished jewellery. A Raman spectrometer can quickly separate gems with overlapping refractive indices. The measurement of refractive index (RI) with a gemmological refractometer requires a flat polished surface; if the RI of a gemstone is above the limit other time consuming gem testing tools and methods have to be used. The quick separation of diamond from its most popular imitations such as Cubic Zirconia and moissanite is illustrated in Figure 2.

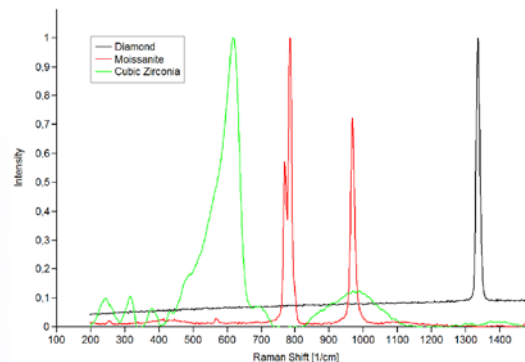


Figure 2: Separation of diamond from simulants.

Garnet varieties cover the full colour spectrum and due to their similarity are difficult to identify; Raman based spectral measurements can give a precise and relatively inexpensive solution for these problems (Serov *et al.*, 2012). The detection of treatments in gemstones is often challenging; for example in Figure 3 the use of extended Raman spectroscopy can detect polymer treatment in jadeite.

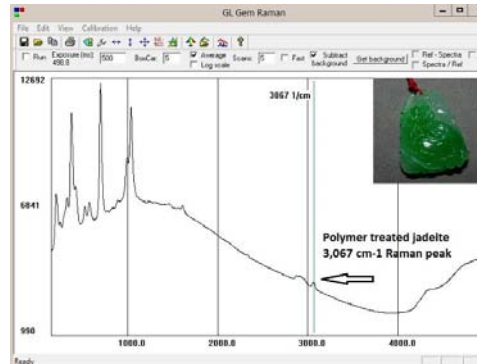


Figure 3: Raman spectrum of polymer treated jadeite

Fluorescence Problems

As seen in Figure 4 the strongly fluorescent flux grown sapphire crystal (Chatham) shows a dramatic signal improvement in Raman mode after insertion of a band pass dielectric filter (GL Gem Raman Band Pass Filter- GLBPF); these filters are not in-expensive and have to be specified for each application.

Combined with the TEC option exposure time was increased to 5,000 ms and the sample could be matched with an entry in the RRUFF database.

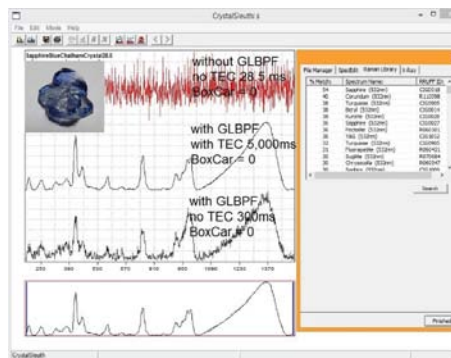


Figure 4: Suppression of fluorescence with GLBPF

Photoluminescence (PL)

In some cases luminescence features are so intense that one can no longer see the Raman peaks associated with the atomic vibrations of the mineral. Luminescence spectroscopy is used to measure the energy levels of luminescence centers (Jasinevicious, 2009). PL Applications

PL Applications

The GL Gem Raman PL532 TEC is a dual purpose Raman spectrometer with an adjustable 532 nm laser source (200 mW) and is suitable for PL studies in the range from 530 – 750 nm. After reducing the laser output to approximately 30% of full power photoluminescence patterns become visible. In Figure 5 a synthetic red flux grown spinel is quickly separated from natural red spinel; to arrive at the same conclusion the use of a microscope and other gem testing tools would have been necessary.

In a similar manner emerald types (whether natural or synthetic, also geological provenance) can be determined by observing chromium PL peak locations.

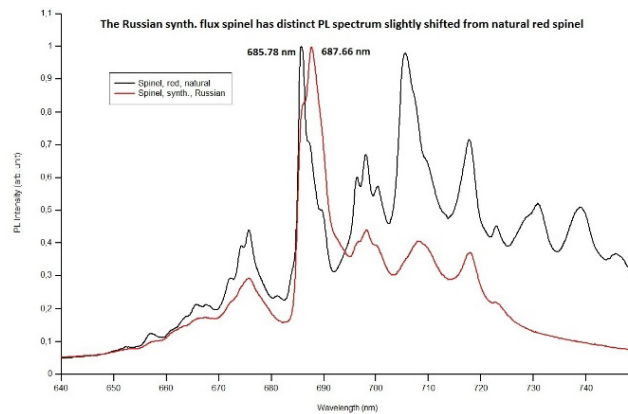


Figure 5: Separation of syn. and natural red spinel (685 nm)

Current Challenges

Synthetic materials, treatments, imitations and fakes are problems facing not only dealers, buyers and collectors but the entire jewellery industry. With the advent of small synthetic diamonds mixed in parcels with natural diamonds scientists are urgently working on methods and instrumentation to properly identify synthetic and treated diamonds.

One area of great interest are photoluminescence studies for diamond type screening and detecting HPHT treatments (Dobrinets *et al.*, 2013). However, this method should be supported with other instrumentation and not be used alone.

Figure 6 illustrates a synthetic HPHT treated diamond with a nitrogen-vacancy defect at 637 nm; it also shows the suppression of the 558, 566 and 576 nm bands which usually indicate an untreated diamond if the 637 nm peak is missing as well. Strong silicon-vacancy peak at about 737 nm may indicate CVD (chemical vapor deposition) grown synthetic diamond. Crystallographic defects causing the above mentioned PL peaks for natural untreated diamonds are not fully understood.

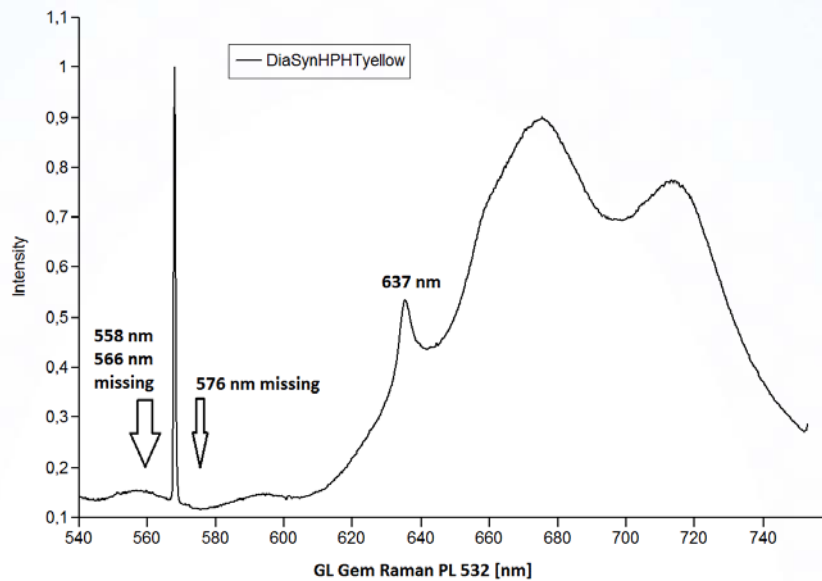


Figure 6: Synthetic HPHT treated diamond

Conclusion

Several economically priced Raman spectrometer systems are now available and allow for rapid identification of gems and minerals. In general polished surfaces of gemstones produce good Raman scattering with high percentage matches in the RRUFF data-bases. For rough surfaces spectrometers with thermo-electric cooling (TEC) allow for low signal detection at exposure times of 1,000 ms and higher.

For the detection of synthetic diamonds and HPHT (high pressure high temperature) treatments the PL option of the Raman spectrometer is of particular value. With experience it may even provide a semi-quantitative estimate of trace elements such as chromium. The analysis of Gr1 and SiV centers in CVD-grown yellow diamonds and the comparison with existing published data indicate that other impurities like Xe, Ni or Cr may produce other colours as well; more research is required (Zaitsev et al., 2014).

Acknowledgements

Raman and PL spectra were obtained with a GL Gem Raman PL532 TEC ($175\text{-}5,470\text{ cm}^{-1}$) system from Gemlab Research & Technology; spectra were edited in Spekwin32 (Menges, 2012). Sample gemstones courtesy Canadian Institute of Gemmology.

References

- Dobrinets, I.A., Vins, V.G., and Zaitsev, A.M., 2013, HPHT-treated Diamonds, Springer 2013 ed., 257 p.
- Jasinevicious, R., 2009, Characterization of vibrational and electronic features in the Raman spectra of gemstones (MS thesis, unpublished), 147 p.
- Menges, F., 2012, Spekwin32 - optical spectroscopy software, Version 1.71.6.1, 2012, Available

from <http://www.efemm2.de/spekwin> RRUFF Project at www.rruff.info

Serov, R., Shelementiev, Y., and Mashkina, A., 2012, Identification of the Garnet Chemical Composition and Color Causes by Express Raman and Visible Spectroscopy, GIT2012 Proceedings, p.214-216.

Zaitsev, A.M., Deljanin, B., Peretti, A., Alessandri, M., and Bieri, W., 2014, New Generation of Synthetic Diamonds Reaches the Market Part C: Origin of Yellow Color in CVD-grown Diamonds and Treatment Experiments, Contributions to Gemology (March Issue), No.14, p.41-55.

Corresponding Author

Full name: J. Wolfgang Kuehn

Affiliation: Gemlab Research & Technology, c/o Canadian Institute of Gemmology, P.O. Box 57010, Vancouver, B.C., V5K 5G6, Canada.

Phone: +16045308569

Email: gemlab@cigem.ca

Raman Spectroscopic Identification of Geographical Origins of Sapphires

Siwon Lee,¹Jinyoung Hwang,²Daun Sul,² and Hoeil Chung²

¹Department of Material Sciences and Engineering, Hanyang University, Seoul, 133-791, Korea

²Department of Chemistry, Hanyang University, Seoul, 133-791, Korea

Extended Abstract

Sapphire, one of most popular gemstones, is basically aluminum oxide (Al_2O_3) incorporating trace amounts of metals such as Fe^{2+} , Fe^{3+} , Ti^{4+} , Cr^{3+} and V^{3+} (Kim *et al.*, 2006). As generally known, Al_2O_3 has several structural phases such as water-free, $\alpha\text{-Al}_2\text{O}_3$ and $\alpha\text{-Al}_2\text{O}_3$ (Zaw *et al.*, 2014). Various colors of sapphires originate from the change in band gap between conduction and valence band depends on incorporated metals. Due to the recent increase in the global trade of gemstones, the demand for rapid and non-destructive identification of geographical origin has been increased to ensure the fair evaluation and distribution of products. For this purpose, Raman spectroscopy could be a potential method since it provides sensitive spectral information pertinent to lattice structure of gemstones and measurement is intrinsically non-destructive, that is one of most critically concerning issues in analysis of gemstones.

Here, we have attempted to differentiate sapphires from 6 different origins (Laos, Rwanda, Congo, Mozambique, Madagascar and Australia) using Raman spectroscopy. Since sapphires are usually inhomogeneous in structure and/or composition, it is critically necessary to acquire representative spectra of a whole sapphire rather than localized area for a reliable spectroscopic evaluation of the shown sapphires. To acquire representative Raman spectra, a wide area illumination (WAI) scheme (Kim *et al.*, 2006) capable of covering a large sample area (28.3 mm^2 , laser illumination diameter: 6 mm) was used. A sapphire was simply positioned at the focal point of laser (wavelength: 785 nm) illumination for spectral collection. Each Raman spectrum (resolution: 4 cm^{-1}) was acquired by an accumulation of 10 scans with 25 seconds exposure at each scan.

Figure 1 shows the pictures of selected samples from each origin and the corresponding baseline-corrected Raman spectra. As shown, the differentiation of the samples only by color could be difficult; therefore, Raman spectra providing structural and compositional information is helpful. Raman spectral features of the samples from 6 different geographical origins are generally similar with each other, while minor spectral differences in peak shape and intensity among them are observed.

To simply compare the spectral features of samples together, principal component analysis (PCA) was performed using the spectra in the 1000-300 cm^{-1} range and the resulting scores were examined. Figure 2 shows the scatter plot constructed by the first and second scores. The first and second factors described 79.29% and 8.45% of total spectral variation present in the dataset. As known, the first factor recognizes the most significant spectral features and the following factors describe relatively detail spectral variations. As shown, the score groups of each geographical origin are identifiable with some degree of overlapping. The result demonstrates that the structure and/or composition of sapphires are obviously different from the origin to origin. The overall result suggests that Raman spectroscopic identification of geographical origins of sapphire is feasible.

In future, the more detail structural and compositional analysis of the samples using other analytical methods such as XPS and UV/Vis spectroscopy will be accomplished to provide supplementary information for the identification. Further, to impose statistical significance on the identification of geographical origins, more diverse samples will be included. Finally, sapphire samples will be classified according to their origins using support vector machine (SVM) and the resulting accuracy will be evaluated. SVM is a popular and powerful supervised classifier, which finds the best hyper-plane to classify samples by maximizing the distance between class boundaries.

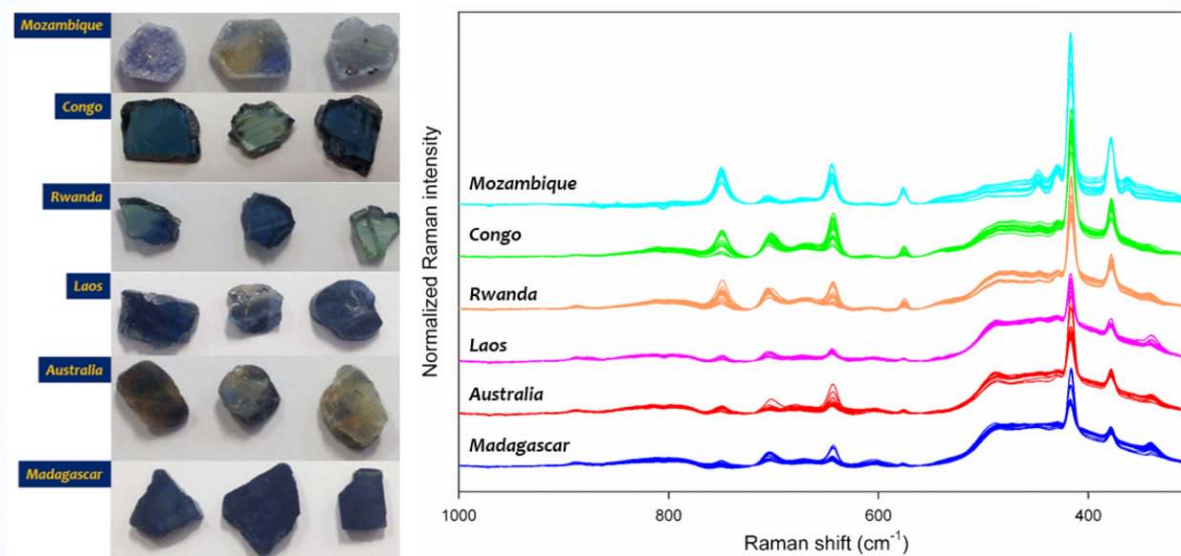


Figure 1: The pictures of selected samples from each origin and the corresponding baseline-corrected Raman spectra.

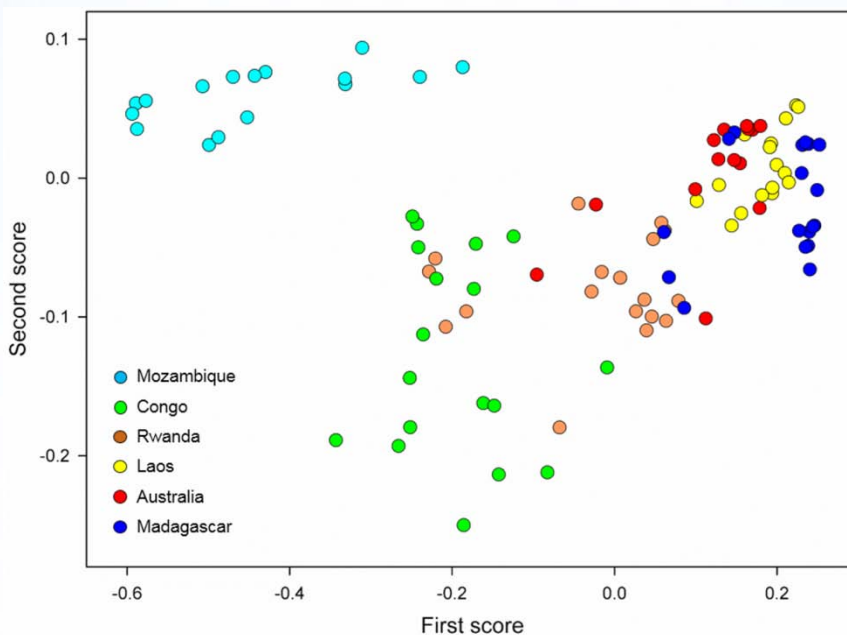


Figure 2: The scatter plot constructed by the first and second scores. The first and second factors described 79.29% and 8.45% of total spectral variation present in the dataset.

References

- Kim, M., Chung, H., Woo, Y., and Kemper, M., 2006, New reliable Raman collection system using the wide area illumination (WAI) scheme combined with the synchronous intensity correction standard for the analysis of pharmaceutical tablets, *Analytica Chimica Acta*, 2006, Vol.579, No.2, p.209-216.
- Zaw, K., Sutherland, L., Yui, T., Meffre, S., and Thu, K., 2014, Vanadium-rich ruby and sapphire within Mogok Gemfield, Myanmar: implications for gem color and genesis, *Mineralium Deposita*, 2014, Ahead of print, 15 p.

Corresponding Author

Full name: Hoeil Chung
 Affiliation: Department of Chemistry, College of Natural Sciences, Hanyang University, 17 Haengdang-dong, Seongdong-gu, Seoul, 133-791, Korea.
 Phone: +82-2-2220-0937
 Email: hoeil@hanyang.ac.kr

Rubies, Sapphires and Quartzes with Double Stars

Karl Schmetzer¹, Martin P. Steinbach², Hans A. Gilg³ and A.R. Blake⁴

¹Petershausen, Germany

²Idar-Oberstein, Germany

³Technische Universität München, Munich, Germany

⁴Chevy Chase, MD, USA

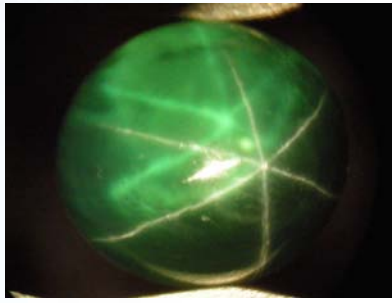
Extended Abstract

Asterism involving a single silvery white six-rayed star, due to the presence of three series of oriented needle-like inclusions, is frequently observed in natural and synthetic rubies and sapphires and in natural quartz cabochons. "Double" or multiple star patterns of several stars with identical whitish colour have also been seen in corundum and quartz and can be attributed to additional series of inclusions (in quartz) or twinning (in ruby and sapphire).

Corundum and quartz samples showing a further type of double star, consisting of two differently coloured six-rayed stars, have occasionally been noted or depicted as well. For example, upon examination of a Verneuil-grown synthetic ruby in reflected light, the cabochon showed the ordinary whitish six-rayed star and a second orange-red star which seemed to originate from the back of the sample (Schmetzer and Hainschwang, 2012). In a rose quartz sphere, an analogous double star pattern consisting of two differently coloured stars (white and pink) was observed in reflected light (Killingback, 2006). However, in absence of any comprehensive study of the mode of formation for this latter type of double star, the instant project was undertaken to elucidate the optical phenomenon.

Diffusion-treated synthetic rubies and sapphires

Synthetic corundum cabochons that had undergone diffusion treatment exhibited the three intersecting light bands of an ordinary silvery white six-rayed star such as is commonly seen in asteriated natural and synthetic rubies and sapphires. In addition, three intersecting light bands producing a second, variously coloured six-rayed star could be observed under fibre optic illumination (Figure 1a, 1b). The ordinary silvery white star was confined to the dome of the cabochons. In all samples, the second six-rayed star showed the body colour of the host corundum crystals, e.g. red, orange, yellow or green. This second body-coloured star seemed to emanate from the curved or almost flat base of the cabochons. After grinding and re-polishing the base of certain of these cabochons, all such samples showed only one remaining silvery white six-rayed star (Figure 2a). The second star having the body colour of the cabochon was no longer observed. Upon grinding and re-polishing the curved dome of others of these synthetic corundum cabochons, the samples so tested showed only the second six-rayed star with the body colour of the sapphire, but the ordinary silvery white star had disappeared (Figure 2b).

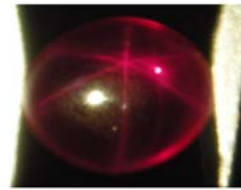
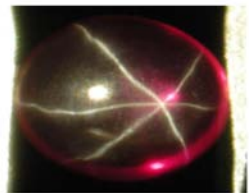
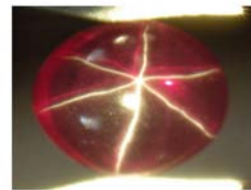
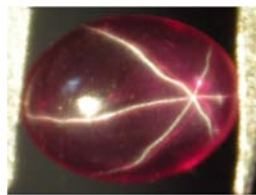


(a)



(b)

Figure 1: (a) (b) These two synthetic sapphires show a white six-rayed star and a second, body-coloured green or orange star. The green cabochon measures 15.6 x 14.1 mm and weighs 26.80 ct; the orange cabochon measures 10.0 x 8.0 mm and weighs 3.85 ct; photos by K. Schmetzer.



(2a)

(2b)

Figure 2a: (left) This diffusion-treated synthetic ruby shows a silvery white six-rayed star and a second red-purple star (**above**); after grinding and re-polishing the base of the cabochon and removing the diffusion-treated layer, the red-purple star is removed and only the remaining silvery white star is observed (**below**). The sample measures 8.1 x 6.3 mm and weighs 1.44 ct; photos by K. Schmetzer.

Figure 2b: (right) This diffusion-treated synthetic ruby shows a silvery white six-rayed star and a second red-purple star (**above**); after grinding and re-polishing the dome of the cabochon and removing the diffusion-treated layer, the silvery white star is removed and only the remaining red-purple star is observed (**below**). The sample measures 10.3 x 8.1 mm and weighs 3.51 ct; photos by K. Schmetzer.

Non-diffusion-treated natural and synthetic rubies and sapphires

A similar double star pattern was observed in a natural transparent purplish pink sapphire. The sample reportedly originated from Mogok, Myanmar. The gemstone showed two clearly separated six-rayed stars: one silvery white star reflected from the dome of the cabochon and one purplish pink star confined to the curved base of the sample (Figure 3).

Transparent synthetic sapphires produced by Linde in the early 1970s also showed a similar double star pattern. For most of these samples, neither the silvery white star confined to the dome nor the body-coloured second star confined to the base was removed or altered by the grinding and re-polishing process (Figure 4).

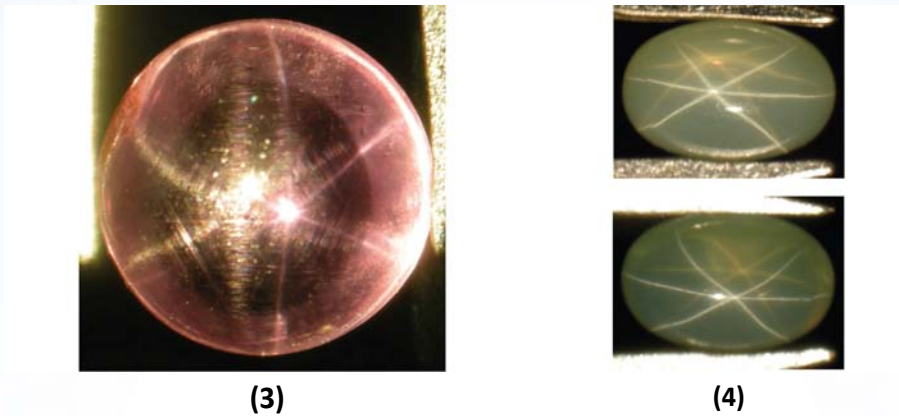


Figure 3: (left) This purplish pink sapphire from Myanmar shows a silvery white star reflected from the dome of the cabochon and a body-coloured star reflected from the curved base of the sample. The sample measures 7.0 mm in diameter and weighs 1.62 ct; photo by K. Schmetzer.

Figure 4: (right) This light yellowish green synthetic sapphire shows a silvery white six-rayed star and a second body-coloured star (**above**); after three grinding and re-polishing steps at the base of the cabochon, the body-coloured star is not removed and both stars are still observed (**below**). The sample measures 6.0 x 4.1 mm, with thickness 2.6 mm, and weighs 0.54 ct; photos by K. Schmetzer.

Diffusion treatment of ruby and sapphire

According to information from former employees of Union Carbide (Linde) and from the directors of Wiede's Carbidwerk, Freyung, Germany, diffusion treatment to create or improve asterism and to improve colour has been performed commercially for various types of corundum since the early 1970s, at least for part of the production.

Natural quartz and rose quartz

Quartzes from two sources revealed an analogous double star pattern. Specifically, examinations of two almost colourless, very slightly pink rose quartz cabochons from Brazil and two slightly brownish pink quartz cabochons from India were performed. These transparent asteriated quartzes showed, in addition to the normal white six-rayed star, a second star confined to the base of the cabochons (Figure 5).

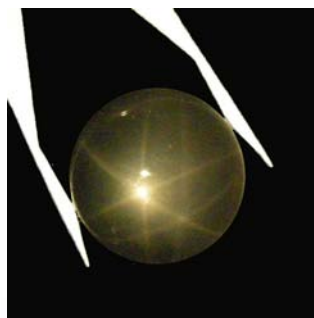


Figure 5: Very light rose quartz cabochon from Brazil showing double stars in reflected light. The cabochon measures 21.0 mm in diameter and weighs 26.18 ct; photo by K. Schmetzer.

Mode of star formation

Through comparison of commonalities between the different types of materials studied, it was determined that the following mechanism could be applied to explain the phenomenon in all groups of samples examined:

- a) The ordinary silvery white star is formed by reflection and scattering of light at a layer confined to the curved dome of the cabochons consisting of a matrix of corundum or quartz containing minute needle-like inclusions.
- b) The body-coloured second star is formed by reflection and scattering of light at a layer confined to the base of the cabochons consisting of a matrix of corundum or quartz containing minute needle-like inclusions.
- c) The light forming the second star travels twice through the body of the cabochons and is absorbed by trace elements or other features, e.g. lattice defects that are responsible for the body colour of the corundum or quartz crystals. Thus, the colour of the second star is identical to the body colour of the host.

In diffusion-treated corundum samples, it is possible to remove the silvery white or the body-coloured star by grinding and re-polishing the outermost (upper or lower) surface, thus removing the diffusion-treated layer.

References

- Killingback, H., 2006, Diasterism in rose quartz, *Gems & Jewellery*, Vol.15, No.3, p.64.
Schmetzer, K., and Hainschwang, T., 2012, Star ruby, *Gems & Jewellery*, Vol.20, No.4, p.14-17.

Corresponding Author

Full name: Karl Schmetzer
Affiliation: Petershausen, Germany.
Phone: +4981377770
Email: SchmetzerKarl@hotmail.com

Smoky Quartz from Hod, Chiang Mai, Northern Thailand

Phisit Limtrakun and Naphithiphorn Manoli

Gemology Program, Department of Geological Sciences, Faculty of Science, Chiang Mai University, 50200, Thailand

Extended Abstract

Introduction

Quartz is silicon dioxide, SiO₂, the second most common mineral in the crust of the earth. Although found in abundance in nearly all rock types, gem quartz nearly always comes from igneous rocks, principally pegmatites and cavities in volcanic rock, or from hydrothermal veins. Gemologists recognize two categories of quartz, coarsely crystalline and finely crystalline. The former varieties include amethyst, citrine, smoky quartz, and occur as relatively large, single crystals that can be faceted. The latter varieties, called chalcedony, are composed of intergrown aggregates of microcrystalline quartz crystals such as agate, onyx, carnelian, and are commonly translucent to opaque. In this study, smoky quartz samples from Hod, Chiang Mai, northern Thailand were investigated for their gemological characteristics and cause of coloration.

Methodology

A total of 16 quartz samples used in this study were collected from Hod, Chiang Mai, northern Thailand. The samples were classified as smoky quartz based on their color. The color of samples can be described with the GIA Gem Set. The basic gemological instruments were applied to determine gemological properties of the studied samples including specific gravity, refractive index, birefringence, ultraviolet fluorescence and inclusion features. UV-VIS-NIR spectroscopy (250-1500 nm) was performed to investigate cause of coloration. All samples were carried out using instruments at the Department of Geological Sciences, Faculty of Science, Chiang Mai University, Chiang Mai, Thailand.

Results

The gemological properties of smoky quartz samples are summarized as followed. The studied quartz samples are subhedral to euhedral crystals, exhibiting crystal forms of hexagonal prism, hexagonal dipyrramids and rhombohedral. The Dauphine twins are also observed in few samples (Figure 1). The smoky samples range from transparent to translucent, having grayish brown to yellowish brown in color. Their specific gravity is in the ranges of 2.57-2.65, and inert to both short and long wave UV radiation. Microscopic features contain fluid inclusions, hollow tubes, fingerprints, healed fracture and iron stains. UV-VIS-NIR absorption spectra of the representative samples were investigated the cause of coloration in smoky quartz. They show absorption broad bands in the range of 400-800 nm with intense bands at 450 nm, and this spectral range are attributed to color center.

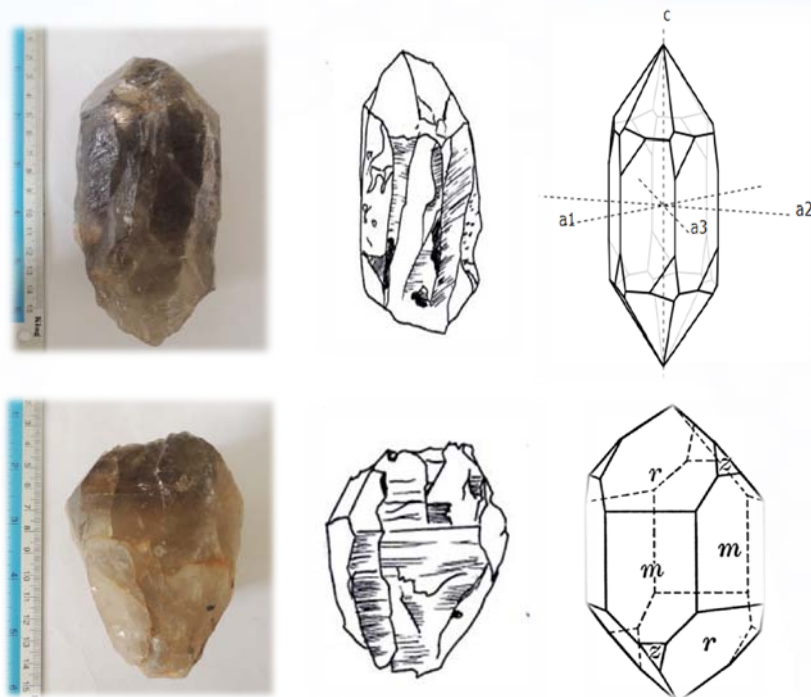


Figure 1: Crystal morphology of the studied smoky quartz.

Summary

The study presents information on the gemological properties and the cause of coloration in smoky quartz from Hod, Chiang Mai, northern Thailand. Crystal forms, color and transparency of the smoky quartz are common compared to other localities. The UV-VIS-NIR spectroscopy analyses indicate that cause of coloration due to color center.

Acknowledgements

This work was granted by the undergraduate senior project fund and the Igneous and Related Ore Deposits Research Laboratory (IROL), Department of Geological Sciences, Faculty of Science, Chiang Mai University, Thailand.

Reference

Deer, W.A., Howie, R.A. and Zussman, J., 1992, An Introduction to the Rock-Forming Minerals, 2nd edition, Longman Group Limited, London, 549 p.

Corresponding Author

Full name: Phisit Limtrakun
 Affiliation: Department of Geological Sciences, Faculty of Sciences, Chiang Mai University, 239 Huaykaew Road, Suthep, Chiang Mai, 50200, Thailand.
 Phone: +66-53-943417
 Fax: +66-53-943444
 Email: phisitlim@gmail.com

Spectroscopic Characterization of Zircon Inclusions in Gem Corundum from Mercaderes, Cauca, Colombia

Manuela Zeug¹, Lutz Nasdala¹, and Andrés Ignacio Rodríguez Vargas²

¹Institut für Mineralogie und Kristallographie, Universität Wien, Althanstr. 14, 1090 Wien, Austria

²Minerlab Limitada, Calle 51 Sur N° 80 i-34, Bogotá, D.C. Colombia

Abstract

Raman micro-spectroscopy is an excellent method for (i) the non-destructive estimation of the degree of radiation damage of zircon crystals confined within corundum of metamorphic origin, and (ii) the determination of pressures acting on such inclusions. Here we present preliminary results of an in-situ study of solid inclusions in alluvial gem corundum originating from Mercaderes, Cauca, Colombia. Among other inclusion minerals, we have analyzed several zircon inclusions whose sizes are in the range 10–90 μm .

The accumulation of self-irradiation damage by zircon leads to increasingly irregular bond lengths in the structure, which is observed from increased widths of vibrational bands (Nasdala *et al.*, 1995). Zircon inclusions in the Mercaderes corundum yielded Raman spectra with rather mild band broadening. The FWHMs (full width at half band maximum) of the $\nu_3(\text{SiO}_4)$ Raman band (assigned to the anti-symmetric stretching of SiO_4 tetrahedrons; Dawson *et al.* 1971) were found to vary between 1.7 ± 0.3 and 5.7 ± 0.5 cm^{-1} . These values correspond to very low to at most moderate degrees of self-irradiation damage (Nasdala *et al.*, 1995). This in turn is in accordance with the young age of about 10 Ma of the Mercaderes corundum reported by Sutherland *et al.*, (2008). Furthermore, the observation of broadened Raman bands of zircon was found to be predominantly due to radiation damage, whereas compressive stress does not cause significant band broadening (Nasdala *et al.*, 2008). Exposure of zircon to elevated temperatures causes structural annealing and hence narrowing of Raman bands, which was however not observed here. The Raman-band broadening detected for zircon included in the Mercaderes corundum specimens investigated, therefore allows us to exclude high-temperature gem enhancement.

Damage-induced Raman-band broadening is accompanied by certain band-downshifts (reflecting a general increase in bond lengths; Nasdala *et al.*, 1995). The band broadening detected was used to calculate theoretical band positions that correspond to the current structural state of zircon inclusions. The amount of compressive stress (also referred to as “fossilized pressure”) acting on the zircon inclusions was then calculated based on the pressure dependence of the $\nu_3(\text{SiO}_4)$ Raman band of zircon. In a DAC (diamond anvil cell) study, Nasdala *et al.*, (2008) have observed a band-upshift of about 5.4 – 5.9 cm^{-1} per GPa. In our analyses we have determined band upshifts (relative to the theoretical positions) in the range 4.7 – 7.2 cm^{-1} , which indicates recent zircon pressures between 8.3 ± 2.5 and 12.7 ± 2.5 kbar. These values may provide an estimate of the pressure under which metamorphic corundum has formed.

References

- Dawson, P., Hargreave, M., and Wilkinson, G.R., 1971, The vibrational spectrum of zircon ($ZrSiO_4$), *Journal of Physics C: Solid State Physics*, Vol.4, No.2, p.240-256.
- Nasdala, L., Irmer, G., and Wolf, D., 1995, The degree of metamictization in zircons: a Raman spectroscopic study, *European Journal Mineralogy*, Vol.7, No.3, p.471-478.
- Nasdala, L., Miletich, R., Ruschel, K., and Vácz, T., 2008, Raman study of radiation-damaged zircon under hydrostatic compression, *Physics and Chemistry of Minerals*, Vol.35, No.10, p.597–602.
- Sutherland, F.L., Duroc-Danner, J.M., and Meffre, S., 2008, Age and origin of gem corundum and zircon megacrysts from the Mercaderes-Rio Mayo area, South - West Colombia, South America, *Ore Geology Review*, Vol.34, No.1-2, p.155-168.

Corresponding Author

- Full name: Manuela Zeug
Affiliation: Institut für Mineralogie und Kristallographie, Universität Wien, Althanstr.
14, 1090 Wien, Austria.

Surface Morphology of Untreated and Irradiated Diamond Samples

Muzdareefah Thudsanapbunya, Jidapa Mogmued, and Somruedee Satitkune

The Gem and Mineral Sciences Special Research Unit, Department of Earth Sciences, Faculty of Science, Kasetsart University, Bangkok, 10900, Thailand

Extended Abstract

Introduction

The diamond industry has developed methods to enhance yellow and brown diamond to colorless and fancy colors to satisfy market demand. Natural blue-to-green colors in diamond are the effects of the exposure to natural radiation which is usually alpha or beta particles. The limited penetrating ability of these particles results in partial coloring of the polished diamond's surface (King, 2006). Irradiation is a common method to treat the diamond color. The colors of irradiated diamond are different shades depending on trace elements and types of radiation (Hainschwang *et al.*, 2009).

After irradiation, non-repolished diamond is usually annealed. This process is helpful to enhance the stability of diamond color. Irradiated diamond has the similar basic gemological properties compared to the natural one. The effect of irradiation on diamond surfaces will be analyzed by Atomic Force Microscopy (AFM).

Materials and Methods

A 0.1540 ct. untreated brown diamond, 0.1370 ct. green irradiated diamond (30,000 KGy electron dose) and 0.1825 ct. bluish green irradiated diamond from gem market (Figure 1) were selected for this experiment. Their surface features focused on the table of diamond samples were examined by AFM (ARMFP-3D model), a machine at Scientific Equipment Center, Faculty of Science, Kasetsart University, Bangkok, Thailand (Figure 2). AFM offers a 3D profile of the surface by measuring the force between a sharp probe (tip) and surface applied in gemstone research (Lhuaamporn *et al.*, 2010; Sanguanphun *et al.*, 2013). Tapping mode of operation in AFM allows high resolution of samples and it is suitable for diamond samples (Wilson and Bullen, 2007). The roughness and atomic step of the samples from AFM were analyzed by using "Igor Pro 6.30A" software.

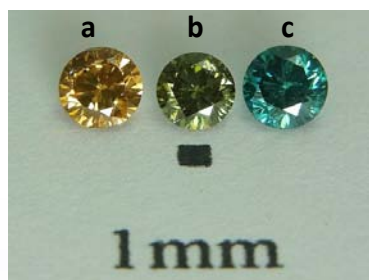


Figure 1: Diamond samples; (a) Untreated diamond, (b) and (c) Irradiated diamonds.



Figure 2: Atomic Force Microscope (ARMFP-3D model).

Results and Discussions

According to the surface feature in a nanometer scale, the average step height of natural diamond sample, irradiated diamond sample with 30,000 KGy electron dose and irradiated diamond sample from gem market are 0.42, 1.26 and 0.56 nm, respectively (Table 1). RMS roughness refers to the mathematical Root Mean Square, which is an average of peaks or baseline correction of a materials surface profile, recorded inside the evaluation length (Oliveira *et al.*, 2012).

The Figure 3, 4 and 5 show the AFM images of samples, the AFM images of the untreated samples exhibit with sharper edges and clearer step patterns than irradiated samples, they have different surface roughness shown in Table 2. That is an effect of irradiation on diamond surfaces. Any particle with sufficient energy (electron, neutrons, γ -rays, ions, etc.) can produce vacancies in diamond, it is the cause of the hole or color center (Collins, 2007). High levels of ionizing radiation can alter the atomic structure of the gemstone's crystal lattice, effecting to the optical properties of gemstone (Hurlbut and Kammerling, 1991). The change of atomic structure may alter the atomic step and may also be related to the difference of untreated diamond and irradiated diamond.

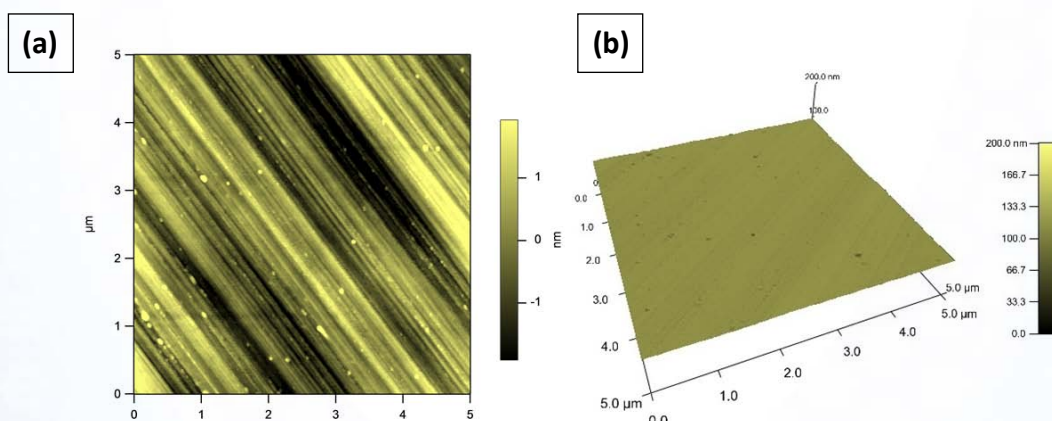


Figure 3: (a) 2D and (b) 3D AFM images of untreated diamond sample.

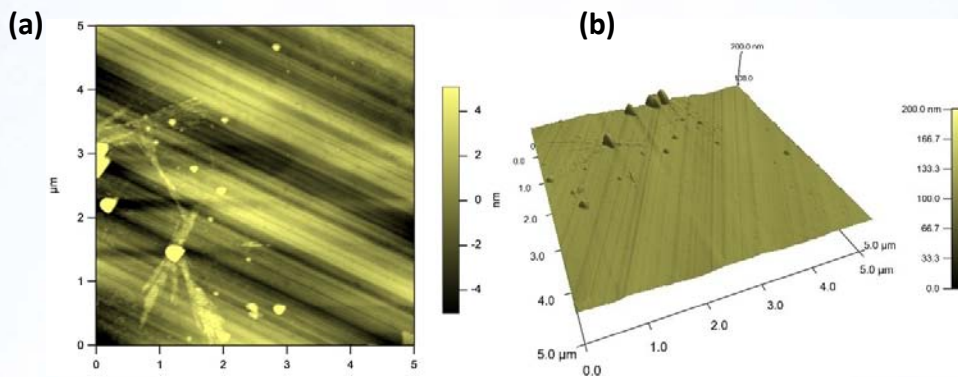


Figure 4: (a) 2D and (b) 3D AFM images of irradiated diamond sample with 30,000 KGy electron dose.

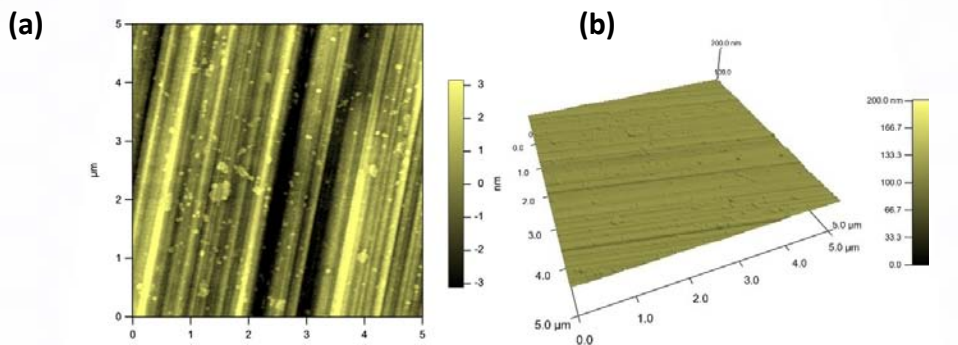


Figure 5: (a) 2D and (b) 3D AFM images of irradiated diamond sample from gem market.

Table 1: Average Step heights of diamond samples

Sample	Step heights (nm)			Average step heights (nm)
	Line A	Line B	Line C	
Untreated diamond	0.87, 0.31, 0.20, 0.45	0.18, 0.45, 0.47, 0.24	0.34, 0.88, 0.46, 0.16	0.42
Irradiated diamond with 30,000 KGy electron dose	1.11, 0.83, 1.38, 3.59	0.65, 0.32, 0.58, 0.42	0.42, 2.07, 1.08, 2.75	1.26
Irradiated diamond from gem market	0.33, 0.47, 0.85, 0.25	0.25, 0.61, 0.82, 0.22	0.63, 0.94, 0.91, 0.48	0.56

Table 2: Average roughness of diamond samples

Sample	RMS roughness(nm)					Average of the RMS roughness (nm)	Standard deviation (SD)
	1	2	3	4	5		
Untreated diamond	0.775	1.093	0.725	0.798	0.896	0.857	±0.15
Irradiated diamond with 30,000 KGy electron dose	1.880	1.510	1.890	1.880	1.720	1.776	±0.16
Irradiated diamond from gem market	1.096	1.567	2.005	1.414	1.351	1.486	±0.34

Conclusions

The result of this experiment shows that the average step height and the average roughness of untreated diamond are lower than those of irradiated diamonds. The difference of step height and roughness is one of reliable characteristics that may be helpful to identify irradiated diamond, although more samples need to be studied to confirm AFM as an identification technique.

Based on this research, the samples of this experiment are possibly not enough. Plans for future work include experimenting with several samples, analyzing the results among before and after irradiation.

Acknowledgments

Faculty of science, Kasetsart university is gratefully acknowledged for granting the research project. The AFM facility was provided by the Scientific Equipment Center, Faculty of Science, Kasetsart University. Special thanks are due to Mr.Chakkrich Boonmee and Ms.Sermrak Ingavanija for their support in the laboratory and I would like to thank Mr.Natthapong Monarumit, for his advice.

References

- Collins, A.T., 2007, Optical Centres Produced in Diamond by Radiation Damage, New Diamond and Frontier Carbon Technology MY Tokyo, Vol.17, No.2, p.47-61.
- Hainschwang, T., Respinger, A., Notari, F., Hartmann, H.J., and Günthard, C., 2009, A comparison of diamonds irradiated by high fluence neutrons, before and after annealing, Diamond and Related Materials, Vol.18, No.10, p.1223-1234.
- Hurlbut, C.S., and Kammerling, R.C., 1991, Gemology, Wiley Interscience, p.170.
- King, John, M., 2006, Gems & Gemology in Review: Colored Diamonds, Gemological Institute of America, p.48.
- Lhuaamporn, T., Pongkrapan, S., and Wathanakul, P., 2010, Micro-nano Scaled Surface Features of Synthetic Ruby at Different Orientation before and After Anneal,ⁱⁿ Proceedings of Provenance and Properties of Gems and Geo-Materials, 17-24 October 2010, Hanoi University, Vietnam, p.179-181.
- Oliveira, R.R.L., Albuquerque, D.A.C., Cruz, T.G.S., Yamaji, F.M., and Leite, F.L., 2012. Measurement of the Nanoscale Roughness by Atomic Force Microscopy: Basic Principles and Applications, Federal University of São Carlos, Campus Sorocaba, Brazil, p.147-174.
- Sanguanphun, C., Monarumit, N., Lhuaamporn, T., Wongkokua, W., Satitkune, S., and Wathanakul, P., 2013, Micro-nano Effect of electron irradiation on Diamond surfaces using Atomic Force Microscope, Abstract proceedings in the International gemological Conference 2013, 12-16 October 2013, Hanoi, Vietnam, p.161-163.
- Wilson, R.A. and Bullen, H.A., 2007, Basic Theory Atomic Force Microscopy (AFM), Department of Chemistry, Northern Kentucky University, Highland Heights, KY., Available from http://asdlb.org/onlineArticles/ecourseware/Bullen/SPMModule_BasicTheoryAFM.pdf

Corresponding Author

Full name: Muzdareefah Thudsanapbunya
Affiliation: The Gem and Mineral Sciences Special Research Unit, Department of Earth Sciences, Faculty of Science, Kasetsart University, Bangkok, 10900, Thailand.
Email: muzdareefah.t@gmail.com

Three-phase Inclusions in Emerald and Their Impact on Origin Determination

Sudarat Saeseaw, Vincent Pardieu and Supharat Sangsawong

GIA Research (Thailand), 10th Floor, U-Chu-Liang Building, 968 Rama IV Road, Bangkok, 10500, Thailand

Extended Abstract

Three-phase inclusions in emerald have been considered a potential indicator of Colombian origin. Nowadays, emeralds from Afghanistan (Panjshir Valley), China (Davdar), and Zambia (Kafubu and a new deposit at Musakashi) may also contain three-phase inclusions resembling those often found in specimens from Colombian deposits (Muzo, Chivor, La Pita, Coscuez, and Peñas Blancas). This presentation will present detailed photomicrographs of samples from these localities, with a focus on their multiphase inclusions. In addition to, UV-Vis-NIR spectroscopy and LA-ICP-MS will be presented as they are potential tools to aid for geographic origin determination.

Materials and Methods

A total of 84 emeralds consisted of 35 emeralds from different Colombian deposits; 13 emeralds from Davdar, China; 15 emeralds from Panjshir, Afghanistan; 11 emeralds from Musakashi, Zambia; and 10 emeralds from Kafubu, Zambia were studied. 55 emeralds were rough samples with one or two polished surface windows, 28 were fabricated as optical wafers oriented either perpendicular or parallel to the crystal's c-axis, and one was faceted. Color ranged from light to deep green. Standard gemological properties including refractive index, birefringence, and fluorescence were measured. Microscopic examination was performed with GIA binocular microscopes at 10×–70× magnification. Photomicrographs were captured at up to 180× magnification with a Nikon SMZ 1500 system using darkfield, brightfield, and oblique illumination with a fiber-optic light. Ultraviolet through visible and near-infrared (UV-Vis-NIR) spectra were collected with a Hitachi U-2900 spectrophotometer (for polarized ordinary ray spectra) at 1 nm resolution. For laser ablation–inductively coupled plasma–mass spectrometry (LA-ICP-MS) chemical analysis, we used a Thermo Scientific X Series II ICP-MS combined with a Nd:YAG-based laser ablation device operating at a wavelength of 213 nm. For the ICP-MS operations, the forward power was set at 1300 W and the typical nebulizer gas flow was approximately 0.90 L/min. The carrier gas used in the laser ablation unit was He, set at approximately 0.78 L/min. The alignment and tuning sequences were set to maximize Be counts and keep the ThO/Th ratio below 2%. Laser ablation conditions consisted of a 40 μm diameter laser spot size, a fluence of 10 ± 1 J/cm², and a 7 Hz repetition rate. For quantitative analysis, samples must be calibrated against an external standard of known composition, which meant measuring the signals for the elements of interest in the sample and comparing them to the signals for a standard with known concentrations of those elements. Generally, NIST 610 and 612 glasses were used for calibration standards. All elemental concentrations were calculated by applying ²⁹Si as an internal standard, with Si concentration calculated from the theoretical value of beryl (31.35 wt.%). Laser spots were applied in the same area where UV-Vis spectra were collected, which was usually clean and had an even color distribution, though color-zoned areas were also sampled.

Results

Physical properties, microscopic characteristic, UV-Vis-NIR absorption data, and trace-element chemistry of emeralds from five different localities has summarized in Table 1.

Locality	Refractive index	Color filter reaction	Microscopic characteristics	UV-Vis Spectroscopy (Cations in addition to Cr ³⁺)	Trace element analysis (84 samples)
Musakashi, Zambia	1.572-1.582	Strong pink	Multiphase inclusions tend to be more irregular than those in Colombian gems; Multiphase inclusions with at least two crystals associated with a gas bubble might indicate Zambian rather than Colombian origin	No significant Fe ²⁺ related absorption features in the NIR region, and no Fe ³⁺ observed.	Low alkali metal concentrations (1,530-6,060ppmw) Cr > V; Cr/V ratio 1.7 - 5.3 Fe concentration: 680 - 1,490 ppmw [Li vs. Cs log-log plot can help separate Musakashi from Kafubu and slightly separate from Colombia] [Fe vs. K log-log plot can help separate Musakashi from Colombia]
Kafubu, Zambia	1.582-1.593 (RI values typically higher than other localities)	Inert	Multiphase inclusions usually rectangular in shape, but might be irregular in outline; solid crystals of pyrolusite, chlorite, mica, amphibole, and tourmaline	Strong broad Fe ²⁺ band at approximately 810 nm O-ray: narrow Fe ³⁺ band at approximately 372 nm	High alkali metal concentrations (15,834 - 23,294 ppmw) Cr >> V; Cr/V ratio 8 - 40 Fe concentration: 5,900 - 11,600 ppmw [Li vs. Cs log-log plot can help separate Kafubu from others.]
Panjsher Valley, Afghanistan	1.572-1.590	Inert to pink	Multiphase inclusions tend to be more elongated or needle-shaped than other localities; each might host several cubic to rounded transparent crystals, and sometimes small, dark opaque crystals.	Medium broad Fe ²⁺ band at approximately 810 nm O-ray: Fe ³⁺ peak at 372 nm in some samples	Moderate to high alkali metal concentrations (3,946-17,505ppmw) Cr and V concentrations might be similar: Cr/V ratio 0.3 - 3-3 Fe concentration: 1,010 - 9,820 ppmw [Li vs. Cs log-log plot can help separate Panjsher from Kafubu, Davdar, Musakashi and Colombia]
Davdar, China	1.577-1.588	Pink	Multiphase inclusions usually jagged or irregular in outline and some needle-like in shape.	Similar to Musakashi: Small broad Fe ²⁺ band at approximately 810 nm Similar to Colombia: Strong V ³⁺ bands at approximately 400 and 654 nm	Low to moderate alkali metal concentrations (5,190-12,620 ppmw) Slightly more V than Cr; Cr/V ratio 0.1 - 1.0 Fe concentration: 1,230 - 4,350 ppmw [Li vs. Cs log-log plot can help separate Davdar from Panjsher] [Fe vs. K log-log plot can help separate Davdar from Musakashi and Colombia]
Colombian localities: (Muzo, Coscuez, La Pita, Peñas Blancas, Chivor)	1.570-1.580 (RI values typically lower than other localities)	Pink to strong pink	Classic jagged multiphase inclusions hosting a gas bubble and one or more cubic crystals; gas bubble usually smaller than the whole inclusion and also smaller or about the same size and the associated cubic crystal	No Fe ²⁺ or Fe ³⁺ observed Weak to medium V ³⁺ bands at approximately 400 and 654 nm	Low alkali metal concentrations (1,515 to 8,115 ppmw) Cr and V concentrations might be similar: Cr/V ratio 0.04 and 3.5 Fe concentration: 117 to 2,030 ppmw [Fe vs. Ga and Fe vs. K log-log plot can help separate Colombia from others]

Corresponding Author

Full name: Sudarat Saeseaw

Affiliation: GIA Research (Thailand), 10th Floor, U-Chu-Liang Building, 968, Rama IV
Road, Bangkok, 10500, Thailand.

Email: ssaeseaw@gia.edu

Update on the Characteristics of Amber from Indonesia

***Nalin Narudeesombat¹, Papawarin Ounorn¹, Pimtida Bupparaenoo¹, Arne Christopherse²,
Visut Pisutha-Arnond¹ and Chakkaphan Sutthirat^{1,3}***

¹The Gem and Jewelry Institute of Thailand (Public Organization), Bangkok, 10500, Thailand

²Starborn Creations, USA

³Department of Geology, Faculty of Science, Chulalongkorn University, Bangkok, 10330, Thailand

Extended Abstract

Introduction

Amber is an organic gem material that is a fossilized tree resin. Plant resins usually take over a million years to transform into amber. Amber is usually yellow, red or milky yellow in color, light in weight, and can be either opaque or transparent. The well-known ambers come from the Baltic Sea; however, amber is also found in other places, such as Lebanon, northern Myanmar, Spain, French, China, Indonesia, Dominican Republic and Mexican (Ross and Sheridan, 2013). Recently, plenty of amber samples claimed to be from Indonesia were circulated in gem markets and their preliminary characteristics were studied by Leelawatanasuk *et al.*, (2013). The Indonesian amber was reportedly found in the Tertiary (Miocene and Oligocene; 23-30 Million years old) coal layers of the Central Sumatra Basin on the Island of Sumatra. The Sumatra fossil amber resin was found in a primary deposit (in original location as opposed to alluvial or secondary deposits) in between three distinct coal layers in open strip mines. The amber is a byproduct of the coal mining and solely mining the amber would not be economically feasible since the amber is recovered from deep layers under 30-80 m of sediments and rocks. The Sumatra amber is a Glessite type of amber, which formed from the resin of the deciduous tree Dipterocarpaceae. Since a lot of rocks and earth is being moved by the mining of coal, several tons of amber can be recovered per month. However, most of the amber collected from the site is very brittle or very dark, already damaged by geological processes (geothermal heat, pressure, seismic activity etc.) or heavily damaged by the machinery used in coal mining so that only a small percentage of the total production can be used as gem or decorative material. Complete large pieces are quite rare and hard to find.

Material and Methods

In this study, thirteen amber samples from Sumatra, Indonesia were provided by a co-author (AC). All of them appear as tumbled freeform pieces that are transparent to opaque. Their weights vary from 6.66 cts. (sample no.8) to 41.89 cts. (sample no.3). The colors range from brownish yellow to greenish yellow to yellowish brown (Figure 1). One sample shows distinct blue sheen effect under strong daylight (Figure 2). This effect is similar to blue amber from Dominican Republic which is called "blue amber" (Erichson and Weitschat, 2008). As usual, they were recorded for basic gemological properties. In addition, these samples were also analyzed by advanced instruments, such as Laser Raman Spectroscopy (Renishaw InVia equipped with 785 nm laser) and an Attenuate Total Reflection (ATR)-FTIR spectroscope (Thermo-Nicolet In10 attached with germanium tip for ATR analysis). All analyzes were performed at The Gem and Jewelry Institute of Thailand-Gem Testing Laboratory (GIT-GTL).

Results

General properties

The refractive Indices (RI) of amber samples used in this study vary approximately from 1.54-1.53 (spot reading). Their Specific Gravity (SG) ranges from 0.999 (sample no.9) – 1.018 (sample no.1). Only one sample (sample no.13) can float on distilled water which may be due to the presence of plentiful cotton-like inclusions inside. The samples are fluoresced blue and green in LWUV (Figure 3) and blue in SWUV lights.



Figure 1: Thirteen samples of amber from the Central Sumatra Basin, Indonesia.
Photo by Jakkawanvibul.



Figure 2: Blue sheen effect under strong daylight (Sample no. 1). Photo by Jakkawanvibul.



Figure 3: Strong bluish fluorescence under LWUV. Photo by Jakkawanvibul.

Microscopic observation revealed that ten out of thirteen samples contain patches of typical round-to-oval-shaped inclusions or nodules apparently in white and yellow to brown colors (Figure 4). Swirl lines and swirly brown inclusions aligned in zonal pattern were found in some samples (Figure 5). In addition, white cotton-like inclusions and white material were seen in some samples as well (Figures 6 and 7). Moreover, a fossilized insect was also encountered in a sample from this study (Figure 8).



Figure 4: Patches of round-to-oval-shaped inclusions in white and yellow to brown colors (**left**, Sample no. 10 magnified 6.5x; **right**, Sample no. 11 magnified 10.0x). Photomicrographs by Ounorn.



Figure 5: Swirly brown inclusions aligned in zonal pattern (Sample no. 9). Photo by Jakkawanvibul.

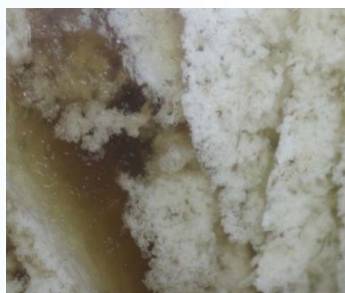


Figure 6: Cotton-like inclusions (Sample no. 13). Photomicrograph by Ounorn; magnified 12.5X



Figure 7: White material at the contact boundary between transparent and opaque parts of sample no. 2 with a zone of round-to-oval-shaped inclusions. Photomicrograph by Ounorn; magnified 6.5X



Figure 8: A fossilized Insect (Sample no. 3). Photomicrograph by Ounorn; magnified 10X

Advanced Instrument Testing

The Mid-IR spectra in the range of 4,000-700 cm^{-1} were collected using ATR technique for all studied samples. The spectra appear in three different patterns. All those three patterns similarly show two regions of absorption, the low wavenumber absorption region between 1800-700 cm^{-1} and the high wavenumber absorption region between 3000 – 2800 cm^{-1} . In the low wavenumber region, the first pattern shows many characteristic absorption peaks and bands at around 752, 833, 1026, 1164, 1380, 1454 and 1708 cm^{-1} , whereas the second pattern shows many characteristic absorption peaks and bands at around 798, 1041, 1261, 1454, 1542 and 1650 cm^{-1} , while the third pattern gives peaks and bands not only those found in the second pattern but also has an additional peak at 1743 cm^{-1} together with several low-intensity peaks and bands around 1600 – 1715 cm^{-1} . In the high wavenumber region, all three patterns show similarly distinct peak positions at around 2850, 2919 and 2954 cm^{-1} (Figure 9).

The samples were also analyzed by Raman spectroscopic technique in range of 250-3500 Raman Shift (cm^{-1}) using 785 nm laser. The spectra show major Raman shift peaks at 724, 790, 946, 1307, 1430, 1653 cm^{-1} with broader peaks around 2800-3000 cm^{-1} (Figure 10). In addition, Photoluminescence technique was used with 325 nm laser in range 300-700 nm^{-1} .

The photoluminescence spectra of the Indonesian amber show broader emission with humps at around 411, 443, 504, 525 and 551 nm. In comparison, The photoluminescence spectra of Baltic amber display narrower emission with humps at around 528, 549 and 572 nm only (Figure 11).

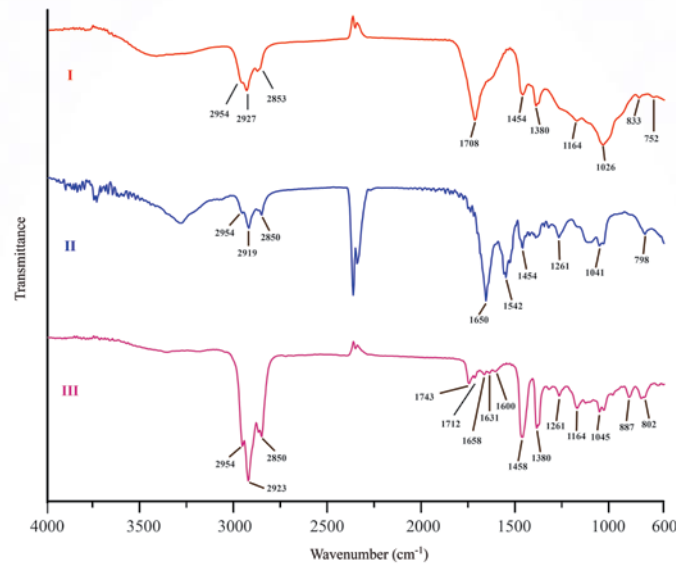


Figure 9: Three different Mid-IR spectra of Indonesia ambers; 1, 2 and 3 Patterns (recorded from Sample no. 1, 2 and 5) shown from top to bottom, respectively.

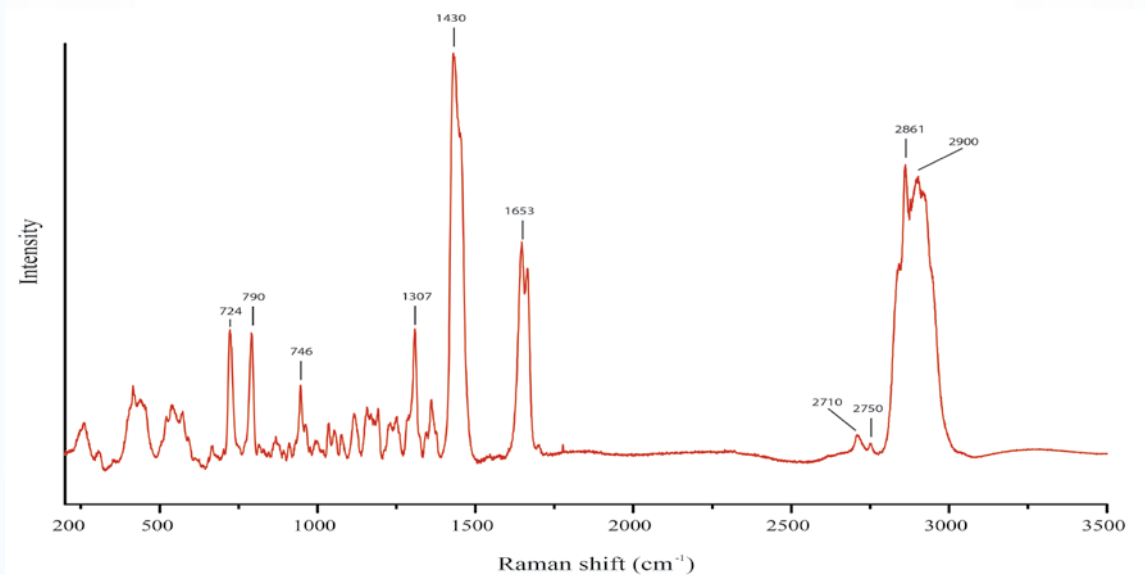


Figure 10: Representative Raman spectrum of Indonesia amber.

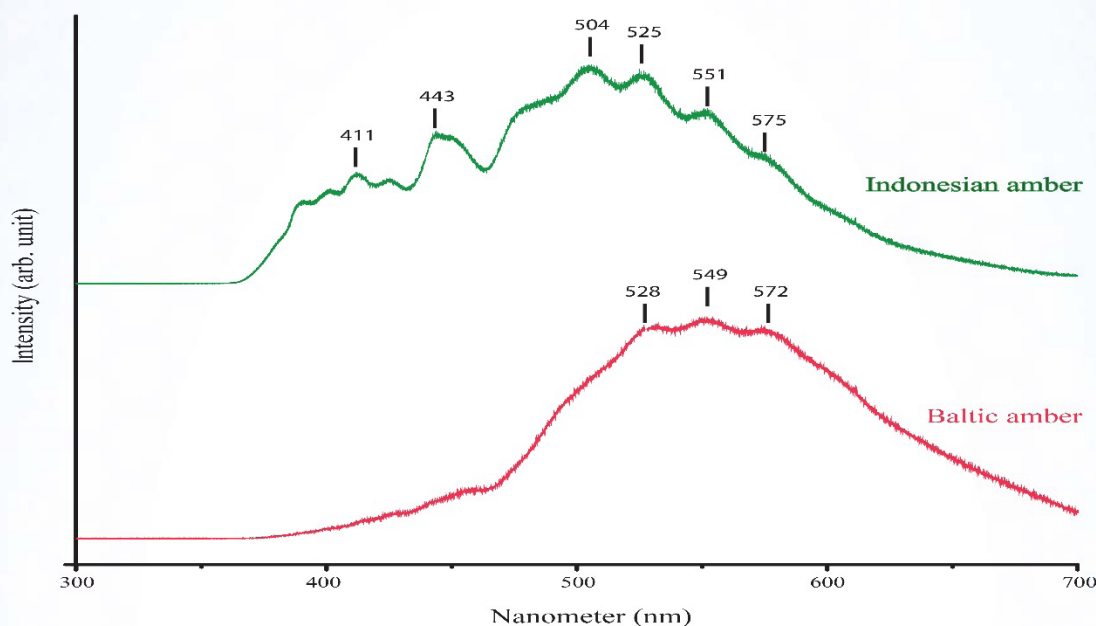


Figure 11: Comparison of photoluminescence spectra of Indonesia amber, sample no.1 (**top**) and Baltic amber (**bottom**).

Conclusions

This study has revealed that the basic gemmological properties fit well with the properties of true amber and are also similar to those reported in previous study (Leelawatanasuk *et al.*, 2014). Moreover, there are many inclusion features such as fossilized insect found in samples from this study. Even though the IR and Raman spectra obtained from this study show a similarity with the pattern previous reported by Leelawatanasuk *et al.*, (2014), several new absorption peaks and bands in the IR spectra are newly found and never been reported elsewhere. In addition, the photoluminescence spectra of Indonesian amber are distinctly different from those of Baltic amber. Besides, the characteristic FTIR spectrum of baltic amber, referred to as baltic shoulder ($1175\text{-}1250\text{ cm}^{-1}$) flanked by an absorbance peak at 1160 cm^{-1} (Wolfe *et al.*, 2009), also appears in the FTIR spectrum of Indonesian amber.

Based on the information provided by the co-author (AC), the amber with blue sheen or the so-called “Blue Amber” is found in all three layers of the mining site, but best specimens usually come from the deepest layers. Gem quality specimens are rare and make up less than 5-10% of the production. Very blue pieces and very clear pieces are hard to find and only a fraction of one percent of the recovered material shows very strong blue color. The Sumatra amber takes a good polish and is quite hard, Sumatra amber currently sold in the market is generally untreated. Compared to other ambers, the untreated Sumatra amber has a slight waxy feel to it and will lose the polish sooner if worn everyday and directly on the skin. It has a very nice aromatic smell when cut and the smell can even be detected if polished pieces are rubbed by hand. In the fu-

ture, treatments might be developed to harden this amber (autoclave or heat treatments as commercially used with Baltic amber or Columbian copal) and extend the duration of the polish. As with all other ambers, oxidative color change of the surface can be observed and over long periods of time some of the amber might get a little darker.

Acknowledgements

The authors would like to thank Mr. Thanong Leelawatanasuk, Chief of GIT-GTL, for his advices and inspiration for this study. Besides, Mr. Jirapit Jakkawanvibul took the photos and Mr. Vigo Christophersen from Starborn Creations, for supplying samples used in this study as well as their locality information.

References

- Erichson, U., and Weitschat, W., 2008, Baltic Amber, German Amber Museum Ribnitz-Damgarten, 191 p.
- Leelawatanasuk, T., Wathanakul, P., Paramita, S., Sutthirat, C., Sriprasert, B., and Bupparenoo, P., 2013, The characteristics of amber from Indonesia, The Australian Gemmologist, Vol. 25, No.4, p.142-145.
- Ross, A., and Sheridan A., 2013, Amazing Amber, NMSE- Publishing Ltd, United Kingdom, 48 p.
- Wolfe, A.P., Tappert, R., Muehlenbachs, K., Boudreau, M., McKellar, R. C., Basinger, J. F., and Garrett, A., 2009, A new proposal concerning the botanical origin of Baltic amber, Proceedings of the Royal Society: B, Vol.276, No.1672, p.3403-3412.

Corresponding Author

Full name : Nalin Narudeesombat
Affiliation : The Gem and Jewelry Institute of Thailand (Public Organization), Bangkok, 10500, Thailand.
Phone: (662) 634-4999 ext. 409
Fax: (662) 634-4970
Email : nnalin@git.or.th

XRF Analysis in Thai's Ivory Samples from Lampang Province, Northern Thailand

***Chakkrich Boonmee¹, Natthapong Monarumit¹, Sermrak Ingavanija¹,
Somruedee Satitkune¹ and Pornsawat Wathanaku²***

¹The Gem and Mineral Sciences Special Research Unit, Department of Earth Sciences, Faculty of Science, Kasetsart University, Bangkok 10900, Thailand

²The Gem and Jewelry Institute of Thailand (Public Organization), Bangkok, Thailand

Extended Abstract

Introduction

Ivory is an organic gemstone which demanded in the market for jewelry making, crafting, and other ornaments around the world. Many elephants have been chased for ivory hunting. The ivory trade has been banned in world wide. There are three species of elephant in the world consisting of Savannah elephant (*Loxodonta africana africana*), Forest African elephant (*Loxodonta africana cyclotis*), and Asian elephant (*Elephas maximus*). Elephants and their ivories were safeguarded under the Convention on International Trade in Endangered Species (CITES) and were listed in appendix I since 1975 (Banerjee *et al.*, 2008).

Ivory is formed by biomineralisation of the connective tissue in the teeth of some animals such as mammoth and elephant. The hydroxlyapatite ($\text{Ca}_{10}(\text{PO}_4)_6(\text{OH})_2$) is the main organic composition in ivory. The geographic origins of ivory can be identified by studying the physical and chemical properties that related to the different food from their origins (Banerjee *et al.*, 2008; Reifenstein *et al.*, 2008).

X-ray fluorescence (XRF), a non destructive method, was selected to study the elemental analysis in ivory. The characteristic of X-ray spectrum could be guided to distinguish the origins of ivory due to their unique intensity of the elements. The African ivories were determined by XRF presenting high Sr, Fe, S, and Si (Kautenburger *et al.*, 2004).

Materials and Methods

The ivory samples were donated from the Timber Center, Lampang Province. The samples were cut and prepared for chemical analysis by using the advance scientific equipment.



Figure 1: Ivory sample from the Timber Center, Lampang Province.

X-ray fluorescence is caused by excited atom from X-ray. The inner shell atom is excited and produced the electron hole in the inner shell. The outer shell electron moves to replace the inner shell electron vacancy. This phenomenon splits out the photons with characteristic energy which can be used to identify the quantity of the element in the sample (Brouwer, 2003).



Figure 2: EDXRF at The Gem and Jewelry Institute of Thailand (Public Organization)-GIT.

Result

The chemical composition of Lampang's ivory samples have been analyzed by EDXRF showing Mg, Si, P, S, K, Ca, Fe, Zn, and Sr. This result applies to support and confirm the Thai's ivory database.

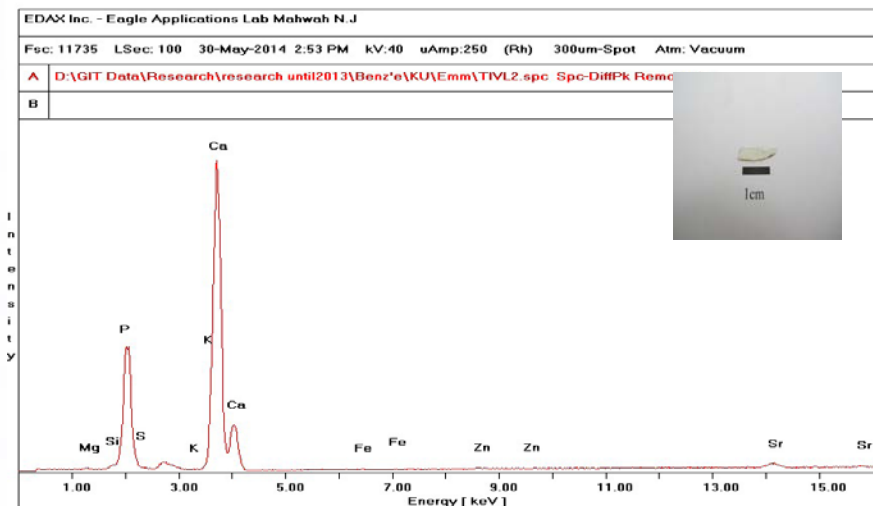


Figure 3: Elements composition result of Lampang's ivory.

Conclusions

The XRF result of Thai's Ivory from Lampang Province is very helpful for database creating that is the evidence to confirm and distinguish the Thai's Ivory from other origins. The most important is useful to support the police for capturing the ivory smuggler or illegal trader.

References

- Banerjee, A., Bortolaso, G., and Dindorf, W., 2008, Distinction between African and Asian Ivory, in Proceedings of INCENTIVS-Meeting (2004-2007), Vol.228, p.37-49.
- Banerjee, A., Bortolaso, G., Hofmeister, W., Petrovic-Prelevic, I., and Keiwisch, B., 2008, Investigation of quality of commercial mammoth ivory by means of X-ray Powder Diffraction (Rietveld method) and FTIR Spectroscopy, in Proceedings of INCENTIVS-Meeting (2004-2007), Vol.228, p.51-63.
- Brouwer, P., 2003, Theory of XRF, PANanalytical BV, The Netherlands, 59 p.
- Kautenburger, R., Wannemacher, J., and Müller, P., 2004, Multi element analysis by X-ray Fluorescence: A powerful tool of ivory identification from various origins, Journal of Radioanalytical and Nuclear Chemistry, Vol.260, No.2, p.399-404.
- Reifenstein, V., Kitschke, C., and Ziegler, S., 2008, Elephant Conservation and the Ivory Trade, in Proceedings of INCENTIVS-Meeting (2004-2007), Vol.228, p.13-25.

Acknowledgments

The authors appreciate various supports from the Department of Earth Sciences, Faculty of Science, Kasetsart University; the Timber Center, Lampang Province for supporting the ivory samples, and The Convention on International Trade in Endangered Species (CITES) of Thailand. Special thanks are due to The Gem and Jewelry Institute of Thailand (Public Organization)-GIT for XRF analyses; Kasetsart University Research and Development Institute (KURDI) for the research fund.

Corresponding Author

Full name: Chakkrich Boonmee
Affiliation: The Gem and Mineral Sciences Special Research Unit, Department of Earth Sciences, Faculty of Science, Kasetsart University, Bangkok, 10900, Thailand.

About Bead Nucleus Used for Pearl Culturing

Shigeru Akamatsu

Central Gem Laboratory, Miyagi Bldg, 5-15-14 Ueno, Taito-Ku, Tokyo, 110-0005, Japan

Extended Abstract

Introduction

When discussing the quality of cultured pearl, the quality of bead nucleus has rarely been mentioned. Recently, however, the need to discuss the quality of bead nucleus has arisen, since bead nucleus often causes problems affecting pearl quality. One example shows when a pearl is drilled, nucleus cracks and this crack causes subsequent crack of the pearl nacre. The material of the bead nucleus also causes problems. At present many bead nuclei are made of *Giant clam* (*Tridacna gigantea*). However catching Giant clam is against CITES, so the use of Giant clam bead nucleus is illegal. Some other bead nuclei are made of Chinese freshwater mussel shells by bleaching with strong toxic bleaching chemicals that may injure our health. Such problematic nuclei are appearing in the markets. Observing the present situation, it is time to consider what materials should be allowed as bead nuclei.

Historical aspect of the bead nucleus

In 1919, when Mr. Kokich Mikimoto started to sell his cultured pearls for the first time in European markets, Gemstone Importing Association in Paris made a complaint about Mikimoto pearls as “fake” and started a big boycott campaign. Against this movement, Mikimoto took this matter to court and it was fought in the court whether cultured pearls are real or fake. In 1924 a decision was made that cultured pearl was a real pearl. For the decision, famous French university professor, Louis Boutan, played a very important role. After his differential research work, he announced that “cultured pearl is made by covering a bead nucleus made of freshwater mussel shell nacre. The difference between natural and cultured pearl is that the formation started naturally in oyster body or a bead was inserted by the aid of human action. There is no difference in subsequent pearl formation between them”. At that time the bead nucleus was made of the nacre of freshwater mussel shell, it was recognized the same substance as natural pearl. Thus substance of the bead nucleus helped to prove cultured pearl was real. Since then Japanese pearl cultivators observed the tradition to use freshwater mussel shell as the material of bead nucleus. (Figure 1).



Figure 1: Traditional bead nucleus made of American freshwater mussel shell

Present situation

The tradition to use bead nuclei made of freshwater mussel shell has been observed over 100 years by Japanese pearl cultivators. However, this tradition is gradually collapsing according to following reasons.

The first reason is the change toward bead nucleus. As the globalization of pearl culturing has developed, the tradition to use bead nucleus made of freshwater mussel shell, kept over 100 years by Japan, is dwindling. In many pearl producing countries, they think whichever bead material is accepted if pearl sac is formed in oyster body and pearl is formed in it. As the result, as aforementioned bead nuclei made of Giant clam shell are used, that is against CITES. And other bead nuclei may be found so heavily bleached that it affects human body, are appearing in the markets.

The second reason is resource problem of freshwater mussels. At present huge amount of freshwater mussels such as Wash board (*Megalonaias gigantea*), Maple leaf (*Quadrulla quadrulla*), Pig toe (*Fusconaia flava*), Three ridge (*Amblyma plicata*) and Ebony shell (*Fusconaia ebena*) are imported from USA by Japanese bead nucleus manufacturers. Recently, however, The US Government has started to regulate the catch of freshwater mussels by the reason of resource protection and except for several species for bead nucleus manufacturing, to catch mussels was totally prohibited, since they are designated as Appendix I of CITES. Even though the need for bead nucleus is increasing by globalization of pearl culturing, if supply of the bead nucleus cannot satisfy the demands of pearl cultivators, it is natural to shift from conventional bead nucleus to cheaper substitutes. The more the need for bead nucleus increases, the higher the price of it becomes. Consequently, price hike of the bead nucleus begins to affect pearl culturing cost. Especially for the cultivators of Silver and Black lipped pearl who have to use high priced bigger sized bead nucleus, it becomes inevitable to use cheaper substitutes.

The third reason is globalization of bead nucleus manufacturing. As well as pearl culturing, globalization of bead nucleus manufacturing has become remarkable. Bead nucleus is manufactured by comparatively simple technique such as shell sawing, cutting and rounding. If high technology is not needed for the production, it is natural that bead nucleus manufacturing transfers from Japan to China, Hong Kong and Vietnam where labor cost is cheaper, and bead nucleus made in these countries is exported directly, not via Japan to pearl culturing countries. Now bead nucleus production got utterly out of Japanese control. Japan can only notice the present situation of the bead nuclei from imported cultured pearls.

Problems about substitute bead nucleus

At present there are many substitutes for bead nuclei. The following paragraph shows examples of main substitutions and their problems.

Bead nucleus made of Giant clam

Though catching giant clam is restricted by Appendix II of CITES, many shells are caught illegally to make bigger sized bead. Bead nucleus made of Giant clam often cracks by drilling, since it does not possess nacreous structure but cross-lamellar structure. (Figure 2)



Figure 2: Bead nucleus made of Giant clam. It is cracked when drilled.

Glued bead nucleus

Three to five freshwater mussel shell plates are glued to increase the width, and bigger sized bead nucleus is made. The same procedure has also been witnessed with saltwater *P. maxima* shells. When such bead nuclei are drilled, glued parts sometimes separates. Glued bead nucleus also separates by endurance tests.

Bleached bead nucleus

As Chinese freshwater “Triangle” mussel shell usually contains pigments in its nacre. So, when bead nucleus is made by this freshwater mussel shell, colored product is obtained. In order to make the color of the nucleus white, toxic bleaching agent Rongalite ($\text{NaHSO}_2 \cdot \text{CH}_2\text{O} \cdot 2\text{H}_2\text{O}$) is used. Rongalite emits formaldehyde that injures our health. (Figure 3)



Figure 3: Bead nucleus made of freshwater “Triangle” mussel shell. Colored nucleus (**left**) is bleached by Rongalite.

Bead nucleus treated with fluorescence whitening agent

In order to whiten the color of bead nucleus made of freshwater “Triangle” mussel shell, it is treated with fluorescence whitening agent. By the treatment pearls emit fluorescence that they do not originally possess.

Future Prospect

Observing pearls cultured using various kinds of bead nuclei, definition is needed after all. Bead nucleus amounts over 60% of the pearl. In case of thinly coated pearl, percentage becomes nearly 90%. The pearl quality cannot be discussed without judging the quality of bead nucleus. Cultured pearls should be jewellery. They should not be mere accessory. If so, we should observe traditional bead nucleus and the idea of “which ever bead nucleus is accepted if pearl sac is formed in an oyster body and pearl is formed in the sac” should be denied. Japan Pearl Promotion Society has recently revised Pearl Standard 2014. In it bead nucleus is defined as “the product by cutting, rounding and polishing freshwater mussel shell nacre”. In order to make jewelry pearl, Japanese pearl cultivators still continue to use traditional bead nucleus. We have to pay more attention to the quality of bead nuclei.

References

- Hänni, H.A., Krzemnicki, M.S., and Cartier, L.E., 2010, Appearance of new bead material in cultured pearls, *Journal of Gemmology*, Vol.32, No.1-4, p.31-37.
- Pearl standard, 2014, The Definition and Nomenclature of Pearls, CIBJO Pearl Book 2014 CIBJO (International Jewelry Confederation).
- Japan Pearl Promotion Society, Japan Jewellery Association.
- Superchi, M., Castaman, E., Donini, A, Gambini, E., and Marzola, A., 2008, Nucleated Cultured Pearls: What is there inside? *Zeitschrift der Deutschen Gemmologischen Gesellschaft* Vol.57, No.1-2, p.33–40.

Corresponding Author

Full name: Shigeru Akamatsu
Affiliation: Central Gem Laboratory, Miyagi Bldg, 5-15-14 Ueno, Taito-Ku, Tokyo, 110-0005, Japan.
Phone: +81-3-38363219
Email: s-akamatsu@mikimoto.net

Ancient Glass Beads: A Gemstone of the Log Coffin Culture at Pang Mapha, Mae Hong Son, Thailand

Seriwat Saminpanya, Natamon Bavornyospiwat, Sunisa Homklin and Sumalee Danyutthapolchai

Department of General Science, Faculty of Science, Srinakharinwirot University, Bangkok, 10110, Thailand

Extended Abstract

The ancient glass beads from a log coffin cave at Pang Ma, Mae Hong Son as well as from Sa Kaeo, Thailand have been studied for certain gemological characteristics and their chemical compositions were analyzed by EDXRF. The samples have the SG ranging from 1.67 to 3.00 with an average of 2.22, and the RI ranging from 1.51 to 1.60 with an average of 1.54. The glasses show typical inclusions of swirls and gas bubbles suggesting the drawn production. The copper and iron play the major role for the blue and green colors in the glasses, as confirmed by the UV-Vis-NIR spectra, whereas iron is responsible for the yellow and black beads. Lead as a color intensifier, is dominant gradually from yellow, green to blue samples, respectively. The major raw materials could possibly be silica sand, reh and stannate. The results suggest that people on the northern highland of the log coffin culture had a connection to the low land community in the central and eastern regions of the country during ~260-560 AD. The technology of glass making was probably the same as those used in Khao Sam Kaeo, a manufacturer site in southern Thailand.

Introduction

The log coffin culture in northern Thailand has been very well-known for the tourism and archaeological aspects. There are several caves and some rock-shelters where people of this culture loaded the corpses into the teak-coffins and placed into them. The age based on radiocarbon dating of log coffins is 2,100- 1,200 BP or 1st century- 800 AD. (contemporaneous with the late prehistoric to Dvaravati kingdom) (Grave *et al.*, 1994; Treerayapiwat, 2005). The artifacts and jewelries were put into the coffins associated with the corpses and some of those include the gem glass beads.

Material and Methods

Eight ancient glass-beads of this study have been exhumed from the soil associated with the log-coffins in a cave at Pang Mapha, Mae Hong Son, Thailand. The samples are in greenish blue and green with the diameter ranging from <3 to 4 mm (Figure.1). They were observed for their gemological properties and analyzed for their chemical characteristics with standard gemological equipments and advanced techniques (UV-Vis-NIR and EDXRF). The results were compared with those of the ancient glass beads from central, eastern and southern Thailand.

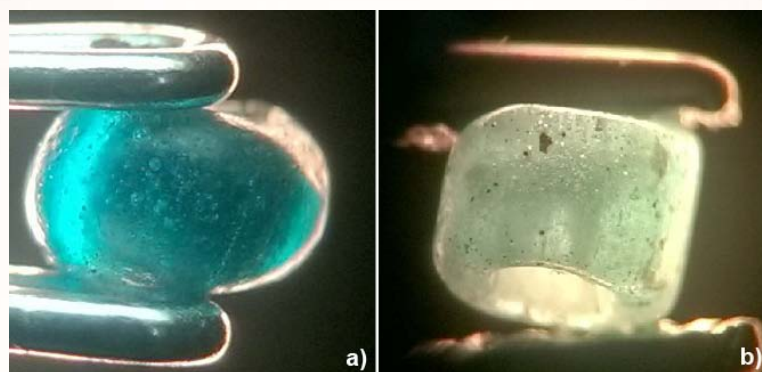


Figure 1: Ancient glass-bead samples from a log-coffin cave, **(a)** PMP5 and **(b)** PMP2. The gas bubbles align in row, suggesting the drawn production.

Results and Discussion

The samples typically show surface pits (so called orange peel appearance) due to cut bubbles or weathered surface. The beads from the log coffin cave contain more abundant dark brown inclusions. The glasses show typical inclusions of swirls and rows of gas bubbles parallel to the length of the drilled hole, suggesting a production by drawing (Figure 1). Samples from the log coffin cave have the SG ranging from 1.67 to 3.00 with an average of 2.22 and the RI ranging from 1.51 to 1.60 with an average of 1.54. An average composition is presented in Table 1.

Table 1: Average concentration for elements of the ancient gem glass-beads from a log coffin cave at Pang Mapha.

Oxide:	Na ₂ O	MgO	Al ₂ O ₃	SiO ₂	K ₂ O	CaO	TiO ₂	V ₂ O ₅	MnO	Fe ₂ O ₃	CuO	PbO	SrO	ZrO ₂	SnO ₂	ZnO
wt%:	1.83	0.86	9.88	69.07	1.97	7.54	0.76	0.05	0.09	0.94	2.14	3.53	0.12	0.3	1.26	0.09

Copper and iron play the major role for the blue and green colors in the glass, confirmed by the UV-Vis-NIR spectra, whereas iron is responsible for the yellow and black beads. Lead as a color intensifier, is dominant gradually from yellow, green to blue samples, respectively. The major raw materials could possibly be silica sand, reh, and stannate. There are some evidences reflecting the recycled raw materials. The glass beads found in the soil associated with log coffins in the cave at Pang Mapha has the major chemical composition similar to those of the lower land glass beads (eastern and central regions of the country). This indicates that people living in the log coffin culture had a link or contemporary trade with the people of the low land areas during 1750-1450 BP or 260-560 AD (Dvaravati Kingdom). The beads from the log coffin culture, Sa Kaeo and most localities in central Thailand, could have used the same technology as- or possibly manufactured - from the Khao Sam Kaeo, a production site in southern Thailand.

Acknowledgements

We would like to offer our special thanks to the Thailand Research Fund (TRF) for financial support and the Gem and Jewelry Institute of Thailand (GIT) for EDXRF and spectroscopy analyses.

References

Grave, P., Spies, J., Barrbetti, M., and Hotchkis. M., 1994, Dating of Log Coffins of Northwestern Thailand, IPPA Conference, January 5-12, 1994, Chiang Mai.

Treerayapiwat, C., 2005, Pattern of the Habitation and Burial Activity in the Ban Rai Rockshelter, Northwest Thailand, Asian Perspectives, Vol.44, No.1, p.231-245.

Corresponding Author

Full name: Seriwat Saminpanya

Affiliation: Department of General Science, Faculty of Science, Srinakharinwirot University, 114 Sukhumvit 23, Bangkok 10110, Thailand.

Phone: +6626495000 ext 18668

Email: seriwat@hotmail.com

Dynamic Korea, Dynamic Jewelry Design by Ye Myungji

Myungji Ye¹, Sora Shin² and Jongwan Park²

¹4504 Trade tower, samsungdong kangnam-Gu, seoul, Korea

²Material Science and Engineering, Hanyang University, seoul Korea

Extended Abstract

Korea, the country where the sun does not set. Korea, where the glorious civilization and the advanced technologies are combined, is a country characterized by dynamic economic growth and culture. Korea led a dynamic development including Korean wave and IT in line with the remarkable economic growth based on its long history. Dynamic Korea is Korea's representative image and contains a symbolic meaning: dynamic, positive, and future-oriented. My dynamic design with dynamic KOREA Image is a really striking resemblance

Dynamic I (Jewelry show)

From My debut as a designer, I am quite interested in creating jewelry culture in a new way. In 1998, Ye Myungji's launching show started with a cyber jewelry show where a cyber human wore jewelry in cyber space. In Millenium Show of 2000, king and queen of the future welcomed the new era for all of us. Besides the cyber jewelry show and the millennium jewelry show, I have been featuring various jewelry shows so far. (Seoul, Tokyo, Shanghai, Italy etc). I also participates in related projects through diverse collaborations (Lotte vvip credit cards. Glamorous necklace for Ralph Lauren, and a limited edition jewelry bag for MCM)

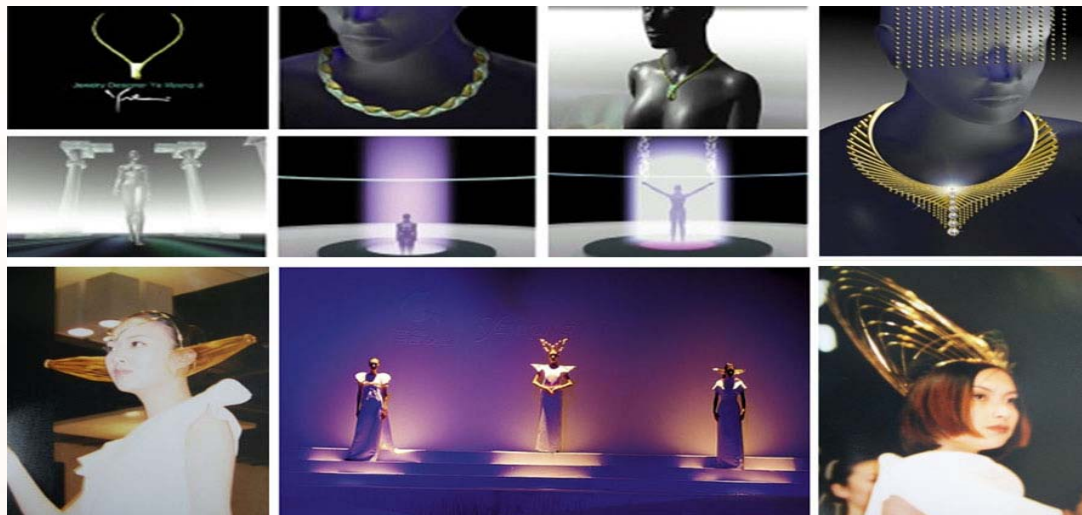


Figure 1: 1998 Ye Myungji Cyber Jewelry Show, 2000 Ye Myungji New Millenium Jewelry Show.



Figure 2: I have been featuring various jewelry shows so far. (Seoul, Tokyo, shanghai, Italy etc)

Dynamic II (Line)

It has been tabbed that color is beautiful in China, plane in Japan, and line in Korea. I am a Korean designer who loves line and have pursued more dynamic design than anyone else. I used dynamic lines from the beginning. And from it, I felt vitality. My design starts with lines. Although the life force in nature and the tension in civilisation are dynamic, they are manifested in the orderly repetition of lines," It is the dynamic lines as my wavy design, represented by the series to go, in harmony with nature and beauty to an expression of Korean traditional beauty that produces



Figure 3: I've heard an assessment that my series represented by dynamic lines resembled the graceful and dynamic lines of the eaves of Korea. It's a beauty of Korea that is created with sculpture in tune with nature.



Figure 4: It is the dynamic lines as my wavy design, represented by the series to go, in harmony with nature and beauty to an expression of Korean image that is the feeling of consensus and harmony.

Dynamic III (Space)

I was one of the first jewelry designers to design jewelry using Cad/Cam in 1998. As designer of Korea, IT power, I was very interested in technology and also took interest in Cad/Cam early to express the beauty of limited lines by hand. The technique is to transform the existing heavy and opaque jewelry into clear and light one. The things that have fascinated me are woven lines to create voluminous shapes and dynamic repeating lines to create energetic forms and spaces. Especially, the use of lines by my own 3D knitting methods has given me entire collections uniqueness.



Figure 5,6: With jewelry, I expressed the universe and the space between fine lines created a new design under the harmony of line and space through 3D knitting methods.(millenium ball in 1999, blooming space in 2001).

Dynamic III (Mineral)

I approach jewelry from the concept of 'highlight.' I use jewelry, the most beautiful material in nature and celebrate the most wonderful moment in life. I took interest in the crystal structure of mineral which is a growth of mineral as well as dynamic lines and shapes. It was about natural ecological geometry and wonder of color. The growth of crystal of mineral and the mystery of color were associated with something fundamental in the universe. I'd like to keep expressing something supernatural into my works through dynamic design and minerals

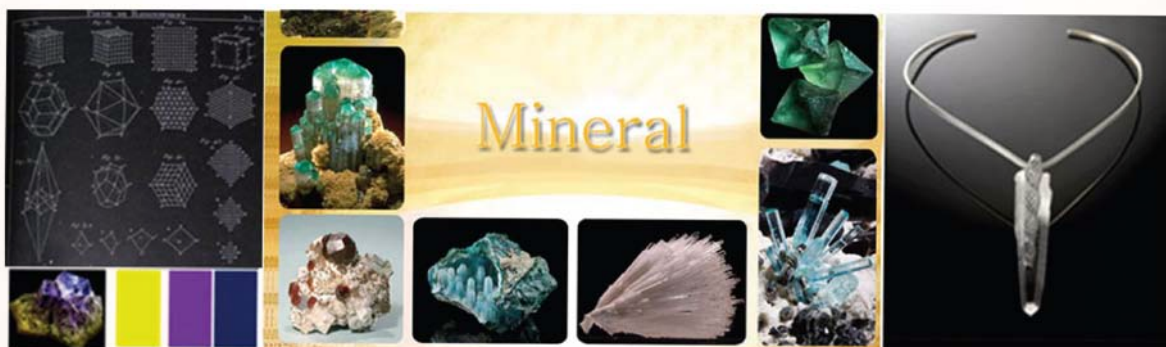


Figure 7: Growth of geometric crystal of mineral and color contrast of mineral.

Dynamic V (Tradition)

Korea's glorious metal works can be found from a long history of 5000 years. Over the last few years, I have been focusing on a reinterpretation of Korean traditional jewelry such as queens' formal outfit. Lately, I finished the exhibition, 'Glowing Lines', with great success at Burlington Arcade in London. I introduced my unique pieces meaning of the harmony of cross culture based on transcendental thought, and it received a lot of attention during the exhibition. I aim to create awareness on Korean culture through my jewelry.



Figure 8: Golden crown and diadem ornament in Shilla Dynasty.



Figure 9: In London Burlington Arcade Ye myungji Glowing Line Exhibition of 2014, applied the Jewelry of royal family such as hair in wedding ceremony, bride's headpiece, and dragon-headed hairpin, unfolded the dynamic designs of Korean traditional Jewelry in royal family to introduce my unique works under the theme of the tradition meets the modern and the east meets the west.

My design pursues the co-existence of nature and culture as well as the harmony of past and future by a reinterpretation of traditional Korean elements in a contemporary way. It also stands for the harmony of eastern culture and western culture based on the super-cosmic outlook. My works will be produced continuously for the ultimate happiness of humans, something transcending all these. I keep my work to make art jewelry stand for its natural sublimity. Ultimately, I hope that I can lead the new culture of Jewelry.

Jewelry resembles a country's history and culture. As Korea has consistently achieved a miracle of culture, My jewelry design will also continue to repeat dynamic development, like Korea achieved a new culture of miracle with dynamic growth



Figure 10: My jewelry design will also continue to repeat dynamic development, like Korea achieved a new culture of miracle with dynamic growth. (WWW.YEMYUNGJI.COM)

Corresponding Author

Full name: Jongwan Park
 Affiliation: Division of Materials Science & Engineering, Hanyang UV Seoul 133-791, Korea.
 Phone : +82-2-2220-0386,
 Fax : +82-2-2298-2850
 Email: jwpark@hanyang.ac.kr myungji.ye@hotmail.com

Forests and Trees: 10 Lessons in Gemology

Richard W. Hughes

Lotus Gemology Co. Ltd., Bangkok, 10500, Thailand

Extended Abstract

Introduction

Gemologists are largely involved with exploring the minutiae of the substances they work with. In this program, the author will step back away from the subject, discussing ten broad lessons he has learned over his 35-year career in gemology. Many of these are personal mistakes he has made. By telling the stories it is hoped that some broad truths can be gleaned that will be of use for both students and practicing gemologists, alike.

10 Lessons in Gemology

The ten lessons that the author will touch upon in his talk are:

- 1. The Importance of Psychology**
- 2. Searching for Significant Differences**
- 3. Embracing Pressure**
- 4. Avoiding Prejudice**
- 5. Beware of Contradictions**
- 6. Grabbing Opportunities**
- 7. Altering your Perspective**
- 8. Choosing the Appropriate Tool (and Understanding its Limitations)**
- 9. Learning to Self-Edit**
- 10. Losing the Ego**
- 11. Increasing one's Field of View**

Acknowledgements

The author would like to thank John Saul for supplying much of the inspiration for this talk.

Corresponding Author

Full name: Richard W. Hughes
Affiliation: Lotus Gemology Co. Ltd., Silom 19 Building, Suite 413, 45/1 Soi 19, Silom
Bangkok, 10500, Thailand.
Phone: (662) 117 3616
Web: www.lotusgemology.com
Email: richard@lotusgemology.com

Gemological Research Status on Jades in China

Jie Ke, Taijin Lu, Hua Chen, Yan Lan, Yong Zhang, and Jian Zhang

National Gems & Jewelry Technology Administrative Center (NGTC), 22F Tower C, Global Trade Center, 36# North 3rd Ring East Road, Beijing, 100013, P.R.China

Extended Abstract

In China, the concept and understanding of jade are of broad meanings referring to those mineral aggregates or rocks with commercial interest and value. Nephrite, jadeite jade, Dushan jade, and turquoise are the famous jade varieties in Chinese jade markets. With the rapid economical development, the impelled cultural industry, and the improvement of cutting technology, the jade market has risen to an unprecedented boom recently. Then, many new jade varieties with beautiful appearance have been emerged in the market, such as colorful quartzite jade, vivid green 'xi'an lv' vivid red 'southern red agate'.

In recent years, various research activities on the gemology of jades have been performing by the researchers of NGTC and other gemologists in China. The gemological research activities focus mainly on fundamental research, standardization, and identification of jades.

Materials and Methods

1. The fundamental research of jades

(1.1) Research on the mineralogical characterization of light colored jadeite

With the industry facing a serious shortage of rough jadeite jade due to the political and economic instability in Myanmar, there are more and more rocks consisting mainly of jadeite and many other light colored minerals in Chinese jade market. Their appearances look like to jadeite jade, but some gemological properties are different. So it is controversial and urgent to identify and provide right name(s) for this kind of materials for gem testing laboratories in China.

After systematically mineralogical investigation for the mineral compositions and structures for hundreds of the rock specimens, the mineralogical features and gemological properties of this materials were summarized and discussed. Fast identification/testing method and procedure using spectroscopic and S.G. value measuring techniques has been developed.

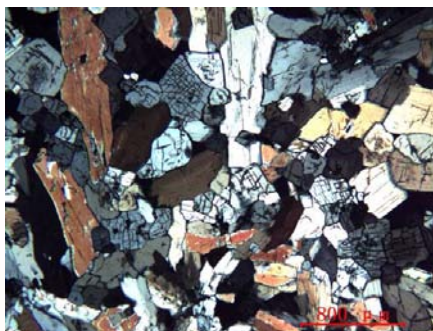


Figure 1: A polarization image of jadeite.

(1.2) Research on the coloration of quartzite jade

The colorful quartzite jade is one of the most important jade varieties emerged in the gem and jewelry market recently. The coloration and microstructures of the jade have been investigated in China. In order to distinguish the natural and treated color of the material, a lot of research work has been done by NGTC. The results suggested that the red coloration of quartzite jade is caused mainly by nano-sized hematite, while the yellow coloration could result from lepidocrocite and goethite crystallized during the post crystal growth stage of the quartzite veins.



Figure 2: Rough material of yellow colored quartzite jade with typical dendrite

(1.3) Study on whiteness of nephrite

White colored nephrite is the most valued and widely loved nephrite variety in China, however, it is difficult to determine the boundaries among the white, gray, greenish white, brownish white colored nephrites. Based on study of various colored nephrites using Raman scattering spectroscopic techniques, it was found that the peaks of Mg/Fe ratio reflecting the changes of tremolite-actinolite in nephrite, which could be used as a new effective method to differentiate white jade, greenish jade, and green jade.

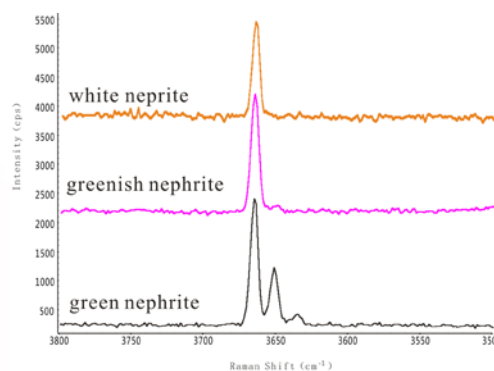


Figure 3: As the Fe ions substitute for Mg ions in tremolite lattice, the 3661 cm⁻¹ and 3645 cm⁻¹ appear sequentially.

2. Research on Standardization

(2.1) Jadeite jade grading standard

Jadeite jade (Fei Cui) still dominates jade market in China. To meet the demand of market, NGTC formulated jadeite jade grading standard, which consists of color, texture, transparency, clarity, cut and crafts. The development and application of the standard have been playing a positive role in promoting jadeite trading, and guide the jadeite jade trading to become simpler and more standardized



Figure 4: Jadeite jade grading standard

(2.2) Dushan jade standard

Dushan jade is a traditional jade in China, this kind of jade consist of anorthose and zoisite. This year, a national standard of Dushan jade has been formulated, based on a systematic investigation from the mineral assemblage to the gemological properties including the identification features of Dushan jade. This standard will play a positive role in protecting this special kind of jade, standardizing the identification name, and promoting the healthy and orderly development of the market. (Elaborate: Definition of Dushan Jade)

(2.3) Nomenclature standard of quartzite jade

Recent years, yellow/red colored quartzite jades with good quality have being found in more than ten provinces in China, and the gemological features of the jades are slightly different depending on the localities. The local governments formulated their own regional or local standards and provided different names for this kind of material, which confuse the consumers. In order to standardizing the name of quartzite jade and stabilizing the consuming market, the foundational research and formulation of quartzite jade have being performing by NGTC.

3. Study on identification challenges

(3.1) Identification of new type treated jadeite jade



Figure 5: The colorful quartzite jade from Hezhou, Guangxi province



Figure 6: Hetian jade pebble

Wax-filled is a normal process during the jadeite jade cutting/crafting processing. However, a kind of “new” wax-impregnated jadeite has appeared on jadeite market recently. Because its structure is not destroyed, it’s difficult to distinguish it from natural jadeite by naked eyes, excepting slightly abnormal fluorescence under an UV lamp irradiation. Through a systematic investigation by NGTC researchers, the identification characteristics are summarized and applied in the labs.

(3.2) Identification of nephrite (Hetian jade) pebble

Nephrite pebble from Xinjiang province is most favorite by the collectors, and its price is much higher than the jade from other localities. Many treated nephrite pebbles by dyeing or other artificial techniques appeared in the market. In order to protect the interests of consumers, the detailed investigation on the natural surface microstructures of the jade are carried out using a three-dimensional microscope system at NGTC. Now, the natural and treated pebbles could be effectively distinguished.

(3.3) Identification of the treated turquoise

It is still a challenge for gem laboratories to identify turquoise treated by polymer-impregnated, wax-impregnated, epoxy-impregnated, Zachery process, as well as dyed turquoise. After systematic investigation for various natural and treated turquoises by the gemologists in China, it was found that dyed turquoise could be identified by an absorption band centered at 677 nm, and the polymer-impregnated jade could be accurately identified using a curve-fitting technique for the IR absorption spectra of turquoise.

Conclusion

“Jade study” is the historical mission for gemologists in China. The study involves all aspects related to jades, such as deposit geology, petrology, mineralogy, material science, gemology, and processing aesthetics etc. The gems & jewelry academic conference held regularly in China has become a popular communication platform for gemologists to exchange and discuss the recently development and currently topics and/or interested subjects. The next conference will be around November, 2015 in Beijing, China.



Figure 7: The 2013 China Gem & Jewelry academic conference.

Corresponding Author

Full name: Taijin Lu
 Affiliation: National Gems & Jewelry Technology Administrative Center (NGTC), 22F Tower C, Global Trade Center, 36# North 3rd Ring East Road, Beijing, 100013, P.R.China.
 Phone: +861058276120
 Email: taijinlu@hotmail.com

Laminated Type Zirconia Ceramics

Min Woo Park

Advanced Materials & Chemical Engineering Building 522, 222 Wangsimni-ro, Seongdong-gu, Seoul, 133-791, Korea

Extended Abstract

The zirconia ceramics have been utilized as structural materials and semiconductor materials because of its high toughness, high strength and excellent electric insulation. Furthermore, with high abrasion resistance, it is necessary materials for various industries and even daily life. The zirconia ceramics are given a higher utilization as environment-friendly materials. As beauty and personality are considered high value in modern society, a color is the important method for expression of individuality. To use of zirconia ceramics in various fields, the color expression is vital element for individual esthetic demands. Therefore, zirconia ceramics should be expressed not only a single color but also various colors of complex zirconia ceramics. This structural ceramics are called laminate type ceramics. For the laminate type with black and white zirconia ceramics, it is critical that colored zirconia has a thermal stability at high temperature and its physical/chemical characteristics are not damaged in manufacturing process.

In this experiment, the composition optimization of complex zirconia and making zirconia ceramics of better characteristics are fulfilled through the mechanical densification process. First, to strengthen white zirconia, reasonable amount of Y_2O_3 , Al_2O_3 and SiO_2 were mixed with pure zirconia powder. Then black zirconia powder was made by white zirconia with spinel pigment consisted of Fe_2O_3 - Cr_2O_3 - CoO - NiO . We found out the optimum composition by analysis of physical and optical qualities from 5 wt.% to 30 wt.% of black pigment at 1400°C sintering temperature.

After that we formed laminate structure of optimum black and white zirconia powder by compression molding using Cold Isostatic Press (CIP) with 500 Mpa. Then, laminate zirconia was sintered at a temperature of 1400°C for 5 h to the mechanical densification process. The sintered zirconia was also measured optical characteristics by UV spectroscopy, hardness by Vicker's durometer, density by pycnometer. The densification of interface between two color zirconia was analyzed by cross-section image with scanning electron microscopy (SEM). Figure 1 shows the cut results accessory of laminate structured zirconia ceramics.

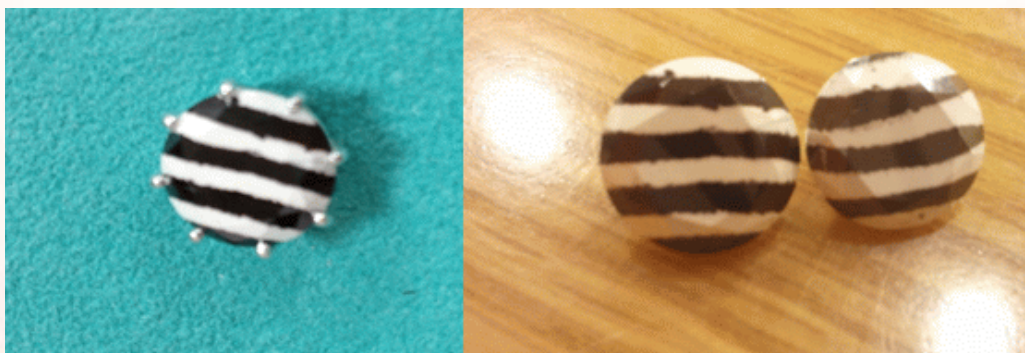


Figure 1: Application for accessories of zirconia ceramics with laminate structure.

This study assured that the laminate type ceramics of black and white zirconia has the possibility as high functional, high added value product of accessories. Also, in view of considerable mechanical hardness, it is also expected to utilize in more various field as mechanical parts.

References

- Ahn, Jeong-hwa, Effect of SiO_2 and Al_2O_3 on Characteristics of Yttria Stabilized zirconia ceramics.
Butler, E.P., and Drennan, J., 1982, Microstructural Analysis of Sintered High-Conductivity Zirconia with Al_2O_3 Additions, Journal of the American Ceramic Society, Vol.65, No.10, p.474478.

Corresponding Author

Full name: Min Woo Park
Affiliation: Advanced Materials & Chemical Engineering Building 522, 222 Wangsimni-ro, Seongdong-gu, Seoul, 133-791, Korea.
Phone: +82-10-31201315
Email: yupgisun@naver.com

Micro-Raman Technology with Fast Imaging and its Applications

Y. Y. Yang

Technical Director for Spectroscopy Products – Far East Renishaw (Hong Kong) Ltd.

Abstract

Analysis of Raman scattered light, as a Raman spectrum, reveals key information about a sample's chemical structure. Until late 90's, Raman spectroscopy was rarely used outside a specialist research laboratory because of low sensitivity, instability and difficult-of-use of traditional double or triple grating Raman spectrometers.

In recent years, a novel confocal micro-Raman spectrometer system equipped with a combination of new technologies such as Raleigh rejection edge filters, CCD detector and research grade microscope, has been developed first by Renishaw and Leeds university of UK. Its high sensitivity (2~3 orders of magnitude higher than traditional Raman spectrometers), spatial resolution (down to < 1 μm), accuracy/ repeatability and easy of use make it available for many applications in various of research and developments areas. It is particularly useful when an application requires no sample preparation, non-destructive and non-contacting analysis.

Samples as small as submicron can be analysed in seconds, non-destructively and non-intrusively, with high spectral resolution. Micro size particles, inclusions, and even single nano tube/wire could be analyzed without destroying them. Larger samples can also be imaged for their Raman or PL distributions.

An unique development of Renishaw's Global imaging technology provides the fastest way to acquire a Raman spectral image of whole sampling area at the same time without touching or moving the sample. The recent innovation of Renishaw's StreamLinePlus™ rapid Raman mapping/ imaging system makes it possible to collect spatially resolved chemical information from samples as large and complex as whole pharmaceutical tablets in about 4 minutes. With StreamlineHR™ the spatial resolution of a Raman image can be as good as 250 nm.

Corresponding Author

Full name: Y. Y. Yang

Affiliation: Technical Director for Spectroscopy Products- Far East Renishaw (Hong Kong) Ltd.

Myanmar - The Past, Present and Future

Kennedy Ho and Simon Wingate

AIGS Laboratory, 919/1 Jewlery Trade Center, Level B1 (Unit B24), Silom Road, Bangrak, Bangkok, 10500, Thailand

Abstract

While most eyes have been on Africa- especially eastern Africa- during these past few decades, the ancestral home of highly prolific and varied deposits, Myanmar, still remains an integral part of the modern day gemstone industry.

Home to over 50 different gemstone species- including being the primary source of three of the most important; ruby, spinel and jadeite- Myanmar is throwing off the shackles of its recent past as it continues on a path towards liberalization and openness.

With the Ho family's Burmese roots, the Asian Institute of Gemological Sciences (AIGS) – though the work of its founder, Mr. W.K. Ho, his sons Henry and Kennedy Ho and past and present laboratory directors such as Vincent Pardieu and Dietmar Schwarz- has always been at the forefront of locating, researching and publicizing Myanmar's vast mineral wealth. However, 2015 will be year when this close association is taken to a whole new level with the upcoming opening of our new fully-equipped laboratory in Yangon.

Company CEO, Kennedy Ho, will use his decades of experience as a central character within the ongoing Burmese gemstone story to provide a first-person perspective of the country's past, present and future with regards to its prolific and varied production, and how his rapidly-modernizing country of birth can continue to rebuild bridges with the wider international gemstone community- especially the United States, with whom Myanmar still remains under a ruby and jade embargo.

Corresponding Author

Full name: Kennedy Ho

Affiliation: AIGS Laboratory, 919/1 Jewlery Trade Center, Level B1 (Unit B24), Silom Road, Bangrak, Bangkok, 10500, Thailand.

Email: info@aigsthailand.com

Preliminary Study on the Use of Lead Free Fire Assay for the Determination of Gold Fineness

Kageporn Wongpreedee¹, Panphot Ruethaitananon², Khumsing Vichapoon³, Jakraphan Suwanvijit³, Thidarat Muangthai³, and Narong Praphairaksit^{3,4}

¹Gems and Jewelry Program, Faculty of Science, Srinakharinwirot University, Bangkok, 10110, Thailand

²Materials Science Program, Faculty of Science, Srinakharinwirot University, Bangkok, 10110, Thailand

³The Gem and Jewelry Institute of Thailand (Public Organization), Bangkok, 10500, Thailand

⁴Department of Chemistry, Faculty of Science, Chulalongkorn University, Bangkok, 10330, Thailand

Extended Abstract

A fire assay method replacing lead with bismuth had been known in smelted industries. However, the technique has neither been used in jewelry applications nor adopted as a standard testing procedure. In this research, a lead free fire assay method was developed for the determination of gold fineness using bismuth in an attempt to eliminate the use of toxic lead. The method was then applied to verify the purity of gold bars and gold jewelry items with 96.50% gold content, the most common fineness of gold used in Thailand. Various parameters affecting the accuracy and precision of the technique were optimized, i.e. means of silver addition, silver content, bismuth content, addition of copper, as well as the cupellation temperature. The results indicated that the combination of silver at 450 mg as a thin wrapping sheet, 1 g of bismuth, 5-10 mg of copper and the melting temperature of 1,050 degree Celsius provided the best result with errors within the range of ± 0.05 %.

Introduction

The fire assay process has been well known as a testing method for gold purity since the sixteenth century (Bugbee, 1922; Corti, 2001). Originally, fire assay was used in the hydro-metallurgical of gold mining. Later on, it has been modified to characterize gold purity in jewelry industry and adopted as an internationally recognized standard method for the determination of gold fineness, i.e. ISO 11426 and ASTM E1335, with the accuracy in the range of ± 0.02 % (ISO/CD 11426, 2010) Several works have been experimented to replace lead with bismuth (Appelhans, 1993; Weiss, 1996; Kelly and Ojebuoboh, 2002) for such determination; nevertheless, none has yet been successfully demonstrated as a good alternative for jewelry application.

This work aims to develop the bismuth (lead free) fire assay technique as an analytical tool for the determination of gold purity in gold jewelry applications. Several operating parameters have been optimized to achieve the best accuracy and precision and evaluated against those obtained from the traditional fire assay method.

Methodology

Two alloys of approximately 96.50 weight% gold, one with silver and the other with silver and copper as base elements, were used to verify the test results during the optimization. The experiment was designed to evaluate the composition of mixing ingredients in the cupels, i.e. silver grain and sheet at 400-500 mg, bismuth powder at 0.5-2 g and copper grain at 5-20 mg, as well as the cupellation temperature in the range of 1,000-1,100 degree Celsius.

There were two methods of placing alloys in the cupels. The first method was to place gold, silver, and copper grains together and cover with bismuth powder. The second method was to put gold and copper grains and bismuth powder into a silver wrapping sheet. Then, they were placed in the magnesium cupels and heated at the desired temperature. The resulting dore beads were then rolled into flat sheets and boiled in the acid to remove the remaining silver. The obtained cornets were then dried and accurately weighed. The calculation of gold fineness were done according to the ISO 11426 standard. The other evaluation aspects were performed by physical properties of the button and sheet rolling as well as the X-ray fluorescence on the magnesium cupel to check for the gold residue.

Results and Discussion

The first technique of placing all metal grains with bismuth powder covering shows the disintegration of an alloy button. The purity of gold was substantially lost after the verification process apparently due to the scatter of gold in the cupel surface as shown in Figure 1.



Figure 1: The scattering of gold around the magnesium cupel.

The second method of using silver sheet wrapping around the gold grain, copper grain, and bismuth powder shows nice round shape of dore bead especially with 0.5 mg of bismuth. A slight distortion of round shape was noticed with increasing amount of bismuth powder at 1.0 mg and 1.5 mg, respectively, as shown in Figure 2.

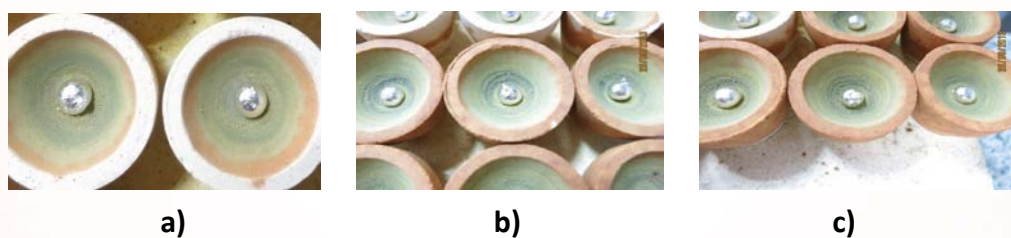


Figure 2: The dore beads of alloys using bismuth at **a)** 0.5 g, **b)** 1.0 g, and **c)** 1.5 g

The rolled sheets of temperature at 1,050 and 1,100 degree Celsius shows nice and smooth surface as shown in Figure 3a. However, uneven and tearing surface was produced when melted at 1,000°C presumably because the mixing alloy was unable to melt and combine readily at such low temperature.



Figure 3: The gold and silver rolling sheets obtained at **a)** 1,050°C and 1,100°C and **b)** 1,000°C

The various weight of silver sheets were assessed to observe the errors of gold purities. It was shown that no significant differences of error was observed for 400, 450, and 500 mg of silver when used with bismuth in the range of 0.5-1 g as shown in Figure 4.

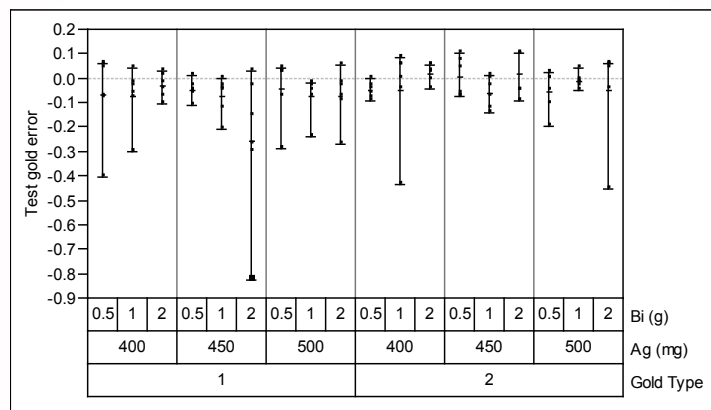


Figure 4: The variability graph showing insignificant differences of error obtained with Ag at various composition.

The addition of copper at 5 and 10 mg show less deviation comparing to those using copper at 15 and 20 mg. (Figure 5)

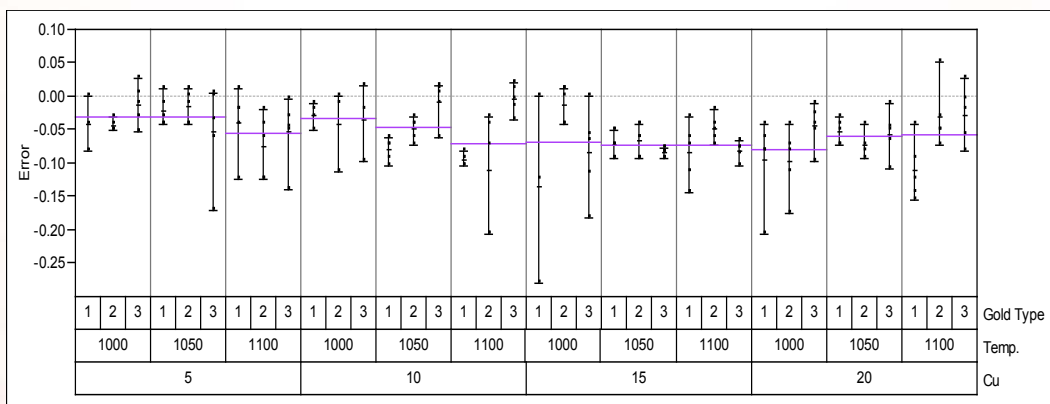


Figure 5: The variability graph showing deviation obtained with varying amount of copper.

Others

Following this optimization, the method was successfully applied to determine the gold fineness in 20 samples of commercial gold bars and gold jewelry items with errors merely within the range of ± 0.05 %.

Conclusion

The fire assay technique using bismuth as a substituent for the undesired and toxic lead was developed and successfully employed for the determination of gold fineness in commercial gold products with satisfactory results. This research is still under further investigation.

References

- Appelhans, D.J., 1993, The Environmental and Economic Aspects of Lead-Free Fire Assaying, in Randol Gold Forum, Golden, CO, 1993, p.39-42.
- Bugbee, E.E., 1922, A text book of Fire Assaying, John Wiley & Sons Inc. New York, 254 p.
- Corti, C.W, 2001, Assaying of Gold Jewellery – Choice of Technique, Gold Technology Magazine, Vol. 32, p.20-30 (Available from http://www.utilisegold.com/assets/file/discover/sci_indu/GTech/2001_32/WOR82071.PDF).
- ISO/CD 11426, 2010, Jewellery- Determination of Gold in Goldjewellery alloys – Cupellation method (fire assay), ISO/TC 174 N 229, 7 p.
- Kelly, Z., and Ojebuoboh, F., 2002, Producing Bismuth Trioxide and Its Application in Fire Assaying, Journal of the Minerals, metals, and Materials Society, Vol.54, No.4, p.42-45.
- Weiss, W.L., 1996, Development of the Bismuth Five Assay Ton Fire Assay, in the 10th Annual Conference of the Society of Mineral Analysts, Moscow, ID, April 1996.

Corresponding Author

Full name: Kageeporn Wongpreedee
Affiliation: Gems and Jewelry Program, Faculty of Science, Srinakharinwirot University, Bangkok, 10110, Thailand.

Should Laboratories Make Clarity Enhancement Calls? Controversy and Consequence

Shane F. McClure

GIA GTL, Carlsbad, California, USA

Extended Abstract

Clarity enhancement has been common in emeralds for a very long time – possibly centuries. While the practice was widely known in the jewelry industry, it was for the most part not mentioned to the consumer. The trade seldom spoke of it and considered it an “accepted trade practice”, never considering what the public might think if it found out it was being sold treated stones and not being told. Of course the public eventually did find out through a series of expose’s that painted the emerald trade in a very unfavorable light. This resulted in emerald sales dropping dramatically, a situation which lasted for many years.

Better disclosure was clearly needed. Laboratories had been disclosing clarity enhancement for some time but more was necessary. It became apparent that the fact that an emerald was clarity enhanced or what specific filler was being used for the enhancement was less important than how much it was enhanced. This was the consensus reached by emerald dealers and producers attending the first World Emerald Congress in Colombia in 1998 (Johnson and Koivula, 1998). Emeralds were almost always clarity enhanced, but the degree to which they were enhanced varied greatly. In fact, it got to the point that highly fractured rough emeralds were being filled with hardened resin before they were cut, allowing larger finished stones, some of which that were essentially ‘glued’ together.

Laboratories developed systems to quantify clarity enhancement (SSEF Swiss Gemmological Institute, 1998). Several different ones were developed, but many settled on a four tiered system – none, minor, moderated and significant. These divisions are admittedly subjective and unfortunately they are not coordinated very well between laboratories, even though there have been several attempts to do so. There has been a lot of research devoted to this issue and GIA performed a lengthy study of removing the filler from emeralds, documenting them and then refilling them with different substances to observe the change in appearance (McClure *et al.*, 1999).

As inevitably happens, the trade started to develop a pricing structure around these designations. It wasn’t long before “none” or “minor” carried a premium because most emeralds did not fall into these categories. This of course led to the filler being cleaned out of some emeralds so the dealers could get the better calls. After all, these systems described in broad terms how many fractures in an emerald were filled and how well they were filled. If a stone had many fractures but they were not filled then there was no enhancement taking place and the appropriate designation would be none.

Of course, cleaning out the filler from the fractures defeats the whole purpose of the treatment, which is to make large reflective fractures less visible by replacing the air in them with an oil or resin. The fractures once again become very visible, making them harder to sell, even though they have a preferred designation on a lab report.

Now we come to the unfortunate part of this story. Once the coveted “none” or “minor” designation is reached there was nothing to stop the stone from being re-filled to make it look nice again and sell it with the now inaccurate report. This intentional misrepresentation is fraud. We know it is happening but we don’t know how much. The labs seldom see these emeralds again so it is hard for us to know. However, we have heard many reports of this practice from the trade and some labs have actually seen evidence of it. Of course, there are many honest and ethical dealers who would never dream of doing this. But there are those who are not concerned with ethics if it gets in the way of making money. This lack of concern about honesty and the resulting misrepresentation to the public could severely damage the emerald trade. It has happened before. It could easily happen again.

It has been suggested by some that the labs cannot accurately make these decisions anyway. After all, the fractures are being intentionally hidden, with varying degrees of success depending on what filler is being used. It has even been suggested that the labs should stop making these distinctions. They should go back to what they used to do – declare the treatment – clarity enhancement – and that’s all.

It is unclear to me how this would serve the public. We would go back to a situation where emeralds that have an average or even small amount of filler would be considered in the same light as those that are virtually glued together. Furthermore, would the industry ever accept this change? It is difficult to go back on something so firmly established.

I have my opinions on these issues of course. I do not agree that we cannot do this service with a reasonable degree of accuracy within the broad categories that have been described. We can identify these fractures and have a reasonable idea of their extent. The issue is more where individual laboratories decide to draw the boundaries between the categories. These can vary significantly between labs and some are considerably more lenient than others.

While this is clearly a point of concern, the remaining issue is potentially far more serious. What can be done about those who intentionally commit fraud by re-treating an emerald after it has gotten a favorable lab report? There is no easy answer to this.

This presentation raises more questions than it provides answers. It was intended to be that way. These issues affect the whole industry and do not have simple solutions. Maybe a debate can provide some answers. The questions are:

- Should laboratories stop providing degree of clarity enhancement information?
- If so then what should they provide?
- If they continue to provide such information, what can be done about the apparent disparity between the calls in different labs?

- What, if anything, can be done about those who re-treat emeralds after they get reports and sell them knowing the reports are no longer accurate?

What do you think?

References

Johnson, M.L., and Koivula J.I., Eds., 1998, A Preliminary Report From the First World Emerald Congress, Gem News, Gems & Gemology, Vol.34, No.1, p.56-57.

McClure, S., Moses, T., Tannous, M., and Koivula, J., 1999, Classifying Emerald Clarity Enhancement at the GIA Gem Trade Laboratory, Gems & Gemology, Vol.35, No.4, p.176-185.

SSEF Swiss Gemmological Institute, 1998, Standards and Applications for Diamond Report/ Gemstone Report/Test Report, SSEF, Basel, Switzerland, 118 p.

Corresponding Author

Full name: Shane McClure

Affiliation: GIA GTL, 5345 Armada Dr, Carlsbad, California, 92008, USA.

Phone: +911412568221

Email: smcclure@gia.edu

The Stars fall from Heaven: Gems with Asterism: An update

Martin P. Steinbach

Tiefensteiner Str. 281b, D-55743 Idar-Oberstein, Germany

Extended Abstract

About 50 different well-known gem mineral varieties such as star ruby, star sapphire, (Figure 1a left) star garnet, star quartz and rarer varieties such as star bronzite, star iolite (Figure 1b right), star peridot, star spinel - display the phenomenon of asterism (greek: "star") whereas about 10 gemstone varieties show a "fixed" star also known as "trapiche".



(a)



(b)

Figure 1: a (left) Star sapphire, Myanmar, 33.20 ct. and **b (right)** Gigantic star iolite, India, 199 ct. Photo by M.P. Steinbach.

Origin of Asterism

Oriented inclusions arranged in accordance with the crystal system of the host mineral can cause the desired phenomenon displayed mostly as 4 and 6 rayed stars. In addition to these star formations, also stars with 12 (Figure 2a left), 18, or even 24 rays are observed. Very rare, however, are twin stars/double stars (Figure 2b right) or parallel stars with apparently two parallel rays in each direction of the asterism.



(a)



(b)

Figure 2: a (left) 12-ray star sapphire, Myanmar, 10.82 ct and **b (right)** Black star sapphire, Thailand, with two stars, 15.60 ct. Photo by M.P. Steinbach.

Stars can either be seen in reflected light (epiasterism) or in transmitted light (diasterism). Rutile inclusions (as “silk”) are responsible for most stars in gems. Other mineral inclusions can be hematite, ilmenite, sillimanite and growth irregularities.

Asteriated gems have to be cut as a cabochon or an object with a rounded, smooth surface, like a double cabochon or a sphere. In order to be able to observe the phenomenon there should be a contrast between the star and the colour of the stone. An asterism of high quality is defined by the sharpness of the rays whereas the rays have to be complete and reach the girdle of the gem. The star should be centered and the gem cut in good proportions.

History

Asteriated gems are known for more than 2000 years, starting with Dionysius Periegetes’ description of “Asterios” (1st c. BC). From Pliny the Elder, (1st c. AD) to the Middle Ages, to De Boodt (1609) and Brueckmann (1783), asterism was known in corundum and feldspar varieties only.

Famous Stars

Some of the most famous star rubies are the DeLong Star Ruby (100.32 ct), the Rosser Reeves Star Ruby (138.72 ct), the Eminent Star Ruby (6465 ct) and as the largest 12-rayed star ruby- the Neelanjali (1370 ct).

Among the most famous star sapphires are the Midnight Star (116.75 ct), the Star of Bombay (182 ct), the Star of Lanka (193 ct), the Star of Asia (330 ct) and the Star of India (563.35 ct). The largest black star sapphire is currently the Black Star of Queensland (733 ct).

Deposits

Both, primary and secondary as well as magmatic and metamorphic deposits are possible as sources for asteriated rough. Most often however, are gems displaying asterism found in secondary, alluvial deposits. By far the most important country for asteriated gems – commercially and rare – is Sri Lanka. Other important sources are Brazil, India, Madagascar (Figure 3a left), Myanmar (Burma) (Figure 3b right) and Vietnam. Thailand is famous for black star sapphires, along with some golden stars (star thong or star butt), and yellowish to greenish stars.

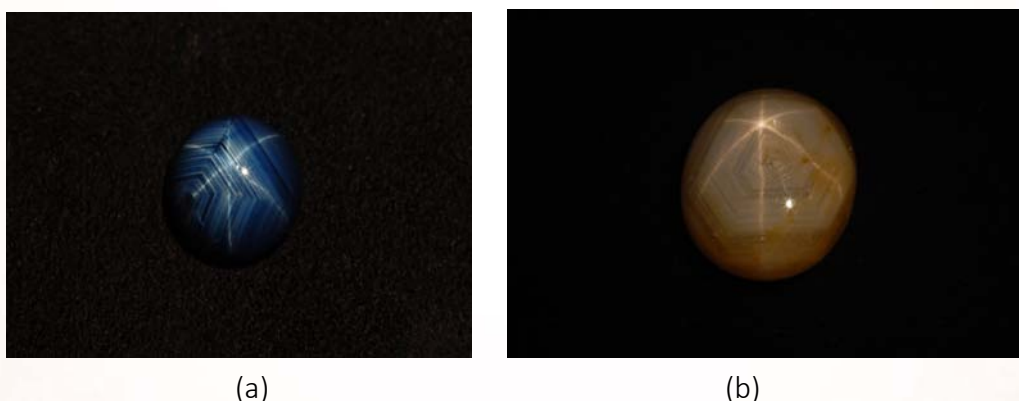


Figure 3: a (left) Star sapphire with nice color banding, Madagascar, 10.82 ct. and **b (right)** Star sapphire with complete hexagonal color banding, Myanmar, 22.30 ct. Photo by M.P. Steinbach.

Synthetics/Treatments/Imitations

Synthetic star corundum was first created in 1947 by Linde – the Linde stars. At the beginning, red and blue stars were produced by the Verneuil flame fusion method (Figure 4a left) and then other colours followed. Further known in the market are doublets with a synthetic top and a natural base and gems with scratched, artificial stars. Most recently diffusion-treated blue star sapphires and glass-filled star rubies (Figure 4b right) drew the attention of the market.



Figure 4: a (left) Synthetic star sapphire, Verneuil boule, 42 gms. and **b (right)** Star ruby, glassfilled, Madagascar, 9.80 ct. Photo by M.P. Steinbach.

World Premieres

In addition to the quoted well-known and rare star gemstones two extremely rare and yet unknown gems with displaying asterism are introduced here: star tanzanite and 8-rayed star zircon.

How to observe asterism in gemstones

Epiasterism

Hold the stone in the palm of your hand or between thumb and finger and let a light (as a spot or narrow beam) or the sun shine on it. The light has to be perpendicular (90°) to the surface of the stone (Figure 5a left).

Diasterism

In order to allow the light beam travelling through the stone (transmitted light), hold or rotate the stone between your fingers and let a strong, spot-like light source illuminate the gemstone. As an optional light source you can also use the sun. Star quartz or star rose quartz spheres (Figure 5b right) have to be handled carefully due to the strong stars displayed in transmitted

light. Note: Only translucent or transparent gemstones show diasterism.



(a)



(b)

Figure 5: a (left) Star quartz in reflected light, Brazil, 75.56 ct. and **b (right)** Star rose quartz sphere in transmitted light, Madagascar, 225 gms. Photo by M.P. Steinbach.

References

Hughes, R.W., 1997, Ruby & Sapphire, RWH Publishing, Boulder, Colorado, USA, 512 p.

Steinbach, M.P., 2011, Neue künstlich geritzte Sternsteine und ihre natürlichen Gegenstücke, Zeitschrift der Deutschen Gemmologischen Gesellschaft, Vol.60, No.1-2, p.25-36.

Corresponding Author

Full name: Martin P. Steinbach

Affiliation: Tiefensteiner Str. 281b, D-55743 Idar-Oberstein, Germany.

Phone: +0049-6781-509942

Fax: +0049-6781-569627

Email: gstargems@aol.com

Top Ten Trends and Colors in Designer Jewelry for 2015

Cynthia Unninayar

CIJ Trends & Colours magazine

Extended Abstract

As a luxury accessory, jewelry is closely linked to fashion. It is important for manufacturers and retailers to gain insight into the top trends and colors that will be popular in 2015 in both areas in order to better meet the needs and desires of their customers. This presentation offers a dynamic description of the top ten trends in designer jewelry with examples from some of the world's most creative brands and individuals. It also features the top fashion colors, as depicted by Pantone in their Spring Fashion Report for 2015, and jewelry from around the world that goes with these colors.

Jewelry designs are as individual and particular as are their creators. Trends arise when designers are inspired and influenced by cultural, economic, and social factors. Most trends are gradual and happen over time, while some occur relatively rapidly for a variety of reasons. The directions for 2015 in terms of designer jewelry can be divided into ten general trends, along with a few minor ones. While none are dramatically new, they offer revisited styling and new, innovative interpretations.

Four of the ten general trends to be discussed in the presentation are the following:

1. Flora and Fauna... Nature-inspired designs have been favorites in fine jewelry, both stylized and realistic, since time immemorial. For 2015, the most prevalent motifs are flowers and butterflies, followed by birds, bees, snakes, spiders, and creatures of the deep.

2. Lacy Looks... A trend resulting from the economic times of the day is the lacy look, with its open spaces, that offers airy elegance while creating a luxurious look for less.



3. Geometrics... One of today's most popular design directions in fashion, home decor, and designer jewelry involves geometric patterns. Anything goes, as long as the angles are sharp, defined, and aesthetically interesting.

4. Digital Expression... Jewels for the fingers are taking on new dimensions. Not only are rings adorning two, three, or even four fingers at a time, but designers are embellishing a single finger with precious metals, set with diamonds and gemstones.



Color is everywhere in jewelry and in fashion. For the last 20 years, Pantone—the global authority on color—has surveyed the designers of New York Fashion Week and beyond to provide insight into the season’s most important color trends. For Spring/Summer 2015, Pantone forecasts the following top ten tones, which are also featured in this presentation along with jewelry that aligns with these colors.

Pantone’s predictions for S/S 2015

This season there is a move toward the cooler and softer side of the color spectrum. An eclectic, ethereal mix of understated brights, pale pastels and nature-like neutrals take center stage as designers draw from daydreams of simpler times. Remembrances of retro delights, folkloric and floral art, and the magical worlds of tropical landscapes restore a sense of well-being as we head into warmer months.

“Many feel compelled to be connected around the clock because we are afraid we’ll miss something important. There is a growing movement to step out and create ‘quiet zones’ to disconnect from technology and unwind, giving ourselves time to stop and be still,” stated Leatrice Eiseman, executive director of the Pantone Color Institute®. “Color choices follow the same minimalistic, ‘en plein air’ theme, taking a cue from nature rather than being reinvented or mechanically manipulated. Soft, cool hues blend with subtle warm tones to create a soothing escape from the everyday hustle and bustle.”

On one end of the women’s palette sits **Aquamarine**, an airy, ethereal blue with a cool, dreamy feel that mixes well with the other blues and greens in the Top 10. Evoking thoughts of soothing, tropical waters, **Scuba Blue** restores our sense of carefree playfulness, while invigorating the body and mind, and **Lucite Green**, a soft, serene green offers a fresh sense of clarity. Pair **Lucite Green** with bold **Classic Blue** for a balanced and refreshed look. As the name implies, **Classic Blue** is a strong and reliable anchor and, with its waterborne qualities, is perceived as thoughtful and introspective.

Bringing balance to the coolness of the Spring/Summer color range, **Toasted Almond**, a sun-tanned neutral, offers timeless, comforting warmth. Reminiscent of the sun on our skin in the spring and summer months, **Toasted Almond** pairs well with both **Strawberry Ice**, a light, nurturing coral tone, and **Tangerine**, an energizing, non-jarring take on orange that adds a bold pop of color for spring. Combine all three for a delicious, almost retro-inspired look.

Emanating warmth and happiness, **Custard** serves as an all-encompassing yellow for the spring palette, which can be combined with **Classic Blue** for a maritime look. Much like the fortified wine that gives **Marsala** its name, this compelling and cordial hue incorporates the satisfying richness of a tastefully fulfilling meal while its grounding red-brown roots point to a sophisticated, natural earthiness. **Marsala** works well with Glacier Gray, a timeless and unobtrusive gray that adds a sense of graceful relaxation as another practical neutral. Bring **Marsala** and Glacier Gray together with **Aquamarine** for an unexpected and exciting pairing that is perfect for spring.



Corresponding Author

Full name: Cynthia Unnayar
Affiliation: Editor in Chief, CIJ Trends & Colours magazine
Email: cynthiau@gmail.com

Building Consumer Confidence in Dubai Gem and Jewelry Industry

Sutas Singbamroong¹ and Ismail Abdulla Almas²

¹ Gemstone and Precious Metal Laboratory Unit, Consumer Product Laboratory Section, Dubai Central Laboratory Department, Dubai Municipality, Dubai, United Arab Emirates, P.O. Box: 67,

² Inspection Unit, Inspection and Certification Section, Dubai Central Laboratory Department, Dubai Municipality, Dubai, United Arab Emirates

Extended Abstract

Dubai Municipality by Dubai Central Laboratory department (DCL), in its effort to enhance Dubai's reputation as a prestigious place where one can be assured of the quality of purchased jewelry items, has established many policies to build consumer confidence and protect consumer and trader as following;

- Inspection Campaign of Gem and Jewelry,
- Good Jewelry Trading Practice (GJTP) or Bareeq Certification,
- Verification on Weighing Balances of Gold and Jewelry Traders
- Gemstone and Precious Metal Testing Services.

Inspection Campaign of Gem and Jewelry

In support to the United Arab Emirates Federal Regulation Number (9/1993) regarding hallmarking of precious metals and gemstone testing. The inspection unit implements inspection scheme of surveillance and monitoring purpose for gold and jewelry shops operating in Dubai. The purpose of the inspection is to ensure the all pieces of gold and jewelry sold in Dubai are stamped with the correct fineness mark (indicating purity of gold content) and tagged/labeled with correct information (weight, type of gemstone, quality of diamond).

DM inspector carry out a systematic inspection of gold and jewelry shops and collect samples for laboratory test in orders to verify the correctness of the fineness marks and jewelry description. In case of non-compliance, the inspectors may issue warning or violation notice to the concerned establishment. Implementation of the Federal Regulation will further enhance the reputation of the Emirates of Dubai as the "City of Gold" and "Jewellery Destination of the World" as supplier of good quality gold and jewelry items.

Good Jewellery Trading Practice (GJTP) or Bareeq Certification

A voluntary quality management system certification scheme for jewelry shops called "Good Jewelry Trading Practice (GJTP) – Bareeq (Arabic word means Brilliant) in short" is an independent endorsement by a third party (Dubai Municipality) given to a jewelry trading establishment after it complies with the certification requirements.

An evaluation of the retail establishment's operation shall be conducted to ensure that the following requirements are effectively implemented; Compliance with existing applicable local and federal regulations, Personnel competence, Appropriated environment, Appropriated tags and labels, Records and documents control, Product quality assurance, Customers' complaint and product warranty arrangement. When the certification assessors are satisfied that the establishment, a GJTP "BAREEQ" Certificate shall be granted after which regular monitoring and surveillance visits shall be conducted to ensure continuous compliance by the certified establishment.

Bareeq certification provides confidence on the quality of customers' purchased jewelry items. This scheme was developed in order to give recognition to jewelry shops that operates to the highest level of quality in terms of products and service. A jewelry shop that is certified under the scheme can display "Bareeq Conformity Mark" in their premises and in their marketing and advertising campaigns. It is a marketing tool that jewelry establishments can take advantage of. Having the Bareeq certification is an assurance from an independent certification body that the shop will provide excellent service and quality products. Under this scheme, Dubai Municipality assessors carry out rigid evaluation of applicant shops to ensure that they operate in accordance with the criteria set by the scheme. Compliance with the criteria will assure the customers of the quality of goods and services being offered by the certified shops.

Verification on Weighing Balances of Gold and Jewelry Traders

The Metrology Section of Dubai Central Laboratory Department – Dubai Municipality has been authorized by Emirates Authority for Standardization and Metrology (ESMA) to perform legal verification of electronic balances in the Emirate of Dubai. This is to ensure that measuring instruments that are being used in the businesses are giving accurate measurements and within the acceptable limits based on the applicable international standards.

Dubai Central Laboratory send trained Legal Metrology officers who holding in the judicial police to visit retail shops and complete series of verifications on the balances that the retailers/wholesalers are using by means of standard reference weights & advanced PDA to verify its competency and to make sure they conform to the UAE regulation. In particular, they ensure that the balances are accurate to international standards, that the measurements they show are clearly and correctly visible to the customer and that they use the international metric system. Upon completion of the series of tests, the legal metrology officer determines if the scale is passed or failed. He will then put sticker on the scale as per the following:



Verified – The verified sticker means that the balance has been inspected by Dubai Municipality / Dubai Central Lab. and verified to be accurate as per the UAE and international standards.



Rejected – The rejected sticker means that the balance has been inspected by Dubai Municipality / Dubai Central Lab. and verified to be not fit for the purpose due to technical specifications or condition of the machine and not allowed to be used for trade in the Emirate of Dubai.

Retailer/Wholesalers that continue to use rejected scales or try to tamper the Government seals will be breach of Federal and Emirates laws.

Gemstone and Precious Metal Testing Services.

The Gemstone and Precious Metals Laboratory was set up in the year 1998 and since then it had been offering gemstone identification, precious metal (gold, silver and platinum) testing and hallmarking services to the industry and publics by issuing identification and grading reports for diamonds, colored stones, pearls and test report and hallmarking for precious metals.

The laboratory plays vital role in protecting the customer and trader of Dubai by supervising and testing the items collected by the Inspectors of Inspection and Certification Section of the DCL. For accomplishing this task, the gemstone and precious metal laboratory has acquired a number of update advanced equipments in order to ensure the adherence to the required technical specification. The test methods employed are either International standards or laboratory developed methods; all are accredited by Dubai Accreditation Center (DAC) to ISO 17025:2005. The Gemstone and Precious Metals Laboratory is also recognized as National Gem and Jewelry Reference Testing Center by the United Arab Emirates Ministry of Economy.

The Microstructures and Bending Test of Cu-based Shape Memory Alloy for Jewelry Application

Chutimun Chanmuang, O. Juntakool, B. Kumnerdponpittaya, Saisamorn Niyomsoan and Natthaphol Chomsaeng

Jewelry Materials Research and Development Center (JMAT), Faculty of Gems, Burapha University, Chanthaburi Campus, 22170, Thailand

Extended Abstract

The microstructure and phase formation of an experimental Cu-Zn-Al shape memory alloys containing different amount of In addition prepared by conventional lost-wax casting using an induction furnace was investigated. Vickers microhardness, optical microscope, scanning electron microscope (SEM), energy x-ray diffraction spectroscopy (EDS) and bending test were used for microstructural observation and shape memory effect test. Vickers microhardness in the as-cast state revealed the significantly difference in hardness between matrix and copper enriched α -phase. The small size needle-like structures were found in the matrix phase. The shape recovery ration was improved with In addition.

Introduction

Shape Memory Alloys (SMAs) is one among smart materials that can-remember its original shape and ability to return to a pre-deformed shape when being heated. It is very different from conventional elastic/plastic materials because it exhibits reversible thermo-mechanical behavior. Shape memory effect derives from a martensitic transformation induced by stress and/or temperature changes (Otsuka and Wayman, 1998). Since the martensitic transformation is a diffusionless transition so their structures change extremely fast. It is dependent on temperature, stress and history, but not on time (Malard *et al.*, 2012). Although there is a relatively wide variety of SMAs, Ti-Ni alloys and Cu-based alloys are in commercial interest (Hodgson, 1999). Ti-Ni SMAs are the most commonly used especially in commercial applications because they combine excellent functional properties such as shape memory effect and superelasticity with good mechanical strength and ductility (Asanovic *et al.*, 2008; Zhou *et al.*, 2006). Recently, Cu-based alloys provide a more economical alternative to Ni-Ti for some purposes such as an actuator, temperature sensor and spring (Dia *et al.*, 2008). In the present study, the purpose is to investigate effect of In addition on the microstructure and shape memory effect of the Cu-Zn-Al for jewelry application.

Materials and Methods

An experimental Cu-Zn-Al-In SMAs were made by melting all metals in the induction casting machine under a protective atmosphere of high purity Nitrogen gas. Master alloys of Cu-Zn (Cu:Zn = 67:33 wt.%) and pure commercial-grade aluminum were used to introduce the Zn and Al into the melt. The nominal amount of 0-2.0 wt% indium additive elements was added to the melt to prepare the Cu-Zn-Al-In alloys. The molten metal was cast by investment casting by pouring at a temperature of 1,100°C into a gypsum-bonded investment mould preheated at 650°C. After pouring, the mould was held for 2 minutes under vacuum in the flask chamber, then

Shape memory effect was tested by bending method. The hardness measurements were carried out using a Vickers microhardness tester with a load of 100 gf and a dwell time of 10 s. Optical microscope and Scanning electron microscope (SEM) were used to examine the microstructures of the alloys. Microanalysis was performed by using energy dispersive X-ray spectroscopy (EDS).

Discussion

Four alloys with nominal compositions, given in Table 1, were prepared. Small amount of In addition was added to these alloys. Figure 2 shows the bending test for shape memory effect measurement.

Table 1: Compositions of the Cu-Zn-Al-In alloys

Alloy No.	Nominal Composition (wt %)			
	Cu	Zn	Al	In
Alloy 1	Bal.	20.8	5.8	0
Alloy 2	Bal.	20.8	5.8	x
Alloy 3	Bal.	20.8	5.8	y
Alloy 4	Bal.	20.8	5.8	z



Figure 1: Typical tree set-up for lost-wax casting.

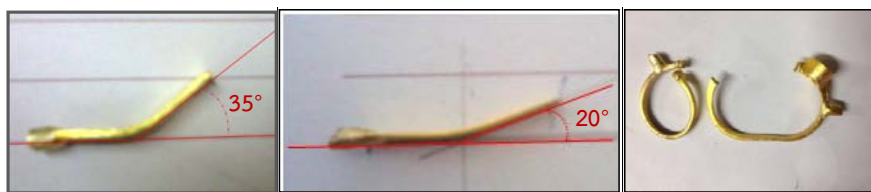


Figure 2: A bent sample for shape memory testing

Initially, the optical microscopes of the as-cast Cu-Zn-Al-In alloys (Figure 3a and 3c) revealed the needle-like phase in the matrix. Upon bending and heating the samples for shape memory test, the needle-like structure was deformed (Figure 3b and 3d), this could relate to the reduction of shape recovery effect. EDS revealed that the a-phase was enriched with Cu, while Al was more soluble in the matrix phase.

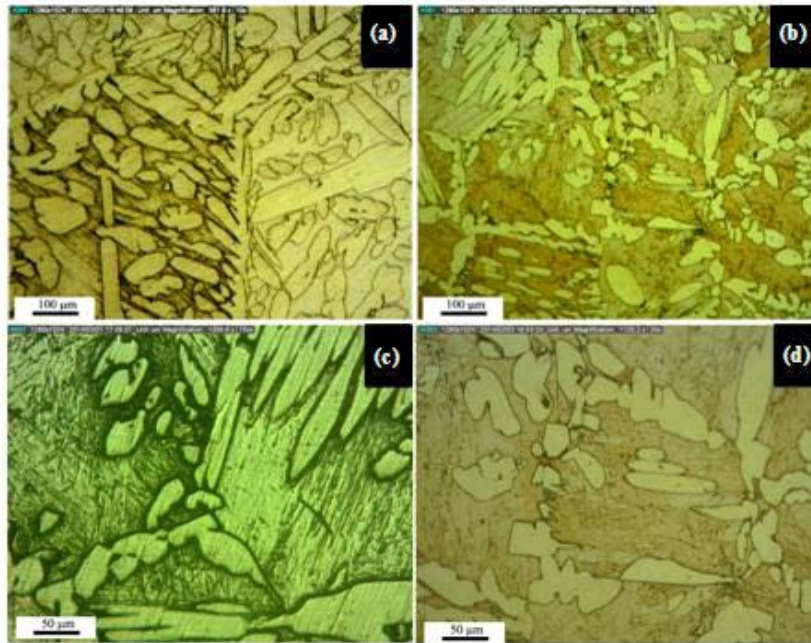


Figure 3: Optical microstructure of Alloy 3 **(a,c)** as-cast condition and **(b,d)** after shape memory test.

Conclusions

- (1) The Cu-based shape memory alloy with Zn, Al and In addition was successfully cast with the conventional jewelry casting process.
- (2) In addition has a significant effect on an improvement of shape memory effect, but within a limit. The excess In addition could induced a brittle and severe crack to the alloy.
- (3) Maximum strain recovery of this experimental alloy was 42%.
- (4) The needle-like structure was deformed after bending and heating the sample, this transformation could relate to a reduction of shape recovery.
- (5) EDS revealed that the a-phase was enriched with Cu. Al was more soluble in the matrix phase, while the same amount of Zn was found in both matrix and a-phase.

Acknowledgements

Author would like to thank Faculty of Gems, Burapha University, Chanthaburi campus for financial support.

References

- Asanovic, V., Delijic, K., and Jaukovic, N., 2008, A study of transformations of b-phase in Cu–Zn–Al shape memory alloys, *Scripta Materialia*, Vol.58, No.7, p.599-601.
- Dia, V., Bujoreanu, L. G., Stanciu, S., and Munteanu, C., 2008, Study of the shape memory effect in lamellar helical springs made from Cu–Zn–Al shape memory alloy, *Materials Science and Engineering: A*, Vol.481-482, p.697-701.

- Hodgson, D. E., 1999, Shape Memory Applications, ASM Handbook, Volume 2: Properties and Selection: Nonferrous Alloys and Special-Purpose Materials, p.897-902.
- Malard, B., Sittner, P., Berveiller, S., and Patoor, E., 2012, Advances in martensitic transformations in Cu-based shape memory alloys achieved by in situ neutron and synchrotron X-ray diffraction methods, Comptes Rendus Physique, Vol.13, No.3, p.280-292.
- Otsuka, K., and Wayman, C.M., 1998, Shape Memory Materials, Cambridge University Press, 282 p.
- Zhou, Y., Fan, G., Zhang, J., Ding, X., Ren, X., Sun, J., and Otsuka, K., 2006, Understanding of multi-stage R-phase transformation in aged Ni-rich Ti–Ni shape memory alloys, Materials Science and Engineering: A, Vol.438-440, p.602-607.

Corresponding Author

Full name: Chutimun Chanmuang
Affiliation: Jewelry Materials Research and Development Center (JMAT), Faculty of Gems, Burapha University, Chanthaburi Campus, 22170, Thailand.
Email: chutimun@buu.ac.th

Phrae Sapphire Deposit Style

Pornsawat Wathanakul¹, PrayathNantasin², SomruedeeSatitkune², Krit Won-In², Prakarn Buenkhuntod², Kachane Kraissittipong², and Marute Lekkean²

¹The Gems and Jewelry Institute of Thailand (Public Organization), Bangkok, 10500, Thailand

²Department of Earth Sciences, Kasetsart University, Bangkok, 10900, Thailand

Extended Abstract

Gem corundum occurrences in Thailand are related to basaltic rocks. Among the five localities namely Chanthaburi-Trat, Kanchanaburi, Phrae-Sukhothai, Srisaket-Ubonratchathani and Wichianburi, the Phrae-Sukhothai was believed to be abandoned for nearly twenty years.

In 1998 the first author and students from the Department of Earth Sciences, Kasetsart University stopped by the road number 101 at Ban Bo Kaeo as attracted by its name (Ban = village, Bo = pond/pit, Kaeo = gem or jewel in the northern Thai dialect)(Figure 1). As being the last sapphire deposit of the country, the area has been explored for education and geotourism purposes. The deposit has shown its unique characteristics of both the blue sapphires and the deposit style. Since the rainy days of mid 2014, the villagers have found blue sapphires at basaltic columnar area so called Mon Hin Lan Pi (Mon = little hill, Hin = rock, Lan = million, Pi = year) near Ban Bo Kaeo with megacrysts of black spinel and rare blue sapphire.

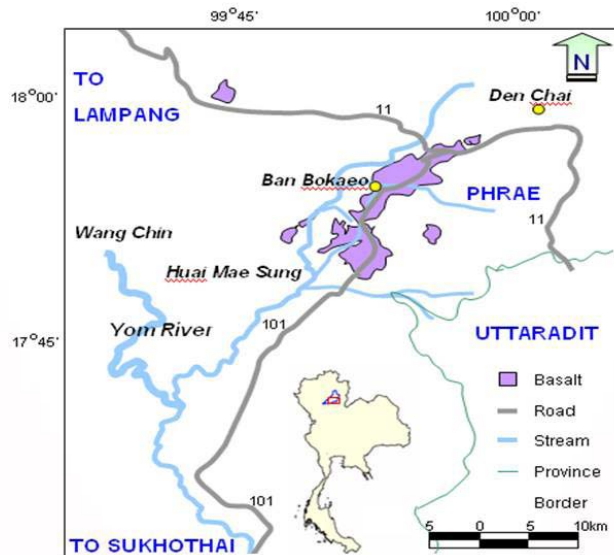


Figure 1: Map of the Ban Bo Kaeo sapphire deposit, Phrae.

Gem Corundum Deposit Style

- The occurrence of blue sapphires in Phrae indicates two main styles: the alluvial placer and residual deposits. The research investigation shows that the small individual sapphire deposits were commonly found and scattered along the Huay Mae Sung and its tributaries (Huay = stream), typically at terraces and point bars of about 1-2 m thick

(Figure 2); blue sapphires, black spinel and other heavy minerals are associated. The sporadic residual deposits can also be found in some weathered alkaline basalts exposed in the area.

- At Ban Bo Kaeo vicinity, there is a distinctive gravel bed (approx. 1m thick) inter-layered between two basaltic flows (Figure 3), This conglomeratic inter-layered bed is very poor-sorted and composed of 1-12 cm rounded sediments made of tuff, sandstone, basalt and chert. The bed contains spinel, zircon, olivine and corundum, which reveals Phrae typical deposit style.
- Based on field evidences, it can be revealed that there were at least two basaltic episodes in Denchai, Phrae, which brought the gem corundum up to the surface at different time. Therefore, the deposition of gem corundum there should be multi episodes rather than a single episode as previous concept.

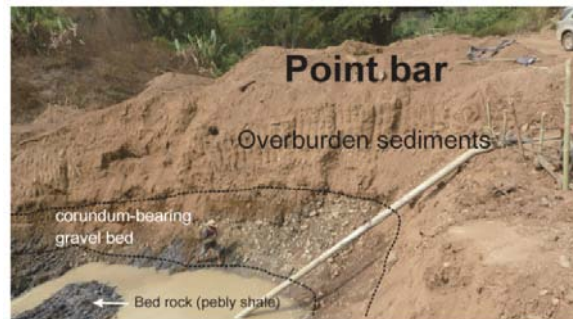


Figure 2: Corundum-bearing gravel bed at a point bar of Huay Mae Sung.



Figure 3: Corundum-bearing gravel bed interlayered by basaltic flows at Ban BoKaeo vicinity.

Corresponding Author

Full name: Pornsawat Wathanakul
Affiliation: The Gems and Jewelry Institute of Thailand (Public Organization),
Bangkok, 10500, Thailand.
Email: pwathanakul2@gmail.com

The GIT Standard Color Master Sets for 'Pigeon Blood' Ruby, 'Royal blue' and 'Cornflower blue' Sapphires

PongchanChandayot¹, Wilawan Atichat², Sakrapee Saejoo², Pimtida Bupparenoo², Marisa Maneekrajangsaeng², Oraphan Tongchaung² and Sasiwimon Chaiyathed²

¹Asian University, Banglamung, Chonburi, 20260, Thailand

²The Gem and Jewelry Institute of Thailand (Public Organization), Bangkok, 10500, Thailand

Extended Abstract

The Gem and Jewelry Institute of Thailand (Public Organization) or GIT has conducted the research on color quality standard of gemstones, especially corundum, since 1999. The collected data and standard master sets for color communication of gemstones have been used in the gem identification report of the institute ever since. Mostly, the varieties of corundum studied include the major hue such as red, blue, yellow, and green. Lately, the institute was requested by the traders to include certain popular trade names which are related to the gem quality into the report, such as 'Pigeon Blood' ruby, 'Royal Blue' sapphire, etc. The traders suggested that the gem identification report which included these trade names could enhance the sales for the local and the international markets. However, it was observed that there has been ambiguity and confusion on the above mentioned trade names. The GIT then decided to conduct the research project "The Study of the Trade Names for Certain Important Gemstones in Thai Market" in 2007. The gemstones included in the study were ruby and sapphire in which master sets for 'Pigeon Blood' and 'Royal Blue' were established in the GIT Lab. Nowadays because of the rarity, unbalance supply and demand of top quality ruby and sapphire in gemstone business, which is reflected in the overall high prices of these gem materials. The GIT has decided to revise and improve the existing standard master set of 'Pigeon Blood' ruby and 'Royal Blue' sapphire as well as establishing a "Cornflower Blue" color master set.

In this research project, the researchers have conducted the literature search and once again surveyed the traders' opinion on the 'Pigeon Blood', 'Royal Blue' and 'Cornflower Blue' colors. Then the reference stones were procured from the experienced traders. All reference samples were submitted to the color analysis using standard Munsell color chips in the standard light box, GretagMacbeth, model The Judge II, under the fluorescent lamp which has the color temperature 5000-5500 Kelvin. Results from this research are summarized as follows:

- The 'Pigeon Blood' ruby standard master set: red to pinkish red hue, medium to medium-dark tone and vivid saturation, Munsell hue between 5R to 2.5R, Munsell value between 2.5 to 3 and Munsell chroma more than 11.
- The 'Royal Blue' sapphire standard master set: blue to slight violetish blue, medium-dark tone and vivid saturation, Munsell hue of 6.25PB, Munsell value between 2.5 to 3 and Munsell chroma more than 10.
- The 'Cornflower Blue' sapphire standard master set: blue to violetish blue, medium tone and strong to vivid saturation, sleepy transparency, Munsell hue between 7.5PB to 6.25PB, Munsell value between 2.5 to 3.5 and Munsell chroma more than 10.

The result of the study is of great value to support GIT's gem identification certificate. It will also be useful for the general public who are interested in gem and jewelry industry. However, this project is still an on-going research for the industry in the future.

Acknowledgements

The authors would like to express the thankfulness to the GIT for the financial support on this research. The authors are also grateful to all GIT research staff and Thai gemstone traders for the cooperation and assistance.

References

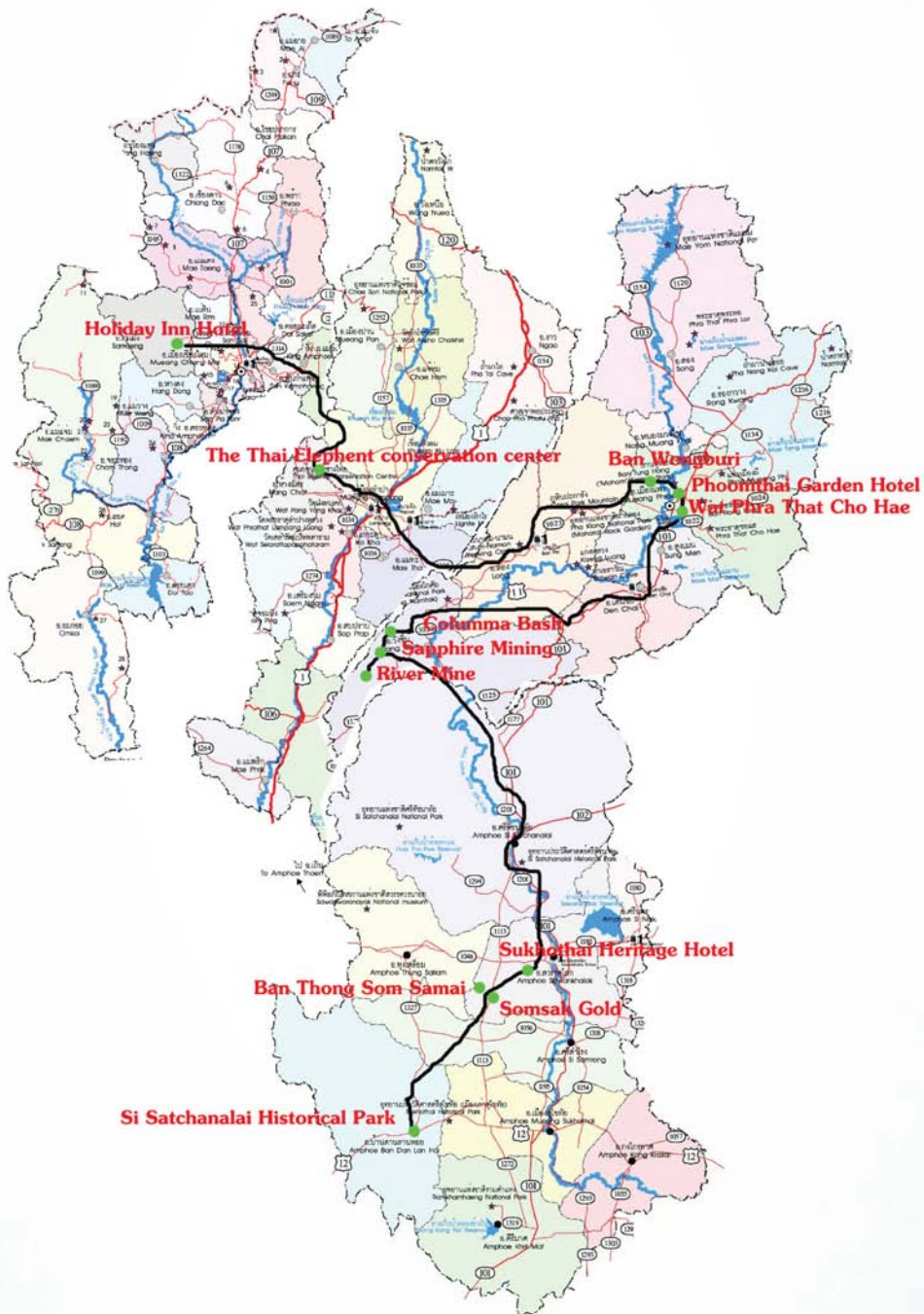
- Chandayot, P., Kankaew, Y., and Singbamroong, S., 2001, Color Grading System of Ruby, The Gem and Jewelry Institute of Thailand (Public Organization) Bangkok, Thailand, 58 p. (In Thai)
- Chandayot, P., Saejoo, S., Kaewmanee, S., and Singbamroong, S., 2003, Color Grading System of Blue Sapphire and other Sapphires, The Gem and Jewelry Institute of Thailand (Public Organization) Bangkok, Thailand, 200 p. (In Thai)
- Chandayot, P., Atichat, W., Suriyachod, C., Saejoo, S., and Saengbuangarmlum, S., 2007, The Improvement of Gem Corundum Color Communication System, The Gem and Jewelry Institute of Thailand (Public Organization) Bangkok, Thailand, 105 p. (In Thai)
- Chandayot, P., Atichat, W., Leelawathanasuk, T., Saengbuangarmlum, S., and Bupparenoo, P., 2007, The Study of the Trade Names for Certain Important Gemstones in Thai Market, The Gem and Jewelry Institute of Thailand (Public Organization) Bangkok, Thailand, 50 p. (In Thai)

Corresponding Author

Full name: PongchanChandayot
Affiliation: Asian University, 89 Moo 12, Highway 331, HuayYai, Banglamung, Chonburi 20260 Thailand. Bangkok Office, 15th Floor, Srijulsup Building, 44 Rama I Road, Pathumwan, Bangkok, 10330, Thailand.

Post-Conference Excursion Lampang-Phrae-Sukhothai 10-12 December 2014

Travel Route



Post-Conference Excursion Lampang-Phrae-Sukhothai 10-12 December 2014

Schedule

Date	Departure	Arrival	Attractions
10 Dec. 2014	08:00	17:30	Chiang Mai to Phrae The Thai Elephant Conservation Center (TECC) – Ban Wongburi – Phra That Cho Hae
11 Dec. 2014	08:00	17:30	Phrae – Basalt Area, River Mine & Sapphire Mining – Sukhothai
12 Dec. 2014	08:00	20:00	Ban Thong Somsak & Ban Thong Som Samai – Si Satchanalai Historical Park – Chiang Mai

Itinerary

Day 1 Wednesday 10 December, 2014

Set of Chiang Mai to Lampang and Phrae by bus; visit the Thai Elephant Conservation Center (TECC), Ban Wongburi & Phra Thai Cho Hae; evening get-together party at the hotel.

0700	Rendez-vous at the Lobby of Holiday Inn Hotel. Staff will be on hand to check baggage before leaving
0800	Depart for Lampang
0930	Arrival at the Thai Elephant Conservation Center (TECC).
1130	Lunch at a Restaurant en Route.
1500	Arrive at Ban Wongburi. After that, visit Wat Phra That Cho Hae (The Royal Temple).
1730	Check-in at Phoomthai Garden Resort
1800	Dinner Party, enjoy Thai Cultural foods, shows and Karaoke till late.

Day 2 Thursday 11 December, 2014

Visit Sapphire & Basalt Area; Phrae to Sukhothai

0700	Breakfast at the Hotel
0800	Depart from hotel to visit Columma Basalt (Mon Hin Lan Pee)
0900	Reach at Columma Basalt (Mon Hin Lan Pee), then the participants are divided into two groups Group 1: Visit River Mine Group 2: Visit Sapphire Mining

1200	Lunch at Basalt Area Group 1: Visit Sapphire Mining Group 2: Visit River Mine Continue the journey to Sukhothai
1800	Be greeted at Sukhothai Heritage Hotel
1900	Dinner on the Hotel grounds

Day 3 Friday 12 December, 2014

Sukhothai to Si Satchanalai Historical Park, then return to Chiang Mai

0700	Breakfast at the Hotel
0800	Visit the heritage (Sukhothai-style) Gold-Jewelry Making at Ban Thong Som Samai, and Ban Thong Somsak. Then, visit Si Satchanalai Historical Park
1130	Lunch at a Restaurant, adjacent to The Park. After lunch, depart for Chiang Mai
1830	Return to Chiang Mai and Dinner at a Restaurant
2000	Back to Holiday Inn Hotel

LAMPANG



<http://en.wikipedia.org/wiki/Lampang>

Geography

Lampang is located in the broad river valley of the Wang River, surrounded by mountain chains. In the Mae Mo district lignite is found and mined in open pits. To the north of the province is the 1,697-metre (5,568 ft) high Doi Luang.



Within the province are the national parks Chae Son and Doi Khun Tan National Park in the Khun Tan Range, as well as Tham Pha Thai, Doi Luang National Park and the Huay Tak Teak Biosphere Reserve in the Phi Pan Nam Range

History

Starting in the 7th century Lampang was part of the Dvaravati period Haripunchai kingdom of the Mon. In the 11th century the Khmer empire occupied the Lampang area, but it was King Mengrai of Lanna who incorporated the complete Haripunchai kingdom into his kingdom in 1292. Lampang or Nakhon Lampang or Lakhon, was under the Burmese rule after the fall of Lanna Kingdom from the sixteenth century to eighteenth century. During the uprising against Burmese rule by Siam's new kings in the late eighteenth century, a Lampang's local leader became Siam's ally. After the victory, the leader was named to be the ruler of Chiang Mai, the former center of Lanna, while his relative ruled Lampang. The city continues to be one of the most important economic and political centers in the north. Lampang was announced as a province in Thailand in 1892

Symbols

The provincial seal shows a white rooster inside the entrance to the. According to local legend, Buddha visited the province in his lifetime. The god Indra worried that the people would not get up by themselves to show respect to Buddha, and therefore woke them by transforming himself into a white rooster.

The provincial flower is the Heliconia (*Heliconia* sp.), and the provincial tree is the Indian Elm (*Holoptelea integrifolia*). According to the legend, this tree was planted in the temple during Buddha's visit.

Tourism Kaeo Don Tao - it used to be the place where the



Emerald Buddha was once enshrined (the same statue now installed in Bangkok). Interesting structures include the large Chedi containing the hair of the Lord Buddha, a Burmese-style Mondop, an ancient Viharn and a museum exhibiting ancient relics of the Lanna era. Wat Phra That Lampang Luang- a paradigm of temple building of Lanna. The temple itself is prominently sited on a hillock surrounded by walls. The entrance arches, called Pratu Khong, is adorned with fine plaster designs. The wall-less main Viharn houses a bronze Buddha statue called the Phra Chao Lan Thong.

Wat Phra That Chom Ping - The amazing aspect of this temple is the natural-coloured reflection of the Phrathat passing through the hole of the window and appearing on the floor inside the Phra Ubosot all the time when there is light, both during the day and at night (see Camera obscura).



Thai Elephants Conservation Centre - It is the only facility in the world devoted to the training of elephants for timber work using these pachyderms as labourers. There are performances and training demonstrations.

The Khun Tan mountain range, where the Doi Khun Tan National Park is located, forms a natural boundary between Lamphun and Lampang provinces. The Khun Tan Range has deciduous Dipterocarp forest and dry evergreen forest on the mountain sides, as well as hill evergreen forests and wide

stretches of grasslands combined with pine tree clumps at higher altitudes.

Local Products

Hand-made Cotton comes in different patterns designed by different villages.

Wood-carving is a major industry at Tambon Na Khrua of Mae Tha district which is about 25 kilometres from the provincial town. Most of the local people make their living by producing wooden figures of animals in various sizes. It has been a cottage industry in this locality for generations.



Terra-cotta or **Ceramics** produced in Lamphang are of the best quality in Thailand. The indigenous clay, added by the local craftsmanship, has helped to make Lamphang the centre of such products, with scores of factories and shops dealing in this beautiful craft.

Sa Paper is a fine product made from a type of soft wood. The process is purely traditional and the major producing center is the village of Ban Nam Thong. The Sa is mainly made into parasols, lampshades, decorative flowers and other souvenir items.

Culture **Festivals**

Luang Wiang Lakhon Fair is held just prior to the annual Loi Krathong event around Wat Phra Kaeo Don Tao and Wat Phra That Lamphang Luang, featuring Lamphang's own historical backgrounds and long-established customs and traditions. A Khrua Than procession is organized with local people dressed in native attires carrying various traditional household appliances, some of which are of ancient vintage.

Khantok Chang Fair is organised on the first Friday-Saturday period of February each year at the Thai Elephant conservation Centre. There is an elephant show and the pachyderms are feasted with their popular fruits and vegetables which are placed on the Tok, a traditional food tray of the Lanna people.

Salung Luang Procession and Songkran Festival is the unique Songkran festival of Lamphang, organized during 12-14 April every year. On the 12 April, the Salung Luang procession will be beautifully decorated (Salung means a water bowl and Luang means large). The participants in the parade will dress up in the ancient Lanna style and carry a giant silver bowl around the city to receive lustral water soaked with turmeric and acacia from the people to be poured onto the Phra Kaeo Don Tao, the revered Buddha image of the town enshrined at Wat Phrathat Lamphang Luang. Then, during 13-14 April every year, there will be a merit making ceremony at the temple, sand pagoda making, ceremony of pouring water onto the elderly, splashing of water, fairs and various forms of entertainment.

PHRAE



http://en.wikipedia.org/wiki/Phrae_Province

Geography

Phrae is located in the valley of the river Yom. The Phi Pan Nam Range runs across the province from North to south in the west and the Phlueng Range in the east.

Climate

Phrae Province has a tropical savanna climate (Köppen climate classification Aw). Winters are dry and warm. Temperatures rise until April, which is very hot with the average daily maximum at 37.6 °C (99.7 °F). The monsoon season runs from May through October, with heavy rain and somewhat cooler temperatures during the day, although nights remain warm.

History

The history of Phrae dates back to the Haripunchai kingdom of the Mon. It became part of the Lannathai kingdom in 1443, when King Tilokaraj was on an expedition to capture Nan.

Symbols

Provincial seal: According to legend the two cities of Phrae and Nan were once ruled by brothers. When they met to divide the land between them the one from Phrae rode on a horse, the one from Nan on a buffalo to the meeting point on top of a mountain. Hence Phrae uses a horse in their seal, while Nan uses a buffalo. When the provincial government proposed the seal in 1940, the Fine Arts Department suggested adding a historic building to the seal in addition to the horse, thus it now has the stupa of Phra Tat Cho Hae on the back of the horse. This temple is located about 9 kilometers south-east of the city Phrae.

Tourism

Wat Luang Some of its major features include the Viharn and Chiang Saen-style Chedi enshrining a Holy Relic brought over from Myanmar. Others are the museum housing various antiquities including several 500-year-old Buddha statues and an ancient Lanna-style wooden structure.

To the west of Wat Luang is Wat Phra Non near the site of the old city walls. Some of the architectural works include the Chiang Saen-style Ubosot with narrow openings to let in light instead of normal windows. Inside is a 9 metre-long plaster Reclining Buddha.

Wat Phra Bat Ming Mueang was built in 1955 by combining two ancient temples. There is an old Chedi containing a replica of the Holy Footprint inside.



The City Pillar Shrine of Phrae features an inscription stone with ancient Thai scripts of the Sukhothai period describing the construction of a temple in the town.

Wat Chom Sawan, a Burmese architectural style temple. Antiquities found here include marble Buddha statues, statues made of woven bamboos coated with lacquer, and Buddha statues made from ivory, as well as ivory scripture slabs with Burmese scripts.

Phae Mueang Phi is a wide area with no large trees. Because of subsidence and erosion of the soil, the harder elements remain and are formed into the shapes of exotic-looking mushrooms. Wat Phra That Cho Hae A major religious site of the province, it was built since the time of Sukhothai. The 33 metre-tall Chiang Saen-style Chedi housed a Holy Relic. It was built of bricks and covered with bright brass sheets.

Wat Phra That Chom Chaeng The golden Chedi is 29 metres tall and enshrined a Holy Relic. There is also a museum of rare ancient relics.

Wat Phra That Suthon Mongkhon Khiri The Ubosot in particular is noted for its delicate sculptures with fine designs. There is also the golden teak structure in the Lanna-style which houses valuable relics of the North, including Buddha statues, lacquer ware, Lanna musical instruments, ancient weapons and pictures depicting past events.

Local Products

Mo Hom is a well-known hand-crafter material made in Phrae. Considered a quality product, using traditional methods in the weaving, dyeing and tailoring processes.

Another famous product is **Pha Tin Chok**, a fine and well-made material with distinctive design. Apart from being widely used as material to make dresses, today it is also used to make items such as hand-bags, shoes, household decorative items, etc.

Culture

Festivals

The Phra That Cho Hae Fair, held in around March, involves a procession to carry robes to cover the Chedi. The procession follows the Lanna style. All participants are decked out in traditional Lanna attires.

Doklomlaengban Songkran Muangphrae Nung Mohhom Tae Ngam Ta or Songkran Festival in Phrae on 13-17 April every year at Chareun Muang Road, Yantarakit Kosol Road and Around the City.



SUKHOTHAI



Sukhothai Province



http://en.wikipedia.org/wiki/Sukhothai_Province

Geography

Sukhothai is located in the valley of the Yom River on the lower edge of the northern region, 427 kilometres north of Bangkok, and covers some 6,596 square kilometres.

The Khao Luang Mountain Range, with its four main peaks: Khao Phu Kha, Khao Phra Mae Ya, Khao Chedi, and Pha Narai, lies within the Ramkhamhaeng National Park in the south of the province. [1] The Si Satchanalai National Park is located in the north-west, protecting the mountainous forest areas of the Phi Pan Nam Range at the northern end of the province.

History

Sukhothai, meaning the Dawn of Happiness, was a town founded in the 13th century on the fringe of the Khmer empire. The exact year is unknown, but according to the Fine Arts Office it was between 1238 and 1257. Founded by Phokhun Si Intharathit, it was the first truly independent Thai (Siamese) Kingdom after defeating the Khmers. Sukhothai enjoyed a golden age under their third king, King Ramkhamhaeng, who was credited with creating the Khmer-derived Thai alphabet which is essentially the same as that in use today. He also laid the foundation for politics, the monarchy and religion, as well as expanding its boundary of influence. Sukhothai was later ruled by many



kings. The province is most famous for the historic city of Sukhothai, the capital of the Sukhothai kingdom. It is located about 12 km from the modern New Sukhothai city. Not far from Sukhothai are the Si Satchanalai historical park and the Kamphaeng Phet Historical Park. Both were cities within the former Sukhothai kingdom and of the same time period.

The province was at first known as Sawankhalok; it was renamed to Sukhothai in 1939.

Symbols

The provincial seal shows King Ramkhamhaeng the Great sitting on the Managkhasila Asana throne. Under King Ramkhamhaeng the kingdom of Sukhothai flourished the most. Provincial tree is *Azelia xylocarpa*; provincial flower is the Lotus (*Nymphaea lotus*).

The provincial slogan is Source of national heritage, the Thai alphabets, the best Loy Krathong celebrations, firm foundation of Buddhism, the fine Teen Jok cloth, ancient chinaware, holy Pho Khun Ramkhamhaeng's mother, dawn of happiness.



Tourism

Sukhothai province is most famous for its historical city of Sukhothai, the first capital of Siam, founded by King Ramkhamhaeng. The province's temples and monuments have been restored well and Sukhothai Historical Park – a place with numerous sites of historical interest – has been made into a UNESCO World Heritage Site. Other interesting places include Ramkhamhaeng National Museum, Ramkhamhaeng National Park, Sri Satchanalai National Park, and The Royal Palace and Wat Mahathat.

Si Satchanalai historical park is registered by the UNESCO as the world's heritage like Sukhothai historical park. It is situated at Kaeng Luang in Tambon Sri Sachanalai, Amphur Sri Sachanalai, about fifty-two kilometres away from town centre. It was formerly called "Muang Chaliang," the name changed to "Si Satchanalai" during the reign of Phra Ruang when a new administrative centre was established to replace Chaliang.[4] Ruins of 134 monuments have been discovered within the park.

Ramkhamhaeng National Park is widely known as Pa Kho Luang. It covers an area of about 341 square kilometers, or 213,125 rai. It is blessed with wildlife, birds, and natural beauties, including fertile tropical jungles and mountain. Ramkhamhaeng National Park, within the province of Sukhothai, is surrounded by the districts of Kirimas, Ban Dan Lan Hoi, and the provincial capital of Sukhothai.

The Centre for Study and Preservation of Sangkhalok Kilns (is considered the industrial area of Si Satchanalai. Numerous celadon wares in broken, as well as perfect, condition have been discovered. The kiln is oval in shape with a curved roof like that of a ferryboat and is 7–8 metres long. The centre consists of two buildings situated on the kiln site area with two kilns Nos. 42 (ground level) and 61 (underground) exhibited in situ. There are also exhibitions on artifacts, academic documents, and on the evolution of ancient ceramic wares.

Local Products

Sangkhalok ceramics These replicas arguably look as good as the originals.

Thung Luang terra cotta of Khiri Mat district come in unique patterns. The products include flower pots, vases, basin, water jar, lamps, with perforated decorations of animal figures like frogs, bullfrogs, and dogs.

Butter-baked Banana A well-known snack of Amphoe Khiri Mat, it resembles another local sweet called Khanom Rang Nok made from sweet potato. This butter-baked banana snack is made from slicing raw banana horizontally, left to dry for half a day, seasoned with salt, deep fried, adding sugar, and giving it a good stir. Sprinkle with sesame seeds and add butter. This product is available everywhere.



Fried peanuts of Si Samrong district, also called “200- year fried peanuts”, are a tribute to a technique which has been inherited for many generations.

The recipe is a mixture of rice flour, wheat flour, eggs, coconut milk, salt, pepper, chopped wild yam, which are then deep fried.

Ancient gold reproductions (of Si Satchanalai district) are entirely hand-made by skilled workers. These replicas of the Sukhothai style products include necklaces, wristlets, bangles, earrings, rings, etc.

Ancient silver reproductions These replicas are entirely hand-made with distinctive skill. They are available at all silver shops in Amphoe Si Satchanalai.



Local Culture

Lifestyle

The Thais are a friendly, laid-back, non-aggressive, and non-confrontational people who are known world wide for their impressive smiles – even to complete strangers. The Thai-Chinese make up the majority of Sukhothai’s new town urban folk while the original Thai-Thais prefer their more traditional rural roots in the Sukhothai countryside. The northern Thais in Sukhothai are Lanna in origin and their ancient roots lie in Burma, Tibet and southern China.

The people of Sukhothai are very proud of their heritage and do not take easily to tourists there who don’t show any interest in wishing to learn about their history. Since they look up to King Ramkhamhaeng the Great as their adopted father, all foreign tourists should only mention him with respect.

Festivals

Phor Khun Ramkhamhaeng's Day Festival (or King Ramkhamhaeng the Great Memorial Fair Phor Khun Ramkhamhaeng's Day Festival), annually held on January 17. It honors of the Great King of Sukhothai Kingdom. In this day, people will visit the Monument of Phor Khun Ramkhamhaeng the Great for praising Phor Khun Ramkhamhaeng. People will make merit and present food to a Buddhist priest. At night, there is merrymaking and many shows that all people can enjoy. There are fireworks, too.

Song Nam Aui Than Festival Song Nam Aui Than Festival is annually held on April 12, Songkran Ceremony in the SriSathanalai Historical Park. It exhibits the Buddha image procession from Wat Phra Prang to the Historical Park for people who want to pour the water over the Buddha image.

Si Sachanalai Ordination Celebration Si Sachanalai Ordination Celebration is called by Thais as "Buat Chang Hat Siao", held annually during 7–8 April at Ban Hat Siao, Ampher Si Sachanalai. It features a spectacular procession of ordination candidates in colourful costumer on the backs of some 20-30 decorated elephants.



Phor Khun Ramkhamhaeng's Day Festival (or King Ramkhamhaeng the Great Memorial Fair)

Sukhothai Loi Krathong and Candle Festival The tradition derived from traditional beliefs common to communities living along the banks of a river or waterway. It has become a need to worship and supplicate the Khongkla to avoid bad luck, to worship the gods in the Brahmin tradition, or to revere the Buddha's footprint. The celebrations are normally organized in the 12th month when the tide is high and the air is cool. Sukhothai's Loi Krathong is held annually on the full moon night of the 12th lunar month at the Sukhothai Historical Park. The Krathongs, or floats, have been made in the form of lotus. There is also a reference, in the Sila Charuek, to candle lighting and playing with firework in a grand festival believed to be similar to the candle lighting and firework as practiced in



the current Loi Krathongs Festival.[4] In this festival, there are Nang Nopphamat procession, exhibitions, lighting of lantern at the historical site, Loi Krathong, fireworks over all waterways, and Krathong competition.



Songkran and Mueang Sawankhalok Festival This takes place during 11–15 April annually on the bank of the Yom River, in front of Wat Sawang Arom, by the Yom River, and at the Stadium of the Sawankhalok Municipal School. The procession of Miss Songkran, the Sawankhalok Food Festival, ceremonies of giving alms to monks and bathing rituals for Buddha images and monks are performed in the festival.

Local Food

Sukhothai has its very own specialty noodle dish simply called Sukhothai Noodles. They are a blend of Thai rice noodles (khanom chin) mixed with crispy pork, garlic, green beans, coriander, chili, and peanuts in a broth flavored with dark soy sauce.



The Thai Elephant Conservation Center

<http://www.thailandelegant.org/en/>



The Thai Elephant Conservation Center (TECC), founded in 1993 under Royal Patronage, cares for more than 50 Asian elephants in a beautiful forest conveniently located near the famous city of Chiang Mai. Beyond being an exciting tourist experience, the TECC is also known for its pioneering work in conservation and science. The TECC also proudly houses six of HM King Bhumibol's ten white elephants in the Royal Elephant Stables.

As Thailand's only government-owned elephant camp, the TECC promotes affordability and accessibility. The admission price is only 200 baht for adults) and 100 baht for children. Being often visited by Thai families and schoolchildren, the TECC's foreign guests never feel caught on the tourist trail. Guidebooks consistently praise the TECC for its relaxed, non-commercial atmosphere.

The TECC offers many enjoyable Activities. Day trip "musts" include watching elephant bathing, the elephant show and a visit to see our baby elephants. Most guests take an elephant-back ride and tour our hospital. Overnight activities include our popular Home stay program and trekking in the forest.

Active in Conservation, the TECC operates an onsite Hospital and manages Thailand's first mobile clinic, treating needy elephants free of charge. The TECC has an excellent natural breeding rate, usually producing at least two baby elephants a year.

The TECC has also done cutting-edge research in Science, especially in reproduction and artificial insemination as well as major studies in the biomechanics of how elephants move ("locomotion").

The TECC has broken new ground in Arts & Culture. It was the first place in Thailand where elephants learned painting. It is also the home of the internationally famous Thai Elephant Orchestra. The TECC is operated by the Forest Industry Organization, a State Enterprise of the government of Thailand. It houses the National Elephant Institute of Thailand, a center of learning which shares its vast library and trained specialists with other agencies and organizations working to help the country's 2,700 domesticated elephants.

Baan Wong Buri (Wong Buri Old House)

[http://www.tripadvisor.com/Travel-g982710-c150110/
Phrae:Thailand:Baan.Wong.Buri.Wong.Buri.Old.House.html](http://www.tripadvisor.com/Travel-g982710-c150110/Phrae:Thailand:Baan.Wong.Buri.Wong.Buri.Old.House.html)



Baan Wong Buri (Wong Buri Old House) is located in 50 Kham Leu Road (Road behind Phrae Governor House, Phra Non Neu intersection), and near Wat Pong Su Nan. It was built in 2450 B.E. by Chao Phrom (Luang Phongpiboon) and Chao Sunantha Wong Buri, the daughter of Chao Buri (Phraya Burirat). Technicians who build this house come from Guangdong, China and also the local carpenter. House made of wood in two-story, European-style. Brick and cement base are one meter above the ground floor with two roof vents air between two layers to increase the flow of air due to house facing south-west winds were so cool in the summer. House was shaped in Pan Ya style, 2 storeys which have high ceiling, and high roof. The prominent point of the building is wood carving patterns at gable, roof, terrace, doors, windows, and vents. At the front door is a goat stucco image, representing of Luang Phongpiboon and Mae Chao Sunantha which were born in the year of goat. Later, it was in reparation, but carving patterns remain the same. Household items decorated with old appliances that convey the same family for several generations, including furniture, silver ware, and important documents such as documents of slave trade. Baan Wong Buri won the Conservation Award in 2536 B.E. by the Association of Siamese Architects under Royal Patronage. The house was used as a filming location many times and published in various books. Moreover, Baan Wong Buri set menu in the traditional foods serving in northern style (Khan Tok) for all local and overseas travelers.



Wat Phra That Cho Hae (the Royal Temple)

<http://www.tripadvisor.com/Travel-g982710-c149958/Phrae:Thailand:Wat.>

[Phra.That.Cho.Hae.The.Royal.Temple.html](http://www.tripadvisor.com/Travel-g982710-c149958/Phrae:Thailand:Wat.Phra.That.Cho.Hae.The.Royal.Temple.html)



Wat Phra That Cho Hae, the Royal Temple, is a sacred ancient temple in Phrae and a temple of people who have the year of birth in year of the Tiger.

Wat Phra That Cho Hae, the Royal Temple, spread on an area of 175 rai (1 rai = 1,600 square meter). Everyone who visit Phrae province must not miss to worship Phra That Cho Hae for auspiciousness themselves. A statement that “If you come to Phrae, but do not worship Phra That Cho Hae, you do not yet reach to Phrae”

His Majesty the King addressed the Wat Phra That Cho Hae as a royal temple third class the ordinary type on 23 June 2549, which announced in a common issue of the Government Gazette Vol. 123 Part 96, dated September 19, 2549.

The temple is located in a hill about 28 meters high. The body is a Pagan pagoda, octagon shape, wood inoamuum twelve, and Chiang Saen art. Lined with gold, high 33 meters, square base wide 11 meters each side, it is situate on a square base, then next floor is octagonal base 3-storey, and next is a lotus base upside down. Overlap each degradation over 7 floors, the shape then is like a bell in lotus shape and then change to octagonal shape bell. Next up is the twelfth Inoamuum wood.

The top decorate in Lanna style. The body covered with gold throughout. A steel fence surrounding the Holy element has 4 directions, 4 doors, creating each door's arch in the beautiful Lanna style.

Fine Arts Department has announced the registration Wat Phra That Cho Hae as the archaeological site in the Government Gazette Volume 52 Part 75, dated March 8, 2478 and announced the historic scope in the Government Gazette Volume 97 Part 159, dated October 14, 2523.

Chronicles of His Majesty on the Sukhothai period in the National Library said to Wat Phra That Cho Hae, the Royal Temple that year of built between 1879-1881 B.E. during the reign of King Maha Dhamaracha (Lithai). He like to build the place of Buddhist religion as it appears in history and select Doi Go Sataya Chucka Banpot (Go Sataya Chucka Banpot Hill) to build a pagoda, Phra That Cho Hae.

According to legend, His Majesty Maharaja Lithai gave the Lord Buddha relics (the hair elements) to Khun Lua Ai Kom (Phra That Cho Hae builder) to be contained in the pagoda base. When Khun Lua Ai Kom arrived to Doi Go Sataya Chucka Banpot, he found that it has a good location to build the pagoda. He put the casket containing the relics in the Golden Lion statue, and built a podium of the casket by silver and gold. After set up the Golden Lion statue, he used the cement waved over for another layer. After that, he set a celebration event 7 days and 7 nights. Later Phrae was assembled into the Kingdom of Lanna Thai, Lanna King has renovated Phra That Cho Hae continuously. Until the fall of dynasty, Phra That Cho Hae was so deliplied respectively. In 2467 B.E., Kruba Srivijaya (Saint of Lanna) restored Phra That Cho Hae with Phrae Province Minstry, which had Phra Maha Methang Gon (Prom Prom Dhe Vo), a former dean of Phrae Province Monk as a president of restoration. Phra That Cho Hae returned to grace as a pride of Phrae city.

Another legend of Phra That Cho Hae say that the Lord Buddha came to Phrae, sat at Doi Go Sataya Chucka Banpot (Go Sataya Chucka Banpot Hill). Khun Lua Ai Kom (Phra That Cho Hae builder) has come to worship the Lord Buddha on this hill. Lord Buddha has shown him the Four Noble Truths and the Eightfold Noble Path, and then given him the relics (the hair elements) as a gift. Lord Buddha ordered Khun Lua Ai Kom to put the relics in a cave nearby, and said that after his nirvana, do remove the relics of left elbow to put in this place as well. After Lord Buddha's nirvana 218 years, the Great King Asoka and all saint of Lord Buddha join prayer, and summon the urn, which contain the relics, and then provided that to places where the Lord Buddha was predestined. At the end of prayers went out, all relics from the urn came out into the air and went to the defined places. For the remaining relics, the saint brought to 84,000 pagodas, announced to the angels to defend all forever until the end of the Buddhist 5,000 years.

For the name of Phra That Cho Hae, some say that it comes from fine woven gauze from Xishuangbanna, which villagers use to band the pagoda for worship. Some say that it is from the satin, which Lua Ai Ko offer to the Lord Buddha. Every year, the worship festival is on 9- 15 in the fourth lunar month (around March). Phra That Cho Hae Temple is the temple of one who was born in Tiger year, 1 of 12 zodiacs. There is a belief that if you worship by three color satin, your life will have the power and can protect from enemies.

Sapphire Deposits Area

The origin of sapphire deposits in Thailand associated to the basaltic rock which is basanitoid or basanite basalt. The chemical compositions of this basalt contain a high level of titanium but a low level of silica indicating that the source of the basaltic magma is probably from the depth basalt (Sutthirat *et al.*, 1994). The corundum megacrysts are commonly associated to pyroxenitic and spinel lherzolitic xenoliths in the basalt bearing gem at high pressures between 15 and 20 kbar. (Yaemniyom S., 1982).

Only in Phrae and Sukhothai Provinces in the northern Thailand region, are found the deposits of blue sapphire of good quality. They are the last gem deposits in Thailand which are not yet fully developed by the mining industry. In the past, Ban Bo Kaew gem deposits (in Den Chai district, Phrae province) were well known as the deposits of sapphire and gemstone of good quality in the northern Thailand. Thus the local people name this gem deposit “Ban Bo Keaw” (meaning the gem deposit village) (Vichit, 1994). Since 1972, the miners (local people) have started to develop many pitting mines in Ban Bo Kaew and surrounding areas. They found the new gem deposit in “Huai E- Tor” from the name of the stream “E-Tor”. From Huai E- Tor area, the local got big sapphires of good color and quality.



During 1975 to 1977, many gem hunters attempted to find the new deposits in Den Chai district and they found the sapphire of good quality at Khao Nam Tok and Huai Mae Khanueng deposits in Ban Bo Kaew area and Huai Mae Sung at Na Poon sub district, Wang Chin district. In 1985 to 1988, the local numerates the gem deposits so as to be easier to understand. For example, “Ban Hnong Yao” gem deposit was “Bo 1”, “Huai Si Siat” gem deposit was “Bo 2”, “Huai E-Tor” gem deposit was “Bo 3” and “Huai Mae Khanueng” gem deposit was “Bo 4”. The gems and associate minerals found in these areas were corundum (sapphire), black spinel, garnet, zircon, pyroxene, quartz and olivine.

Geological characteristic of Den Chai gem



deposit consists of the Cenozoic basalt which covers the Permo-Carboniferous sedimentary rock (sandstone, shale, siltstone and chert) (Chareonprawat A., 1968 and Piyasilpa S., 1975). These basalts are divided into 7 flows base on the physical and chemical properties (Bar and Mcdonald, 1979). The first to fourth flows are the Transition Hawaiite, the fifth and sixth flow are Hawaiite and the seventh flow is Basanite. The grains of the first to sixth basalt flow are of fine to medium sizes and compose of more olivine, less plagioclase (labradorite) and a few clinopyroxene. The grain of the seventh basalt flow is of dark color, dense and very fine crystal. They comprise of more ultramafic nodules (spinel lherzolite) xenolith. The olivine and plagioclase are usually found to be phenocrysts in vesicular basalt. The age of the uppermost basalt flow is 5.64±0.28 Ma by K-Ar dating (Bar and Mcdonald, 1981). The width of basalt flow is about 1.5 to 5 km and the thickness of basalt is about 20 to 50 m (Maneenai D., Chareonprawat A. and Phuenda C., 1987). The basalt bearing gem is the uppermost flow which is commonly associated to lherzolite



xenolith (Vichit, 1994) and there are 7 potential gem deposits such as Huai Si Siat, Kha Nam Tok, Ban Hnong Yao, Huai Wao deang, in Den Chai district and Huai E-Tor, Huai Mae Sung in Wang Chin district.

Wathanakul et. al. (2000) studied the gem deposits at Den Chai area, Phrae province and Si Satchanalai area, Sukhothai province and found the gemstone deposits to be the residual deposit and paleo –channel deposit (vertical distance above modern stream level 10 to 20 m). The layer of the paydirt is about 0.3 to 1 m thick and consists of various rock gravels such as shale, pyroclastic rock, phyllite and slate.

Ban Bo Keaw (บ้านบ่อแก้ว) and Ban Na Poon (บ้านนาพูน) sapphire deposits in Phrae Province is the last gem field in northern Thailand. The prominent characteristic of the blue sapphire from Ban Bo Keaw is its dark blue colour known as Morhom (มอฮ่อม), which is the colour of the traditional blue clothes from Phrae. The shapes of the sapphire crystals are euhedral, subhedral hexagonal, broken barrel. Most samples have broken ends. The biggest crystal ever found in Ban Bo Keaw deposit is 257 ct. beside blue sapphire, black spinel, garnet, zircon and ruby also have been found, but the last is rare.

References & further reading

Barr, S.M., and Macdonald, A.S., 1978, Geochemistry and petrogenesis of late Cenozoic alkaline basalts of Thailand: Geological Society of Malaysia Bulletin, v.10, p.25-52

Barr, S.M., and Macdonald, A.S., 1981, Geochemistry and geochronology of late Cenozoic basalts of Southeast Asia: The Geological Society of America Bulletin, v.92, part II, p.1066-1142

Charoenpravat, A., 1967, Geology reports of Amphoe Wangchin and Ban Bo Keaw 1:50000, Geological survey section, Department of Mineral and Resource, 70p. (in Thai)

Maneenai, D., Charoenpravat, A., Puenda, J., 1978, Geology reports of Sheet Amphoe Maewang (4945III), Ban Bo Keaw (4944 I) and Changwat Phrae (5054 III). Geological survey section, Department of Mineral and Resource, 70p. (in Thai)

Piyasin, S., 1975, Geological map of Changwat Uttaradit 1:250,000, Report no. 15, Geological survey section, Department of Mineral and Resource, 68p. (in Thai)

Sutthirat, C., Charusiri, P., Farrar, F. and Clark, A.H., 1994, New $^{40}\text{Ar}/^{39}\text{Ar}$ geochronology and characteristics of some Cenozoic basalt in Thailand : in Proceedings of International Symposium on Stratigraphic Correlation of Southeast Asia, Bangkok, p.306-321.

Vichit, P., 1989 Gem deposits in Phrae-Sukhothai, ruby-sapphire deposits in Thailand, Information section, Department of Mineral and Resource, p.55-61. (in Thai)

Wathanakul, P., Kraisthipong, K., Yamnert, S. Sirisayant, S., Lomthong, P., Sakkaravej, S. and Chanthip, N., 1990, Final report of gem deposit in Phrae – Sukhothai potential area. Kasetsart University. (in Thai)

Yaemniyom, S., 1982, The Petrochemical Study of Corundum-bearing Basalt at Bo Phloi District, Kanchanaburi: Thesis, Dept. of Geology, Chulalongkorn University, Thailand, 100p.

Sukhothai Gold Jewelry From Ancient Wisdom to Contemporary Craft

Gem and Jewelry Information Center
The Gem and Jewelry Institute of Thailand (Public Organization)
July 2014

In spite of the increasing prices in the global market, gold still has inherent value which everyone wants to acquire. It is a precious metal used as investment asset due to its ability in value preservation and high market liquidity, while being held as country's international reserves for economic stability and security in the financial system. Gold is also a material with distinctive qualities: it has bright, shiny yellow color, and its malleability allows for versatile applications, most commonly as raw material for jewelry making. Unsurprisingly, gold and gold jewelry still maintain their high popularity around the world throughout history, especially in Asia, where people still recognize the importance of gold-ornament wearing has deeply rooted in their old tradition. Gold jewelry has long been used as a dowry in engagement or marriage or as a gift in special occasions or festive seasons. On the other hand, modern consumers wear gold jewelry not only for emotional or aesthetic value, but also as an indication of their social status and their fashion styles. Additionally, gold also plays a major role as an asset for wealth accumulation and investment.



Gold Jewelry in Thai Culture

In Thailand, the making of gold ornaments began to prosper in Sukhothai period and continued on into Ayutthaya period. Initially, these ornaments were produced only for kings, royal members and noblemen. When jewelry wearing was controlled by strict regulations. Ordinary people were not allowed to have jewelry in their possession. Later, in the middle of Rattanakosin period, a large number of European and Chinese merchants started their businesses in Thailand, while some foreign goldsmiths also settled in the country and set up their workshops. At that point, jewelry use became more liberal to wear; its production and wearing have proliferated more widely among the public.

From its original state as one of the rare metals, gold is molded, carved and polished to show its beauty in exquisite forms of jewelry. Local knowledge acquired from experience and skill development has established this valuable craft heritage, which has been carried on live through various periods in Thai history. As a result, Thai gold creativity now have unique regional characteristics thanks to the techniques develop locally which have been passed on through generations. Along the way, we also prosper the advancement of traditional knowledge, the perfect blend of ancient and contemporary designs, a significant approach in adding value to the

piece while preserving and restoring the art of jewelry making from its glorious past.

Today, gold jewelry in Thailand can be divided into three categories: gold ornaments or “red gold cabinet” with 96.50% purity (23.16 karat), which is the standard of Thai gold. The another popular combination of gold is 18-karat or 75% gold, widely use decorated with gemstones. And the significant one is antique gold jewelry, which is considered as wearable high art with 99.99% gold purity (24 karat). In this case, “antique” does not refer to old-fashioned designs, but implies exquisite craftsmanship incorporated into each piece of jewelry through meticulous processes and require advanced techniques for creating pattern exclusively by expert goldsmiths, a quality unachievable by no automatic machines. One of Thailand’s highly valuable cultural heritages in antique gold ornaments is “Sukhothai gold jewelry”, which is renowned for its unique quality from its entirely handmade process and 99.99% gold. With manufacturing techniques restored from traditional gold weaving methods in Sukhothai period, while development and integration of new creative inventions, these precious pieces of jewelry feature outstanding patterns and design elements, such as gold-weaving methods, bead designs, openwork patterns, colorful enamel. Furthermore the manufacturing process requires imagination, expertise and patience. The result is contemporary gold jewelry inspired by motifs found in antiquities, local objet d’art, including sculptures, icons, stucco works and mural paintings. For example, Nangpaya pattern was inspired by a stucco work in Nangpaya Temple, and Krueawal pattern is an imitation of the natural vines.



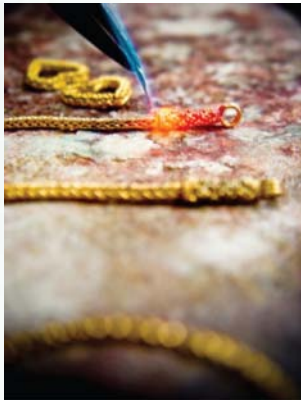
The Making of Sukhothai Gold Jewelry

The production process of Sukhothai gold jewelry has several steps, all of which require meticulous craftsmanship. It begins with melting gold bars, which must have 99.99% purity without any alloy contamination, in order to achieve the effectiveness in jewelry shaping. Pure gold is dense and soft, making it suitable for traditional designs, while its almost 100% purity gives brighter golden color compared to general gold ornaments made of 96.50% gold. After the goldsmith melts gold bars by blowing fire in a crucible until solid gold has been transformed into liquid, it will be poured into square molds and left to cool down and become hardened. Then the gold ingots will be flattened or rolled with rolling or drawing machines into different sizes of sheets or threads as needed.



The next step is jewelry making in traditional Sukhothai’s methods, which primarily include shaping and forming gold into various designs and patterns. Gold weaving, similar to crochet, can be divided into tubular patterns, which use a small number of gold threaded from three to ten. As for the flat patterns, there are number of patterns such as braided pattern, 20-thread pattern and 24-thread pattern, which are mostly used for bracelets. Customary gold beads are also produced in round or oval shape obtain by hammering gold sheets into round molds to make pairs of hemispherical shapes and place them together before perforating them for thread-

ing. Cork Fruit Pattern is a method of soldering the same size rectangular gold sheets with borax. These gold parts are assembled into Thai-styled jewelry, limited only by the goldsmith's artistic imagination. Gold jewelry can also be developed by many other processes, one of which is enamel. It is mostly comply only three colors which are red, green and blue, to add colorful patterns into the piece instead of decorating with diamonds or colored gemstones. This has become one of the unique features in Sukhothai's gold jewelry. The knowledge in gold jewelry making has been passed on through generations, leading to the growth of goldsmith



communities, namely Tachai and Sri Satchanalai in Sri Satchanalai district, Sukhothai province for longer than 20 years. Now there are dozen of well-known goldsmiths' workshops or "gold house" in the area, most prominent one is Somsamai Gold House, which is a pioneer in Sukhothai gold jewelry making. Then, others such as Somsak Gold House, On-anong Goldsmith and Nantana Goldsmith, to name but a few.

From delicate hands that create gold jewelry in the tradition of antique gold ornaments, nowadays, there are precious crafts in various patterns and types, including jewelry such as necklaces, bracelets, bangles, rings, earrings, pendants, belts, Buddha image cases; custom works such as breast-plates, tiaras, and armlets as well as, decorative elements on antique objects like Buddha images. These products gain popularity among enthusiasts in antique gold pieces, who recognize unique patterns made by Sri Satchanalai craftsmen in Sukhothai as differently from those found in antique pieces available in other regions of Thailand, particularly Bangkok, or in gold ornaments sold in general shops. With this outstanding feature, Sukhothai gold jewelry is widely recognized among Thais and foreigners, many of whom travel to manufacturing sites to personally select them from a wider range of choices, as well as to take an opportunity to explore and observe its manufacturing processes.

Si Satchanalai Historical Park

http://en.wikipedia.org/wiki/Si_Satchanalai_Historical_Park

The **Si Satchanalai Historical Park** is a historical park in Si Satchanalai district, Sukhothai Province, northern Thailand. The park covers the ruins of Si Satchanalai and Chaliang. Si Satchanalai, which literally means "City of good people", was founded in 1250 as the second center of Sukhothai Kingdom and a residence of the crown prince in the 13th and 14th centuries. The city was rectangular in shape. In the 16th century, a 5-metre high wall with an upstream moat was built to fend off the growing Burmese attacks. The location of the town was facilitated by two the neighborhood dominant hill. The park is maintained by the Fine Arts Department of Thailand with help from UNESCO, which has declared it a World Heritage Site together with the associated historic parks in Kamphaengphet and Sukhothai. Similar to Sukhothai Historical Park, Si Satchanalai Historical Park attracts thousands of visitors each year, who marvel at the ancient Buddha figures, palace buildings and ruined temples. The park is easily toured by bicycle or even on foot.



Wat Chang Lom

Wat Chang Lom was built in 1286 by order of Ramkhamhaeng after the discovery of Buddha's relic on the site. The main structure of the temple is a two tiers square base round Sri Lanka style laterite stupa. The name of the temple come from the statues of 39 standing elephants around the first tier of stupa base. The elephants are remarkably full size in front of the wall. Normally only the front half of the body is shown like in Wat Chang Rop and Wat Chang Lom in Sukhothai Historical Park. Also on the second tier of stupa base has 20 niches that were originally filled with 1.4 m high Buddha images. Some Buddha images can still be seen today. There is a ruin of vihara in front of stupa as well as other smaller structures in the temple compound. The main sanctuary is surrounded by a thick wall made of laterite stones.



Wat Nang Paya

Wat Nang Paya means the temple of queen. In Phra Ruang City Journey, Vajiravudh reported that, according to local legend, the temple was built by Pasuja Devi, a daughter of the Emperor of China; however, there is no archaeological evidence to support such a legend. The temple ground is fairly extensive. There is a large laterite stupa and remains of seven rooms vihara, a typical style of Sukhothai and Lanna architecture, in the center of the compound. The temple is famous for remains of beautiful stucco-reliefs on the wall of Vihara. The stucco-reliefs are protected under the tin roof shelter.



Wat Chedi Chet Thaeo

Wat Chedi Chet Thaeo means the temple of seven rows of stupa. The temple is one of the most important historic sights inside the town wall of Si Satchanalai. The temple is located in front of Wat Chang Lom and is considered unique than other temples in Sukhothai Kingdom, because the temple consists of 32 stupas of different sizes in different styles. The gigantic size of the temple in the town center indicating that this temple was built for the royal family. Vajiravudh wrote in his Phra Ruang City



Journey that a local claimed that the temple was once called Wat Kalayanimit and was built by a daughter of Lithai. Damrong Rajanubhab believed that the temple was the burial place for the ruler family of Si Satchanalai. Pattern of Stupas at Wat Chedi Chet Thaeo are influenced from various arts such as Sri Lanka, Lanna and Bagan stupa which has unique square tower base with spherical

top and arched hall facade stucco for standing Buddha image in beautiful Sukhothai style. Inside the temple, there were vihara, ordination hall, five mandapas and sacred pond. There was also a defensive wall around the temple which was originally surrounded by a moat.

Thuriang Kilns

The Thuriang Kilns are ruins of the old celadon factory, located about 5 km north of the old town of Si Satchanalai. In an area of about 1.5 square kilometers about 200 kilns have been found. This is a site where Sukhothai celadons were produced since the 13th century, they are probably the oldest kilns in Thailand. The vaulted brick kilns measure 1.5 – 2 metres wide and 4.5 metres long. The ceramic wares found here are generally large bowls and jars; they have a matt yellowish grey glaze, and a design, usually of a flower, a fish, or a whirling circle, painted in black in Chinese designs. A group of Thai-Australian archaeologists from University of Adelaide found that the ceramic wares in Si Satchanalai had been produced more than a millennium even before the Sukhothai Kingdom which contradict with general views that the Chinese brought the production in the 13th century.





Thailand CONNECT

Your Global Business Events Connection

Connect Thailand and discover a global success through your business events. Here, we offer endless opportunities to expand your global business networks. With the strategic location as a gateway for business success in Asia, you will find complete satisfaction from advanced infrastructure and facilities, variety of venues, and gracious hospitality that link you to global connection.

With Thailand Convention and Exhibition Bureau (TCEB) as your strategic business partner, we build strong connections for collaborations at all levels, leading you to the strong expansion of business connections.

Connect Thailand and be part of the world's success.

www.businesseventsthailand.com

Thailand





AIGS Lab Co Ltd

Asian Institute of Gemological Sciences

Gemstone Identification, Grading and Research Laboratory

Fast

Accurate

Value for Money

AIGS
Bangkok, Tokyo, Yangon

Master Gemstone Report

Report No. : MGR9999999

Date : 18 February 2014

Weight : 18.63 cts

Shape : Cushion

Dimensions : 19.62 x 15.10 x 9.35 mm

Color Grade : Very Good

Color Hue : Red

Clarity Grade : Very Good - Excellent

Clarity : Eye Clean

Cut Grade : Very Good

Cutting Style : Faceted

Symmetry : Very Good

Polish : Very Good

Proportions : Very Good

AIGS Rarity Scale : Extremely Rare (RRR)

AIGS Star Rating : ★★★★★

Probable Origin : Myanmar (Burma)

Identification : Natural Ruby

Comment
No indications of heating.

MGR9999999

18.63 cts

photo not at actual size

Instruments Used:

Microscope FTIR EDXRF

UV/VIS/NIR LIBS

AIGS Lab Co Ltd 8191 Sothi Rd., Jewelry Trade Center, Level B1 (JW4) Bangkok 10500 Thailand

Asian Institute of Gemological Sciences T: (66) 267 4221 F: (66) 267 4227 E: info@aigslab.com www.aigslab.com

The item described in this Report has been examined by at least two qualified AIGS staff Gemologists. This Report is limited in accordance with the agreement printed on its inside covers. The cover being an integral part of this report. Copyright © Asian Institute of Gemological Sciences





Beauty Gems

*Bangkok Thailand Tel. (66) 0 2237 8680-99 Fax. (66) 0 2237 5664-65
E-mail : info@beautygems.co.th Website : www.beautygems.com*

CONFIDENCE COMES WITH PROOF OF QUALITY



EDUCATION. RESEARCH. LABORATORY SERVICES.

Education

U Chu Liang Building, 2nd Floor
968 Rama IV Road, Silom, Bangrak, Bangkok, 10500 Thailand
T +66 2632 4590 F +66 2632 4595
giabkkedu@gia.edu

Laboratory

U Chu Liang Building, 10th Floor
968 Rama IV Road, Silom, Bangrak, Bangkok, 10500 Thailand
T +66 2632 4090 F +66 2632 4096
giabkklab@gia.edu



GIA[®]

WWW.GIA.EDU

人生の宝物に、もうひとつ確かなブランドを。

Depend on CGL for exacting precision and flawless analysis. For over 40 years, we have been satisfying clients worldwide with our highly accurate gem inspections.



CGL (Central Gem Laboratory), JAPAN

Miyagi Bldg. 5-15-14 Ueno Taito-ku, Tokyo 110-0005 JAPAN
<http://www.cgl.co.jp>

LEE SENG JEWELRY



L.S. ORIENTAL JEWELRY ♦ L.S.GEMS

SINCE 1932

nd
82 year Anniversary

รับประกันซื้อคืนตลอดอายุการใช้งาน

เราคือ ผู้ผลิต ผู้จำหน่ายส่ง-ปลีก-ส่งออกจิวเวลรี่เพชรคุณภาพสูงสุด ทั้งเพชรเหลี่ยม HEART & ARROW และเหลี่ยมรัชเซียน และพลอยคุณภาพสูงสุดทุกชนิด จำหน่ายส่งจิวเวลรี่คุณภาพสูงสุดโดยตรง ยินดีให้คำปรึกษาสำหรับผู้สนใจลงทุนในธุรกิจจิวเวลรี่

ตัวอย่างเพชร GIA, HRD คัดสรรเฉพาะคุณภาพสูงสุดระดับ Triple Excellent / Heart & Arrow / None Fluorescent เท่านั้น (เชิญเลือกชมสินค้าอีกกว่าหนึ่งหมื่นรายการ)

เพชร **GIA 3EX 10.34** กะรัต **D Color** (น้ำ100%) / **IF** (บริสุทธิ์ 100%) ราคาพิเศษ Pls. CALL

เพชร **HRD 3EX 6.49** กะรัต **G Color** (น้ำ 97%) / **VVS2** ราคาพิเศษ Pls. CALL

เพชร **HRD 3EX 3.01** กะรัต **H Color** / **VVS2** ราคาพิเศษ Pls. CALL

เพชร **GIA 3EX 1.23** กะรัต **D Color** (น้ำ100%) / **VVS2** ราคาพิเศษ Pls. CALL

เพชร **GIA 3EX 1.02** กะรัต **E Color** (น้ำ99%) / **VVS1** ราคาพิเศษ Pls. CALL



L.S. JEWELRY GROUP

171, 177-179 ถนนพระสุเมรุ โกลด์สแก็กบางลำภู เขตพระนคร กรุงเทพฯ 10200

Tel. 0 2629 1444 (10 Lines) Fax 0 2629 1717

E-mail : info@LSjewelrygroup.com

WWW.LSJEWELRYGROUP.COM

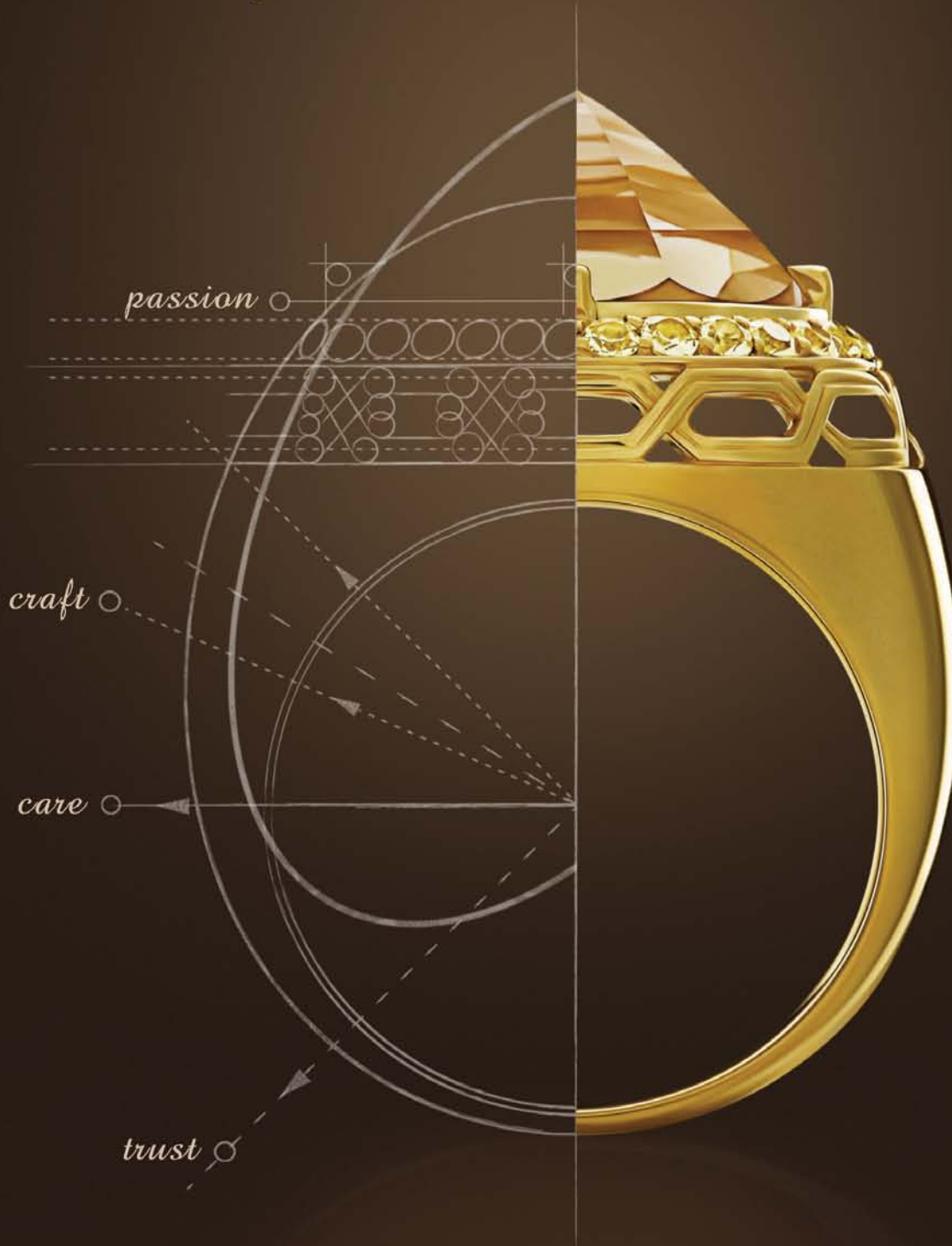


มีเพชรราคาต้นกุ่มเก่า (ก่อนราคาเพชรขึ้นเนื่องจากราคาตลาดโลกขึ้น) จำหน่ายในราคาเก่า ต่ำกว่าต้นกุ่มปัจจุบันนี้

L.S. Jewelry Group ร่วมกับ DTC (Debeers) Sightholder (Belgium) จึงสามารถจำหน่ายส่ง-ปลีกเพชร Heart & Arrow น้ำหนึ่งถึงสามกะรัตในราคาต่ำกว่า 50%



The Emergence of Architecture and Craftsmanship



At Pranda, every piece we create realizes that inspiration. From sketches through prototypes to complete mass craftsmanship, our expert craftsmen unite decades of caring experience with a deep passion from the heart. It's what we call the PRANDA PROCESS.

For over 40 years, Pranda has been committing to bring success to our partners and care to their customers. Taking inspiration to perfection of jewelry making, that is Pranda.

PLQI THAI

Gems & Jewelry from Thailand

Bangkok Gems & Jewelry Fair

DUTY FREE

**FREEDOM
OF TRADE**

No Taxes, Maximum Trade Freedom


The Gems Jewelry &
Precious Metal
Confederation of Thailand


Thai Gem & Jewelry
Traders Association


BANGKOK GEMS
& JEWELRY FAIR

THAI GEM & JEWELRY TRADERS ASSOCIATION

Jewelry Trade Center, 52nd Fl., 919/616, Silom Rd., Bangrak, Bangkok 10500, THAILAND

Tel : (662) 630-1390-7 Fax : (662) 630-3257

E-mail : samai@bangkokgemsfair.com

Website : www.bangkokgemsfair.com, www.thaigemjewelry.or.th

Power of **FREE** **TRADE**
Connect the **WORLD** WITH **FREE** **TAX**


**BANGKOK GEMS
& JEWELRY FAIR**



The Gems Jewelry &
Precious Metal
Confederation of Thailand

สมาพันธ์อัญมณี เครื่องประดับ และโลหะมีค่า แห่งประเทศไทย
The Gems, Jewelry and Precious Metal
Confederation of Thailand



Thai Gem & Jewelry
Traders Association

สมาคมผู้ค้าอัญมณีไทยและเครื่องประดับ
Thai Gem and Jewelry Traders Association

Jewelry Trade Center, 52th floor, 919/616, Silom Rd., Bangrak, Bangkok 10500 THAILAND

Tel: (662) 630 1390-7 Fax: (662) 630 3257

Email: tgjta@thaigemjewelry.or.th www.thaigemjewelry.or.th



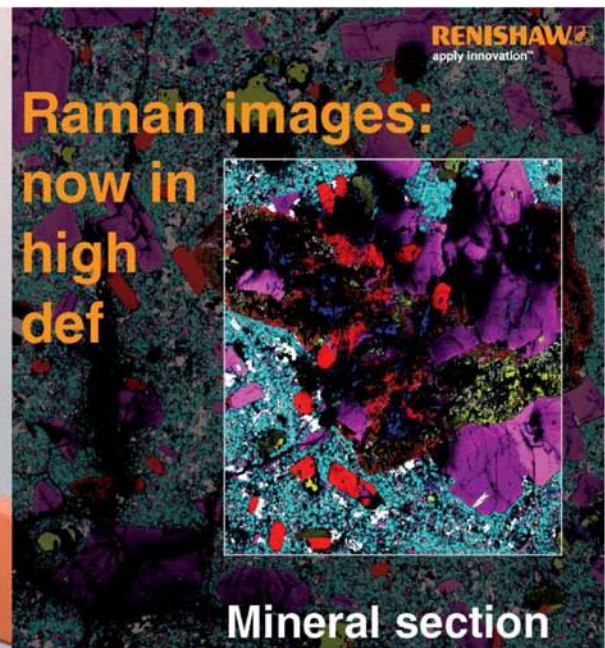
SUKHADIA STONES CO., LTD.

**Our Expertise - Calibrated Color Stones
with Consistent Assortment**



30-38 KBS Bldg., 4th Floor, Room # 401-6
Mahesak Soi 3 Road, Suriyawong, Bangrak
Bangkok 10500 Thailand
Tel: (662) 237 0922-24 Fax: (662) 237 0925
E-mail: sukhadia@sukhadiastones.net www.sukhadiastones.net

**Contact Persons:
Mr Chiku & Mr Kaimesh**



**Raman images:
now in
high
def**

Mineral section

**High performance
Raman spectroscopy**

inVia™ Raman microscope

www.renishaw.com/raman

Renishaw (Hong Kong) Ltd.
28/F Tower Two, Ever Gain Plaza,
88 Container Port Road,
Kwai Chung, Hong Kong

T +852 2753 0638
F +852 2756 8786
E hongkong@renishaw.com

Synchrotron Golden Pearls

...and...

Micro-Pattern Imprinted Pearls

Innovation from

Synchrotron Technology



Synchrotron Golden Pearls, disclosed for the first time at GIT 2014, is a brand-new valuable jewellery from synchrotron technology. The optimal synchrotron light can change white colour of freshwater pearls to metallic-gold. The changed colour possesses a beauty of natural pearl with an improved lustre like gold. This innovation can be applied for a high-resolution pattern printing process that yields Micro-Pattern Imprinted Pearls. The technique can create a unique and beautiful golden pattern on pearls with the streaks in micrometre level, which is ideal for a unique and valuable gift that suits your special ones.

Synchrotron Light Research Institute
(Public Organization)

Sirindhornwitothai Building, 111 University Avenue,
Muang District, Nakhon-Ratchasima, Thailand 30000
Tel. +66 44 21 70 40 ext. 1607-8 Fax. +66 44 21 70 47
E-mail : bds@slri.or.th Website : www.slri.or.th
Facebook : <http://www.facebook.com/SLRI.THAILAND>

Fischer[®]

Analysis of Precious Metals Quick, precise and non-destructive

Coins and Bullions

REAL or FAKED ?

**FISCHERSCOPE
X-RAY XAN Series**



SIGMASCOPE GOLD Product Line

Helmut Fischer (Thailand) Co.,Ltd.
www.helmut-fischer.com

*Your partner of Coating Thickness
and Material Analysis Instrument ...*



Ferrari Logistics Asia (Thailand) Co. Ltd.
 1249/146 Gems Tower Building, 16/F, Charoenkrung Road
 Suriyawongse, Bangrak, Bangkok 10500, Thailand
 Tel: +66 2 2674 755-8 Fax: +66 2 2674 759

www.ferrarigroup.net

**Worldwide Logistics Services
 for Your Valuables**



Malca-Amit (Thailand) Ltd.

5th Floor, Jewelry Trade Center Building,
 919/6 Silom Road, Bangkok 10500
 Tel +662-267 4400 Fax +662-630 1350
 email: info.BKK@malca-amit.com

www.malca-amit.com



Ninety-Three S P N Group Limited Partnership

สร้างสรรค์ ผลิตภัณฑ์คุณภาพครบวงจร

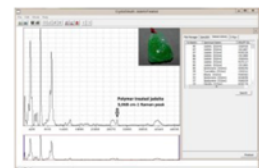
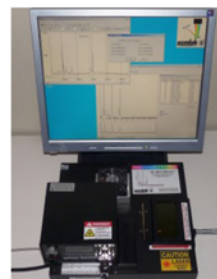
Gemlab Research and Technology

Manufacturer of Advanced Spectrometer Systems

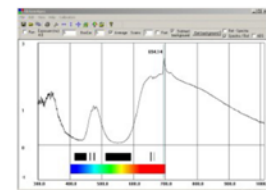
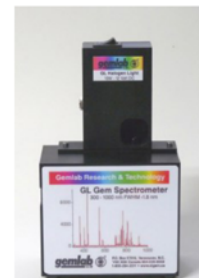
P.O. Box 57010, Vancouver, B.C. V5K 5G6 CANADA

Telephone +1 .604.530.8569 • Toll free 1.800.294.2211

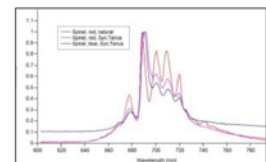
www.gemlab.ws



GL Gem Raman PL 532 TEC (100 – 5440 cm⁻¹) and
 Photoluminescence Spectrometer (530 – 750 nm)
 with Band Pass Filter (GLBPF)



GL Gem Spectrometer UV-VIS-NIR (300 – 1000 nm)
 with GL Halogen 10W Gem Holder



GL Gem Spectrometer NIR PL405 (600–1050 nm)
NEW Advanced Luminescence Analyzer System



Conceptual Plan

GEMOPOLIS **FREE ZONE**
complex

NO DUTY NO TAX !!!

The gateway to AEC's light industrial hub

- Prime location
- Prime advantage
- Prime facility & infrastructure



www.gemopolis.com

Tel. +662 727 0000

E-mail: chitwalai@gemopolis.com

GIT

Author Index

Author Index	Page (Theme)
A.R. Blake	256
A.Serova	109
Aatish Panjekar	145
Adolf Peretti	113
Andrés Ignacio Rodríguez Vargas	262
Andrea Marzola	228
Antonello Donini	228
Aram Ham	134
Arne Christopherse	271
Aumaparn Phlayrahan	122,161,211
B. Kummerdponpittaya	317
Bhuwadol Wanthanachaisaeng	97,101,172
Boontarika srithai	157
Boontawee Sriprasert	126, 232
Branko Deljanin	113
Bui Sinh Vuong	172
Carina Bagola	76
Chakkaphan Sutthirat	97, 165,271
Chakkrich Boonmee	122,161,277
Chandana P. Udawatte	142
Christian Muellen	76
Christoph Hauzenberger	76,195,217
Chutimun Chanmuang	317
Claudio C. Milisenda	79
Cynthia Unninayar	311
Dmitry Filimonov	109
Dongwook Shin	134, 149,177
Dorrit E. Jacob	207,240
Duong Anh Tuan	91,195,217
Elena Gambini	228
Emanuela Castaman	228
Frieder Enzmann	207
Gagan Choudhary	191
Giuliano Radice	228
Hans A. Gilg	256

Hasintha Wijesekara	142
Hauzenberger Christoph Anton ⁴ and	91
Hermann Götz	240
Hiroshi Kitawaki	203,244
Hua Chen	292
Hunhyeong Lee	177
Huong Le	76,172
Hyeonki Kim	169
Hyun-Min Choi	104
Ismail Abdulla Almas	314
Jakraphan Suwanvijit	300
Janyaporn Witthayarat	184
JAYSHREE PANJIKAR	145
Jian Zhang	292
Jidapa Mogmued	264
Jie Ke	292
Jinhee Jeon	177
Jirapit Jakkawanvibul	232
Jochen Knigge	79
John Chapman	63
Jongwan Park	91,118,217,287
Kageeporn Wongpreedee	300
Kanyarat Kwansirikul	199
Karl Schmetzer	256
Katrien De Corte	95
Kennedy Ho	299
Kentaro Emori	203,244
Khumsing Vichapoon	300
Krit Won-in	65,153
Kyungjin Kim	221
Laura M. Otter	207,240
Loke Hui Ying	131
Lore Kiefert	237
Lutz Nasdala	262
Majken D. Poulsen	180
Manuela Zeug	262
Marisa Maneekrajangsaeng	232
Martin Steinbach	256,307
Masahiro Yamamoto	244

Meththika Vithanage	142
Mimi C. M. Ouyang	137
Minwoo Park	296
Mio Hisanaga	244
Miro F. Y. Ng	137
Muzdareefah Thudsanapbunya	264
Myungji Ye	287
Nalida Jaiboon	224
Nalin Narudeesombat	271
Namrawee Susawee	126
Nantharat Bunnag	97,101
Naphithiphorn Manoli	260
Narong Praphairaksit	300
Natamon Bavornyospiwat	284
Nataya Nilhud	69,165
Natthaphol Chomsaeng	82,122,153,161,211,277,317
Nguyen Ngoc Khoi	76,91,195,217
Nguyen Thuy Duong	91
Nicharee Atsawatanapirom	126
Nirawat Thammajak	187
Nisa Sukkee	165
Nutwatcharee Noirawee	161
Nynke Keulen	180
O. Juntakool	317
Padon Tangulrat	65
Panjawan Thanasuthipitak	106,184
Panphot Ruethaitananon	300
Papawarin Ounorn	97,271
Parichart Puangcharoen	157
Phan Thi Minh Diep	195,217
Phisit Limtrakun	260
Pierre Hardy	237
Pimtida Bupparaenoo	271
Pornsawat Wathanakul	82,153,211,277
Prayath Nantasin	153
Rattanawalee Chooyoung	122
Richard Hughes	291
Roman Serov	109
Saengthip Saengbuangamlam	129

Saisamorn Niyomsoan	317
Sandun Illangasinghe	142
Sasithorn Ya-in	199
Seriwat Saminpanya	284
Sermrak Ingavanija	153,277
Shane McClure	304
Shigeru Akamatsu	280
Simon Wingate	299
Siwon Lee	253
Somruedee Satitkune	65,82,97,122,153,161,172,211,264,277
Sora Shin	91,118,217,287
Sorapong Pongkrapan	187
Suchart Kiatwattanacharoen	106
Sudarat Saeseaw	268
Sumalee Danyutthapolchai	284
Sungjae Kim	149
Sungwon Park	118
Sunisa Homklin	284
Sun-Ki Kim	82
Supharat Sangsawong	268
Supparat Promwongnan	129
Sutas Singbamroong	314
Taijin Lu	292
Tasnara Sripoonjan	69,165
Tatjana M. Gluhak	240
Tay Thye Sun	131
Tewodros Siantayehu	237
Thanapong Lhuaamporn	82,165,232
Thanong Leelawatanasuk	69,126,131,232
Thidarat Muangthai	300
Thitiporn Kaewlungka	65
Tobias Haeger	76,91,195,217
U Tin Hlaing	221
Ursula Wehrmeister	207,240
Vincent Pardieu	268
Visut Pisutha-arnond	69,97,129,271
Wantana Klysubun	187
Weerapan Srichan	157,224
Wilawan Atichat	69,126,131,232
Wiwat Wongkokua	82

Wolf Kuehn	248
Wolfgang Hofmeister	195
Wuyi Wang	87
Y.Y. Yang	298
Yan Lan	292
Yong Zhang	292
Yongkil Ahn	221
Young-Chool Kim	104
Yuri Shelementiev	109



สถาบันวิจัยและพัฒนาอัญมณีและเครื่องประดับแห่งชาติ (องค์การมหาชน)
The Gem and Jewelry Institute of Thailand (Public Organization)

GIT 2014

